IN THE UNITED STATES PATENT AND TRADEMARK OFFICE

Applicant:Fong et al.
Serial No.:10/791,618
Filing Date: March 2, 2004

Docket No.: P1192-2C1
Group Art Unit: 1647
Examiner: Deberry, Regina M.

DECLARATION OF SHERMAN FONG, Ph.D. UNDER 37 C.F.R. § 1.132

Commissioner for Patents
P.O. Box 1450
Alexandria, VA 22313-1450

Sir:

I, Sherman Fong, Ph.D. declare as follows:-

1. I was awarded a Ph.D. in Microbiology by the University of California at Davis, CA in 1975.

2. After postdoctoral training and holding various research positions at Scripps Clinic and Research Foundation, La Jolla, CA, I joined Genentech, Inc., South San Francisco, CA in 1987. I am currently a Senior Scientist at the Department of Immunology/Discovery Research of Genentech, Inc.

3. My scientific Curriculum Vitae is attached to and forms part of this Declaration.

4. I am familiar with the Mixed Lymphocyte Reaction (MLR) assay, which has been used by me and others under my supervision, to test the immune stimulatory or immune inhibitory activity of novel peptides discovered in Genentech's Secreted Protein Discovery Initiative project.

5. The MLR assay is a well known and widely used proliferative assay of T-cell function, the basic protocols of which are described, for example, in Current Protocols in Immunology Vol. 1, Richard Coico, Series Ed., John Wiley & Sons, Inc., 1991, Unit 3.12 (Exhibit A). This publication is incorporated by reference in the description of the MLR protocol in the present application.

6. The T-lymphocytes or "T-cells" of our immune system can be induced to proliferate by a variety of agents. The MLR assay is designed to study a particularly important induction mechanism whereby responsive T-cells are cultured together (or "mixed"), with other lymphocytes that are "allogeneic", e.g. lymphocytes that are taken from different individuals of the same species. In the MLR protocol of the present application, a suspension of PBMCs that includes responder T-cells, is cultured with allogeneic PBMCs that predominantly contain dendritic cells. According to the protocol, the allogeneic "stimulator" PBMCs are irradiated at a dose of 3000 Rad. This irradiation is done in order to create a sample of cells that has mainly dendritic cells. It is known that the dendritic cell population among the PBMCs are differentially affected by irradiation. At low doses (500-1000 Rad), the proliferation of most cells, including the B cells in the PBMCs, is preserved, however, at doses above 2000 Rad, this function of B cells is abolished. Dendritic cells on the other hand, maintain their antigen presentation function even at a 3000 Rad dose of radiation. (See, e.g. Current Protocols in Immunology, *supra*, at 3.12.9). Accordingly, under the conditions of the MLR assay used to test the PRO polypeptides of the present invention, the stimulator PBMCs remaining after irradiation are essentially dendritic cells.

7. Dendritic cells are the most potent antigen-presenting cells, which are able to "prime" naive T cells *in vivo*. They carry on their surface high levels of major histocompatibility complex (MHC) products, the primary antigens for stimulating T-cell proliferation. Dendritic cells provide the T-cells with potent and needed accessory or costimulatory substances, in addition to giving them the T-cell maturing antigenic signal to begin proliferation and carry out their function. Once activated by dendritic cells, the T-cells are capable of interacting with other antigen presenting B cells and macrophages to produce additional immune responses from these cells. For further details about the properties and role of dendritic cells in immune-based therapies see, e.g. Steinman, Drug News Perspect. 13(10):581-586 (Exhibit B).

8. The MLR assay of the present application is designed to measure the ability of a test substance to "drive" the dendritic cells to induce the proliferation of T-cells that are activated, or co-stimulated in the MLR, and thus identifies immune stimulants that can boost the immune system to respond to a particular antigen that may not have been immunologically active previously.

9. Such immune stimulants find important clinical applications. For example, IL-12 is a known immune stimulant, which has been shown to stimulate T-cell proliferation in the MLR assay. IL-12 was first identified in just such an MLR .[Gubler et al. PNAS 88, 4143 (1991) (Exhibit C)]. In a recent cancer vaccine trial, researchers from the University of Chicago and Genetics Institute (Cambridge, MA) have demonstrated the efficacy of the approach, relying on the immune stimulatory activity of IL-12, for the treatment of melanoma. [Peterson et al. Journal of Clinical Oncology 21 (12). 2342-48 (2003) (Exhibit D)] They extracted circulating white blood cells carrying one or more markers of melanoma cells, isolated the antigen, and returned them to the patients. Normally patients would not have an immune response to his or her own human antigens. The patients were then treated with different doses of IL-12, an immune stimulant capable of inducing the proliferation of T cells that have been co-stimulated by dendritic cells. Due to the immune stimulatory effect of IL-12, the treatment provided superior results in comparison to earlier work, where patients' own dendritic cells were prepared from peripheral blood mononuclear cells (PBMCs), treated with antigens, then cultured *in vitro* and returned to the patient to stimulate anti-cancer response. [Thurner et al. J. Exp. Med. 190 (11), 1669-78 (1999) (Exhibit E)].

10. It is my considered scientific opinion that a PRO polypeptide shown to stimulate T-cell proliferation in the MLR assay of the present invention with an activity at least 180% of the control, as specified in the present application, is expected to have the type of activity as that exhibited by IL-12, and would therefore find practical utility as an immune stimulant. Some PRO polypeptides do the reverse, and give inhibition of T-cell proliferation in the MLR assay. It is my considered scientific opinion that a PRO polypeptide shown to inhibit T-cell proliferation in the MLR assay where the activity is observed as 80% or less of the control, as specified in the present application, would be expected to find practical utility when an inhibition of the immune response is desired, such as in autoimmune diseases.

Dated: 6/16/04

By: Sherman Fong

Sherman Fong, Ph.D.

2041362

Sherman Fong, Ph.D.

Senior Scientist
Department of Immunology
Genentech Inc.
1 DNA Way.
South San Francisco, California 94080-4990

19 Basinside Way
Alameda, California 94502

Work Telephone: (650) 225-2783 FAX: (650) 225-8221
Home Telephone: (510) 522-5411

Education:

1978 - 1980 Postdoctoral Fellow in Immunology, Scripps Clinic and Research Foundation, La Jolla, California

1975 - 1978 Postdoctoral Fellow in Immunology, University of California at San Francisco, San Francisco, California

1970 - 1975 Ph.D. in Microbiology, University of California at Davis, California

1966 - 1970 B.A. in Biology/Microbiology, San Francisco State University, San Francisco, California

Professional Positions:

Currently: Senior Scientist, Department of Immunology/Discovery Research, Genentech, Inc., South San Francisco, California

8/00-8/01 Acting Director, Department of Immunology, Genentech, Inc. South San Francisco, California

10/89 Senior Scientist in the Department of Immunology/Discovery Research, Genentech, Inc. South San Francisco, California

3/89 - 10/89 Senior Scientist and Immunobiology Group Leader, Department of Pharmacological Sciences, Immunobiology Section/Medical Research and Development, Genentech, Inc., S. San Francisco, California

9/87 - 3/89 Scientist, Department of Pharmacological Sciences, Immunopharmacology Section/Medical Research and Development, Genentech, Inc., S. San Francisco, California

1/82 - 9/87 Assistant Member (eq. Assistant Professor level), Department of Basic and Clinical Research, Division of Clinical Immunology, Scripps Clinic and Research Foundation, La Jolla, California

6/80 - 12/81 Scientific Associate in the Department of Clinical Research, Division of Clinical Immunology, Scripps Clinic and Research Foundation, La Jolla, California

7/78 - 6/80 Postdoctoral training in the laboratory of Dr. J. H. Vaughan, Chairman, Department of Clinical Research, Division of Clinical Immunology, Scripps Clinic and Research Foundation, La Jolla, California

2/75 - 6/78 Postdoctoral training in the laboratory of Dr. J. W. Goodman, Department of Microbiology and Immunology, School of Medicine, University of California, San Francisco, California

7/71 - 12/74 Research Assistant and Graduate Student, Department of Medical Microbiology, School of Medicine, University of California, Davis, California, under Dr. E. Benjamini

Awards:

Recipient: National Institutes of Health Postdoctoral Fellowship Award (1975).

Recipient: Special Research Award, (New Investigator Award), National Institute of Health (1980).

Recipient: P.I., Research Grant Award, National Institute of Health (1984).

Recipient: Research Career Development Award (R01), National Institutes of Health (1985).

Recipient: P.I., Multi-Purpose Arthritis Center Resarch Grant, NIH (1985)

Recipient: P.I., Resarch Grant Award, (R01 Renewal), National Institute of Health (1987).

Scientific Associations:

Sigma Xi, University of California, Davis, California Chapter

Member, The American Association of Immunologists

Committee Service and Professional Activities:

Member of the Immunological Sciences Study Section, National Institutes of Health Research Grant Review Commitee, (1988-1992).

Advisory Committee, Scientific Review Committee for Veteran's Administration High Priority Program on Aging, 1983.

Ad Hoc member of Immunological Sciences Study Section, National Institutes of Health, 1988.

Ad Hoc Reviewer: Journal of Clinical Investigations, Journal of Immunology, Arthritis and Rheumatism, International Immunology, Molecular Cell Biology, and Gastroenterology

Biotechnology Experience

Established at Genentech in 1987-1989 within the Immunobiology Laboratory, in the Department of Pharmcological Sciences, group to study the immunogenicity of recombinant hGH (Protropin®) in hGH transgenic mice.

Served as Immunologist on the **Biochemical Subteam for Protropin® Project** team.

Served as Immunologist on the **Met-less hGH and Dnase project teams**, two FDA approved biological drugs: second generation hGH Nutropin® and Pulmozyme® (DNase).

Served immunologist in1989-1990 on the **CD4-IgG project team** carrying out in vitro immunopharmacological studies of the effects of CD4-IgG on the in vitro human immune responses to mitogens and antigens and on neutrophil responses in support of the filing of IND to FDA in 1990 for use of CD4-IgG in the prevention of HIV infection. Product was dropped.

In 1989-1991, initiated and carried research and development work on antibodies to CD11b and CD18 chains of the leukocyte β2 integrins. Provided preclinical scientific data to **Anti-CD18 project team**

supporting the advancement of humanized anti-CD18 antibody as anti-inflammatory in the acute setting. IND filed in 1996 and currently under clinical evaluation.

1993-1997, **Research Project Team leader** for small molecule α4β1 integrin antagonist project. Leader for collaborative multidisciplinary team (N=11) composed of immunologists, molecular/cell biologists, protein engineers, pathologists, medicinal chemists, pharmacologists, pharmaceutical chemists, and clinical scientists targeting immune-mediated chronic inflammatory diseases. Responsible for research project plans and execution of strategy to identify lead molecules, assessment of biological activities, preclinical evaluation in experimental animals, and identification of potential clinical targets. Responsible for identification, hiring, and working with outside scientific consultants for project. Helped established and responsible for maintaining current research collaboration with Roche-Nutley. Project transfered to Roche-Nutley.

1998-present, worked with Business Development to identify and create joint development opportunity with LeukoSite (currently Millennium) for monoclonal antibody against α4β7 intergin (LDP-02) for therapeutic treatment for inflammatory bowel disease (UC and Crohn';s disease). Currently, working as scientific advisor to the core team for phase II clinical trials for LDP-02.

Currently, **Research Project Team Biology Leader** (1996-present) for small molecule antagonists for α4β7/MAdCAM-1 targeting the treatment of human inflammatory bowel diseases and diseases of the gastrointestinal tract. Responsible for leading collaborative team (N=12) from Departments of Immunology, Pathology, Analytical Technology, Antibody Technology, and Bio-Organic Chemistry to identify and evaluate lead drug candidates for the treatment of gastrointestinal inflammatory diseases.

Served for nearly fifteen years as **Ad Hoc reveiwer** on Genentech Internal Research Review Committee, Product Development Review Committee, and Pharmacological Sciences Review Committee.

Worked as Scientific advisor with staff of the **Business Development** Office on numerous occasions at Genentech, Inc. to evaluate the science of potential in-licensing of novel technologies and products.

2000-2001 Served as Research Discovery representative on Genentech Therapeutic Area Teams (Immunology/Endocrine, Pulmonary/Respiratory Disease Task Force)

Invited Symposium Lectures:

Session Chairperson and speaker, American Aging Association 12th Annual National Meeting, San Francisco, California, 1982.

Invited Lecturer, International Symposium, Mediators of Immune Regulation and Immunotherapy, University of Western Ontario, London, Ontario, Canada, 1985.

Invited Lecturer, workshop on Human IgG Subclasses, Rheumatoid Factors, and Complement. American Association of Clinical Chemistry, San Francisco, California, 1987.

Plenary Lecturer, First International Waaler Conference on Rheumatoid Factors, Bergen, Norway, 1987.

Invited Lecturer, Course in Immunorheumatology at the Universite aux Marseilles, Marseilles, France, 1988.

Plenary Lecturer, 5th Mediterranean Congress of Rheumatology, Istanbul, Turkey, 1988.

Invited Lecturer, Second Annual meeting of the Society of Chinese Bioscientist of America, University of California, Berkeley, California, 1988.

Lecturer at the inaugural meeting of the Immunology by the Bay sponsored by The Bay Area Bioscience Center. The β2 Integrins in Acute Inflammation, July 14, 1992.

Lecturer, "Research and Development -- An Anatomy of a Biotechnology Company", University of California, Berkeley, Extension Course, given twice a year--March 9, 1995 to June 24, 1997.

Lecturer, "The Drug Development Process – Biologic Research - Genomics", University of California, Berkeley Extension, April 21, 1999, October, 1999, April 2000, October, 2000.

Lecturer, "The Drug Development Process – Future Trends/Impact of Pharmacogenomics", University of California Berkeley Extension, April 2001, October 2001, April 2002.

Invited Speaker, "Targeting of Lymphocyte Integrin α4β7 Attentuates Inflammatory Bowel Diseases", in Sympoium on "Nutrient effects on Gene Expression" at the Institute of Food Technology Symposium, June, 2002.

Patents:
Dennis A. Carson, Sherman Fong, Pojen P. Chen.
U.S. Patent Number 5,068,177: Anti-idiotype Antibodies induced by Synthetic Polypeptides, Nov. 26, 1991

Sherman Fong, Caroline A. Hebert, Kyung Jin Kim and Steven R. Leong.
U.S. Patent Number 5,677,426: Anti-IL-8 Antibody Fragments, Oct. 14, 1997

Claire M. Doerschuk, Sherman Fong, Caroline A. Hebert, Kyung Jin Kim, Steven R. Leong. U.S. Patent Number 5,686,070: Methods for Treating Bacterial Pneumonia, Nov. 11, 1997

Claire M. Doerschuk, Sherman Fong, Caroline A. Hebert, Kyung Jin Kim, Steven R. Leong. U.S. Patent 5,702,946: Anti-IL-8 Monoclonal Antibodies for the Treatment of Inflammatory Disorders, Dec. 30, 1997

Sherman Fong, Caroline A. Hebert, Kyung Jin Kim, Steven R. Leong.
U.S. Patent Number 5,707,622: Methods for Treating Ulcerative Colits, Jan. 13, 1998

Sherman Fong, Napoleone Ferrara, Audrey Goddard, Paul Godowski, Austin Gurney, Kenneth Hillan, and Mickey Williams. U.S. Patent Number 6,074,873: Nucleic acids encoding NL-3, June 13, 2000

Sherman Fong, Napoleone Ferrara, Audrey Goddard, Paul Godowski, Austin Gurney, Kenneth Hillan, and Mickey Williams. U.S. Patent Number 6,348,351 B1: The Receptor Tyrosine Kinase Ligand Homologues. February 19, 2002

Patent Applications:

Sherman Fong, Kenneth Hillan, Toni Klassen
U.S. Patent Application: "Diagnosis and Treatment of Hepatic Disorders"

Sherman Fong, Audrey Goddard, Austin Gurney, Daniel Tumas, William Wood
U.S. Patent Application: Compositions and Methods for the Treatment of Immune Related Diseases.

Sherman Fong, Mary Gerritsen, Audrey Goddard, Austin Gurney, Kenneth Hillan, Mickey Williams, William Wood . U.S. Patent Application: Promotion or Inhibition of Cardiovasculogenesis and Angiogenesis

Avi Ashkenazi, Sherman Fong, Audrey Goddard, Austin Gurney, Mary Napier, Daniel Tumas, William Wood. US Patent Application: Compounds, Compositions and Methods for the Treatment of Diseases Characterized by A33-Related Antigens

Chen, Filvaroff, Fong, Goddard, Godowski, Grimaldi, Gurney, Hillan, Tumas, Vandlen, Van Lookeren, Watanabe, Williams, Wood, Yansura
US Patent Application: IL-17 Homologous Polypeptides and Therapeutic Uses Thereof

Ashkenazi, Botstein, Desnoyers, Eaton, Ferrara, Filvaroff, Fong, Gao, Gerber, Gerritsen, Goddard, Godowski, Grimaldi, Gurney, Hillan, Kljavin, Mather, Pan, Paoni, Roy, Stewart, Tumas, Williams, Wood
US Patent Application: Secreted And Transmembrane Polypeptides And Nucleic Acids Encoding The Same

Publications:

1. Scibienski R, Fong S, Benjamini E: Cross tolerance between serologically non-cross reacting forms of egg white lysozyme. J Exp Med 136:1308-1312, 1972.

2. Scibienski R, Harris M, Fong S, Benjamini E: Active and inactive states of immunological unresponsiveness. J Immunol 113:45-50, 1974.

3. Fong S: Studies on the relationship between the immune response and tumor growth. Ph D Thesis, 1975.

4. Benjamini E, Theilen G, Torten M, Fong S, Crow S, Henness AM: Tumor vaccines for immunotherapy of canine lymphosarcoma. Ann NY Acad Sci 277:305, 1976.

5. Benjamini E, Fong S, Erickson C, Leung CY, Rennick D, Scibienski RJ: Immunity to lymphoid tumors induced in syngeneic mice by immunization with mitomycin C treated cells. J Immunol 118:685-693, 1977.

6. Goodman JW, Fong S, Lewis GK, Kamin R, Nitecki DE, Der Balian G: T lymphocyte activation by immunogenic determinants. Adv Exp Biol Med 98:143, 1978.

7. Goodman JW, Fong S, Lewis GK, Kamin R, Nitecki DE, Der Balian G: Antigen structure and lymphocyte activation. Immunol Rev 39:36, 1978.

8. Fong S, Nitecki DE, Cook RM, Goodman JW: Spatial requirements of haptenic and carrier determinants for T-dependent antibody responses. J Exp Med 148:817, 1978.

9. Fong S, Chen PP, Nitecki DE, Goodman JW: Macrophage-T cell interaction mediated by immunogenic and nonimmunogenic forms of a monofunctional antigen. Mol Cell Biochem 25:131, 1979.

10. Tsoukas CD, Carson DA, Fong S, Pasquali J-L, Vaughan JH: Cellular requirements for pokeweed mitogen induced autoantibody production in rheumatoid arthritis. J Immunol 125:1125-1129, 1980.

11. Pasquali J-L, Fong S, Tsoukas CD, Vaughan JH, Carson DA: Inheritance of IgM rheumatoid factor idiotypes. J Clin Invest 66:863-866, 1980.

12. Fong S, Pasquali J-L, Tsoukas CD, Vaughan JH, Carson DA: Age-related restriction of the light chain heterogeneity of anti-IgG antibodies induced by Epstein-Barr virus stimulation of human lymphocytes in vitro. Clin Immunol Immunopathol 18:344, 1981.

13. Fong S, Tsoukas CD, Frincke LA, Lawrance SK, Holbrook TL, Vaughan JH, Carson DA: Age-associated changes in Epstein-Barr virus induced human lymphocyte autoantibody responses. J Immunol 126:910-914, 1981.

14. Tsoukas CD, Fox RI, Slovin SF, Carson DA, Pellegrino M, Fong S, Pasquali J-L, Ferrone S, Kung P, Vaughan JH: T lymphocyte-mediated cytotoxicity against autologous EBV-genome-bearing B cells. J Immunol 126:1742-1746, 1981.

15. Fong S, Tsoukas CD, Pasquali J-L, Fox RI, Rose JE, Raiklen D, Carson DA, Vaughan JH: Fractionation of human lymphocyte subpopulations on immunoglobulin coated petri dishes. J Immunol Methods 44:171-182, 1981.

16. Pasquali J-L, Tsoukas CD, Fong S, Carson DA, Vaughan JH: Effect of Levamisole on pokeweed mitogen stimulation of immunoglobulin production in vitro. Immunopharmacology 3:289-298, 1981.

17. Pasquali J-L, Fong S, Tsoukas CD, Hench PK, Vaughan JH, Carson DA: Selective lymphocyte deficiency in seronegative rheumatoid arthritis. Arthritis Rheum 24:770-773, 1981.

18. Fong S, Fox RI, Rose JE, Liu J, Tsoukas CD, Carson DA, Vaughan JH: Solid- phase selection of human T lymphocyte subpopulations using monoclonal antibodies. J Immunol Methods 46:153-163, 1981.

19. Pasquali J-L, Fong S, Tsoukas CD, Slovin SF, Vaughan JH, Carson DA: Different populations of rheumatoid factor idiotypes induced by two polyclonal B cell activators, pokeweed mitogen and Epstein-Barr virus. Clin Immunol Immunopathol 21:184-189, 1981.

20. Carson DA, Pasquali J-L, Tsoukas CD, Fong S, Slovin SF, Lawrance SK, Slaughter L, Vaughan JH: Physiology and pathology of rheumatoid factors. Springer Semin Immunopathol 4:161-179, 1981.

21. Fox RI, Fong S, Sabharwal N, Carstens SA, Kung PC, Vaughan JH: Synovial fluid lymphocytes differ from peripheral blood lymphocytes in patients with rheumatoid arthritis. J Immunol 128:351-354, 1982.

22. Seybold M, Tsoukas CD, Lindstrom J, Fong S, Vaughan JH: Acetylcholine receptor antibody production during leukoplasmapheresis for Myasthenia Gravis. Arch Neurol 39:433-435, 1982.

23. Tsoukas CD, Fox RI, Carson DA, Fong S, Vaughan JH: Molecular interactions in human T-cell-mediated cytotoxicity to Epstein-Barr virus. I. Blocking of effector cell function by monoclonal antibody OKT3. Cell Immunol 69:113-121, 1982.

24. Sabharwal UK, Vaughan JH, Fong S, Bennett P, Carson DA, Curd JG: Activation of the classical pathway of complement by rheumatoid factors: Assessment by radioimmunoassay for C4. Arthritis Rheum 25:161-167, 1982.

25. Fox RI, Carstens SA, Fong S, Robinson CA, Howell F, Vaughan JH: Use of monoclonal antibodies to analyze peripheral blood and salivary gland lymphocyte subsets in Sjogren's Syndrome. Arthritis Rheum 25:419, 1982.

26. Fong S, Miller JJIII, Moore TL, Tsoukas CD, Vaughan JH, Carson DA: Frequencies of Epstein-Barr virus inducible IgM anti-IgG B lymphocytes in normal children and in children with Juvenile Rheumatoid Arthritis. Arthritis Rheum 25:959-965, 1982.

27. Goodman JW, Nitecki DE, Fong S, Kaymakcalan Z: Antigen bridging in the interaction of T helper cells and B cells. Adv Exp Med Biol 150:219-225, 1982.

28. Goodman JW, Nitecki DE, Fong S, Kaymakcalan Z: Antigen bridging in T cell-B cell interaction: Facts or fiction. In: Protein Conformation as Immunologic Signal. EMBO Workshop, Portonenere, Italy, 1982.

29. Tsoukas CD, Carson DA, Fong S, Slovin SF, Fox RI, Vaughan JH: Lysis of autologous Epstein-Barr virus infected B cells by cytotoxic T lymphocytes of rheumatoid arthritis patients. Clin Immunol Immunopathol 24:8-14, 1982.

30. Fong S, Vaughan JH, Tsoukas CD, Carson DA: Selective induction of autoantibody secretion in human bone marrow by Epstein-Barr virus. J Immunol 129:1941-1945, 1982.

31. Sabharwal UK, Fong S, Hoch S, Cook RD, Vaughan JH, Curd JG: Complement activation by antibodies to Sm in systemic lupus erythematosus. Clin Exp Immunol 51:317-324, 1983.

32. Tsoukas CD, Carson DA, Fong S, Vaughan JH: Molecular interactions in human T cell mediated cytotoxicity to EBV. II. Monoclonal antibody OKT3 inhibits a post-killer-target recognition/adhesion step. J Immunol 129:1421-1425, 1982.

33. Welch MJ, Fong S, Vaughan JH, Carson DA: Increased frequency of rheumatoid factor precursor B lymphocytes after immunization of normal adults with tetanus toxoid. Clin Exp Immunol 51:299-305, 1983.

34. Fong S, Vaughan JH, Carson DA: Two different rheumatoid-factor producing cell populations distinguished by the mouse erythrocyte receptor and responsiveness to polyclonal B cell activators. J Immunol 130:162-164, 1983.

35. Fox RI, Hueniken M, Fong S, Behar S, Royston I, Singhal SK, Thompson L: A novel cell surface antigen (T305) found in increased frequency on acute leukemia cells and in autoimmune disease states. J Immunol 131:762-767, 1983.

36. Fong S: Solid-phase panning for the fractionation of lymphoid cells. In: Cell separation: methods and selected applications. Pretlow TG, Pretlow TP (eds.) pp. 203-219. Academic Press, New York, 1983.

37. Carson DA, Fong S: A common idiotype on human rheumatoid factors identified by a hybridoma antibody. Mol Immunol 20:1081-1087, 1983.

38. Fong S, Gilbertson TA, Carson DA: The internal image of IgG in cross- reactive anti-idiotypic antibodies against human rheumatoid factors. J Immunol 131:719-724, 1983.

39. Fox RI, Adamson TC, Fong S, Young C, Howell FV: Characterization of the phenotype and function of lymphocytes infiltrating the salivary gland in patients with primary Sjogren syndrome. Diagn Immunol 1:233-239, 1983.

40. Fox RI, Adamson III TC, Fong S, Robinson CA, Morgan EL, Robb JA, Howell FV: Lymphocyte phenotype and function in pseudolymphoma associated with Sjogren's syndrome. J Clin Invest 72:52-62, 1983.

41. Fong S, Gilbertson TA, Chen PP, Vaughan JH, Carson DA: Modulation of human rheumatoid factor-specific lymphocyte responses with a cross- reactive anti-idiotype bearing the internal image of antigen. J Immunol 132:1183-1189, 1984.

42. Chen PP, Houghten RA, Fong S, Rhodes GH, Gilbertson TA, Vaughan JH, Lerner RA, Carson DA: Anti-hypervariable region antibody induced by a defined peptide. A new approach for studying the structural correlates of idiotypes. Proc Natl Acad Sci USA 81:1784-1788, 1984.

43. Fox RI, Fong S, Tsoukas CD, Vaughan JH: Characterization of recirculating lymphocytes in rheumatoid arthritis patients: Selective deficiency of natural killer cells in thoracic duct lymph. J Immunol 132:2883-2887, 1984.

44. Chen PP, Fong S, Normansell D, Houghten RA, Karras JG, Vaughan JH, Carson DA: Delineation of a cross-reactive idiotype on human autoantibodies with antibody against a synthetic peptide. J Exp Med 159:1502-1511, 1984.

45. Fong S, Carson DA, Vaughan JH: Rheumatoid factor. In: Immunology of Rheumatic Diseases. Gupta S, Talal N (eds.): Chapter 6. pp. 167-196. Plenum Publishing Corp., New York, 1985.

46. Fong S: Immunochemistry. In: Immunology as applied to Otolaryngology. Ryan AF, Poliquis JF, Harris A (eds.): pp. 23-53. College Hill Press, San Diego, 1985.

47. Fong S, Chen PP, Vaughan JH, Carson DA: Origin and age-associated changes in the expression of a physiologic autoantibody. Gerontology 31:236-250, 1985.

48. Chen PP, Fong S, Houghten RA, Carson DA: Characterization of an epibody: An anti-idiotype which reacts with both the idiotype of rheumatoid factors (RF) and the antigen recognized by RFs. J Exp Med 161:323, 1985.

49. Chen PP, Goni F, Fong S, Jirik F, Vaughan JH, Frangione B, Carson DA: The majority of human monoclonal IgM rheumatoid factors express a primary structure-dependent cross-reactive idiotype. J Immunol 134:3281-3285, 1985.

50. Lotz M, Tsoukas CD, Fong S, Carson DA, Vaughan JH: Regulation of Epstein- Barr virus infections by recombinant interferon. Selected sensitivity to interferon-gamma. Eur J Immunol 15:520-525, 1985.

51. Chen PP, Kabat EA, Wu TT, Fong S, Carson DA: Possible involvement of human D-minigenes in the first complementarity-determining region of kappa light chains. Proc Natl Acad Sci USA 82:2125-2127, 1985.

52. Goldfien RD, Chen PP, Fong S, Carson DA: Synthetic peptides corresponding to third hypervariable region of human monoclonal IgM rheumatoid factor heavy chains define an immunodominant idiotype. J Exp Med 162:756-761, 1985.

53. Fong S, Chen PP, Gilbertson TA, Fox RI, Vaughan JH, Carson DA: Structural similarities in the kappa light chains of human rheumatoid factor paraproteins and serum immunoglobulins bearing a cross-reactive idiotype. J Immunol 135:1955-1960, 1985.

54. Chen PP, Goni F, Houghten RA, Fong S, Goldfien RD, Vaughan JH, Frangione B, Carson DA: Characterization of human rheumatoid factors with seven antiidiotypes induced by synthetic hypervariable-region peptides. J Exp Med 162:487-500, 1985.

55. Fong S, Gilbertson TA, Hueniken RJ, Singhal SK, Vaughan JH, Carson DA: IgM rheumatoid factor autoantibody and immunoglobulin producing precursor cells in the bone marrow of humans. Cell Immunol 95:157-172, 1985.

56. Fong S, Chen PP, Goldfien RD, Jirik F, Silverman G, Carson DA: Recurrent idiotypes of human anti-IgG autoantibodies: their potential use for immunotherapy. In: Mediators of Immune Regulation and Immunotherapy. Singhal SK, Delovitch TL (eds.): pp. 232-243. Elsevier Science Publishing Co., New York, 1986.

57. Fox RI, Chen PP, Carson DA, Fong S: Expression of a cross reactive idiotype on rheumatoid factor in patients with Sjogren's syndrome. J Immunol 136:477-483, 1986.

58. Jirik FR, Sorge J, Fong S, Heitzmann JG, Curd JG, Chen PP, Goldfien R, Carson DA: Cloning and sequence determination of a human rheumatoid factor light-chain gene. Proc Natl Acad Sci USA, 83:2195-2199, 1986.

59. Lotz M, Tsoukas CD, Fong S, Dinarello CA, Carson DA, Vaughan JH: Release of lymphokines following Epstein-Barr virus infection in vitro. I. The sources and kinetics of production of interferons and interleukins in normal humans. J Immunol, 136:3636-3642, 1986.

60. Lotz M, Tsoukas CD, Fong S, Dinarello CA, Carson DA, Vaughan JH: Release of lymphokines following infection with Epstein-Barr virus in vitro. II. A monocyte dependent inhibitor of interleukin-1 downregulates the production of interleukin-2 and gamma interferon in rheumatoid arthritis. J Immunol, 136:3643-3648, 1986.

61. Fong S, Chen PP, Gilbertson TA, Weber JR, Fox RI, Carson DA: Expression of three cross reactive idiotypes on rheumatoid factor autoantibodies from patients with autoimmune diseases and seropositive adults. J Immunol, 137:122-128, 1986.

62. Fong S, Gilbertson TA, Chen PP, Karras JG, Vaughan JH, Carson DA: The common occurrence of internal image type anti-idiotypic antibodies in rabbits immunized with monoclonal and polyclonal human IgM rheumatoid factors. Clin Exp Immunol, 64:570-580, 1986.

63. Fox RI, Carson DA, Chen P, Fong S: Characterization of a cross reactive idiotype in Sjogren's syndrome. Scand J Rheum S61:83-88, 1986.

64. Silverman GJ, Carson DA, Solomon A, Fong S: Human kappa light chain subgroup analysis with synthetic peptide-induced antisera. J Immunol Methods 95:249-257, 1987.

65. Goldfien R, Chen P, Kipps TJ, Starkebaum G, Heitzmann JG, Radoux V, Fong S, Carson DA: Genetic analysis of human B cell hybridomas expressing a rheumatoid factor-associated cross-reactive idiotype. J Immunol 138:940- 944, 1987.

66. Carson DA, Chen PP, Fox RI, Kipps TJ, Jirik F, Goldfien RD, Silverman G, Radoux V, Fong S: Rheumatoid factors and immune networks. Annu Rev Immunol 5:109-126, 1987.

67. Kipps TJ, Fong S, Tomhave E, Chen PP, Goldfien RD, Carson DA: High frequency expression of a conserved kappa variable region gene in chronic lymphocytic leukemia. Proc Natl Acad Sci USA 84:2916-2920, 1987

68. Fong S, Chen PP, Fox RI, Goldfien RD, Silverman GJ, Radoux V, Jirik F, Vaughan JH, Carson DA: Rheumatoid factors in human autoimmune disease: Their origin, development and function. Path Immunopath Res 5:407-449, 1987.

69. Goldfien RD, Fong S, Chen P, Carson DA: Structure and function of rheumatoid factor: Implications for its role in the pathogenesis of mixed cryoglobulinemia. In: Antiglobulins, cryoglobulins and glomerulonephritis, Proceedings of 2nd International Milano Meeting of Nephrology. Ponticelli C, Minetti L, D'Amico G (eds.) Martinus Nijhoff, Dordrecht pp. 17-27, 1986.

70. Silverman GJ, Carson DA, Patrick K, Vaughan JH, Fong S: Expression of a germline human kappa chain associated cross reactive idiotype after in vitro and in vivo infection with Epstein-Barr virus. Clin Immunol Immunopathol 43:403-411, 1987.

71. Silverman GJ, Fong S, Chen PP, Carson DA: Clinical update: Cross reactive idiotype and the genetic origin of rheumatoid factors. J Clin Lab Anal, 1:129-135, 1987.

72. Chen PP, Fong S, Carson DA: Molecular basis of reactivity of epibodies. In: Elicitation and use of anti-idiotypic antibodies and their biological applications. Bona C (ed.), CRC Press, Boca Raton, Fla, in press.

73. Fong S, Chen PP, Carson DA, Fox, RI: Rheumatoid factor in Sjogren's syndrome. In: Sjogren's Syndrome: Clinical and Immunological Aspects. Talal N, Moutsopoulos HM, Kassan SS (eds.), Springer-Verlag, New York, pp. 203-217, 1987.

74. Chen PP, Fong S, Carson DA: The use of defined peptides in characterizing idiotypes. Int Rev Immunol 2:419-432, 1987.

75. Chen PP, Fong S, Goni F, Houghten RA, Frangione B, Liu F, Carson DA: Analyses of human rheumatoid factors with anti-idiotypes induced by synthetic peptides. Monogr Allergy 22:12-23, 1987.

76. Carson DA, Chen PP, Radoux V, Jirik F, Goldfien RD, Silverman GJ, Fong S: Molecular basis for the cross-reactive idiotypes on human anti-IgG autoantibodies (rheumatoid factors) In: Autoimmunity and Autoimmune Disease. Ciba Foundation Symposium 129 pp. 123-130, 1987.

77. Radoux V, Fong S, Chen PP, Carson DA: Rheumatoid factors: current concepts. In: Advances in Inflammation Research. Lewis, A. (Ed), Raven Press, New York, pp.295-304, 1987.

78. Kipps TJ, Fong S, Chen PP, Miller WE, Piro LD, Carson DA: Immunoglobulin V gene utilization in CLL. In: Chronic lymphocytic leukemia: recent progress and future direction, Alan R Liss, Inc., New York, pp. 115-126, 1987.

79. Fong S, Chen PP, Fox RI, Goldfien RD, Radoux V, Silverman GJ, Crowley JJ, Roudier J, Carson DA: The diversity and idiotypic pattern of human rheumatoid factors in disease. Concepts in Immunopath 5: 168-191, 1988.

80. Fox RI, Fong S, Chen PP, Kipps TJ: Autoantibody production in Sjogren's syndrome: a hypothesis regarding defects in somatic diversification of germline encoded genes. In Vivo 2: 47-56, 1988.

81. Chen PP, Fong S, Goni F, Silverman GJ, Fox RI, Liu M-K, Frangione B, Carson DA: Cross-reacting idiotypes on cryoprecipitating rheumatoid factor. Springer Seminar Series in Immunopath 10: 35-55, 1988.

82. Chen PP, Fong S, Carson DA: Rheumatoid factor. Rheumatic Diseases of North America 13:545-568, 1987.

83. Carson DA, Chen PP, Kipps TJ, Radoux V, Jirik FR, Goldfien RD, Fox RI, Silverman GJ, Fong S. Idioytpic and genetic studies of human rheumatoid factors. Arthritis Rheum 30: 1321-1325, 1987.

84. Fong S, Chen PP, Crowley JJ, Silverman GJ, Carson DA: Idiotypic characteristics of rheumatoid factors. Scand J Rheumatol, Suppl. 75: 58-65, 1988.

85. Crowley JJ, Goldfien RD, Schrohenloher RE, Spiegelberg HL, Silverman GJ, Mageed RA, Jefferis R, Koopman WJ, Carson DA, Fong S: Incidence of three cross reactive idiotypes on human rheumatoid factor paraproteins. J Immunol 140: 3411-3418, 1988.

86. Fong S, Chen PP, Crowley JJ, Silverman GJ, Carson DA: Idiotypes and the structural diversity of human rheumatoid factors. Springer Seminar Series in Immunopath 10: 189-201, 1988.

87. Silverman GJ, Goldfien, Chen PP, Mageed RA, Jefferis R, Goni F, Frangione B, Fong S, Carson DA. Idiotypic and subgroup analysis of human monoclonal rheumatoid factors: implications for structural and genetic basis of autoantibodies in humans. J Clin Invest 82: 469-475, 1988.

88. Fox RI, Chan E, Benton L, Fong S, Friedlander M. Treatment of primary Sjogren' syndrome with hydroxychloroquine. American Journal of Medicine 85 (suppl 4A): 62-67, 1988.

89. Fong S. La Diversite Structurale Des Facteurs Rhumatoides Humains. In Immunorhumatologie. Roux H, Luxembourg A, Roudier J, (Eds.). Solal, editeurs, Marseille, pp 162-166, 1989.

90. Fu, Y., Arkin, S., Fuh, G., Cunningham, B.C., Wells, J.A., Fong, S., Cronin, M., Dantzer, R., Kelley, K. Growth hormone augments superoxide anion secretion of human neutrophils by binding to the prolactin receptor. J. Clin. Invest 89: 451-457, 1992.

91. Weber, J.R., Nelson, C., Cunningham, B.C., Wells, J.A., Fong, S. Immunodominant structures of human growth hormone identified by homolog-scanning mutagenesis. Mol. Immunol. 29: 1081-1088, 1992.

92. Bushell, G., Nelson, C., Chiu, H., Grimley, C., Henzel, W., Burnier, J., Fong, S. The role of cathepsin B in the generation of T cell antigenic epitopes of human growth hormone. Mol. Immunol. 30:587-591, 1993.

93. Bednarczyk, J.L., Wygant, J.N., Szabo, M.C., Molinari-Storey, L., Renz, M., Fong, S., McIntyre, B.W. Homotypic leukocyte aggregation triggered by a monoclonal antibody specific for novel epitope expressed by the integrin β1 subunit: Conversion of non-responsive cells by transferring human α4 subunit cDNA. J. Cell. Biochem. 51: 465-478, 1993.

94. Berman, P.W., Nakamura, G., Riddle, L., Chiu, H., Fisher, K., Champe, M., Gray, A., Ward, P., Fong, S. Biosynthesis and function of membrane bound and secreted forms of recombinant Mac-1. J. Cell. Biochem. 52:183-195, 1993.

95. Crowe, D.T., Chiu, H., Fong, S., Weissman, I.L. Regulation of the avidity of integrin α4β7 by the β7 cytoplasmic domain. J. Biol. Chem. 269:14411-14418, 1994.

96. Renz, M.E., Chiu, H.H., Jones, S., West, C., Fox, J., Kim, J.K., Presta, L.G., Fong, S. Structural requirements for adhesion of soluble recombinant murine VCAM-1 to α4β1. J. Cell Biol. 125:1395-1406, 1994.

97. Chiu, H. H., Crowe, D. T., Renz, M. E., Presta, L. G., Jones, S., Weissman, I. L., and Fong, S. Similar but non-identical amino acid residues on vascular cell adhesion molecule-1 are involved in the interaction with α4β1 and α4β7 under different activity states. J. Immunol. 155:5257-5267, 1995.

98. Viney, J. L., Jones, S., Chiu, H., Lagrimas, B., Renz, M., Presta, L., Jackson, D., Hillan, K., Fong, S. Mucosal Addressin Cell Adhesion Molecule-1. A structural and functional analysis demarcates the integrin binding motif. J. Immunol. 157: 2488-2497, 1996.

99. Fong, S., Jones, S., Renz, M.E., Chiu, H.H., Ryan, A.M., Presta, L. G., and Jackson, D. Mucosal Addressin Cell Adhesion Molecule-1 (MAdCAM-1)--Its binding motif for α4β7 and role in experimental colitis. Immunologic Research 16: 299-311, 1997.

100. Jackson, D.Y., Quan, C., Artis, D.R., Rawson, T., Blackburn, B., Struble, M., Fitzgerald, G., Chan K., Mullin, S., Burnier, J.P., Fairbrother, W.J., Clark, K., Beresini, M., Chiu, H., Renz, M., Jones, S., and Fong, S. Potent α4β1 Peptide Antagonists as Potential Anti-Inflammatory Agents. J. Med. Chem. 40: 3359-3368, 1997.

101. Viney, J.L. and Fong, S. β7 Integrins and Their Ligands in Lymphocyte Migration to the Gut. Chemical Immunology: 'Mucosal T Cells' . Chemical Immunology 71;64-76, 1998.

102. Bradley, L.M., Malo, M.E., Fong, S., Tonkonogy, S.L., and Watson, S.R. Blockade of both L-selectin and α4 Integrins Abrogate Naïve CD4 Cell Trafficking and Responses in Gut-Associated Lymphoid Organs. International Immunology 10, 961-968, 1998.

103. Quan, C., Skelton, N., Clark, K., Jackson, D.Y., Renz, M., Chiu, H.H., Keating, S.M., Beresini, M.H., Fong, S., and Artis D.R. Transfer of a Protein Binding Epitope to a Minimal Designed Peptide. Bioploymers (Peptide Science);47,265-275, 1998.

104. Hillan, K.J., Hagler, K.E., MacSween, R.N.M., Ryan, A.M., Renz, M.E., Chiu, H.H., Ferrier, R.K., Bird, G.L., Dhillon, A.P., Ferrell, L.D., Fong, S. Expression of the Mucosal Vascular Addressin, MAdCAM-1, in Inflammatory Liver Disease. Liver 19, 509-518, 1999

105. Pender, S.L.F., Salmela, M.T., Monteleone, G., Schnapps, D., McKenzie, C., Spencer, J., Fong, S., Saarialho-Kere, U., and MacDonald, T.T. Ligation of alpha 4 beta 1 integrin on human intestinal mucosal mesenchymal cells selectively upregulates membrane type-1 matrix metalloproteinase and confers a migratory phenotype. American Journal of Pathology 157, 1955-1962, 2000.

106. Liang, T.W., DeMarco, R., Gurney, A., Hooley, J., Huang, A., Klassen, T., Mrsny, R., Tumas, D., Wright, B.D., and Fong, S. Characterization of Human Junctional Adhesion Molecule (huJAM): Evidence for involvement in cell-cell contact and tight junction regulation. American Journal of Physiology; Cell Physiology 279, C1733-C1743, 2000.

107. Liang, T.W., Chiu, H.H., Gurney, A., Sidle, A., Tumas, D.B., Schow, P., Foster, J., Klassen, T., Dennis, K., DeMarco, RA.., Pham T., Frantz, G., Fong, S. VE-JAM/JAM 2 interacts with T, NK, and dendritic cells through JAM 3. J.Immunology 168, 1618-1626, 2002.

107. Dupree,N., Artis, D.R., Castanedo, G., Marsters, J., Sutherlin, D., Caris, L., Clark, K., Keating, S.,Beresini, M., Chiu, H., Fong, S., Lowman, H., Skeleton, N., and Jackson, D. Selective $\alpha 4\beta 7$ Antagonists and Their Potential as Anti-Inflammatory Agents. J. Med. Chem. 45, 3451-3457, 2002.

108. Castanedo, G.M., Sailes, F.C., Dubree, N., Nicholas, J., Caris, L., Keating, S., Chiu, H., Fong, S., Marsters, J., Jackson, D.Y., Sutherlin, D.P. The Solid Phase Synthesis of Dual $\alpha 4\beta 1/\alpha 4\beta 7$ Antagonists: Two Scaffolds with Overlapping Pharmacophores. Bioorganic and Medicinal Chemistry Letters 12, 2913-2917, 2002.

EXHIBIT A

Exhibit A

CURRENT PROTOCOLS IN IMMUNOLOGY

VOLUME 1

John Wiley & Sons, Inc.

Library of Congress Cataloging in Publication Data:

Current protocols in immunology / edited by John E. Coligan ... [et al.].
p. cm.
Kept up to date by quarterly supplements.
4 vols. Includes index.
ISBN 0-471-52276-7
1. Immunology—Laboratory manuals. I. Coligan, John E.
[DLM: 1. Clinical Protocols. 2. Immunologic Techniques. QW 525 C976]

QR183.C87 1991
616.07'0'072—dc20
DNLM/DLC
for Library of Congress 90-15726
CIP

Printed in the United States of America

10

Proliferative Assays for T Cell Function

A number of agents can specifically or nonspecifically induce T cell activation, resulting in cytokine production, cytokine receptor expression, and ultimately proliferation of the activated T cells. Although proliferation is not a specific effector function of T lymphocytes—in contrast to helper function for B lymphocytes (*UNIT 3.10*) or cytotoxicity (*UNIT 3.11*)—proliferation assays are reliable, simple, and easy to perform and have been widely used to assess the overall immunocompetence of an animal. In addition, the assays described in this unit form the basis for identifying the appropriate cellular population that might be used to obtain T cell clones (*UNIT 3.13*) or T cell hybridomas (*UNIT 3.14*).

The assays have been divided into two groups on the basis of whether they are used to stimulate primed or unprimed T lymphocytes. The first basic protocol describes the use of agents that are capable of activating unprimed T lymphocytes in culture either by pharmacologic means (calcium ionophore and phorbol ester stimulation), by direct cross-linking of the T cell receptor (TCR) on a large percentage of responder cells (anti-CD3, anti-TCR-γδ, or anti-TCR-αβ monoclonal antibodies), by cross-linking the receptors on certain subpopulations of T cells with monoclonal antibodies specific for the *V* regions of β chains of the TCR (anti-Vβ) or with enterotoxins specific for certain *V*β-chain regions, or by indirectly cross-linking the TCR (lectins or monoclonal antibodies to non-TCR antigens). The first alternate protocol describes the use of plate-bound antibodies specific for the TCR to stimulate proliferation. The second alternate protocol describes the activation of unprimed T cells to cell-associated antigens in the mixed leukocyte reaction (MLR). The first support protocol describes the preparation and use of T cell–depleted accessory or stimulator cells and the second support protocol describes methods for blocking accessory cell proliferation. Finally, the second basic protocol describes the induction of a T cell proliferative response to soluble protein antigens or to cell-associated antigens against which the animal has been primed in vivo.

The assays in this unit employ murine T lymphocytes. Induction of proliferative responses of murine B lymphocytes is described in *UNIT 3.10*. Related assays for use with human peripheral blood lymphocytes are described in *UNIT 7.9*.

NOTE: All solutions and equipment coming into contact with cells must be sterile, and proper sterile technique should be used accordingly.

ACTIVATION OF UNPRIMED T CELLS

BASIC PROTOCOL

Unprimed T cells can be induced to proliferate by a variety of agents, including pharmacological agents, anti-CD3/TCR or anti-Thy-1 monoclonal antibodies, enterotoxins and lectins. The commentary briefly describes the specificities of these agents, while Table 3.12.1 lists sources and concentrations for use in this protocol. Although this procedure is intended to measure proliferation of T cells specifically, in many cases induction of T cell proliferation is dependent on the presence of non–T cells that function as accessory cells. The latter provide additional costimulatory signals for T cell proliferation as well as cross-link (via their Fc receptors) monoclonal antibodies bound to cell-surface antigens. The requirement for non–T accessory cells varies with the nature of the stimulatory ligand and can range from absolute dependence to accessory cell–independent T cell activation (see Table 3.12.1). The activation is calculated after determining the difference in incorporation of [^{3}H]thymidine between stimulated and control cells.

Contributed by Ada M. Kruisbeek and Ethan Shevach
Current Protocols in Immunology (1991) 3.12.1-3.12.14

Table 3.12.1 Agents Used to Activate Unprimed T Cells in Proliferative Assays

Agent[a]	Source/ cat. no.[b]	Concentration	Accessory cells[c]	Mode of action, etc.
PMA	SIG P8139	1-10 ng/ml	No	Use with ionomycin or A23187; pharmacologic
Ionomycin	CAL 407950	200-500 ng/ml	No	Use with PMA; pharmacologic
A23187	CAL 100105	100-500 ng/ml	No	Use with PMA; pharmacologic
PHA	WD HA16	1-5 μg/ml	Yes	Indirect TCR cross-linking
Con A	PH 17-0450-01	1-10 μg/ml	Yes	Indirect TCR cross-linking
Anti-Thy-1	PG mAb-G7	1-50 μg/ml	Yes[c]	Indirect TCR cross-linking
Anti-CD3	PG HM-CD3	0.1-5 μg/ml	Yes[c]	Use plate-bound or soluble; direct TCR cross-linking
Anti-TCR-αβ	PG HM-AB-TCR	0.1-10 μg/ml	Yes[c]	Use plate-bound or soluble; direct TCR cross-linking
Anti-TCR-γδ	PG HM-GD-TCR-1; HM-GD-TCR-3	0.1-100 μg/ml	No	Use plate-bound; direct TCR cross-linking
Anti-Vβ-8.1, 8.2[c]	PG MM-Vβ-TCR-1	0.1-100 μg/ml	No	Use plate-bound; direct TCR cross-linking
Anti-Vβ-6[c]	PG RM-Vβ-TCR-2	0.1-100 μg/ml	No	Use plate-bound; direct TCR cross-linking
Anti-Vβ-11	PG RM-Vβ-TCR-3	0.1-100 μg/ml	No	Use plate-bound; direct TCR cross-linking
Staph tox A	TT AT101	1-10 μg/ml	Yes[c]	Vβ-1,3,10,11,17-receptor specificity
Staph tox B	TT BT202; SIG S4881	1-100 μg/ml	Yes[c]	Vβ-3,7,8,17-receptor specificity
Staph tox E	TT ET404	1-10 μg/ml	Yes[c]	Vβ-11,15,17-receptor specificity

[a]Abbreviations: PMA, phorbol 12-myristate 13-acetate; PHA, phytohemagglutinin; Con A, concanavalin A; Staph tox A, B, & E, *Staphylococcus* enterotoxins A, B, & E.

[b]Supplier addresses and phone numbers are provided in *APPENDIX 5*. Abbreviations: CAL, Calbiochem; PG, Pharmingen; PH, Pharmacia LKB; SIG, Sigma; TT, Toxin Technology; WD, Wellcome Diagnostics.

[c]When using anti-CD3 and anti-TCR antibodies in soluble form (rather than plate-bound), accessory cells are required. When using Staph enterotoxins, accessory cells must express appropriate MHC class II molecules. Accessory cell dependence is not absolute with anti-Thy-1 antibodies.

Materials

Complete RPMI-5 and RPMI-10 media (*APPENDIX 2*)
Responder cells: lymphocytes from nonimmunized mouse thymus, spleen, or lymph nodes (*UNIT 3.1*)
Activating agent(s) (Table 3.12.1)
Phosphate-buffered saline (PBS; *APPENDIX 2*)
Accessory cells: unfractionated mouse spleen cell suspension, irradiated or treated with mitomycin C (second support protocol) or T cell–depleted (first support protocol)
[^{3}H]thymidine (*APPENDIX 3*)

15- and 4-ml disposable, polystyrene conical tubes with screw caps
Low-speed centrifuge with Sorvall H-1000B rotor (or equivalent)
1-, 5-, and 10-ml disposable polystyrene pipets
96-well flat- or round-bottom microtiter plates with lids (Costar #3596 or #3799)
25- to 100-µl single- and multichannel pipettors with disposable tips

Additional reagents and equipment for removing organs (*UNIT 1.9*), preparing single-cell suspensions (*UNIT 3.1*), and counting, labeling, and harvesting cells (*APPENDIX 3*)

1. Prepare responder leukocyte suspensions from thymus, spleen, or lymph node in complete RPMI-5 as described in *UNIT 3.1*.

   The size of the intended experiment dictates the number of organs to be collected. See annotation to step 3 for an indication of cell number required, and UNIT 3.1 for number of cells per organ. Spleen, thymus, and lymph node can be used as responder cells, while only spleen is a source of accessory cells. Purified T cells or subpopulations of T cells (i.e., CD4$^+$ or CD8$^+$) cells may also be used. See UNITS 3.1-3.6 for enrichment/depletion methods.

2. Centrifuge single-cell suspensions in 15-ml conical tubes for 10 min in Sorvall H-1000B rotor at ~1000 rpm (200 × *g*), room temperature, and discard supernatant.

3. Resuspend cell pellet in complete RPMI-5. Count responder cells and adjust to ~10^6 cells/ml with complete RPMI-10.

   While this concentration (1×10^6 cells/ml or 2×10^5 cells/well) will give satisfactory responses with most cell populations, it is useful to compare 2, 4, and 8×10^5 cells per well in initial pilot experiments. If unfractionated spleen or lymph node cells are used as the responder population, sufficient accessory cells are present and there is no need to supplement the cultures with additional cells. However, if highly purified T cells or T cell subpopulations are used as responders, it will be necessary to add non–T accessory cells depending on the nature of the activating agent (see Table 3.12.1). This is most easily accomplished by adding increasing numbers (0.1, 0.5, and 1.0×10^5) of syngeneic spleen (accessory) cells in 0.1 ml to 2×10^5 T cells in 0.1 ml (see first support protocol). Also, a meaningful comparison of the responsiveness of different cell populations requires titrations of both the activating agents as well as the responding cell populations, and a kinetic experiment.

4. Prepare working solutions of activating agents in 4-ml conical tubes at room temperature as follows. For MAb, toxin, or lectin, make a series of four dilutions from 1 mg/ml stock solutions—e.g., 100, 30, 10, and 3 µg/ml in PBS. For the pharmacological agent, make single dilutions of 100 ng/ml solution of PMA and 1 µg/ml A23187 (or 4 µg/ml ionomycin) in PBS.

   If MAb in supernatant or ascites form are being used, at least four dilutions should also be used. Working solutions should be used immediately, since the various proteins, especially MAb, may bind to the plastic.

See Table 3.12.1 for Vβ specificities of staphylococcal enterotoxins. It is essential to verify that the mouse strain employed expresses the MHC class II surface molecules for which the enterotoxin has a specific binding affinity. See Marrack and Kappler (1989) for further discussion of various enteroxins and their specificities.

5. Add 20 µl of each dilution of activating reagent (MAb, enterotoxin or lectin) to each of three wells of a 96-well flat- or round-bottom microtiter plate. Include control wells with 20 µl of PBS only. Add 20 µl PMA or calcium ionophore at the single concentration indicated in step 4, as the dose-response curve for these agents is extremely narrow.

   A series of four dilutions will form one row of each microtiter plate, allowing for efficient organization of the plates.

6. To the wells of the 96-well microtiter plate containing activating agent, add 2×10^5 cells in 0.2 ml.

7. Place microtiter plates in a humidified 37°C, 5% CO_2 incubator for 2 to 4 days.

   Optimum culture periods for stimulating cells will vary depending on cell type and laboratory conditions and must be determined empirically (see critical parameters).

8. Add [^{3}H]thymidine to each well. Return the plates to CO_2 incubator to pulse 18 to 24 hr. Harvest cells using a semiautomated sample harvester and measure cpm in β scintillation counter.

9a. Compute the data as the difference in cpm of stimulated (experimental) and control (no activating agent added) cultures. This is done by subtracting the arithmetic mean of cpm from triplicate control cultures from the arithmetic mean of cpm from corresponding stimulated cultures. The results are referred to as "Δ cpm."

9b. Alternatively, compute the data as the ratio of cpm of stimulated and control cultures. This is done by dividing the arithmetic mean of cpm from stimulated cultures by the arithmetic mean of cpm from control cultures. The results are referred to "SI" (stimulation index).

   The second method (step 9b) has the disadvantage that small changes in background values will result in large changes in SI and should be interpreted with caution. In most publications, Δ cpm rather than SI values are preferred.

ALTERNATE PROTOCOL

ACTIVATION OF UNPRIMED T CELLS WITH PLATE-BOUND ANTIBODIES

Although it is possible to induce T cell activation with monoclonal antibodies to the CD3/TCR complex in solution during culture, such activation depends on cross-linking of the antibody by Fc receptor–bearing accessory cells. This protocol describes the use of monoclonal antibodies to the CD3/TCR complex by coupling them to the wells of the microtiter plates. The T cell proliferative response induced under these conditions does not require the presence of significant numbers of accessory cells, although the responses obtained may be suboptimal (Jenkins et al., 1990).

Use of this protocol is recommended for use with those antibodies to the CD3/TCR complex which bind poorly to the Fc receptor present on murine accessory cells and which do not induce T cell activation in soluble form. Although all monoclonal antibodies readily couple to plastic under these conditions, it is very difficult to induce a proliferative response with certain antibodies such as the G7, anti-Thy-1 monoclonal antibody. In such cases, the conditions described in the basic protocol should be followed.

Additional Materials

PBS (*APPENDIX 2*), room temperature and 4°C
1 mg/ml purified anti-CD3 or anti-TCR MAb in PBS (for nonspecific activation of T cells) *or* 1 mg/ml purified anti-Vβ or anti-TCR-γδ MAb in PBS (for activation of T cells with specific receptors; see Table 3.12.1)

1. In 4-ml conical polystyrene tubes, prepare a series of four dilutions of MAb from sterile 1 mg/ml stock solutions—e.g., 100, 10, 1, and 0.1 μg/ml—using room temperature PBS.

   Sources and recommended concentrations of monoclonal antibodies can be found in Table 3.12.1; since MAb will bind to plastic, the working dilutions should be used immediately.

   The ability of anti-TCR antibodies to cross-link receptor molecules varies depending on the purity of the MAb preparation and the affinity of the MAb for the TCR/CD3 complex. Optimum dilutions will have to be determined in dose-response experiments. Alternatively, preparations of ascites fluid from the MAb can be tested at different dilutions (e.g., 1:100, 1:200, 1:400, and 1:800), but use of purified antibody will allow for better standardization of the assay.

   Because the efficacy of MAb-induced activation depends on the amount of antibody bound to the bottom of the wells, it is crucial to make the dilutions in a buffer without any additional source of proteins such as FCS or albumin; these would compete with the binding of the antibody, and therefore reduce the responsiveness. For this reason, it is also not recommended to perform the assay with culture supernatants of the appropriate hybridomas.

2. Add 30 μl of each concentration of MAb solution to each of three wells of a 96-well round-bottom microtiter plate. Include control wells of 30 μl PBS only.

   A series of four dilutions will form one row of each plate, allowing for efficient organization of the plates. Consistently better responses are seen with round-bottom (compared with flat-bottom) plates in antibody-mediated experiments.

   Most often, optimal responses are seen with 10 μg/ml antibody. There is no point in adding more than the indicated amount of antibody, since the maximum amount that can bind to surface of the wells is ~2 to 3 μg (A.M.K., unpub. observ.).

3. Cover the plate and gently tap its side to ensure complete covering of the bottom of the wells. Incubate plates 90 min at 37°C. During incubation, proceed to step 4.

   During this incubation, the antibodies bind to the plastic in the wells for subsequent cross-linking of the T cell receptors on responding T cells. Plates can also be prepared the night before an experiment and kept in the refrigerator overnight, after the 37°C incubation.

4. Prepare responder cell suspensions as in steps 1 to 3 of the basic protocol.

   Highly purified T cell populations can be used in these studies as the proliferative response induced is accessory cell–independent. However, the presence of non–T accessory cells does not interfere with the proliferative response.

5. Wash the wells of the incubated plates by adding 200 μl cold PBS and inverting the plates with a flick of the hand on a stack of paper towels placed in a tissue culture hood. Repeat washing procedure two more times to remove excess antibody.

6. To the wells of the washed plates, add ~2×10^5 cells in 0.2 ml.

   If cells are not ready at this stage, plates may be kept in the refrigerator overnight after 100 μl PBS has been added. Presumably, longer storage periods should be acceptable, but our experience is limited to ≤4 day periods. The PBS should be removed before the cells are added.

Most cell populations will give peak responsiveness at this cell dosage, but pilot experiments should be performed to establish optimal conditions.

7. Proceed as in steps 7 to 9 of the basic protocol, but incubate cultures for 2 to 3 days before adding [^{3}H]thymidine.

Kinetic assays should be performed to determine the optimum culture period.

ALTERNATE PROTOCOL

T CELL PROLIFERATION IN MIXED LYMPHOCYTE CULTURES

In the mixed lymphocyte culture (MLC) or reaction (MLR), suspensions of responder T cells are cultured with allogeneic stimulator lymphocytes. The activating stimulus is the foreign histocompatibility antigen (usually MHC class I or class II molecules) expressed on the allogeneic stimulator cells. Responder cells need not be primed because a sufficiently high number of T cells in the MLC will respond to the stimulator population. If the stimulator cell population contains T cells, their uptake of [^{3}H]thymidine must be prevented by irradiation or treatment with mitomycin C; alternatively the stimulator cell suspension can be depleted of T cells (see support protocols).

Additional Materials

Responder cells: lymphocytes from nonimmunized mouse thymus, spleen, or lymph nodes (*UNITS 1.9 & 3.1*) *or* purified T cells or T cell subpopulations (*UNITS 3.1-3.6*)

Stimulator cells: allogeneic mouse spleen cells that differ from the responder cells at *H-2* or *Mls* loci, irradiated or treated with mitomycin C (second support protocol) or T cell–depleted (first support protocol)

1. Prepare responder cell populations as in steps 1 to 3 of the basic protocol. Although unfractionated cell populations can be used as responders in certain situations, it may be preferable to use purified T cells or T cell subsets.

To estimate the MLR of a cell population, it is necessary to perform a dose-response assay with different numbers of responder cells. Typically, three replicate wells are set up containing each of the following: 0.5, 1, 2, and 4 × 10^5 cells (optimal responses are usually obtained with the latter two densities). The setup for these four cell densities will occupy one row (12 wells) of a microtiter plate.

For thymocytes, it may be necessary to use 8 × 10^5 cells per well because the frequency of responding T cells is lower; the lowest number of responder cells could then be 1 × 10^5 and the doses in between would be 2 and 4 × 10^5. Using this range of higher numbers of responder cells may also be preferred when experimental manipulations are expected to reduce the frequency of responding T cells.

2. To a 96-well microtiter plate, add 5 × 10^4 to 4 × 10^5 responder cells in 0.1 ml to each well. For each experimental group, set up three replicate wells.

Stimulation of leukocytes for proliferation in 96-well microtiter plates can be run in parallel with cytotoxic T lymphocyte (CTL) generation (UNIT 3.11), which is performed in 24-well microtiter plates. For example, cells can be diluted to 4 × 10^6 cells/ml and added to 24-well plates in 1.0 ml/well for CTL generation and to 96-well plates in 0.1 ml/well for proliferation.

3. Prepare a single-cell suspension of irradiated or mitomycin C–treated stimulator cells. Alternatively, prepare a suspension of T-cell depleted stimulator cells. Add 0.1 ml to each well of the plates containing responder cells.

The optimum number of stimulator cells must be determined for each MLC and for different responder cells. For a range of responder cells from 0.5-4 × 10^5, test stimulator cells at densities of 2, 4, and 8 × 10^6/ml (i.e., 2, 4, and 8 × 10^5/well). It should be noted that the stimulator cell suspension provides both the specific antigen to be recognized by the responder T cells as well as nonspecific accessory cells. If

highly purified T cells are used as the responder population, it is therefore not necessary to supplement the cultures with non–T accessory cells syngeneic to the responder T cells.

Separate wells with control cultures should be set up that include—for each dose of responder and stimulator cells—replicate wells of responder cells with irradiated or mitomycin C–treated syngeneic stimulator cells. Values obtained from these controls reflect "background" proliferation values (see step 9 of basic protocol). Other negative controls often included are wells with stimulator cells alone and wells with responder cells alone. These are not used for the calculation of the data, but are useful to compare with the background proliferation values; the latter should not be much higher (<2-fold) than those obtained with stimulator or responder cells alone. Higher background values indicate potential autoreactivity.

4. Follow steps 7 to 9 of the basic protocol, but incubate the cultures for 3 to 6 days.

Optimum culture periods for stimulating cells will vary depending on cell type and laboratory conditions, and must be determined empirically (see critical parameters).

DEPLETION OF T CELLS FROM ANTIGEN-PRESENTING/STIMULATOR CELL SUSPENSIONS

SUPPORT PROTOCOL

Although normal unfractionated spleen cell populations can be used as a source of accessory cells, in certain types of experiments it may be preferable to use spleen cell populations from which the T cells have been removed. This procedure ensures that none of the observed proliferative responses of the responder population result from T cell factors derived from the accessory cell population. For example, even T cells whose cell division has been blocked (second support protocol) can produce cytokines. In the following steps, T cell–depleted spleen cell suspensions are prepared using a lytic monoclonal antibody to the T cell antigen, Thy-1. Because almost all the antigen presentation or stimulator cell activity in spleen resides in the non–T cell fraction, this procedure also leads to enrichment of functional antigen-presenting cell function. Further enrichment of antigen-presenting cells (APC) by flotation of the T cell-depleted spleen cells on Percoll gradients is also described. Other procedures leading to enrichment of APC are described elsewhere; the method described in *UNIT 3.7* does not deplete T cells and therefore is not recommended here; the method described in *UNIT 3.15* leads to higher levels of enrichment that are not required in the protocols presented here.

Additional Materials

Spleen cells from nonimmunized mice
Hanks balanced salt solution (HBSS; *APPENDIX 2*)
Low-Tox rabbit complement (Cedarlane #CL3051), reconstituted with ice-cold distilled water and filter-sterilized
Anti-Thy-1.2 ascites (HO-13-4; ATCC #TIB 99) or anti-Thy-1.1 ascites (HO-22-1; ATCC #TIB 100; alternatively, see Table 3.4.1 for other anti-Thy-1 MAb and *UNIT 2.6* for production of ascites)
70% Percoll solution (*UNIT 3.8* and reagents and solutions)

1. Centrifuge the spleen cell suspension derived from single spleen down to a pellet.

The spleen cells should always be from nonprimed animals and should be syngeneic to the responder T cells unless they are to be used as stimulator cells in the MLC.

2. To the pellet, add 0.9 ml HBSS, 0.1 ml complement, and 25 µl anti-Thy-1 ascites.

If cells from more than a single spleen are needed, the procedure should be scaled up accordingly.

The choice of anti-Thy-1 reagent to be used depends on the strain of animal from which the spleen was derived. The great majority of commonly available mouse strains (except AKR) express the Thy-1.2 allele.

3. Incubate the mixture at 45 min in a 37°C water bath.
4. Centrifuge 10 min in Sorvall H-1000B rotor at ~1000 rpm (200 × *g*), room temperature, and discard supernatant. Resuspend pellet in HBSS and wash two more times.
5. Count viable cells (*APPENDIX 3*) and resuspend in complete RPMI-10 or PBS for inactivation as in the second support protocol, or in HBSS to prepare low-density accessory cells (see below).

   The T cell–depleted spleen cell population is comprised of B cells, macrophages, and dendritic cells. Further enrichment of cells with enhanced accessory cell function can be obtained by fractionation of this population on Percoll.

6. Dilute 70% Percoll solution to 55% by mixing 23.58 ml of the 70% Percoll with 6.42 ml HBSS. Resuspend T cell–depleted spleen cells from step 5 in HBSS at 20×10^6 cells/ml.
7. Layer 3 ml cell suspension over 3 ml of 55% Percoll solution in a 15-ml conical centrifuge tube.
8. Spin 13 min in H-1000B rotor at 3000 rpm (1900 × *g*), room temperature.
9. Remove cells that band at the Percoll/HBSS interface with a 5-in. Pasteur pipet and wash 3 times in HBSS as in step 4.
10. Count viable cells and resuspend in complete RPMI-10 for inactivation according to the second support protocol.

    The population obtained from steps 6 to 10 is comprised of large cells including macrophages, dendritic cells, and activated B lymphocytes. This population of cells is enriched in accessory cell function. When used in either of the basic protocols with purified T responder cells, fewer of the Percoll-purified cells should be needed to provide accessory function.

SUPPORT PROTOCOL

BLOCKING CELLULAR DIVISION OF ACCESSORY/STIMULATOR CELLS

There are two situations in which inhibition of accessory or stimulator cell division should be blocked. When purified T cells rather than unfractionated lymphoid populations are used in the basic protocol, cultures are frequently supplemented with accessory cells syngeneic to the responder T cells. If accessory cell DNA synthesis is inhibited, one can then be certain that the resultant proliferative response is comprised entirely of responder T cells and does not contain a component of recruited B cell proliferation derived from the accessory cell populations. In the MLR, the stimulator cells are spleen cells from mice that differ from the responder cells in *H-2* and/or *Mls* gene expression (see *APPENDIX 1*, Tables A.1C.1 and A.1F.1) and they can also recognize alloantigens on the responder cells. This responsiveness of stimulator cells against responder cells in an MLR (so-called back-stimulation) must be prevented by blocking cellular division. This can be done by treatment of stimulator cells with mitomycin C (a DNA cross-linking reagent) or by g irradiation. Many investigators prefer mitomycin C treatment when antigenic differences encoded for by *Mls* genes are to be measured, or when an irradiation source is not available. For more information on the loci encoding *Mls* genes, see Tables A.1F.2 and A.1F.3.

Mitomycin C Treatment

Additional Materials

Mitomycin C (Sigma #M-0503; store in dark)

1. In a 15-ml aluminum foil–wrapped tube, prepare a solution of mitomycin C in PBS at 0.5 mg/ml and filter sterilize.

   Since mitomycin C is very light-sensitive, it is necessary to prepare a fresh stock solution each day for each experiment.

2. Prepare spleen cell suspension as described in steps 1 and 2 of the basic protocol at a concentration of 5×10^7 cells/ml in PBS.

3. Add mitomycin C to a final concentration of 50 μg/ml (100 μl/ml of cell suspension) and wrap the tube in aluminum foil. Incubate 20 min at 37°C.

4. Add an excess of complete RPMI-5 (i.e., fill tube with ~12 ml) and centrifuge 10 min in Sorvall H-1000B rotor at 1200 rpm (300 × *g*). Discard supernatant and repeat washing procedure two more times.

   Three washes are crucial, because any traces of mitomycin C left among the cells will reduce proliferative responses when the cells are added to an MLC.

5. Resuspend pellet in complete RPMI-10. Count cells with hemacytometer. Adjust to desired concentration as described in the annotation to step 6 of the basic protocol.

Irradiation Treatment

Prepare a spleen cell suspension as described in steps 1 to 3 of the basic protocol, at a final concentration of $5\text{-}10 \times 10^6$ cells/ml in complete RPMI-10. Using a source of ionizing irradiation (^{60}Co or ^{137}Cs γ-irradiator; e.g., Gammacell 1000, Nordion), deliver 1000 to 2000 rad of irradiation to the cells.

This dose range of irradiation is suitable for most immunologic applications employing spleen cell suspensions. However, antigen presentation by different spleen cells is differentially affected by irradiation (Ashwell et al., 1984): at low doses (500 to 1000 rad), antigen-presenting function of B cells is preserved; after doses of 1100 to 2000 rad, a substantial decline is observed; and doses >2000 rad abolish the participation of B cells as APC. Macrophages and dendritic cells, on the other hand, maintain antigen presentation through doses of 3000 rad. To ensure that B cells do not participate in the responses measured, some investigators prefer to use doses of 2000 rad. However, responsiveness to *Mls* antigens can best be measured with stimulator cells that received doses of <1000 rad, since B cells present *Mls* more effectively. Alternatively, *Mls* responsiveness can be measured after mitomycin C treatment of stimulator cells, since it also preserves the antigen-presentation function of B cells.

When transformed cell lines are used as antigen-presenting or accessory cells, higher doses must be used to ensure blockage of cell division. The appropriate dose will have to be determined empirically for each cell line, but is likely to be at least 5000 rad; some transformed cell lines require as much as 10,000 to 12,000 rad, and may be more sensitive to mitomycin C treatment.

ACTIVATION OF PRIMED T CELLS

BASIC PROTOCOL

Proliferative responses to viruses, protein antigens, minor transplantation antigens, and the male H-Y antigen require in vivo immunization followed by in vitro stimulation. Furthermore, enhanced proliferative responses to those antigens that will generate primary in vitro responses (i.e., MHC antigens) can be obtained by in vivo priming. Multiple immunizations usually elevate in vitro responses.

To immunize animals for in vitro secondary responses to soluble protein antigens or peptides, dissolve antigens and emulsify in complete Freunds adjuvant (*UNIT 2.5*). For strong responses by draining lymph node cells, immunize animals in a hind footpad. For

strong responses by spleen cells, immunize intraperitoneally. Tail-base immunization also can be used as an efficient route of immunization; follow procedure for intradermal injection. To prime animals against cellular antigens, inject intraperitoneally with 1-5 × 10^7 cells that express the antigen. Immunization protocols are described in *UNIT 1.6*.

Within 2 to 3 weeks after in vivo priming, in vitro responsiveness of primed T cells can usually be measured. This assay is often used as a preparation for subsequent in vitro cloning procedures (*UNIT 3.14*) and T cell hybridoma preparation (*UNIT 3.13*).

Materials

Complete RPMI-10 medium (*APPENDIX 2*)
Responder cells: Purified T cells isolated from lymph nodes (*UNITS 3.1-3.6*) of in vivo primed mice
Antigen: 1 mg/ml sterile protein antigen(s) (*UNIT 3.13*), in PBS *or* suspension of irradiated or mitomycin C–treated stimulator cells expressing alloantigens at 8 × 10^6 cells/ml (*UNIT 3.11*, support protocol) in complete RPMI-10 medium (*APPENDIX 2*)
Accessory cells: suspension of irradiated or mitomycin C–treated (or T cell–depleted) spleen cells syngeneic to the responding T cells at 5 × 10^6 cells/ml in complete RPMI-10 medium
4-ml conical tubes
96-well flat-bottom microtiter plates with lids

1. Follow steps 1 to 3 of the first basic protocol for preparation of responder cells.
2. Prepare 4-fold dilution series of the antigens in 4-ml conical tubes, using complete RPMI-10.

   The following dilutions are recommended: 100, 10, 1, and 0.1 μg/ml protein antigens and 8, 4, 2, and 1 × 10^6 cells/ml of stimulator cells in complete medium.

3. Add antigens to 96-well flat-bottom microtiter plates, at 30 μl/well for protein antigens or 100 μl/well for cellular antigens. For each experimental group, set up three replicate wells and include control wells with medium only (no antigen).

   By using four concentrations of antigens and three replicate wells for each dose, one row of a microtiter plate will cover the entire tested range.

4. Add responder T cells in 0.1 ml to each well.

   Purified T cells are recommended; otherwise extremely high background values may be obtained. This appears to be due in part to proliferation of recruited cells (T and non–T) that are not antigen-specific. If unfractionated lymph node cells from recently primed mice are used, add 1-2 × 10^5 cells per well and proceed to step 6.

5. If purified lymph node T cells specific for protein antigens are used, add 0.1 ml of accessory spleen cells syngeneic to the donor of the responder T cells at 5 × 10^5 cells per well.

   Purified T cells require an exogenous source of accessory non–T cells. Accessory cells function both as antigen-presenting cells and as a source of undefined "second signals." They are not required for cell preparations primed against cellular antigens, because accessory cell function is provided by the stimulator cells.

6. Proceed as in steps 7 to 9 of the basic protocol.

   Culture periods before labeling can vary widely and kinetic assays should be performed. In general, for T cells from primed mice, it is likely that the response will peak at day 4 or 5.

REAGENTS AND SOLUTIONS

Percoll solution

Diluent:
45 ml 10× PBS, pH 7.4 (*APPENDIX 2*)
3 ml 0.6 M HCl
132 ml H_2O
Filter sterilize

70% Percoll solution:
63 ml Percoll (Pharmacia LKB #170891-01)
37 ml sterile diluent (above)
Final osmolarity should be 310 to 320 osM

COMMENTARY

Background Information

Proliferative assays for measuring T cell function have certain advantages and disadvantages compared to the cytotoxic T lymphocyte (CTL) assay described in *UNIT 3.11* or the lymphokine production assays in *UNITS 3.15 & 6.3*. Advantages are that proliferative assays are less time-consuming, less labor-intensive, less cell-consuming, and less expensive than "true" effector T cell function assays. A disadvantage is that antigen specificity is not as easily demonstrated in proliferative assays as in CTL assays, unless antigen-specific clones of proliferating cells are used. Furthermore, the proliferative assay only detects dividing cells instead of measuring true effector T cell function.

It is not clear which T cell function is measured in proliferative assays; the proliferative response should therefore be used solely as general indicators of T cell reactivity. Data obtained in proliferative assays might variously reflect proliferation of CTL, lymphokine-producing T cells, or nonactivated "bystander" cells, and will be severely affected by the function of non–T cells such as accessory cells (see below). Since the majority of T cells respond to and produce IL-2 upon activation, differences in responsiveness in a proliferative assay in part reflect differences in IL-2 production by the responding T cells. Proliferative assays therefore become more meaningful when combined with the lymphokine detection assays presented in *UNITS 3.15 & 6.3*. Since responsiveness to IL-2 is also determined by the levels and functionality of IL-2 receptors, further information will be added by including measurements of IL-2 receptors (*UNIT 6.1*) or by flow cytometry (*UNIT 5.4*). Yet, as a first approximation of cellular activation, proliferative assays are valuable.

Critical Parameters and Troubleshooting

Parameters affecting the magnitude of T cell proliferative responses include cell concentration, type of medium, source of serum, incubator conditions (CO_2 level and humidity), type and concentration of activating agent, type of responding T cells, type of accessory/ stimulator cells, mouse strain, and culture time. Optimal conditions for individual laboratories and experiments must be derived empirically with respect to these variables, but general guidelines are provided below.

A number of agents can be employed in the first basic protocol to induce T cell proliferation (Table 3.12.1). T cells may be activated by pharmacologic means by producing an elevation of intracellular free calcium with a calcium ionophore combined with activation of protein kinase C with a phorbol ester. The most direct means of inducing T cell activation involves stimulation with monoclonal antibodies that interact with the CD3/TCR complex—i.e., anti-CD3, anti-TCR-αβ or -γδ, as well as anti-Vβ antibodies that are capable of interacting with a subset of cells bearing a specific TCR. A vigorous T cell proliferative response of defined subsets can also be induced with certain bacterial toxins known as staphylococcal enterotoxins. These toxins are often referred to as "superantigens" (Marrack and Kappler, 1989) because they stimulate T cells via the variable (*V*) gene segment of the TCR. Different toxins have affinities for different *V*β chains and these specificities make them valuable reagents for activating T cells. The activating capacity of toxins is also dependent on their ability to bind to MHC class II molecules (i.e., responding T cells react with the toxin/class II complex); thus, responsiveness varies with the

mouse strain used. Lectins such as phytohemagglutinin (PHA) and concanavalin A (Con A) have been widely used for many years to activate T cells. Although the precise mechanism of action of these agents is unknown, it is likely that lectins activate T cells by indirectly cross-linking the TCR because TCR-negative cells will not respond to these agents. Lastly, it is also possible to induce T cell activation with monoclonal antibodies to cell-surface antigens other than the TCR; this protocol employs the G7 monoclonal antibody, one of the most effective of the anti-Thy-1 activators (Gunter et al., 1984).

When comparing the reactivity of different cell populations, it is essential to perform dose-response assays for responder T cells and activating agents and for both responder and stimulator T cells (in MLR), since each population may yield optimal responses at different cell numbers. This may reflect differences in frequency of responding cells, and hence may indicate a need to perform limiting dilution assays (*UNIT 3.15*). Since peak responsiveness of different populations of T cells may occur at different times, it is also essential to perform kinetic experiments—i.e., compare responsiveness at days 2, 3, 4, and 5.

Differences in responsiveness need not necessarily be due to differences in the frequency of responding T cells, but may also indicate differences in the efficacy with which co-stimulatory activity or "second signals" are delivered by the accessory cells present in different cell populations. The type of interactions pertinent to the generation of primary responses by T cells is explained in the commentaries of *UNITS 3.8, 3.11, & 3.13*. Specific requirements for inducing activation with immobilized antibodies have been described (Staerz and Bevan, 1986; Hathcock et al., 1989; Jenkins et al., 1990). A responding cell population completely devoid of accessory cells (such as purified populations of splenic or lymph node T cells or cloned T cells) will yield fine responsiveness in an MLC, since accessory cell function is provided by the stimulator cells; however, the same population will generally not yield responses when mitogens, antigens, or enterotoxins are used. In such a setting, accessory cells may also function as antigen-presenting cells (APC). Addition of irradiated or mitomycin C–treated syngeneic sources of accessory cells (either whole spleen cells or purified APC; see first support protocol) can be used to restore responsiveness in purified T cells. The need for accessory cells can sometimes be bypassed when anti-TCR monoclonal antibodies are coupled to plastic, or when certain anti-Thy-1 monoclonal antibodies are used; however, these conditions do not necessarily result in optimal responsiveness (Jenkins et al., 1990).

The level of [^{3}H]thymidine incorporation should not be regarded only as a reflection of cellular proliferation: some nondividing cells will synthesize DNA and "cold" thymidine released by disintegrating cells will compete with incorporation of labeled thymidine. Therefore, measurements of DNA synthesis should be accompanied by counting viable cells over the length of the culture period if a true estimate of cellular proliferation is to be obtained. Of course, cell death of nonactivated cells will also interfere with the accuracy of this last parameter.

The sensitivity of proliferation assays is such that small errors in cell numbers will result in large differences in [^{3}H]thymidine incorporation values. When values obtained in triplicate cultures correspond poorly (e.g., >5% difference in cpm values >1000), technical problems such as cell clumping, dilution, and pipetting should be considered. Excessively high values may be obtained from contaminated wells, as [^{3}H]thymidine will be incorporated into replicating bacteria; therefore, it is good practice to check the wells from microtiter plates under an inverted microscope for contamination. Contamination may also interfere with proliferation of the activated lymphocytes.

It is also useful to check for blast formation by microscopic examination of the cultures: activated lymphocytes will tend to enlarge, and detection of blasts will give a general indication of successful activation.

The main problem that may occur with proliferative response assays is high levels of background [^{3}H]thymidine incorporation in control cultures without antigens. This problem is frequently due to the fetal calf serum (FCS) used to supplement the cultures, which may be mitogenic for B cells. Different lots of FCS should be screened to select those that are nonstimulatory or only weakly stimulatory in the absence of other stimuli, and that support strong proliferative responses upon antigenic stimulation of T cells.

If flat-bottom microtiter plates are used in the procedure and weak responses occur, it may be useful to switch to round-bottom plates. Our laboratory has found consistently better responses in round-bottom plates when

thymocytes are used as responder cells or with slight alloantigenic differences between responding and stimulating cells. In addition, antibody-mediated experiments yield better results with round-bottom plates. Presumably, this reflects better cell contact obtained in such plates; optimal responses will almost certainly occur at different cell numbers than in flat-bottom plates and densities will have to be adjusted accordingly.

Although satisfactory responses to most alloantigens can be obtained with complete RPMI-10 medium, it may be necessary to compare different media. This need arises when the proliferative responses are weak (i.e., when [^{3}H]thymidine values for activated cultures are <10-fold higher than those for control cultures) and may occur under various circumstances: weak alloantigenic differences between responder and stimulator cells, weak T cell proliferative function in the responder cells or diminished APC function in the stimulator cells due to experimental manipulations, or a low precursor frequency of responding T cells. Thymocytes in particular do not contain a high level of responding T cells. Frequently, proliferation can be improved when complete Clicks or Dulbeccos media are used (with additives as described in *APPENDIX 2*), presumably because these media contain additional nutrients and have an osmolarity more compatible with mouse serum than RPMI.

When RPMI is used as medium, 5% CO_2 will be sufficient, but for other media, a 7.5% CO_2 concentration in the incubator will be more satisfactory. Generally, the buffering capacity of DMEM is insufficient at 5%, but fine at 7.5%. Much will also depend on the proliferative activity of the responding population of T cells (e.g., vigorous proliferation will reduce the pH in the cultures); it is therefore recommended to compare responsiveness in initial pilot experiments in incubators set at different CO_2 concentrations.

The culture period required for stimulation—after which the cells are to be labeled—varies for different laboratories, media, and types of responding and stimulator cells. Conditions eliciting weak responses, such as those obtained with thymocytes or a weak alloantigenic difference, will require a longer culture period (5 to 6 days) than those which elicit a higher frequency of responding T cells (3 to 4 days). Because laboratory conditions vary, it will be necessary to run a kinetic assay to determine the optimal time for T cell proliferation. Addition of [^{3}H] thymidine on days 2, 3, 4, 5, and 6 will provide a useful test; further extension of the culture period will not yield any improvements, due to exhaustion of nutrients in the medium.

Anticipated Results

For proliferative assays described in the basic protocol, which activate the majority of the responding T cells, responses of 100,000 cpm should be obtained; in the MLR or following activation with monoclonal antibodies to subpopulations of T cells (anti-Vβ), responses up to 100,000 cpm may be observed; however, measurements of 20,000 cpm (with tight standard errors) can be quite satisfactory. Background values of <1000 cpm should be expected. Reported results (as described in step 9a) should be mean cpm of experimental wells minus background cpm (Δ cpm).

Time Considerations

The time required to set up proliferative assays is not more than a day, with the number of hours depending on the number of different groups of responder cells that must be prepared. The time required for incubation of cells ranges from 2 to 6 days, as noted above in critical parameters. Following an additional 18- to 24-hr incubation period for pulsing, harvesting the cells and measuring cpm will require several hours depending on the number of plates (~15 min for harvesting each plate and ~100 min for counting each plate at 1 min/sample).

Literature Cited

Ashwell, J.D., DeFranco, A.L., Paul, W.E., and Schwartz, R.H. 1984. Antigen presentation by resting B cells: Radiosensitivity of the antigen-presentation function and two distinct pathways of T cell activation *J. Exp. Med.* 159:861-869.

Gunter, K.C., Malek, T.R., and Shevach, E.M. 1984. T cell activating properties of an anti-Thy-1 monoclonal antibody: Possible analogy to OKT3/Leu-4. *J. Exp. Med.* 159:716-730.

Hathcock, K.S., Segal, D.M., and Hoder, R.J. 1989. Activation of Lyt2$^+$ (CD8$^+$) and Lyt2$^-$(CD4$^+$) T cell subsets by anti-receptor antibody. *J. Immunol.* 142:2181-2186.

Jenkins, M.K., Chen, C., Jung, G., Mueller, D.L., and Schwartz, R.H. 1990. Inhibition of antigen-specific proliferation of type 1 murine T cell clones after stimulation with immobilized anti-CD3 monoclonal antibody. *J. Immunol.* 144:16-22.

Marrack, P. and Kappler, J. 1989. The staphylococcal enterotoxins and their relatives. *Science* 248:705-711.

Staerz, U.D. and Bevan, M.J. 1986. Activation of resting T lymphocytes by a monoclonal antibody directed against an allotypic determinant on the T cell receptor. *Eur. J. Immunol.* 16:263-268.

Key References

Corradin, G., Etlinger, H.M., and Chiller, M. 1977. Lymphocyte specificity to protein antigens. I. Characterization of the antigen-induced in vitro T cell dependent proliferative response with lymph node cells from primed mice. *J. Immunol.* 119:1048-1055.

Rosenwasser, L.J. and Rosenthal, A.S. 1978. Adherent cell function in murine T lymphocyte antigen recognition. I. A macrophage-dependent T cell proliferation assay in the mouse. *J. Immunol.* 120:1991-1998.

Both of the above describe how specific proliferation of antigen-primed T cells can be measured.

Strong, D.M., Ahmed, A.A., Thurman, G.B., and Sell, K.W. 1973. In vitro stimulation of murine spleen cells using a microculture system and a multiple automated sample harvester. *J. Immunol. Methods* 2:279-287.

Details the MLC proliferation assay.

Contributed by Ada M. Kruisbeek
Netherlands Cancer Institute
Amsterdam, The Netherlands

Ethan Shevach
National Institute of Allergy and Infectious Diseases
Bethesda, Maryland

Exhibit 8

Dendritic cells are allowing scientists to overcome a longstanding obstacle to research in immunology by extending the playing field beyond antigens to immunogens and beyond models to pathogens that cause disease.

The Dendritic Cell Advantage: New Focus For Immune-Based Therapies

by Ralph M. Steinman

Summary

Dendritic cells (DCs) provide a much earlier and antigen-specific means for manipulating the immune response. The best-studied function of DCs is to convert antigens into immunogens for T cells. The "DC advantage" entails a myriad of functions. DCs are more than antigen-presenting cells; they are accessories or adjuvants or catalysts for triggering and controlling immunity. Another special feature of DCs is their location and movement in the body; DCs are stationed at surfaces where antigens gain access to the body. The events that make up the life history of DCs are now being unraveled in molecular terms. As research on DCs expands, more potential functions and more sites for their manipulation are becoming apparent.

The focus of immune therapeutics has been on lymphocytes, the cellular mediators of immunity, and the suppression of lymphocyte function. The drug ciclosporin (cyclosporine) is an excellent and successful example. However, medicine needs therapies that enhance immunity or resistance to infections and tumors. Medicine also needs strategies, whether suppressive or enhancing, that are specific to the disease-causing stimulus or antigen. In contrast to lymphocytes, dendritic cells (DCs) provide a much earlier and antigen-specific means for manipulating the immune response. DCs capture antigens and then initiate and control the activities of lymphocytes, including the development of resistance to infections and tumors (reviewed in references 1–3).

The controlling role of DCs is best known for thymus-dependent lymphocytes or T cells which are important in many diseases, the most poignant being the AIDS epidemic (Table 1). DCs were identified in a few laboratories that were focusing on the induction of immunity from resting T cells. It was noted that immune tissues (spleen, lymph nodes, lymph, blood) had a small fraction of cells with unusual "tree-like" or "dendritic" processes. These distinctive cells had not been recognized previously and they proved to have distinct functions. Most importantly, DCs were potent inducers of immunity even in animals, not just the test tube, and now even in patients (reviewed in references 1–3).

The DC field was held back by the fact that there were so few cells relative

  CCC: 0214-0934/2000

TABLE I: HUMAN DISEASES THAT INVOLVE T CELLS

- Rejection of organ transplants and graft-vs.-host disease in bone marrow transplantation
- Resistance to many infections including vaccine design
- Vaccines against tumors and immune therapies for existing tumors
- Allergy
- AIDS
- Autoimmune diseases like insulin-dependent (juvenile) diabetes, multiple sclerosis, rheumatoid arthritis and psoriasis

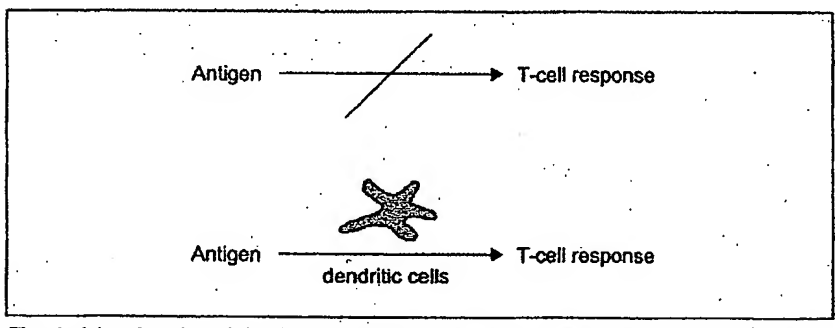

Fig. 1. A key function of dendritic cells. Antigens within tumors, transplants and infectious agents need to be presented by DCs to become immunogens, i.e., to make T cells begin to grow and exhibit their helper and killer functions.

to other players in the immune system such as B cells, T cells and macrophages. In reality, DCs are quite abundant for the job they have to do, namely, to initiate immune responses from antigen-specific T cells. In immune system organs like lymph nodes, DCs form an extensive network throughout the T cell-rich regions and physically outnumber any given antigen-reactive T cell by at least 100 to 1. The DC field was also held back because many thought that the cells were no different from macrophages, thus keeping investigators from working on the active DCs. In reality, DCs were identified on the basis of profound differences from macrophages, and their many distinct properties and functions were only uncovered by separating DCs from macrophages.

The best-studied function of DCs is to convert antigens into immunogens for T cells. The antigen receptors on T cells do not focus on intact proteins in microbes and tumors, but instead recognize fragmented or processed proteins, that is, peptides. The processing of protein antigens into peptides occurs within cells, and then the peptides are displayed or presented at the cell surface affixed to products of the major histocompatibility complex (MHC). The ensuing interaction between a T-cell receptor (TCR) and its specific MHC–peptide complex allows a T cell to detect peptides formed within cells in transplants, tumors, sites of infection and self tissues attacked during autoimmune disease (Table I). "Antigens" refers to specific substances recognized by the immune system, while "immunogens" refers to antigens that effectively induce responses either by themselves or together with enhancing materials called "adjuvants." For T cells in particular, antigens and immunogens are not one and the same (Fig. 1). Even preprocessed peptides and MHC–peptide complexes are weak immunogens. This was evident early on in the work of Peter Medawar, the great scientist who discovered the immune basis of transplantation. He spent many years trying to purify functioning transplantation antigens. These efforts were to little avail.

What was not known in Medawar's time is that transplantation antigens (later shown to be MHC–peptide complexes) become immunogenic when presented by DCs.[4] In other words, transplantation antigens when presented on many cell types are weak immunogens, but on DCs they become powerful inducers of immunity.[4] The same is true of peptides that become much more immunogenic when presented on DCs. DCs activate T cells by getting them to divide and express their helper and killer functions. Then the activated T cells interact with other antigen-presenting cells to eliminate the antigen in question. DCs are also called "nature's adjuvant," because prior adjuvants were artificial substances used to enhance immunity. The DC advantage entails a myriad of functions, some of which will be considered below.

Potency of dendritic cells in initiating immunity in tissue culture

What are some specific features of DCs that warrant attention? The first is their potency. Very small numbers of DCs are sufficient to trigger strong T-cell responses in test tubes. Immune assays are generally carried out with impure antigen-presenting cells, applied at a dose of one presenting cell for every T cell, the latter often preactivated. In contrast, roughly one DC per 30–100 T cells is more than sufficient to induce optimal responses, including responses by resting T cells. A single DC can simultaneously activate 10–20 T cells nestled within its sheet-like processes. Therefore, DCs are more than antigen-presenting cells; they are accessories or adjuvants or catalysts for triggering and controlling immunity.

It has always been clear that the accessory function of DCs did not depend exclusively on their capacity to process antigens to form MHC–peptide complexes. This is because the stimuli that were used to define the potency and immune-activating role of DCs did not require that the DCs process an applied antigen. Such stimuli included major transplantation antigens, mitogens, contact allergens, anti-

T-cell antibodies and superantigens. Furthermore, once resting T cells were activated by DCs, the T cells responded vigorously to antigens presented by other cell types, showing that the latter were not deficient in forming ligands for the antigen receptor on T cells, but instead lacked accessory properties.

The word "accessory" has since been replaced by the terms "professional" and "co-stimulatory," but the basic concept is unchanged by shifting terminology. T cells need stimuli other than their specific trigger or ligand (MHC–peptide complexes) to begin to grow and function, for example, to produce the interleukins and killer molecules mentioned above. DCs are potent in providing the needed accessory or co-stimulatory functions. For example, DCs produce an adhesion molecule called DC-SIGN that binds to a target on resting T cells called ICAM-3,[5] and DCs express very high levels of a stimulatory molecule called CD86 that binds to CD28 on resting T cells.[6] These are but two examples of the specialized activities of DCs. These cells do not operate as a single magic bullet.

Position of dendritic cells *in vivo*

Another special feature of DCs is their location and movement in the body. As criteria were developed to identify DCs, it became feasible to go back into the animal and patient to look for the corresponding cells in different tissues. DCs are stationed at surfaces where antigens gain access to the body (Fig. 2, left). The skin and the airway have been the best studied. DCs are found in afferent lymphatic vessels, special channels that allow cells to move from peripheral tissues to lymphoid organs, primarily the T-cell areas (Fig. 2, middle and right). This migration is most readily observed in models of skin transplantation and contact allergy, which are the two most powerful immune responses known.

DC migration is likely to be very important. The body's pool of T cells primarily traffics through the T-cell areas of lymph nodes, rather than through tissues where antigens are usually deposited. So when DCs capture antigens in the skin, airway or another peripheral tissue, their migration to the T-cell areas gives them a chance to select the corresponding rare specific T cells from the assembled repertoire (Fig. 2). The selected T cells then increase in numbers (clonal expansion) and function, enabling the specific immune response to begin. The initial frequency of T cells that recognize an antigen is very small. Only one in 10,000–100,000 of T cells in the repertoire responds to a specific MHC–peptide complex. Therefore, it is so precise and efficient for DCs to be able to pick up an antigen in the periphery and then initiate the immune response from rare T-cell clones in lymphoid organs.

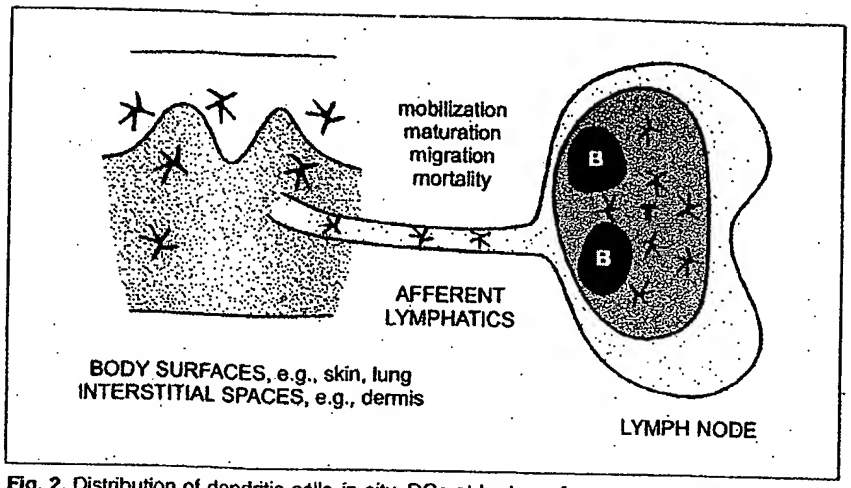

Fig. 2. Distribution of dendritic cells *in situ*. DCs at body surfaces and in solid organs can pick up antigens, move to the lymphoid tissues to find antigen-specific T cells and initiate immunity. Molecular mechanisms are being uncovered that govern the mobilization, maturation, migration and mortality of these DCs. In the lymph node, T lymphocytes are selected for expansion and differentiation into helper and killer T cells. The activated T cells then leave the lymph node to return to the body surface or peripheral organ to eliminate the antigen.

The events that make up the life history of DCs (Figs. 2 and 3) are now being unraveled in molecular terms. For example, scientists are figuring out how to expand antigen-capturing precursors to DCs using flt3 ligand and granulocyte colony-stimulating factor (G-CSF). Key players for the mobilization of DCs from the periphery to lymph nodes are the multidrug resistance receptors, usually studied for their capacity to mediate resistance to chemotherapeutic agents rather than movement of DCs. Migration of DCs is controlled by chemokines produced in the lymphatic vessels and lymphoid organs (Fig. 2). These act on DC chemokine receptors to orchestrate their movement to the T-cell areas. Then within the lymphoid tissue, several members of the tumor necrosis factor (TNF) and TNF-receptor families, such as TRANCE and CD40 ligand, trigger DC production of cytokines like interleukin-12. The TNF family also maintains DC viability. Otherwise the cells die within a day or two. Each of these components of DC function provides targets for manipulating immunity.

Priming of T-cell immunity via dendritic cells

Animal studies

During the early research on DCs, several labs administered antigens to experimental animals and then tried to identify the cells that had captured the antigens in a form that was immunogenic. Regardless of the route of antigen administration (blood, muscle, skin, intestine and airway), DCs were the major reservoir of immunogen.

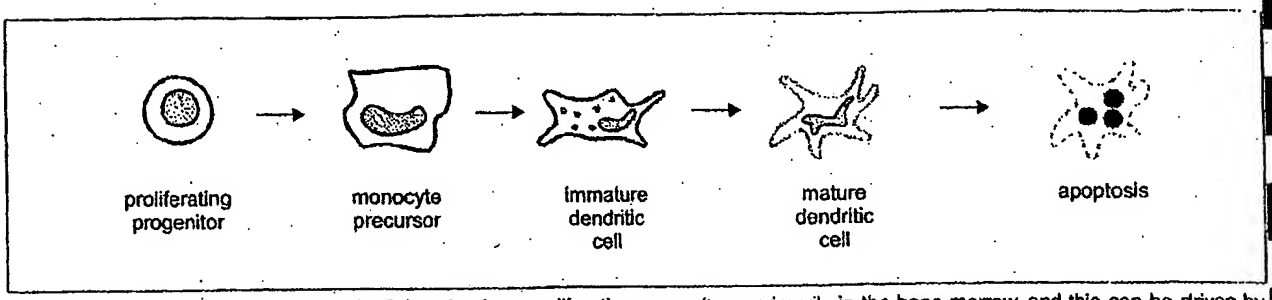

Fig. 3. The life history of dendritic cells. DCs arise from proliferating progenitors, primarily in the bone marrow, and this can be driven by cytokines like flt-3 ligand and G-CSF. Precursors are formed, such as the monocytes in blood, which then give rise to immature DCs. The immature DCs are capable of producing large amounts of antigen-presenting MHC products and capturing antigens. Multidrug resistance receptors are newly recognized players in the mobilization of immature DCs. DCs mature in response to various stimuli such as infection and inflammation, and migrate under the influence of chemokines to the lymphoid tissues. There the DCs die within a day unless their life-span is prolonged by TNF-family molecules expressed by the activated T cells.

Next, DCs were used as nature's adjuvant to immunize animals. The DCs were taken from mice or rats, exposed to antigens *ex vivo* and injected back into immunologically naive recipients. The animals became immunized to the antigens that had been captured by the DCs, and the immunization took place in the lymph nodes draining the site of DC injection. Genetic proof was provided that the DCs were priming the animal directly and not simply handing off their antigen to other cells.[7,8]

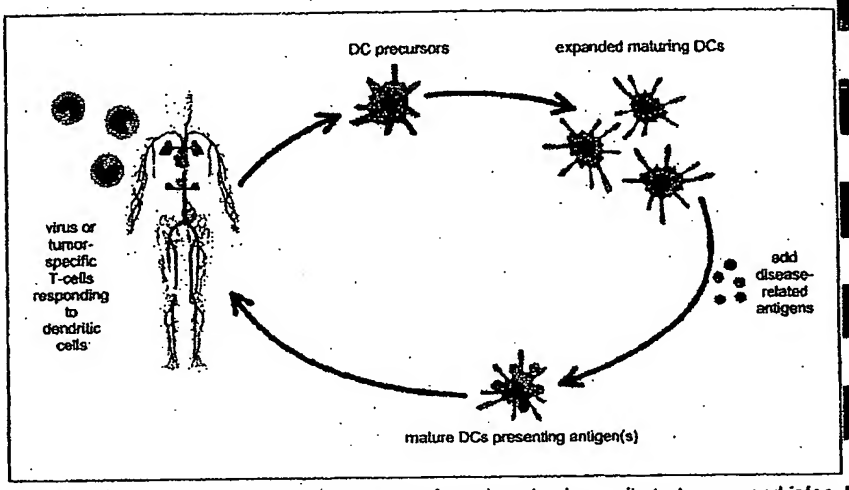

Fig. 4. The use of dendritic cells as adjuvants for enhancing immunity to tumors and infectious agents in humans. This new form of immune therapy begins with the isolation of DC precursors from the patient, usually from blood. The precursors develop *ex vivo* (in relatively simple tissue culture systems) into large numbers of more mature DCs. During this time, the DCs are charged with antigens from the tumor or infection. Then the DCs are reinfused to elicit immunity and thereby resistance to the disease.

DC-based immunization is really very different from all prior attempts at cell therapy. Immunology has had extensive experience with "passive immunization," whereby a recipient is given large numbers of cells that are activated prior to injection. It is hard to produce such large numbers of cells, and their lifespan, diversity and efficacy are all finite. In contrast, when relatively small numbers of antigen-charged DCs are used to induce immunity, this produces "active immunization." Now the animals (and patients, see below) can make their own diverse and longer lasting immune response to the antigen-bearing DCs.

Human studies

The above experiments made it clear that DCs, pulsed *ex vivo* with antigens, actively immunized animals and raised the exciting possibility that scientists would be able to induce resistance to tumors, infections and transplants in patients. For example, could one expose patients' DCs *ex vivo* to antigens in their tumors and then reinfuse the antigen-bearing DCs to elicit tumor-specific immunity (Fig. 4)? This approach is actually not terribly complicated, but one first had to overcome a major obstacle and learn to generate large numbers of DCs. These techniques became available in the 1990s. They have energized the field and, accordingly, clinical trials for the immunization of humans against cancer have begun on most continents.

It is evident that DCs can serve as adjuvants for humans, converting antigens into immunogens.[9,10] Even in advanced cancer, immune responses already have been observed that are similar to or better than immune responses obtained with other approaches. However, this approach is still in its preliminary stages, since a good deal of science remains to be developed. On the one hand, there are critical unknowns in terms of overall DC biology. Many of the clinical studies to date, for example, have overlooked key features that could improve DC function, such as the need for DCs

to be sufficiently mature (see below) to be effective *in vivo*. Also, DC biology has to be placed in the context of specific tumors and pathogens and patients for DC-based therapies to be optimized.

To summarize and further illustrate the role of DCs in the context of human disease (Table I), consider the need to harness T cells to resist tumors and chronic infections. Protein antigens often are known for a tumor-like melanoma, or for a virus like HIV-1 whose genetic sequence has been available for more than 15 years. However, this knowledge about antigens from melanoma and HIV-1 antigens remains to be converted into methods that provide better immunogens either for immune therapy of melanoma or for the design of HIV-1 vaccines. This is because some important facts of immunological life are being overlooked. When antigens are injected, they also need to gain access to the right DCs to become immunogens (Fig. 1).

Delivering antigens to dendritic cells

Broadly speaking, a central goal is to learn how to deliver or "target" antigens to DCs and simultaneously to differentiate or "mature" the cells to their most potent state. These two challenges, antigen targeting and DC maturation, prove to be intertwined.

Targeting means that the antigen should be in a form that the DCs can recognize. Without such recognition, the uptake and subsequent processing of antigen to form MHC–peptide complexes is suboptimal. DCs have a number of special mechanisms for capturing antigens and converting these into MHC–peptide complexes (Table II). For example, DCs have a receptor called DEC-205 whose binding partners or ligands are still unknown. Nonetheless, it is clear that DEC-205 greatly increases the capacity of DCs to form MHC–peptide complexes.[11] DCs also carry out a fascinating process called "cross-presentation." DCs can take up dying cells and efficiently extract peptides from them, so antigens "cross" from the dying cell to the DC. The discoverers of this phenomenon called it "resurrecting the dead."[12] Cross-presentation allows DCs to efficiently form MHC–peptide complexes from dead cells in tumors, transplants and tissues under autoimmune attack.

TABLE II: DENDRITIC CELL SPECIALIZATION TO INCREASE MHC–PEPTIDE COMPLEX FORMATION

- Receptors for antigen uptake, e.g., DEC-205
- Processing of dying cells, nonreplicating microbes and immune complexes onto MHC class I ("cross-presentation")
- Regulation of antigen processing by maturation stimuli
- Clustering of T-cell receptor ligands with co-stimulators like CD86

Special uptake and processing mechanisms allow DCs to tailor a protein antigen, as well as the proteins in a complex microbe or tumor cell, into peptides that bind to an individual's MHC products. The latter are exceptionally polymorphic, differing genetically from one individual to another. As a result, the relevant immunizing peptides differ from one individual to another. One reason why peptides are not ideal immunogens is that they must be individualized. DCs, in contrast, can capture antigens with high efficiency and likewise extract peptides that are relevant for any individual.

A second DC advantage is that these cells have the many required accessory or co-stimulatory properties for converting the selected peptides ("antigens") into effective immunogens. A third DC advantage is that these cells position themselves in a way that leads to the identification of rare antigen-reactive T lymphocytes *in vivo* (Fig. 2). DCs thus overcome many of the difficult obstacles in initiating immunity.

In order for an antigen to be a strong immunogen, one needs to provide a stimulus for the final differentiation or maturation of the DCs (Fig. 3). Most DCs in the body are in an immature state and lack many features that lead to a strong T-cell response. Immature DCs, for example, lack the CD86 and CD40 molecules that greatly boost the DC–T cell interaction. Immature DCs also lack a chemokine receptor called CCR7 that seems very important for proper migration and homing to lymph nodes to start immunity. For cancer immunology, it is unlikely that tumors provide maturation stimuli. Tumors may even block DC maturation induced by other stimuli. Therefore it is important to learn how to deliver tumor cells to DCs and bypass the normal obstacles to effective antitumor immunity.

Surprising recent evidence actually links DC maturation to the efficient formation of MHC–peptide complexes or TCR ligands (Table II). Immature DCs take up antigens, but they do not make abundant MHC–peptide complexes until they receive a maturation stimulus.[13,14] Maturation also up-regulates CD86 co-stimulators, but the CD86 actually travels together with the TCR ligands to the surface of the DCs. At the DC surface, the MHC molecules and CD86 remain clustered with each other, keeping the machinery for T-cell activation juxtaposed. This phenomenon will help explain the potency of DCs, because TCR ligands and co-stimulators are displayed together on the cell surface and in high levels.

Control points beyond antigen targeting and maturation of DCs

Research on DCs is moving more vigorously, because the cells are more readily available and because their role in the immune system is considered essential. Nonetheless, researchers in this field are just beginning to find ways to manipulate DCs *in situ*. Putting together an antigen that targets

to DCs with a stimulus for DC maturation will be a major step in improving the conversion of antigens into immunogens, as in immune-based therapies against tumors and infectious agents.

Additional challenges and questions are evident:

- How can DC numbers be increased *in situ* and how can active DCs be mobilized to a cancer or site of chronic infection?
- Can DCs induce strong immune memory to make vaccination long lasting and effective (we have only been reviewing the role of DCs in the initiation of immunity)?
- Can DCs change the quality of the immune response? "Quality" refers to recent evidence for different types of DCs, especially a subset that induces Th1-type T cells for resistance to infectious agents and strong memory.
- Is it possible to move beyond DC-based immunization experiments and use DCs to either regulate or tolerize the immune system, as frequently required in transplantation and autoimmune diseases?
- Can DCs influence elements of the immune system other than T cells; for example, B cells and the innate defenses provided by natural killer (NK) and NK-T cells?

The answer to all these questions is a preliminary "yes." As research on DCs expands, more potential functions and more sites for their manipulation are becoming apparent.

Dendritic cells and better control of disease

DCs provide important avenues for the investigation of human disease. Many labs are exploiting DCs to identify antigens relevant for immunity against human pathogens. In these experiments, one introduces complex but clinically important antigens to DCs and then identifies which components are best presented to the immune system. We have recently used this approach to identify previously unknown immune responses to the Epstein-Barr virus,[15] a virus we all carry that has the potential to cause cancer like Hodgkin's lymphoma. Other laboratories have been using DCs to identify new antigens in other infectious agents, in transplants and in cancers like melanoma.

Investigators are also manipulating DCs *ex vivo* and then reinfusing the cells to identify conditions leading to strong immunity in patients (Fig. 4). In particular, DC-mediated active immunization against cancer is being vigorously pursued, as mentioned above. Instead of manipulating DCs *ex vivo*, a more desirable goal would be able to alter DCs directly *in situ*. Some approaches are under way. An example is the injection of cytokines like flt3 ligand and G-CSF to mobilize various precursor populations of DCs. One should also develop methods to control DC mobilization, migration and maturation. In sum, DCs are allowing scientists to overcome a longstanding obstacle to research in immunology by extending the playing field beyond antigens to immunogens and beyond models to pathogens that cause disease.

References

1. Hart, D.N.J. *Dendritic cells: Unique leukocyte populations which control the primary immune response.* Blood 1997, 90: 3245–87.
2. Banchereau, J. and Steinman, R.M. *Dendritic cells and the control of immunity.* Nature 1998, 392: 245–52.
3. Banchereau, J., Briere, F., Caux, C., Davoust, J., Lebecque, S., Liu, Y.-J., Pulendran, B. and Palucka, K. *Immunobiology of dendritic cells.* Annu Rev Immunol 2000, 18: 767–811.
4. Steinman, R.M. and Witmer, M.D. *Lymphoid dendritic cells are potent stimulators of the primary mixed leukocyte reaction in mice.* Proc Natl Acad Sci USA 1978, 75: 5132–6.
5. Geijtenbeck, T.B.H., Torensma, R., van Vliet, S.J., van Duijnhoven, G.C.F., Adema, G.J., van Kooyk, Y. and Figdor, C.G. *Identification of DC-SIGN, a novel dendritic cell-specific ICAM-3 receptor that supports primary immune responses.* Cell 2000, 100: 575–85.
6. Inaba, K., Witmer-Pack, M., Inaba, M., Hathcock, K.S., Sakuta, H., Azuma, M., Yagita, H., Okumura, K., Linsley, P.S., Ikehara, S., Muramatsu, S., Hodes, R.J. and Steinman, R.M. *The tissue distribution of the B7-2 costimulator in mice: Abundant expression on dendritic cells in situ and during maturation in vitro.* J Exp Med 1994, 180: 1849–60.
7. Inaba, K., Metlay, J.P., Crowley, M.T. and Steinman, R.M. *Dendritic cells pulsed with protein antigens in vitro can prime antigen-specific, MHC-restricted T cells in situ.* J Exp Med 1990, 172: 631–40.
8. Liu, L.M. and MacPherson, G.G. *Antigen acquisition by dendritic cells: Intestinal dendritic cells acquire antigen administered orally and can prime naive T cells in vivo.* J Exp Med 1993, 177: 1299–307.
9. Dhodapkar, M., Steinman, R.M., Sapp, M., Desai, H., Fossella, C., Krasovsky, J., Donahoe, S.M., Dunbar, P.R., Cerundolo, V., Nixon, D.F. and Bhardwaj, N. *Rapid generation of broad T-cell immunity in humans after single injection of mature dendritic cells.* J Clin Invest 1999, 104: 173–80.
10. Thurner, B., Haendle, I., Röder, C., Dieckmann, D., Keikavoussi, P., Jonuleit, H., Bender, A., Maczek, C., Schreiner, D., von den Driesch, P., Bröcker, E.B., Steinman, R.M., Enk, A., Kämpgen, E. and Schuler, G. *Vaccination with Mage-3A1 peptide-pulsed mature, monocyte-derived dendritic cells expands specific cytotoxic T cells and induces regression of some metastases in advanced stage IV melanoma.* J Exp Med 1999, 190: 1669–78.
11. Mahnke, K., Guo, M., Lee, S., Sepulveda, H., Swain, S., Nussenzweig, M. and Steinman, R.M. *The dendritic cell receptor for endocytosis, DEC-205, can recycle and enhance antigen presentation major histocompatibility complex class II-positive lysosomal compartments.* J Cell Biol 2000, 151: 673–84.
12. Albert, M.L. and Bhardwaj, N. *Resurrecting the dead: DCs cross-present antigen derived from apoptotic cells on MHC I.* Immunologist 1998, 6: 194–8.
13. Inaba, K., Turley, S., Iyoda, T., Yamaide, F., Shimoyama, S., Reis e Sousa, C., Germain, R.N., Mellman, I. and Steinman, R.M. *The formation of immunogenic MHC class II-peptide ligands in lysosomal compartments of dendritic cells is regulated by inflammatory stimuli.* J Exp Med 2000, 191: 927–36.
14. Turley, S.J., Inaba, K., Garrett, W.S., Ebersold, M., Untermaehrer, J., Steinman, R.M. and Mellman, I. *Transport of peptide-MHC class II complexes in developing dendritic cells.* Science 2000, 288: 522–7.
15. Munz, C., Bickham, K.L., Subklewe, M., Tsang, M.L., Chahroudi, A., Kurilla, M.G., Zhang, D., O'Donnell, M. and Steinman, R.M. *Human CD4(+) T lymphocytes consistently respond to the latent Epstein-Barr virus nuclear antigen EBNA1.* J Exp Med 2000, 191: 1649–60.

Ralph M. Steinman, M.D., is Henry G. Kunkel Professor and Senior Physician, Laboratory of Cellular Physiology and Immunology, The Rockefeller University, 1230 York Ave., New York, New York 10021–6399, U.S.A.

Proc. Natl. Acad. Sci. USA
Vol. 88, pp. 4143–4147, May 1991
Immunology

Exh C

Coexpression of two distinct genes is required to generate secreted bioactive cytotoxic lymphocyte maturation factor

(heterodimeric lymphokine/T-cell growth factor/lymphokine-activated killer cells/coordinate gene regulation/interleukin-12)

UELI GUBLER*†, ANNE O. CHUA*, DAVID S. SCHOENHAUT*, CYNTHIA M. DWYER‡, WARREN MCCOMAS*, RICHARD MOTYKA*, NASRIN NABAVI§, AIMEE G. WOLITZKY§, PHYLLIS M. QUINN§, PHILIP C. FAMILLETTI‡, AND MAURICE K. GATELY§

Departments of *Molecular Genetics, ‡Bioprocess Development, and §Immunopharmacology, Roche Research Center, Hoffmann–La Roche, Inc., Nutley, NJ 07110

Communicated by John J. Burns, February 4, 1991

ABSTRACT Cytotoxic lymphocyte maturation factor (CLMF) is a disulfide-bonded heterodimeric lymphokine that (*i*) acts as a growth factor for activated T cells independent of interleukin 2 and (*ii*) synergizes with suboptimal concentrations of interleukin 2 to induce lymphokine-activated killer cells. We now report the cloning and expression of both human CLMF subunit cDNAs from a lymphoblastoid B-cell line, NC-37. The two subunits represent two distinct and unrelated gene products whose mRNAs are coordinately induced upon activation of NC-37 cells. Coexpression of the two subunit cDNAs in COS cells is necessary for the secretion of biologically active CLMF; COS cells transfected with either subunit cDNA alone do not secrete bioactive CLMF. Recombinant CLMF expressed in mammalian cells displays biologic activities essentially identical to natural CLMF, and its activities can be neutralized by monoclonal antibodies prepared against natural CLMF. Since this heterodimeric protein displays the properties of an interleukin, we propose that CLMF be given the designation interleukin 12.

The molecular cloning and expression of recombinant cytokines has made possible both significant advances in our understanding of the molecular basis of immune responses and the development of new approaches to the treatment of disease states. As an example, recombinant interleukin 2 (recombinant IL-2) has been shown to be capable of causing regression of established tumors in both experimental animals (1) and in man (2); however, its clinical use has been associated with significant toxicity (2). One potential approach to improving the therapeutic utility of recombinant cytokines is to use them in combination (3, 4). With this concept in mind, we initiated a search for novel cytokines that would synergize with suboptimal concentrations of recombinant IL-2 to activate cytotoxic lymphocytes *in vitro* and thus might have synergistic immunoenhancing effects when administered together with recombinant IL-2 *in vivo*. This led to the identification of a factor, designated cytotoxic lymphocyte maturation factor (CLMF), that synergized with recombinant IL-2 to facilitate the generation of both cytolytic T lymphocytes (CTLs) and lymphokine-activated killer (LAK) cells *in vitro* (5, 6). CLMF was subsequently purified to homogeneity from a human lymphoblastoid B-cell line (NC-37) and was shown to be a 75-kDa disulfide-bonded heterodimer composed of two subunits with molecular masses of 40 kDa and 35 kDa (7).¶ We now report the molecular cloning and expression of CLMF.

The publication costs of this article were defrayed in part by page charge payment. This article must therefore be hereby marked "*advertisement*" in accordance with 18 U.S.C. §1734 solely to indicate this fact.

MATERIALS AND METHODS

cDNA Cloning. A subline of NC-37 cells selected for its ability to produce high levels of CLMF (7), NC-37.98, was induced with phorbol 12-myristate 13-acetate (PMA) and calcium ionophore A23187 for 16 hr. Poly(A)$^+$ RNA was isolated, and random hexamer-primed cDNA libraries were established in phage λgt10 by standard procedures. Mixed-primer polymerase chain reaction (PCR) using controlled ramp times (8) was performed as follows. PCR primers contained all possible codons and were 14 or 15 nucleotides long (Fig. 1) with a 5' extension of 9 nucleotides containing an *Eco*RI site for subcloning. Degeneracies varied from 1 in 32 to 1 in 4096; 0.5–4 pmol per permutation of forward and reverse primer was used in a 50- to 100-μl PCR mixture with 40 ng of cDNA made from NC-37.98 cells that had been activated by culture with 10 ng of PMA and 25 ng of calcium ionophore A23187 per ml for 16 hr (40-kDa subunit) or with 3 μg of human genomic DNA (35-kDa subunit). PCR cycling parameters were as follows. Initial denaturation was at 95°C for 7 min. Low-stringency annealing was performed by cooling to 37°C over 2 min, incubating 2 min at 37°C, heating to 72°C over 2.5 min, extending at 72°C for 1.5 min, heating to 95°C over 1 min, and denaturing at 95°C for 1 min. This cycle was repeated once. Thirty standard cycles (40-kDa subunit) or 40 standard cycles (35-kDa subunit) were performed as follows: 95°C for 1 min, 55°C for 2 min, and 72°C for 2 min. Final extension was at 72°C for 10 min. "Amplicons" of the expected size were gel-purified, subcloned, and sequenced. The 40-kDa subunit cDNAs were isolated by hybridizing the 54-mer amplicon in 5× SSC (1× SSC = 0.15 M NaCl/0.015 M sodium citrate, pH 7) containing 20% formamide at 37°C overnight. Filters were washed in 2× SSC at 42°C for 30 min and exposed to x-ray film. The 35-kDa subunit cDNAs were isolated by hybridizing the 51-mer amplicon in 5× SSC/20% formamide at 37°C overnight. The filters were washed in 2× SSC at 40°C for 30 min and exposed to x-ray film. Positive clones were plaque-purified, their inserts were subcloned into the pBluescript plasmid, and their sequences were determined by using Sequenase.

Expression. cDNAs were separately engineered for expression in vectors containing the simian virus 40 early promotor essentially as described (9). COS cells were transfected with both CLMF subunit expression plasmids mixed together or

Abbreviations: CLMF, cytotoxic lymphocyte maturation factor; rCLMF and nCLMF, recombinant and natural CLMFs; CTL, cytolytic T lymphocyte; IL, interleukin; LAK, lymphokine-activated killer; PHA, phytohemagglutinin; PMA, phorbol 12-myristate 13-acetate; n, natural; PCR, polymerase chain reaction.

†To whom reprint requests should be addressed.

¶The cDNA sequences reported in this paper have been deposited in the Genbank data base [accession nos. M38443 (35-kDa CLMF subunit) and M38444 (40-kDa CLMF subunit)].

```
                                                ---->          <----
  1  MCPARSLLLV ATLVLLDHLS LARNLPVATP DPGMFPCLHH SQNLLRAVSN
 51  MLQKARQTLE FYPCTSEEID HEDITKDKTS TVEACLPLEL TKNESCLNSR
101  ETSFITNGSC LASRKTSFMM ALCLSSIYED LKMYQVEFKT MNAKLLMDPK
151  RQIFLDQNML AVIDELMQAL NFNSETVPQK SSLEEPDFYK TKIKLCILLH
201  AFRIRAVTID RVTSYLNAS

                                          ---->          <-----
  1  MCHQQLVISW FSLVFLASPL VAIWELKKDV YVVELDWYPD APGEMVVLTC
 51  DTPEEDGITW TLDQSSEVLG SGKTLTIQVK EFGDAGQYTC HKGGEVLSHS
101  LLLLHKKEDG IWSTDILKDQ KEPKNKTFLR CEAKNYSGRF TCWWLTTIST
151  DLTFSVKSSR GSSDPQGVTC GAATLSAERV RGDNKEYEYS VECQEDSACP
201  AAEESLPIEV MVDAVHKLKY ENYTSSFFIR DIIKPDPPKN LQLKPLKNSR
251  QVEVSWEYPD TWSTPHSYFS LTFCVQVQGK SKREKKDRVF TDKTSATVIC
301  RKNASISVRA QDRYYSSSWS EWASVPCS
```

FIG. 1. Amino acid sequences of the 35-kDa (*Upper*) and 40-kDa (*Lower*) CLMF subunits as deduced from the respective cDNAs and shown in single-letter code. Signal peptides are overlined, cysteine residues are marked by a caret, and N-linked glycosylation sites (NXS, NXT, where X is another amino acid) are underlined. The peptide sequences used to generate PCR probes are overlined with arrows indicating the direction of amplification.

with each one separately by the DEAE-dextran method. Twenty-four hours after transfection, the serum-containing medium was replaced with medium containing 1% Nutridoma-SP (Boehringer Mannheim), and supernatant fluids were collected from the cultures after 40 hr. These fluids were stored at 4°C until tested in the bioassays.

General Methods. Standard molecular biological procedures were used as described (10). CLMF bioassays were performed as detailed (7).

Computer Searches. The National Biomedical Research Foundation protein data base (Release 26.0) as well as the Genbank and European Molecular Biology Laboratory databases (Releases 65.0 and 24.0, respectively) were searched for sequences homologous to CLMF cDNAs. The two subunit sequences were compared to each other using the ALIGN program (mutation data matrix, break penalty of 6; see ref. 11).

RESULTS

Partial N-terminal amino acid sequences of the two CLMF subunits (7) were used to generate completely defined 51- to 54-base-pair (bp)-long oligonucleotide probes by means of mixed primer PCR. These probes were used to screen cDNA libraries made from RNA from activated NC-37.98 cells, and cDNAs encoding the two subunits were isolated and characterized. Both cDNAs encode secreted proteins with a classical hydrophobic N-terminal signal peptide immediately followed by the N terminus of the mature protein as determined by protein sequencing (7). Two independent cDNA clones for the 40-kDa subunit were shown to be identical. Both encode the mature 40-kDa subunit that is composed of 306 amino acids (calculated M_r = 34,699) and contains 10 cysteine residues and four potential N-linked glycosylation sites (Fig. 1). Two of these sites are within isolated tryptic peptides derived from the purified 40-kDa CLMF subunit protein. Amino acid sequence analysis has shown that Asn-222 is glycosylated, whereas Asn-125 is not (Fig. 1; F. Podlaski, personal communication). The mature 35-kDa subunit is composed of 197 amino acids (calculated M_r = 22,513), with 7 cysteine residues and three potential N-linked glycosylation sites (Fig. 1). When purified CLMF is reduced with 2-mercaptoethanol and analyzed by SDS/PAGE, the 35-kDa subunit appears to be heterogeneous, suggesting that it may be heavily glycosylated (7). Two variants of 35-kDa subunit-encoding cDNAs were isolated. The first type had the sequence shown in Fig. 1. Additional isolates contained what is probably an allelic variation, replacing Thr-213 with a methionine residue.

Computer searches of sequence databases showed that the amino acid sequences of the two subunits are not related to any known protein. The subunit sequences are also not related to each other, since a comparison using the ALIGN program (11) gave a score of 1.27; only scores >3 are considered to indicate significant evolutionary relationship (12). The genes encoding the subunits appear to be unique, since low- and high-stringency hybridizations of genomic blots revealed identical banding patterns (data not shown). RNA blots showed the size of the 40-kDa subunit mRNA to be 2.4 kb, whereas the 35-kDa subunit was encoded by a 1.4-kb transcript (Fig. 2). Expression of the two mRNAs encoding the subunits was coordinately regulated upon induction (Fig. 2). When NC-37.98 cells were activated with PMA and calcium ionophore for 72 hr, mRNA encoding each of the CLMF subunits was minimally detectable at 6 hr after the beginning of induction but was readily detected at 24 hr and continued to accumulate until maximal levels were reached at 72 hr (normalized to GAPDH mRNA levels; see the legend to Fig. 2). In contrast, the mRNA for IL-2 in activated NC-37.98 cells was already at high levels at 6 hr and subsequently decreased, whereas the mRNAs for the low-affinity IL-2 receptor (p55) followed the induction pattern seen for the CLMF subunits. Scanning of RNA blots also revealed that steady-state mRNA levels for the 40-kDa

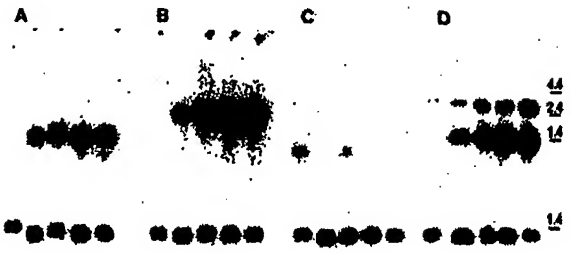

FIG. 2. RNA blots showing the coordinate induction of the 35-kDa (*A*) and 40-kDa (*B*) CLMF subunit mRNAs and IL-2 mRNA (*C*) and its p55 receptor mRNA (*D*). Poly(A)$^+$ RNA (5 μg) from NC-37.98 cells activated with 10 ng of PMA and 25 ng of calcium ionophore A23187 per ml were loaded in each lane. Lanes from left to right in each panel show RNAs isolated 6, 24, 30, 48, and 72 hr after induction, respectively. (*Upper*) Four-day exposures. (*Lower*) Two-hour exposure of the same blots after stripping and rehybridization with a GAPDH probe. Marker sizes are in kb (BRL RNA ladder).

CLMF subunit were severalfold higher than those for the 35-kDa subunit expressed by the same cells. This finding parallels the observation that activated NC-37 cells secrete excess free 40-kDa subunit protein (7). The 3′ untranslated sequences of both CLMF subunit mRNAs contain several copies of the octamer motif TTATTTAT (data not shown). This sequence is present in other transiently expressed mRNAs and is involved in regulating mRNA stability (13).

Coexpression of the 40-kDa and 35-kDa CLMF subunit cDNAs in COS cells was required to generate secreted biologically active CLMF (Table 1 and Fig. 3). COS cells transfected with cDNA encoding either the 40-kDa subunit alone or the 35-kDa subunit alone did not secrete biologically active CLMF (Table 1). Mixing media conditioned by COS cells that had been separately transfected with one or the other of the two CLMF subunit cDNAs also did not give rise to bioactive CLMF (Table 1).

Two types of assays were used to compare rCLMF and nCLMF. The first assay measures the proliferation of phytohemagglutinin (PHA)-activated human peripheral blood lymphocytes, whereas the second assay evaluates the synergy between CLMF and suboptimal concentrations of IL-2 in the generation of LAK cells in hydrocortisone-containing cultures (7). The data in Fig. 3 show that rCLMF as expressed in COS cells and nCLMF as purified from NC-37 cells are essentially identical. Dose–response curves for rCLMF and nCLMF were superimposable in each of the two assays, and rCLMF was neutralized by a monoclonal antibody raised against nCLMF. Conditioned media from cultures of mock-transfected COS cells displayed no activity in these assays (Table 1 and data not shown).

DISCUSSION

In a previous report (7), we described the purification of a heterodimeric cytokine, CLMF, that synergized with low amounts of IL-2 to cause the generation of LAK cells in the presence of hydrocortisone and stimulated the proliferation of activated T cells independent of IL-2. In the present report, we have used the N-terminal amino acid sequence information previously obtained to clone the two subunit cDNAs of CLMF. Protein purification of NC-37 cell line-derived CLMF had shown that the protein was composed of two disulfide-bonded subunits with different N-terminal amino acid sequences (7). However, it was not clear from our previous results whether the two subunits were processed from one common gene product and whether proteolytic posttranslational processing other than signal peptide cleavage was occurring. The molecular cloning and sequencing of

Table 1. Coexpression of both CLMF subunit cDNAs is required for secretion of biologically active CLMF by COS cells

Addition	Conc., units/ml	Dilution	[^{3}H]Thymidine incorporated by PHA-activated lymphoblasts, mean cpm ± 1 SEM
Cytokine*			
None	—		11,744 ± 514
nCLMF	200		68,848 ± 878
nCLMF	40		48,827 ± 605
nCLMF	8		26,828 ± 594
nCLMF	1.6		17,941 ± 196
Culture fluid from COS cells transfected with			
A. 35-kDa CLMF subunit cDNA		1:20	11,912 ± 660
		1:100	10,876 ± 232
B. 40-kDa CLMF subunit cDNA		1:20	11,699 ± 931
		1:100	11,666 ± 469
C. 35-kDa + 40-kDa CLMF subunit cDNAs		1:20	58,615 ± 587
		1:100	38,361 ± 828
1:1 mix of culture fluids A and B		1:10†	11,544 ± 483
		1:50	10,503 ± 259
CM from mock-transfected control‡		1:20	11,503 ± 286
		1:100	10,751 ± 303

PHA-activated lymphoblasts were prepared from human peripheral blood mononuclear cells as described (7). Lymphoblast proliferation was measured in a 48-hr assay (7) in which 2×10^4 lymphoblasts were incubated in 100-μl cultures containing the indicated amounts of natural CLMF (nCLMF) or COS cell culture fluids. [^{3}H]Thymidine was added to each culture 18 hr prior to harvest. Conc., concentration.

*nCLMF is purified NC-37-derived CLMF.

†1:10 dilution of the 1:1 mixture of culture fluids A and B was equivalent to a 1:20 final dilution of each of the individual culture fluids.

‡Conditioned medium (CM) from cultures of mock transfected COS cells.

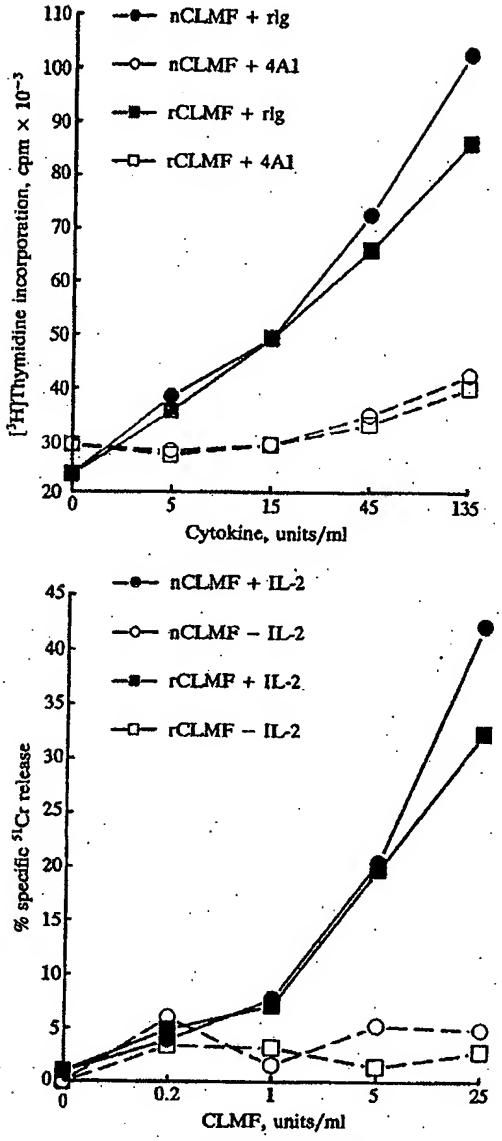

FIG. 3. Comparison of biologic activities of nCLMF (circles) and recombinant CLMF (rCLMF, squares). nCLMF was purified from NC-37 cell-conditioned media; rCLMF was purified from conditioned media from cultures of COS cells transfected with cDNAs encoding the 40-kDa and 35-kDa human CLMF subunits. (*Upper*) T-cell growth factor assay. The ability of CLMF to stimulate the proliferation of human PHA-activated lymphoblasts in 48-hr cultures was assayed as described (7). CLMF preparations were mixed with neutralizing rat monoclonal anti-human CLMF antibody 4A1 (ref. 7; open symbols) or with normal rat IgG (Sigma; rIg, closed symbols) at a final concentration of 20 μg of IgG/ml and were incubated for 30 min at 37°C prior to addition of PHA blasts. All values are means of triplicate determinations. (*Lower*) LAK cell induction assay. The ability of CLMF, alone or in combination with recombinant IL-2, to induce the generation of LAK cells in 4-day cultures was assessed as described (7). Low-density peripheral blood lymphocytes were incubated in the presence of various amounts of nCLMF or rCLMF with (closed symbols) or without (open symbols) recombinant IL-2 at 7.5 units/ml. Units of CLMF activity were based on previous titrations in the T-cell growth factor assay. Hydrocortisone sodium succinate (Sigma) was included at a concentration of 0.1 mM to minimize triggering of endogenous cytokine cascades. Lysis of ^{51}Cr-labeled Daudi cells was assessed at an effector/target ratio of 5:1. The data shown represent the means of quadruplicate determinations. The spontaneous ^{51}Cr release was 20%.

the corresponding cDNAs now has demonstrated that there is no common precursor for the two CLMF subunits; rather, they are encoded by completely different genes. The predicted and actual amino acid composition for the two subunits are strikingly similar; differences in predicted versus actual molecular weights are accounted for by glycosylation (F. Podlaski, personal communication). Thus, the only major posttranslational proteolytic event that appears to take place in the maturation of the CLMF subunits is signal peptide cleavage.

The kinetics of expression of the individual CLMF subunit mRNAs were examined and compared to the expression of mRNAs for IL-2 and the IL-2 receptor p55. Previously it had been observed that NC-37 cells, like certain murine (14) and marmoset (15) B-cell lines, secreted IL-2 when activated (M.K.G., unpublished results). RNA blots demonstrated that upon activation of NC-37 cells, both CLMF subunit mRNAs were coordinately induced with kinetics similar to the IL-2 receptor (p55) mRNAs. On the other hand, IL-2 mRNA levels peaked much earlier. Similar differences in induction kinetics were also seen at the level of IL-2 and CLMF bioactivity secreted from NC-37 cells (M.K.G., unpublished data). These kinetic differences are consistent with our previous observation that in a cytolytic lymphocyte response, IL-2 appears to act earlier than CLMF (5).

Transfection studies with COS cells established that only coexpression of both subunit cDNAs gives rise to secreted bioactive CLMF. Thus, it appears that the two proteins have to interact within the endoplasmic reticulum to assemble properly into bioactive secreted CLMF. By comparing the activity of rCLMF to that of nCLMF in the T-cell growth factor and LAK cell induction assays (Fig. 3) and assuming that the specific activity of rCLMF is similar to that of nCLMF [8×10^7 units/mg (7)], we estimate that the amount of rCLMF heterodimer produced in these experiments was 5–50 ng/ml. The finding that COS cells, which are fibroblast-like cells, are able to assemble correctly the two CLMF subunits to form bioactive CLMF indicates that this secretion and processing pattern is not limited to cells of the lymphoid lineage.

Western blot analysis using an anti-CLMF antibody specific for the 40-kDa subunit has allowed confirmation that (*i*) COS cells transfected with both CLMF subunit cDNAs secrete CLMF with the expected heterodimeric structure and (*ii*) COS cells transfected with the 40-kDa subunit cDNA alone secrete that subunit (F. Podlaski, personal communication). Since no bioactivity was detected in media conditioned by COS cells transfected with only the 40-kDa subunit, that subunit by itself appears either to have a much reduced specific activity compared with heterodimeric CLMF or to be completely inactive.

Because of the lack of a high-affinity antibody specific for the 35-kDa subunit, we have not yet been able to determine definitively whether COS cells transfected with only the 35-kDa subunit cDNA secrete that subunit. Since no bioactivity was detected in the media, secretion of a bioactive 35-kDa subunit by itself could be very inefficient; alternatively, similar to the 40-kDa subunit, the protein could be much less active or inactive altogether. Intracellular 35-kDa protein in the absence of the other subunit could be inherently unstable; there is precedence for this phenomenon, since it has been reported that 90% of the β chains of lutropin (LH), when expressed in the absence of α chains, are retained in the endoplasmic reticulum and are slowly degraded (16). Simple mixing of media conditioned by COS cells transfected separately with either one of the two CLMF subunit cDNAs did not yield bioactive CLMF. One possible explanation would be that the cells do not secrete the 35-kDa CLMF subunit by itself. More likely, our experimental conditions did not allow proper heterodimer formation. One would expect that only

carefully controlled renaturation and oxidation conditions would allow the disulfide bond formation required for generation of bioactive CLMF.

Normal human peripheral blood lymphocytes under the appropriate induction conditions produce both CLMF subunit mRNAs and secrete the active protein (N.N. and M.K.G., unpublished data). There is some evidence suggesting that CLMF is produced predominantly by B cells. In preliminary experiments, B-cell mitogens have appeared to be more effective than T-cell mitogens in eliciting CLMF production from peripheral blood lymphocytes (M.K.G., unpublished results). When screening human cell lines for their ability to produce CLMF activity (7), we observed that four of eight B-cell lines tested produced CLMF after activation with PMA and calcium ionophore, whereas none of five T-cell lines produced CLMF. Nevertheless, three of these T-cell lines secreted large amounts of IL-2 and tumor necrosis factor activity after activation (M.K.G., unpublished results). Likewise, natural killer cell stimulatory factor (NKSF), a heterodimeric cytokine similar or identical to CLMF, was isolated from RPMI 8866 lymphoblastoid B cells (17). A recent report (18) has indicated that B lymphocytes can secrete a cytokine(s) distinct from IL-2 that facilitates virus-specific cytolytic T-lymphocyte responses. It is possible that CLMF may have been the cytokine active in those studies. Thus, although B lymphocytes have not traditionally been viewed as cytokine-producing helper cells, it is conceivable that CLMF production constitutes a novel mechanism whereby B lymphocytes contribute to the amplification of T-lymphocyte responses. In addition to the biologic activities described in this report, CLMF by itself has been shown (*i*) to activate NK cells in an 18–22 hr assay, (*ii*) to facilitate the generation of specific allogeneic CTL responses, and (*iii*) to stimulate the secretion of γ interferon by resting peripheral blood lymphocytes (M.K.G., unpublished results). It can also synergize with low concentrations of recombinant IL-2 in the latter two assays and in causing the proliferation of resting peripheral blood lymphocytes. In view of its production by peripheral blood lymphocytes and its diverse actions on lymphoid cells, it appears that CLMF constitutes a new interleukin. We propose that CLMF be given the provisional designation IL-12. The availability of recombinant CLMF will now make possible a broader and more detailed characterization of its biology.

1. Rosenberg, S. A., Mule, J. J., Speiss, P. J., Reichert, C. M. & Schwartz, S. L. (1985) *J. Exp. Med.* **161**, 1169–1188.
2. Rosenberg, S. A., Lotze, M. T., Muul, L. M., Leitman, S., Chang, A. E., Ettinghausen, S. E., Matory, Y. L., Skibber, J. M., Shiloni, E., Vetto, J. T., Seipp, C. A., Simpson, C. & Reichert, C. M. (1985) *N. Engl. J. Med.* **313**, 1485–1492.
3. Iigo, M., Sakurai, S., Tamura, T., Saijo, N. & Hoshi, A. (1988) *Cancer Res.* **48**, 260–264.
4. Winklehake, J. L., Stampfl, S. & Zimmerman, R. J. (1987) *Cancer Res.* **47**, 3948–3953.
5. Gately, M. K., Wilson, D. E. & Wong, H. L. (1986) *J. Immunol.* **136**, 1274–1282.
6. Wong, H. L., Wilson, D. E., Jenson, J. C., Familletti, P. C., Stremlo, D. L. & Gately, M. K. (1988) *Cell Immunol.* **111**, 39–54.
7. Stern, A. S., Podlaski, F. J., Hulmes, J. D., Pan, Y.-C. E., Quinn, P. M., Wolitzky, A. G., Familletti, P. C., Stremlo, D. L., Truitt, T., Chizzonite, R. & Gately, M. K. (1990) *Proc. Natl. Acad. Sci. USA* **87**, 6808–6812.
8. Compton, T. (1990) in *PCR Protocols*, eds. Innis, M. A., Gelfand, D. H., Sninsky, J. J. & White, T. J. (Academic, New York), pp. 39–45.
9. Cullen, B. (1987) *Methods Enzymol.* **152**, 684–703.
10. Maniatis, T., Fritsch, E. F. & Sambrook, J. (1989) *Molecular Cloning: A Laboratory Manual* (Cold Spring Harbor Laboratory Press, Cold Spring Harbor, NY).
11. Dayhoff, M. O., Barker, W. C. & Hunt, L. T. (1983) *Methods Enzymol.* **91**, 524–545.
12. Williams, A. F. (1987) *Immunol. Today* **8**, 298–303.
13. Shaw, G. & Kamen, R. (1986) *Cell* **46**, 659–667.
14. Taira, S., Matsui, M., Hayakawa, K., Yokoyama, T. & Nariuchi, H. (1987) *J. Immunol.* **139**, 2957–2964.
15. Brent, L. H., Miyawaki, T., Everson, M. P. & Butler, J. L. (1990) *Eur. J. Immunol.* **20**, 1125–1129.
16. Corless, C. L., Matzuk, M. M., Ramabhadran, T. P., Krichevsky, A. & Boime, I. (1987) *J. Cell Biol.* **104**, 1173–1181.
17. Kobayashi, M., Fitz, L., Ryan, M., Hewick, R. M., Clark, S. C., Chan, S., Loudon, R., Sherman, F., Perussia, B. & Trinchieri, G. (1989) *J. Exp. Med.* **170**, 827–845.
18. Liu, Y. & Mullbacher, A. (1989) *Proc. Natl. Acad. Sci. USA* **86**, 4629–4633.

Exh D

Immunization With Melan-A Peptide-Pulsed Peripheral Blood Mononuclear Cells Plus Recombinant Human Interleukin-12 Induces Clinical Activity and T-Cell Responses in Advanced Melanoma

By Amy C. Peterson, Helena Harlin, and Thomas F. Gajewski

Purpose: Preclinical studies showed that immunization with peripheral blood mononuclear cells (PBMC) loaded with tumor antigen peptides plus interleukin-12 (IL-12) induced CD8+ T-cell responses and tumor rejection. We recently determined that recombinant human (rh) IL-12 at 30 to 100 ng/kg is effective as a vaccine adjuvant in patients. A phase II study of immunization with Melan-A peptide-pulsed PBMC + rhIL-12 was conducted in 20 patients with advanced melanoma.

Patients and Methods: Patients were HLA-A2–positive and had documented Melan-A expression. Immunization was performed every 3 weeks with clinical re-evaluation every three cycles. Immune responses were measured by ELISpot assay before and after treatment and through the first three cycles, and were correlated with clinical outcome.

Results: Most patients had received prior therapy and had visceral metastases. Nonetheless, two patients achieved a complete response, five patients achieved a minor or mixed response, and four patients had stable disease. The median survival was 12.25 months for all patients and was not yet reached for those with a normal lactate dehydrogenase. There were no grade 3 or 4 toxicities. Measurement of specific CD8+ T-cell responses by direct ex vivo ELISpot revealed a significant increase in interferon gamma–producing T cells against Melan-A ($P = .015$) after vaccination, but not against an Epstein-Barr virus control peptide ($P = .86$). There was a correlation between the magnitude of the increase in Melan-A–specific cells and clinical response ($P = .046$).

Conclusion: This immunization approach may be more straightforward than dendritic cell strategies and seems to have clinical activity that can be correlated to a biologic end point.

J Clin Oncol 21:2342-2348.

MOST MELANOMA tumors express antigens that can be recognized by CD8+ T cells.[1,2] Nonetheless, tumors frequently escape immune destruction, either from a failure to generate an optimal tumor antigen-specific T-cell response or from development of resistance to the T-cell response induced. One strategy to overcome the former hurdle is through active immunization, the opportunity for which has been facilitated by the molecular definition of melanoma antigens.[3] Specific CD8+ T cells that are properly activated can home to tumor sites and kill tumor cells, to the extent to which they can overcome negative immunoregulatory pathways and tumor resistance.[4]

The optimal immunization strategy for inducing tumor antigen-specific CD8+ effector T cells in humans remains undefined. However, antigen-presenting cell-based strategies have shown promise. Both monocyte-derived[5,6] and bone marrow–derived[7] dendritic cells (DCs) have been loaded with melanoma tumor antigens and administered in the advanced-disease setting, with evidence for immunization and tumor regression in subsets of patients. However, DCs are cumbersome to generate and alternative approaches that are more straightforward yet equally as effective would be useful. One cofactor produced by DCs that contributes to their efficacy is interleukin-12 (IL-12), which facilitates the induction of interferon gamma (IFN-γ)–producing cytolytic effector cells.[8-10] Endogenous IL-12 seems necessary for optimal rejection of immunogenic murine tumors[11,12] and provision of exogenous IL-12, either alone[13] or combined with tumor antigen-based vaccines,[14-19] can induce rejection of pre-established tumors in murine models. We previously have shown that coadministration of IL-12 with peripheral blood mononuclear cells (PBMCs) loaded with tumor antigen peptides induced specific cytolytic T-lymphocyte responses and tumor protection in mice, circumventing the need to generate dendritic cells.[20] The ease by which PBMC can be isolated from patients has made this an attractive approach for clinical translation. We recently conducted a phase I clinical study to determine the dose of recombinant human (rh) IL-12 necessary to induce T-cell responses in combination with antigen-loaded PBMCs, and found that doses from 30 to 100 ng/kg administered subcutaneously (sc) at the vaccine site were optimal and well tolerated.[21] The effective range of doses indicated that a straight dose of 4 μg might be used.

In this article, we describe results of a phase II clinical study of immunization with Melan-A/MART-1[3] peptide-pulsed autologous PBMCs + rhIL-12 in HLA-A2–positive patients with

From the University of Chicago, Departments of Pathology and Medicine, Section of Hematology/Oncology, and the Ben May Institute for Cancer Research, Chicago, IL.

Submitted December 26, 2002; accepted March 26, 2003.

Supported by the Burroughs Wellcome Fund, Research Triangle Park, NC, and the Cancer Research Institute, New York, NY.

A.P. and H.H. contributed equally to this work.

Address reprint requests to Thomas F. Gajewski, MD, PhD, University of Chicago, 5841 S. Maryland Ave., MC2115, Chicago, IL 60637; email: tgajewsk@medicine.bsd.uchicago.edu.

0732-183X/03/2112-2342/$20.00

advanced melanoma. Immune responses were analyzed using a direct ex vivo ELISpot assay. We show that this vaccine approach had clinical activity and that the magnitude of increased T-cell response correlated with clinical outcome.

PATIENTS AND METHODS

Patient Enrollment and Eligibility

This was an open-label, nonrandomized, single-institution study of Melan-A peptide-pulsed autologous PBMCs + rhIL-12.[4] The protocol was approved by the University of Chicago Institutional Review Board and all patients signed written informed consent. Patients who were both HLA-A2–positive and showed Melan-A tumor expression by reverse transcriptase polymerase chain reaction (RT-PCR) were considered for inclusion. Additional inclusion criteria were life expectancy more than 12 weeks, Karnofsky performance status ≥70, and adequate hematopoietic, renal, and hepatic function. Delayed-type hypersensitivity (DTH) skin testing was performed against mumps, *Candida*, and *Trichophytin*, not for eligibility but to correlate subsequently with clinical outcome and immunization potential. Patients were excluded if they had severe cardiovascular disease or arrhythmia, were pregnant or nursing, had biologic therapy received within 4 weeks, tested positive for hepatitis B surface antigen or human immunodeficiency virus (HIV), had clinically significant autoimmune disease or any illness requiring immunosuppressive therapy, had a psychiatric illness that would interfere with patient compliance and informed consent, had active gastrointestinal bleeding or uncontrolled peptic ulcer disease, or had uncontrolled brain metastases. Patients with treated brain metastases who were clinically and radiographically stable and did not require corticosteroids were allowed to enter onto the trial.

Patient Characteristics

Twenty patients with metastatic melanoma were enrolled after giving written informed consent. Patient characteristics are outlined in Table 1. All patients had advanced disease; the majority had at least three sites of metastasis, 60% of which were visceral (ie, noncutaneous and nonpulmonary metastases). Approximately two thirds of the patients had received prior therapy, and 10 patients had an elevated lactate dehydrogenase (LDH) level, which is an important negative prognostic factor.[22] Only 45% were positive for at least one recall antigen (mumps, *Candida*, or *Trichophytin*) by DTH skin testing.

Table 1. Patient Characteristics

Patient Characteristic	Patients (n = 20) No.	%
Age, years		
Median	58	
Range	35-79	
Sex		
Male	9	45
Female	11	55
Karnofsky performance status (ECOG)		
90%-100% (0)	10	50
70%-80% (1)	9	45
60%-70% (2)	1	5
No. of metastatic sites		
1	2	10
2	None	
≥3	18	90
Location of metastases		
Visceral	13	65
Brain (treated)	4	20
Prior therapy		
None	6	30
Chemotherapy or immunotherapy	7	35
As only prior therapy	5	25
Chemotherapy	1	5
As only prior therapy	1	5
Immunotherapy	4	20
As only prior therapy	1	5
Other*	2	10
As only prior therapy	None	
Adjuvant IFN-α	5	25
As only prior therapy	3	15
Elevated LDH	10	50
DTH recall positive	9	45

Abbreviations: ECOG, Eastern Cooperative Oncology Group; IFN-α, interferon alfa-2b; LDH, lactate dehydrogenase; DTH, delayed-type hypersensitivity.

*Experimental therapy other than a melanoma vaccine, immunomodulatory cytokine, or chemotherapy.

RT-PCR Analysis

RNA was isolated from fresh tumor cells using guanidine and cesium chloride. cDNA was synthesized and PCR was performed for Melan-A and beta-actin using the primer pairs and reaction conditions described previously.[21] Control reactions without reverse transcriptase were performed to rule out a contribution of genomic DNA. PCR products were visualized using a 1.5% ethidium bromide–stained agarose gel. No formal quantitation was performed.

Vaccine Preparation

Therapy consisted initially of three 21-day cycles. Vaccinations were given on the first day of each cycle and rhIL-12 was administered subcutaneously on days 1, 3, and 5. Approximately 100 to 150 mL of peripheral blood from patients was collected on day 1 of each cycle into heparinized 60-mL syringes using sterile technique. PBMCs were isolated over a Lymphoprep gradient (Lymphoprep; Axis-Shield PoC, Oslo, Norway), counted, washed, and resuspended in Dulbecco's phosphate-buffered saline (DPBS) at 40×10^6 cells/mL. At least 10×10^6 cells from each sample were cryopreserved to prepare $CD8^+$ and $CD8^-$ fractions for subsequent correlative immunologic studies. The Melan-A_{27-35} peptide (AAGIGILTV) was produced according to good manufacturing practice standards by Multiple Peptide Systems (San Diego, CA) and provided in lyophilized vials. Aliquots of peptide were prepared at 5 mmol/L in dimethyl sulfoxide and stored at −80°C for up to 3 months. Peptide preparations were quality controlled for HLA-A2 binding, sterility, and identity by high-performance liquid chromatography and mass spectrometry. An aliquot of peptide was diluted to 20 μmol/L in DPBS and mixed with an equal volume of patient PBMCs (final peptide concentration, 10 μmol/L; target number of PBMCs, 10^8) followed by incubation at 37°C for 1 hour in 10 mL DPBS. The cells were then irradiated (20 Gy), washed in DPBS, and resuspended in 1 mL DPBS. The suspension of peptide-loaded PBMCs was injected sc using a 1-mL syringe and a 21-gauge needle, divided evenly into two sites. Preferred sites were those near draining lymph node basins but not near a tumor mass. The actual number of PBMCs administered per vaccine ranged from 78 to 100×10^6.

rhIL-12 was provided by Genetics Institute (Cambridge, MA) as a lyophilized powder of 10 μg under vacuum. Each vial was intended for single use only and was stored as a powder in our research pharmacy at 2 to 8°C until reconstituted with sterile water for injection. Once reconstituted, rhIL-12 was loaded into 3-mL syringes and used within 4 hours. rhIL-12 (4 μg) was administered sc with a 25-gauge needle just after pulsed PBMC inoculation and immediately adjacent to one of the two immunization sites on days 1, 3, and 5. The same approximate location was used for each injection of peptide-pulsed PBMCs and rhIL-12 for each cycle.

Toxicity Assessment and Criteria for Clinical Response

Toxicities were determined using the National Cancer Institute common toxicity criteria scale version 2.0. A complete response (CR) was assigned if there was disappearance of all lesions without the appearance of any new

lesions; a partial response (PR) was defined as ≥ 50% reduction in total tumor volume; a minor response (MR) was defined as less than 50% reduction in total tumor volume; progressive disease (PD) was assigned if new lesions appeared, any tumor reappeared, or if a 25% increase in tumor area was observed; a mixed response was assigned if at least one tumor decreased in size with other or new tumors growing; stable disease (SD) was anything that did not fit the aforementioned criteria. When possible, cutaneous lesions were photographed.

$CD8^+$ T-Cell Preparation

$CD8^+$ and $CD8^-$ fractions from PBMC were isolated at the time of preparation of each vaccine and cryopreserved until analysis in batch fashion. $CD8^+$ T lymphocytes were isolated by positive selection using CD8 microbeads and magnetic columns (MACS system; Miltenyi Biotech, Auburn, CA). The unbound $CD8^-$ fraction was cryopreserved for use as antigen-presenting cells for in vitro expansion of specific $CD8^+$ T cells. Although the primary ELISpot analysis was performed directly with thawed cells, a secondary assay was carried out after in vitro expansion. For in vitro expansion, $CD8^-$ cells were thawed from each time point and pooled, pulsed with 50 μmol/L Melan-A peptide in serum-free Iscove's modified Dulbecco's medium (IMDM) with $beta_2$-microglobulin, irradiated (3,000 rad), washed, and plated at 2×10^6 cells/well in 24-well plates. $CD8^+$ T cells were thawed and cultured with the irradiated $CD8^-$ cells at 4×10^5 cells/well in IMDM medium containing 10% human AB serum. After 5 days, the cells were collected and plated with a new batch of Melan-A–pulsed irradiated $CD8^-$ cells. After an additional 5 days the cells were collected and tested.

ELISpot Assays

Briefly, 96-well membrane bottomed plates (MAHA S4510; Millipore, Bedford, MA) were coated with 15 μg/mL of antihuman IFN-γ antibody (Mabtech, Cincinnati, OH) in PBS. The plates were washed and $CD8^+$ T cells, either freshly thawed at 5×10^4 cells/well or after in vitro expansion at 5×10^3 cells/well, were plated in triplicate in IMDM medium with 10% human AB serum. T2 cells (transporter associated with antigen processing–deficient cell line, American Type Culture Collection no. CRI 1992) were pulsed for 1 hour at 37°C with 50 μmol/L peptide (either derived from HIV [ILKEPVHGV], Epstein-Barr virus [EBV; GLCTLVAML], or Melan-A [AAGIGILTV]), washed, and plated at a 5-to-1 ratio to the T cells. A replicate of $CD8^+$ T cells was stimulated with PMA (phorbol 12-myristate 13-acetate) (50 ng/mL) + ionomycin (0.5 μg/mL) as a positive control. After 24 hours, the cells were removed by washing with PBS + 0.05% Tween (wash buffer), and biotinylated antihuman IFN-γ antibody was added in PBS + 0.5% fetal calf serum. The plates were incubated for 2 to 4 hours at room temperature, washed, and streptavidin–alkaline phosphatase was added for 1 hour at room temperature. The plates were then washed, BCIP-NBT (5-bromo-4-chloro-3-indolyl phosphate/nitro-blue tetrazolium) was added, and the plates were finally washed with water and allowed to air dry. Plates were scanned with an ELISpot reader (CTL Technologies, Cleveland, OH) and the number of spots per well was enumerated after the background was set on the basis of wells that had been incubated with medium alone; spot separation was adjusted using Immunospot software (CTL Technologies). For each sample, the number of T cells producing IFN-γ in response to EBV or Melan-A peptides was determined by subtracting the number of spots seen in response to HIV peptide. The mean and SD were determined for each triplicate sample. After immunization, the time point at which peak frequencies among the first three cycles were observed was used for data analysis.

Statistical Analysis

Comparisons between pre- and post-ELISpot frequencies were performed using a paired *t* test, and comparisons of augmented ELISpot frequencies between responders and nonresponders were made using an unpaired two-sided *t* test. Correlations between various dichotomous variables and clinical outcome were made using Fisher's exact test (two-sided). Survival data were determined using the Kaplan-Meier method, with differences among subgroups assessed by the log-rank test. All analyses were performed using SPSS software (version 8.0; SPSS Inc, Chicago, IL).

Table 2. Adverse Events

Adverse Event	Grade 1	Grade 2	Grade 3
Fatigue	16	0	0
Anorexia	6	0	0
Fever	7	0	0
Rash	3	0	0
Headache	3	0	0
Nausea	2	0	0
Injection site reaction	5	0	0
Neutropenia	1	2	0
Thrombocytopenia	2	0	0
Hepatic	5	2	0
Creatinine	1	0	0

NOTE. Adverse events were determined using the National Cancer Institute common toxicity criteria scale version 2.0.

RESULTS

Immunization Treatment and Toxicities

Each 3-week cycle consisted of immunization on day 1 and sc rhIL-12 administration on days 1, 3, and 5, as described in Methods. Three cycles constituted one course of therapy and patients were evaluated for response after each course. Patients were observed as inpatients in our General Clinical Research Center for the first 24 hours of each cycle.

Adverse reactions are listed in Table 2. All but one patient completed at least three cycles of therapy. There were no grade 3 to 4 toxicities; two patients had grade 2 neutropenia and two patients had grade 2 ALT or AST elevations, which were reversible. The most common adverse reactions were fatigue and fever.

Clinical Outcome

Clinical response outcomes are listed in Table 3. Two patients had a CR, for an overall response rate of 10%. In addition, four patients (20%) had a mixed response, one patient (5%) had an MR, four patients (20%) had SD, and the remaining nine patients (45%) had PD. The sites of tumor response were diverse. The two patients who experienced a CR both had numerous metastases of 2 cm or less and a normal LDH. One patient was female, had multiple cutaneous lesions, and no prior therapy; the other patient was male, had multiple lung lesions, and had experienced prior treatment failure from chemoimmunotherapy. Neither patient experienced a recurrence with a mean follow-up time of 28 months at the time of data analysis. Of the five other patients who showed a decrease in size of at least one tumor mass, three had responses in skin, one had a response in bone, and one had a response in an adrenal lesion. Three of the four patients with SD had visceral metastases.

Table 3. Clinical Outcome

Best Response	No. of Patients	%
Complete response	2	10
Partial response	0	0
Minor response	1	5
Mixed response	4	20
Stable disease	4	20
Progressive disease	9	45

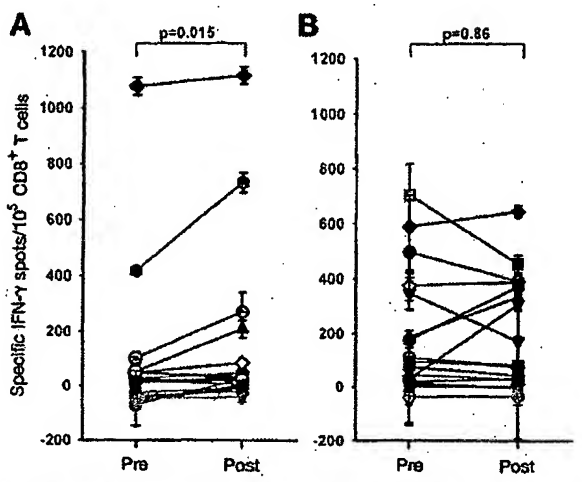

Fig 1. Interferon gamma ELISpot frequencies by $CD8^+$ T cells against Melan-A and (A) Epstein-Barr virus (EBV) (B) pre- and postimmunization. Control values with HIV peptide were subtracted out. Post- and pretreatment values were compared using a paired *t* test.

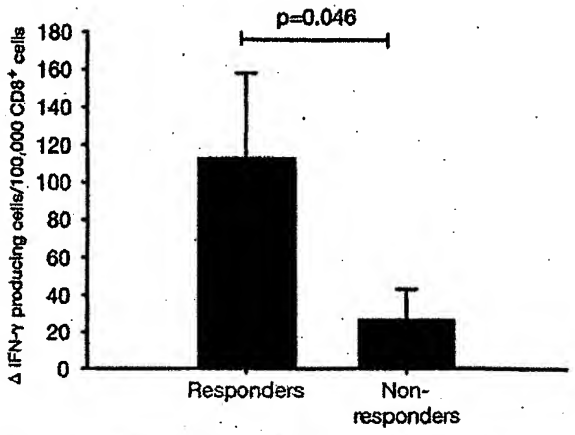

Fig 2. Comparison of increased Melan-A ELISpot frequencies after immunization between clinical responders and nonresponders. The absolute difference between Melan-A-specific ELISpot frequencies post- and pretreatment was compared between responders and nonresponders using a two-sided, unpaired *t* test.

Peptide-Specific T-Cell Responses by ELISpot

A carefully controlled IFN-γ ELISpot assay was used to monitor the immune response to immunization. Cryopreserved $CD8^+$ T cells were thawed in batch fashion and stimulated in triplicate directly ex vivo with T2 cells loaded with peptides derived from either HIV, EBV, or Melan-A. The HIV values were subtracted from those obtained with either Melan-A or EBV as an internal control at each time point. Seventeen of the enrolled patients had adequate cryopreserved material with which to perform immunologic assessments.

As shown in Fig 1, some patients displayed a high frequency of Melan-A–specific $CD8^+$ T cells before vaccination, with as high as 1% of $CD8^+$ cells responding to this peptide. These T cells were functional because they produced IFN-γ. The majority of patients showed an increase in the frequency of Melan-A–specific cells after immunization ($P = .015$). In contrast, the frequencies of specific $CD8^+$ T cells responding to the EBV peptide did not vary significantly overall ($P = .86$). Although the changes in T-cell frequency were modest, these results demonstrate an antigen-specific response after immunization with Melan-A peptide-pulsed PBMC + rhIL-12.

The changes in Melan-A–specific ELISpot frequencies were compared among patients who had a mixed response or better and those who had no clinical response. As shown in Fig 2, the mean increase in Melan-A–specific T cells for the clinical responders was 112 ± 45 and for nonresponders was 26 ± 16, indicating that a greater absolute increase in Melan-A–specific T cells was associated with tumor regression ($P = .046$).

Survival and Associations Between Immunologic Parameters and Clinical Outcome

The overall median survival was 12.25 months and is shown in Fig 3A. Seven patients remained alive at the time of data analysis, with all patients followed beyond 12 months. Because the presence of elevated levels of serum LDH is a known negative prognostic factor,[23] survival was also compared in response to this vaccine on the basis of LDH level (Fig 3B). The median survival for patients with an elevated LDH level was 9.25 months, whereas the median had not yet been reached for those with a normal LDH ($P = .005$). In addition, the median survival for patients who experienced a significant increase in Melan-A–specific T cells was not yet reached, compared with 8.5 months for patients without a significant increase in Melan-A–specific cells (Fig 3C; $P = .120$).

Additional immunologic parameters that had been measured were also analyzed for associations with either clinical response or survival and are summarized in Table 4. Neither a positive recall DTH to standard antigens nor a relatively high number of EBV- or Melan-A–specific $CD8^+$ T cells before immunization correlated with either outcome. The median pretreatment Melan-A–specific T cell frequency was 23 in clinical nonresponders and −26 in responders. To increase the sensitivity of the assay to detect Melan-A–specific T cells, an in vitro expansion was performed on the preimmunization samples and analyzed by ELISpot as described in Methods. Ten patients showed high Melan-A–specific T cell frequencies after in vitro expansion. However, this also failed to correlate with clinical outcome. Finally, although a normal LDH level was associated with survival, it did not correlate with clinical response and also did not correlate with immune response. Collectively, these results reinforce the specificity of the result showing a significant association between an increased number of Melan-A–specific T cells and clinical outcome.

Expression of Melan-A in Resected Tumors After Immunization

It was conceivable that some patients developed PD despite immunization because of outgrowth of Melan-A–negative tumor cells. Posttreatment tumor samples were obtained from progressing tumors from three patients and analyzed by RT-PCR. Although the new metastasis that developed in patient 1 was negative for

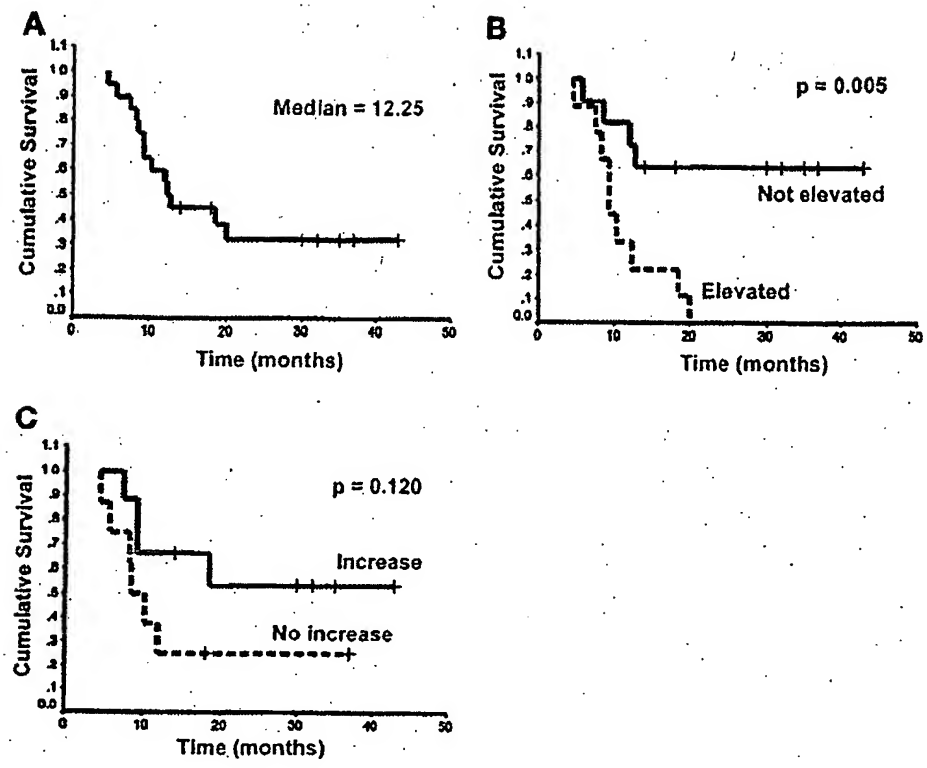

Fig 3. Overall survival for all patients (A), on the basis of serum lactate dehydrogenase greater than 200 U/L (B), and on the basis of increased Melan-A-specific interferon gamma-producing $CD8^+$ T cells (C) was determined using the Kaplan-Meier method. Differences between groups were compared using the log-rank test.

Melan-A expression, those samples from patients 4 and 6 retained detectable expression of Melan-A mRNA (Fig 1). These results indicate that, although outgrowth of antigen-negative tumors can occur, other mechanisms of resistance to immune destruction likely explain the lack of clinical response in other patients.

DISCUSSION

In this study we used Melan-A peptide-pulsed autologous PBMC + rhIL-12 as a vaccine to treat HLA-A2–positive patients with advanced melanoma. We observed a significant increase in Melan-A–specific IFN-γ–producing $CD8^+$ T cells after immunization, and found a statistical association between clinical response and the magnitude of the specific T-cell increase. Although it is difficult to compare across individual, small phase II studies, these results are similar to those that have been reported using antigen-loaded dendritic cells, but with a strategy that may be more straightforward to execute.

Preparation of the peptide-loaded PBMCs typically took 5 hours from phlebotomy to injection, and quality control of the cell product was facilitated by the lack of an extended in vitro culture period and absence of exposure to culture medium or serum proteins that is required for dendritic cell preparations. Conversely, dendritic cell vaccines have been prepared in batches and cryopreserved in individual doses in some studies, which obviates the need to prepare a fresh vaccine at each time point. Cryopreservation of vaccines has not yet been examined with our current approach. A comparative trial between PBMC/rhIL-12 and dendritic cell-based vaccination may, therefore, be of interest as the technologies continue to develop. Our results support the notion developed in preclinical models that IL-12 can contribute to effective antitumor immunity, and are consistent with the results of a recent adjuvant vaccine study using rhIL-12 in melanoma.[24]

We used a direct ex vivo ELISpot assay to assess antigen-specific T-cell responses in this study. Control experiments testing EBV reactivity from normal donors revealed that ELISpot analysis could be performed accurately on cryopreserved $CD8^+$ T cell samples immediately after thawing (H. Harlin and T. Gajewski, unpublished data). We found that background reactivity against the control HIV peptide varied among patients and to some extent among time points for an individual patient. The magnitude of increase in apparent Melan-A–reactive T cells would have been greater in some patients had the values obtained with the HIV control peptide not been subtracted. We believe that this experimental detail is critical because it normalizes the samples for background differences and provides an internal control for minor variation between individual vials of cryopreserved T cells. We also compared the Melan-A frequencies to those against an EBV control peptide, to determine whether the treatment was altering ELISpot results. We performed our analyses on purified $CD8^+$ T cells to control for variable numbers between patients and across time points. It is possible that we excluded subpopulations of $CD8^-$ T cells, $CD4^+$ T cells, and natural killer T cells that could have produced IFN-γ in response to Melan-A. Nonetheless, our results revealed a measurable and significant increase in Melan-A–specific T cells posttreatment. Our currently employed ELISpot assay is distinct from the assay used in our phase I trial of peptide-pulsed

Table 4. Statistical Correlates With Response or Survival

Parameter	Correlation With Response (P)	Correlation With Survival (P)
Positive DTH recall	.642	.130
Strong EBV pre-Rx*	.131	.491
Increased EBV post versus pre†	.290	.644
Strong Melan-A pre-Rx†	.644	.481
Increased Melan-A post versus pre†	.046	.120
Strong in vitro expansion of Melan-A§	.304	.565
LDH levels < 200	.99	.005

NOTE. Associations with response were determined using Fisher's exact test (two sided), except the differences between pre- and posttreatment, which were determined using an unpaired *t* test. Associations with survival were determined using the Kaplan-Meier method and log-rank test. Significant values are indicated in boldface.

Abbreviations: DTH, delayed-type hypersensitivity; EBV, Epstein-Barr virus; Rx, immunization; LDH, lactate dehydrogenase; HIV, human immunodeficiency virus; IL-2, interleukin-2.

*At least 90 spots per 10^5 $CD8^+$ T cells after subtraction of background against a control HIV peptide.

†Changes between post- and prevaccination samples were calculated as the difference between the absolute number of specific spots and compared using an unpaired *t* test between clinical responders and nonresponders.

‡At least 40 spots per 10^5 $CD8^+$ T cells after subtraction of background against a control HIV peptide.

§At least 90 spots per 10^5 $CD8^+$ T cells after subtraction of background against a control HIV peptide, after a 10-day in vitro expansion with Melan-A peptide-pulsed autologous $CD8^-$ cells and IL-2.

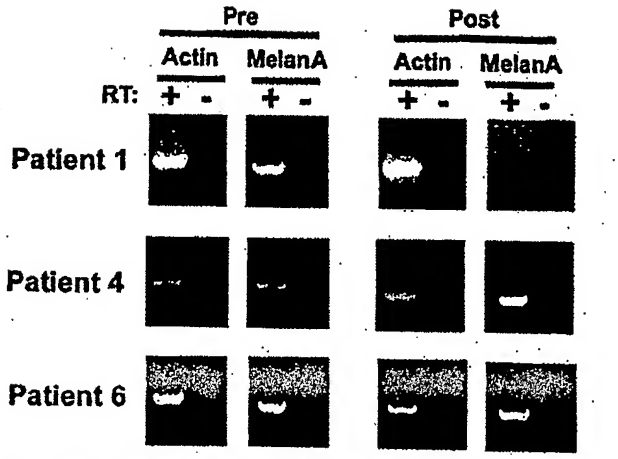

Fig 4. Melan-A expression in tumors that persisted after immunization. Three patients underwent surgical resection of lesions (after discontinuing the study), which were analyzed for Melan-A expression by qualitative reverse transcriptase polymerase chain reaction. Controls were analyzed without reverse transcriptase or with beta-actin primers.

PBMC + rhIL-12 and in other trials[21,25] in which in vitro expansion had been performed before assessment of IFN-γ production. Analysis of T-cell responses with minimal in vitro manipulation should most accurately reflect the status of those cells in vivo.

High frequencies of Melan-A–specific, IFN-γ–producing $CD8^+$ T cells were observed in some patients at study entry when they clearly had progressively growing melanoma. This observation indicates that the absolute frequency of functional T cells against a tumor antigen does not correlate with the behavior of the tumor. We also found no statistical association between this high frequency and clinical outcome; in fact, the two patients who experienced a CR had undetectable Melan-A–specific T cells before therapy. Although high frequencies of T cells reacting with a Melan-A tetramer have been detected in some normal donors,[26] those cells had a naïve surface phenotype and did not produce high levels of IFN-γ. What did correlate with clinical response in our current study is a meaningful increase in Melan-A–specific T cells posttreatment. These increases were modest (a net gain of 112 spots per 10^5 $CD8^+$ T cells on average), indicating either that a subtle alteration in the steady-state between the immune response and a growing tumor in favor of increased T-cell frequencies is sufficient to translate into tumor regression, or that another immune function that we are not measuring is contributing to the final event of tumor shrinkage. Tumor regressions without detectable increases in T-cell frequencies using standard assays have been observed in other studies.[27]

The median overall survival in our study was 12.25 months from treatment initiation, which is greater than the expected 6 to 9 months for this patient population. Although it was a relatively small study and subject to selection bias, most patients were pretreated and had visceral disease, one half of the patients had elevated serum LDH levels, and four patients had treated brain metastases. As has been seen in melanoma patients treated with standard therapies, we found that an elevated serum LDH level was a negative prognostic factor for survival. Whether this is reflective of tumor burden or the metabolic state of the tumor cells that have adapted to an anaerobic environment is unclear.

Some patients developed increases in Melan-A–specific T cells and developed progressive tumor growth despite retained expression of the antigen on posttreatment biopsies. This observation is similar to that seen in murine studies[28] and indicates mechanisms of tumor resistance downstream from initial T-cell priming, presumably within the tumor microenvironment. Potential explanations include poor T-cell trafficking to tumor sites, presence of negative regulatory cells, T-cell anergy or death, expression of inhibitory molecules by tumor cells, or downregulation of class I major histocompatibility complex or antigen-processing molecules.[29,30] Future studies should investigate definable mechanisms of tumor escape that allow tumor cells to resist elimination by antigen-specific T cells in vivo.

ACKNOWLEDGMENT

We thank Genetics Institute/Wyeth for rhIL-12, and T. Karrison, M. Sherman, S. Swiger, and M. Posner for important contributions.

REFERENCES

1. Boon T, Cerottini JC, Van den Eynde B, et al: Tumor antigens recognized by T lymphocytes. Annu Rev Immunol 12:337-365, 1994

2. Kawakami Y, Robbins PF, Wang RF, et al: Identification of tumor-regression antigens in melanoma. Important Adv Oncol 3-21, 1996

3. Coulie PG, Brichard V, Van Pel A, et al: A new gene coding for a differentiation antigen recognized by autologous cytolytic T lymphocytes on HLA-A2 melanomas. J Exp Med 180:35-42, 1994

4. Gajewski TF, Fallarino F: Rational development of tumor antigen-specific immunization in melanoma. Ther Immunol 2:211-225, 1995

5. Nestle FO, Alijagic S, Gilliet M, et al: Vaccination of melanoma patients with peptide- or tumor lysate-pulsed dendritic cells. Nat Med 4:328-332, 1998

6. Thurner B, Haendle I, Roder C, et al: Vaccination with MAGE-3A1 peptide-pulsed mature, monocyte-derived dendritic cells expands specific cytotoxic T cells and induces regression of some metastases in advanced stage IV melanoma. J Exp Med 190:1669-1678, 1999

7. Banchereau J, Palucka AK, Dhodapkar M, et al: Immune and clinical responses in patients with metastatic melanoma to CD34(+) progenitor-derived dendritic cell vaccine. Cancer Res 61:6451-6458, 2001

8. Gajewski TF, Renauld JC, Van Pel A, et al: Costimulation with B7-1, IL-6, and IL-12 is sufficient for primary generation of murine antitumor cytolytic T lymphocytes in vitro. J Immunol 154:5637-5648, 1995

9. Mehrotra PT, Wu D, Crim JA, et al: Effects of IL-12 on the generation of cytotoxic activity in human CD8+ T lymphocytes. J Immunol 151:2444-2452, 1993

10. Trinchieri G: Interleukin-12: A proinflammatory cytokine with immunoregulatory functions that bridge innate resistance and antigen-specific adaptive immunity. Annu Rev Immunol 13:251-276, 1995

11. Fallarino F, Uyttenhove C, Boon T, et al: Endogenous IL-12 is necessary for rejection of P815 tumor variants in vivo. J Immunol 156:1095-1100, 1996

12. Fallarino F, Gajewski TF: Cutting edge: Differentiation of antitumor CTL in vivo requires host expression of Stat1. J Immunol 163:4109-4113, 1999

13. Brunda MJ, Luistro L, Warrier RR, et al: Antitumor and antimetastatic activity of interleukin 12 against murine tumors. J Exp Med 178:1223-1230, 1993

14. Hallez S, Detremmerie O, Giannouli C, et al: Interleukin-12-secreting human papillomavirus type 16-transformed cells provide a potent cancer vaccine that generates E7-directed immunity. Int J Cancer 81:428-437, 1999

15. Fallarino F, Ashikari A, Boon T, et al: Antigen-specific regression of established tumors induced by active immunization with irradiated IL-12-but not B7-1-transfected tumor cells. Int Immunol 9:1259-1269, 1997

16. Vagliani M, Rodolfo M, Cavallo F, et al: Interleukin 12 potentiates the curative effect of a vaccine based on interleukin 2-transduced tumor cells. Cancer Res 56:467-470, 1996

17. Cavallo F, Signorelli P, Giovarelli M, et al: Antitumor efficacy of adenocarcinoma cells engineered to produce interleukin 12 (IL-12) or other cytokines compared with exogenous IL-12. J Natl Cancer Inst 89:1049-1058, 1997

18. Rao JB, Chamberlain RS, Bronte V, et al: IL-12 is an effective adjuvant to recombinant vaccinia virus-based tumor vaccines: Enhancement by simultaneous B7-1 expression. J Immunol 156:3357-3365, 1996

19. Sumimoto H, Tani K, Nakazaki Y, et al: Superiority of interleukin-12-transduced murine lung cancer cells to GM- CSF or B7-1 (CD80) transfectants for therapeutic antitumor immunity in syngeneic immunocompetent mice. Cancer Gene Ther 5:29-37, 1998

20. Fallarino F, Uyttenhove C, Boon T, et al: Improved efficacy of dendritic cell vaccines and successful immunization with tumor antigen peptide-pulsed peripheral blood mononuclear cells by coadministration of recombinant murine interleukin-12. Int J Cancer 80:324-333, 1999

21. Gajewski TF, Fallarino F, Ashikari A, et al: Immunization of HLA-A2+ melanoma patients with MAGE-3 or MelanA peptide-pulsed autologous peripheral blood mononuclear cells plus recombinant human interleukin 12. Clin Cancer Res 7:895s-901s, 2001

22. Balch CM, Buzaid AC, Atkins MB, et al: A new American Joint Committee on Cancer staging system for cutaneous melanoma. Cancer 88:1484-1491, 2000

23. Eton O, Legha SS, Moon TE, et al: Prognostic factors for survival of patients treated systemically for disseminated melanoma. J Clin Oncol 16:1103-1111, 1998

24. Lee P, Wang F, Kuniyoshi J, et al: Effects of interleukin-12 on the immune response to a multipeptide vaccine for resected metastatic melanoma. J Clin Oncol 19:3836-3847, 2001

25. Rosenberg SA, Yang JC, Schwartzentruber DJ, et al: Immunologic and therapeutic evaluation of a synthetic peptide vaccine for the treatment of patients with metastatic melanoma. Nat Med 4:321-327, 1998

26. Pittet MJ, Valmori D, Dunbar PR, et al: High frequencies of naive Melan-A/MART-1-specific CD8(+) T cells in a large proportion of human histocompatibility leukocyte antigen (HLA)-A2 individuals. J Exp Med 190:705-715, 1999

27. Marchand M, van Baren N, Weynants P, et al: Tumor regressions observed in patients with metastatic melanoma treated with an antigenic peptide encoded by gene MAGE-3 and presented by HLA-A1. Int J Cancer 80:219-230, 1999

28. Wick M, Dubey P, Koeppen H, et al: Antigenic cancer cells grow progressively in immune hosts without evidence for T cell exhaustion or systemic anergy. J Exp Med 186:229-238, 1997

29. Ferrone S, Marincola FM: Loss of HLA class I antigens by melanoma cells: Molecular mechanisms, functional significance and clinical relevance. Immunol Today 16:487-494, 1995

30. Marincola FM, Jaffee EM, Hicklin DJ, et al: Escape of human solid tumors from T-cell recognition: Molecular mechanisms and functional significance. Adv Immunol 74:181-273, 2000

Exh E

Vaccination with Mage-3A1 Peptide–pulsed Mature, Monocyte-derived Dendritic Cells Expands Specific Cytotoxic T Cells and Induces Regression of Some Metastases in Advanced Stage IV Melanoma

By Beatrice Thurner,* Ina Haendle,* Claudia Röder,* Detlef Dieckmann,* Petra Keikavoussi,‡ Helmut Jonuleit,§ Armin Bender,* Christian Maczek,* Doris Schreiner,* Peter von den Driesch,* Eva B. Bröcker,‡ Ralph M. Steinman,‖ Alexander Enk,§ Eckhart Kämpgen,‡ and Gerold Schuler*

*From the *Department of Dermatology, University of Erlangen-Nuremberg, D-91052 Erlangen, Germany; the ‡Department of Dermatology, University of Würzburg, D-97080 Würzburg, Germany; the §Department of Dermatology, University of Mainz, D-55131 Mainz, Germany; and the ‖Laboratory of Cellular Physiology and Immunology, The Rockefeller University, New York, New York 10021*

Summary

Dendritic cells (DCs) are considered to be promising adjuvants for inducing immunity to cancer. We used mature, monocyte-derived DCs to elicit resistance to malignant melanoma. The DCs were pulsed with Mage-3A1 tumor peptide and a recall antigen, tetanus toxoid or tuberculin. 11 far advanced stage IV melanoma patients, who were progressive despite standard chemotherapy, received five DC vaccinations at 14-d intervals. The first three vaccinations were administered into the skin, 3×10^6 DCs each subcutaneously and intradermally, followed by two intravenous injections of 6×10^6 and 12×10^6 DCs, respectively. Only minor (less than or equal to grade II) side effects were observed. Immunity to the recall antigen was boosted. Significant expansions of Mage-3A1–specific $CD8^+$ cytotoxic T lymphocyte (CTL) precursors were induced in 8/11 patients. Curiously, these immune responses often declined after the intravenous vaccinations. Regressions of individual metastases (skin, lymph node, lung, and liver) were evident in 6/11 patients. Resolution of skin metastases in two of the patients was accompanied by erythema and $CD8^+$ T cell infiltration, whereas nonregressing lesions lacked $CD8^+$ T cells as well as Mage-3 mRNA expression. This study proves the principle that DC "vaccines" can frequently expand tumor-specific CTLs and elicit regressions even in advanced cancer and, in addition, provides evidence for an active $CD8^+$ CTL–tumor cell interaction in situ as well as escape by lack of tumor antigen expression.

Key words: dendritic cells • vaccination • active immunotherapy • melanoma • cytotoxic T lymphocytes

It is now established that the immune system has cells, particularly $CD8^+$ CTLs, that can recognize tumor antigens and kill tumors (1, 2). Nevertheless, a major problem is that these T cells are either not induced or only weakly induced, i.e., the T cells are not evident in the systemic circulation. One possibility is that there is inadequate tumor antigen presentation by dendritic cells (DCs),[1] "nature's adjuvant" for eliciting T cell immunity (3). Another is that tumor-reactive T cells are tolerized by the tumors (1, 4). Melanoma provides a compelling setting in which to pursue a current goal of cancer immunotherapy, the generation of stronger tumor-specific T cell immunity, particularly with CTLs (4). The majority of tumor antigens identified so far are expressed by melanomas (2). Limited antimelanoma CTL responses have been detected (5), and infusions of IL-2 expanded killer cells can lead to rejection of melanoma (6).

Conventional adjuvants promote antibody rather than CTL responses. Therefore, several novel strategies are being explored to induce tumor-specific T cell immunity. DC vaccination is one of these (3). Immature DCs capture

[1] *Abbreviations used in this paper:* CNS, central nervous system; DCs, dendritic cells; DTH, delayed-type hypersensitivity; MCM, monocyte-conditioned medium; RT, reverse transcriptase; TT, tetanus toxoid.

J. Exp. Med. © The Rockefeller University Press • 0022-1007/99/12/1669/10 $5.00
Volume 190, Number 11, December 6, 1999 1669–1678
http://www.jem.org

antigens but lack full T cell–stimulatory activity (7). In the presence of appropriate stimuli, such as inflammatory cytokines, the DCs mature. DCs upregulate T cell adhesion and costimulatory molecules as well as select chemokine receptors that guide DC migration into lymphoid organs for priming of antigen-specific T cells. The use of DCs as adjuvants is supported by many animal experiments with primarily mature DCs (3, 8). These studies have shown that the injection of tumor antigen–loaded DCs reliably induces tumor-specific CTL responses, tumor resistance, and in some cases, regression of metastases (3, 8). In the few pilot trials reported so far for humans, *immature* DCs have been employed (9–11). Scattered tumor responses are reported, but evidence for the induction of tumor-specific CTLs by DC vaccination has not been shown.

We have developed a technique to generate large numbers of homogenous populations of *mature* and stable DCs from monocytes in the absence of nonhuman proteins (12, 13). We are now exploring the use of these DCs as vaccine adjuvants in humans. Here we provide the proof of the principle by demonstrating that three intracutaneous injections of Mage-3A1 peptide–pulsed mature DCs reliably enhance Mage-3A1–specific $CD8^+$ and recall $CD4^+$ T cell immunity in heavily pretreated, progressive stage IV melanoma patients with large tumor loads. Expansions of Mage-3A1–specific CTL responses have not been previously detected after Mage-3A1 peptide vaccination in less advanced melanoma patients (14), underscoring the potent adjuvant properties of DCs. As regressions of metastases also occurred upon DC-mediated immunization and were accompanied by $CD8^+$ T cell infiltration, we propose that the induced Mage-3A1–specific CTLs are active in vivo.

Materials and Methods

Patient Eligibility Criteria

Patients were eligible if they suffered from stage IV (i.e., distant metastases) cutaneous malignant melanoma (1988 American Joint Committee on Cancer/Union Internationale Contre Cancer pTNM staging system) that was not curable by resection and was progressive despite chemo(immuno)therapy. Further inclusion criteria were an expected survival ≥4 mo, Karnofsky index ≥60%, age ≥18 yr, measurable disease, HLA-A1 positivity, expression of Mage-3 gene shown by reverse transcriptase (RT)-PCR in at least one excised metastasis, and no systemic chemo-, radio-, or immunotherapy within 4 wk (6 wk in the case of nitrosurea drugs) preceding the first DC vaccination. A positive skin test to recall antigens was *not* required. Important exclusion criteria were active central nervous system (CNS) metastasis, any significant psychiatric abnormality, severely impaired organ function (hematological, renal, liver), active autoimmune disease (except vitiligo), previous splenectomy or radiation therapy to the spleen, organ allografts, evidence for another active malignant neoplasm, pregnancy, lactation, or participation (or intent to participate) in any other clinical trial. Concomitant treatment (chemo- or immunotherapy, corticosteroids, investigational drugs, paramedical substances) was prohibited. Palliative radiation or surgical therapy of selected metastases and certain medications (acetaminophen/paracetamol, nonsteroidal antiinflammatory drugs, opiates) to control symptoms were allowed.

Clinical Protocol and Study Design

The study was performed at the Departments of Dermatology in Erlangen, Würzburg, and Mainz, Germany according to standards of Good Clinical Practice for Trials on Medicinal Products in the European Community. The protocol was approved by the Protocol Review Committee of the Ludwig Institute for Cancer Research (New York, NY) and performed under supervision of its Office of Clinical Trials Management as study LUD #97-001. The protocol was also approved by the ethics committees of the involved study centers.

The study design is shown in Table II. All patients gave written informed consent before undergoing a screening evaluation to determine their eligibility. Extensive clinical and laboratory assessments were conducted at visits 1, 5, and 8 (Table II) and consisted of a complete physical examination, staging procedures, and standard laboratory values as well as special ones (pregnancy test, free testosterone in males, autoantibody profile, and antibodies to HIV-1/2, human T cell lymphotropic virus type I, hepatitis B virus, and hepatitis C virus). Patients were hospitalized and examined the day before each vaccination and were monitored for 48 h after the DC injections. Adverse events and changes in laboratory values were graded on a scale derived from the Common Toxicity Criteria of the National Cancer Institute, National Institutes of Health, Bethesda, MD.

Production of the DC Vaccine

During prestudy screening, we tested a small amount of fresh blood to verify that appropriate numbers of mature DCs could be generated from the patient's monocytes (12). Sufficient DC numbers could be successfully generated in all patients, but in some patients the test generation revealed that TNF-α had to be added to assure full maturation. To avoid repetitive blood drawings, we performed a single leukapheresis during visit 2 to generate DCs as described (13). In short, PBMCs from the leukapheresis ($\geq 10^{10}$ nucleated cells) were isolated on Lymphoprep™ (Nycomed Pharma) and divided into three fractions. The first fraction of 10^9 PBMCs was cultured on bacteriological petri dishes (Cat. #1005; Falcon Labware) coated with human Ig (100 μg/ml; Sandoglobin™; Sandoz GmbH) in complete RPMI 1640 medium (BioWhittaker) supplemented with 20 μg/ml gentamicin (Refobacin 10; Merck), 2 mM glutamine (BioWhittaker), and 1% heat-inactivated human plasma for 24 h to generate monocyte-conditioned medium (MCM) for later use as the DC maturation stimulus. The second fraction of 3×10^8 PBMCs was used for the generation of DCs for vaccination 1 and delayed-type hypersensitivity (DTH) test I. Adherent monocytes were cultured in 1,000 U/ml GM-CSF (10×10^7 U/mg; Leukomax™; Novartis) and 800 U/ml IL-4 (purity >98%; 4.1×10^7 U/mg in a bioassay using proliferation of human IL-4R$^+$ CTLL; CellGenix; expressed in *Escherichia coli* and produced under good laboratory practice conditions but verified for good-manufacturing practice [GMP] safety and purity criteria by us) for 6 d, and then MCM was added to mature the DCs. MCM was supplemented in patients 04, 06, 09, 11, and 12 with 10 ng/ml GMP-rhu TNF-α (purity >99%; 5×10^7 U/mg in a bioassay using murine L-M cells; a gift of Dr. G.R. Adolf, Boehringer Ingelheim Austria, Vienna, Austria) to assure full maturation of DCs. Mature DCs were harvested on day 7. The third fraction of PBMCs was frozen in aliquots and stored in the gas phase of liquid nitrogen to generate DCs for later vaccinations and DTH tests.

DCs for vaccinations were pulsed with the Mage-3A1 peptide (15) (EVDPIGHLY, synthesized at GMP quality by Clinalfa) as tumor antigen, and as a recall antigen and positive control, tetanus toxoid (TT) or tuberculin (if at visit 1 the DTH to TT in the

Multitest Merieux was >10 mm; both purchased from the Bacterial Vaccines Department of the Statens Serum Institute, Copenhagen, Denmark). The recall antigen was added at 10 μg/ml for the last 24 h, and the Mage-3A1 peptide was added at 10 μM directly to the cultures for the last 8 h (if immunity to recall antigens was strongly boosted, the dose of recall antigen was reduced to 1.0 or 0.1 μg/ml or was omitted for the intravenous DC injections to avoid a cytokine release syndrome). On day 7, mature DCs were harvested, resuspended in complete medium, washed, and pulsed once more with Mage-3A1 peptide (now at 30 μM) for 60 min at 37°C. DCs were finally washed and resuspended in PBS (GMP quality PBS; BioWhittaker) for injection. DCs to be used for Mage-3A1 DTH tests were pulsed with Mage-3A1 (but no recall antigen); DCs that served as negative control in the DTH tests were not pulsed at all. An aliquot of the DCs to be used for vaccinations was analyzed as described (13) to assure that functionally active and mature DCs were generated. The features of the DCs are described in Results. Release criteria were typical morphology (>95% nonadherent veiled cells) and phenotype (>95% HLA-DR^{+++}CD86^{+++}CD40^{+}CD25^{+}CD14^{-} and >65% homogenously CD83^{++}).

Immunization Schedule

A total of five vaccinations (three into the skin followed by two intravenously) with antigen-pulsed DCs were given at 14-d intervals (Table II). This design was chosen to explore the toxicity and efficacy of various routes in this trial. For vaccinations 1–3, 3×10^6 DCs were given subcutaneously at two sites (1.5×10^6 DCs in 500 μl PBS per site) and 3×10^6 intradermally at 10 sites (3×10^5 DCs in 100 μl PBS per site). The injection sites were the ventromedial regions of the upper arms and the thighs close to the regional lymph nodes and were rotated clockwise. Limbs where draining lymph nodes had been removed and/or irradiated were excluded. For intravenous vaccinations 4 and 5, a total of 6 and 12×10^6 antigen-pulsed DCs (resuspended in 25 or 50 ml PBS plus 1% autologous plasma) was administered over 5 and 10 min, respectively. Premedication with an antipyretic (500 mg acetaminophen/paracetamol p.o.) and an antihistamine (2.68 mg clemastinhydrogenfumarat i.v.) was given 30 min before intravenous DC vaccination.

Evaluation of Immune Status

Recall Antigen–specific Proliferation and Cytokine Production. PBMCs were cultured in triplicate at two dose levels (3×10^4 and 1×10^5 PBMCs/well) plus or minus TT or tuberculin (at 0.1, 1, and 10 μg/ml) and pulsed on day 5 with [^{3}H]thymidine for 12 h. In all cases, the highest cpms were obtained with the highest doses of PBMCs and antigen and are shown in Fig. 2. IL-4 and IFN-γ levels were measured in culture media by ELISA (Endogen, Inc.). In a separate plate, staphylococcal enterotoxin (SEA; Serva) was added at 0.5, 1, and 5 ng/ml, and proliferation was assessed after 3 d to provide a positive control for helper T cell viability and responsiveness.

Enzyme-linked Immunospot Assay for IFN-γ Release from Single Antigen–specific T Cells. To quantitate antigen-specific, IFN-γ–releasing, Mage-3A1–specific effector T cells, an enzyme-linked immunospot (ELISPOT) assay was used as described (16). PBMCs (10^5 and 5×10^5/well) or in some cases CD8$^+$ or CD4$^+$ T cells (isolated by MACS™ according to the manufacturer, Miltenyi Biotec) were added in triplicate to nitrocellulose-bottomed 96-well plates (MAHA S4510; Millipore Corp.) precoated with the primary anti–IFN-γ mAb (1-D1K; Mabtech) in 50 μl ELISPOT medium (RPMI 1640 and 5% heat-inactivated human serum) per well. For the detection of Mage-3A1–reactive T cells, the APCs were irradiated T2.A1 cells (provided by P. van der Bruggen, Ludwig Institute of Cancer Research, Brussels, Belgium) pulsed with MHC class I–restricted peptides (Mage-3A1 peptide and the HIV-1 p17-derived negative control peptide GSEELRSLY) added at 7.5×10^4/well (final volume 100 μl/well). After incubation for 20 h, wells were washed six times, incubated with biotinylated second mAb to IFN-γ (7-B6-1; Mabtech) for 2 h, washed, and stained with Vectastain Elite kit (Vector Labs.). For detection of TT-reactive T cells, TT was added at 10 μg/ml directly to the PBMCs (1 or 5×10^5 PBMCs/flat-bottomed 96-well plate). Assays were performed on fresh PBMCs. Spots were evaluated and counted using a special computer-assisted video imaging analysis system (Carl Zeiss Vision) as described (16).

Semiquantitative Assessment of CTL Precursors. The multiple microculture method developed by Romero et al. (17) was used to obtain a semiquantitative assessment of CTLp (precursors) specific for Mage-3A1 peptide. Aliquots of frozen PMBCs were thawed and assayed together. CD8$^+$ T cells were isolated with magnetic microbeads (MACS™ separation columns; Miltenyi Biotec) and seeded at 10^4/well in 96-well round-bottomed plates in RPMI 1640 with 10% heat-inactivated human serum. The CD8$^-$ PBMCs were pulsed with peptide Mage-3A1 or the influenza PB1 control peptide VSDGGPNLY (10 μg/ml; 30 min at room temperature), irradiated (30 Gy from a cesium source), and added as an APC population at 10^5/well together with IL-2 (10 IU/ml final) and IL-7 (10 ng/ml final) in a total volume of 200 μl/well. On day 7, 100 μl fresh medium was substituted, and peptide Mage-3A1 or PB1 (1 μg/ml final) and IL-2 (10 U/ml) was added. On day 12, each microwell was divided into three equal samples to test cytolytic activity in a standard 4-h ^{51}Cr-release assay on peptide-pulsed (10 μg/ml for 1 h at 37°C) T2A1 cells, nonpulsed T2A1 cells, and K562 target cells, respectively. All of the assays were performed with an 80-fold excess of nonlabeled K562 to block NK activity. Microwells were scored positive if lysis of T2A1 targets with peptide minus lysis without peptide was ≥12% and this specific lysis was greater than or equal to twice the lysis of T2A1 targets without peptide plus six as described (18). We aimed at testing 30 microwells of 10^4 CD8$^+$ T cells. Therefore, 1/30 positive wells equals at least one CTLp in 3×10^5 (i.e., 30 wells at 10^4 CTLp per well) CD8$^+$ T cells (corresponding to ~3×10^6 PBMCs).

DTH. DTH to Mage-3A1 peptide was assessed by intradermal injection at two sites of each 3×10^5 Mage-3A1 peptide–loaded DC in 0.1 ml PBS. Negative controls were nonpulsed autologous DCs in 0.1 ml PBS and 0.1 ml PBS. DTH to seven common recall antigens (Multitest Merieux) including TT and tuberculin was performed on visits 1, 5, and 8 (Table II).

Assessment and Analysis of Tumor Tissue

For recruitment into the study, Mage-3 gene expression in at least one metastatic deposit had to be demonstrated by RT-PCR as described (14). Accessible superficial skin metastases were removed whenever possible after the vaccinations and subjected to Mage-3 RT-PCR as well as routine histology and immunohistology (to characterize cellular infiltrates).

Statistical Analysis

For analysis of the immune response, pre- and postimmunization values were compared by paired *t* test after logarithmic transformation of the data. Significance was set at $P < 0.05$.

Results

Patient Characteristics

All 13 patients were HLA-A1$^+$, had proven Mage-3 mRNA expression in at least one excised metastasis, and suffered from advanced stage IV melanoma, i.e., distant metastases that were progressive despite chemotherapy and, in some cases, chemoimmunotherapy (Table I). We offered DCs to all patients who fulfilled the inclusion and exclusion criteria, i.e., we did not select for subsets of patients. Two patients (numbers 01 and 03) succumbed to melanoma after two and three vaccinations, respectively. 11 patients received all five planned DC vaccinations in 14-d intervals (Table II) and were thus fully evaluable.

Quality of the Vaccine

All vaccine preparations were highly enriched in mature DCs. More than 95% of the cells were large and veiled in appearance, expressed a characteristic phenotype by flow cytometry (HLA-DR^{+++}CD86^{+++}CD40$^+$CD25$^+$CD14$^-$), and acted as strong stimulators of an MLR at DC/T cell ratios of ≤1:300 (13). Most (mean 80%) expressed the CD83 mature DC marker (19). These features were stable upon removal of cytokines and culture for one to two more days (13). The DCs were pulsed with Mage-3A1 peptide as a tumor antigen and TT or tuberculin as a recall antigen. The latter were internal controls for immunization and possibly provided help for CTL responses (20).

Toxicity

No major (above grade II) toxicity or severe side effects were observed in any patient, including the two patients who were not fully evaluable. We noticed, however, local reactions (erythema, induration, pruritus) at the intracuta-

Table I. *Patients' Characteristics, Status before DC Vaccination, and Response to DC Vaccination*

Patient code	Sex-Age	Onset stage IV	Previous therapy	Metastases at study entry[δ]							Clinical Response	Survival
				regional		distant					14 days after the 5th vaccination	
				skin	LN	Skin	LN	Lung	Liver	Other		
Patients with objective tumor regression												
04	M48	1/98	PCI				1/15	m/30		CNS 2/12*	complete regression of all but 1 lung metastasis, overall progression	10 + >9
06	F61	10/97	CI			3/19		m/20	2/10		complete regression# of 1 lung + 4 s.c.& metastases, overall progression	6 + >16
07	F48	6/97	C			1/7				ovary 1/30 bone 3/70	complete regression# of 1 lung& + 2 s.c.& metastases, overall progression	13 + 12†
08	M67	11/97	PC		2/54		m/30	5/20	2/30		complete regression° of lung + liver + 4 s.c.& metastases, overall progression"	8 + 3†
09	F43	5/98	C					1/26		mediast 1/45 bone 2/n.d.	Partial regression of 1 lung metastasis, overall progression	4 + >11
12	M54	9/96	CI			2/80	m/35	3/20			partial regression of axillary LN metastases, overall progression	26 + >9
Patients without objective tumor regression												
02	F73	5/98	PCI	3/50/40			m/26	m/10	m/85	pancr 1/10	continuous progression	18 + 5†
05	F49	10/97	CI		1/10		2/15	m/10			continuous progression	5+>17
10	M62	8/98	C	3/70		1/30					continuous progression	1+ 6†
11	F72	7/98	C		1/25	2/n.d.		3/12		bone 1/n.d.	continuous progression	4+ 9†
13	M34	12/97	CI				1/25		M/25	spleen 1/n.d.	continous progression	12 + 5†

Treatment centers: three patients (04, 08, and 12) were treated in Wuerzburg, two in Mainz (patients 10 and 13), and the others in Erlangen.
Pretreatment therapy: PCI, polychemoimmuno. Preceding excisions and radiotherapies are not listed.
Metastases at study entry: the number and diameter of the largest metastases present at study entry are listed (number/diameter in millimeters). m, multiple (>3 metastases).
Survival: (since onset of stage IV and as of 5 August 1999) is listed as months since onset stage IV until study entry + number of months since study entry. †Patient deceased.
*CNS metastases were regressing at study entry after gamma knife treatment.
&Developed (in part) after study entry.
°Determined by autopsy.
"Sudden death from bleeding into CNS metastasis on visit 8.
#The regressions of lung metastases in patients 06 and 07 were documented at a staging 3 mo after visit 8.
mediast., mediastinum; pancr., pancreas.

Table II. *Study Design*

Activities	Screen	Leuka pheresis	Vacc. #1 3 Mio s.c. 3 Mio i.d.	Vacc. #2 3 Mio s.c. 3 Mio i.d.	Vacc. #3 3 Mio s.c. 3 Mio i.d.	Vacc. #4 6 Mio i.v.	Vacc. #5 12 Mio i.v.	Final Evaluation
Clinical visit	1	2	3	4	5	6	7	8
Day	-28/-14	-9	+1	+14	+28	+42	+56	+70
Vaccination			X	X	X	X	X	
Multitest Merieux	X				X			X
DTH to Mage-3 A1 peptide-loaded DC			X		X		X	
Recall-antigen proliferation		X						X
CTLp analysis		X				X		X
ELISPOT Mage-3A1		X	X	X	X	X	X	X
ELISPOT recall antigen		x	x	x	x	x	x	x

X, prespecified in the protocol as obligatory; x, optional.

neous vaccination sites that increased with the number of vaccinations. In 9/11 patients, strong DTH reactions (induration >10 mm in diameter) were noted to DCs carrying a recall antigen (Fig. 1). Elevation of body temperature (grade I and II fever) was observed in most (9/11) patients and was also related to pulsing DCs with recall antigen. The most striking example was patient 02, who progressively developed fever (up to 40°C) upon successive vaccinations but did not show a rise in body temperature when TT was omitted for the final (fifth) vaccination. We observed slight lymph node enlargement, clinically in 63% and by sonography in 83% of patients, after the intracutaneous DC injections. Interestingly, these were delayed, being inapparent during the 2 d of monitoring after vaccinations but detected when patients were investigated again the day before the next vaccination (Table II).

Immunological Responses

Boosting of Recall Antigen-specific Immunity. PBMCs that had been frozen before vaccination and 14 d after vaccination 5 were thawed and assayed together, as specified in the protocol (Table II). In most patients, a significant boost of antigen-specific immunity developed to TT (and tuberculin in patient 10) ($P < 0.004$; Fig. 2). Supernatants from the proliferative assays contained large amounts of IFN-γ (mean 1,679 pg/ml, range 846–4,325) but little IL-4 (IFN-γ/IL-4, 317:1). In five patients, we studied the kinetics of the immune response to TT by IFN-γ ELISPOT analysis. We found an increase after the intracutaneous vaccinations ($P < 0.02$) but a peculiar decrease after the intravenous vaccinations ($P < 0.008$; Fig. 3). Thus, comparing recall immunity before and after all five vaccinations (Fig. 2) as prespecified in the protocol (Table II) obviously underestimated the extent of boosting.

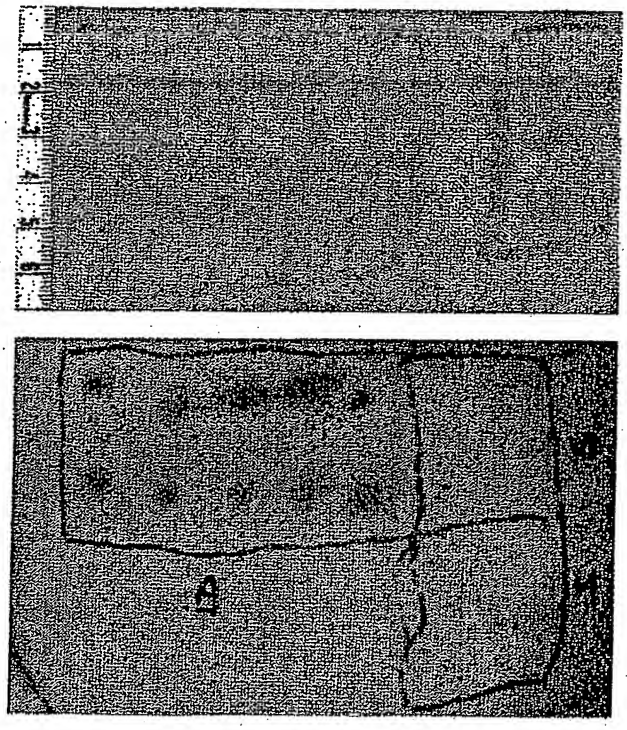

Figure 1. Local reactions to DCs carrying Mage-3A1 peptide and TT at the intradermal and subcutaneous vaccination sites in patient 09 (24 h after vaccination 2; top panel) and 02 (48 h after vaccination 3; bottom panel). Erythema at the 10 intradermal (left) and 2 subcutaneous (right) vaccination sites was followed by induration >10 mm in diameter (with secondary purpura in patient 02). These local reactions represent strong DTH reactions to DCs carrying TT, as such strong reactions did not occur in response to unpulsed DCs or DCs pulsed with Mage-3A1 peptide alone in DTH tests I–III (Table II; reactions not shown).

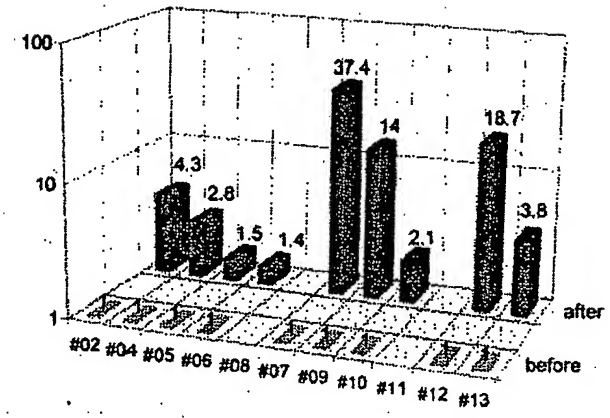

Figure 2. Recall antigen-specific immunity (tuberculin in patient 10; TT in all others) as assayed by antigen-specific proliferation. The cpm values determined after therapy (14 d after vaccination 5) are shown as multiples of pretherapy cpm values. Absolute cpm (cpm with recall antigen minus cpm without antigen) after therapy was 68,917 in patient 02, 85,225 in patient 04, 16,759 in patient 05, 7,913 in patient 06, 16,367 in patient 07, 107,923 in patient 09, 22,790 in patient 10, 4,507 in patient 12, and 1,831 in patient 13 (SEM for all measurements was <20%). Patients 08 and 11 could not be evaluated due to shortage of cells after therapy.

Expansion of Mage-3A1-specific CTLp. Aliquots of PBMCs, frozen before the first and after the third and fifth vaccinations, were thawed at the same time (Table II) and subjected to a semiquantitative recall assay for CTLp (reference 17; Fig. 4). Before vaccination, CTLp frequencies were low or undetectable. In 8/11 patients, we found a significant expansion of Mage-3A1-specific CTLp as indicated by the increase (mean, eightfold; $P < 0.008$) of positive microcultures in the multiple microculture procedure employed for the semiquantitative assessment of CTLp (17). Interestingly, in six patients, the CTLp frequencies were maximal after the three intracutaneous vaccinations ($P < 0.0013$) but then decreased after the two additional intravenous vaccinations in all but one of these patients ($P < 0.026$). Only in 1/11 patients did we observe an increase of CTLp to an irrelevant PB1 influenza peptide that served as a specificity control (not shown).

ELISPOT Analysis for IFN-γ-releasing, Mage-3A1-specific T Cells. We also tried to detect Mage-3A1-specific CTL effectors in uncultured fresh, nonfrozen PBMCs by performing ELISPOT analyses at 14-d intervals on all patients. A significant increase of Mage-3A1-reactive IFN-γ spot-forming cells was apparent only in patients 07 and 09 after the first and second vaccinations, respectively, but the frequency of Mage-3A1-specific effectors was very high (~5,000 and 10,500/10^7 $CD8^+$ T cells; not shown).

DTH Test to Mage-3A1 Peptide-loaded DCs. Tests of DTH to Mage-3A1 peptide-loaded DCs yielded erythema and/or induration (>5 mm diameter) in 7/11 patients (not shown). The results were, however, equivocal due to the frequently observed background to nonpulsed DCs (up to 10 mm in diameter) and the variability from test site to test site.

Clinical Responses

At the end of the trial, i.e., ~2 wk after the fifth vaccination (Table II), we observed temporary growth cessation of some individual metastases, but more intriguingly, in 6/11 patients, complete regression of individual metastases in skin, lymph nodes, lung, and liver (Table I and Fig. 5). Resolution of skin metastases was found in three patients (Table I, patients 06, 07, and 08) and in two of them (06 and 07), it was preceded by local pain, itching, and slight erythema. The six regressing skin lesions of patients 06 and 07 (Table I) were also excised and examined by immunohistology. Clusters of $CD8^+$ T cells were seen around and in the tumor, the latter often necrotic, suggesting an immune attack (Fig. 6).

In patients 06 and 08, the metastases excised at study entry (four and two, respectively) proved to be Mage-3 $mRNA^+$. However, all of the samples removed at the end (two and six, respectively) were Mage-3 $mRNA^-$, suggesting immunoselection for antigen-negative tumor cells. Remarkably, significant infiltration of $CD8^+$ T cells was not found in any of these lesions.

Discussion

In deciding on the source of DCs for this phase I trial, we selected *mature*, monocyte-derived DCs for the follow-

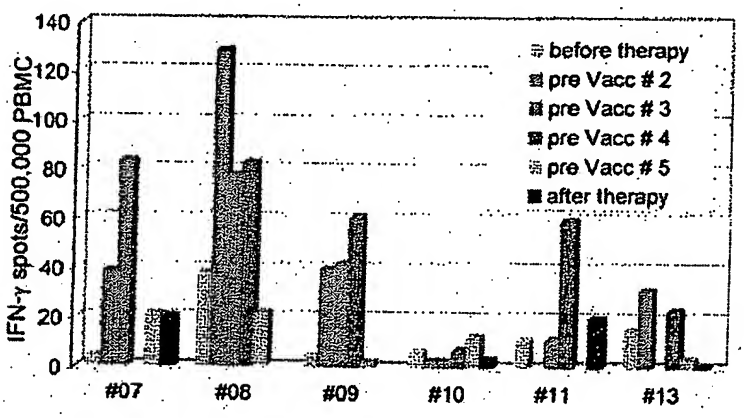

Figure 3. Kinetic analysis of immunity to recall antigens as assessed by TT-specific IFN-γ ELISPOT (SEM for all measurements was <20%). Blood was drawn (see Table II, Study Design) before the first DC vaccination and then every 14 d just before administration of the next DC vaccination (e.g., pre Vacc # 2 means immediately *before* vaccination 2, i.e., 14 d *after* vaccination 1), and finally after therapy. Time points at which vaccinations were not performed lack bars. Note the increase after the intracutaneous vaccinations and the decline upon the two vaccinations after intravenous ones. Patient 10, who received tuberculin-pulsed DCs, exhibited no significant change in the TT-specific IFN-γ ELISPOT as expected.

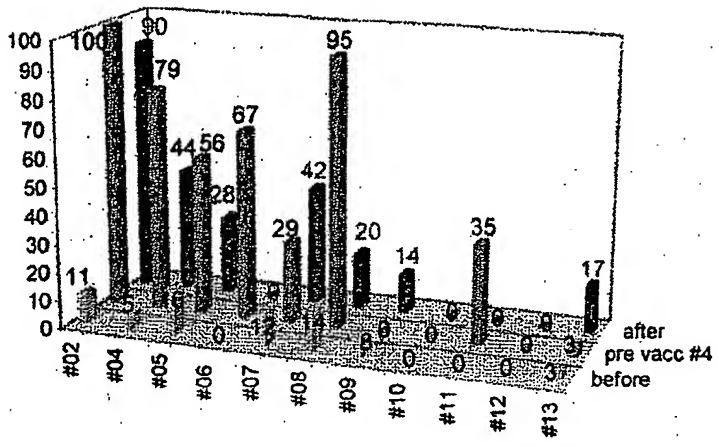

Figure 4. Mage-3A1 CTLp frequency analysis as assessed by semiquantitative recall assay. The y-axis and the numbers above the bars indicate the percentage of positive wells found before vaccination 1, before vaccination 4 (14 d after vaccination 3), and after therapy (usually 14 d after vaccination 5).

ing reasons. Monocyte-derived DCs currently represent the most homogenous and potent DC populations, with several defining criteria and quality controls (12, 13, 21). The method for generating production of these DCs is very reproducible and allows the cryopreservation of large numbers of cells at an identical stage of development (12, 13). Furthermore, these DCs can be produced in the absence of potentially hazardous FCS (12, 13, 21). FCS exposure also leads to large syngeneic T cell responses in culture, so their clinical use (11) might produce nonspecific immunostimulatory effects. Unlike other investigators (9–11), we chose to use mature rather than immature DCs for our first melanoma trial. The DCs that have been used with efficacy in animal experiments were primarily mature (3, 8). Mature DCs are much more potent in inducing CTL and Th1 responses in vitro (reference 22 and Jonuleit, H., A. Gieseke, A. Kandemir, L. Paragnik, J. Knop, and A.H. Enk, manuscript in preparation), and the DCs are also resistant to the immunosuppressive effects of IL-10 (23) that can be produced by tumors (24–26). Mature DCs also display an extended half-life of antigen-presenting MHC class I (26a) and class II molecules (27). Finally, mature DCs have a high migratory activity (21) and express CCR7 (28), a receptor for chemokines produced constitutively in lymphoid tissues (28). Mature DCs, as used in this cancer therapy trial, have recently also been shown to rapidly generate broad T cell immunity in healthy subjects (28).

Mature DCs were loaded with only one melanoma peptide, Mage-3A1, to avoid uncertainties regarding loading of DCs with multiple peptides (11) of varying affinity and off rate. Successful loading was verified with a Mage-3A1–specific CTL clone and ELISPOT analysis (not shown). The Mage-3A1 peptide (15) was selected for several reasons. It is essentially tumor specific (2) and expressed in tumors other than melanoma (2), and the Mage-3A1 epitope is likely a rejection antigen (14). Moreover, the Mage-3A1 CTLp frequency is exceedingly low in noncancer patients (reference 18; 0.4–3 per 10^7 $CD8^+$ T cells) as well as in cancer patients, even after peptide vaccination (14). Thus, any induction or boost of Mage-3A1 $CD8^+$ T cell responses would indicate a significant superiority in the adjuvant capacities of DCs.

DTH assays with peptide-pulsed DCs were carried out as described by Nestle et al. (11) to detect Mage-3A1 immunity (not shown). However, we did not detect unequivocal DTH. This was due to the frequently observed background to nonpulsed DCs (possibly due to cytokine production by DCs) and the noteworthy variability from test site to test site. As Mage-3A1–specific T cells are $CD8^+$

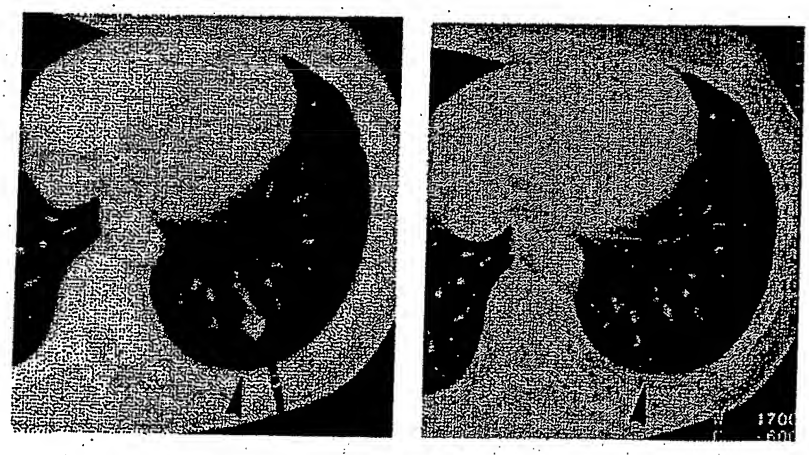

Figure 5. Regression (arrows) of a globular (13 mm in diameter) lung metastasis in patient 07 that was then no longer detectable in serial 6-mm-thick computed tomography scans.

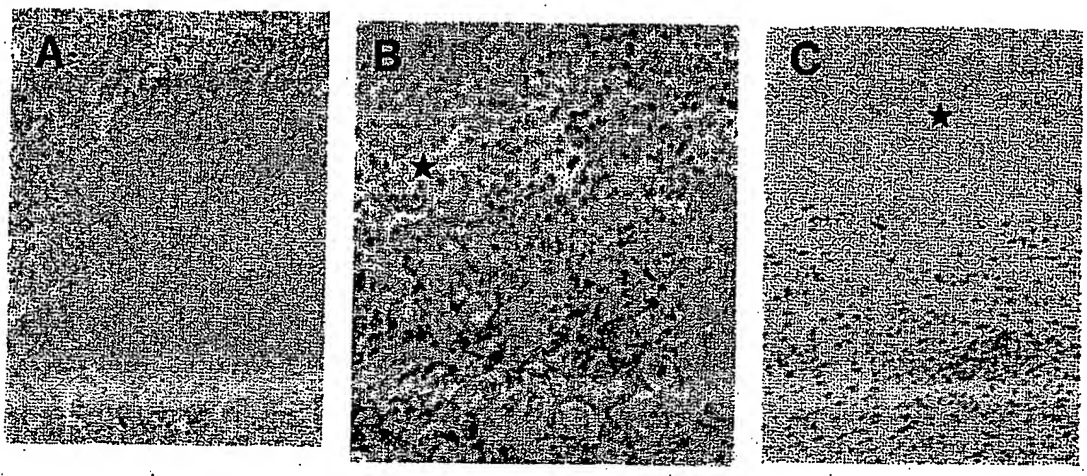

Figure 6. Regressing subcutaneous metastases in patient 06 display a $CD8^+$ lymphocytic infiltrate (alkaline phosphatase/antialkaline phosphatase immunohistochemical staining with anti-CD8 mAb) that surrounds (A) and infiltrates (B) the tumor. Areas of damaged (B, ★) and necrotic (C, ★) melanoma cells are obvious in the vicinity of the $CD8^+$ T cell infiltrate. The metastasis expressed Mage-3, as demonstrated by RT-PCR (data not shown). Magnifications: A, 100; B, 250; C, 160.

T cells and DTH assays typically detect primed $CD4^+$ T cells, we suspect that DTH to MHC class I peptide–pulsed DCs may also for this reason prove not to be a sensitive or reliable way to monitor specific $CD8^+$ T cell–mediated immunity.

In contrast, we found sizable expansions of Mage-3A1–specific CTL precursors in PBMCs from a majority (8/11) of patients ($P < 0.008$; Fig. 4). This is an important proof of the principle of DC-based immunization, and it is also significant from the point of view that tumors can induce tolerance or anergy. It is very promising that CTLp expansions can be induced in far advanced and heavily pretreated stage IV melanoma patients. However, active Mage-3A1–specific effectors were generally not observed in ELISPOT assays, except for in two patients with high frequencies (>5,000/10^7 $CD8^+$ T cells). Perhaps active $CD8^+$ effectors were rapidly sequestered in the numerous metastases, as suggested by the biopsy studies illustrated in Fig. 6. An alternative explanation is that looking for effectors in peripheral blood 14 d after a preceding vaccination might simply be too late.

Interestingly, in six patients, CTLp had increased to their highest levels after the three intracutaneous vaccinations ($P < 0.0013$) and then decreased ($P < 0.026$) with subsequent intravenous immunizations (Fig. 4). The decrease in CTLp might be due to emigration of activated Mage-3–reactive CTLs into tissues, tolerance induction, or clonal exhaustion via the intravenous route. We also observed decreased responses to recall antigens in the five patients that we studied before and after intravenous vaccination (Fig. 3). The effect of the intravenous route requires additional study, as it may be counterproductive. In contrast, our results clearly demonstrate that the intracutaneous route is effective, so that the less practical intranodal injection propagated by other investigators (11) does not seem essential. It will, however, be necessary to compare subcutaneous and intradermal routes to find out if one is superior.

We found regression of individual metastases in 6/11 patients when patients were staged 14 d after the fifth vaccination (Table I). This percentage of responses was unexpected in far advanced stage IV melanoma patients who were *all* progressive despite standard chemotherapy and even chemoimmunotherapy. In the study by Nestle et al. (11), chemotherapy was only given to 4/16 melanoma patients, and objective tumor responses were observed in 5/16. Therefore, we attribute the regressions to DC-mediated induction of Mage-3A1–specific CTLs. This interpretation is supported by the heavy infiltration with $CD8^+$ T cells of regressing but not nonregressing (skin) metastases. The observation that all of the metastases in patients 06 and 08 that were excised at the end of the study were Mage-3 $mRNA^-$ (whereas those removed at the onset were uniformly positive) suggests immune escape of and selection for Mage-3 antigen–negative tumors. Immune escape might also have been responsible for the lack of tumor response in those nonresponders that had mounted a Mage-3A1–specific CTL response.

After the end of the trial, surviving patients received further vaccinations with DCs and several tumor peptides (Mage-1, tyrosinase, and Mage-3) that were no longer part of the protocol. It is encouraging that 5/11 patients are still alive (Table I) 9–17 mo after study entry, as the expected median survival in patients progressive after chemo(immuno)therapy is only 4 mo (29, 30). One of the initial responders (patient 06) has recently experienced a complete response and has now been disease free for 2 mo. It is interesting that Marchand et al. (14) have also observed that regressions, once they have started, proceed slowly and may take months to complete.

In conclusion, the use of a defined DC vaccine combined with detailed immunomonitoring provides proof that vaccination with mature DCs expands tumor-specific T cells in advanced melanoma patients. In addition, we have found some evidence for the direct interaction between

$CD8^+$ CTLs and tumor cells as well as for escape of antigen-negative metastases. We are convinced that DC-mediated immunization can be intensified further to reveal the presence of expanded populations of effector cells. Efficacy might be increased at the level of the DC, e.g., by optimizing variables such as DC maturational state, route, dose, and schedule or by improving the short life span of DCs in vivo (31, 32); at the level of the T cell, e.g., by providing melanoma-specific $CD4^+$ T cell help (33, 34) or IL-2 (35); and by treating patients earlier in their disease course.

We are grateful to all patients for their confidence and cooperation. We appreciate the support of J. Knop, Head of the Department of Dermatology in Mainz. We thank our colleagues H.B.-R. Balda, H. Hintner, F.S.M. Meurer, and C.R. Neumann for referring patients and T.L. Diepgen for statistical analysis. We are particularly grateful to T. Boon and P. van der Bruggen, who helped us in many ways, and to A. Knuth and T. Woelfel for help in establishing the semiquantitative CTL and ELISPOT assays, respectively. We are obliged to the Protocol Review Committee and Office of Clinical Trials Management of the Ludwig Institute for Cancer Research, in particular H.F. Oettgen and E. Hoffman, for their suggestions on improving the protocol and for supervising the trial.

This work was supported by a grant from the Deutsche Krebshilfe (project #70-2291). B. Thurner was supported by the Training and Mobility of Researchers (TMR) programme of the European Union (EUNIDI).

Address correspondence to Gerold Schuler, Dermatologische Klinik mit Poliklinik, Hartmannstr. 14, D-91052 Erlangen, Germany. Phone: 49-9131-85-0, ext. 33661; Fax: 49-9131-85-6175; E-mail: schuler@derma.med.uni-erlangen.de

Submitted: 1 June 1999 Revised: 21 September 1999 Accepted: 24 September 1999

References

1. Schreiber, H. 1999. Tumor Immunology. *In* Fundamental Immunology. W.E. Paul, editor. Lippincott-Raven Publishers, Philadelphia. 1237–1270.
2. Van den Eynde, B.J., and P. van der Bruggen. 1997. T cell defined tumor antigens. *Curr. Opin. Immunol.* 9:684–693.
3. Schuler, G., and R.M. Steinman. 1997. Dendritic cells as adjuvants for immune-mediated resistance to tumors. *J. Exp. Med.* 8:1183–1187.
4. Pardoll, D.M. 1998. Cancer vaccines. *Nat. Med.* 4(Suppl.): 525–531.
5. Romero, P., P.R. Dunbar, D. Valmori, M. Pittet, G.S. Ogg, D. Rimoldi, J.L. Chen, D. Lienard, J.C. Cerottini, and V. Cerundolo. 1998. Ex vivo staining of metastatic lymph nodes by class I major histocompatibility complex tetramers reveals high numbers of antigen-experienced tumor-specific cytolytic T lymphocytes. *J. Exp. Med.* 188:1641–1650.
6. Rosenberg, S.A. 1998. New opportunities for the development of cancer immunotherapies. *Cancer J. Sci. Am.* 4(Suppl.):S1–4.
7. Banchereau, J., and R.M. Steinman. 1998. Dendritic cells and the control of immunity. *Nature.* 393:245–252.
8. Lotze, M.T., H. Farhood, C.W. Wilson, and W.J. Storkus. 1999. Dendritic cell therapy of cancer and HIV infection. *In* Dendritic Cells: Biology and Clinical Applications. M.T. Lotze and A. Thomson, editors. Academic Press, San Diego, CA. 459–485.
9. Hsu, F.J., C. Benike, F. Fagnoni, T.M. Liles, D. Czerwinski, B. Taidi, E.G. Engleman, and R. Levy. 1996. Vaccination of patients with B-cell lymphoma using autologous antigen-pulsed dendritic cells. *Nat. Med.* 2:52–58.
10. Murphy, G., B. Tjoa, H. Ragde, G. Kenny, and A. Boynton. 1996. Phase I clinical trial: T-cell therapy for prostate cancer using autologous dendritic cells pulsed with HLA-A0201-specific peptides from prostate-specific membrane antigen. *Prostate.* 29:371–380.
11. Nestle, F.O., S. Alijagic, M. Gilliet, Y. Sun, S. Grabbe, R. Dummer, G. Burg, and D. Schadendorf. 1998. Vaccination of melanoma patients with peptide- or tumor lysate-pulsed dendritic cells. *Nat. Med.* 4:328–332.
12. Romani, N., D. Reider, M. Heuer, S. Ebner, E. Kämpgen, B. Eibl, D. Niederwieser, and G. Schuler. 1996. Generation of mature dendritic cells from human blood. An improved method with special regard to clinical applicability. *J. Immunol. Methods.* 196:137–151.
13. Thurner, B., C. Röder, D. Dieckmann, M. Heuer, M. Kruse, A. Glaser, P. Keikavoussi, E. Kämpgen, A. Bender, and G. Schuler. 1999. Generation of large numbers of fully mature and stable dendritic cells from leukapheresis products for clinical application. *J. Immunol. Methods.* 223:1–15.
14. Marchand, M., N. van Baren, P. Weynants, V. Brichard, B. Dreno, M.H. Tessier, E. Rankin, G. Parmiani, F. Arienti, Y. Humblet, et al. 1999. Tumor regressions observed in patients with metastatic melanoma treated with an antigenic peptide encoded by gene MAGE-3 and presented by HLA-A1. *Int. J. Cancer.* 80:219–230.
15. Gaugler, B., B. Van den Eynde, P. van der Bruggen, P. Romero, J.J. Gaforio, E. De Plaen, B. Lethe, F. Brasseur, and T. Boon. 1994. Human gene MAGE-3 codes for an antigen recognized on a melanoma by autologous cytolytic T lymphocytes. *J. Exp. Med.* 179:921–930.
16. Herr, W., B. Linn, N. Leister, E. Wandel, K.H. Meyer zum Buschenfelde, and T. Wölfel. 1997. The use of computer-assisted video image analysis for the quantification of $CD8^+$ T lymphocytes producing tumor necrosis factor alpha spots in response to peptide antigens. *J. Immunol. Methods.* 203:141–152.
17. Romero, P., J.C. Cerottini, and G.A. Waanders. 1998. Novel methods to monitor antigen-specific cytotoxic T-cell responses

in cancer immunotherapy. *Mol. Med. Today.* 4:305–312.
18. Chaux, P., V. Vantomme, P. Coulie, T. Boon, and P. van der Bruggen. 1998. Estimation of the frequencies of anti-MAGE-3 cytolytic T-lymphocyte precursors in blood from individuals without cancer. *Int. J. Cancer.* 77:538–542.
19. Zhou, L.J., and T.F. Tedder. 1995. Human blood dendritic cells selectively express CD83, a member of the immunoglobulin superfamily. *J. Immunol.* 154:3821–3835.
20. Lanzavecchia, A. 1998. Immunology. Licence to kill. *Nature.* 393:413–414.
21. Jonuleit, H., U. Kuhn, G. Muller, K. Steinbrink, L. Paragnik, E. Schmitt, J. Knop, and A.H. Enk. 1997. Pro-inflammatory cytokines and prostaglandins induce maturation of potent immunostimulatory dendritic cells under fetal calf serum-free conditions. *Eur. J. Immunol.* 27:3135–3142.
22. Dhodapkar, M.V., R.M. Steinman, M. Sapp, H. Desai, C. Fossella, J. Krasovsky, S.M. Donahoe, P.R. Dunbar, V. Cerundolo, D.F. Nixon, et al. 1999. Rapid generation of broad T-cell immunity in humans after a single injection of mature dendritic cells. *J. Clin. Invest.* 104:173–180.
23. Steinbrink, K., H. Jonuleit, G. Müller, G. Schuler, J. Knop, and A.H. Enk. 1999. Interleukin-10-treated human dendritic cells induce a melanoma-antigen-specific anergy in $CD8^+$ T cells resulting in a failure to lyse tumor cells. *Blood.* 93:1634–1642.
24. Enk, A.H., H. Jonuleit, J. Saloga, and J. Knop. 1997. Dendritic cells as mediators of tumor-induced tolerance in metastatic melanoma. *Int. J. Cancer.* 73:309–316.
25. Sato, T., P. McCue, K. Masuoka, S. Salwen, E.C. Lattime, M.J. Mastrangelo, and D. Berd. 1996. Interleukin 10 production by human melanoma. *Clin. Cancer Res.* 2:1383–1390.
26. Dummer, W., J.C. Becker, A. Schwaaf, M. Leverkus, T. Moll, E.B. Bröcker. 1995. Elevated serum levels of interleukin-10 in patients with metastatic malignant melanoma. *Melanoma Res.* 5:67–68.
26a. Keikavoussi, P., C. Carstens, C. Scheicher, F. Koch, W. Fries, E.B. Brocker, N. Koch, and E. Kämpgen. 1999. Full maturation of human monocyte derived dendritic cells results in stable expression of MHC class I molecules. *Arch. Dermatol. Res.* 291:110. (Abstr.)
27. Cella, M., A. Engering, V. Pinet, J. Pieters, A. Lanzavecchia. 1997. Inflammatory stimuli induce accumulation of MHC class II complexes on dendritic cells. *Nature.* 388:782–787.
28. Dieu, M.C., B. Vanbervliet, A. Vicari, J.M. Bridon, E. Oldham, S. Ait-Yahia, F. Briere, A. Zlotnik, S. Lebecque, and C. Caux. 1998. Selective recruitment of immature and mature dendritic cells by distinct chemokines expressed in different anatomic sites. *J. Exp. Med.* 188:373–386.
29. Balch, C.M., A.N. Houghton, A.J. Sober, and S. Soong. 1998. Cutaneous Melanoma. 3rd ed. Quality Medical Publishing Corporation, St. Louis, MO. 596.
30. Kamanabrou, D., C. Straub, M. Heinsch, C. Lee, and A. Lippold. 1999. Sequential biochemotherapy of INF-α/IL-2, cisplatin (CDDP), dacarbacine (DTIC) and carmustine (BCNU). Result of a monocenter phase II study in 109 patients with advanced metastatic malignant melanoma (MMM). *Proc. Am. Soc. Clin. Oncol.* 18:2044a. (Abstr.)
31. Caux, C., C. Massacrier, B. Vanbervliet, B. Dubois, C. Van Kooten, I. Durand, and J. Banchereau. 1994. Activation of human dendritic cells through CD40 cross-linking. *J. Exp. Med.* 180:1263–1272.
32. Wong, B.R., R. Josien, S.Y. Lee, B. Sauter, H.L. Li, R.M. Steinman, and Y. Choi. 1997. TRANCE (tumor necrosis factor [TNF]-related activation-induced cytokine), a new TNF family member predominantly expressed in T cells, is a dendritic cell-specific survival factor. *J. Exp. Med.* 186:2075–2080.
33. Topalian, S.L., M.I. Gonzales, M. Parkhurst, Y.F. Li, S. Southwood, A. Sette, S.A. Rosenberg, and P.F. Robbins. 1996. Melanoma-specific $CD4^+$ T cells recognize nonmutated HLA-DR-restricted tyrosinase epitopes. *J. Exp. Med.* 183:1965–1971.
34. Chaux, P., V. Vantomme, V. Stroobant, K. Thielemans, J. Corthals, R. Luiten, A.M. Eggermont, T. Boon, and P. van der Bruggen. 1999. Identification of MAGE-3 epitopes presented by HLA-DR molecules to CD4(+) T lymphocytes. *J. Exp. Med.* 189;767–778.
35. Shimizu, K., R.C. Fields, M. Giedlin, and J.J. Mule. 1999. Systemic administration of interleukin 2 enhances the therapeutic efficacy of dendritic cell-based tumor vaccines. *Proc. Natl. Acad. Sci. USA.* 96:2268–2273.

IN THE UNITED STATES PATENT AND TRADEMARK OFFICE

Applicant:	Fong et al.	Docket No.:	P1192-2C1
Serial No.:	10/791,618	Group Art Unit:	1647
Filing Date:	March 2, 2004	Examiner:	Deberry, Regina M.
For:	*NovelPolypeptides and Nucleic Acids Encoding Bolekine*		

DECLARATION OF SHERMAN FONG, Ph.D. UNDER 37 C.F.R. § 1.132

Commissioner for Patents
P.O. Box 1450
Alexandria, VA 22313-1450

Sir:

I, Sherman Fong, Ph.D. declare and say as follows: -

1. I am an inventor of the above-identified patent application.

2. I was awarded a Ph.D. in Microbiology by the University of California at Davis, CA in 1975.

3. After postdoctoral training and holding various research positions at Scripps Clinic and Research Foundation, La Jolla, CA, I joined Genentech, Inc., South San Francisco, CA in 1987. I am currently a Senior Scientist at the Department of Immunology/Discovery Research of Genentech, Inc.

4. My scientific Curriculum Vitae is attached to and forms part of this Declaration.

5. I am familiar with the skin vascular permeability assay (Assay #64), which has been used by me and others under my supervision, to test the activities of novel polypeptides discovered in Genentech's Secreted Protein Discovery Initiative project.

6. The skin vascular permeability assay, is also known in the art as the Miles assay and was first described by Miles and Miles in 1952 when they studied vascular responses to histamine (Miles A.A., and Miles E.M., J. Physiol., 1952, 118: 228-257; see **Exhibit A**). Since then it has been reliably used for identifying proinflammatory molecules.

7. Proinflammatory molecules can directly or indirectly cause vascular permeability by causing immune cells to exit from the blood stream and move to the site of injury or infection. These proinflammatory molecules recruit cells like leukocytes which includes monocytes, macrophages,

basophils, and eosinophils. These cells secrete a range of cytokines which further recruit and activate other inflammatory cells to the site of injury or infection. How leukocytes exit the vasculature and move to their appropriate destination of injury or infection is critical and is tightly regulated. Leukocytes move from the blood vessel to injured or inflamed tissues by rolling along the endothelial cells of the blood vessel wall and then extravasate through the vessel wall and into the tissues (see **Exhibit B**). This diapedesis and extravasation step involves cell activation and a stable leukocyte-endothelial cell interaction.

8. Hence, proinflammatory molecules are useful in treating infections, as local administration of the proinflammatory polypeptide would stimulate immune cells already present at the site of infection and induce more immune cells to migrate to the site, thus removing the infection at a faster rate. Examples of proinflammatory molecules that induce neutrophils to extravasate are MIP-1 and MIP-2. Other proinflammatory may be able to activate immune cells, as shown with the CXC chemokines activation of neutrophils, and the non-CXC chemokines which are chemotactic for T lymphocytes (Baggiolini *et al.*, Adv Immunology 1994; 55:97-179 see **Exhibit C**).

Inappropriate expression of proinflammatory molecules may cause an abnormal immune cell reponse and lead tissue destruction. Examples of such abnormal immune reponses include at least the following conditions: psoriasis, inflammatory bowel disease, renal disease, arthritis, immune-mediated alopecia, stroke, encephalitis, Multiple Sclerosis, hepatitis, and others. Therefore, inhibitors of such proinflammatory molecules find use in the treatment of these conditions. Further, proinflammatory molecules with angiostatic properties are useful in the inhibition of angiogenesis during abnormal wound healing or abnormal inflammation during infection. Further, proinflammatory molecules that are also angiostatic are useful in treating tumors, by inhibiting the neovascularization that accompanies tumor growth (Strieter RM. *et al.*, J. Biol. Chem. 1995; 270: 27348-27357 see **Exhibit D**). Administration of the proinflammatory polypeptide, either alone or in combination with another angiostatic factor such as anti-VEGF, would be useful for limiting or reducing tumor growth.

9. The Skin Vascular Permeability Assay was used to identify such proinflammatory and immune related molecules. Miles and Miles described this assay initially in 1952, in their work on vascular response to histamine (Miles A.A., and Miles E.M., J. Physiol. 1952; (118) 228-257 *supra*). Miles and Miles solved the critical variables in the assay, such as performing the intradermal injection, where to inject, effects of temperature, effects of dosage, and effects of anesthetic used. Using this assay, Miles and Miles proved that histamine increased the capillary permeability in the skin, thus allowing cells to exit the vasculature. The assay was used qualitatively until other investigators quantitated it by

extracting the amount of accumulated marker dye and measuring its absorbance at 620 nm (Udaka et al., Proc Soc Exp Biol Med 1970; (133) 1384-1387 see **Exhibit E**).

10. The Skin Vascular permeability assay was used in the clinic in determining if blood coagulation factor XIII (FXIII) could be used in treating Shonlein Henoch Purpura (SHP) (Hirahara K., et al., Thrombosis Res 1993; 71(2) 139-148 see **Exhibit F**). SHP is an immunovascular disease, characterized by hemorrhagic skin lesions, gastro-intestinal bleeding and hematuria. The physiology of SHP was undetermined, but destruction of FXIII by leukocytes that migrated into the area and secreted destructive proteases was believed to play a role. This hypothesis was tested by using antibodies raised to guinea pig endothelial cells. These antibodies were specific for endothelial cells and not for fibroblasts, and when injected into the skin of a guinea pig, caused increased vascular permeability. When FXIII was mixed with this antibody and injected, the marker dye showed less spreading, indicating that FXIII was suppressing the vascular permeability and did so in a dose dependant manner. The conclusion was that FXIII was stabilizing the microvasculature, leading to less permeability, and therefore FXIII may be useful in the treatment of SHP.

11. The Skin Vascular Permeability assay has been confirmed by alternate experimental methods. Senger et al., used the Skin Vascular Permeability assay as described by Miles and determined that a secreted factor they called VPF (later determined to be VEGF), caused vascular permeability (Senger D.R., et al., Science 1983; (219) 983-985 see **Exhibit G**). In these experiments VPF was subjected to the Skin Vascular Permeability assay, the sites of injection were analyzed by light and electron microscopy and VPF caused vascular permeability without damaging endothelial cells or causing mast cell degranulation.

12. Yeo et al., confirmed the viability of the Skin Vascular Permeability assay by correlating it with disassociation enhanced lanthanide fluoroimmunoassay (DELFIA) results (Yeo K.T., Clin. Chem 1992; (38) 71-75 see **Exhibit H**). VPF (VEGF) was first measured using the Skin Vascular Permeability assay by quantifiying the amount of accumulated dye in the skin as described in Udaka et al., (supra). Anti-VPF antibodies were used to quantitate the amount of VPF in the DELFIA. This assay has increased sensitivity as the result is read by a fluorometer, instead of dye absorbance. The investigators found that the sensitivity of the DELFIA was greater than the Skin Vascular Permeability assay, but there was an excellent linear correlation (r^2= 0.94) between the two assays.

13. The Applicant's Skin Vascular Permeability assay was conducted using anesthetized Hairless guinea pigs. A sample of a purified PRO polypeptide or a conditioned media test sample was injected intradermally onto the backs of the test animals with 100 µL per injection site. It was possible to have up to about 24 injection sites per animal. One mL of Evans Blue dye (1% in physiologic buffered saline), was injected intracardially as the marker dye. Blemishes at the injection sites were then measured (mm diameter) after 1 hr, 6 hrs and 24 hrs post injection. Animals were sacrificed at the appropriate time after injection, and each skin injection site was biopsied and fixed in paraformaldehyde. The biopsies were then prepared for histopathalogic evaluation. Each site was evaluated for inflammatory cell infiltration into the skin. Sites with visible inflammatory cell inflammation were scored as positive. Polypeptides tested stimulated an immune response and induced mononuclear cell, eosinophil and PMN infiltration at the site of injection of the animal. Perivascular infiltrate at the injection site was scored as positive; no infiltrate at the site of injection is scored as negative.

An example of a positive reaction is shown in **Exhibit I**. The top row is injected with Interleukin-8 (IL-8) control and shows no increased vascular permeability. The 2nd row from the top is VEGF as a positive control. The 2 bottom rows show a positive result from a PRO polypeptide, performed in duplicate.

14. It is my opinion that the PRO polypeptide that shows activity in the Skin Vascular permeability assay has specific, substantial and credible utilities. In the experiments performed in the instant application, the results of the skin vascular permeability assay were further analyzed by histopathological examination to rule out inflammation due to endothelial cell damage or mast cell degranulation. Hence, the vascular permeability observed was not due to histamine release or endothelial cell damage. Examples of utilities include, enhancing immune cell recruitment to sites of injury or infection, or inhibitors to treat autoimmune diseases such as psoriasis etc. as discussed above. Furthermore, the angiogenic or angiostatic properties of proinflammatory molecules would also find practical utility in controlling tumorigenesis.

15. I declare further that all statements made in this Declaration of my own knowledge are true and that all statements made on information and belief are believed to be true and further, that these statements are made with the knowledge that willful statements and the like so made are punishable by fine or imprisonment, or both, under Section 1001 of Title 18 of the United States Code and that such willful false statements may jeopardize the validity of the application or any patent granted thereon.

Date: 8/27/04

By: Sherman Fong
Sherman Fong, Ph.D.

Sherman Fong, Ph.D.

Senior Scientist
Department of Immunology
Genentech Inc.
1 DNA Way.
South San Francisco, California 94080-4990

19 Basinside Way
Alameda, California 94502

Work Telephone: (650) 225-2783 FAX: (650) 225-8221
Home Telephone: (510) 522-5411

Education:

1978 - 1980 Postdoctoral Fellow in Immunology, Scripps Clinic and Research Foundation, La Jolla, California

1975 - 1978 Postdoctoral Fellow in Immunology, University of California at San Francisco, San Franciso, California

1970 - 1975 Ph.D. in Microbiology, University of California at Davis, California

1966 - 1970 B.A. in Biology/Microbiology, San Francisco State University, San Francisco, California

Professional Positions:

Currently: Senior Scientist, Department of Immunology/Discovery Research, Genentech, Inc., South San Francisco, California

8/00-8/01 Acting Director, Department of Immunology, Genentech, Inc. South San Francisco, California

10/89 Senior Scientist in the Department of Immunology/Discovery Research, Genentech, Inc. South San Francisco, California

3/89 - 10/89 Senior Scientist and Immunobiology Group Leader, Department of Pharmacological Sciences, Immunobiology Section/Medical Research and Development, Genentech, Inc., S. San Francisco, California

9/87 - 3/89 Scientist, Department of Pharmacological Sciences, Immunopharmacology Section/Medical Research and Development, Genentech, Inc., S. San Francisco, California

1/82 - 9/87 Assistant Member (eq. Assistant Professor level), Department of Basic and Clinical Research, Division of Clinical Immunology, Scripps Clinic and Research Foundation, La Jolla, California

6/80 - 12/81 Scientific Associate in the Department of Clinical Research, Division of Clinical Immunology, Scripps Clinic and Research Foundation, La Jolla, California

7/78 - 6/80 Postdoctoral training in the laboratory of Dr. J. H. Vaughan, Chairman, Department of Clinical Research, Division of Clinical Immunology, Scripps Clinic and Research Foundation, La Jolla, California

2/75 - 6/78 Postdoctoral training in the laboratory of Dr. J. W. Goodman, Department of Microbiology and Immunology, School of Medicine, University of California, San Francisco, California

7/71 - 12/74 Research Assistant and Graduate Student, Department of Medical Microbiology, School of Medicine, University of California, Davis, California, under Dr. E. Benjamini

Awards:
Recipient: National Institutes of Health Postdoctoral Fellowship Award (1975).

Recipient: Special Research Award, (New Investigator Award), National Institute of Health (1980).

Recipient: P.I., Research Grant Award, National Institute of Health (1984).

Recipient: Research Career Development Award (R01), National Institutes of Health (1985).

Recipient: P.I., Multi-Purpose Arthritis Center Resarch Grant, NIH (1985)

Recipient: P.I., Resarch Grant Award, (R01 Renewal), National Institute of Health (1987).

Scientific Associations:

Sigma Xi, University of California, Davis, California Chapter

Member, The American Association of Immunologists

Committee Service and Professional Activities:

Member of the Immunological Sciences Study Section, National Institutes of Health Research Grant Review Commitee, (1988-1992).

Advisory Committee, Scientific Review Committee for Veteran's Administration High Priority Program on Aging, 1983.

Ad Hoc member of Immunological Sciences Study Section, National Institutes of Health, 1988.

Ad Hoc Reviewer: Journal of Clinical Investigations, Journal of Immunology, Arthritis and Rheumatism, International Immunology, Molecular Cell Biology, and Gastroenterology

Biotechnology Experience

Established at Genentech in 1987-1989 within the Immunobiology Laboratory, in the Department of Pharmcological Sciences, group to study the immunogenicity of recombinant hGH (Protropin®) in hGH transgenic mice.

Served as Immunologist on the **Biochemical Subteam for Protropin® Project** team.

Served as Immunologist on the **Met-less hGH and Dnase project teams**, two FDA approved biological drugs: second generation hGH Nutropin® and Pulmozyme® (DNase).

Served immunologist in1989-1990 on the **CD4-IgG project team** carrying out in vitro immunopharmacological studies of the effects of CD4-IgG on the in vitro human immune responses to mitogens and antigens and on neutrophil responses in support of the filing of IND to FDA in 1990 for use of CD4-IgG in the prevention of HIV infection. Product was dropped.

In 1989-1991, initiated and carried research and development work on antibodies to CD11b and CD18 chains of the leukocyte β2 integrins. Provided preclinical scientific data to **Anti-CD18 project team**

supporting the advancement of humanized anti-CD18 antibody as anti-inflammatory in the acute setting. IND filed in 1996 and currently under clinical evaluation.

1993-1997, **Research Project Team leader** for small molecule α4β1 integrin antagonist project. Leader for collaborative multidisciplinary team (N=11) composed of immunologists, molecular/cell biologists, protein engineers, pathologists, medicinal chemists, pharmacologists, pharmaceutical chemists, and clinical scientists targeting immune-mediated chronic inflammatory diseases. Responsible for research project plans and execution of strategy to identify lead molecules, assessment of biological activities, preclinical evaluation in experimental animals, and identification of potential clinical targets. Responsible for identification, hiring, and working with outside scientific consultants for project. Helped established and responsible for maintaining current research collaboration with Roche-Nutley. Project transfered to Roche-Nutley.

1998-present, worked with Business Development to identify and create joint development opportunity with LeukoSite (currently Millennium) for monoclonal antibody against α4β7 intergin (LDP-02) for therapeutic treatment for inflammatory bowel disease (UC and Crohn';s disease). Currently, working as scientific advisor to the core team for phase II clinical trials for LDP-02.

Currently, **Research Project Team Biology Leader** (1996-present) for small molecule antagonists for α4β7/MAdCAM-1 targeting the treatment of human inflammatory bowel diseases and diseases of the gastrointestinal tract. Responsible for leading collaborative team (N=12) from Departments of Immunology, Pathology, Analytical Technology, Antibody Technology, and Bio-Organic Chemistry to identify and evaluate lead drug candidates for the treatment of gastrointestinal inflammatory diseases.

Served for nearly fifteen years as **Ad Hoc reveiwer** on Genentech Internal Research Review Committee, Product Development Review Committee, and Pharmacological Sciences Review Committee.

Worked as Scientific advisor with staff of the **Business Development** Office on numerous occasions at Genentech, Inc. to evaluate the science of potential in-licensing of novel technologies and products.

2000-2001 Served as Research Discovery representative on Genentech Therapeutic Area Teams (Immunology/Endocrine, Pulmonary/Respiratory Disease Task Force)

Invited Symposium Lectures:

Session Chairperson and speaker, American Aging Association 12th Annual National Meeting, San Francisco, California, 1982.

Invited Lecturer, International Symposium, Mediators of Immune Regulation and Immunotherapy, University of Western Ontario, London, Ontario, Canada, 1985.

Invited Lecturer, workshop on Human IgG Subclasses, Rheumatoid Factors, and Complement. American Association of Clinical Chemistry, San Francisco, California, 1987.

Plenary Lecturer, First International Waaler Conference on Rheumatoid Factors, Bergen, Norway, 1987.

Invited Lecturer, Course in Immunorheumatology at the Universite aux Marseilles, Marseilles, France, 1988.

Plenary Lecturer, 5th Mediterranean Congress of Rheumatology, Istanbul, Turkey, 1988.

Invited Lecturer, Second Annual meeting of the Society of Chinese Bioscientist of America, University of California, Berkeley, California, 1988.

Lecturer at the inaugural meeting of the Immunology by the Bay sponsored by The Bay Area Bioscience Center. The β2 Integrins in Acute Inflammation, July 14, 1992.

Lecturer, "Research and Development -- An Anatomy of a Biotechnology Company", University of California, Berkeley, Extension Course, given twice a year--March 9, 1995 to June 24, 1997.

Lecturer, "The Drug Development Process – Biologic Research - Genomics", University of California, Berkeley Extension, April 21, 1999, October, 1999, April 2000, October, 2000.

Lecturer, "The Drug Development Process – Future Trends/Impact of Pharmacogenomics", University of California Berkeley Extension, April 2001, October 2001, April 2002.

Invited Speaker, "Targeting of Lymphocyte Integrin α4β7 Attentuates Inflammatory Bowel Diseases", in Sympoium on "Nutrient effects on Gene Expression" at the Institute of Food Technology Symposium, June, 2002.

Patents:

Dennis A. Carson, Sherman Fong, Pojen P. Chen.
U.S. Patent Number 5,068,177: Anti-idiotype Antibodies induced by Synthetic Polypeptides, Nov. 26, 1991

Sherman Fong, Caroline A. Hebert, Kyung Jin Kim and Steven R. Leong.
U.S. Patent Number 5,677,426: Anti-IL-8 Antibody Fragments, Oct. 14, 1997

Claire M. Doerschuk, Sherman Fong, Caroline A. Hebert, Kyung Jin Kim, Steven R. Leong. U.S. Patent Number 5,686,070: Methods for Treating Bacterial Pneumonia, Nov. 11, 1997

Claire M. Doerschuk, Sherman Fong, Caroline A. Hebert, Kyung Jin Kim, Steven R. Leong. U.S. Patent 5,702,946: Anti-IL-8 Monoclonal Antibodies for the Treatment of Inflammatory Disorders, Dec. 30, 1997

Sherman Fong, Caroline A. Hebert, Kyung Jin Kim, Steven R. Leong.
U.S. Patent Number 5,707,622: Methods for Treating Ulcerative Colits, Jan. 13, 1998

Sherman Fong, Napoleone Ferrara, Audrey Goddard, Paul Godowski, Austin Gurney, Kenneth Hillan, and Mickey Williams. U.S. Patent Number 6,074,873: Nucleic acids encoding NL-3, June 13, 2000

Sherman Fong, Napoleone Ferrara, Audrey Goddard, Paul Godowski, Austin Gurney, Kenneth Hillan, and Mickey Williams. U.S. Patent Number 6,348,351 B1: The Receptor Tyrosine Kinase Ligand Homologues. February 19, 2002

Patent Applications:

Sherman Fong, Kenneth Hillan, Toni Klassen
U.S. Patent Application: "Diagnosis and Treatment of Hepatic Disorders"

Sherman Fong, Audrey Goddard, Austin Gurney, Daniel Tumas, William Wood
U.S. Patent Application: Compositions and Methods for the Treatment of Immune Related Diseases.

Sherman Fong, Mary Gerritsen, Audrey Goddard, Austin Gurney, Kenneth Hillan, Mickey Williams, William Wood . U.S. Patent Application: Promotion or Inhibition of Cardiovasculogenesis and Angiogenesis

Avi Ashkenazi, Sherman Fong, Audrey Goddard, Austin Gurney, Mary Napier, Daniel Tumas, William Wood. US Patent Application: Compounds, Compositions and Methods for the Treatment of Diseases Characterized by A33-Related Antigens

Chen, Filvaroff, Fong, Goddard, Godowski, Grimaldi, Gurney, Hillan, Tumas, Vandlen, Van Lookeren, Watanabe, Williams, Wood, Yansura
US Patent Application: IL-17 Homologous Polypeptides and Therapeutic Uses Thereof

Ashkenazi, Botstein, Desnoyers, Eaton, Ferrara, Filvaroff, Fong, Gao, Gerber, Gerritsen, Goddard, Godowski, Grimaldi, Gurney, Hillan, Kljavin, Mather, Pan, Paoni, Roy, Stewart, Tumas, Williams, Wood
US Patent Application: Secreted And Transmembrane Polypeptides And Nucleic Acids Encoding The Same

Publications:

1. Scibienski R, Fong S, Benjamini E: Cross tolerance between serologically non-cross reacting forms of egg white lysozyme. J Exp Med 136:1308-1312, 1972.

2. Scibienski R, Harris M, Fong S, Benjamini E: Active and inactive states of immunological unresponsiveness. J Immunol 113:45-50, 1974.

3. Fong S: Studies on the relationship between the immune response and tumor growth. Ph D Thesis, 1975.

4. Benjamini E, Theilen G, Torten M, Fong S, Crow S, Henness AM: Tumor vaccines for immunotherapy of canine lymphosarcoma. Ann NY Acad Sci 277:305, 1976.

5. Benjamini E, Fong S, Erickson C, Leung CY, Rennick D, Scibienski RJ: Immunity to lymphoid tumors induced in syngeneic mice by immunization with mitomycin C treated cells. J Immunol 118:685-693, 1977.

6. Goodman JW, Fong S, Lewis GK, Kamin R, Nitecki DE, Der Balian G: T lymphocyte activation by immunogenic determinants. Adv Exp Biol Med 98:143, 1978.

7. Goodman JW, Fong S, Lewis GK, Kamin R, Nitecki DE, Der Balian G: Antigen structure and lymphocyte activation. Immunol Rev 39:36, 1978.

8. Fong S, Nitecki DE, Cook RM, Goodman JW: Spatial requirements of haptenic and carrier determinants for T-dependent antibody responses. J Exp Med 148:817, 1978.

9. Fong S, Chen PP, Nitecki DE, Goodman JW: Macrophage-T cell interaction mediated by immunogenic and nonimmunogenic forms of a monofunctional antigen. Mol Cell Biochem 25:131, 1979.

10. Tsoukas CD, Carson DA, Fong S, Pasquali J-L, Vaughan JH: Cellular requirements for pokeweed mitogen induced autoantibody production in rheumatoid arthritis. J Immunol 125:1125-1129, 1980.

11. Pasquali J-L, Fong S, Tsoukas CD, Vaughan JH, Carson DA: Inheritance of IgM rheumatoid factor idiotypes. J Clin Invest 66:863-866, 1980.

12. Fong S, Pasquali J-L, Tsoukas CD, Vaughan JH, Carson DA: Age-related restriction of the light chain heterogeneity of anti-IgG antibodies induced by Epstein-Barr virus stimulation of human lymphocytes in vitro. Clin Immunol Immunopathol 18:344, 1981.

13. Fong S, Tsoukas CD, Frincke LA, Lawrance SK, Holbrook TL, Vaughan JH, Carson DA: Age-associated changes in Epstein-Barr virus induced human lymphocyte autoantibody responses. J Immunol 126:910-914, 1981.

14. Tsoukas CD, Fox RI, Slovin SF, Carson DA, Pellegrino M, Fong S, Pasquali J-L, Ferrone S, Kung P, Vaughan JH: T lymphocyte-mediated cytotoxicity against autologous EBV-genome-bearing B cells. J Immunol 126:1742-1746, 1981.

15. Fong S, Tsoukas CD, Pasquali J-L, Fox RI, Rose JE, Raiklen D, Carson DA, Vaughan JH: Fractionation of human lymphocyte subpopulations on immunoglobulin coated petri dishes. J Immunol Methods 44:171-182, 1981.

16. Pasquali J-L, Tsoukas CD, Fong S, Carson DA, Vaughan JH: Effect of Levamisole on pokeweed mitogen stimulation of immunoglobulin production in vitro. Immunopharmacology 3:289-298, 1981.

17. Pasquali J-L, Fong S, Tsoukas CD, Hench PK, Vaughan JH, Carson DA: Selective lymphocyte deficiency in seronegative rheumatoid arthritis. Arthritis Rheum 24:770-773, 1981.

18. Fong S, Fox RI, Rose JE, Liu J, Tsoukas CD, Carson DA, Vaughan JH: Solid- phase selection of human T lymphocyte subpopulations using monoclonal antibodies. J Immunol Methods 46:153-163, 1981.

19. Pasquali J-L, Fong S, Tsoukas CD, Slovin SF, Vaughan JH, Carson DA: Different populations of rheumatoid factor idiotypes induced by two polyclonal B cell activators, pokeweed mitogen and Epstein-Barr virus. Clin Immunol Immunopathol 21:184-189, 1981.

20. Carson DA, Pasquali J-L, Tsoukas CD, Fong S, Slovin SF, Lawrance SK, Slaughter L, Vaughan JH: Physiology and pathology of rheumatoid factors. Springer Semin Immunopathol 4:161-179, 1981.

21. Fox RI, Fong S, Sabharwal N, Carstens SA, Kung PC, Vaughan JH: Synovial fluid lymphocytes differ from peripheral blood lymphocytes in patients with rheumatoid arthritis. J Immunol 128:351-354, 1982.

22. Seybold M, Tsoukas CD, Lindstrom J, Fong S, Vaughan JH: Acetylcholine receptor antibody production during leukoplasmapheresis for Myasthenia Gravis. Arch Neurol 39:433-435, 1982.

23. Tsoukas CD, Fox RI, Carson DA, Fong S, Vaughan JH: Molecular interactions in human T-cell-mediated cytotoxicity to Epstein-Barr virus. I. Blocking of effector cell function by monoclonal antibody OKT3. Cell Immunol 69:113-121, 1982.

24. Sabharwal UK, Vaughan JH, Fong S, Bennett P, Carson DA, Curd JG: Activation of the classical pathway of complement by rheumatoid factors: Assessment by radioimmunoassay for C4. Arthritis Rheum 25:161-167, 1982.

25. Fox RI, Carstens SA, Fong S, Robinson CA, Howell F, Vaughan JH: Use of monoclonal antibodies to analyze peripheral blood and salivary gland lymphocyte subsets in Sjogren's Syndrome. Arthritis Rheum 25:419, 1982.

26. Fong S, Miller JJIII, Moore TL, Tsoukas CD, Vaughan JH, Carson DA: Frequencies of Epstein-Barr virus inducible IgM anti-IgG B lymphocytes in normal children and in children with Juvenile Rheumatoid Arthritis. Arthritis Rheum 25:959-965, 1982.

27. Goodman JW, Nitecki DE, Fong S, Kaymakcalan Z: Antigen bridging in the interaction of T helper cells and B cells. Adv Exp Med Biol 150:219-225, 1982.

28. Goodman JW, Nitecki DE, Fong S, Kaymakcalan Z: Antigen bridging in T cell-B cell interaction: Facts or fiction. In: Protein Conformation as Immunologic Signal. EMBO Workshop, Portonenere, Italy, 1982.

29. Tsoukas CD, Carson DA, Fong S, Slovin SF, Fox RI, Vaughan JH: Lysis of autologous Epstein-Barr virus infected B cells by cytotoxic T lymphocytes of rheumatoid arthritis patients. Clin Immunol Immunopathol 24:8-14, 1982.

30. Fong S, Vaughan JH, Tsoukas CD, Carson DA: Selective induction of autoantibody secretion in human bone marrow by Epstein-Barr virus. J Immunol 129:1941-1945, 1982.

31. Sabharwal UK, Fong S, Hoch S, Cook RD, Vaughan JH, Curd JG: Complement activation by antibodies to Sm in systemic lupus erythematosus. Clin Exp Immunol 51:317-324, 1983.

32. Tsoukas CD, Carson DA, Fong S, Vaughan JH: Molecular interactions in human T cell mediated cytotoxicity to EBV. II. Monoclonal antibody OKT3 inhibits a post-killer-target recognition/adhesion step. J Immunol 129:1421-1425, 1982.

33. Welch MJ, Fong S, Vaughan JH, Carson DA: Increased frequency of rheumatoid factor precursor B lymphocytes after immunization of normal adults with tetanus toxoid. Clin Exp Immunol 51:299-305, 1983.

34. Fong S, Vaughan JH, Carson DA: Two different rheumatoid-factor producing cell populations distinguished by the mouse erythrocyte receptor and responsiveness to polyclonal B cell activators. J Immunol 130:162-164, 1983.

35. Fox RI, Hueniken M, Fong S, Behar S, Royston I, Singhal SK, Thompson L: A novel cell surface antigen (T305) found in increased frequency on acute leukemia cells and in autoimmune disease states. J Immunol 131:762-767, 1983.

36. Fong S: Solid-phase panning for the fractionation of lymphoid cells. In: Cell separation: methods and selected applications. Pretlow TG, Pretlow TP (eds.) pp. 203-219. Academic Press, New York, 1983.

37. Carson DA, Fong S: A common idiotype on human rheumatoid factors identified by a hybridoma antibody. Mol Immunol 20:1081-1087, 1983.

38. Fong S, Gilbertson TA, Carson DA: The internal image of IgG in cross- reactive anti-idiotypic antibodies against human rheumatoid factors. J Immunol 131:719-724, 1983.

39. Fox RI, Adamson TC, Fong S, Young C, Howell FV: Characterization of the phenotype and function of lymphocytes infiltrating the salivary gland in patients with primary Sjogren syndrome. Diagn Immunol 1:233-239, 1983.

40. Fox RI, Adamson III TC, Fong S, Robinson CA, Morgan EL, Robb JA, Howell FV: Lymphocyte phenotype and function in pseudolymphoma associated with Sjogren's syndrome. J Clin Invest 72:52-62, 1983.

41. Fong S, Gilbertson TA, Chen PP, Vaughan JH, Carson DA: Modulation of human rheumatoid factor-specific lymphocyte responses with a cross- reactive anti-idiotype bearing the internal image of antigen. J Immunol 132:1183-1189, 1984.

42. Chen PP, Houghten RA, Fong S, Rhodes GH, Gilbertson TA, Vaughan JH, Lerner RA, Carson DA: Anti-hypervariable region antibody induced by a defined peptide. A new approach for studying the structural correlates of idiotypes. Proc Natl Acad Sci USA 81:1784-1788, 1984.

43. Fox RI, Fong S, Tsoukas CD, Vaughan JH: Characterization of recirculating lymphocytes in rheumatoid arthritis patients: Selective deficiency of natural killer cells in thoracic duct lymph. J Immunol 132:2883-2887, 1984.

44. Chen PP, Fong S, Normansell D, Houghten RA, Karras JG, Vaughan JH, Carson DA: Delineation of a cross-reactive idiotype on human autoantibodies with antibody against a synthetic peptide. J Exp Med 159:1502-1511, 1984.

45. Fong S, Carson DA, Vaughan JH: Rheumatoid factor. In: Immunology of Rheumatic Diseases. Gupta S, Talal N (eds.): Chapter 6. pp. 167-196. Plenum Publishing Corp., New York, 1985.

46. Fong S: Immunochemistry. In: Immunology as applied to Otolaryngology. Ryan AF, Poliquis JF, Harris A (eds.): pp. 23-53. College Hill Press, San Diego, 1985.

47. Fong S, Chen PP, Vaughan JH, Carson DA: Origin and age-associated changes in the expression of a physiologic autoantibody. Gerontology 31:236-250, 1985.

48. Chen PP, Fong S, Houghten RA, Carson DA: Characterization of an epibody: An anti-idiotype which reacts with both the idiotype of rheumatoid factors (RF) and the antigen recognized by RFs. J Exp Med 161:323, 1985.

49. Chen PP, Goni F, Fong S, Jirik F, Vaughan JH, Frangione B, Carson DA: The majority of human monoclonal IgM rheumatoid factors express a primary structure-dependent cross-reactive idiotype. J Immunol 134:3281-3285, 1985.

50. Lotz M, Tsoukas CD, Fong S, Carson DA, Vaughan JH: Regulation of Epstein- Barr virus infections by recombinant interferon. Selected sensitivity to interferon-gamma. Eur J Immunol 15:520-525, 1985.

51. Chen PP, Kabat EA, Wu TT, Fong S, Carson DA: Possible involvement of human D-minigenes in the first complementarity-determining region of kappa light chains. Proc Natl Acad Sci USA 82:2125-2127, 1985.

52. Goldfien RD, Chen PP, Fong S, Carson DA: Synthetic peptides corresponding to third hypervariable region of human monoclonal IgM rheumatoid factor heavy chains define an immunodominant idiotype. J Exp Med 162:756-761, 1985.

53. Fong S, Chen PP, Gilbertson TA, Fox RI, Vaughan JH, Carson DA: Structural similarities in the kappa light chains of human rheumatoid factor paraproteins and serum immunoglobulins bearing a cross-reactive idiotype. J Immunol 135:1955-1960, 1985.

54. Chen PP, Goni F, Houghten RA, Fong S, Goldfien RD, Vaughan JH, Frangione B, Carson DA: Characterization of human rheumatoid factors with seven antiidiotypes induced by synthetic hypervariable-region peptides. J Exp Med 162:487-500, 1985.

55. Fong S, Gilbertson TA, Hueniken RJ, Singhal SK, Vaughan JH, Carson DA: IgM rheumatoid factor autoantibody and immunoglobulin producing precursor cells in the bone marrow of humans. Cell Immunol 95:157-172, 1985.

56. Fong S, Chen PP, Goldfien RD, Jirik F, Silverman G, Carson DA: Recurrent idiotypes of human anti-IgG autoantibodies: their potential use for immunotherapy. In: Mediators of Immune Regulation and Immunotherapy. Singhal SK, Delovitch TL (eds.): pp. 232-243. Elsevier Science Publishing Co., New York, 1986.

57. Fox RI, Chen PP, Carson DA, Fong S: Expression of a cross reactive idiotype on rheumatoid factor in patients with Sjogren's syndrome. J Immunol 136:477-483, 1986.

58. Jirik FR, Sorge J, Fong S, Heitzmann JG, Curd JG, Chen PP, Goldfien R, Carson DA: Cloning and sequence determination of a human rheumatoid factor light-chain gene. Proc Natl Acad Sci USA, 83:2195-2199, 1986.

59. Lotz M, Tsoukas CD, Fong S, Dinarello CA, Carson DA, Vaughan JH: Release of lymphokines following Epstein-Barr virus infection in vitro. I. The sources and kinetics of production of interferons and interleukins in normal humans. J Immunol, 136:3636-3642, 1986.

60. Lotz M, Tsoukas CD, Fong S, Dinarello CA, Carson DA, Vaughan JH: Release of lymphokines following infection with Epstein-Barr virus in vitro. II. A monocyte dependent inhibitor of interleukin-1 downregulates the production of interleukin-2 and gamma interferon in rheumatoid arthritis. J Immunol, 136:3643-3648, 1986.

61. Fong S, Chen PP, Gilbertson TA, Weber JR, Fox RI, Carson DA: Expression of three cross reactive idiotypes on rheumatoid factor autoantibodies from patients with autoimmune diseases and seropositive adults. J Immunol, 137:122-128, 1986.

62. Fong S, Gilbertson TA, Chen PP, Karras JG, Vaughan JH, Carson DA: The common occurrence of internal image type anti-idiotypic antibodies in rabbits immunized with monoclonal and polyclonal human IgM rheumatoid factors. Clin Exp Immunol, 64:570-580, 1986.

63. Fox RI, Carson DA, Chen P, Fong S: Characterization of a cross reactive idiotype in Sjogren's syndrome. Scand J Rheum S61:83-88, 1986.

64. Silverman GJ, Carson DA, Solomon A, Fong S: Human kappa light chain subgroup analysis with synthetic peptide-induced antisera. J Immunol Methods 95:249-257, 1987.

65. Goldfien R, Chen P, Kipps TJ, Starkebaum G, Heitzmann JG, Radoux V, Fong S, Carson DA: Genetic analysis of human B cell hybridomas expressing a rheumatoid factor-associated cross-reactive idiotype. J Immunol 138:940- 944, 1987.

66. Carson DA, Chen PP, Fox RI, Kipps TJ, Jirik F, Goldfien RD, Silverman G, Radoux V, Fong S: Rheumatoid factors and immune networks. Annu Rev Immunol 5:109-126, 1987.

67. Kipps TJ, Fong S, Tomhave E, Chen PP, Goldfien RD, Carson DA: High frequency expression of a conserved kappa variable region gene in chronic lymphocytic leukemia. Proc Natl Acad Sci USA 84:2916-2920, 1987

68. Fong S, Chen PP, Fox RI, Goldfien RD, Silverman GJ, Radoux V, Jirik F, Vaughan JH, Carson DA: Rheumatoid factors in human autoimmune disease: Their origin, development and function. Path Immunopath Res 5:407-449, 1987.

69. Goldfien RD, Fong S, Chen P, Carson DA: Structure and function of rheumatoid factor: Implications for its role in the pathogenesis of mixed cryoglobulinemia. In: Antiglobulins, cryoglobulins and glomerulonephritis, Proceedings of 2nd International Milano Meeting of Nephrology. Ponticelli C, Minetti L, D'Amico G (eds.) Martinus Nijhoff, Dordrecht pp. 17-27, 1986.

70. Silverman GJ, Carson DA, Patrick K, Vaughan JH, Fong S: Expression of a germline human kappa chain associated cross reactive idiotype after in vitro and in vivo infection with Epstein-Barr virus. Clin Immunol Immunopathol 43:403-411, 1987.

71. Silverman GJ, Fong S, Chen PP, Carson DA: Clinical update: Cross reactive idiotype and the genetic origin of rheumatoid factors. J Clin Lab Anal, 1:129-135, 1987.

72. Chen PP, Fong S, Carson DA: Molecular basis of reactivity of epibodies. In: Elicitation and use of anti-idiotypic antibodies and their biological applications. Bona C (ed.), CRC Press, Boca Raton, Fla, in press.

73. Fong S, Chen PP, Carson DA, Fox, RI: Rheumatoid factor in Sjogren's syndrome. In: Sjogren's Syndrome: Clinical and Immunological Aspects. Talal N, Moutsopoulos HM, Kassan SS (eds.), Springer-Verlag, New York, pp. 203-217, 1987.

74. Chen PP, Fong S, Carson DA: The use of defined peptides in characterizing idiotypes. Int Rev Immunol 2:419-432, 1987.

75. Chen PP, Fong S, Goni F, Houghten RA, Frangione B, Liu F, Carson DA: Analyses of human rheumatoid factors with anti-idiotypes induced by synthetic peptides. Monogr Allergy 22:12-23, 1987.

76. Carson DA, Chen PP, Radoux V, Jirik F, Goldfien RD, Silverman GJ, Fong S: Molecular basis for the cross-reactive idiotypes on human anti-IgG autoantibodies (rheumatoid factors) In: Autoimmunity and Autoimmune Disease. Ciba Foundation Symposium 129 pp. 123-130, 1987.

77. Radoux V, Fong S, Chen PP, Carson DA: Rheumatoid factors: current concepts. In: Advances in Inflammation Research. Lewis, A. (Ed), Raven Press, New York, pp.295-304, 1987.

78. Kipps TJ, Fong S, Chen PP, Miller WE, Piro LD, Carson DA: Immunoglobulin V gene utilization in CLL. In: Chronic lymphocytic leukemia: recent progress and future direction, Alan R Liss, Inc., New York, pp. 115-126, 1987.

79. Fong S, Chen PP, Fox RI, Goldfien RD, Radoux V, Silverman GJ, Crowley JJ, Roudier J, Carson DA: The diversity and idiotypic pattern of human rheumatoid factors in disease. Concepts in Immunopath 5: 168-191, 1988.

80. Fox RI, Fong S, Chen PP, Kipps TJ: Autoantibody production in Sjogren's syndrome: a hypothesis regarding defects in somatic diversification of germline encoded genes. In Vivo 2: 47-56, 1988.

81. Chen PP, Fong S, Goni F, Silverman GJ, Fox RI, Liu M-K, Frangione B, Carson DA: Cross-reacting idiotypes on cryoprecipitating rheumatoid factor. Springer Seminar Series in Immunopath 10: 35-55, 1988.

82. Chen PP, Fong S, Carson DA: Rheumatoid factor. Rheumatic Diseases of North America 13:545-568, 1987.

83. Carson DA, Chen PP, Kipps TJ, Radoux V, Jirik FR, Goldfien RD, Fox RI, Silverman GJ, Fong S. Idioytpic and genetic studies of human rheumatoid factors. Arthritis Rheum 30: 1321-1325, 1987.

84. Fong S, Chen PP, Crowley JJ, Silverman GJ, Carson DA: Idiotypic characteristics of rheumatoid factors. Scand J Rheumatol, Suppl. 75: 58-65, 1988.

85. Crowley JJ, Goldfien RD, Schrohenloher RE, Spiegelberg HL, Silverman GJ, Mageed RA, Jefferis R, Koopman WJ, Carson DA, Fong S: Incidence of three cross reactive idiotypes on human rheumatoid factor paraproteins. J Immunol 140: 3411-3418, 1988.

86. Fong S, Chen PP, Crowley JJ, Silverman GJ, Carson DA: Idiotypes and the structural diversity of human rheumatoid factors. Springer Seminar Series in Immunopath 10: 189-201, 1988.

87. Silverman GJ, Goldfien, Chen PP, Mageed RA, Jefferis R, Goni F, Frangione B, Fong S, Carson DA. Idiotypic and subgroup analysis of human monoclonal rheumatoid factors: implications for structural and genetic basis of autoantibodies in humans. J Clin Invest 82: 469-475, 1988.

88. Fox RI, Chan E, Benton L, Fong S, Friedlander M. Treatment of primary Sjogren' syndrome with hydroxychloroquine. American Journal of Medicine 85 (suppl 4A): 62-67, 1988.

89. Fong S. La Diversite Structurale Des Facteurs Rhumatoides Humains. In Immunorhumatologie. Roux H, Luxembourg A, Roudier J, (Eds.). Solal, editeurs, Marseille, pp 162-166, 1989.

90. Fu, Y., Arkin, S., Fuh, G., Cunningham, B.C., Wells, J.A., Fong, S., Cronin, M., Dantzer, R., Kelley, K. Growth hormone augments superoxide anion secretion of human neutrophils by binding to the prolactin receptor. J. Clin. Invest 89: 451-457, 1992.

91. Weber, J.R., Nelson, C., Cunningham, B.C., Wells, J.A., Fong, S. Immunodominant structures of human growth hormone identified by homolog-scanning mutagenesis. Mol. Immunol. 29: 1081-1088, 1992.

92. Bushell, G., Nelson, C., Chiu, H., Grimley, C., Henzel, W., Burnier, J., Fong, S. The role of cathepsin B in the generation of T cell antigenic epitopes of human growth hormone. Mol. Immunol. 30:587-591, 1993.

93. Bednarczyk, J.L., Wygant, J.N., Szabo, M.C., Molinari-Storey, L., Renz, M., Fong, S., McIntyre, B.W. Homotypic leukocyte aggregation triggered by a monoclonal antibody specific for novel epitope expressed by the integrin β1 subunit: Conversion of non-responsive cells by transferring human α4 subunit cDNA. J. Cell. Biochem. 51: 465-478, 1993.

94. Berman, P.W., Nakamura, G., Riddle, L., Chiu, H., Fisher, K., Champe, M., Gray, A., Ward, P., Fong, S. Biosynthesis and function of membrane bound and secreted forms of recombinant Mac-1. J. Cell. Biochem. 52:183-195, 1993.

95. Crowe, D.T., Chiu, H., Fong, S., Weissman, I.L. Regulation of the avidity of integrin α4β7 by the β7 cytoplasmic domain. J. Biol. Chem. 269:14411-14418, 1994.

96. Renz, M.E., Chiu, H.H., Jones, S., West, C., Fox, J., Kim, J.K., Presta, L.G., Fong, S. Structural requirements for adhesion of soluble recombinant murine VCAM-1 to α4β1. J. Cell Biol. 125:1395-1406, 1994.

97. Chiu, H. H., Crowe, D. T., Renz, M. E., Presta, L. G., Jones, S., Weissman, I. L., and Fong, S. Similar but non-identical amino acid residues on vascular cell adhesion molecule-1 are involved in the interaction with α4β1 and α4β7 under different activity states. J. Immunol. 155:5257-5267, 1995.

98. Viney, J. L., Jones, S., Chiu, H., Lagrimas, B., Renz, M., Presta, L., Jackson, D., Hillan, K., Fong, S. Mucosal Addressin Cell Adhesion Molecule-1. A structural and functional analysis demarcates the integrin binding motif. J. Immunol. 157: 2488-2497, 1996.

99. Fong, S., Jones, S., Renz, M.E., Chiu, H.H., Ryan, A.M., Presta, L. G., and Jackson, D. Mucosal Addressin Cell Adhesion Molecule-1 (MAdCAM-1)--Its binding motif for α4β7 and role in experimental colitis. Immunologic Research 16: 299-311, 1997.

100. Jackson, D.Y., Quan, C., Artis, D.R., Rawson, T., Blackburn, B., Struble, M., Fitzgerald, G., Chan K., Mullin, S., Burnier, J.P., Fairbrother, W.J., Clark, K., Beresini, M., Chiu, H., Renz, M., Jones, S., and Fong, S. Potent α4β1 Peptide Antagonists as Potential Anti-Inflammatory Agents. J. Med. Chem. 40: 3359-3368, 1997.

101. Viney, J.L. and Fong, S. β7 Integrins and Their Ligands in Lymphocyte Migration to the Gut. Chemical Immunology: 'Mucosal T Cells' : Chemical Immunology 71;64-76, 1998.

102. Bradley, L.M., Malo, M.E., Fong, S., Tonkonogy, S.L., and Watson, S.R. Blockade of both L-selectin and α4 Integrins Abrogate Naïve CD4 Cell Trafficking and Responses in Gut-Associated Lymphoid Organs. International Immunology 10, 961-968, 1998.

103. Quan, C., Skelton, N., Clark, K., Jackson, D.Y., Renz, M., Chiu, H.H., Keating, S.M., Beresini, M.H., Fong, S., and Artis D.R. Transfer of a Protein Binding Epitope to a Minimal Designed Peptide. Bioploymers (Peptide Science);47,265-275, 1998.

104. Hillan, K.J., Hagler, K.E., MacSween, R.N.M., Ryan, A.M., Renz, M.E., Chiu, H.H., Ferrier, R.K., Bird, G.L., Dhillon, A.P., Ferrell, L.D., Fong, S. Expression of the Mucosal Vascular Addressin, MAdCAM-1, in Inflammatory Liver Disease. Liver 19, 509-518, 1999

105. Pender, S.L.F., Salmela, M.T., Monteleone, G., Schnapps, D., McKenzie, C., Spencer, J., Fong, S., Saarialho-Kere, U., and MacDonald, T.T. Ligation of alpha 4 beta 1 integrin on human intestinal mucosal mesenchymal cells selectively upregulates membrane type-1 matrix metalloproteinase and confers a migratory phenotype. American Journal of Pathology 157, 1955-1962, 2000.

106. Liang, T.W., DeMarco, R., Gurney, A., Hooley, J., Huang, A., Klassen, T., Mrsny, R., Tumas, D., Wright, B.D., and Fong, S. Characterization of Human Junctional Adhesion Molecule (huJAM): Evidence for involvement in cell-cell contact and tight junction regulation. American Journal of Physiology; Cell Physiology 279, C1733-C1743, 2000.

107. Liang, T.W., Chiu, H.H., Gurney, A., Sidle, A., Tumas, D.B., Schow, P., Foster, J., Klassen, T., Dennis, K., DeMarco, RA.., Pham T., Frantz, G., Fong, S. VE-JAM/JAM 2 interacts with T, NK, and dendritic cells through JAM 3. J.Immunology 168, 1618-1626, 2002.

107. Dupree,N., Artis, D.R., Castanedo, G., Marsters, J., Sutherlin, D., Caris, L., Clark, K., Keating, S.,Beresini, M., Chiu, H., Fong, S., Lowman, H., Skeleton, N., and Jackson, D. Selective $\alpha 4\beta 7$ Antagonists and Their Potential as Anti-Inflammatory Agents. J. Med. Chem. 45, 3451-3457, 2002.

108. Castanedo, G.M., Sailes, F.C., Dubree, N., Nicholas, J., Caris, L., Keating, S., Chiu, H., Fong, S., Marsters, J., Jackson, D.Y., Sutherlin, D.P. The Solid Phase Synthesis of Dual $\alpha 4\beta 1/\alpha 4\beta 7$ Antagonists: Two Scaffolds with Overlapping Pharmacophores. Bioorganic and Medicinal Chemistry Letters 12, 2913-2917, 2002.

J. Physiol. (1952) 118, 228–257

VASCULAR REACTIONS TO HISTAMINE, HISTAMINE-LIBERATOR AND LEUKOTAXINE IN THE SKIN OF GUINEA-PIGS

By A. A. MILES and E. M. MILES

From the National Institute for Medical Research, Mill Hill, London

(*Received* 3 *April* 1952)

A substantial increase in capillary permeability is a feature of acute inflammation in bacterial infections. The present investigation is part of an attempt to prove an old hypothesis, namely, that this increase in permeability is mediated by histamine. A comparative study was made of histamine, of the histamine-liberator 48/80, a condensation product of *p*-methoxyphenylethylmethylamine and formaldehyde (Baltzly, Buck, de Beer & Webb, 1949), and of leukotaxine (Menkin, 1936, 1938*a*, *b*).

In animals with a recently injected vital dye in their blood, the intradermal injection of substances that increase permeability of the blood vessels is followed by an accumulation of dye at the site of injection, presumably due to the passage of an excess of dye-stained plasma into the tissue spaces. When the blood flow and the vascular bed of the skin are relatively constant, differences in the size and intensity of stained areas of skin reflect differences in vascular permeability, and may be used to investigate the properties of substances that increase permeability in this way. Our work was confined to the skin of guinea-pigs, partly because much is already known about skin reactions to toxins and other inflammatory agents, and partly because it is a tissue readily studied in the intact and unanaesthetized animal—an important consideration with phenomena which, like the passage of dye through vascular endothelium, are peculiarly dependent on the state of the blood vessels in the tissue under test.

MATERIALS AND METHODS

Albino guinea-pigs, 300–450 g in weight, were used throughout. The skin of the trunk was depilated, after clipping away the hair, by a paste consisting of wheat flour, 350 g; talcum powder, 350 g; barium sulphide, 250 g; Castile soap powder, 50 g; and water. The depilated area was thoroughly washed with warm water.

Detection of increased permeability. Neither the intradermal injection nor the pricking-in of histamine or 48/80 produce in the depilated skin any measurable reaction indicating change in

vascular permeability; and there is no trace of the wheal that characterizes the reaction of human skin to histamine. In the skin of animals with circulating dye, however, both substances induce remarkably constant effects. A 5% solution of pontamine sky blue 6X ('pontamine blue') was used, given intravenously in the leg in doses of 65–75 mg/kg body weight. Animals so injected are referred to below as 'blued'. A few minutes after the injection of the dye the sites of wounds, of too-long application of depilating paste, and of recent careless or even firm manipulation of the skin, become blue. Though traumatic blueing of this kind commonly results from depilation, with nice judgement it is possible to depilate cleanly without damage to the skin. Owing to the sensitivity to trauma of blued animals, injections cannot be made into the skin pinched into a fold between thumb and finger; the skin must be steadied by gentle stretching over the underlying tissue.

In the absence of further interference, the skin of a blued animal becomes generally and maximally stained in 10 hr or more; but up to 6 hr after the intravenous dye, the intradermal injection of a substance that increases permeability results in a local increase in the intensity of blueing. The best contrasts were obtained within 1 hr of giving the dye. Unless otherwise stated, all our injections were given into the skin of the trunk posterior to the shoulder blade and anterior to the knee joint in the sitting animal, and omitting the thin skin about 30–40 mm on each side of the ventral mid-line; all solutions for injection were made up in 0·85% saline, which by itself induces no blueing. The volume injected was usually 0·1 ml., which initially raises a bleb 9–11 mm in diameter. With short-bevel no. 26 gauge needles, a small area of traumatic blueing 1–3 mm in diameter develops at the centre of the bleb.

Skin reactions in the ears of blued animals were induced either by free-hand intradermal injections with a no. 28 needle, or by injections with a mechanically manipulated glass micro-needle into animals under light bromethol (avertin) anaesthesia. The micro-injections were either intradermal or made directly into the lymphatic plexus of the ear, which is readily entered via one of the numerous anastomosing lymphatic channels at the margin of the ear. The ears were transilluminated and observed under ×20 and ×40 magnification.

Materials. The acid phosphate of histamine was used; amounts are cited as the weight of the base. The specimen of 48/80 (Wellcome Research Laboratories, U.S.A.) was probably in the form of the dimer, trimer and tetramer (Paton, 1951), with an average molecular weight of about 540 The leukotaxine was a single batch prepared by Dr J. H. Humphrey, by a combination of the methods of Cullumbine & Rydon (1946) and Spector (1951), and corresponded to the fractions described by Spector as active in inducing capillary permeability, containing eight to fourteen amino-acid residues. On this basis its molecular weight is of the order of 1500.

RESULTS

The mechanics of intradermal injection

The behaviour of injected drugs is determined in part by the mechanics of intradermal injection. The skin of the trunk moves loosely over the underlying abdominal and thoracic muscles. For our purpose this movable skin may be described as three layers of about equal thickness (Text-fig. 1*a*). (*A*) Epidermis and dermis which together are about 1·0 mm thick, appearing on cross-section as a dense whitish layer, whiter in the deeper part; the dermis contains an extensive plexus of blood vessels (*sp*) round the main bodies of the glands and hair follicles, and a fine plexus of lymphatic channels, detectable when indian ink is injected into this region by a micro-needle. (*B*) A looser connective tissue about 1·0 mm thick, appearing on cross-section as a grey gelatinous layer; at its base, immediately above *C*, the panniculus carnosus, is a plexus

of blood vessels (*dp*) and a coarse scanty plexus of lymphatic channels, each joined to the corresponding upper plexus in *A* by relatively few vessels. (*C*) The panniculus carnosus, a muscle layer about 1·0 mm thick.

In making an intradermal injection, the depth of the needle-tip to some extent determines the depth at which the bulk of the injected fluid will spread, but not as completely as is generally supposed. The fluid spreads outwards, upwards and downwards to form a lenticular mass of wet tissue (Text-fig. 1*b*). When the needle tip is as low as the deepest part of *B*, the swelling of the skin

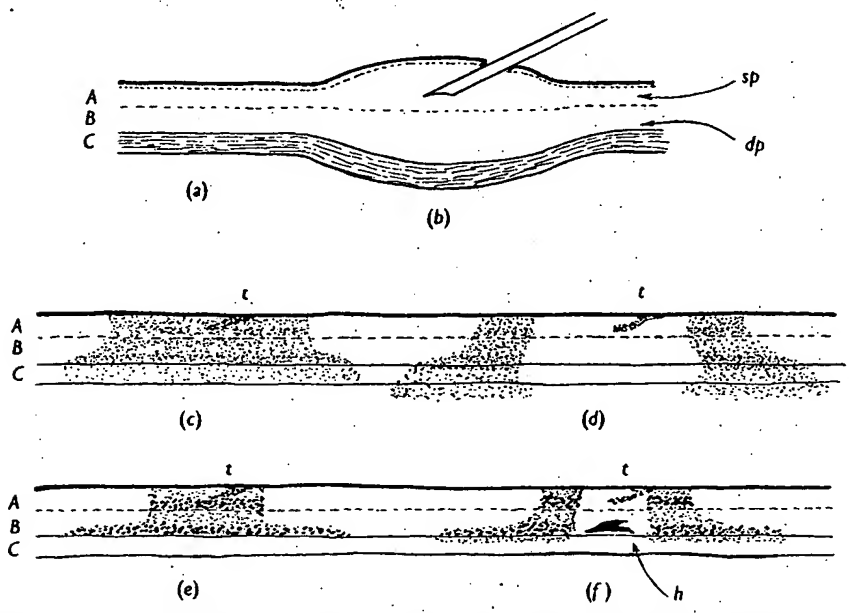

Text-fig. 1. Schematic sections of guinea-pig skin. (*a*) normal; (*b*) intradermal injection bleb; (*c*) blueing with low dose of histamine, showing traumatic blueing *t*, due to needle; (*d*) blueing with high dose of histamine showing central inhibition; (*e*) blueing with low dose of 48/80; (*f*) blueing with high dose of 48/80, showing central inhibition, and haemorrhage, *h*. *sp*, *dp* = superficial and deep plexus of blood vessels. For definition of layers *A*, *B* and *C*, see p. 229.

is due mainly to the distension of that layer, but when it lies in the middle of *B*, or in the dermis, both *B* and the dermis are equally permeated by the injection fluid. The initial diameter of the bleb is a simple function of volume injected; being linearly related to log. volume (Text-fig. 3*a*–*d*).

The initially domed injection-bleb of saline is scarcely visible after 3–4 hr. Some of the fluid is doubtless taken into the blood stream and some into the lymphatic channels; though, judging by the results of intradermal injection of dyes and indian ink, only a very small proportion of the injected substances escapes by the lymphatic channels during the first 2 hr. Other forces must be at work to account for the gradual disappearance of the bleb, which both decreases in thickness and spreads outwards. The diameter of a 0·1 ml. bleb,

measured under illumination by a very oblique beam of light, grows linearly with respect to log. time (Text-fig. 2); and on the average, blebs starting at 10·5 mm are 19·5 mm in diameter after 2 hr and 20·5 mm after 4 hr. The rate of spread is much the same in freshly killed animals. The decrease in thickness is partly due to seepage through the muscle layer into the subcutaneous tissue, which becomes noticeably wet; and partly to the outward spread of the fluid. Of the forces responsible for the outward spread, diffusion is unlikely to play any large part, because the intradermal invasion of diffusible substances applied to the cut edge fo normal skin is small and slow (e.g. the enzyme hyaluronidase, Hechter, 1946). Spread probably takes place by mass movement of the fluid either by reason of the hydrostatic pressures engendered in the tissue during injection or because the tissue has an affinity for water, which moves therefore from the hydrated bleb to the surrounding less hydrated tissue.

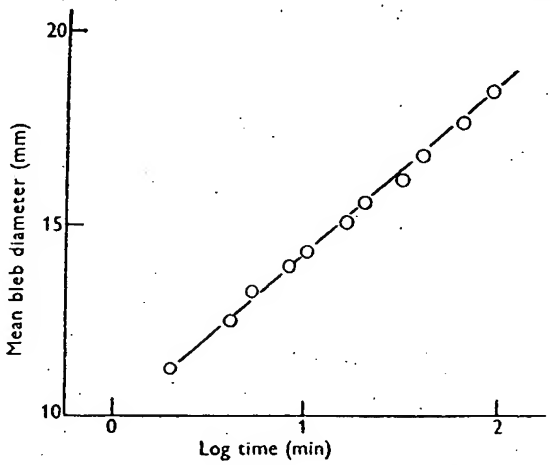

Text-fig. 2. Growth of an intradermal bleb in the guinea-pig formed by 0·1 ml. saline. Each point the mean of three blebs.

Large syringe pressures are required to initiate an intradermal bleb. In a series of measurements on ten guinea-pigs, this pressure varied between 80 and 140 cm Hg; once the bleb was begun, it increased rapidly in size under syringe pressures of 60–100 cm Hg. Only 1–2 cm Hg were required to expel fluid rapidly from the unimpeded syringe needle. The tissues do not, however, store the energy to a degree represented by these pressures, because when the bleb is cut vertically across its middle, fluid oozes only very slowly from the cut surface. Indeed, the pressure within the bleb soon after it is made cannot be higher than that in the small vessels involved, because exudation from the vessels takes place in blebs only 3 min old (see p. 236). At this time the maximum pressure must therefore be less than that in the largest vessels from which exudation takes place; and probably does not exceed 1–2 cm Hg. That the occlusion of the vessels during injection is only short-lived can be seen when

the formation of an intradermal bleb is watched under low-power magnification in a transilluminated hyperaemic ear. The hyperaemia is apparently restored after a few seconds. In arteries 0·4–0·8 mm in diameter, the flow returns in 5–10 sec; and in veins 0·5–2 mm in diameter flow returns in 30–120 sec, and initial diameter is restored in under 3 min. The high injection pressures are apparently needed only to tear apart the tissues at the advancing edge of the bleb.

Fluid may be expressed more rapidly by gently pinching the cut edge of a bleb between finger and thumb. A great deal of the fluid therefore cannot be held by hydration of the tissues. It is presumably held in innumerable small, distended, interconnecting loculi in the connective tissues, and is forced outwards to the periphery of the bleb by contraction of the distended tissue fibres. Hydration, however, may well account for the retention of some of the fluid in a cut bleb, as the following experiment shows. The average water content of pieces of muscle-free, intact skin from the trunk was about 50%; i.e. one part of dry matter holds about one part of water. Pieces of fresh guinea-pig skin were cut into 10μ slices on a freezing microtome, washed in saline to remove damaged cells and the contents of the cells cut open during section, and the washed slices allowed to imbibe water from 0·85% saline for 30 min at 32° C. They were then deposited as a hard cake by centrifugation, and excess fluid removed from the deposit by firm pressing between sheets of filter-paper. The average water content of these masses was about 70%, i.e. one part of dry matter can hold $70/30 = 2{\cdot}3$ parts water. A 0·1 ml. bleb occupies about 160 mg of intact skin, which, if it attained the same degree of hydration as the sliced skin, could hold $80 \times 2{\cdot}3 = 184$ mg water; i.e. not only the 80 mg of natural water, but the injected 100 mg as well.

The dosage-response to intradermally injected substances

The distribution in the skin of an intradermally injected substance will depend on its concentration and the rate at which it is adsorbed or 'fixed' by the tissues during the outward flow of injection fluid from the needle. A substance that was adsorbed very little would spread with the injection fluid, and, according to the evidence in Text-fig. 2, would eventually produce lesions whose diameter was directly proportional to the diameter of the injection bleb; i.e. to the volume of fluid injected. Most substances, however, are adsorbed in some degree, and accumulate at and around the centre of the bleb. The relation of the bleb-diameter to lesion-diameter with different drugs can be used to characterize their adsorption to the tissues. It was explored for histamine, 48/80 and leukotaxine by two methods of injection in blued animals: (*a*) graded concentrations in a constant injection-volume, and (*b*) graded injection-volumes containing a constant dose.

'*Constant-volume*' *measurements.* Four doses of the substance under test in

0·1 ml., were randomized in a 4 × 4 Latin square on the trunk, two rows on each side of the spinal mid-line. Histamine, 48/80 and leukotaxine all produced round blue lesions in the skin and in each case the lesion-diameters measured 30 min after injection were linearly related to the log. dose (cf. Text-fig. 5*a*, *b*). The responses were subjected to analysis of variance, with the results exemplified in Table 1, which records a titration of histamine in three blued animals. The departure from linearity of the regression line of lesion-diameter on log. dose is insignificant. The variation between columns and rows is also insignificant, so that for practical purposes the skin of the more dorsal

TABLE 1. Analysis of variance of a titration of histamine in a 4-fold Latin square in three blued guinea-pigs

	Degrees of freedom	Sum of squares	Mean square	Variance ratio	*P*
Between animals	2	3·2279	1·61395	1·66	>0·05
Between columns	3	3·1275	1·0425	1·07	>0·05
Between rows	3	2·0174	0·6725	—	—
Between doses	3	312·7425	104·2475	107·46	<0·001
Linearity	1	72·8017	72·8017	75·05	<0·001
Curvature	1	3·2939	3·2939	3·40	>0·05
Response	1	235·8784	235·8784	243·15	<0·001
Error	36	34·9239	0·9701	—	—
Total	47	356·0392	—	—	—

part of the guinea-pig's trunk may be considered homogeneous in its sensitivity to histamine. (This is not true of the thinner ventral skin, where lesions tend to be larger.) Each animal yields a mean of four responses per dose. The error term for inter-animal variation is large, but reliable comparisons between various treatments were obtained in other tests by using four to six animals per group. This linear relationship differs from that found by Bain (1949) in the human skin, where *area* of histamine whealing was proportional to log. dose. Linearity of diameter against log. dose holds for many substances in guinea-pig skin: diphtheria toxin (Miles, 1949), tuberculin in tuberculous animals (Wadley, 1949) and appears to hold for other bacterial antigens in hypersensitive animals, and for the lesions produced in the blued animals by various toxins such as the exotoxins of *Clostridium welchii*, *Cl. oedematiens* and *Staphylococcus aureus*, and for cobra venom (unpublished work). The difference in Bain's titration may lie in the modification of histamine spread or of wheal-diameter, by the copious exudation during whealing that occurs in man but not in the guinea-pig.

Full 4 × 4 Latin-square titrations were usually made only when the significance of a result was in doubt; in most of the tests fewer replications of doses were used, partially randomized among three to six animals per group. In these titrations, 48/80 and leukotaxine differed from histamine mainly in the slope of the dosage-response lines. Slopes varied with each experiment, and particularly with the amount of dye injected. Moreover, since the concentration of circulating dye falls rapidly during the first 2 hr, slope decreases with lapse of

time between blueing the animal and the intradermal titration. In guinea-pigs receiving 65 mg/kg tested soon after its injection, the slopes for histamine lay between 2·8 and 3·5, for 48/80 between 1·5 and 2·0 and for leukotaxine between 1·5 and 4·0. The shallow slope of 48/80, which indicates an increase of only 1·5–2·0 mm in lesion-diameter for a 10-fold increase in concentration, suggests that, compared with histamine, it is strongly adsorbed to the tissues. It should be noted that the susceptibility of this linear dosage-response to statistical analysis makes possible an accurate though not very precise measure of the potency of each of the three substances. The method is too insensitive for routine assay, but was well adapted to our investigations of skin reactions. Thus where parallel regression lines can be fitted to two sets of log. dose-diameter responses, the horizontal distance between the two lines is the log. ratio of drug potency; and, for a given specimen of a drug, it is the log. inverse ratio of sensitivity to the drug. For example, in Text-fig. 5*b*, 3 mg neoantergan has shifted the slope to the right by 0·43 = antilog. 2·7. That is, the neoantergan has decreased the 48/80-sensitivity of the animals 2·7-fold, since 2·7 × the dose in normal animals is required to produce the same effect in the treated animal.

'Constant-amount' measurements. In this method a fixed amount of the drug was injected in volumes of 0·05, 0·1, 0·2 and 0·4 ml.; i.e. the concentration of the drug is varied. The diameter of the blebs, measured immediately after the injections, was linear with respect to log. volume (Text-fig. 3*a*, *A*); and, according to the data in Text-fig. 2, after a given period (e.g. 30 min, Text-fig. 3*a*, *B*) the expanded bleb-diameters would be linear, on a line parallel to that for the immediate bleb-diameters (Text-fig. 3*a*, *B*). The slope of the initial bleb-diameters, irrespective of any lesion produced by the drug injected, is relatively constant in the region of 9·0. When the drug has acted the resulting lesion-diameters are also linear with respect to log. injection volume. Text-fig. 3*a*, *C* and *D*, records results with 12·5 and 50 μg pontamine blue in unblued animals. The 'lesion' here is the area of skin coloured by the injected dye. The slope of lesion-diameter is not parallel to that for initial bleb-diameter, which would have indicated no adsorption during injection. Nor is it horizontal, which would have indicated an adsorption so strong that it was independent of concentration within the range tested. The slope of *C* and *D* is in fact 5·5, compared with 9·7 for the initial bleb-diameter. Pontamine blue has a good affinity for skin tissue (Evans, Miles & Niven, 1948), and we would therefore expect slopes like *C* and *D*, which show that as the solutions are forced outwards during injection, adsorption decreases with decreasing concentration of the injection fluid. The magnitude of the slope, compared with that for the initial bleb, is a reasonable inverse indicator of the affinity of the tissues for the drug. Text-fig. 3*b–d*, and Table 2 summarize similar titrations on histamine, 48/80 and leukotaxine; the slopes indicate that the tissue affinity is least for histamine, and greatest for leukotaxine.

V.

The relative p
the 50 μg line *D*
bleb from 0·1 ml

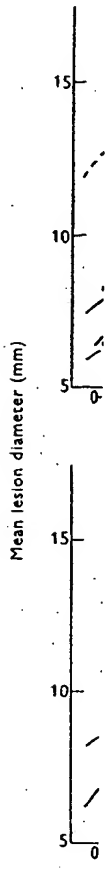

Text-fig. 3. Constar
injected. Each
diameter of the
by the *substanc*
after 30 min c
50 μg dye. (*b*) I
(see pp. 234–6

to fill the 0·2 ml
spreads outward
dye is carried sc
dye has spread c
initial bleb-dian

The relative position of the two slopes is also informative. In Text-fig. 3*a*, the 50 μg line *D* crosses *A* at about 10 mm, i.e. the skin occupied by the initial bleb from 0·1 ml. just adsorbs the dye. The 50 μg of dye is clearly insufficient

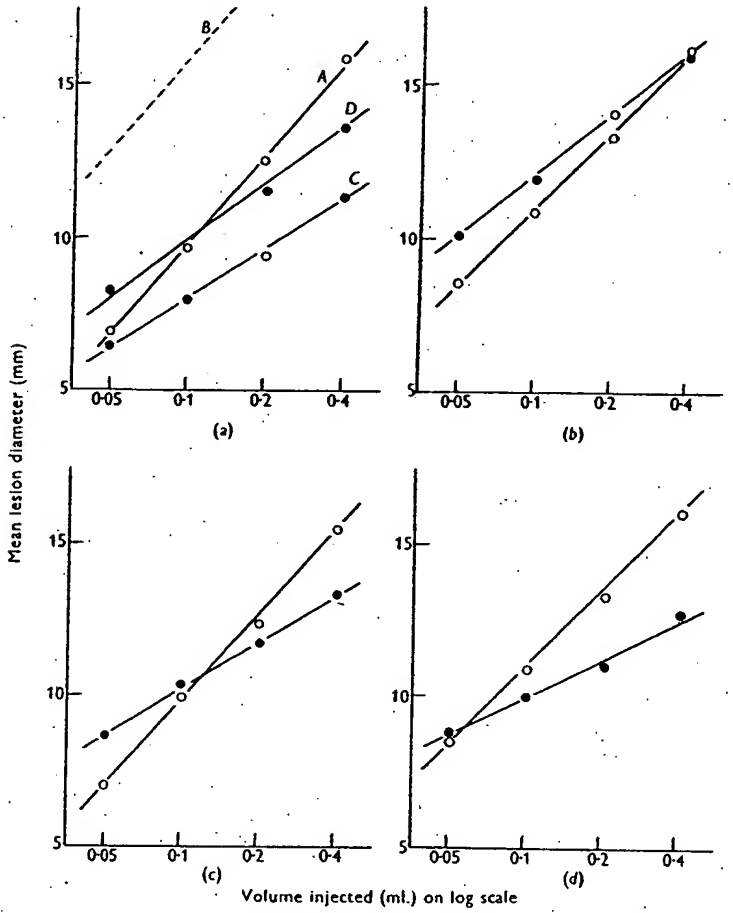

Text-fig. 3. Constant-dose intradermal titrations. Lesion-diameters plotted against log. volume injected. Each point the mean of twelve to sixteen lesions. In all the graphs, O — O, mean diameter of the initial blebs raised by the *fluid* injected; ● — ●, diameter of lesion produced by the *substances* injected. (*a*) pontamine blue: *A*, initial bleb-diameter; *B*, bleb-diameter after 30 min calculated from data in Text-fig. 2. *C* and *D*, lesion-diameters of 12·5 and 50 μg dye. (*b*) Histamine, 8 μg; (*c*) 48/80, 13 μg; and (*d*) leukotaxine, 40 μg, in blued animals (see pp. 234–6 and Table 2).

to fill the 0·2 ml. bleb. It oversaturates the 0·05 ml. bleb so that as the fluid spreads outwards from the region initially filled by the injection, the excess of dye is carried some way with it; at 30 min, when the reading was taken, the dye has spread over 8 mm and the fluid (line *B*) over 12·5 mm. The intersect of initial bleb-diameters and lesion-diameters is thus a convenient measure of the

adsorbing power of the skin for a given dose of drug, though clearly it can give no information about the concentration gradient of the drug within the bleb. It is the volume in which the adsorption of the drug is so balanced that the minimal effective concentration is produced at the edge of the initial bleb; and may be called the critical volume. In Text-fig. 3*a*, the critical volume for 50 μg of pontamine blue is 0·105 ml.

TABLE 2. Slopes and critical volumes in 'constant-amount' titrations of histamine, 48/80 and leukotaxine

Substance	Approx. equimolar dose (μg)	Slope mean diameter		Critical volume (ml.)
		Initial bleb	Lesion	
Histamine	8	8·6	6·6	0·400
48/80	13	9·3	5·2	0·012
Leukotaxine	40	8·6	4·1	0·058
(Pontamine blue	—	9·8	6·2	0·105)

For a valid comparison, the critical volumes of equimolar concentrations of histamine, 48/80 and leukotaxine were determined from the data in Text-fig. 3*c–e* (Table 2). 8 μg of histamine was tested, and the approximate molecular equivalent, 13 μg, of 48/80. The result for an equimolar amount of leukotaxine (40 μg) was extrapolated from the slope for 20 μg using the value 4·0 for the slope of a constant-volume titration. The values both for slope and critical volume must be regarded as very approximate. Histamine (Table 2) has a high 'constant-amount' slope, and a high critical volume; it is thus relatively poorly adsorbed during injection, and the skin is relatively poor in adsorbing sites. Both 48/80 and leukotaxine are more strongly adsorbed, and the skin is richer in adsorbing sites.

Skin reactions to histamine

Histamine even as strong as 1·6% will not induce blueing in dyed animals when applied to undamaged skin. When the skin of blued animals is damaged by rubbing (cf. Matolsty & Matolsty, 1951) or scratching sufficient to produce patches of traumatic blueing, the application of 1% histamine will increase the size and intensity of such blueing, presumably because the drug, having penetrated the damaged skin, diffuses inwards from the damaged area. It is also possible to induce blueing by the electrophoresis of 1% histamine; the histamine is not however driven in uniformly, but produces irregular patches of blueing. In none of these tests was whealing ever observed.

Intradermal injection in the trunk. Histamine injected intradermally into blued animals produces a round area of blueing that appears in 3–5 min and increases slightly in diameter and intensity during the next 7 min. In a volume of 0·1 ml., as little as 0·1–0·2 μg is effective; with increasing dose the blue increases in intensity and area. With amounts greater than 1–3 μg the colour first appears at the edge of the bleb, but gradually fills the centre. With doses

of 4 μg and more, the centre remains uncoloured except for the traumatic blueing round the site of needle-entry, and colour develops at the edge. More than 10–20 μg produces only a narrow band of very faint blue at the edge of the bleb.

On section after 10 min, a 1 μg histamine lesion is seen to be uniformly stained at the skin surface, more widely stained in layer *B* (Text-fig. 1*c*), and feebly stained in the muscle. Occasionally the staining is slightly deeper in the region of the two plexuses of blood vessels. With stronger doses of histamine (Text-fig. 1*d*), the drug has in 10 min spread downwards and outwards so that there is blue exudate in the underlying subcutaneous tissues, and the abdominal and thoracic muscles may be stained. The other feature of the stronger dose, the central inhibition of blueing, is also evident in cross-section, where the colourless zone reaches down to the muscle layer.

The linear response, lesion diameter on log. dose, holds with histamine for diameters between 5 and 17 mm: below 4 mm histamine blueing may be confused with traumatic blueing. In reading the diameters, inhibition of blueing at the centre is ignored even though with the higher concentrations of the drug only faint, thin rings of blue may be produced. The lesion-diameters measured on the under-surface of flayed skin are larger than those on the upper surface, by about 40%. This ratio is approximately constant. There is, however, no advantage in the measurement, because the lesions are less well defined and, with the bigger doses, obscured by subcutaneous blue exudate.

Intradermal injections in the ear. Blueing of the ear, as in the trunk (see below), was partly inhibited by bromethol anaesthesia; but under light anaesthesia it was sufficiently strong for a number of useful observations, though lesion diameters were not such a consistent guide to drug-sensitivity. The ear was found to be less sensitive to histamine than the skin of the trunk. In unblued animals, concentrations of 5–1000 μg/ml. caused immediate flushing of the skin of the bleb, which lasted about 10 min. Stronger histamine, up to 10,000 μg/ml. also caused immediate flush, and after 1½ min an intense vasoconstriction, lasting 3–5 min, of the arteries traversing the bleb area.

In blued animals, the permeability effect is visible in 1½ min. The minimal blueing concentration was about 0·5 μg/ml. Central inhibition of blueing occurred at 50 μg/ml., lasting only 3 min, after which the centre of the bleb became blue. At 1000 μg/ml. it lasted about 16 min, unlike the central inhibition by 50 μg/ml. in the skin of the trunk, which persisted for several hours. The results in Table 6 were obtained from blebs of 3 mm initial diameter; the injection volume was not measured exactly.

With concentrations of 100 μg/ml. the area of blueing of a 3 mm bleb was 10 mm in diameter after 10 min. Histamine in stronger concentrations, 1000–10,000 μg, leaked into the lymphatic plexus, spread both distally and proximally through the freely anastomosing channels, passing back into the

tissues to produce an oedematous wedge-shaped area of intense blueing with its apex at the base of the ear where the main lymphatic ducts leave the ear (Pl. 1A, B). This is a characteristic lymphatic spread of strong histamine in the ear, and is also produced by strong histamine injected directly into the lymphatic plexus. It is evident therefore, that histamine readily passes both ways through lymphatic endothelium.

Factors that change skin-reactivity to histamine in the trunk

Temperature. Depilated animals held at 10° C react poorly to histamine; those at 20° C react well; and those at 37° C poorly and irregularly. Thus, the mean lesion-diameters for 3, 9 and 27 μg histamine were 6·7, 8·3 and 9·6 mm at 20° C, and 4·7, 5·7 and 5·9 mm in animals held at 37° C. The intensity of blueing was considerably less at 37° C. In this reaction to heat the guinea-pig is similar to man in his whealing reaction to histamine (Lewis & Grant, 1924).

Anaesthesia. Under ether, chloroform, chloralose, bromethol, pentobarbitone and urethane anaesthesia, blueing is greatly diminished or even abolished. In general, the deeper the anaesthesia, the greater the inhibition of blueing. After a short period of anaesthesia with ether, bromethol or chloroform, reactivity is sometimes restored on recovery. Loss of reactivity is accompanied by a decline in the pressure of the central arteries of the ear, measured by a modified Grant's capsule (Miles & Niven, 1950), from 40 to 70 mm in the unanaesthetized state, to 20–40 mm Hg. This suggests that in the skin of the trunk also there is in anaesthesia a decline in blood pressure to the point where dye is no longer forced out into the tissues, though the permeability of the vessels may be increased by the histamine. However, in many recovered animals, in which the blood pressures in the ear have returned to normal, the skin of the trunk remains unresponsive; either the anaesthetic has modified histamine-sensitivity, or the circulation is in these areas restored less quickly than in the ear.

Shock. In guinea-pigs given sublethal shocking doses of *Proteus vulgaris* and *Bacterium coli* endotoxins, of adenosine-triphosphate, insulin or intraperitoneal hypertonic glucose, reactivity to histamine is diminished; and, as in anaesthesia, the loss is associated with low blood pressure in the ear, and with low skin temperature (Miles & Niven, 1950). In shocked or anaesthetized blued animals, whose skin does not respond to histamine, it is possible to demonstrate an increase in capillary permeability by indirectly raising the intracapillary pressure. When a suction cup is applied to the skin of these animals, substantial blueing of a histamine-treated area is produced within 5 min, by a suction of 10 mm Hg applied intermittently for 2–3 sec every 10 sec.

Infection and malnutrition. Guinea-pigs suffering from spontaneous chronic infective abscesses, or in poor health because of heavy infection with B.C.G.

(Bacillus of Calmette and Guérin) or as a result of long-term partial deficiency of vitamin C, react poorly to histamine.

Cortisone, preparations of adrenocorticotrophic hormone (ACTH) and posterior pituitary lobe extract (P.P.E.). In an attempt to relate the anti-allergic effect of cortisone and ACTH to an effect on histamine sensitivity, histamine was titrated in blued animals, 2–3 hr after doses of cortisone (2 mg) or ACTH (1 i.u.). These doses had proved effective in diminishing tuberculin allergy in the guinea-pig (Long & Miles, 1950). The cortisone had no effect. The diameters of the lesions were not substantially changed by the ACTH, but intensity of staining was greatly diminished. At this time, the skin of the ACTH-treated animals was slightly colder than those of controls. Nearly all current preparations of ACTH contain some posterior lobe extractives, and these may have been responsible for the ACTH effect we observed. Certainly both 2 and 0·2 i.u. P.P.E., given subcutaneously 2½ hr before the titration, diminished reactivity to histamine (Text-fig. 4); and here again the diminution was probably due to poor blood supply, because the skin was cooler than that of the controls.

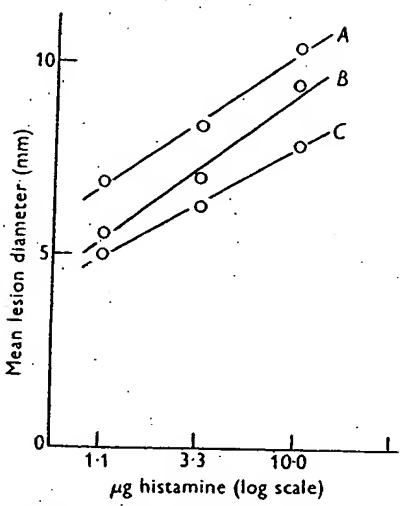

Text-fig. 4. The depressant effect of intramuscular posterior pituitary extract (P.P.E.) on histamine blueing in the guinea-pig. Each point the mean of twelve lesions. *A*, untreated animals; *B*, 0·2 i.u. P.P.E., 2·5 hr earlier; *C*, 2·0 i.u. P.P.E., 2·5 hr earlier.

Neoantergan. 20 μg neoantergan (mepyramine maleate) given intradermally in 0·1 ml. itself induced slight blueing of the skin; 5 μg histamine induced intense blueing 11 mm in diameter; and 20 μg neoantergan mixed with 5 μg histamine gave a pale blue area 10 mm in diameter. Local neutralization by neoantergan is therefore possible, but not very effective. Intravenous neoantergan, on the other hand, is most effective; 0·1 mg/kg almost abolished histamine blueing, and 0·02 mg/kg diminished the efficacy of intradermal histamine about 9-fold (Text-fig. 5*a*).

Excepting inhibition in animals held at high atmospheric temperatures, and by intravenous neoantergan, most of the effects on blueing described above can be attributed to a decline of intravascular pressure, rather than to insensitivity to histamine. The insensitivity of an abnormally warm skin may be due, as Lewis & Grant (1924) suggested for the human subject, to the more rapid removal of histamine in the more physiologically active tissue. The variety of the states in which there is inhibition of blueing is a warning that

absence of local blueing cannot safely be interpreted as absence of increase in capillary permeability unless there is good reason to believe that the blood supply to the skin and the state of the skin vessels have not been altered by the experimental procedure. On the other hand, it is reasonable to assume that a substance like histamine, which rapidly induces a deep blueing in healthy animals held at an atmospheric temperature of about 20° C, does so by an abnormal increase in capillary permeability. Histamine can act as vasodilator, but it is unlikely that the increased blueing in the guinea-pig is due to increased flow and exudation of dye as a result simply of vasodilatation, as suggested by Dekanski (1949). The rate of histamine blueing is too rapid to be attributable to this cause. Histamine induces in 3 min an intensity of blueing reached by untreated skin in 10 hr or more; i.e. the rate of accumulation of the dye is increased by over 200-fold.

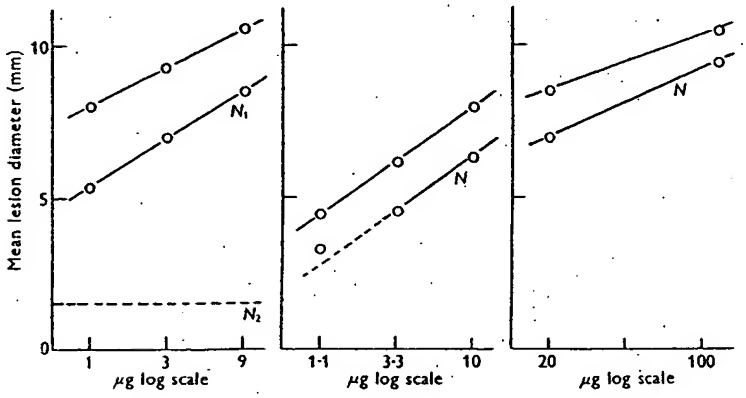

Text-fig. 5. The effect of neoantergan (N) on blueing in the guinea-pig. Each point the mean of twelve or sixteen lesions. (*a*) Histamine, $N_1 = 0{\cdot}02$ mg/kg, N_2 = average diameter of lesion with 0·1 mg/kg; (*b*) 48/80, $N = 8$ mg/kg; (*c*) leukotaxine, $N = 3$ mg/kg.

The time-course of the histamine effect

The rate of 'fixation' of histamine. The 'constant-amount' titration of histamine (Text-fig. 3*b*, Table 2), measuring the blue area developing in 10 min, shows that during injection the drug is lightly adsorbed. Within 5 min, however, some reaction with tissue must have occurred, because the increased permeability is by that time almost fully developed. The rate of that reaction may be estimated by the technique of superinjection (Miles, 1949) in which a substance is injected through a needle painted with a trace of indian ink so that the site of needle entry is exactly marked; and after an interval an injection of saline made into the same site. If any of the injected substance is free, it will be displaced outwards by the superinjected saline beyond the periphery of the initial bleb, with a consequent increase in the size of the lesion; if there is no increase, the injected substance has already been held fixed or destroyed by the tissues.

In applying the method to histamine and histamine-liberators the evidence from increase in lesion-diameter is not unambiguous because the superinjected saline may push, not free histamine, but already-formed blue exudate, beyond its original confines. The ambiguity may be resolved in part by determining the rate at which 'exudate' is fixed to the tissues. To this end, guinea-pig serum was coloured with pontamine blue so that in an unblued animal 0·1 ml. stained the skin to the intensity produced by 3 μg histamine in 0·1 ml. injected into a blued animal. Into the sites of injection of this fluid, 0·2 ml. saline were superinjected after graded intervals of time. The results were variable but indicated that some of the dyed serum was fixed within 3–4 min and the rest could be dislodged by superinjection up to 20 min. later. The best that can be

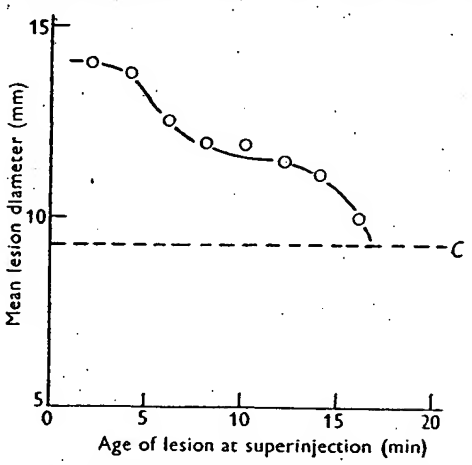

Text-fig. 6. The fixation of 3 μg histamine by guinea-pig skin. Superinjection of histamine lesions by 0·2 ml. saline. C = average diameter of control lesions. Each point the mean of four lesions.

hoped for from the test is that with time the lesion-diameters decline to a steady value, but this will not necessarily be the same as the diameter of lesions left to develop without superinjection. When saline was superinjected into blebs made in blued animals with 3 μg histamine (Text-fig. 6) little was fixed in 3–4 min, a period corresponding to the latent period before blue exudation starts, the greater part was fixed in 4–12 min, and nearly all was fixed in 16 min old lesions. If we allow 3 min for the fixation of the blue exudate, then all the histamine may be fixed in as little as 13 min, and most of it is fixed, as might be expected, during the period when the histamine-induced exudation is taking place.

Duration of increased permeability. The duration of the histamine effect was measured by injecting 2 μg in 0·1 ml. at regular intervals for 30 min in an animal, and giving the dye intravenously immediately after the last intradermal injection; there are thus lesions varying in age from 1 to 30 min when the dye is injected, and lesions in which the vessels are no longer permeable do

not blue. It is clear from Text-fig. 7*b* that after 10 min the capillaries have recovered; only the traumatic blueing caused by the needle remains. A similar result was obtained in the ear (Text-fig. 7*a*). Here the residual traumatic blueing due to the fine micro-needle is minimal.

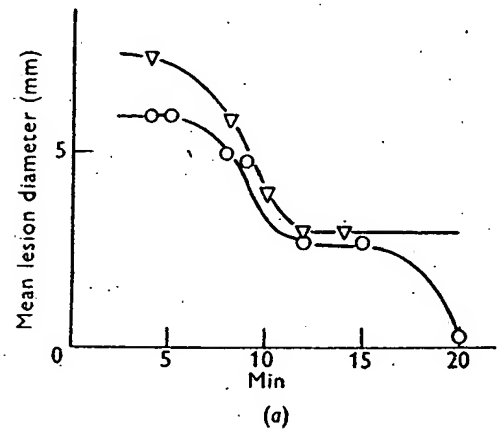

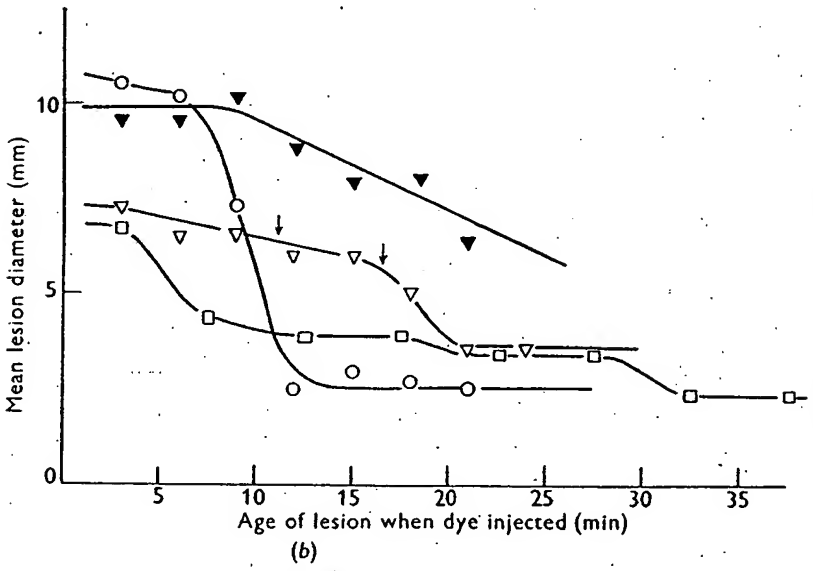

Text-fig. 7. The duration of increased permeability in guinea-pig skin. In each case there is a decline to the level of traumatic blueing induced by the injection needle. (*a*) The ear: histamine, approx. 2 μg in 0·02 ml., ○ — ○; 48/80, 2 μg in 0·02 ml., ▽—▽. (*b*) The trunk: histamine, 1 μg in 0·1 ml., ○ — ○; 48/80, 20 μg in 0·1 ml., ▼—▼; 2 μg in 0·1 ml., ▽—▽; leukotaxine, 10 μg in 0·1 ml., □ — □.

Immunity to histamine. It follows that the site of a histamine injection remains colourless if it is 10–15 min old when dye is given. When more histamine is superinjected into such a site, blueing is either feeble or absent. The

injection site has become refractory—or immune—to further histamine. The immunity is neither solid nor regular in its manifestation; it may take the form of diminished area of feeble staining, as though all the tissue were partly immunized; or of small patches of blue from 1 to 4 mm in diameter, as though the blood vessels in certain areas of the injection site had escaped immunization. This irregularity of response partly spoils measurement of immunity in terms of lesion-diameter, but the differences between immune and non-immune tissues are usually so large that mean lesion-diameters are good enough indices of the change. It is clear, for example, from Table 3, that after 1 hr 9 μg

TABLE 3. Immunizing action of intradermal histamine to injections of histamine made 1 hr later. Means of three lesions

Immunizing dose of histamine (μg)	Mean diameter (mm) and intensity* of reaction to test dose of histamine		
	1 μg	3 μg	9 μg
Nil	8·5 + +	10 + +	11·3 + +
9	0	6 f.	7·8 f.

* f., ±, +, + + = faint, moderate, marked, intense blueing.

induces a solid immunity to 1 μg, and a substantial immunity to 9 μg. A number of similar experiments established that though some immunity is present after 10 min, when the capillaries have recovered from the immunizing dose, it is greatest in lesions 1½–2½ hr old, and is passing off after 4 hr.

Histamine in concentrations of 10–100 μg/ml. immunized the ear vessels to histamine. Immunity was irregular in lesions up to 35 min old, well established after 40 min, maximal at 2–3 hr and lasted up to 5 hr. After 40 min, 50 μg/ml. had immunized to a test dose of 50 μg/ml. so that the diameter and intensity of blueing was reduced from 9 mm + +, in a control area to 4 mm ±, in the immunized area; 20 μg/ml. did not immunize to 50 μg/ml., and the immunity induced by 10 μg/ml., though it protected against 10 μg/ml., lasted only 60 min.

The inhibition of skin-reactivity by high concentrations of histamine

The restriction of blueing to the periphery of blebs containing 4 μg histamine or more may be explained in terms of the recovery of normal impermeability and of immunity, if we also postulate that the histamine at the centre of the bleb was strong enough to induce vasoconstriction of the arterioles for at least 10 min. As a result, the centre of the bleb would not blue during this time because the blood supply is cut off—a state corresponding to the inhibition of whealing in man by pressure-occlusion of the vessels—and by the time the blood supply is re-established, the central capillaries would have recovered from the histamine. Alternatively, the reaction of the vessels with high concentrations of histamine may proceed so rapidly that the immune stage is reached before the preceding stage of permeability can manifest itself by the escape of dye.

Lewis & Grant (1924) inferred that the refractory state was not due to occlusion of the lumen of the vessels by viscous R.B.C. or other material, because it could be induced in a relatively bloodless arm, and because, even though whealing was inhibited, vascular reactions that indicated a fully patent vascular bed could still be elicited. There is no anatomically convenient site in the guinea-pig for occlusion tests as applied by Lewis & Grant, and the dermis is too dense for direct observation of vascular changes. The vessels were proved patent by direct test. Injections of 5 or 10 μg histamine were made at intervals, in the skin over the right scapular region of normal guinea-pigs under urethane anaesthesia. At the end of the series of skin injections, 4 ml. indian ink was put into the right axillary artery. During the preparation of this artery, the blood supply to the skin was interrupted for the last 2–3 min of the experiment. The state of the vascular bed was deduced (*a*) by direct observation of the blackening of the skin; (*b*) from the pattern of the ink-filled vessels seen by low-power microscopy in excised skin areas fixed in 10% formalin, dehydrated and cleared with clove oil; and (*c*) from the distribution of ink in the lumen of capillaries seen in histological section of individual blebs. In tests by these methods on eight animals, there was no evidence of blocked vessels in histamine lesions from 5 to 30 min old.

Skin reactions to 48/80

Intradermal injection in the trunk. In the skin of blued animals, 48/80, like histamine, induces a round area of blueing whose diameter is linearly related to the log. dose injected in a constant volume of 0·1 ml. (Text-Fig. 5*b*). The slope of the dose-response line is much less than that of histamine, varying between 1·5 and 2·0. The blueing develops in 3–5 min and is more intense than that produced by histamine; the minimal effective dose distinguishable from traumatic blueing by the injection needle is about 0·2 μg. With doses of 2–4 μg the blue first appears at the periphery of the bleb and invades the centre. In cross-section of 48/80 lesions the blue area is confined to the two upper layers of the skin (Text-fig. 1*e*). The blueing is not uniform as it is with histamine; it is more intense in the region of the two plexuses of blood vessels, and especially that immediately over the muscle layer. The 48/80 does not spread downwards to the subcutaneous tissues. Even with doses of 30 μg in 0·1 ml., only the upper part of the muscle layer is blued, and there is no blueing of subcutaneous tissues or underlying muscle. This is not due to absence of histamine available for liberation in the muscle or subcutaneous tissues, because direct injection of 48/80 into these sites induced intense localized blueing. This difference in the spread of 48/80 and histamine from the injection site is not likely to be due to the difference in molecular weights, which are of the order of 540 for the trimer of 48/80 and 310 for the acid phosphate of histamine; the difference confirms the conclusions about the greater adsorption of 48/80 derived from the results of the 'constant-amount' titrations (Text-fig. 3*c* and Table 2).

The centre of the 48/80 bleb remains unblued with doses over 5 μg; at most it becomes pink with a purplish tinge, and sometimes there are small patches of haemorrhage (Text-fig. 1*f*). The absence of response may in part be due to temporary vasoconstriction by 48/80 itself or by the histamine it liberates, followed by recovery of normal permeability before the vessels become patent. But it is to a large extent due to a more permanent damage, presumably thrombotic, to the blood vessels, because the pink area remains when the surrounding skin is blackened by intra-arterial injections of indian ink; and the blocking of the vessels is evident in stained sections of the ink-treated skin.

Intradermal injection in the ear. Concentrations of 10 and 100 μg/ml. caused an immediate flushing; with 10 μg/ml. blueing started in 7 min, and with 100 μg/ml. in 1½ min. Blueing in a histamine bleb develops uniformly over the treated area, whereas that due to 48/80 begins at the edge of the bleb and after 5 min, along the course of the large vessels, particularly the arteries, lying under it. These paravascular streaks then coalesce to form a uniformly blue lesion. Above 250 μg/ml. this blueing occurs only at the periphery of the bleb. There is a central area whose size varies with the concentration, in which within 1½ min, the small superficial vessels thrombose without prior constriction. The underlying larger vessels become invisible but refill with circulating blood after about 10 min. By this time there is very slight blueing in the central area, so that by naked eye the lesion is faint purplish pink in the centre surrounded by deep blue (Pl. 2A). This central thrombosis and inhibition persist for over 6 hr.

Though 48/80 spreads outwards to blue an area 50–200 times that of the initial bleb, the resulting lesion is always round. Unlike histamine, 48/80, even at 10,000 μg/ml. does not leak in the lymphatic plexus beyond the confines of the bleb to produce a wedge-shaped blue lesion. Even when 48/80 is injected directly into the plexus, the blue area is approximately round (Pl. 2B). After 15 min or more a blue prolongation towards the base of the ear may develop, but this is observably the coloration of the lymphatic ducts with blue exudate from the bleb; it is not due to an increased permeability of blood vessels adjacent to the channels, as with histamine. These observations confirm the conclusions from the behaviour of 48/80 lesions in the skin of the trunk, that it is fixed firmly and rapidly to the tissue, whereas histamine at first moves freely, and begins to be fixed only after 2–3 min; and that inhibition at the centre is due to thrombosis of the vessels. Moreover, since 48/80 lesions blue as fast as histamine lesions, but no faster, and since the duration of the 48/80 effect is almost identical with that of histamine (Text-fig. 7*a*), it is probable that 48/80 liberates histamine very quickly and its latent period is mainly that of the liberated histamine.

Factors that change the skin-reactivity to 48/80. Blueing by 48/80, like that by histamine, is partly inhibited during anaesthesia and shock, and by

warming the animals in an atmosphere at 37° C. Sickly animals respond poorly to 48/80; this is probably not due to a diminution in the skin of histamine available for liberation, because the same animals are proportionally insensitive to histamine itself. As with histamine, most of the states of apparent insensitivity to 48/80 appear to be due to a poor blood supply to the skin.

Neoantergan intravenously is much less effective with 48/80 than with histamine. The effect of 8 mg/kg body weight 30 min before the injection of 48/80 is shown in Text-fig. 5*b*. Three concentrations of 48/80 and a saline control were titrated in blued animals, the four doses being randomized in a Latin square over sixteen sites. Three animals were used in each group so that each point is the mean of twelve readings. There is a 3-fold decrease in the 48/80 effect. In other tests 6 mg neoantergan/kg decreased the effect 5-fold, and 2 mg decreased it 2·5-fold. In a few animals the neoantergan greatly diminished the intensity but not the area of blueing by 48/80. The relative inefficiency of circulating neoantergan in antagonizing 48/80 suggests that 48/80 may have a more direct action on capillary permeability; histamine activity was reduced 9-fold by 0·02 mg neoantergan/kg, whereas as much as 6 mg/kg was required for a 5-fold decrease of 48/80 activity. Moreover, doses up to 15 mg/kg, which is near the LD50 of neoantergan, did not abolish the response to 48/80. It is possible that at the centre of the bleb, 48/80 itself is in a sufficiently high concentration to increase capillary permeability by direct action. Nevertheless, since the area of the 48/80 lesion is diminished by neoantergan, the drug in the concentrations obtaining at the edge of the lesion clearly act by liberating histamine. In the centre of the lesion, either the increase in permeability is not wholly due to histamine, or the available neoantergan is overwhelmed by histamine rapidly liberated by the high concentration of 48/80.

Fixation of 48/80. Superinjection of 0·2 ml. saline into lesions of various ages made by 2 μg of 48/80, failed to increase the lesion-diameter after 2–3 min. With larger doses, 48/80 remained free for a longer period, and superinjection increased the lesion-diameter after 10 min or more.

Duration. The increased permeability, as tested by late blueing, induced by a single dose, lasts for 7–10 min, after which it declines, so that after 20–25 min no blueing occurs. In the graph illustrating this recovery (Text-fig. 7*b*), the arrows indicate the period between 12 and 15 min, when the blueing ceases to be intense and becomes relatively feeble; the decrease in lesion-diameter does not fully indicate the recovery of the vessels, which is substantially complete at 12–15 min.

Immunity. The three experiments in Table 4 exemplify the immunity induced by 48/80 to test injection of the same substance. Thus in Expt. I, 2 μg partly, and 10 μg almost wholly, immunize to test doses of 10 μg. In Expt. II, 50 μg immunize to 50 μg to some extent after 30 min and well after 3 hr, whereas after 5 hr the immunity is wearing off. Immunity is maximum

between 1·5 and 3·5 hr (Expt. III). In the ear, a concentration of 20 μg/ml. immunizes well to test doses of the same concentration. Here also, the immunity is at a maximum between 1·5 and 3·5 hr, and then passes off gradually and is gone at 5–6 hr.

TABLE 4. Immunizing action of intradermal 48/80 and histamine. Means of four to six lesions

Expt.	Immunizing agent and dose (μg)		Age of primary lesion (hr)	Mean diameter (mm) and intensity* of reaction to test dose of	
				48/80 (10 μg)	Histamine (2 μg)
I	48/80	0	2	8·5 + +	7·0 f.
		2	2	2·0 f.	2·0 f.
		10	2	8·0 f.	2·0 f.
II	48/80	50	0·5	9 +	8·5 +
			3	1·5 f.	2·0 f.
			5	4 +	8·0 f.
	Histamine	5	0·5	9 + +	2±
			3	9 + +	8 f.
			5	8·5 + +	9 +
	Saline		0·5	10 + +	10 + +
			3	10·5 +	10·5 +
			5	10·5 +	10·5 +
III	48/80	30	0·5	5·2±	7·3 +
			1·5	1·8 +	2·0 f.
			2·5	0·0	0·7±
			3·5	3·8±	5·5 +
			4·5	3·3 +	6·5 +
			5·5	7·2 +	6·7 +
			6·5	6·2 +	6·7 +
	Saline		2·5	8·7 + +	6·7 +

* Intensity: symbols as Table 3.

The site of action of 48/80. The accumulation of blue at the level of the two plexuses of blood vessels in skin treated with 48/80, as compared with the more general blueing with histamine (Text-fig. 1) and the visible development of blueing along the larger vessels of similarly treated ears, suggests strongly that the main reservoirs of histamine available for liberation are closely associated with the smaller arteries and veins. The association of this histamine with blood vessels may also be inferred from the intensity of blueing induced in body skin by the two substances. The amount of histamine that can be extracted from the skin of the trunk is about 3 μg/g (Feldberg & Miles, unpublished work); and a 10 mm lesion occupies about 150 mg skin. The intensity of blueing induced by enough 48/80 to give a lesion-diameter of 10 mm is far greater than that produced by injecting 0·5 μg histamine (the amount that 48/80 presumably liberates) in about 0·35 ml. saline, a volume that will give a 10 mm lesion (see Text-fig. 3*b*). We conclude that after injection a great deal of this dose of histamine is ineffective because it is distributed through relatively non-vascular tissue, and that the endogenous histamine which can be liberated by 48/80 must be concentrated near or in the blood vessels.

Cross-immunity with histamine. As already noted, the lesions developing

after the injection of a substance into an already-injected site are variable and not easily measured. Cross-immunity is nevertheless obvious by reason of a decline in intensity or size or both, of the blued area. Tables 3 and 4 exemplify the results usually obtained. Histamine and 48/80 each induces a good immunity to itself; histamine induces only a fair immunity to 48/80, but 48/80 induces a good immunity to histamine. In the ear, concentrations of 20 μg/ml. of both induced a good though not marked cross-immunity between 48/80 and histamine. It appears, therefore, that 48/80 immunizes both by liberating histamine, which in turn immunizes the susceptible vessels, and either by exhausting the histamine which can be liberated in the skin or by interfering with the mechanism of release of the bound histamine not liberated by the immunizing dose.

Skin reactions to leukotaxine

In most respects, the reaction of the blood vessels to leukotaxine were remarkably similar to those produced by 48/80. The chief difference lay in the very high concentration of leukotaxine required to induce thrombosis of the vessels.

Intradermal injection in the trunk and the ear. Like 48/80, leukotaxine induces in 3–5 min a round area of intense blueing, the diameter of which is in proportion to the log. dose in the constant-volume titration (Text-fig. 3*d*) and to the log. volume in the constant-amount titration (Text-fig. 5*c*). Leukotaxine appears to be strongly adsorbed to the skin tissues (Table 2); minimal blueing dose in 0·1 ml. is about 1 μg; inhibition of blueing at the centre of the bleb may occur with amounts from 10 μg upwards, absent in some animals until 100–500 μg is reached. This inhibition is not permanent; the area blues within 15–25 min. With large doses, 2 mg or more, small areas of permanent inhibition are produced. On cross-section, the blue leukotaxine blebs are like those of 48/80 (Text-fig. 1*e*).

In the ear, concentrations of 200 μg/ml. and over induce a general dilatation of the small vessels within 30 sec, and a rapid blueing that starts first along the small vessels, then the larger veins and finally along the larger arteries within the bleb. When concentrations of 300 μg or more per ml. are placed near one of the larger veins or arteries, a narrow band of vasoconstriction may appear within 1 min, disappearing after 1–2 min. With concentrations above 2·5 mg/ml., thrombosis of the vessels may occur at the centre of the bleb, though it is less severe and less regular in occurrence than that induced by 48/80. The blued areas are always approximately round (cf. Pl. 2B) whether made by intradermal or intralymphatic injection.

Effect of anaesthesia and neoantergan. Blueing is diminished in area and intensity during bromethol and urethane anaesthesia. Intravenous neoantergan, 3–8 mg/kg body weight, diminishes the leukotaxine effect from 1·5- to

3-fold (Text-fig. 5*c*); the degree of neutralization is of the same order as that of 48/80, but rather less marked.

Time-course of the leukotaxine effect. By the superinjection method, putting 0·2 ml. saline into 5 μg lesions, all the leukotaxine appeared to be fixed in 16 min and most of it in the first 5–8 min. The capillaries of the skin treated with 10 μg wholly regained their normal impermeability within 25 min; most of them had recovered after 10 min (Text-fig. 7*a*, *b*).

Immunity. Table 5 typifies the results of several tests of leukotaxine immunity. Three immunizing doses of each substance, histamine, 48/80 and leukotaxine were used, and immunity tested after 2 hr by superinjecting the lowest dose again. As is common in all such tests, immunity is best when the

TABLE 5. Immunity and cross-immunity induced in the skin by leukotaxine. Primary lesions 2 hr old. Means of four lesions

Immunizing agent and dose (μg)		Mean diameter (mm) and intensity* of reaction to test dose of: Histamine (2 μg)	48/80 (5 μg)	Leukotaxine (17 μg)
Histamine	8	7·4±	N.T.	7·0++
	4	7·0±	N.T.	6·2++
	2	7·1±	7·0±	7·4++
	0	10·0+	7·8++	7·6++
48/80	20	N.T.	3·4±	2·0+
	10	N.T.	3·5±	2·2+
	5	8·0±	4·6±	5·0+
	0	9·0+	7·2++	8·0++
Leukotaxine	67	N.T.	N.T.	4·0±
	33	N.T.	N.T.	3·4±
	17	9·0±	7·1+	4·8±
	0	9·5+	7·8++	7·4++

* Intensity: symbols as in Table 3.
N.T. = No test.

immunizing dose is 4–10 times greater than the test dose. In this example immunity must be judged as much by decrease in intensity as by decrease in diameter of the blueing. Leukotaxine immunizes well to itself but only moderately to histamine and 48/80. Histamine immunizes moderately to itself and 48/80, and slightly to leukotaxine; whereas 48/80, though immunizing only moderately to histamine, immunizes well to itself and leukotaxine. Leukotaxine immunity is maximal in 1–2 hr, and has passed off by the 4th hr.

DISCUSSION

The study of increased permeability in the skin of the trunk of blued guinea-pigs has shown that after a latent period of 1½–3 min, injected histamine induces a gross increase in capillary permeability, which is maximum within the next 5 min. In concentrations of from 1 to 100 μg/ml. it can be characterized by the response of blued animal to varied doses in constant injection-volume

and to constant doses in varied injection-volume. By the superinjection of saline into histamine lesions of varying ages, and by the intravenous injection of dye at varying periods after the intradermal histamine, it can be shown that from 3 to 10 min free histamine is disappearing from the lesion, and the capillaries are recovering their normal low permeability. By the superinjection of histamine into recovered histamine-treated areas, it can be shown that as they recover, the vessels become partly immune to histamine; the immunity increases up to 2 hr, and declines after 4 hr. This immunity is not due to any interruption of the blood supply to the immunized tissues. With concentrations above 100 μg/ml. no blueing due to increased permeability is detectable.

In the ear, the outstanding peculiarity is the high concentration required to produce even a 15 min inhibition of blueing at the centre of the lesion, and the transience of the effect with lower concentrations (p. 237 and Table 6).

TABLE 6. Comparison of the approximate minimal effective concentrations of histamine, 48/80 and leukotaxine in the skin of the trunk (10 mm blebs) and the ear (3 mm blebs)

Effect	Drug	Minimal effective concentration in μg/ml. Trunk	Ear
Blueing	Histamine	1–2	0·5
	48/80	2	5·0
	Leukotaxine	10	—
Temporary inhibition of blueing, and arterial constriction*	Histamine	10–30	50
	48/80	10–30	250
	Leukotaxine	100	300
Thrombosis of blood vessels	48/80	30–50	250
	Leukotaxine	2500	5000
Leak of free drug into surrounding lymphatic plexus	Histamine	—	1000
	48/80	—	>10000
	Leukotaxine	—	>10000

* Presumed in trunk, demonstrable in ear.

In the skin of the trunk inhibition lasts for hours. For this relative permanence we postulated an arterial vasoconstriction, and therefore an absence of exudation, for periods longer than the duration of increased permeability. This relation does not hold in the ear because vasoconstriction is visibly relaxed within 3–7 min, and increased permeability lasts up to 8 min and may persist, though feebly, for 12–15 min. The relative insensitivity of the ear to this inhibitory effect may be a reflexion of its greater vascularity; either the injected histamine is swept away by the blood and lymph streams more quickly or much of the injected histamine is taken up by receptors in the numerous small vessels, so that on reaching the underlying larger vessels its concentration is too low for vasoconstriction. As Table 6 shows, the ear displays the same relative insensitivity towards 48/80 and leukotaxine, and presumably for the same reasons.

The action of 48/80 in many ways resembles that of histamine. Both substances have a latent period of about 3 min. When blueing starts they become 'fixed' to the tissues; as blueing proceeds, the vessels recover their normal low permeability and are apparently normal at the end of 10–20 min. They are at this time partly immune to second doses of the same size, and the immunity increases for 2 hr; and after 4 hr it begins to decline. But there are marked differences, which raise the question how far the release of histamine accounts fully for the action of 48/80 on capillary permeability? First, the distribution of blueing by histamine is general, but that produced by 48/80 is concentrated in the region of the arteries and veins in both the skin of the trunk and the ear, suggesting that bound histamine is localized in or near these larger vessels. Secondly, whereas high concentrations of histamine inhibit blueing by altering the immunity of the vessels, high concentrations of 48/80 do so by damaging the vessels so that thrombosis occurs. Thirdly, the two substances differ in their susceptibility to circulating neoantergan; we have to assume either that 48/80 has a direct action on capillaries, or that the histamine it releases is less sensitive than injected histamine to neoantergan. Since 48/80 is well established as a potent histamine-liberator (Feldberg & Paton, 1951; Paton, 1951; Paton & Schachter, 1951) the second assumption is the more justified, particularly because insensitivity to antihistaminics is displayed by other known histamine-liberators (MacIntosh & Paton, 1949). Although in our experiments complete extinction of 48/80 blueing by neoantergan was impossible, partial neutralization was achieved by 200 times the dose required to neutralize histamine to the same extent. The parallelism of dosage-response in untreated and neoantergan-treated animals (Text-fig. 5*b*) is consistent with a true neutralization, and with the hypothesis that the unneutralized blueing is due to some 'pharmacological inaccessibility' of the liberated histamine rather than to a direct action of 48/80 on the capillaries. This inaccessibility may result from the ready adsorption of 48/80 to the tissues, and the concentration of the depots of available histamine near the blood vessels. This histamine is perhaps 'intrinsic' in Dale's (1948) sense that it is released from the cells on which it acts. Our observations are not exact enough to decide this point. But whatever reason for the relative inefficacy of neoantergan with 48/80, the fact indicates that we need not demand of a presumed histamine-liberator that its susceptibility to inhibition by neoantergan shall be of the same order as that of histamine.

Our observations on 48/80 provide a pattern of the intradermal behaviour of a histamine-liberator, for comparison with substances like leukotaxine, whose capacity to liberate histamine is in doubt. Menkin (1936, 1938*a*; *b*) isolated leukotaxine from sterile inflammatory exudates, and described its capacity to increase capillary permeability. Later work (Duthie & Chain, 1939; Spector, 1951) proved it to be a family of positively chemotactic

polypeptides, of which the larger members have this action on the capillaries. Rocha e Silva & Dragstedt (1941) postulated that leukotaxine acted via histamine, and Dekanski (1949) showed that on intradermal injection it increased the histamine equivalent in cat's skin, and that its 'blueing' action was neutralized by neoantergan. Menkin (1936, 1938*a*), and Cullumbine & Rydon (1946) deny the mediation of histamine because leukotaxine does not cause contraction in isolated smooth muscle, and the blueing is not antagonized by neoantergan (Cullumbine, 1947). We shall not, however, expect a histamine-liberator to cause isolated smooth muscle to contract. Menkin (1938*a*) showed that leukotaxine did not do so; but neither does 48/80 (Paton, 1951). Nor is Cullumbine's failure to detect a neoantergan effect by roughly quantitative tests unexpected. Leukotaxine in the skin can have a very shallow dosage-response slope, so that as much as a 10-fold drop in potency might diminish the diameter of the lesion by as little as 2 mm. Unless the neutralization test is made at several dose-levels in several animals, a genuine though small neutralization effect might well be missed. The relative insusceptibility of leukotaxine to neoantergan may well be determined by factors responsible for the similar behaviour of 48/80 and other liberators. Leukotaxine differs from histamine in spreading less readily through the tissues after local injection, as first recorded by Menkin, and in failing to induce inhibition at the centre of injection blebs, except in high concentrations. If it acts solely by histamine-liberation, inhibition of blueing may be impossible because there is not enough histamine to reach required concentration, even though it is localized round the vessels upon which it ultimately acts. An inhibiting dose of histamine, say 5 μg, produces a lesion about 8 mm in diameter, involving about 60 mg of skin. Ignoring spread to adjacent tissues, we arrive at an average inhibiting concentration of 83 μg histamine/g skin; whereas the normal content of extractable histamine in the skin of the trunk is of the order of 3 μg/g (W. Feldberg & A. A. Miles, unpublished work). This histamine is presumably all available for liberation. Leukotaxine, except for its inability to induce thrombosis in moderate concentrations, behaves in most respects like 48/80. Both these substances resemble histamine in several respects, notably the similarity of the time-course of blueing (the lag period and duration of permeability) and in the induction and duration of immunity.

We can attach weight to these likenesses as a proof that leukotaxine acts through histamine if the effects are peculiar to histamine. This may well be so, but it should be noted that the time-course of blueing, and duration of permeability is shared by a large number of blueing substances besides 48/80, e.g. neoarsphenamine, stilbamidine, acetylcholine, peptone and hypotonic saline (unpublished work); and though some of these substances are probably histamine-liberators, the time course of their effect may reflect very general properties of vascular endothelium. The evidence obtained from the cross-

immunization tests, which are summarized in Table 7, may be misleading for a similar reason, that in the endothelium there is only one kind of site which is affected, and made resistant, by a wide variety of substances. In addition, cross-immunity between substances other than histamine does not necessarily imply the same site of action. Cross-immunity between histamine and another substance may well be an expression of true histamine immunity; but cross-immunity between two presumed histamine-liberators may be due either to exhaustion of the available histamine, to the immunization of vessels by liberated histamine or to an inhibition of the mechanism of histamine release.

TABLE 7. Summary of tests of immunity and cross-immunity to increased capillary permeability in the skin

	Immunity		
	Tested with		
Induced by	Histamine	48/80	Leukotaxine
Histamine	+ +	+	+
48/80	+ + +	+ + +	+ + +
Leukotaxine	+ +	+	+ + +

+, + +, + + + = moderate, good and marked immunity.

It should be noted here that we have used the very general terms 'immunity' and 'immunization' in this connexion, rather than 'refractoriness' or 'refractory state' because we have applied them generally to drug-resistance induced in the skin by substances other than histamine. The terms can legitimately be extended to cover these phenomena; and though our histamine 'immunity' may be the same phenomenon as Lewis & Grant's (1924) refractoriness to histamine whealing in man, we are not in a position to equate them. The two phenomena have much in common; whealing was inhibited in man by occlusion of the blood supply for 10 min and our blueing is inhibited by withholding the circulating dye for 10 min. Both were relative, never demonstrably absolute. But whereas in man the refractory state lasts 5–10 min, the immune state lasts several hours in the guinea-pig. The immunity induced by histamine, leukotaxine and 48/80 in some respects resembles the immunity to whealing of nervous origin described by Grant, Pearson & Comeau (1935). In both cases it lasts for several hours, and both are explicable in terms of an exhaustion of a substance like histamine or H-substance increasing capillary permeability.

The cross-immunity we demonstrated was never very solid. This may have been due to deviations from the exact superposition of the test injection on the region of immunized tissue, and to the different degrees of tissue affinity of the three substances tested. It may, however, reflect a distinction between the modes of action; though as regards leukotaxine, it is probably significant that the histamine-liberator 48/80 immunized well against leukotaxine. Although cross-immunity should not be accepted as a sufficient single criterion

of similarity of action, in conjunction with other evidence it is strongly suggestive.

Our various tests of the increase of capillary permeability in the skin by the three substances, do not constitute a rigorous proof that the effect of 48/80 and leukotaxine on the capillary endothelium of the skin is mediated by histamine. Nevertheless, taking the evidence as a whole, our observations on these three substances are all consistent with the view that leukotaxine acts as a histamine-liberator in inflammatory lesions. The question whether histamine, through leukotaxine or some other endogenous liberator, is the *sole* mediator of the increased capillary permeability in inflammation, is less easy to answer. A given blood vessel made permeable by histamine or leukotaxine becomes substantially immune to the further action of the drugs within 20 min. The 'perpetuation of increased vessel permeability due to the gradual accumulation of peptides in the tissues' postulated by Spector (1951) in the natural course of inflammation must therefore be produced either by partial stimulation, and consequently only a partial immunization, of some parts of the vessel, leaving other parts for later stimulation; or, what is more consistent with the observed expansion of most progressive inflammatory lesions, by a gradual outward spread of leukotaxine to as yet unaffected vessels, leaving impermeable those already affected. But even with these refinements, the major role of leukotaxine is not necessarily established in inflammation, particularly infective inflammation. For example, the time-course of blueing by several clostridial exotoxins is quite different from that of leukotaxine (unpublished work); blueing may take an hour to develop and permeability persist for several hours; and cross-immunity with histamine and histamine-liberators is difficult to demonstrate. The behaviour of *Cl. oedematiens* exotoxin is singular, because the increased capillary permeability induced by a single dose persists for more than 30 hr. This observation probably has some bearing on the extensive oedema which accompanies infection by this microbe, but in this context it is chiefly interesting as indicating the existence of substances of pathological importance which appear to alter capillary permeability in a manner quite different from that of histamine or histamine-liberators.

SUMMARY

1. The increase in capillary permeability in the skin of the trunk, and ear of guinea-pigs was measured by the size and intensity of the blue lesion induced by the intradermal injection of histamine, the histamine-liberator 48/80, and leukotaxine, in animals with pontamine sky blue 6X in their circulation. In the trunk, the mean lesion-diameter from graded doses of these drugs in a constant volume is proportional to the log. dose; and for a constant dose in graded injection-volumes it is proportional to the log. volume.

2. The linear dosage-response to histamine, 48/80 and leukotaxine forms the basis of an assay method in the 'constant-volume' titration; 'constant-dose' measurements can be used to measure the affinity of skin tissue for the three substances.

3. Histamine has a relatively low, and 48/80 and leukotaxine a relatively high, affinity for skin tissue. Injected histamine spreads readily with the injection fluid to the subcutaneous tissues and lymphatic channels, whereas 48/80 and leukotaxine tend to remain in the skin.

4. All three substances increase capillary permeability within 3–5 min of injection, and their action is mostly finished in 10–15 min, and wholly so in 30 min. Between 15 and 30 min after the injection, the capillaries not only begin to recover their normal low permeability, but become immune to further doses of the drug. The immunity is greatest from 1–3 hr and declines after 4–5 hr.

5. Histamine blueing is general throughout the depth of the skin; 48/80 blueing is most intense in the region of arterioles, venules and the smaller arteries and veins, suggesting that the histamine available for liberation is located in these regions.

6. High local concentrations of histamine inhibit blueing by inducing severe local vasoconstriction during the period of increased permeability, so that by the time the constriction is relaxed the vessel walls have recovered their normal low permeability. High local concentrations of 48/80 inhibit blueing by thrombosing the blood vessels.

7. Anaesthesia, shock and chilling decrease blueing. The effect appears to be secondary to a decline in local intravascular pressures, and not to resistance of the capillaries to permeability-inducing substances.

8. Circulating neoantergan strongly antagonizes histamine blueing. It is over 200 times less effective with 48/80 and leukotaxine, but a definite antagonism to both substances is demonstrable.

9. The three substances induce a substantial cross-immunity to one another. The cross-immunity to histamine is presumably due to histamine liberated by 48/80 and leukotaxine. Cross-immunity between histamine-liberators may be due either to histamine immunization of the blood vessels, exhaustion of histamine or inhibition of the mechanism of histamine release.

10. The similarities in the time-course and duration of the permeability effect, and in the induction of cross-immunity, give strong support to the view that leukotaxine increases capillary permeability by liberating histamine. In all the tests made, the differences between leukotaxine and histamine were paralleled by differences between 48/80 and histamine, excepting the thrombosing effect of strong 48/80. Since 48/80 is an established histamine-liberator, these differences are not good evidence that substances displaying them do not liberate histamine.

We are greatly indebted to Dr E. J. de Beer at the Wellcome Research Laboratories, Tuckahoe, U.S.A., for a generous gift of the compound 48/80, and to our colleague Dr J. H. Humphrey for leukotaxine.

REFERENCES

BAIN, W. H. (1949). The quantitative comparison of histamine antagonists in man. *Proc. R. Soc. Med.* **42**, 615–623.

BALTZLY, R., BUCK, J. S., DE BEER, E. J. & WEBB, F. J. (1949). A family of long-acting depressors. *J. Amer. chem. Soc.* **71**, 1301–1305.

CULLUMBINE, H. (1947). Leukotaxine and histamine. *Nature, Lond.*, **159**, 841–842.

CULLUMBINE, H. & RYDON, H. N. (1946). A study of the formation, properties and partial purification of leukotaxine. *Brit. J. exp. Path.* **27**, 33–46.

DALE, H. H. (1948). Antihistamine substances. *Brit. med. J.* ii, 281–283.

DEKANSKI, J. (1949). The effect of protein hydrolysates (leukotaxine) on skin-histamine in cats. *J. Physiol.* **108**, 233–245.

DUTHIE, E. S. & CHAIN, E. (1939). A polypeptide responsible for some of the phenomena of acute inflammation. *Brit. J. exp. Path.* **20**, 417–429.

EVANS, D. G., MILES, A. A. & NIVEN, J. S. F. (1948). The enhancement of bacterial infections by adrenaline. *Brit. J. exp. Path.* **29**, 20–39.

FELDBERG, W. & PATON, W. D. M. (1951). Release of histamine from skin and muscle in the cat by opium alkaloids and other histamine liberators. *J. Physiol.* **114**, 490–509.

GRANT, R. T., PEARSON, R. S. B. & COMEAU, W. J. (1935). Observations on urticaria provoked by emotion, by exercise and by warming the body. *Clin. Sci.* **2**, 253–272.

HECHTER, O. (1946). Mechanism of hyaluronidase action in skin. *Science*, **104**, 409–411.

LEWIS, T. & GRANT, R. T. (1924). Vascular reactions of the skin to injury. II. The liberation of a histamine-like substance in injured skin; the underlying cause of factitious urticaria and of wheals produced by burning; and observations upon the nervous control of certain skin reactions. *Heart*, **11**, 209–265.

LONG, D. A. & MILES, A. A. (1950). Opposite actions of thyroid and adrenal hormones in allergic hypersensitivity. *Lancet*, i, 492–495.

MACINTOSH, F. C. & PATON, W. D. M. (1949). The liberation of histamine by certain organic bases. *J. Physiol.* **109**, 190–219.

MATOLSTY, A. G. & MATOLSTY, M. (1951). The action of histamine and anti-histaminic substances on the endothelial cells of the small capillaries in the skin. *J. Pharmacol.* **102**, 237–249.

MENKIN, V. (1936). Studies on inflammation. XII. Mechanism of increased capillary permeability. A critique of the histamine hypothesis. *J. exp. Med.* **64**, 485–502.

MENKIN, V. (1938*a*). Studies on inflammation. XIV. Isolation of the factor concerned with increased capillary permeability in injury. *J. exp. Med.* **67**, 129–144.

MENKIN, V. (1938*b*). Studies on inflammation. XV. Concerning the mechanism of cell migration. *J. exp. Med.* **67**, 145–152.

MILES, A. A. (1949). The fixation of diphtheria toxin to skin tissue with special reference to the action of circulating antitoxin. *Brit. J. exp. Path.* **30**, 319–344.

MILES, A. A. & NIVEN, J. S. F. (1950). The enhancement of infection during shock produced by bacterial toxins and other agents. *Brit. J. exp. Path.* **31**, 73–95.

PATON, W. D. M. (1951). Compound 48/80: a potent histamine liberator. *Brit. J. Pharmacol.* **6**, 499–508.

PATON, W. D. M. & SCHACHTER, M. (1951). The influence of an antihistamine drug on the release of histamine in the unanaesthetized dog. *Brit. J. Pharmacol.* **6**, 509–513.

ROCHA E SILVA, M. & DRAGSTEDT, C. A. (1941). Observations on the trypan blue capillary permeability test in rabbits. *J. Pharmacol.* **73**, 405–411.

SPECTOR, W. G. (1951). The role of some higher peptides in inflammation. *J. Path. Bact.* **63**, 93–110.

WADLEY, F. M. (1949). The use of biometric methods in comparisons of acid-fast allergens. *Amer. Rev. Tuberc.* **60**, 131–139.

A

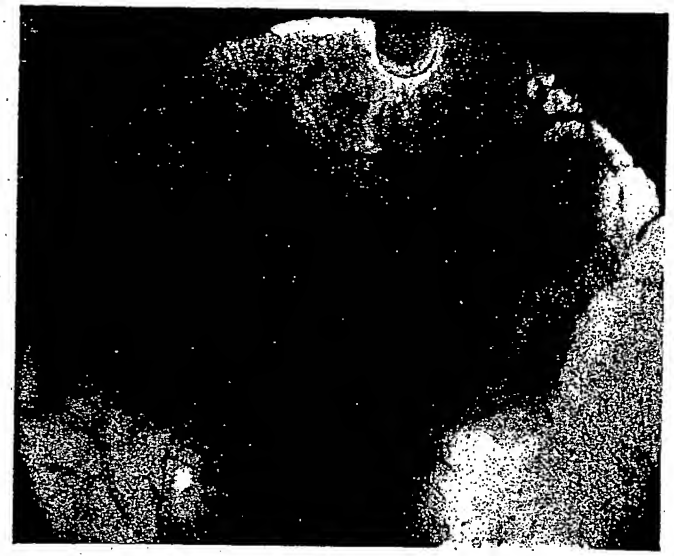

B

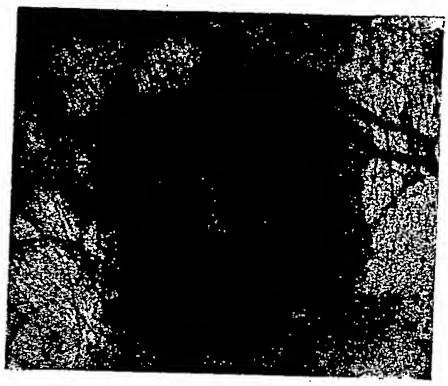

A

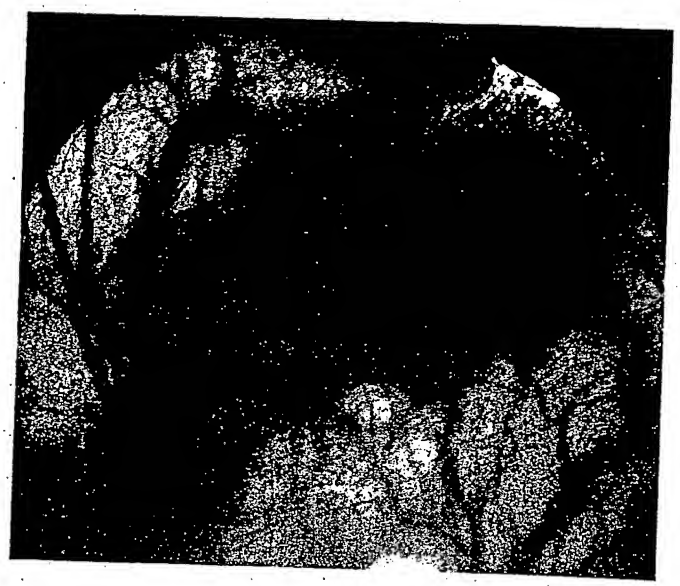

B

A. Untreated ear of blued
due to the relative thi
B. The same ear as in A a
phatic plexus. The ind
of intense blueing is ap

A. Ear of a blued guinea-pi
at the centre of the le
B. Ear of a blued guinea-
phatic plexus. The ops
ear. The area of inten

EXPLANATION OF PLATES

PLATE 1

A. Untreated ear of blued guinea-pig, showing the degree of initial opacity near the main vessels, due to the relative thickness of the ear in that region. ×5.

B. The same ear as in A after injection of strong histamine (1000 μg/mL) directly into the lymphatic plexus. The indian-ink stain on the skin at the top marks the injection site. The area of intense blueing is approximately wedge shaped, with the apex at the base of the ear. ×5.

PLATE 2

A. Ear of a blued guinea-pig injected with strong 48/80 (500 μg/ml.). There is inhibition of blueing at the centre of the lesion, with the thrombosed superficial vessels in sharp focus. ×5.

B. Ear of a blued guinea-pig after injection of strong 48/80 (150 μg/ml.) directly into the lymphatic plexus. The opacity round the main vessels on the left is due to the thickness of the ear. The area of intense blueing is approximately circular. ×5.

EXHIBIT B

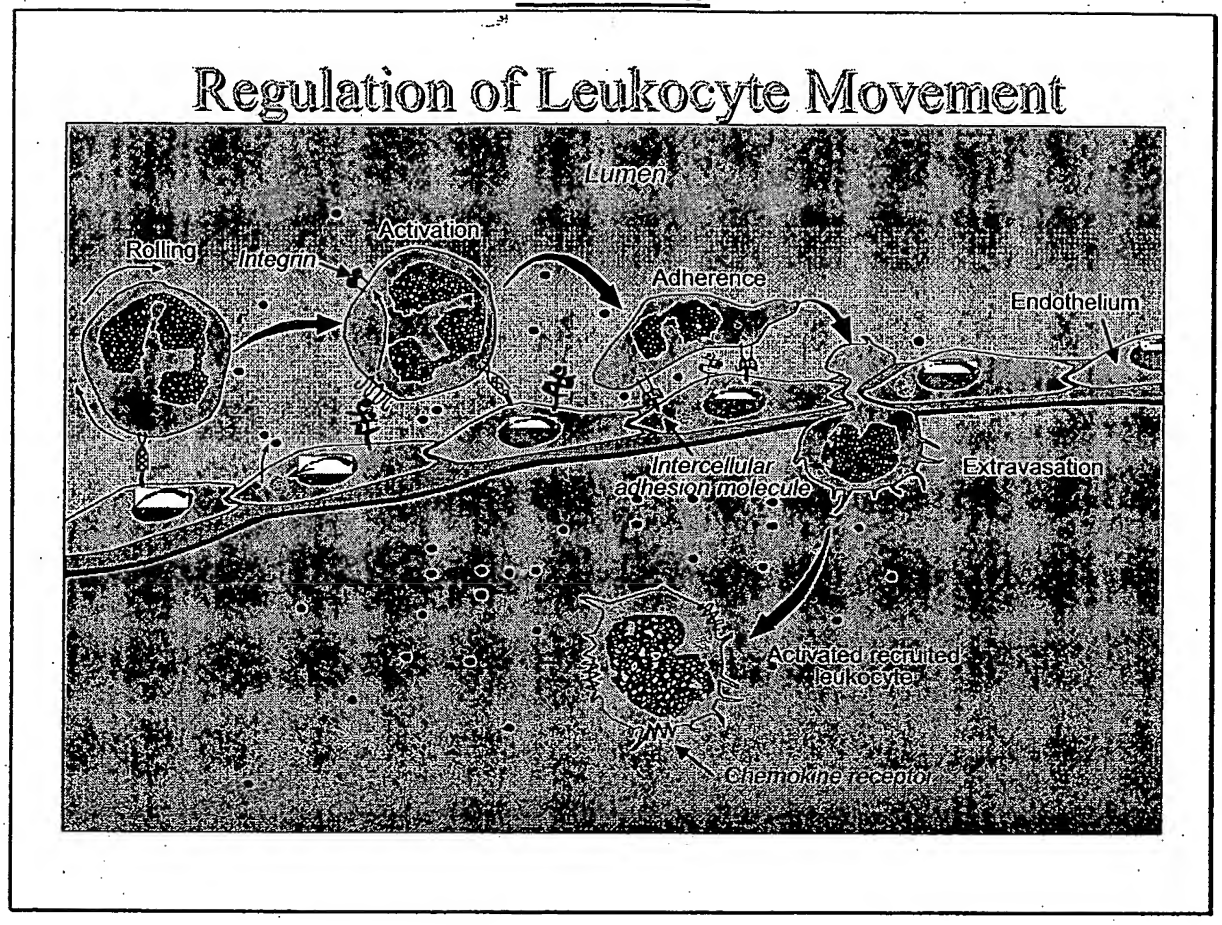
Regulation of Leukocyte Movement
Lumen
Rolling
Integrin
Activation
Adherence
Endothelium
Intercellular adhesion molecule
Extravasation
Activated recruited leukocyte
Chemokine receptor

Annu. Rev. Immunol. 1997. 15:675–705

HUMAN CHEMOKINES: An Update

Marco Baggiolini, Beatrice Dewald, and Bernhard Moser
Theodor Kocher Institute, University of Bern, CH 3000 Bern 9, Switzerland;
e-mail: baggiolini@tki.unibe.ch

KEY WORDS: structure, structure-activity relations, receptors, leukocyte migration, pathophysiology, HIV

ABSTRACT

Interleukin 8, the first chemokine to be characterized, was discovered nearly ten years ago. Today, more than 30 human chemokines are known. They are often upregulated in inflammation and act mainly on leukocytes inducing migration and release responses. The present review deals largely with the new developments of the last three years. Several structural studies have shown that most chemokines form dimers. The dimers, however, dissociate upon dilution, and the monomers constitute the biologically active form. Chemokine activities are mediated by seven-transmembrane-domain, G protein coupled receptors, five of which were discovered in the past three years. The primary receptor-binding domain of all chemokines is near the NH_2 terminus, and antagonists can be obtained by truncation or substitutions in this region. Major progress has been made in the understanding of chemokine actions on T lymphocytes that respond to several CC chemokines but also to IP10 and Mig, two CXC chemokines that selectively attract Tcells via a novel receptor. Effects of chemokines on angiogenesis and tumor growth have been reported, but the data are still contradictory and the mechanisms unknown. Of considerable interest is the recent discovery that some chemokines function as HIV-suppressive factors by interacting with chemokine receptors which, together with CD4, were recognized as the binding sites for HIV-1.

INTRODUCTION

Chemokines constitute a large family of small cytokines with four conserved cysteines linked by disulfide bonds (Figure 1). Two subfamilies, CXC and CC chemokines, are distinguished according to the position of the first two cysteines, which are separated by one amino acid or are adjacent. Most chemokine sequences were derived from cDNAs encoding proteins of 92 to 125 amino acids with leader sequences of 20 to 25 amino acids. In humans, the genes of the CXC chemokines are clustered on chromosome 4, and those of the CC

0732-0582/97/0410-0675$08.00

Table 1 Ligand selectivity of chemokine receptors

Receptors	New	Old nomenclature	Ligands[a]
CXC chemokines	CXCR1	IL-8R1 (type A)	IL-8
	CXCR2	IL-8R2 (type B)	IL-8, GROα,β,γ, NAP-2, ENA78, GCP-2
	CXCR3	IP10/MigR	IP10, Mig
	CXCR4	LESTR, HUMSTR	SDF-1
CC chemokines	CCR1	RANTES/MIP-1αR	RANTES, MIP-1α, MCP-2, MCP-3
	CCR2a/b	MCP-1RA/B	MCP-1, MCP-2, MCP-3, MCP-4
	CCR3	EotaxinR, CC CKR3	eotaxin, RANTES, MCP-3, MCP-4
	CCR4	CC CKR4	RANTES, MIP-1α, MCP-1
	CCR5	CC CKR5	RANTES, MIP-1α, MIP-1β

[a]K_d of 0.1 to 10 nM or Ca^{2+} mobilization at <10 nM.

chemokines on chromosome 17. As indicated by the rapidly expanding literature, chemokines are increasingly studied because of their actions on leukocytes and their role in inflammation and immunity. Additional interest is arising from the recent discovery of a function of chemokines and chemokine receptors in HIV infection. Because of space limitations, we shall concentrate on new, biologically important findings on human chemokines reported during the past three years. For older reports, the reader may turn to our last, comprehensive review, which appeared at the beginning of 1994 and covered the literature up to the middle of 1993 (1). Several other reviews that have appeared since 1994 may also be consulted (2–4). The new, simplified nomenclature for chemokine receptors, which was elaborated at the 1996 Gordon Research Conference on "Chemotactic Cytokines" (Table 1), will be used.

CHEMOKINE STRUCTURE

Three-Dimensional Structure of CXC and CC Chemokines

The first chemokines for which the three-dimensional structure was determined are PF4 and IL-8. Their monomeric structures are very similar and comprise a NH_2-terminal loop, three antiparallel β-strands connected by loops, and a COOH-terminal α-helix. IL-8 forms globular dimers in solution consisting of a six stranded antiparallel β-sheet (made up of the three β-strands of each subunit) and two antiparallel helices lying across the β-sheet. The axis of symmetry is located between residues 26 and 26′ at the center of strands β1 and β1′ (5–7). PF4 forms an asymmetric tetramer by the dimerization of dimers of the IL-8 type (8). The structures of GROα and NAP-2 are similar to that of IL-8, at both the monomer and dimer level (9–12). GROα differs from IL-8 in the NH_2-terminal region containing the ELR motif, the NH_2-terminal loop extending between residues 12 and 23, and the turn between residues 31 and 36,

which is linked to the NH_2-terminal region through the 9 to 35 disulfide bond. These regions are involved in receptor interaction (13), and the differences could determine receptor specificity.

The three-dimensional structure of MIP-1β (14) and RANTES (15, 16) consists of dimers formed by interaction of the NH_2-terminal regions of the monomers yielding an elongated, cylindrical shape. The axis of symmetry is located between residues 10 and 10′ in MIP-1β and 9 and 9′ in RANTES. These residues are part of an additional, short antiparallel β-sheet formed by the strands $\beta 0$ and $\beta 0'$. The distribution of surface hydrophobicity differs markedly between CXC and CC chemokines (17), and this is believed to be the reason for the different mode of dimerization (7, 17). The core hydrophobicity clusters of CXC and CC chemokines, by contrast, are at equivalent positions, in agreement with the similarity of the three-dimensional structure of the monomers.

Monomers and Dimers

Because most chemokines dimerize in solution, the dimer was generally assumed to be the biologically relevant form. Although the biological activities are observed at nanomolar concentrations, while the dissociation constants are mostly in the micromolar range (18, 19), this remained the prevailing view until proof was provided that IL-8 can function as a monomer (20). For this purpose an IL-8 analog was synthesized with N-methyl-Leu instead of Leu at position 25 to disrupt hydrogen bonding between the monomers. The methylated analog remains monomeric even at millimolar concentration and has nonetheless full activity on neutrophils (20). Its three-dimensional structure is similar to that of the subunits of the IL-8 dimer, indicating that the constraints imposed by dimer formation are not critical for the tertiary fold (21). Among the CC chemokines, monomeric forms of MIP-1α were studied extensively and found to be biologically active (22–24). Data obtained by size exclusion HPLC, analytical ultracentrifugation, chemical cross-linking, and titration microcalorimetry support the conclusion that IL-8 and MCP-1, at physiological concentrations, occur predominantly as monomers (18, 25). Platelet basic protein (PBP) and its congeners including NAP-2 appear to behave in a similar manner (10). A different view was presented for MCP-1 based on the observations that chemically cross-linked dimers were active at nanomolar concentrations and that an antagonist obtained by NH_2-terminal truncation formed a heterodimer with wild-type MCP-1 acting as a dominant negative inhibitor (26).

NEW CHEMOKINES AND CHEMOKINE ACTIONS

Many new human chemokines have been discovered in the past few years, and considerable new information has been gathered about their activities on

different types of leukocytes. Several of the more than 30 gene products, however, are known just by the cDNA-deduced amino acid sequence, and little information is available on biological effects. The dendrogram in Figure 1 presents all human chemokines described to date. Although the number has grown considerably, CXC and CC chemokines still fall into completely separate branches. Most new chemokines belong to the CC subfamily. They include: (i) eotaxin (27) and MCP-4 (28), which are structurally closely related to MCP-1; (ii) HCC-1 and a newly identified alternative splicing variant HCC-3, which are similar to MIP-1α (29); (iii) TARC (thymus and activation-regulated chemokine), obtained from thymus-derived RNA, and reported to be chemotactic for T cell lines but not for blood T lymphocytes, monocytes, or neutrophils (30); and (iv) HCC-2, a CC chemokine with six instead of four cysteines located at identical positions as in the murine chemokines C10 (31), CCF18 (32), MRP-2 (33), and MIP-1γ (34). Several new chemokine cDNAs were isolated from human tissues within a large-scale cDNA sequencing program (Human Genome Sciences Ltd, Rockville, MD), and the mature proteins were expressed in insect cells (Figure 1). Some of the new CC chemokines are virtually inactive on granulocytes, monocytes, and lymphocytes, suggesting that they may stimulate precursor cells or other targets. It is important to realize, however, that the actual NH_2 terminus of these chemokines is unknown and that lack of activity may result from incorrect processing upon expression in insect cells.

The following subsections describe several newly discovered chemokines and some known ones for which interesting new properties were found. The chemokine receptors, to which reference is made, are described in a later section and Table 1.

The Monocyte Chemotactic Proteins

MCP-1 was the first CC chemokine to be characterized biologically and shown to attract monocytes but not neutrophils (1). Two related proteins, MCP-2 (HC-14) and MCP-3, were subsequently identified (35), and MCP-4 was described only recently (28). The MCPs share a pyroglutamate proline NH_2-terminal motif and are structurally closely related to each other and to eotaxin (56% to 71% amino acid sequence identity) (Figure 1). They have a broad spectrum of activity and attract monocytes (28, 36), T lymphocytes (37–39), and basophil leukocytes (1, 40–42). MCP-2, MCP-3, and MCP-4, in contrast to MCP-1, are also active on eosinophil leukocytes (28, 40, 42). These patterns can be explained with a minimum of three receptors: CCR1 recognizing RANTES, MCP-2, and MCP-3; CCR2 recognizing all MCPs; and CCR3 recognizing RANTES, MCP-3, MCP-4, and eotaxin. Monocytes and presumably also basophils express CCR1 and CCR2, and eosinophils express CCR1 and CCR3

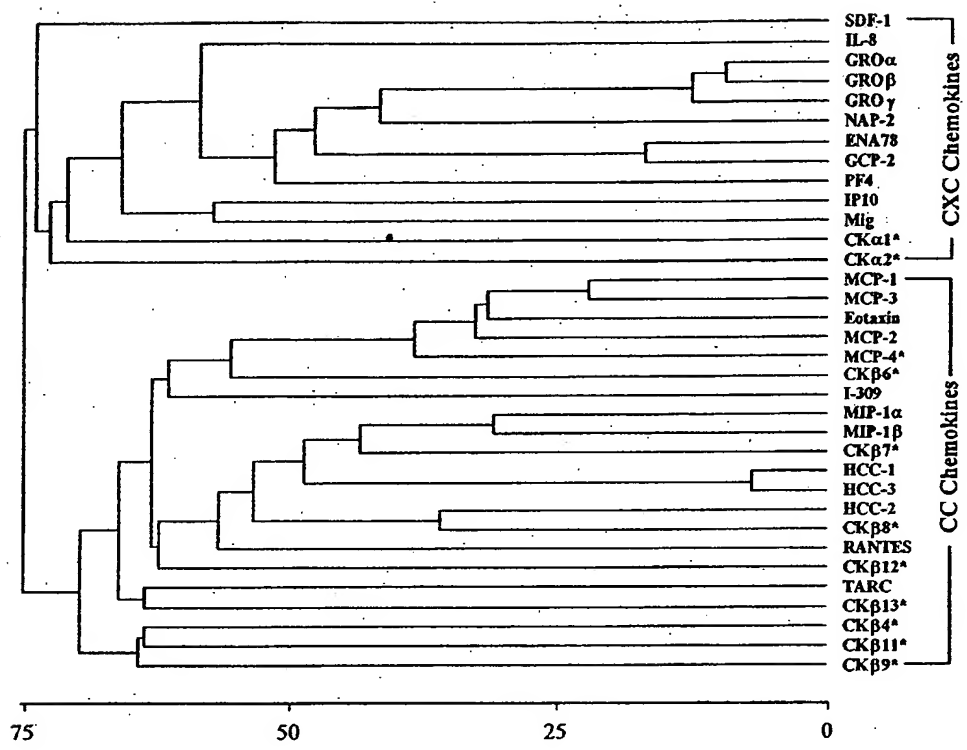

Figure 1 Structure similarity diagram of human CXC and CC chemokines. Similarity scores of the proteins were determined by the average linkage cluster analysis (181). The gap penalty, window size, filtering level, and K-tuple size parameters for pairwise alignments were set at 3, 10, 2.5 and 1, respectively. Distance to the branching points indicates the percent of sequence divergence. Highest pairwise similarity (7.5% divergence) is obtained for the CC chemokines HCC-1 and HCC-3, which differ only in the NH_2-terminal region preceding the adjacent cysteines. Overall similarity between the two subfamilies of chemokines is 24.5% (75.5% divergence). Chemokines from Human Genome Sciences Ltd. are listed by their laboratory abbreviation, CKα or CKβ (for CXC and CC chemokines, respectively) followed by a number. GeneBank accession numbers for the sequences are (from top to bottom): U16752, M17017, J03561, M36820, M36821, M54995, L37036, P80162, M20901, X02530, X72755, X14768, X72308, U18941, P80075, M57502, X03754, J04130, Z49270, Z70293, Z70292, M21121, and D43767. The accession numbers for the chemokines marked with an asterisk are not available.

(2, 3, 43, 44). The picture may become more complex when CCR4 and CCR5 are considered, but the distribution of these receptors and their selectivity must first be studied in more detail. In basophils, MCP-1 is highly effective as a stimulus of histamine and peptido-leukotriene release, but it has only moderate chemotactic activity, whereas RANTES is a strong chemoattractant and a weak inducer of mediator release. This suggests that CCR1 and CCR2 are functionally different, and indeed, maximum migration and release are obtained with MCP-3 that binds to both receptors (2).

Of particular interest are the effects of the MCPs on lymphocytes. Studies on human $CD4^+$ or $CD8^+$ T cell clones (28, 37) and human blood lymphocytes (38, 39) show that all four MCPs are potent attractants for activated T lymphocytes. Under similar conditions, MCP-1, MCP-3, and MCP-4 attract more cells than do RANTES, MIP-1α, and MIP-1β across bare or endothelial cell-coated filters. All MCPs also induce a transient *B. pertussis* toxin–sensitive rise in the cytosolic free Ca^{2+} concentration ($[Ca^{2+}]_i$) in $CD4^+$ and $CD8^+$ T cells (28, 37). Conditioning with IL-2 markedly enhances the expression of CCR1 and CCR2 and the chemotactic responsiveness to RANTES and MCP-1 (45) (see *Lymphocyte Recruitment*). Similar migration responses are observed for natural killer (NK) cells (46) and dendritic cells (47), and the MCPs were also found to induce $[Ca^{2+}]_i$ changes and exocytosis of granzyme A and N-acetyl-β-glucosaminidase in cloned human NK cells (48). In addition, several CC chemokines including the MCPs were reported to enhance target cell lysis by blood-derived NK cells (49).

Eotaxin

A CC chemokine acting on eosinophils and termed *eotaxin* was originally isolated from the bronchoalveolar fluid of allergic guinea-pigs (50). Murine (51) and human homologs (27) were subsequently cloned. They share over 60% sequence identity with guinea-pig eotaxin and are equally selective for eosinophils. Human eosinophils express high numbers of a receptor for eotaxin, CCR3, which was cloned by three independent groups (43, 44, 52). Binding studies have shown that eotaxin as well as RANTES and MCP-3 recognize this receptor (43), in agreement with their ability to attract CCR3-transfected cells (44). In addition, cross-desensitization experiments with eosinophils suggest that CCR3 recognizes MCP-4 as well (27, 28). MCP-4 is very active on eosinophils and is equivalent to eotaxin as chemoattractant and superior to MCP-3 in desensitizing eosinophils toward eotaxin (28). In contrast to other CC chemokines, eotaxin has a high degree of selectivity for its receptor. It is inactive on neutrophils and monocytes, which do not appear to express CCR3 (44, 52, 53) but has weak-to-moderate chemotactic activity toward IL-2-conditioned T lymphocytes (28). Eotaxin exclusively attracts eosinophils when

applied in vivo (27), and its expression is enhanced in animal models of allergic inflammation (50, 54) and in tissue cells at sites of eosinophil accumulation in humans (27). Northern blot analysis showed constitutive expression of eotaxin in human small intestine, colon, heart, kidney, and pancreas; major amounts of this chemokine are believed to be produced by epithelial and endothelial cells as well as eosinophil leukocytes (53). Due to its preferential, powerful action on eosinophils and its occurrence in different species, eotaxin is considered a most relevant chemokine in the pathophysiology of allergic conditions and asthma (55).

IP10 and Mig

IP10 is a CXC chemokine that was identified several years ago as the product of a gene induced by interferon-γ (IFNγ), which was found to be expressed in delayed-type hypersensitivity reactions of the skin (56, 57). For a long time the biological activity of this chemokine remained unclear. Another IFNγ-induced human CXC chemokine, Mig, was later described (58). IP10 was reported to attract human monocytes, T lymphocytes, and NK cells (49, 59), and Mig was shown to attract tumor-infiltrating T lymphocytes (60). A receptor that is specific for IP10 and Mig, CXCR3, was recently cloned (see *CXC Chemokine Receptors*) and found to be selectively expressed on activated T lymphocytes that appear to be the only target cell for the two IFNγ-inducible chemokines (61). The restricted expression and the selectivity for a single receptor on T cells suggest that IP10 and Mig are involved in the regulation of lymphocyte recruitment and the formation of the lymphoid infiltrates observed in autoimmune inflammatory lesions, delayed-type hypersensitivity, some viral infections, and certain tumors.

SDF-1

The CXC chemokine SDF-1 (stromal cell–derived factor 1) occurs in two alternative splicing variants, SDF-1α and SDF-1β, that were cloned from mouse bone marrow stromal cell lines (62, 63). SDF-1α stimulates the proliferation of B cell progenitors and was also termed PBSF (pre-B cell growth stimulating factor (63). Murine SDF-1α was purified as a lymphocyte chemoattractant from a stromal cell culture supernatant (64). A homologous gene of human origin coding for both SDF forms was later characterized, and SDF-1α was shown to be the more abundant variant (64a). Mature human and murine SDF-1α consist of 68 amino acids and differ only at position 18 (valine in the human and isoleucine in the murine protein). Subsequent studies showed that synthetic human SDF-1 stimulates monocytes, neutrophils, and peripheral blood lymphocytes, as is indicated by $[Ca^{2+}]_i$ changes and chemotaxis (64, 65). SDF-1 binds to CXCR4, a former orphan receptor cloned in several laboratories (66–70), (see

CXC Chemokine Receptors), and induces Ca^{2+} mobilization in CHO cells that stably express this receptor (65, 71). No cross-desensitization is observed with other chemokines, which underlines the selectivity of CXCR4. In transfected cell lines coexpressing CXCR4 and CD4 and in blood lymphocytes, SDF-1 is a powerful HIV-suppressive factor (see *HIV Replication*). Mice lacking the SDF-1 gene die perinatally and present multiple defects of development, including a severe reduction of B cell and myeloid progenitors in the bone marrow, in addition to a septal defect in the heart. These findings suggest that SDF-1 may display additional functions that are not typical for chemokines (72).

CHEMOKINE RECEPTORS

Chemokines act via seven-transmembrane-domain (7TM) receptors (1, 3), which form a distinct group of structurally related proteins within the superfamily of receptors that signal through heterotrimeric GTP-binding proteins (Table 1). More than by the overall sequence identity, relatedness is manifested by a number of conserved structural motifs mainly found within the transmembrane domains. The most important of these motifs are: TD(X)YLLNLA (X2)DLLF(X2)TLP(X)W in TM 2, the NH_2- and COOH-terminal extensions of the DRYLAIVHA-motif in TM 3 and the second intracellular loop, PLL(X) M(X2)CY in TM 5, W(X)PYN in TM 6, and HCC(X)NP(X)IYAF(X)G(X2)FR in TM 7. In addition, all chemokine receptors have two conserved cysteines, one in the NH_2-terminal domain and the other in the third extracellular loop (Cys^{30} and Cys^{277} in CXCR1) that are assumed to form a disulfide bond critical for the conformation of the ligand-binding pocket. On the basis of the overall sequence identity, two subgroups can be recognized: CXC chemokine receptors with 36–77% and CC chemokine receptors with 46–89% identical amino acids (Figures 2 and 3).

CXC Chemokine Receptors

Two receptors for IL-8, CXCR1 (IL-8RA/R1) and CXCR2 (IL-8RB/R2), are expressed on neutrophils. They share 77% identical amino acids, and their genes are colocalized on chromosome 2q35 (73, 74). One receptor, CXCR2, has high affinity for IL-8 and all other CXC chemokines that attract neutrophils (e.g. the GRO proteins, NAP-2, etc.), while the other, CXCR1, has high affinity for IL-8 only (1). IL-8 receptors are also found on monocytes, basophils, and eosinophils, but the responses of these cells to IL-8 are much weaker than those of neutrophils (1). In T lymphocytes, expression of both IL-8 receptors is revealed by RT-PCR but not by Northern blotting (75, 76), suggesting that the numbers are low. Using monoclonal antibodies and FACS analysis, it was observed that CXCR1 and CXCR2 are present on all neutrophils and monocytes,

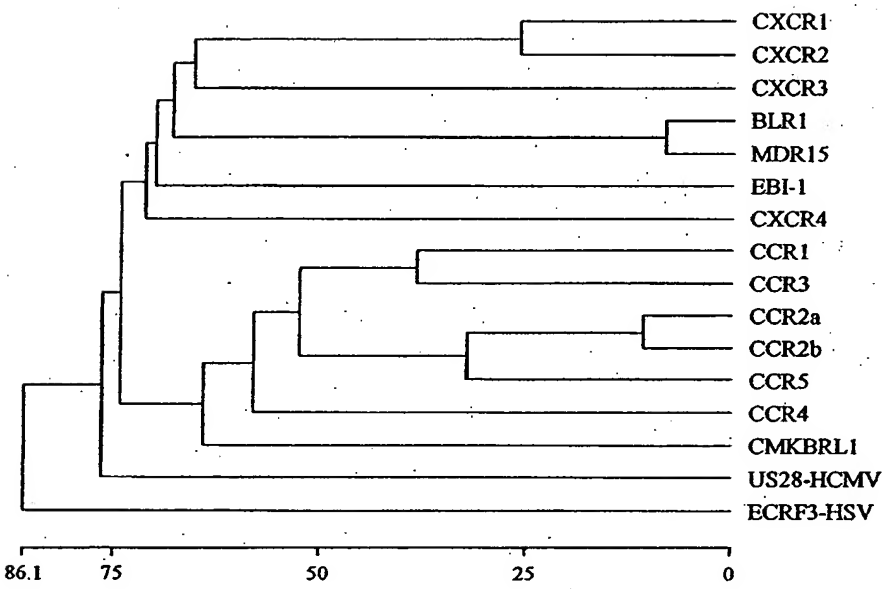

Figure 2 Structure similarity diagram of human chemokine receptors. Similarity scores were determined as described for Figure 1. The highest degree of divergence (86.1%) with respect to all the other receptors is observed for herpesvirus saimiri ECRF3 and the highest pairwise similarity (8.3% divergence) for BLR1 and MDR15. GeneBank accession numbers for the sequences are (from top to bottom): M68932, M73969, X95876, X68149, X68829, L08176, X71635, L10918, U51241, U03882, U03905, X91492, X85740, U28934, L20501, and S76368.

but only on a minority of lymphocytes. They are found in low numbers on NK and $CD8^+$ T cells, with high donor-to-donor variation, but they are absent in $CD4^+$ T cells or B cells (77, 78). Interestingly, while both receptors are present in similar numbers on neutrophils, CXCR2 appears to prevail on other leukocytes (78). Analysis of transendothelial migration shows that MCP-1 attracts $CD26^+$ T cells while the cells responding to IL-8 are CD26-negative (77). Expression of CXCR1 and CXCR2, as assessed by immunocytochemistry or RT-PCR, was also reported in cultured melanocytes and fibroblasts (75), epithelial cells in inflamed skin (79), and fibroblasts and smooth muscle cells of burn lesions (80). There is no evidence for a functional role of the expressed receptors, however.

Chimerae between the rabbit CXCR1 and the human CXCR2 were used to show that the NH_2-terminal domain determines, to a large extent, ligand selectivity (81, 82). Receptors carrying the NH_2-terminal domain of CXCR1 are selective for IL-8, whereas those carrying the NH_2-terminal domain of CXCR2 have high affinity for other CXC chemokines as well. Alanine scanning

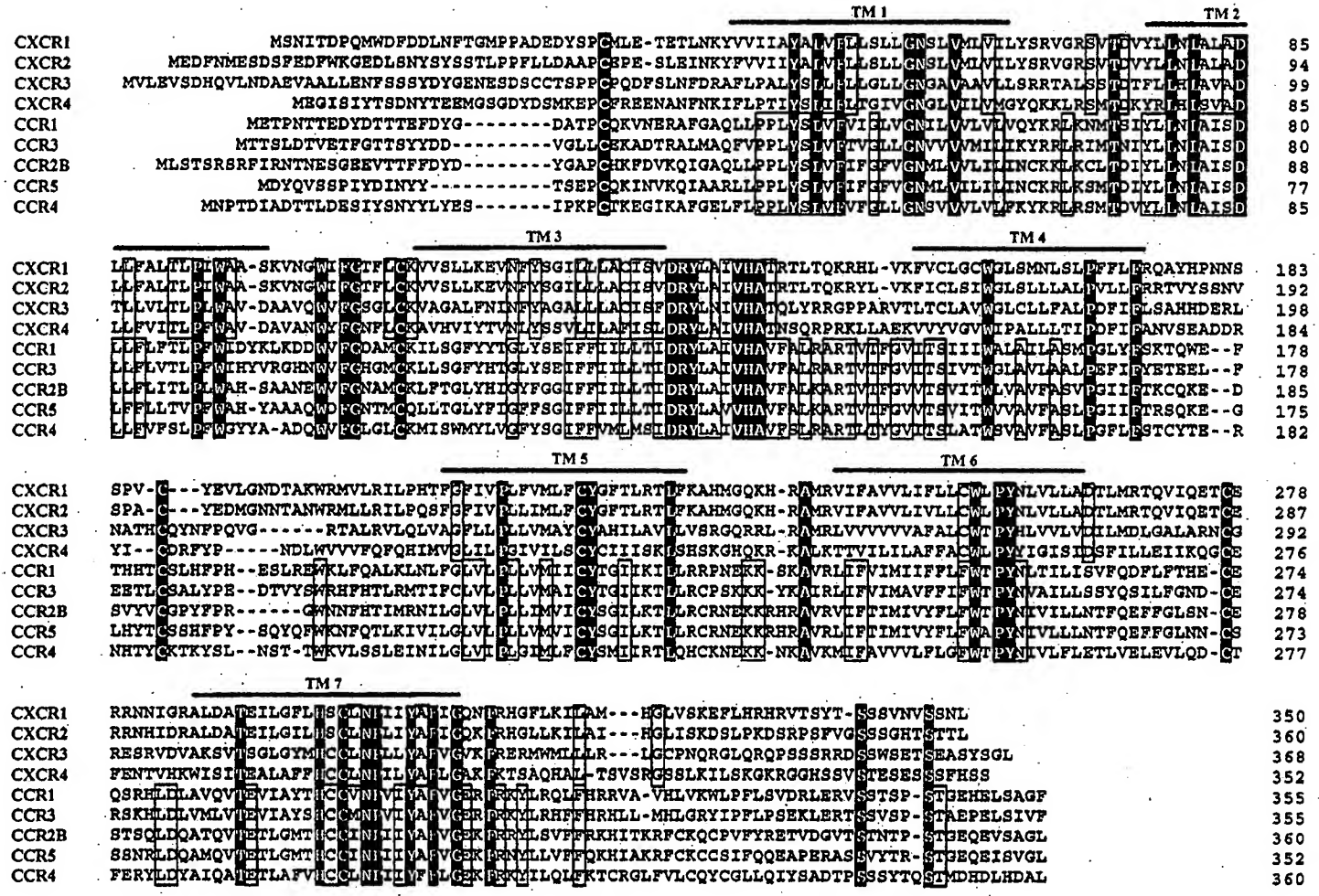
TM 1
TM 2
TM 3
TM 4
TM 5
TM 6
TM 7
CXCR1 MSNITDPQMWDFDDLNFTGMPPADEDYSPCMLE-TETLNKYVVIIAYALVFLLSLLGNSLVMLVILYSRVGRSVTDVYLLNLALAD 85
CXCR2 MEDFNMESDSFEDFWKGEDLSNYSYSSTLPPFLLDAAPCEPE-SLEINKYFVVIIYALVFLLSLLGNSLVMLVILYSRVGRSVTDVYLLNLALAD 94
CXCR3 MVLEVSDHQVLNDAEVAALLENFSSSYDYGENESDSCCTSPPCPQDFSLNFDRAFLPALYSLLFLLGLLGNGAVAAVLLSRRTALSSTDTFLLHLAVAD 99
CXCR4 MEGISIYTSDNYTEEMGSGDYDSMKEPCFREENANFNKIFLPTIYSIIFLTGIVGNGLVIIVMGYQKKLRSMTDKYRLHLSVAD 85
CCR1 METPNTTEDYDTTTEFDYG--------DATPCQKVNERAFGAQLLPPLYSLVFVIGLVGNILVVLVLVQYKRLKNMTSIYLLNLAISD 80
CCR3 MTTSLDTVETFGTTSYYDD---------VGLLCEKADTRALMAQFVPPLYSLVFTVGLLGNVVVVMILIKYRRLRIMTNIYLLNLAISD 80
CCR2B MLSTSRSRFIRNTNESGEEVTTFFDYD--------YGAPCHKFDVKQIGAQLLPPLYSLVFIFGFVGNMLVVLILINCKKLKCLTDIYLLNLAISD 88
CCR5 MDYQVSSPIYDINYY----------TSEPCQKINVKQIAARLLPPLYSLVFIFGFVGNMLVILILINCKRLKSMTDIYLLNLAISD 77
CCR4 MNPTDIADTTLDESIYSNYYLYES-------IPKPCTKEGIKAFGELFLPPLYSLVFVFGLLGNSVVVLVLFKYKRLRSMTDVYLLNLAISD 85
CXCR1 LLFALTLPFWAA-SKVNGWIFGTFLCKVVSLLKEVNFYSGILLLACISVDRYLAIVHATRTLTQKRHL-VKFVCLGCWGLSMNLSLPFFLFRQAYHPNNS 183
CXCR2 LLFALTLPFWAA-SKVNGWIFGTFLCKVVSLLKEVNFYSGILLLACISVDRYLAIVHATRTLTQKRYL-VKFICLSIWGLSLLLALPVLLFRRTVYSSNV 192
CXCR3 TLLVLTLPLWAV-DAAVQWVFGSGLCKVAGALFNINFYAGALLLACISFDRYLNIVHAMQLYRRGPPARVTLTCLAVWGLCLLFALPDFIFLSAHHDERL 198
CXCR4 LLFVITLPFWAV-DAVANWYFGNFLCKAVHVIYTVNLYSSVLILAFISLDRYLAIVHATNSQRPRKLLAEKVVYVGVWIPALLLTIPDFIFANVSEADDR 184
CCR1 LLFLFTLPFWIDYKLKDDWVFGDAMCKILSGFYYTGLYSEIFFIILLTIDRYLAIVHAVFALRARTVTFGVITSIITWGLAVLAALPEFIFYETEEL--F 178
CCR3 LLFLVTLPFWIHYVRGHNWVFGHGMCKLLSGFYHTGLYSEIFFIILLTIDRYLAIVHAVFALRARTVTFGVITSIVTWGLAVLAALPEFIFYETEEL--F 178
CCR2B LLFLITLPLWAH-SAANEWVFGNAMCKLFTGLYHIGYFGGIFFIILLTIDRYLAIVHAVFALKARTVTFGVVTSVITWLVAVFASVPGIIFTKCQKE--D 185
CCR5 LFFLLTVPFWAH-YAAAQWDFGNTMCQLLTGLYFIGFFSGIFFIILLTIDRYLAVVHAVFALKARTVTFGVVTSVITWVVAVFASLPGIIFTRSQKE--G 175
CCR4 LLFVFSLPFWGYYA-ADQWVFGLGLCKMISWMYLVGFYSGIFFVMLMSIDRYLAIVHAVFSLRARTLTYGVITSLATWSVAVFASLPGFLFSTCYTE--R 182
CXCR1 SPV-C---YEVLGNDTAKWRMVLRILPHTFGFIVPLFVMLFCYGFTLRTLFKAHMGQKH-RAMRVIFAVVLIFLLCWLPYNLVLLADTLMRTQVIQETCE 278
CXCR2 SPA-C---YEDMGNNTANWRMLLRILPQSFGFIVPLLIMLFCYGFTLRTLFKAHMGQKH-RAMRVIFAVVLIVLLCWLPYNLVLLADTLMRTQVIQETCE 287
CXCR3 NATHCQYNFPQVG------RTALRVLQLVAGFLLPLLVMAYCYAHILAVTLVSRGQRRL-RAMRLVVVVVVVAFALCWTPYHLVVLVDILMDLGALARNCG 292
CXCR4 YI--CDRFYP-----NDLWVVVFQFQHIMVGLILPGIVILSCYCIIISKLSHSKGHQKR-KALKTTVILILAFFACWLPYYIGISIDSFILLEIIKQGCE 276
CCR1 THHTCSLHFPH--ESLREWKLFQALKLNLFGLVLPLLVMIICYTGIIKILLRRPNEKK-SKAVRLIFVIMIIFFLFWTPYNLTILISVFQDFLFTHE-CE 274
CCR3 EETLCSALYPE--DTVYSWRHFHTLRMTIFCLVLPLLVMAICYTGIIKTLLRCPSKKK-YKAIRLIFVIMAVFFIFWTPYNVAILLSSYQSILFGND-CE 274
CCR2B SVYVCGPYFPR------GWNNFHTIMRNILGLVLPLLIMVICYSGILKTLLRCRNEKKRHRAVRVIFTIMIVYFLFWTPYNIVILLNTFQEFFGLSN-CE 278
CCR5 LHYTCSSHFPY--SQYQFWKNFQTLKIVILGLVLPLLVMVICYSGILKTLLRCRNEKKRHRAVRLIFTIMIVYFLFWAPYNIVLLLNTFQEFFGLNN-CS 273
CCR4 NHTYCKTKYSL--NST-TWKVLSSLEINILGLVIPLGIMLFCYSMIIRTLQHCKNEKK-NKAVKMIFAVVVLFLGFWTPYNIVLFLETLVELEVLQD-CT 277
CXCR1 RRNNIGRALDATEILGFLHSCLNPIIYAFIGQNFRHGFLKILAM---HGLVSKEFLHRHRVTSYT-SSSVNVSSNL 350
CXCR2 RRNHIDRALDATEILGILHSCLNPLIYAFIGQKFRHGLLKILAI---HGLISKDSLPKDSRPSFVGSSSGHTSTTL 360
CXCR3 RESRVDVAKSVTSGLGYMHCCLNPLLYAFVGVKFRERMWMLLLR---LGCPNQRGLQRQPSSSRRDSSWSETSEASYSGL 368
CXCR4 FENTVHKWISITEALAFFHCCLNPILYAFLGAKFKTSAQHALTSVSRGSSLKILSKGKRGGHSSVSTESESSSFHSS 352
CCR1 QSRHLDLAVQVTEVIAYTHCCVNPVIYAFVGERFRKYLRQLFHRRVA-VHLVKWLPFLSVDRLERVSSTSP-STGEHELSAGF 355
CCR3 RSKHLDLVMLVTEVIAYSHCCMNPVIYAFVGERFRKYLRHFFHRHLL-MHLGRYIPFLPSEKLERTSSVSP-STAEPELSIVF 355
CCR2B STSQLDQATQVTETLGMTHCCINPIIYAFVGEKFRKHLSVFFRKHITKRFCKQCPVFYRETVDGVTSTNTP-STGEQEVSAGL 360
CCR5 SSNRLDQAMQVTETLGMTHCCINPIIYAFVGEKFRNYLLVFFQKHIAKRFCKCCSIFQQEAPERASSVYTR-STGEQEISVGL 352
CCR4 FERYLDYAIQATETLAFVHCCLNPILYFFLGEKFKKYILQLFKTCRGLFVLCQYCGLLQIYSADTPSSSYTQSTMDHDLHDAL 360

mutagenesis of acidic residues in CXCR1 led to the identification of several extracellular sites (Asp^{11}, Arg^{199}, Arg^{203}, and Asp^{265}) that are important for IL-8 binding and signaling (83, 84). Similar results were obtained in a more detailed study of chimeric forms of both human receptors, showing that IL-8, GROα, and NAP-2 interact with multiple and partly overlapping sites of the extracellular receptor domains (85).

A new human 7TM receptor that recognizes the CXC chemokines IP10 and Mig has recently been cloned and termed CXCR3 (61). It consists of 368 amino acids and shares 41% sequence identity with the two IL-8 receptors, and 34–36% sequence identity with the five known CC chemokine receptors. CXCR3 is highly expressed in IL-2-activated T lymphocytes but is not detectable in resting T lymphocytes, B lymphocytes, monocytes, or granulocytes. Recombinant CXCR3 expressed in a murine pre-B cell line, the human promyelocytic cell line GM-1, or Jurkat cells mediates $[Ca^{2+}]_i$ changes and chemotaxis in response to IP10 or Mig, but not to other known chemokines or lymphotactin. So far CXCR3 is the only chemokine receptor that is selectively expressed in activated $CD4^+$ and $CD8^+$ T lymphocytes.

Another 7TM receptor, cloned by several groups (66–70) and called LESTR in our laboratory (66), has recently been shown to function as the co-receptor of CD4 for the infection of cell lines or blood lymphocytes by lymphocyte-tropic, syncytium-inducing, HIV-1 strains (86). SDF-1, the newly identified ligand for this receptor (see *SDF-1*), inhibits the infection in a concentration-dependent manner, thereby acting as HIV-suppressive factor (65, 71) (see *HIV Replication*). The SDF-1 receptor, for which the term CXCR4 is proposed, is relatively distant from the other chemokine receptors (32–38% identical amino acids). Its gene, however, is localized on chromosome 2q21 in proximity of the genes of CXCR1 and CXCR2 (1). A feature of CXCR4 that is unusual for chemokine receptors is its wide distribution. High levels of transcripts are found in leukocytes and in a wide variety of tissue cells (66–70). High expression was also found in several tissues from a rhesus monkey, including heart, brain, liver and colon (67).

CC Chemokine Receptors

The first two receptors for CC chemokines, CCR1 and CCR2, were originally designated MIP-1α/RANTES and MCP-1 receptor, respectively (87–89), based

Figure 3 Amino acid sequence alignment of human chemokine receptors. White letters in black boxes designate residues shared by all proteins; amino acids shared by either the CXC or CC chemokine receptors are boxed. Amino acids in one letter code are A, Ala; C, Cys; D, Asp; E, Glu; F, Phe; G, Gly; H, His; I, Ile; K, Lys; L, Leu; M, Met; N, Asn; P, Pro; Q, Gln; R, Arg; S, Ser; T, Thr; V, Val; W, Trp; and Y, Tyr.

on the ligands they bound with high affinity. CCR2 occurs in two RNA-splicing variants, CCR2a and CCR2b, with different COOH-terminal regions, which may affect signal transduction but not ligand selectivity (89, 90). The genes for CCR1 and CCR2 are colocalized on chromosome 3p21 (88, 91), as opposed to chromosome 2 for the IL-8 receptors, showing that the receptor genes, like the genes of CXC and CC chemokines, are segregated on different chromosomes. Subsequent studies demonstrated that CCR1 and CCR2 also recognize MCP-2, MCP-3, and possibly MCP-4 (28, 92–95). However, it was also reported that MCP-2 does not bind to CCR2 (92, 94), a result that may be due to the use of a chemokine preparation with impaired activity (36).

CCR3, the so-called eotaxin receptor, is prominently expressed in eosinophils and is believed to be the principal chemokine receptor for the recruitment of these cells in allergy. CCR3 DNAs were isolated from eosinophil (44) or monocyte (52) cDNA libraries or generated by PCR (43). Transfected cells expressing CCR3 have high affinity for eotaxin, RANTES, and MCP-3 (K_d values of 0.1, 2.7, and 3.1 nM, respectively) but do not bind MCP-1, MIP-1α and MIP-1β (43). MCP-4 completely desensitizes eosinophils toward eotaxin (28), suggesting that it binds with comparably high affinity to CCR3.

Two other CC chemokine receptors, CCR4 and CCR5, bind mainly RANTES and MIP-1α. CCR4 was cloned from a cDNA library obtained from a human basophilic leukemia cell line. When expressed in *Xenopus laevis* oocytes, CCR4 mediated the activation of a Ca^{2+}-dependent chloride channel in response to RANTES, MIP-1α, and MCP-1, but not MIP-1β, MCP-2, or IL-8 (96). HL60 cells transfected with CCR4 cDNA show high affinity for RANTES and MIP-1α (97). Transcripts for CCR4 are detected in IL-5-conditioned basophils, peripheral blood T and B lymphocytes, and monocytes (96). CCR5 was cloned from a human genomic DNA library by low-stringency hybridization with a PCR probe, and the gene was localized on chromosome 3 in close association with the CCR2 gene (98). Binding studies with stably transfected CHO cells indicate that CCR5 recognizes MIP-1β in addition to RANTES and MIP-1α. Although its function in leukocyte recruitment is still unexplored, CCR5 gained considerable attention from recent studies showing that it acts as a HIV-1 coreceptor with selectivity for monocyte/macrophage-tropic strains (see *HIV Replication*).

Orphan and Viral Receptors

Of a large number of orphan 7TM receptors identified by cloning of the respective cDNAs only those with highest similarity to chemokine receptors are listed (Figure 2). BLR1 (Burkitt's lymphoma-derived receptor 1) and MDR15 (monocyte-derived receptor 15) are NH_2-terminal splicing variants of a gene expressed in monocytes, B and T lymphocytes, and tissue cells (99–102). EBI1

was cloned from a cDNA library derived from an Epstein-Barr virus–infected Burkitt's lymphoma, and shown to be expressed exclusively in B and T cell lines (103). Another receptor, CMKBRL1 (chemokine beta receptor-like 1) shows interesting similarities with chemokine receptors. Its gene is located on chromosome 3p21 together with other CC chemokine receptors, and transcripts are found in leukocytes as well as in lymphoid and neural tissues (104, 105).

Some chemokine receptors may mediate functions that are unrelated to cell migration, as is exemplified by two receptors of viral origin. US28 consists of 354 amino acids and is encoded by human cytomegalovirus. It recognizes several CC chemokines, including MCP-1, RANTES, MIP-1α, and MIP-1β (87, 106). Conversely, ECRF3, a 321 amino acid protein encoded by herpesvirus saimiri, recognizes IL-8, GROα, and NAP-2, but not CC chemokines (107). It is interesting that these viral receptors discriminate between CXC and CC chemokines although they share less than 30% identical amino acids with the human chemokine receptors. In human fibroblasts, cytomegalovirus induces the expression of IL-8 receptors and shows enhanced replication in receptor-expressing cells that are exposed to IL-8 (108). This suggests that the expression of chemokine receptors in infected cells may be of advantage for the replication of some viruses (3, 108).

Receptor Function and Signal Transduction

Our review of this topic is largely restricted to neutrophils and cell lines transfected with the IL-8 receptors, which were studied more extensively. Signaling by chemokine receptors depends on coupling to *Bordetella pertussis* toxin-sensitive G-proteins. Experiments with COS-7 cells in which IL-8 receptors were cotransfected with different G-proteins have shown that CXCR1 and CXCR2 couple to $G\alpha_{i2}$, $G\alpha_{i3}$, $G\alpha_{t4}$, $G\alpha_{15}$, and $G\alpha_{16}$ but not to $G\alpha_q$ or $G\alpha_{11}$ (109). Studies on CC chemokine receptors are less advanced. CCR1 was shown to couple to $G\alpha_{14}$ but not $G\alpha_{16}$, while CCR2b couples to both G-proteins. No coupling to these G-proteins was observed for CCR2a, however, suggesting differences in G-protein usage (90).

The function of CXCR1 and CXCR2 was studied in Jurkat cells stably transfected with one or the other cDNA. CXCR1-expressing cells bind IL-8 with high affinity, and GROα and NAP-2 with low affinity, while CXCR2-expressing cells have high affinity for all three ligands. Both types of transfectants respond equally well to IL-8, as shown by $[Ca^{2+}]_i$ changes and chemotaxis, and no difference is observed in the function of CXCR2 after stimulation with IL-8, GROα, or NAP-2. CXCR1-transfected cells migrate in response to GROα and NAP-2, which bind with low affinity, provided that high concentrations are used (110). Similar experiments show that both receptors activate the p42/p44 MAP kinase (111). These results indicate that CXCR1 and CXCR2 signal and

function independently of each other. Monoclonal antibodies that selectively block CXCR1 or CXCR2 were used to study the function of the individual receptors in neutrophils. Both IL-8 receptors trigger $[Ca^{2+}]_i$ changes, chemotaxis and granule exocytosis, whereas phospholipase D activation and the respiratory burst are only observed after stimulation of CXCR1 (112). These observations are in agreement with a study showing that in human neutrophils phospholipase D is activated by stimulation with IL-8, but not with GROα or NAP-2 (113). All three chemokines, on the other hand, induce similar $[Ca^{2+}]_i$ changes and patterns of phosphorylation. Activation of p42/44 MAP kinase is also observed in cells transfected with CCR2 cDNA after stimulation with MCP-1 (114).

There is strong evidence for a role of phosphatidylinositol 3-kinase (PI3K) in chemokine-mediated signal transduction (115, 116). PI3K isoforms may become activated directly by interaction with the G-protein $\beta\gamma$ subunit or by small GTPases, Src-related tyrosine kinases, or phosphotyrosines that bind to the SH2 domain of PI3K. Phosphatidylinositol lipids phosphorylated at the 3-OH position are supposed to trigger a variety of cellular responses (117). A study on murine pre-B cells transfected with CXCR1 showed that the small GTPase Rho is implicated in IL-8-mediated adhesion to fibrinogen (118), suggesting that IL-8 receptors can activate small GTPases, which in turn regulate cytoskeletal rearrangement, phospholipase D activation, and induction of the respiratory burst (117). Leukocyte responses to chemokines are characteristically transient, and the receptors become rapidly desensitized. Phosphorylation of serines and threonines in the COOH-terminal region of CXCR1 and CXCR2 correlates with homologous desensitization after stimulation with IL-8 or GROα, respectively (1, 119, 120). Rat basophilic leukemia cells (RBL-2H3) cotransfected with CXCR1 and the C5a receptor were used to show that heterologous desensitization correlates with COOH-terminal phosphorylation of the receptors (121).

STRUCTURE-ACTIVITY RELATIONS

CXC Chemokines

The short sequence Glu-Leu-Arg (ELR motif), which precedes the first cysteine in all CXC chemokines that act on neutrophils is essential for binding and activation of both IL-8 receptors (CXCR1 and CXCR2). Additional structural domains, however, are required because short peptides containing the ELR motif are inactive, and neither IP10 nor MCP-1 can be converted into neutrophil-activating chemokines by introduction of the ELR motif (1). Active CXC chemokines have a short NH_2-terminal domain, and it has been suggested that if the sequence is extended, it can fold over the ELR motif and prevent its recognition by the receptor (10). Studies with IL-8 have shown that the arginine

adjacent to the first cysteine is very sensitive to substitution (1). It is interesting to note that three CXC chemokines, IP10, Mig, and SDF-1, that were recently shown to act via novel CXC chemokine receptors (61, 65) have a conserved arginine before the first cysteine. The Arg-Cys-X-Cys motif may be a general requirement for the binding to CXC chemokine receptors.

Several attempts have been made to define the structural elements for high-affinity binding to the IL-8 receptors. Studies with synthetic IL-8 analogs with single or double amino acid substitutions and hybrids between IL-8 and the inactive IP 10 have been performed to establish the minimal requirements for activity (13, 122). In addition to the disulfide bridges and the ELR motif, the NH_2-terminal loop region (residues 10–17) and the Gly^{31}-Pro^{32} motif in the β-turn containing the third cysteine (residues 30–35) were found to be of primary importance (13, 19). Single residue mutations and chimeric proteins between IL-8 and CXC chemokines with low affinity for CXCR1, were used to identify the structural determinants for recognition of CXCR1 and CXCR2 (123–127). Of particular interest is the NH_2-terminal loop (residues 10-17 in IL-8), since structural analysis reveals significant differences in this region between monomeric IL-8 and monomeric GROα or NAP-2 (9, 11, 12). Mutations of human and rabbit IL-8 highlight the importance of Tyr^{13} and Lys^{15} for high affinity binding to CXCR1 (123). Mutants of IL-8 and GROα with reversed receptor selectivity were obtained by exchanging the NH_2-terminal loops of the two chemokines (residues 10–17 of IL-8 and 12–18 of GROα) and residues preceding the fourth cysteine (Glu^{48} and Leu^{49} of IL-8, and Ala^{50} of GROα) (127).

The substitution of Tyr^{28} and Arg^{30} in MCP-1 by the corresponding residues in IL-8, Leu and Val, was reported to lower the activity toward monocytes and to confer neutrophil chemotactic activity to the CC chemokine (128). Conversely, replacement of Leu^{25} and Val^{27} in IL-8 by tyrosines, the corresponding residues of RANTES (129), or substitution of Leu^{25} by a modified cysteine were reported to yield mutants with CC chemokine activity (130). Using synthetic mutants, we were unable to confirm the results obtained by substitutions with natural amino acids (128, 129), and we found that the weak activity that IL-8 normally has on monocytes (131) was not affected by the substitutions (I Clark-Lewis, B Dewald, unpublished observation).

CC Chemokines

The NH_2-terminal region of MCP-1 is of critical importance for receptor recognition and activation. The situation is similar to that of IL-8 and its analogs that activate neutrophils, but the structural requirements are more strict because the entire sequence of 10 residues preceding the first cysteine is required for full activity (19, 132). Truncation or elongation of the NH_2-terminal sequence leads to considerable loss of activity, but the NH_2-terminal pyroglutamate can

be replaced by several other noncyclic amino acids. This is particularly interesting because MCP-2, MCP-3, and MCP-4 share with MCP-1 the NH_2-terminal pyroglutamate and high affinity for CCR2.

The role of the NH_2-terminal domain for MCP-1 activity was studied with a series of NH_2-terminally truncated analogs, MCP-1(2–76) to MCP-1(10–76), of the full-length form of 76 residues. Deletion of the NH_2-terminal pyroglutamate, yielding MCP-1(2–76), results in a marked, at least 50-fold decrease in activity on monocytes (132) and basophils (133), and deletion of the next residue leads to total loss of activity. Analogs with deletions of 3 or 4 residues, MCP-1(4-76) and MCP-1(5-76), are active again on both cells, while all further truncation analogs, MCP-1(6-76) through MCP-1(10-76), are inactive. A surprising observation was that MCP-1(2–76), the analog without NH_2-terminal pyroglutamate, is a powerful stimulus for eosinophil leukocytes, which do not express CCR2 and do not respond to full-length MCP-1 (133). On further truncation, the activity on eosinophils changes in the same way as in monocytes and basophils. It can be assumed that the effects on eosinophils are mediated via CCR3, and it is remarkable that MCP-1 acquires activity on these cells only after NH_2-terminal deletion, whereas MCP-2, MCP-3, and MCP-4, which share the NH_2- terminus with MCP-1, are potent attractants in their full-length form.

Several of the truncated MCP-1 analogs, MCP-1(9–76) and MCP-1(10–76) in particular, act as antagonists presumably by blocking CCR2, and they prevent the responses to MCP-1, MCP-2, and MCP-3, but not to RANTES, MIP-1α, or MIP-1β (132). Analogous studies performed with RANTES and MCP-3 yielded antagonists for multiple CC chemokine receptors (95). RANTES(9–68) and MCP-3(10–76) inhibit receptor binding and functional activities of MCP-1, MCP-3, and RANTES. The decreased selectivity of the truncated analogs, RANTES in particular, suggests that receptor specificity is dictated by residues within the NH_2-terminal domain, which are lost upon truncation, while other structural determinants assure the interaction with multiple receptors. Two additional CC chemokine antagonists were reportedly obtained by NH_2-terminal elongation: MCP-3 with three additional residues, Arg-Glu-Phe, which blocks the activity of MCP-3 (134), and RANTES with an additional methionine, which blocks the activity of RANTES and MIP-1α, but not of MCP-1 or IL-8 (135).

These observations demonstrate the critical role of the sequence preceding the first cysteine for the binding and function of MCP-1, MCP-3, and RANTES, and, together with former evidence on CXC chemokines (1), emphasize the overall importance of the NH_2-terminal domain for the biological activity of all chemokines. Interesting differences are nevertheless apparent between CXC and CC chemokines. Minimal modifications of the NH_2 terminus can drastically reduce or even qualitatively change the activity of CC chemokines, while

truncation up to the ELR motif progressively enhances the potency of IL-8 and other CXC chemokines (1). In both cases, elimination of most residues in the short NH_2-terminal stretch or modification of recognition motifs yields derivatives that still recognize the receptor but do not induce functional responses and thus act as antagonists.

PERSPECTIVES

We conclude by highlighting some new developments and concepts of potential interest. For areas where progress has been slow and areas that were reviewed recently, only a few indicative references will be given. Research on chemokines has provided considerable insight into the mechanism of diapedesis, and the ability of endothelial cells to generate attractant chemokines has been recognized as a fundamental process. Outstanding reviews have been published on this subject (136–138). Of interest is the potential activity of chemokines on myeloid progenitor cells. MIP-1α was described early on as a regulator of hematopoiesis (139) and inhibitor of stem cell proliferation (140). Although the disruption of the MIP-1α gene in mice does not appear to cause cellular abnormalities in the bone marrow or blood (141), chemokines are still considered as potential stimuli of leukocyte production and release from the bone marrow. Another major subject is the role of chemokines in tumors. It is well documented that transformed cell lines produce high amounts of different chemokines for which anti-tumor as well as tumor-promoting activities have been suggested (1). The role of chemokines in tumor growth is still unclear, and some new evidence for angiogenic and angiostatic effects will be discussed (see *Angiogenesis*).

Selectivity

Collectively, chemokines and chemokine receptors form a sophisticated system for the regulation of leukocyte and lymphocyte traffic across different compartments from the tissue of origin and the blood to sites of homing, host defense, or disposal. Substantial new information has been obtained about the selectivity and the complexity of the system, and some simplifications are no longer justified. The concept, for instance, that CXC chemokines act primarily on neutrophils, whereas CC chemokines act on the other types of leukocytes must be revised in view of the recent identification of new CXC chemokine receptors, CXCR3 and CXCR4, that mediate lymphocyte recruitment (61, 65, 71). When considering the ligands of the four CXC and five CC chemokine receptors (Table 1), an interesting difference becomes apparent: CXC chemokines have high affinity for single receptors (IL-8 which binds to CXCR1 and CXCR2 is the only exception), whereas most CC chemokines recognize two or more receptors

that differ in ligand specificity and cellular distribution. MCP-1 and eotaxin, which act via CCR2 and CCR3, respectively, are the only CC chemokines with restricted receptor usage. It is conceivable that CXC chemokines elicit more selective leukocyte responses than CC chemokines.

Tissue-Bound Chemokines

The early observation that IL-8 is effective for several hours after intradermal application (142) suggested that chemokines can associate in active form with the tissue matrix. In vitro, IL-8 binds to glycosaminoglycans through its COOH-terminal α-helix and remains active when complexed to heparin or heparan sulfate (143). To some degree, this interaction appears to be selective since IL-8, GROα, NAP-2, and PF4 differ in their binding to heparin subfractions as shown by affinity co-electrophoresis (144). MIP-1β and RANTES also retain activity when bound to the tissue matrix and induce adherence of T cells (145, 146). Together these observations suggest that interaction with matrix glycosaminoglycans may help to confine chemokines within the site of their formation and so support the concept that the migration of leukocytes could be directed by a solid, rather than fluid, chemokine gradient. In situ binding of IL-8 and RANTES, but not of MIP-1α, was observed in venular endothelial cells of the skin, and IL-8 was shown to bind to endothelia of mucosal and serosal sites, but not of parenchymatous tissues (147). It is possible that chemokines bound to the surface of endothelial cells direct diapedesis. The evidence for this attractive hypothesis, however, is still weak because only a few chemokines have been shown to bind, and the binding is restricted to some microvascular beds. In addition, chemokines, like other cationic proteins, can impair the activity of growth factors by competition for their binding sites on heparan sulfate (148, 149), a process that may explain some antiproliferative and angiostatic activities.

Most chemokines associate with the so-called Duffy antigen on erythrocytes (1). The "Duffy antigen receptor for chemokines" (DARC) was cloned and shown to consist of 338 amino acids and to comprise seven putative transmembrane domains. DARC has less than 20% amino acid identity with CXC and CC chemokine receptors and does not signal (150, 151). DARC is also expressed in some B and T cells, the endothelial cells of postcapillary venules and the Purkinje cells in the cerebellum (152). It is not clear, however, whether this promiscuous receptor is functionally relevant on endothelial cells and has a role in chemokine-dependent diapedesis because experiments with erythrocytes have shown that IL-8 is inactive toward neutrophils when bound to DARC (153).

Lymphocyte Recruitment

Chemokines are now generally recognized as the long-sought mediators of lymphocyte recruitment. A first hint came from the early studies on IP10, which is

expressed at sites of lymphocyte accumulation in delayed-type hypersensitivity. Subsequent studies suggested a role for IL-8, but the evidence has repeatedly been questioned, and although papers in support of this concept are still being published, the CC chemokines have emerged as a major force in lymphocyte trafficking. RANTES, MIP-1α, and MIP-1β were shown several years ago to attract T lymphocytes, and, more recently, the monocyte chemotactic proteins were found to perform similar functions (see *The Monocyte Chemotactic Proteins*).

To define conditions for lymphocyte responsiveness, the migration induced by RANTES, MCP-1, and other CC chemokines was studied in relation to the expression of two main receptors, CCR1 and CCR2, in CD45RO$^+$ blood lymphocytes cultured under different stimulatory conditions (45). A close correlation between receptor expression and chemotaxis was observed and found to depend strictly on pretreatment of the cells with IL-2. Receptor expression and responsiveness are rapidly downregulated when IL-2 is withdrawn and are fully restored when IL-2 is supplied again. IL-2 can be substituted partially by IL-4, IL-10, or IL-12, but not by IL-13, IFNγ, IL-1β, or TNFα. Interestingly, treatment with anti-CD3 alone or in combination with anti-CD28 rapidly downregulates receptors and migration. Receptor upregulation by IL-2 and downregulation by other stimuli of activation and proliferation suggest that T cells become responsive to chemokines after IL-2-mediated expansion and not during the early stages of antigen-dependent activation. Other studies showed that phytohemagglutinin-treated lymphocytes do not express CCR1 (88) and that human T cell clones lose migratory capacity after treatment with anti-CD3 (37). The opposite effect, however, was also reported (154).

The CC chemokines that attract lymphocytes are also chemotactic for monocytes, basophils, and eosinophils (2, 36), suggesting that the action of CC chemokines on lymphocytes is not selective. The role of MCP-1 in mononuclear cell recruitment was shown in a model of delayed-type hypersensitivity in rats (155) as well as in mice with *Cryptococcus neoformans* lung infection (156), where neutralizing antibodies against MCP-1 markedly decreased the local infiltration by monocytes and T lymphocytes.

A more selective recruitment of lymphocytes is likely to occur in response to IP10 and Mig, which bind to CXCR3, a receptor that does not recognize other chemokines and is confined to IL-2-activated T cells. Upon viral infection, for instance, IP10 and Mig are upregulated by locally produced IFNγ and thus become available for the recruitment of effector lymphocytes as part of the antiviral response. The potential role of IFNγ-induced chemoattractants in lymphocyte migration is highlighted by a comparison of the influx of radiolabeled neutrophils and lymphocytes in sheep after intradermal injection of chemoattractants and cytokines (157). The ratio of neutrophils to lymphocytes

was 45:1 after injection of IL-8 or C5a, about 5:1 after injection of TNFα or IL-1α, and only 0.1:1 after injection of IFNγ. Lymphotactin, a protein with only two cysteines and some structural similarity to chemokines, was also described as a selective attractant for lymphocytes (158). Such activities, however, have not been confirmed. Recombinant lymphotactin and two synthetic variants were extensively tested on human thymocytes and several preparations of T cells, including T cell clones, monocytes, and neutrophils, but no chemotactic activity nor $[Ca^{2+}]_i$ changes were observed (159).

Angiogenesis

The study of the formation of new blood vessels was greatly encouraged by the recognition of the role of angiogenesis for tumor growth, and the effects of growth factors on endothelial cells (160). Popular models of angiogenesis are the neovascularization of the cornea or the chick chorioallantoic membrane. Angiogenic factors are applied locally in an adsorptive pellet, and angiostatic substances are either added to the pellet or injected systemically. Enhancement or inhibition of endothelial cell proliferation and/or in vitro migration are considered as predictive of angiogenic or angiostatic activity, respectively.

A possible involvement of chemokines in the regulation of angiogenesis was originally suggested by studies showing that PF4 has angiostatic (161) and potential anti-tumor activity (162). Similar effects were observed with other cationic proteins, and recently it was shown that PF4 and IP10 share binding sites on heparan sulfate and inhibit the proliferation of endothelial cells presumably by displacing growth factors (163). The opposite effect, angiogenesis, was reported for IL-8 and several other CXC chemokines with the NH_2-terminal ELR motif (164, 165). Modification of the ELR motif reportedly confers angiostatic properties to IL-8, and introduction of the ELR motif converts the chemokine Mig from angiostatic to angiogenic. The mechanism of these phenomena has not been studied, and no receptors for angiogenic chemokines were described. It is unlikely that angiogenesis depends on neutrophil recruitment because some of the ELR-containing proteins studied, like platelet basic protein and connective tissue-activating peptide III, are inactive on neutrophils (1). In a later study the effects of IL-8 on human umbilical vein and dermal microvascular endothelial cells were examined, but no IL-8 binding nor IL-8-dependent $[Ca^{2+}]_i$ changes were observed, and no CXCR1 or CXCR2 transcripts were detected by PCR (166).

Angiostatic rather than angiogenic activity by CXC chemokines was reported by Cao et al (167) who compared the GRO proteins. They found that GROα, GROβ, and PF4 inhibit the proliferation of capillary endothelial cells stimulated with basic fibroblast growth factor, whereas GROγ was inactive. In vivo GROβ inhibited the neovascularization of the chorioallantoic membrane

and the mouse cornea, and it depressed the growth of murine Lewis lung carcinoma. Most recently, however, an anti-tumor effect was reported in SCID mice bearing human non–small cell lung cancer by neutralizing IL-8 with an antiserum (168). A tumor-promoting effect of IL-8 may also be inferred from the correlation between IL-8 expression and metastatic potential of melanoma cell lines in mice (169). On the other hand, IL-8 inhibits the proliferation of non-small cell cancer lines (170) and reduces tumorigenicity by recruitment of neutrophils in nude mice receiving tumor cells that express the human IL-8 gene (171). Anti-tumor activity was formerly observed in mice inoculated with tumor cells engineered to produce high levels of IP10, and the activity was found to depend on the recruitment of T lymphocytes and other white cells (172). Similar experiments were done with cells overexpressing murine MCP-1 (1). Furthermore, angiogenic properties were reported for soluble E-selectin and VCAM-1, which may be shed from the endothelial surface by enzymes released from adhering leukocytes (173). These and other observations emphasize the complexity of the pathophysiological process and suggest that, in many instances, the angiogenic effects of chemokines may be mediated by products released from the accumulating phagocytes.

HIV Replication

A most exciting new development came from the discovery that some chemokines function as HIV-1-suppressive factors. While searching for factors that delay the outbreak of AIDS, Cocchi et al (174) found that RANTES, MIP-1α, and MIP-1β produced by $CD8^+$ T cell lines are potent inhibitors of infection by monocyte/macrophage-tropic HIV-1 strains. These observations indicated that chemokines may determine the susceptibility to HIV infection and disease progression, and they suggested that chemokine receptors could in some way be involved in the recognition of HIV-1. Shortly thereafter, Feng et al (86) identified by expression cloning a 7TM receptor (termed fusin) that complements CD4 in a cell-fusion model of lymphocyte-tropic HIV-1 infection. Fusin is identical to CXCR4, and its ligand, SDF-1, was found to be a potent inhibitor of infection by lymphocyte-tropic HIV-1 strains in cell lines that coexpress CXCR4 and CD4 and in blood lymphocytes (65, 71). The HIV-suppressive factors RANTES, MIP-1α, and MIP-1β do not prevent the infection of cells expressing CXCR4. Unlike SDF-1, they interact with several receptors (see *CC Chemokine Receptors*) and one of them, CCR5, was shown by several groups to be the main coreceptor for entry of monocyte/macrophage-tropic HIV-1 strains (175–179). CCR3 and CCR2b have similar functions (176–178), but their role as HIV coreceptors is less prominent, suggesting that viral Env proteins have lower affinity for these receptors.

The repertoire of chemokine receptors in $CD4^+$ cells is likely to influence viral tropism, and it will be important to study the regulation of receptor

expression, particularly in T lymphocytes, macrophages, and dendritic cells. Viral entry is assumed to begin with the interaction of the highly variable viral Env protein, gp120, with CD4 and a chemokine receptor. Mutational changes of gp120 could lead to a switch in recognition from CCR5/CCR3 to CXCR4, and a shift from monocyte/macrophage-tropic to lymphocyte-tropic, syncytium-inducing strains. Recognition of CXCR4, which is widely expressed in blood leukocytes (66–70), could contribute to a spreading of the infection. There is already some evidence for a protective role of RANTES, MIP-1α, and MIP-1β in individuals who remain uninfected despite high-risk exposure to HIV (180), and the therapeutic application of chemokines to prevent infection may be considered. Of particular interest is the possibility that SDF-1 in combination with CC chemokines could help to decrease virus load and prevent the emergence of the syncytium-inducing viruses characteristic for the progression to AIDS.

ACKNOWLEDGMENTS

We thank Dr. Mariagrazia Uguccioni and Dr. Marlene Wolf for critical reading of the manuscript. This work was supported by Grant 31-039744.93 to M Baggiolini and B Moser from the Swiss National Science Foundation. B Moser is recipient of a career development award from the Prof. Max Cloetta Foundation.

Literature Cited

1. Baggiolini M, Dewald B, Moser B. 1994. Interleukin-8 and related chemotactic cytokines—CXC and CC chemokines. *Adv. Immunol.* 55:97–179
2. Baggiolini M, Dahinden CA. 1994. CC chemokines in allergic inflammation. *Immunol. Today* 15:127–33
3. Murphy PM. 1994. The molecular biology of leukocyte chemoattractant receptors. *Annu. Rev. Immunol.* 12:593–633
4. Schall TJ, Bacon KB. 1994. Chemokines, leukocyte trafficking, and inflammation. *Curr. Opin. Immunol.* 6:865–73
5. Clore GM, Appella E, Yamada M, Matsushima K, Gronenborn AM. 1990. Three-dimensional structure of interleukin 8 in solution. *Biochemistry* 29:1689–96
6. Baldwin ET, Weber IT, St. Charles R, Xuan J-C, Appella E, Yamada M, Matsushima K, Edwards BFP, Clore GM, Gronenborn AM, Wlodawer A. 1991. Crystal structure of interleukin 8: symbiosis of NMR and crystallography. *Proc. Natl. Acad. Sci. USA* 88:502–6
7. Clore GM, Gronenborn AM. 1995. Three-dimensional structures of α and β chemokines. *FASEB. J.* 9:57–62
8. St. Charles R, Walz DA, Edwards BF. 1989. The three-dimensional structure of bovine platelet factor 4 at 3.0-Å resolution. *J. Biol. Chem.* 264:2092–99
9. Fairbrother WJ, Reilly D, Colby TJ, Hesselgesser J, Horuk R. 1994. The solution structure of melanoma growth stimulating activity. *J. Mol. Biol.* 242:252–70
10. Yang Y, Mayo KH, Daly TJ, Barry JK, La Rosa GJ. 1994. Subunit association and structural analysis of platelet basic protein and related proteins investigated by ^{1}H NMR spectroscopy and circular dichroism. *J. Biol. Chem.* 269:20,110–18
11. Kim K-S, Clark-Lewis I, Sykes BD. 1994. Solution structure of GRO/melanoma

growth stimulatory activity determined by ^{1}H NMR spectroscopy. *J. Biol. Chem.* 269:32,909–15
12. Malkowski MG, Wu JY, Lazar JB, Johnson PH, Edwards BFP. 1995. The crystal structure of recombinant human neutrophil-activating peptide-2 (M6L) at 1.9-Å resolution. *J. Biol. Chem.* 270: 7077–87
13. Clark-Lewis I, Dewald B, Loetscher M, Moser B, Baggiolini M. 1994. Structural requirements for interleukin-8 function identified by design of analogs and CXC chemokine hybrids. *J. Biol. Chem.* 269:16,075–81
14. Lodi PJ, Garrett DS, Kuszewski J, Tsang ML-S, Weatherbee JA, Leonard WJ, Gronenborn AM, Clore GM. 1994. High-resolution solution structure of the β chemokine hMIP-1β by multidimensional NMR. *Science* 263:1762–67
15. Skelton NJ, Aspiras F, Ogez J, Schall TJ. 1995. Proton NMR assignments and solution conformation of RANTES, a chemokine of the C-C type. *Biochemistry* 34:5329–42
16. Chung C, Cooke RM, Proudfoot AEI, Wells TNC. 1995. The three-dimensional solution structure of RANTES. *Biochemistry* 34:9307–14
17. Covell DG, Smythers GW, Gronenborn AM, Clore GM. 1994. Analysis of hydrophobicity in the α and β chemokine families and its relevance to dimerization. *Protein Sci.* 3:2064–72
18. Burrows SD, Doyle ML, Murphy KP, Franklin SG, White JR, Brooks I, McNulty DE, Scott MO, Knutson JR, Porter D, Young PR, Hensley P. 1994. Determination of the monomer-dimer equilibrium of interleukin-8 reveals it is a monomer at physiological concentrations. *Biochemistry* 33:12,741–45
19. Clark-Lewis I, Kim K-S, Rajarathnam K, Gong J-H, Dewald B, Moser B, Baggiolini M, Sykes BD. 1995. Structure-activity relationships of chemokines. *J. Leuk. Biol.* 57:703–11
20. Rajarathnam K, Sykes BD, Kay CM, Dewald B, Geiser T, Baggiolini M, Clark-Lewis I. 1994. Neutrophil activation by monomeric interleukin-8. *Science* 264:90–92
21. Rajarathnam K, Clark-Lewis I, Sykes BD. 1995. ^{1}H NMR solution structure of an active monomeric interleukin-8. *Biochemistry* 34:12,983–90
22. Mantel C, Kim YJ, Cooper S, Kwon B, Broxmeyer HE. 1993. Polymerization of murine macrophage inflammatory protein 1α inactivates its myelosuppressive effects in vitro: the active form is a monomer. *Proc. Natl. Acad. Sci. USA* 90:2232–36
23. Avalos BR, Bartynski KJ, Elder PJ, Kotur MS, Burton WG, Wilkie NM. 1994. The active monomeric form of macrophage inflammatory protein-1α interacts with high- and low-affinity classes of receptors on human hematopoietic cells. *Blood* 84:1790–801
24. Lord BI. 1995. MIP-1α increases the self-renewal capacity of the hemopoietic spleen-colony-forming cells following hydroxyurea treatment in vivo. *Growth Factors* 12:145–49
25. Paolini JF, Willard D, Consler T, Luther M, Krangel MS. 1994. The chemokines IL-8, monocyte chemoattractant protein-1, and I-309 are monomers at physiologically relevant concentrations. *J. Immunol.* 153:2704–17
26. Zhang Y, Rollins BJ. 1995. A dominant negative inhibitor indicates that monocyte chemoattractant protein 1 functions as a dimer. *Mol. Cell. Biol.* 15:4851–55
27. Ponath PD, Qin SX, Ringler DJ, Clark-Lewis I, Wang J, Kassam N, Smith H, Shi XJ, Gonzalo JA, Newman W, Gutierrez-Ramos JC, Mackay CR. 1996. Cloning of the human eosinophil chemoattractant, eotaxin—expression, receptor binding, and functional properties suggest a mechanism for the selective recruitment of eosinophils. *J. Clin. Invest.* 97:604–12
28. Uguccioni M, Loetscher P, Forssmann U, Dewald B, Li HD, Lima SH, Li YL, Kreider B, Garotta G, Thelen M, Baggiolini M. 1996. Monocyte chemotactic protein 4 (MCP-4), a novel structural and functional analogue of MCP-3 and eotaxin. *J. Exp. Med.* 183:2379–84
29. Schulz-Knappe P, Mägert HJ, Dewald B, Meyer M, Cetin Y, Kubbies M, Tomeczkowski J, Kirchhoff K, Raida M, Adermann K, Kist A, Reinecke M, Sillard R, Pardigol A, Uguccioni M, Baggiolini M, Forssmann WG. 1996. HCC-1, a novel chemokine from human plasma. *J. Exp. Med.* 183:295–99
30. Imai T, Yoshida T, Baba M, Nishimura M, Kakizaki M, Yoshie O. 1996. Molecular cloning of a novel T cell-directed CC chemokine expressed in thymus by signal sequence trap using Epstein-Barr virus vector. *J. Biol. Chem.* 271:21,514–21
31. Orlofsky A, Berger MS, Prystowsky MB. 1991. Novel expression pattern of a new member of the MIP-1 family of cytokine-like genes. *Cell. Regulat.* 2:403–12

32. Hara T, Bacon KB, Cho LC, Yoshimura A, Morikawa Y, Copeland NG, Gilbert DJ, Jenkins NA, Schall TJ, Miyajima A. 1995. Molecular cloning and functional characterization of a novel member of the C-C chemokine family. *J. Immunol.* 155:5352–58
33. Youn B-S, Jang I-K, Broxmeyer HE, Cooper S, Jenkins NA, Gilbert DJ, Copeland NG, Elick TA, Fraser MJ Jr, Kwon BS. 1995. A novel chemokine, macrophage inflammatory protein-related protein-2, inhibits colony formation of bone marrow myeloid progenitors. *J. Immunol.* 155:2661–67
34. Poltorak AN, Bazzoni F, Smirnova II, Alejos E, Thompson P, Luheshi G, Rothwell N, Beutler B. 1995. MIP-1gamma: molecular cloning, expression, and biological activities of a novel CC chemokine that is constitutively secreted in vivo. *J. Inflamm.* 45:207–19
35. Van Damme J, Proost P, Lenaerts J-P, Opdenakker G. 1992. Structural and functional identification of two human, tumor-derived monocyte chemotactic proteins (MCP-2 and MCP-3) belonging to the chemokine family. *J. Exp. Med.* 176:59–65
36. Uguccioni M, D'Apuzzo M, Loetscher M, Dewald B, Baggiolini M. 1995. Actions of the chemotactic cytokines MCP-1, MCP-2, MCP-3, RANTES, MIP-1α and MIP-1β on human monocytes. *Eur. J. Immunol.* 25:64–68
37. Loetscher P, Seitz M, Clark-Lewis I, Baggiolini M, Moser B. 1994. The monocyte chemotactic proteins, MCP-1, MCP-2 and MCP-3, are major attractants for human $CD4^+$ and $CD8^+$ T lymphocytes. *FASEB. J.* 8:1055–60
38. Carr MW, Roth SJ, Luther E, Rose SS, Springer TA. 1994. Monocyte chemoattractant protein 1 acts as a T-lymphocyte chemoattractant. *Proc. Natl. Acad. Sci. USA* 91:3652–56
39. Roth SJ, Carr MW, Springer TA. 1995. C-C chemokines, but not the C-X-C chemokines interleukin-8 and interferon-γ inducible protein-10, stimulate transendothelial chemotaxis of T lymphocytes. *Eur. J. Immunol.* 25:3482–88
40. Dahinden CA, Geiser T, Brunner T, von Tscharner V, Caput D, Ferrara P, Minty A, Baggiolini M. 1994. Monocyte chemotactic protein 3 is a most effective basophil- and eosinophil-activating chemokine. *J. Exp. Med.* 179:751–56
41. Alam R, Forsythe P, Stafford S, Heinrich J, Bravo R, Proost P, Van Damme J. 1994. Monocyte chemotactic protein-2, monocyte chemotactic protein-3, and fibroblast-induced cytokine: Three new chemokines induce chemotaxis and activation of basophils. *J. Immunol.* 153:3155–59
42. Weber M, Uguccioni M, Ochensberger B, Baggiolini M, Clark-Lewis I, Dahinden CA. 1995. Monocyte chemotactic protein MCP-2 activates human basophil and eosinophil leukocytes similar to MCP-3. *J. Immunol.* 154:4166–72
43. Daugherty BL, Siciliano SJ, DeMartino JA, Malkowitz L, Sirotina A, Springer MS. 1996. Cloning, expression, and characterization of the human eosinophil eotaxin receptor. *J. Exp. Med.* 183:2349–54
44. Ponath PD, Qin SX, Post TW, Wang J, Wu L, Gerard NP, Newman W, Gerard C, Mackay CR. 1996. Molecular cloning and characterization of a human eotaxin receptor expressed selectively on eosinophils. *J. Exp. Med.* 183:2437–48
45. Loetscher P, Seitz M, Baggiolini M, Moser B. 1996. Interleukin-2 regulates CC chemokine receptor expression and chemotactic responsiveness in T lymphocytes. *J. Exp. Med.* 184:569–77
46. Allavena P, Bianchi G, Zhou D, Van Damme J, Jàlek P, Sozzani S, Mantovani A. 1994. Induction of natural killer cell migration by monocyte chemotactic protein-1, -2 and -3. *Eur. J. Immunol.* 24:3233–36
47. Sozzani S, Sallusto F, Luini W, Zhou D, Piemonti L, Allavena P, Van Damme J, Valitutti S, Lanzavecchia A, Mantovani A. 1995. Migration of dendritic cells in response to formyl peptides, C5a, and a distinct set of chemokines. *J. Immunol.* 155:3292–95
48. Loetscher P, Seitz M, Clark-Lewis I, Baggiolini M, Moser B. 1996. Activation of NK cells by CC chemokines—chemotaxis, Ca^{2+} mobilization, and enzyme release. *J. Immunol.* 156:322–27
49. Taub DD, Sayers TJ, Carter CRD, Ortaldo JR. 1995. α and β chemokines induce NK cell migration and enhance NK-mediated cytolysis. *J. Immunol.* 155:3877–88
50. Jose PJ, Griffiths-Johnson DA, Collins PD, Walsh DT, Moqbel R, Totty NF, Truong O, Hsuan JJ, Williams TJ. 1994. Eotaxin: a potent eosinophil chemoattractant cytokine detected in a guinea pig model of allergic airways inflammation. *J. Exp. Med.* 179:881–87
51. Rothenberg ME, Luster AD, Leder P. 1995. Murine eotaxin: an eosinophil chemoattractant inducible in endothelial

cells and in interleukin 4-induced tumor suppression. *Proc. Natl. Acad. Sci. USA* 92:8960–64
52. Combadiere C, Ahuja SK, Murphy PM. 1995. Cloning and functional expression of a human eosinophil CC chemokine receptor. *J. Biol. Chem.* 270:16,491–94; correction: *J. Biol. Chem.* 270:30,235
53. Garcia-Zepeda EA, Rothenberg ME, Ownbey RT, Celestin J, Leder P, Luster AD. 1996. Human eotaxin is a specific chemoattractant for eosinophil cells and provides a new mechanism to explain tissue eosinophilia. *Nature. Med.* 2:449–56
54. Collins PD, Marleau S, Griffiths-Johnson DA, Jose PJ, Williams TJ. 1995. Cooperation between interleukin-5 and the chemokine eotaxin to induce eosinophil accumulation in vivo. *J. Exp. Med.* 182:1169–74
55. Baggiolini M. 1996. Eotaxin: a VIC (very important chemokine) of allergic inflammation? *J. Clin. Invest.* 97:587
56. Luster AD, Ravetch JV. 1987. Biochemical characterization of a γ interferon-inducible cytokine (IP-10). *J. Exp. Med.* 166:1084–97
57. Kaplan G, Luster AD, Hancock G, Cohn ZA. 1987. The expression of a γ interferon-induced protein (IP-10) in delayed immune responses in human skin. *J. Exp. Med.* 166:1098–108
58. Farber JM. 1993. HuMIG: a new human member of the chemokine family of cytokines. *Biochem. Biophys. Res. Commun.* 192:223–30
59. Taub DD, Lloyd AR, Conlon K, Wang JM, Ortaldo JR, Harada A, Matsushima K, Kelvin DJ, Oppenheim JJ. 1993. Recombinant human interferon-inducible protein 10 is a chemoattractant for human monocytes and T lymphocytes and promotes T cell adhesion to endothelial cells. *J. Exp. Med.* 177:1809–14
60. Liao F, Rabin RL, Yannelli JR, Koniaris LG, Vanguri P, Farber JM. 1995. Human mig chemokine: biochemical and functional characterization. *J. Exp. Med.* 182:1301–14
61. Loetscher M, Gerber B, Loetscher P, Jones SA, Piali L, Clark-Lewis I, Baggiolini M, Moser B. 1996. Chemokine receptor specific for IP10 and Mig: structure, function and expression in activated T lymphocytes. *J. Exp. Med.* 184:963–69
62. Tashiro K, Tada H, Heilker R, Shirozu M, Nakano T, Honjo T. 1993. Signal sequence trap: a cloning strategy for secreted proteins and type I membrane proteins. *Science* 261:600–3
63. Nagasawa T, Kikutani H, Kishimoto T. 1994. Molecular cloning and structure of a pre-B-cell growth-stimulating factor. *Proc. Natl. Acad. Sci. USA* 91:2305–9
64. Bleul CC, Fuhlbrigge RC, Casasnovas JM, Aiuti A, Springer TA. 1996. A highly efficacious lymphocyte chemoattractant, stromal cell-derived factor 1 (SDF-1). *J. Exp. Med.* 184:1101–9
64a. Shirozu M, Nakano T, Inazawa J, Tashiro K, Tada H, Shino hara T, Honjo T. 1995. Structure and chromosomal localization of the human stromal cell-derived factor 1 (SDF-1) gene. *Genomics* 28:495–500
65. Oberlin E, Amara A, Bachelerie F, Bessia C, Virelizier JL, Arenzana-Seisdedos F, Schwartz O, Heard JM, Clark-Lewis I, Legler DF, Loetscher M, Baggiolini M, Moser B. 1996. The CXC chemokine SDF-1 is the ligand for LESTR/fusin and prevents infection by T-cell-line-adapted HIV-1. *Nature.* 382:833–35
66. Loetscher M, Geiser T, O'Reilly T, Zwahlen R, Baggiolini M, Moser B. 1994. Cloning of a human seven-transmembrane domain receptor, LESTR, that is highly expressed in leukocytes. *J. Biol. Chem.* 269:232–37
67. Federsppiel B, Melhado IG, Duncan AMV, Delaney A, Schappert K, Clark-Lewis I, Jirik FR. 1993. Molecular cloning of the cDNA and chromosomal localization of the gene for a putative seven-transmembrane segment (7-TMS) receptor isolated from human spleen. *Genomics* 16:707–12
68. Nomura H, Nielsen BW, Matsushima K. 1993. Molecular cloning of cDNAs encoding a LD78 receptor and putative leukocyte chemotactic peptide receptors. *Int. Immunol.* 5:1239–49
69. Herzog H, Hort YJ, Shine J, Selbie LA. 1993. Molecular cloning, characterization, and localization of the human homolog to the reported bovine NPY Y3 receptor: lack of NPY binding and activation. *DNA Cell. Biol.* 12:465–71
70. Jazin EE, Yoo H, Blomqvist AG, Yee F, Weng G, Walker MW, Salon J, Larhammar D, Wahlestedt C. 1993. A proposed bovine neuropeptide Y (NPY) receptor cDNA clone, or its human homologue, confers neither NPY binding sites nor NPY responsiveness on transfected cells. *Regul. Pept.* 47:247–58
71. Bleul CC, Farzan M, Choe H, Parolin C, Clark-Lewis I, Sodroski J, Springer T. 1996. The lymphocyte chemoattractant SDF-1 is a ligand for LESTR/fusin and blocks HIV-1 entry. *Nature.* 382:829–33
72. Nagasawa T, Hirota S, Tachibana K, Takakura N, Nishikawa S, Kitamura Y,

Yoshida N, Kikutani H, Kishimoto T. 1996. Defects of B-cell lymphopoiesis and bone marrow myelopoiesis in mice lacking the CXC chemokine PBSF/SDF-1. *Nature.* 382:635–38
73. Holmes WE, Lee J, Kuang W-J, Rice GC, Wood WI. 1991. Structure and functional expression of a human interleukin-8 receptor. *Science* 253:1278–80
74. Murphy PM, Tiffany HL. 1991. Cloning of complementary DNA encoding a functional human interleukin-8 receptor. *Science* 253:1280–83
75. Moser B, Barella L, Mattei S, Schumacher C, Boulay F, Colombo MP, Baggiolini M. 1993. Expression of transcripts for two interleukin 8 receptors in human phagocytes, lymphocytes and melanoma cells. *Biochem. J.* 294:285–92
76. Xu L, Kelvin DJ, Ye GQ, Taub DD, Ben-Baruch A, Oppenheim JJ, Wang JM. 1995. Modulation of IL-8 receptor expression on purified human T lymphocytes is associated with changed chemotactic responses to IL-8. *J. Leukocyte. Biol.* 57:335–42
77. Qin SX, LaRosa G, Campbell JJ, Smith-Heath H, Kassam N, Shi XJ, Zeng L, Butcher EC, Mackay CR. 1996. Expression of monocyte chemoattractant protein-1 and interleukin-8 receptors on subsets of T cells: correlation with transendothelial chemotactic potential. *Eur. J. Immunol.* 26:640–47
78. Chuntharapai A, Lee J, Hébert CA, Kim KJ. 1994. Monoclonal antibodies detect different distribution patterns of IL-8 receptor A and IL-8 receptor B on human peripheral blood leukocytes. *J. Immunol.* 153:5682–88
79. Schulz BS, Michel G, Wagner S, Süss R, Beetz A, Peter RU, Kemény L, Ruzicka T. 1993. Increased expression of epidermal IL-8 receptor in psoriasis: down-regulation by FK-506 in vitro. *J. Immunol.* 151:4399–406
80. Nanney LB, Mueller SG, Bueno R, Peiper SC, Richmond A. 1995. Distributions of melanoma growth stimulatory activity or growth-regulated gene and the interleukin-8 receptor B in human wound repair. *Am. J. Pathol.* 147:1248–60
81. LaRosa GJ, Thomas KM, Kaufmann ME, Mark R, White M, Taylor L, Gray G, Witt D, Navarro J. 1992. Amino terminus of the interleukin-8 receptor is a major determinant of receptor subtype specificity. *J. Biol. Chem.* 267:25,402–6
82. Gayle RB III, Sleath PR, Srinivason S, Birks CW, Weerawarna KS, Cerretti DP, Kozlosky CJ, Nelson N, Vanden Bos T, Beckmann MP. 1993. Importance of the amino terminus of the interleukin-8 receptor in ligand interactions. *J. Biol. Chem.* 268:7283–89
83. Hébert CA, Chuntharapai A, Smith M, Colby T, Kim J, Horuk R. 1993. Partial functional mapping of the human interleukin-8 type A receptor. Identification of a major ligand binding domain. *J. Biol. Chem.* 268:18,549–53
84. Leong SR, Kabakoff RC, Hébert CA. 1994. Complete mutagenesis of the extracellular domain of interleukin-8 (IL-8) type A receptor identifies charged residues mediating IL-8 binding and signal transduction. *J. Biol. Chem.* 269:19,343–48
85. Ahuja SK, Lee JC, Murphy PM. 1996. CXC chemokines bind to unique sets of selectivity determinants that can function independently and are broadly distributed on multiple domains of human interleukin-8 receptor B—determinants of high affinity binding and receptor activation are distinct. *J. Biol. Chem.* 271:225–32
86. Feng Y, Broder CC, Kennedy PE, Berger EA. 1996. HIV-1 entry cofactor: functional cDNA cloning of a seven-transmembrane, G protein-coupled receptor. *Science* 272:872–77
87. Neote K, DiGregorio D, Mak JY, Horuk R, Schall TJ. 1993. Molecular cloning, functional expression, and signaling characteristics of a C-C chemokine receptor. *Cell* 72:415–25
88. Gao J-L, Kuhns DB, Tiffany HL, McDermott D, Li X, Francke U, Murphy PM. 1993. Structure and functional expression of the human macrophage inflammatory protein 1α/RANTES receptor. *J. Exp. Med.* 177:1421–27
89. Charo IF, Myers SJ, Herman A, Franci C, Connolly AJ, Coughlin SR. 1994. Molecular cloning and functional expression of two monocyte chemoattractant protein 1 receptors reveals alternative splicing of the carboxyl-terminal tails. *Proc. Natl. Acad. Sci. USA* 91:2752–56
90. Kuang YN, Wu YP, Jiang HP, Wu DQ. 1996. Selective G protein coupling by C-C chemokine receptors. *J. Biol. Chem.* 271:3975–78
91. Raport CJ, Schweickart VL, Chantry D, Eddy RL Jr, Shows TB, Godiska R, Gray PW. 1996. New members of the chemokine receptor gene family. *J. Leuk. Biol.* 59:18–23
92. Franci C, Wong LM, Van Damme J, Proost P, Charo IF. 1995. Monocyte chemoattractant protein-3, but not mono-

cyte chemoattractant protein-2, is a functional ligand of the human monocyte chemoattractant protein-1 receptor. *J. Immunol.* 154:6511–17
93. Ben-Baruch A, Xu LL, Young PR, Bengali K, Oppenheim JJ, Wang JM. 1995. Monocyte chemotactic protein-3 (MCP3) interacts with multiple leukocyte receptors—C-C CKR1, a receptor for macrophage inflammatory protein-1α/Rantes, is also a functional receptor for MCP3. *J. Biol. Chem.* 270:22,123–28
94. Combadiere C, Ahuja SK, Van Damme J, Tiffany HL, Gao JL, Murphy PM. 1995. Monocyte chemoattractant protein-3 is a functional ligand for CC chemokine receptors 1 and 2B. *J. Biol. Chem.* 270:29671–75
95. Gong JH, Uguccioni M, Dewald B, Baggiolini M, Clark-Lewis I. 1996. RANTES and MCP-3 antagonists bind multiple chemokine receptors. *J. Biol. Chem.* 271:10,521–27
96. Power CA, Meyer A, Nemeth K, Bacon KB, Hoogewerf AJ, Proudfoot AEI, Wells TNC. 1995. Molecular cloning and functional expression of a novel CC chemokine receptor cDNA from a human basophilic cell line. *J. Biol. Chem.* 270:19495–500
97. Hoogewerf AJ, Black D, Proudfoot AEI, Wells TNC, Power CA. 1996. Molecular cloning of murine CC CKR-4 and high affinity binding of chemokines to murine and human CC CKR-4. *Biochem. Biophys. Res. Commun.* 218:337–43
98. Samson M, Labbe O, Mollereau C, Vassart G, Parmentier M. 1996. Molecular cloning and functional expression of a new human CC-chemokine receptor gene. *Biochemistry* 35:3362–67
99. Dobner T, Wolf I, Emrich T, Lipp M. 1992. Differentiation-specific expression of a novel G protein-coupled receptor from Burkitt's lymphoma. *Eur. J. Immunol.* 22:2795–99
100. Kaiser E, Förster R, Wolf I, Ebensperger C, Kuehl WM, Lipp M. 1993. The G protein-coupled receptor BLR1 is involved in murine B cell differentiation and is also expressed in neuronal tissues. *Eur. J. Immunol.* 23:2532–39
101. Förster R, Emrich T, Kremmer E, Lipp M. 1994. Expression of the G-protein-coupled receptor BLR1 defines mature, recirculating B cells and a subset of T-helper memory cells. *Blood* 84:830–40
102. Barella L, Loetscher M, Tobler A, Baggiolini M, Moser B. 1995. Sequence variation of a novel heptahelical leucocyte receptor through alternative transcript formation. *Biochem. J.* 309:773–79
103. Birkenbach M, Josefsen K, Yalamanchili R, Lenoir G, Kieff E. 1993. Epstein-Barr virus-induced genes: first lymphocyte-specific G protein-coupled peptide receptors. *J. Virol.* 67:2209–20
104. Combadiere C, Ahuja SK, Murphy PM. 1995. Cloning, chromosomal localization, and RNA expression of a human β chemokine receptor-like gene. *DNA Cell. Biol.* 14:673–80
105. Raport CJ, Schweickart VL, Eddy RL Jr, Shows TB, Gray PW. 1995. The orphan G-protein-coupled receptor-encoding gene V28 is closely related to genes for chemokine receptors and is expressed in lymphoid and neural tissues. *Gene* 163:295–99
106. Gao J-L, Murphy PM. 1994. Human cytomegalovirus open reading frame US28 encodes a functional β chemokine receptor. *J. Biol. Chem.* 269:28539–42
107. Ahuja SK, Murphy PM. 1993. Molecular piracy of mammalian interleukin-8 receptor type B by herpesvirus saimiri. *J. Biol. Chem.* 268:20,691–94
108. Murayama T, Kuno K, Jisaki F, Obuchi M, Sakamuro D, Furukawa T, Mukaida N, Matsushima K. 1994. Enhancement of human cytomegalovirus replication in a human lung fibroblast cell line by interleukin-8. *J. Virol.* 68:7582–85
109. Wu D, LaRosa GJ, Simon MI. 1993. G protein-coupled signal transduction pathways for interleukin-8. *Science* 261:101–3
110. Loetscher P, Seitz M, Clark-Lewis I, Baggiolini M, Moser B. 1994. Both interleukin-8 receptors independently mediate chemotaxis. Jurkat cells transfected with IL-8R1 or IL-8R2 migrate in response to IL-8, GROα and NAP-2. *FEBS Lett.* 341:187–92
111. Jones SA, Moser B, Thelen M. 1995. A comparison of post-receptor signal transduction events in Jurkat cells transfected with either IL-8R1 or IL-8R2: chemokine mediated activation of p42/p44 MAP-kinase (ERK-2). *FEBS Lett.* 364:211–14
112. Jones SA, Wolf M, Qin S, Mackay CR, Baggiolini M. 1996. Different functions for the interleukin 8 receptors of human neutrophil leukocytes. NADPH oxidase and phospholipase D are activated through IL-8R1 but not IL-8R2. *Proc. Natl. Acad. Sci. USA* 93:6682–86
113. L'Heureux GP, Bourgoin S, Jean N, McColl SR, Naccache PH. 1995. Diverging signal transduction pathways activated by interleukin-8 and related chemokines in

human neutrophils: interleukin-8, but not NAP-2 or GROα, stimulates phospholipase D activity. *Blood* 85:522–31
114. Dubois PM, Palmer D, Webb ML, Ledbetter JA, Shapiro RA. 1996. Early signal transduction by the receptor to the chemokine monocyte chemotactic protein-1 in a murine T cell hybrid. *J. Immunol.* 156:1356–61
115. Thelen M, Uguccioni M, Bösiger J. 1995. PI 3-kinase-dependent and independent chemotaxis of human neutrophil leukocytes. *Biochem. Biophys. Res. Commun.* 217:1255–62
116. Turner L, Ward SG, Westwick J. 1995. RANTES-activated human T lymphocytes: a role for phosphoinositide 3-kinase. *J. Immunol.* 155:2437–44
117. Bokoch GM. 1995. Chemoattractant signaling and leukocyte activation. *Blood* 86:1649–60
118. Laudanna C, Campbell JJ, Butcher EC. 1996. Role of Rho in chemoattractant-activated leukocyte adhesion through integrins. *Science* 271:981–83
119. Mueller SG, Schraw WP, Richmond A. 1994. Melanoma growth stimulatory activity enhances the phosphorylation of the class II interleukin-8 receptor in non-hematopoietic cells. *J. Biol. Chem.* 269:1973–80
120. Richardson RM, DuBose RA, Ali H, Tomhave ED, Haribabu B, Snyderman R. 1995. Regulation of human interleukin-8 receptor A: identification of a phosphorylation site involved in modulating receptor functions. *Biochemistry* 34:14193–201
121. Richardon RM, Ali H, Tomhave ED, Haribabu B, Snyderman R. 1995. Cross-desensitization of chemoattractant receptors occurs at multiple levels—evidence for a role for inhibition of phospholipase C activity. *J. Biol. Chem.* 270:27829–33
122. Rajarathnam K, Clark-Lewis I, Sykes BD. 1994. ^{1}H NMR studies of interleukin 8 analogs: characterization of the domains essential for function. *Biochemistry* 33:6623–30
123. Schraufstätter IU, Ma M, Oades ZG, Barritt DS, Cochrane CG. 1995. The role of Tyr^{13} and Lys^{15} of interleukin-8 in the high affinity interaction with the interleukin-8 receptor type A. *J. Biol. Chem.* 270:10428–31
124. Heinrich JN, Bravo R. 1995. N51 competes ^{125}I-interleukin (IL)-8 binding to IL-8Rβ but not IL-8Rα—structure-function analysis using N51/IL-8 chimeric molecules. *J. Biol. Chem.* 270:28,014–17
125. Hammond MEW, Shyamala V, Siani MA, Gallegos CA, Feucht PH, Abbott J, Lapointe GR, Moghadam M, Khoja H, Zakel J, Tekamp-Olson P. 1996. Receptor recognition and specificity of interleukin-8 is determined by residues that cluster near a surface-accessible hydrophobic pocket. *J. Biol. Chem.* 271:8228–35
126. Williams G, Borkakoti N, Bottomley GA, Cowan I, Fallowfield AG, Jones PS, Kirtland SJ, Price GJ, Price L. 1996. Mutagenesis studies of interleukin-8—identification of a second epitope involved in receptor binding. *J. Biol. Chem.* 271:9579–86
127. Lowman HB, Slagle PH, DeForge LE, Wirth CM, Gillece-Castro BL, Bourell JH, Fairbrother WJ. 1996. Exchanging interleukin-8 and melanoma growth-stimulating activity receptor binding specificities. *J. Biol. Chem.* 271:14,344–52
128. Beall CJ, Mahajan S, Kolattukudy PE. 1992. Conversion of monocyte chemoattractant protein-1 into a neutrophil attractant by substitution of two amino acids. *J. Biol. Chem.* 267:3455–59
129. Lusti-Narasimhan M, Power CA, Allet B, Alouani S, Bacon KB, Mermod J-J, Proudfoot AEI, Wells TNC. 1995. Mutation of Leu^{25} and Val^{27} introduces CC chemokine activity into interleukin-8. *J. Biol. Chem.* 270:2716–21
130. Lusti-Narasimhan M, Chollet A, Power CA, Allet B, Proudfoot AEI, Wells TNC. 1996. A molecular switch of chemokine receptor selectivity—chemical modification of the interleukin-8 Leu25⟶Cys mutant. *J. Biol. Chem.* 271:3148–53
131. Walz A, Meloni F, Clark-Lewis I, von Tscharner V, Baggiolini M. 1991. $[Ca^{2+}]_i$ changes and respiratory burst in human neutrophils and monocytes induced by NAP-1/interleukin-8, NAP-2, and gro/MGSA. *J. Leuk. Biol.* 50:279–86
132. Gong J-H, Clark-Lewis I. 1995. Antagonists of monocyte chemoattractant protein 1 identified by modification of functionally critical NH_2-terminal residues. *J. Exp. Med.* 181:631–40
133. Weber M, Uguccioni M, Baggiolini M, Clark-Lewis I, Dahinden CA. 1996. Deletion of the NH_2-terminal residue converts monocyte chemotactic protein 1 from an activator of basophil mediator release to an eosinophil chemoattractant. *J. Exp. Med.* 183:681–85
134. Masure S, Paemen L, Proost P, Van Damme J, Opdenakker G. 1995. Expression of a human mutant monocyte chemotactic protein 3 in *Pichia pastoris* and characterization as an MCP-3

receptor antagonist. *J. Interferon Cytokine Res.* 15:955–63
135. Proudfoot AEI, Power CA, Hoogewerf AJ, Montjovent MO, Borlat F, Offord RE, Wells TNC. 1996. Extension of recombinant human RANTES by the retention of the initiating methionine produces a potent antagonist. *J. Biol. Chem.* 271:2599–603
136. Springer TA. 1995. Traffic signals on endothelium for lymphocyte recirculation and leukocyte emigration. *Annu. Rev. Physiol.* 57:827–72
137. Butcher EC, Picker LJ. 1996. Lymphocyte homing and homeostasis. *Science* 272:60–66
138. Luscinskas FW, Gimbrone MA Jr. 1996. Endothelial-dependent mechanisms in chronic inflammatory leukocyte recruitment. *Annu. Rev. Med.* 47:413–21
139. Broxmeyer HE, Sherry B, Lu L, Cooper S, Carow C, Wolpe SD, Cerami A. 1989. Myelopoietic enhancing effects of murine macrophage inflammatory proteins 1 and 2 on colony formation in vitro by murine and human bone marrow granulocyte/macrophage progenitor cells. *J. Exp. Med.* 170:1583–94
140. Graham GJ, Wright EG, Hewick R, Wolpe SD, Wilkie NM, Donaldson D, Lorimore S, Pragnell IB. 1990. Identification and characterization of an inhibitor of haemopoietic stem cell proliferation. *Nature* 344:442–44
141. Cook DN. 1996. The role of MIP-1α in inflammation and hematopoiesis. *J. Leuk. Biol.* 59:61–66
142. Colditz IG, Zwahlen RD, Baggiolini M. 1990. Neutrophil accumulation and plasma leakage induced in vivo by neutrophil-activating peptide-1. *J. Leukocyte. Biol.* 48:129–37
143. Webb LMC, Ehrengruber MU, Clark-Lewis I, Baggiolini M, Rot A. 1993. Binding to heparan sulfate or heparin enhances neutrophil responses to interleukin 8. *Proc. Natl. Acad. Sci. USA* 90:7158–62
144. Witt DP, Lander AD. 1994. Differential binding of chemokines to glycosaminoglycan subpopulations. *Curr. Biol.* 4:394–400
145. Tanaka Y, Adams DH, Shaw S. 1993. Proteoglycans on endothelial cells present adhesion-inducing cytokines to leukocytes. *Immunol. Today* 14:111–15
146. Gilat D, Hershkoviz R, Mekori YA, Vlodavsky I, Lider O. 1994. Regulation of adhesion of $CD4^+$ T lymphocytes to intact or heparinase-treated subendothelial extracellular matrix by diffusible or anchored RANTES and MIP-1β. *J. Immunol.* 153:4899–4906
147. Rot A, Hub E, Middleton J, Pons F, Rabeck C, Thierer K, Wintle J, Wolff B, Zsak M, Dukor P. 1996. Some aspects of IL-8 pathophysiology. 3. Chemokine interaction with endothelial cells. *J. Leuk. Biol.* 59:39–44
148. Watson JB, Getzler SB, Mosher DF. 1994. Platelet factor 4 modulates the mitogenic activity of basic fibroblast growth factor. *J. Clin. Invest.* 94:261–68
149. Brown KJ, Parish CR. 1994. Histidine-rich glycoprotein and platelet factor 4 mask heparan sulfate proteoglycans recognized by acidic and basic fibroblast growth factor. *Biochemistry* 33:13,918–27
150. Chaudhuri A, Polyakova J, Zbrzezna V, Williams K, Gulati S, Pogo AO. 1993. Cloning of glycoprotein D cDNA, which encodes the major subunit of the Duffy blood group system and the receptor for the *Plasmodium vivax* malaria parasite. *Proc. Natl. Acad. Sci. USA* 90:10793–97
151. Horuk R, Chitnis CE, Darbonne WC, Colby TJ, Rybicki A, Hadley TJ, Miller LH. 1993. A receptor for the malarial parasite *Plasmodium vivax*: the erythrocyte chemokine receptor. *Science* 261:1182–84
152. Horuk R, Martin A, Hesselgesser J, Hadley T, Lu ZH, Wang ZX, Peiper SC. 1996. The Duffy antigen receptor for chemokines: structural analysis and expression in the brain. *J. Leuk. Biol.* 59:29–38
153. Darbonne WC, Rice GC, Mohler MA, Apple T, Hébert CA, Valente AJ, Baker JB. 1991. Red blood cells are a sink for interleukin 8, a leukocyte chemotaxin. *J. Clin. Invest.* 88:1362–69
154. Taub DD, Conlon K, Lloyd AR, Oppenheim JJ, Kelvin DJ. 1993. Preferential migration of activated $CD4^+$ and $CD8^+$ T cells in response to MIP-1α and MIP-1β. *Science* 260:355–58
155. Rand ML, Warren JS, Mansour MK, Newman W, Ringler DJ. 1996. Inhibition of T cell recruitment and cutaneous delayed-type hypersensitivity-induced inflammation with antibodies to monocyte chemoattractant protein-1. *Am. J. Pathol.* 148:855–64
156. Huffnagle GB, Strieter RM, Standiford TJ, McDonald RA, Burdick MD, Kunkel SL, Toews GB. 1995. The role of monocyte chemotactic protein-1 (MCP-1) in the recruitment of monocytes and $CD4^+$ T cells during a pulmonary

Cryptococcus neoformans infection. *J. Immunol.* 155:4790–97
157. Colditz IG, Watson DL. 1992. The effect of cytokines and chemotactic agonists on the migration of T lymphocytes into skin. *Immunology* 76:272–78
158. Kennedy J, Kelner GS, Kleyensteuber S, Schall TJ, Weiss MC, Yssel H, Schneider PV, Cocks BG, Bacon KB, Zlotnik A. 1995. Molecular cloning and functional characterization of human lymphotactin. *J. Immunol.* 155:203–9
159. Müller S, Dorner B, Korthäuer U, Mages HW, D'Apuzzo M, Senger G, Kroczek RA. 1995. Cloning of ATAC, an activation-induced, chemokine-related molecule exclusively expressed in $CD8^+$ T lymphocytes. *Eur. J. Immunol.* 25:1744–48
160. Leek RD, Harris AL, Lewis CE. 1994. Cytokine networks in solid human tumors: regulation of angiogenesis. *J. Leuk. Biol.* 56:423–35
161. Maione TE, Gray GS, Petro J, Hunt AJ, Donner AL, Bauer SI, Carson HF, Sharpe RJ. 1990. Inhibition of angiogenesis by recombinant human platelet factor-4 and related peptides. *Science* 247:77–79
162. Sharpe RJ, Byers HR, Scott CF, Bauer SI, Maione TE. 1990. Growth inhibition of murine melanoma and human colon carcinoma by recombinant human platelet factor 4. *J. Natl. Cancer. Inst.* 82:848–53
163. Luster AD, Greenberg SM, Leder P. 1995. The IP-10 chemokine binds to a specific cell surface heparan sulfate site shared with platelet factor 4 and inhibits endothelial cell proliferation. *J. Exp. Med.* 182:219–31
164. Koch AE, Polverini PJ, Kunkel SL, Harlow LA, DiPietro LA, Elner VM, Elner SG, Strieter RM. 1992. Interleukin-8 as a macrophage-derived mediator of angiogenesis. *Science* 258:1798–801
165. Strieter RM, Polverini PJ, Kunkel SL, Arenberg DA, Burdick MD, Kasper J, Dzuiba J, Van Damme J, Walz A, Marriott D, Chan SY, Roczniak S, Shanafelt AB. 1995. The functional role of the ELR motif in CXC chemokine-mediated angiogenesis. *J. Biol. Chem.* 270:27348–57
166. Petzelbauer P, Watson CA, Pfau SE, Pober JS. 1995. IL-8 and angiogenesis: evidence that human endothelial cells lack receptors and do not respond to IL-8 in vitro. *Cytokine* 7:267–72
167. Cao YH, Chen C, Weatherbee JA, Tsang M, Folkman J. 1995. gro-β, a -C-X-C- chemokine, is an angiogenesis inhibitor that suppresses the growth of Lewis lung carcinoma in mice. *J. Exp. Med.* 182:2069–77
168. Arenberg DA, Kunkel SL, Polverini PJ, Glass M, Burdick MD, Strieter RM. 1996. Inhibition of interleukin-8 reduces tumorigenesis of human non-small cell lung cancer in SCID mice. *J. Clin. Invest.* 97:2792–802
169. Singh RK, Gutman M, Radinsky R, Bucana CD, Fidler IJ. 1994. Expression of interleukin 8 correlates with the metastatic potential of human melanoma cells in nude mice. *Cancer. Res.* 54:3242–47
170. Wang JY, Huang M, Lee P, Komanduri K, Sharma S, Chen G, Dubinett SM. 1996. Interleukin-8 inhibits non-small cell lung cancer proliferation: a possible role for regulation of tumor growth by autocrine and paracrine pathways. *J. Interferon Cytokine Res.* 16:53–60
171. Hirose K, Hakozaki M, Nyunoya Y, Kobayashi Y, Matsushita K, Takenouchi T, Mikata A, Mukaida N, Matsushima K. 1995. Chemokine gene transfection into tumour cells reduced tumorigenicity in nude mice in association with neutrophilic infiltration. *Br. J. Cancer* 72:708–14
172. Luster AD, Leder P. 1993. IP-10, a -C-X-C- chemokine, elicits a potent thymus-dependent antitumor response in vivo. *J. Exp. Med.* 178:1057–65
173. Koch AE, Halloran MM, Haskell CJ, Shah MR, Polverini PJ. 1995. Angiogenesis mediated by soluble forms of E-selectin and vascular cell adhesion molecule-1. *Nature* 376:517–19
174. Cocchi F, DeVico AL, Garzino-Demo A, Arya SK, Gallo RC, Lusso P. 1995. Identification of RANTES, MIP-1α, and MIP-1β as the major HIV-suppressive factors produced by $CD8^+$ T cells. *Science* 270:1811–15
175. Dragic T, Litwin V, Allaway GP, Martin SR, Huang YX, Nagashima KA, Cayanan C, Maddon PJ, Koup RA, Moore JP, Paxton WA. 1996. HIV-1 entry into $CD4^+$ cells is mediated by the chemokine receptor CC-CKR-5. *Nature* 381:667–73
176. Deng HK, Liu R, Ellmeier W, Choe S, Unutmaz D, Burkhart M, Di Marzio P, Marmon S, Sutton RE, Hill CM, Davis CB, Peiper SC, Schall TJ, Littman DR, Landau NR. 1996. Identification of a major co-receptor for primary isolates of HIV-1. *Nature* 381:661–66
177. Choe H, Farzan M, Sun Y, Sullivan N, Rollins B, Ponath PD, Wu L, Mackay CR, LaRosa G, Newman W, Gerard N, Gerard C, Sodroski J. 1996. The β-chemokine

receptors CCR3 and CCR5 facilitate infection by primary HIV-1 isolates. *Cell* 85:1135–48

178. Doranz BJ, Rucker J, Yi Y, Smyth RJ, Samson M, Peiper SC, Parmentier M, Collman RG, Doms RW. 1996. A dual-tropic primary HIV-1 isolate that uses fusin and the β-chemokine receptors CKR-5, CKR-3, and CKR-2b as fusion cofactors. *Cell* 85:1149–58
179. Alkhatib G, Combadiere C, Broder CC, Feng Y, Kennedy PE, Murphy PM, Berger EA. 1996. CC CKR5: A RANTES, MIP-1α, MIP-1β receptor as a fusion cofactor for macrophage-tropic HIV-1. *Science* 272:1955–58
180. Paxton WA, Martin SR, Tse D, O'Brien TR, Skurnick J, VanDevanter NL, Padian N, Braun JF, Kotler DP, Wolinsky SM, Koup RA. 1996. Relative resistance to HIV-1 infection of CD4 lymphocytes from persons who remain uninfected despite multiple high-risk sexual exposures. *Nature Med.* 2:412–17
181. Sneath PHA, Sokal RR. 1973. *Numerical Taxonomy*. New York: Freeman

THE JOURNAL OF BIOLOGICAL CHEMISTRY
Vol. 270, No. 45, Issue of November 10, pp. 27348–27357, 1995
Printed in U.S.A.

The Functional Role of the ELR Motif in CXC Chemokine-mediated Angiogenesis*

(Received for publication, July 7, 1995, and in revised form, August 11, 1995)

Robert M. Strieter‡§, Peter J. Polverini¶, Steven L. Kunkel‖, Douglas A. Arenberg‡, Marie D. Burdick‡, James Kasper**, Judith Dzuiba‡‡, Jo Van Damme§§, Alfred Walz¶¶, David Marriott‖‖, Sham-Yuen Chan‖‖, Steven Roczniak**, and Armen B. Shanafelt**

*From the Departments of ‡Internal Medicine (Division of Pulmonary and Critical Medicine) and ‖Pathology, the University of Michigan Medical School, Ann Arbor, Michigan 48109-0360, the ¶University of Michigan Dental School, Section of Oral Pathology, Ann Arbor, Michigan 48109, the §§Rega Institute, University of Leuven, B-3000 Leuven, Belgium, the ¶¶Theodor Kocher Institut, University of Bern, CH-3000, Bern 9, Switzerland, the **Institute of Molecular Biologicals and ‡‡Institute of Research Technologies, Bayer Corporation, West Haven, Connecticut 06516, and the ‖‖Department of Molecular and Cellular Biology, Bayer Corporation, Berkeley, California 94701*

In this study, we demonstrate that the CXC family of chemokines displays disparate angiogenic activity depending upon the presence or absence of the ELR motif. CXC chemokines containing the ELR motif (ELR-CXC chemokines) were found to be potent angiogenic factors, inducing both *in vitro* endothelial chemotaxis and *in vivo* corneal neovascularization. In contrast, the CXC chemokines lacking the ELR motif, platelet factor 4, interferon γ-inducible protein 10, and monokine induced by γ-interferon, not only failed to induce significant *in vitro* endothelial cell chemotaxis or *in vivo* corneal neovacularization but were found to be potent angiostatic factors in the presence of either ELR-CXC chemokines or the unrelated angiogenic factor, basic fibroblast growth factor. Additionally, mutant interleukin-8 proteins lacking the ELR motif demonstrated potent angiostatic effects in the presence of either ELR-CXC chemokines or basic fibroblast growth factor. In contrast, a mutant of monokine induced by γ-interferon containing the ELR motif was found to induce *in vivo* angiogenic activity. These findings suggest a functional role of the ELR motif in determining the angiogenic or angiostatic potential of CXC chemokines, supporting the hypothesis that the net biological balance between angiogenic and angiostatic CXC chemokines may play an important role in regulating overall angiogenesis.

Angiogenesis, characterized by the neoformation of blood vessels, is an essential biological event encountered in a number of physiological and pathological processes, such as embryonic development, the formation of inflammatory granulation tissue during wound healing, chronic inflammation, and the growth of malignant solid tumors (1–5). Neovascularization can be rapidly induced in response to diverse pathophysiologic stimuli. Under conditions of homeostasis, the rate of capillary endothelial cell turn-over is typically measured in months or years (6, 7). However, the process of angiogenesis during normal wound repair is rapid, transient, and tightly controlled. During neovascularization, normally quiescent endothelial cells are stimulated, degrade their basement membrane and proximal extracellular matrix, migrate directionally, divide, and organize into new functioning capillaries invested by a basal lamina (1–5). The abrupt termination of angiogenesis that accompanies the resolution of the wound repair suggests two possible mechanisms of control: a marked reduction in angiogenic mediators coupled with a simultaneous increase in the level of angiostatic factors that inhibit new vessel growth (8). In contrast to neovascularization of normal wound repair, tumorigenesis is associated with exaggerated angiogenesis, suggesting the existence of augmented angiogenic and reduced levels of angiostatic mediators (3, 9). Although most investigations studying angiogenesis have focused on the identification and mechanism of action of angiogenic factors, recent evidence suggests that angiostatic factors may play an equally important role in the control of neovascularization (8, 10–26).

Recently, platelet factor 4 (PF4),[1] a member of the CXC chemokine family, has been found to be an inhibitor of angiogenesis (27). In contrast, interleukin-8 (IL-8), another member of the CXC chemokine family, has been shown to have potent angiogenic properties (28–30). Although these CXC chemokines have significant homology on the amino acid level, one of the major differences between IL-8 and PF4 is the presence in IL-8 of the sequence Glu-Leu-Arg (the ELR motif), which is not found in PF4 (31–34). These three amino acids appear to be important in ligand/receptor interactions on neutrophils (35, 36) and are highly conserved in all members of the CXC chemokine family that demonstrate biological activation of neutrophils (35, 36).

In this study, we demonstrate that members of the CXC chemokine family that contain the ELR motif, as compared with members that lack these three amino acids, are potent inducers of angiogenic activity. In addition, we show that CXC chemokines that lack the ELR motif, PF4, interferon γ-inducible protein 10 (IP-10), and monokine induced by γ-interferon (MIG) are potent inhibitors of both CXC (ELR) chemokine and

*This work was supported, in part, by National Institutes of Health Grants HL50057, CA66180, and 1P50HL46487 (to R. M. S.), HL39926 (to P. J. P.), and HL31693 and HL35276 (to S. L. K.) and by the General Savings and Retirement Fund (ASLK) Cancer Foundation, Belgium (to J. V. D.). The costs of publication of this article were defrayed in part by the payment of page charges. This article must therefore be hereby marked "*advertisement*" in accordance with 18 U.S.C. Section 1734 solely to indicate this fact.

§To whom correspondence should be addressed: Dept. of Internal Medicine, Div. of Pulmonary and Critical Care, Box 0360, University of Michigan Medical Center, 3916 Taubman Dr., Ann Arbor, MI 48109-0360. Tel.: 313-764-4554; Fax: 313-764-4556.

[1] The abbreviations used are: PF4, platelet factor 4; IL-8, interleukin-8; IP-10, interferon γ-inducible protein 10; MIG, monokine induced by γ-interferon; bFGF, basic fibroblast growth factorbasic fibroblast growth factor; PAGE, polyacrylamide gel electrophoresis; GRO, growth-related oncogene; ENA-78, epithelial neutrophil activating protein-78; GCP-2, granulocyte chemotactic protein-2; PBS, phosphate-buffered saline; GST, glutathione *S*-transferase; HPF, high power field(s); IFN, interferon.

basic fibroblast growth factor (bFGF)-induced angiogenesis. Moreover, substitution of the ELR motif in IL-8, generated proteins that antagonized the angiogenic effects of ELR-CXC chemokines and bFGF, while a mutant of MIG containing the ELR motif was angiogenic. These results suggest that the presence or absence of the ELR motif in CXC chemokines functionally defines the angiogenic (ELR containing) or angiostatic (non-ELR) characteristics of these proteins. These findings support the notion that CXC chemokines play an important role in the regulation of angiogenesis by acting as either angiogenic or angiostatic factors.

MATERIALS AND METHODS

Reagents—Human recombinant IP-10 (lyophilized protein with no additives) was purchased from Pepro Tech Inc. (Rocky Hill, NJ). IP-10 was >98% pure by SDS-PAGE analysis. Human recombinant bFGF (lyophilized protein with no additives) was purchased from R&D Systems Inc. (Minneapolis, MN). bFGF was >97% pure, as determined by NH_2 terminus analysis and SDS-PAGE. Recombinant human PF4, natural NH_2-terminal truncated forms of platelet basic protein (connective tissue activating protein-III, β-thromboglobulin, and neutrophil-activating protein-2), recombinant IL-8 (72 amino acids), recombinant human growth-related oncogene (GRO-α), recombinant human GRO-β, recombinant human GRO-γ, and recombinant human epithelial neutrophil activating protein-78 (ENA-78) were provided by A. Walz. These chemokines were lyophilized proteins with no additives and were >97% pure, as determined by NH_2 terminus analysis and SDS-PAGE. Natural granulocyte chemotactic protein-2 (GCP-2; Ref. 34) was provided by J. Van Damme and was >98% pure, as determined by NH_2 terminus analysis and SDS-PAGE. Endotoxin levels were less than 0.1 ng/μg for the above cytokines. The proteins were either reconstituted in Dulbecco's modified Eagle's medium with 0.1% bovine serum albumin for analysis in endothelial cell chemotaxis assays, Hanks' balanced salt solution with calcium/magnesium for analysis in neutrophil cell chemotaxis assays, or 1 × PBS for the corneal micropocket model of angiogenesis.

Bacterial Host Strains and Vectors—The *Escherichia coli* K12 strain DH5αF′ (Life Technologies, Inc.) was used as host for the propagation and maintenance of M13 DNA, and for expression of IL-8 and MIG proteins. Strain CJ236 was used to prepare uracil-DNA for use in site-directed mutagenesis (37). pGEX 4T-1 (Pharmacia Biotech Inc.) was used as the expression vector for all MIG cDNAs (38). pMAL-c2 (New England BioLabs) was used as the expression vector for all IL-8 cDNAs.

Mutagenesis, Recombinant DNA, and Sequencing Protocols—Site-directed mutagenesis was followed the protocol described by Kunkel *et al.* (37). Individual clones were sequenced using the dideoxynucleotide method (39) with modifications described in the Sequenase® (U. S. Biochemical Corp.) protocol. M13 (replicative form) DNA (40) containing confirmed MIG mutations was cleaved with *Bam*HI and *Xba*I (New England Biolabs) and subcloned into pGEX 4T-1. A 197-base pair *Sac* I (New England Biolabs) fragment from pMAL.hIL-8 (maltose binding protein-Ile-Glu-Gly-Arg-human IL-8 fusion protein expression vector) containing the coding sequence for the NH_2-terminal 49 amino acids of the 72-amino acid form of human IL-8 sequence was subcloned to pUC118 (ATCC) digested with *Sac*I for site-directed mutagenesis. Clones containing confirmed IL-8 mutations were cleaved with *Sac*I and subcloned into pMAL.hIL-8 digested with *Sac*I.

Cloning, Expression, and Purification of Human MIG—The open reading frame of human MIG (38) was amplified from cDNA generated from interferon γ-stimulated (1000 units/ml for 16 h) THP-1 cells by polymerase chain reaction. The 5′-primer used, 5′-CAAGGTGGATCCATGAAGAAAAAGTGGTGTTC-3′, encodes a *Bam*HI restricition site immediately upstream of the ATG start site. The 3′-primer, 5′-GCAAGCTCTAGATTATGTAGTCTTCTTTTGACGAGAACG-3′, encodes a *Xba*I restriction site immediately downstream of the TAA stop codon. The 402-base pair fragment was subcloned to M13mp19 and was confirmed as the human MIG open reading frame by sequencing. Thr^{23} of the open reading frame sequence is the predicted NH_4-terminal amino acid of the mature, secreted MIG protein (38) and will be referred to here as amino acid position 1. Amino acids Lys^6 and Gly^7 were modified to Glu and Leu, respectively, by site-directed mutagenesis, generating the MIG mutein ELR-MIG. A *Bam*HI restriction site was introduced overlapping Gly^{-1} and Thr^1 by site-directed mutagenesis (37), resulting in mutein MIG or ELR-MIG cDNAs encoding a Thr^1 to Ser substitution. 324-base pair fragments obtained from correct M13 RF clones digested with *Bam*HI/*Xba*I were subcloned to pGEX 4T-1 to generate glutathione *S*-transferase-MIG fusion DNAs (GST-MIG or GST-ELR-MIG). The sequence encoded by these DNAs contains the thrombin recognition sequence LVPRGS between the GST and MIG sequences. Digestion of GST-MIG fusion protein with thrombin is predicted to release MIG protein having an NH_4-terminal sequence Gly-Ser-Pro, *versus* the predicted nonmodified NH_4-terminal sequence Thr-Pro.

Cultures of *E. coli* strain DH5αF′ harboring GST-MIG or GST-ELR-MIG plasmid were grown in 1 liter of LB media containing 50 μg/ml ampicillin to $A_{600} \sim 0.5$ at 22 °C with aeration, and protein expression was induced by the addition of 0.1 mM final isopropyl-1-thio-β-D-galactoside and continued incubation at 22 °C for 5–6 h. After induction, the cells were harvested by centrifuging at 6,000 × *g* for 10 min and the pellet was washed once in ice-cold PBS and resuspended in 10 ml of ice-cold 10 mM HEPES, 30 mM NaCl, 10 mM EDTA, 10 mM EGTA, 0.25% Tween 20, 1 mM phenylmethylsulfonyl fluoride (added fresh), pH 7.5 (lysis buffer). The resulting suspension was quick-frozen in liquid nitrogen. After thawing, phenylmethylsulfonyl fluoride was again added to yield a final concentration of 2 mM. The suspension was sonicated using a Branson Sonifier 250 equipped with a microtip for 2 min at output setting 5 with a 40% duty cycle. Triton X-100 was added to a final concentration of 1%, and the lysate was mutated for 30 min at room temperature to aid in the solubilization of the fusion protein. The lysate was then centrifuged at 34,500 × *g* for 10 min, and the supernatant was transferred to a fresh tube.

The GST-MIG protein was purified using the Pharmacia GST purification module (Pharmacia) essentially as described in the manufac-

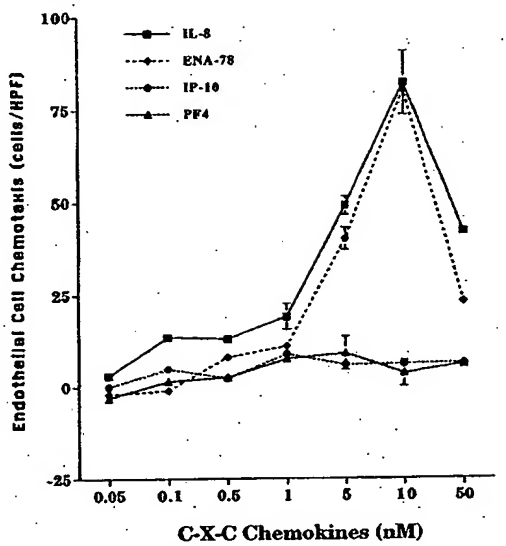

FIG. 1. **Endothelial cell chemotaxis in response to CXC chemokines (50 pM to 50 nM).** To demonstrate specific migration, background (unstimulated control) migration (cells/HPF) was subtracted.

TABLE I

Endothelial cell chemotaxis in response to CXC chemokines

Experimental $n = 3$.

Condition (10 nM)	Increase over control
	-fold
IL-8	5.1 ± 0.7
ENA-78	6.5 ± 0.8
GCP2	6.2 ± 0.4
GRO-α	5.3 ± 0.3
GRO-β	3.5 ± 0.2
GRO-γ	4.5 ± 0.5
PBP	3.4 ± 0.1
CTAP-III	5.2 ± 0.3
β-TG	1.6 ± 0.2
NAP-2	3.9 ± 0.1
IP-10	0.1 ± 0.1
PF4	0.1 ± 0.0
MIG	0.1 ± 0.0

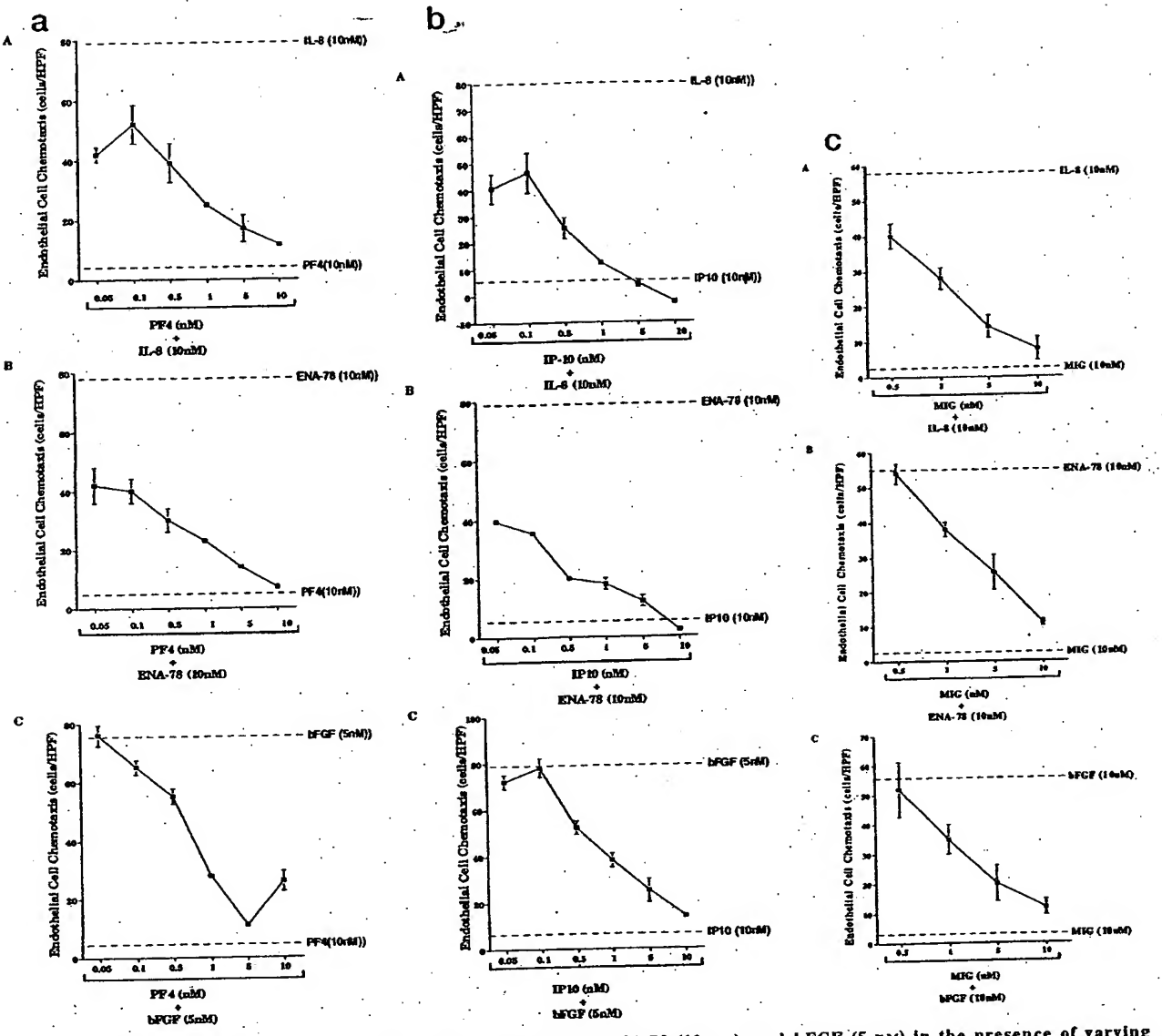

FIG. 2. **Endothelial cell chemotaxis in response to IL-8 (10 nM), ENA-78 (10 nM), and bFGF (5 nM) in the presence of varying concentrations PF4 (50 pM to 10 nM; *part a*), IP-10 (50 pM to 10 nM; *part b*), and MIG (500 pM to 10 nM; *part c*).** To demonstrate specific migration, background (unstimulated control) migration (cells/HPF) was subtracted.

turer's protocol. GST-fusion protein sonicate was passed over a 2-ml glutathione-Sepharose 4B column equilibrated in PBS. After washing with PBS, the GST-fusion protein was eluted with 3 column volumes of 10 mM reduced glutathione, 50 mM Tris-HCL, pH 8.0. 10 units of thrombin/A_{280} unit of fusion protein was added to the eluted GST-MIG or GST-ELR-MIG fusion protein and incubated at room temperature with occasional gentle mixing for 2–3 h. MIG or ELR-MIG protein was ≥95% cleaved from the GST protein under these conditions as monitered by SDS-PAGE (41). The pH of the MIG-containing solution was adjusted to 4.0 using 0.5 M sodium acetate, pH 4.0, filtered through a cellulose acetate 0.45-μm filter (Costar) and passed over a Mono S column (Pharmacia) equilibrated with 20 mM sodium acetate, pH 4.0. MIG protein was eluted as a single peak using a 0–2 M NaCl gradient, and dialyzed against 0.5 mM $NaPO_4$, 20 mM NaCl, pH 7.0. Purified MIG and ELR-MIG was obtained endotoxin-free (<1.0 enzyme units/ml; QCL-1000 test, BioWhittaker), and yields ranged from 100–200 μg/liter (quantitated by amino acid analysis) with a purity of >95% (determined by SDS-PAGE, with apparent molecular mass of 16 kDa; amino acid analysis accuracy > 90%). Mass spectrometry of the purified MIG and ELR-MIG proteins confirmed their predicted mass.

Cloning, Expression, and Purification of Human IL-8—The 72-amino acid mature form of IL-8 was amplified using polymerase chain reaction from an IL-8 cDNA in pET3a (kindly provided by I. U. Schraufstatter, Scripps Clinic). The 5′-primer used, 5′-AGTGCTAAAGAACTTAGATG-3′, encodes the beginning reading frame of IL-8, and the 3′ primer, 5′-GGGATCCTCATGAATTCTC-3′, contains a *Bam*HI restriction site immediately after the stop codon. The 220-base pair PCR product was purified by gel electrophoresis, digested with *Bam*HI (New England Biolabs), subcloned into pMal-c2 previously digested with *Xmn*I and *Bam*HI (New England Biolabs) to generate pMal.hIL-8. Clones containing inserts were confirmed by sequencing. Site-directed mutagenesis was used to modify amino acids Glu^4-Leu^5-Arg^6 to Thr-Val-Arg or Asp-Leu-Gln, generating TVR-IL-8 or DLQ-IL-8, respectively. Correct clones were identified by sequencing and subcloned as *Sac*I fragments from pUC118 into pMal.hIL-8 digested with *Sac*I.

Cultures of *E. coli* strain DH5αF′ harboring pMal.hIL-8, pMal.TVR-IL-8, or pMal.DLQ-IL-8 were grown in 1-liter LB media containing 50 μg/ml ampicilin to A_{600} ~ 0.5 at 37 °C with aeration, and protein expression was induced by the addition of 0.3 mM final isopropyl-1-thio-β-D-galactoside and continued incubation at 37 °C for 2 h. Cells were harvested by centrifuging at 5800 × *g* for 10 min and the pellet was washed once in ice-cold PBS and resuspended in 10 ml of ice-cold lysis buffer. The resulting suspension was quick-frozen in liquid nitrogen.

After thawing, the suspension was sonicated using a Branson Soni-

TABLE II
The IC50 of PF4, IP-10, and MIG for the inhibition of the agonists IL-8, ENA-78, and bFGF

Experimental $n = 3$.

Agonist	IL-8 (10 nM)	ENA78 (10 nM)	bFGF (5 nM)
	M	M	M
PF4	5×10^{-11}	5×10^{-11}	1×10^{-9}
IP-10	5×10^{-11}	5×10^{-11}	1×10^{-9}
MIG	5×10^{-10}	5×10^{-9}	1×10^{-9}

fier 250 equipped with a microtip for 2 min at output setting 5 with a 40% duty cycle. The suspension was clarified by centrifugation at 9000 $\times g$, the supernatant was diluted 5-fold in 10 mM $NaPO_4$, 500 mM NaCl, 1 mM EGTA, 0.25% Tween 20, pH 7.0 (column buffer), and loaded onto a 10-ml amylose resin (New England Biolabs) affinity column. After extensive washing with column buffer, the maltose binding protein fusion protein was eluted with column buffer containing 10 mM maltose. Mutein or wild-type IL-8 proteins were released by incubation with 1 μg of Factor Xa (New England Biolabs)/A_{280} maltose binding protein fusion protein at room temperature overnight and were then passed over a Mono S column (Pharmacia) equilibrated in 10 mM $NaPO_4$, pH 6.2, and eluted in a 0–1 M NaCl gradient. 1 ml of amylose resin was added to fractions containing mutant or wild-type IL-8 protein to remove residual free maltose binding protein by incubation for 30 min at room temperature with gentle shaking. The resin was removed by centrifugation, and the supernatant was dialyzed against 0.5 mM $NaPO_4$, 20 mM NaCl, pH 7.5. Yields were ranged from 0.2 to 3.5 mg for wild-type or mutant IL-8 proteins and were ≥95% pure as assessed by SDS-PAGE and endotoxin-free (<1.0 enzyme units/ml). Proteins were quantitated by amino acid analysis, and had accuracies between 88–93%.

Endothelial Cell Chemotaxis—Endothelial cell chemotaxis was performed in 48-well chemotaxis chambers (Nucleopore Corp.) as described previously (28, 42). Briefly, bovine adrenal gland capillary endothelial cells were suspended at a concentration of 10^6 cells/ml in Dulbecco's modified Eagle's medium with 0.1% bovine serum albumin and placed into each of the bottom wells (25 μl). Nucleopore chemotaxis membranes (5-μm pore size) were coated with 0.1 mg/ml gelatin. The membranes were placed over the wells and the chambers were sealed, inverted, and incubated for 2 h to allow cells to adhere to the membrane. The chambers were then reinverted; 50 μl of sample (containing media alone, ELR-CXC chemokines, non-ELR-CXC chemokines, bFGF, or combinations of ELR-CXC and non-ELR-CXC chemokines or non-ELR-CXC chemokines and bFGF) was dispensed into the top wells and reincubated for an additional 2 h. Membranes were then fixed and stained with Diff-Quik staining kit (American Scientific Products), and cells that had migrated through the membrane were counted in 10 high power fields (HPF; 400×). Results were expressed as the number of endothelial cells that migrated per HPF after subtracting the background (unstimulated control) to demonstrate specific migration. Each sample was assessed in triplicate. Experiments were repeated at least three times.

Neutrophil Chemotaxis—Heparinized venous blood was collected from healthy volunteers and mixed 1:1 with 0.9% saline, and mononuclear cells were separated by Ficoll-Hypaque density gradient centrifugation. Human neutrophils were then isolated by sedimentation in 5% dextran, 0.9% saline (Sigma) and separated from erythrocytes by hypotonic lysis. After washing twice, neutrophils were suspended in Hanks' balanced salt solution with calcium/magnesium (Life Technologies, Inc.) at a concentration of 2×10^6 cells/ml. Neutrophils were >95% viable as determined by trypan blue exclusion. Neutrophil chemotaxis was performed as described previously (43, 44). 150 μl of sample (ELR-CXC, non-ELR-CXC, or combination of ELR-CXC and non-ELR-CXC chemokines), 1×10^{-7} M formylmethionyleucylphenylalanine (Sigma), or Hanks' balanced salt solution (Life Technologies, Inc., Grand Island, NY) alone were placed in duplicate bottom wells of a blind well chemotaxis chamber. A 3-μm pore size polycarbonate filter (polyvinylpyrrolidone-free, Nucleopore Corp.) was placed in the assembly, and 250 μl of human neutrophil was suspension placed in each of the top wells. Chemotaxis chamber assemblies were incubated at 37 °C in humidified 95% air, 5% CO_2 for 60 min. The filters were removed, fixed in absolute methanol, and stained with 2% toluidine blue (Sigma). Neutrophils that had migrated through to the bottom of the filter were counted in 10 HPF (400×) using a Javelin chromachip camera (Javelin Electronics, Japan) attached to a Olympus BH-2 microscope interfaced with a MacIntosh II computer containing an Image Capture 1000 frame grabber (Scion Corp., Walkersville, MD) and NIH Image, version 1.40 software (National Institutes of Health Public Software, Bethesda, MD). Each sample was assessed in triplicate. Experiments were repeated at least three times.

TABLE III
Neutrophil chemotaxis in response to CXC chemokines. Control is media alone

Experimental $n = 3$.

Condition (10 nM)	Cells/HPF
Control	18.4 ± 1.8
IP10	20.7 ± 4.2
MIG	8.6 ± 1.5
IL-8	96.4 ± 6.5
IL-8 + IP10	94.1 ± 9.3
IL-8 + MIG	78.6 ± 10.5

Corneal Micropocket Model of Angiogenesis—*In vivo* angiogenic activity was assayed in the avascular cornea of Long Evans rat eyes, as described previously (28, 29, 42). Briefly, cytokines were combined with sterile Hydron (Interferon Sciences Inc.) casting solution, and 5-μl aliquots were air-dried on the surface of polypropylene tubes. Prior to implantation, pellets were rehydrated with normal saline. Animals were anesthetized with an intraperitoneal injection of ketamine (150 mg/kg) and atropine (250 μg/kg). Rat corneas were anesthetized with 0.5% proparacaine hydrochloride ophthalmic solution followed by implantation of the Hydron pellet into an intracorneal pocket (1–2 mm from the limbus). 6 days after implantation, animals were pretreated intraperitoneally with 1000 units of heparin (Elkins-Sinn, Inc., Cherry Hill, NJ), anesthetized with ketamine (150 mg/Kg), and perfused with 10 ml of colloidal carbon via the left ventricle. Corneas were then harvested and photographed. No inflammatory response was observed in any of the corneas treated with the above cytokines. Positive neovascularization responses were recorded only if sustained directional ingrowth of capillary sprouts and hairpin loops toward the implant were observed. Negative responses were recorded when either no growth was observed or when only an occasional sprout or hairpin loop displaying no evidence of sustained growth was detected.

Statistical Analysis—Data were analyzed by a Macintosh IIfx computer using the Statview II statistical package (Abacus Concepts, Inc., Berkeley, CA). Data were expressed as mean ± S.E. and compared using the nonparametric analysis with the Wilcoxon signed rank test. Data were considered statistically significant if p values were ≤0.05.

RESULTS

CXC Chemokines Display Disparate Angiogenic Activity—Endothelial cell chemotaxis was performed in the presence or absence of IL-8, ENA-78, PF4, and IP-10 at concentrations of 50 pM to 50 nM. Both IL-8 and ENA-78 demonstrated a dose-dependent increase in endothelial migration that was significantly greater ($p < 0.05$) than control (background) at concentrations equal to or above 0.1 and 1 nM, respectively, with evidence of a "bell-shape" curve seen with other chemotactic factors (Fig. 1). In contrast, neither PF4 nor IP-10 induced significant ($p > 0.05$) endothelial cell chemotaxis (Fig. 1). Similar findings were also observed using either human umbilical or dermal microvascular endothelial cells (data not shown). The migration seen in response to IL-8 or ENA-78 was due to chemotaxis, not chemokinesis, as checkerboard analysis demonstrated directed, not random, migration (data not shown). Other CXC chemokines were tested for their ability to induce endothelial cell chemotaxis, including ELR-CXC chemokines IL-8, ENA-78, GCP-2, GRO-α, GRO-β, GRO-γ, platelet basic protein, connective tissue activating protein-III, and neutrophil-activating protein-2 or the non-ELR CXC chemokines IP-10, PF4, and MIG (Table I). In a similar fashion to IL-8 or ENA-78, all of the ELR-CXC chemokines tested demonstrated significant ($p < 0.05$) endothelial cell chemotactic activity over the background control, whereas the endothelial cell chemotactic activity induced by MIG was either similar to background control or to the endothelial cell chemotactic activity seen with either PF4 or IP-10. These findings suggested that CXC chemokines could be divided into two groups with defined biolog-

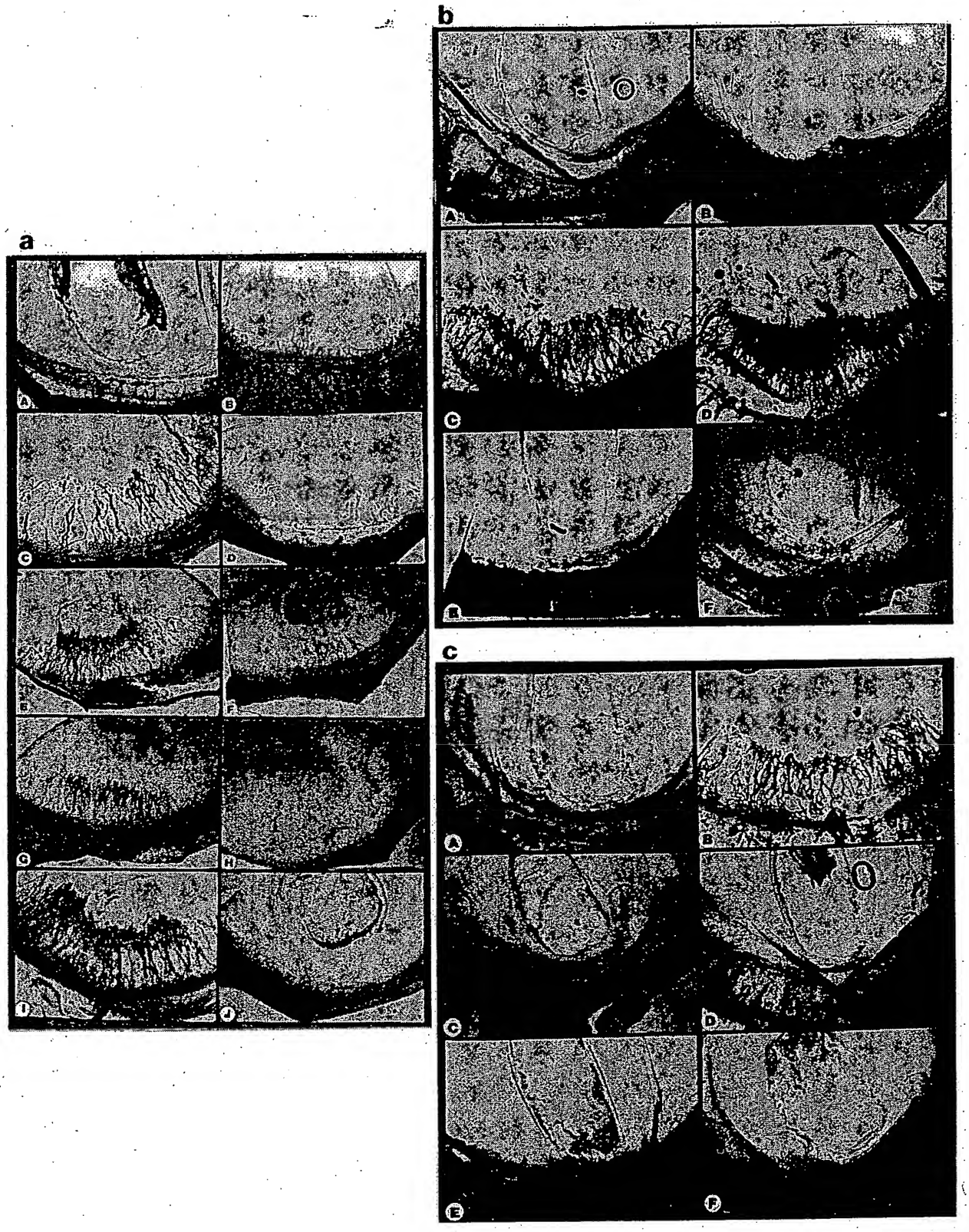

FIG. 3. **Rat cornea neovascularization in response to ELR-CXC chemokines, non-ELR-CXC chemokines, bFGF, or combinations of these cytokines.** *Part a, panels A, B, C, E, G,* and *I,* respectively, represent the corneal neovascular response to a hydron pellet alone (vehicle control), IP-10 (10 nM), IL-8 (10 nM), ENA-78 (10 nM), GRO-α (10 nM), or GCP-2 (10 nM); *part a, panels D, F, H,* and *J,* respectively, represent the combination of IL-8 with IP-10, ENA-78 with IP-10, GRO-α with IP-10, or GCP-2 with IP-10. *Part b, panels A–D,* respectively, represent the corneal neovascular response to a hydron pellet alone (vehicle control), MIG (10 nM), IL-8 (10 nM), or ENA-78 (10 nM); *part b, panels E* and *F,* respectively,

ical activities, one that contains the ELR-motif and is chemotactic for endothelial cells and the other that lacks the ELR motif and does not induce endothelial chemotaxis.

PF4, IP-10, or MIG Inhibit IL-8-, ENA-78-, or bFGF-induced Angiogenic Activity—While the above experiments suggested that PF4, IP-10, and MIG were not significant chemotactic factors for endothelial cells, we postulated that these CXC chemokines may be potent inhibitors of angiogenesis. To test this hypothesis, endothelial cell chemotaxis was performed in the presence or absence of IL-8 (10 nM), ENA-78 (10 nM), or bFGF (5 nM) with or without varying concentrations of PF4, IP-10, or MIG from 0 to 10 nM (Fig. 2, *a–c*, respectively). Endothelial cell migration in response to either IL-8, ENA-78, or bFGF was significantly inhibited by PF4, IP-10, or MIG in a dose-dependent manner (Fig. 2). PF4 and IP-10 in a concentration of 50 pM inhibited either IL-8- or ENA-78-induced endothelial chemotaxis by 50%, whereas, PF4 and IP-10 in a concentration of 1 nM attenuated the response to bFGF by 50% (Fig. 2, *a* and *b*, and Table II). MIG at a concentration of 1, 5, and 1 nM inhibited the endothelial cell chemotactic response to IL-8, ENA-78, and bFGF, respectively, by 50% (Fig. 2*c* and Table II). Interestingly, while IP-10 and MIG inhibited IL-8-induced endothelial cell chemotactic activity, neither IP-10 nor MIG were effective in attenuating IL-8-induced neutrophil chemotactic activity ($p > 0.05$) (Table III).

The rat corneal micropocket model of neovascularization was used to determine whether IP-10 or MIG could inhibit the angiogenic activity of either the ELR-containing CXC chemokines or bFGF *in vivo*. Hydron pellets alone, pellets containing IL-8, ENA-78, GRO-α, GCP-2, IP-10, MIG, or bFGF in a concentration of 10 nM, or pellets containing combinations of 10 nM each of IL-8 + IP-10, ENA-78 + IP-10, GRO-α + IP-10, GCP-2 + IP-10, IL-8 + MIG, ENA-78 + MIG, bFGF + IP10, or bFGF + MIG were embedded into the normally avascular rat cornea and assessed for a neovascular response (Fig. 3, *a–c*). The CXC chemokines (IL-8, ENA-78, GRO-α, or GCP-2) or bFGF-induced positive corneal angiogenic responses in six of six corneas, without evidence for significant leukocyte infiltration (assessed by light microscopy). In contrast, hydron pellets alone ($n = 6$ corneas) or pellets containing either IP-10 or MIG (10 nM) ($n = 6$ corneas for each chemokine) only resulted in a positive neovascular response in less than one of six corneas tested for each variable. When IP-10 was added in combination with the ELR-CXC chemokines (IL-8, ENA-78, GRO-α, or GCP-2) or bFGF (Fig. 3, *a* and *c*, respectively), IP-10 significantly abrogated the ELR-CXC chemokine and bFGF-induced angiogenic activity in five of six corneas ($n = 6$ corneas for each manipulation). In addition, MIG inhibited IL-8, ENA-78, and bFGF-induced corneal angiogenic activity in a similar manner to IP-10 (Fig. 3, *b* and *c*).

ELR Muteins of IL-8 and MIG Generate Angiostatic and Angiogenic Proteins, Respectively—Muteins of IL-8 lacking the ELR motif and a mutant of MIG containing the ELR motif were generated to delineate its functional role in CXC chemokine-induced angiogenesis. The ELR motif in wild-type IL-8 was mutated to either TVR (TVR-IL-8; corresponding IP-10 sequence) or DLQ (DLQ-IL-8; corresponding to PF4 sequence) by site-directed mutagenesis and expressed in *E. coli*. TVR-IL-8 and DLQ-IL-8 alone failed to induce endothelial cell chemotactic activity (Fig. 4, *A* and *B*, respectively), yet these muteins inhibited the maximal endothelial chemotactic activity of wild-type IL-8 by 83 and 88% ($p < 0.05$), respectively (Fig. 4, *A* and *B*). Endothelial cell viability, as determined by the exclusion of trypan blue, was unchanged in the presence or absence of either of the IL-8 muteins (data not shown). Neither TVR-IL-8 nor DLQ-IL-8 induced neutrophil chemotaxis, nor were they effective in attenuating neutrophil chemotaxis in response to IL-8 (data not shown).

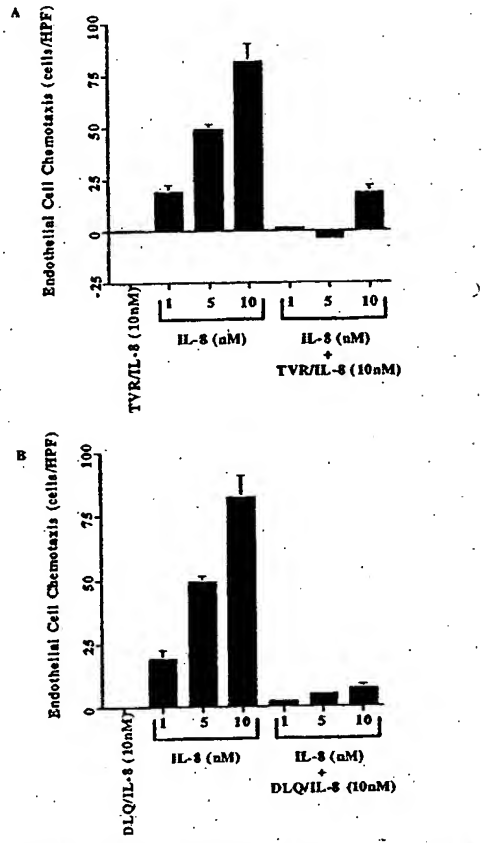

FIG. 4. **Endothelial cell chemotaxis in response to the presence or absence of varying concentrations of IL-8 and IL-8 muteins, TVR-IL-8, and DLQ-IL-8.** *Panel A* is endothelial cell chemotaxis in response to the presence or absence of varying concentrations of IL-8 (1–10 nM), TVR-IL-8 (10 nM), or in combination of varying concentrations of IL-8 with TVR-IL-8 (10 nM). *Panel B* is endothelial cell chemotaxis in response to the presence or absence of varying concentrations of IL-8 (1–10 nM), DLQ-IL-8 (10 nM), or in combination of varying concentrations of IL-8 with DLQ-IL-8 (10 nM). To demonstrate specific migration, background (unstimulated control) migration (cells/HPF) was subtracted.

Using the *in vivo* rat cornea micropocket model of neovascularization, TVR-IL-8 (10 nM) alone did not induce a positive neovascular response in any of the six corneas tested. However, TVR-IL-8 (10 nM) in combination with either IL-8 (10 nM) or ENA-78 (10 nM) resulted in 83% reduction (only one of six corneas positive) in the ability of either IL-8 or ENA-78 to induce cornea neovascularization, as compared with 100% (six of six) of the corneas positive in the presence of either IL-8 or ENA-78 alone (Fig. 5). Moreover, the angiostatic activity of the IL-8 muteins was not only unique to inhibition of ELR-CXC chemokine-induced angiogenic activity, as TVR-IL-8 (10 nM)

represents the corneal neovascular response to the combination of IL-8 with MIG or ENA-78 with MIG. *Part c, panels A–D*, respectively, represents the corneal neovascular response to a hydron pellet alone (vehicle control), bFGF (5 nM), MIG (10 nM), or IP-10 (10 nM); *part c, panels E* and *F*, respectively, represents the corneal neovascular response to the combination of bFGF with MIG or bFGF and IP-10. All panels are at 25× magnification.

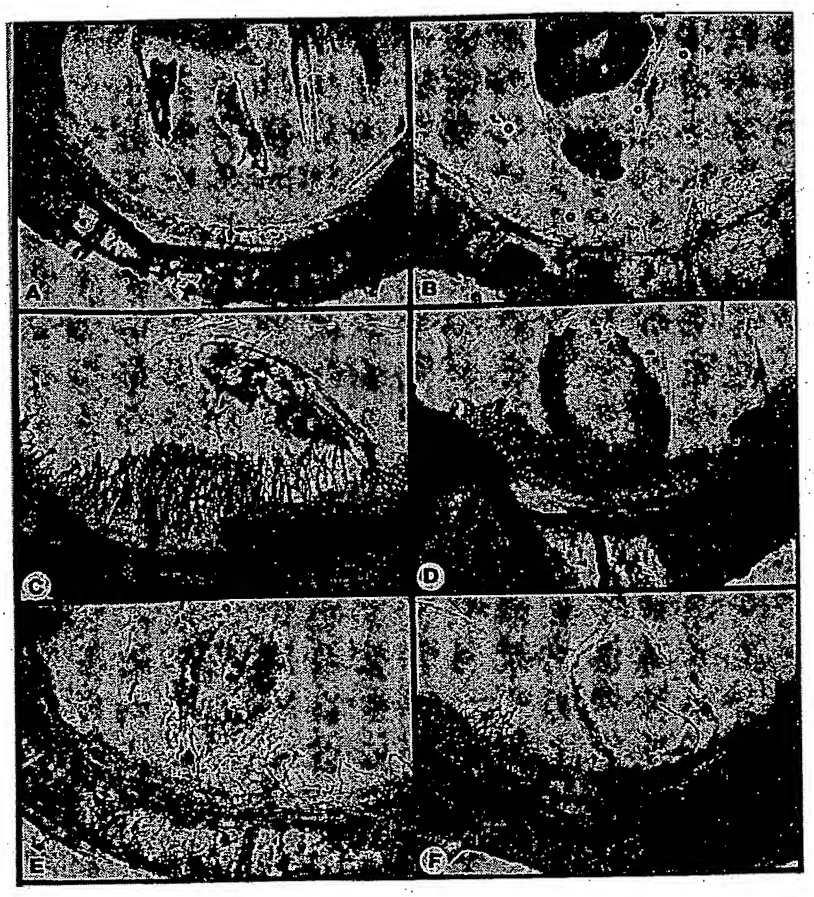

FIG. 5. Rat cornea neovascularization in response to the IL-8, ENA-78, the IL-8 mutein (TVR-IL-8), and combinations of ENA-78 and TVR-IL-8 or IL-8 and TVR-IL-8. *Panels A–D* represent a hydron pellet alone, TVR-IL-8 (10 nM), ENA-78 (10 nM), and IL-8 (10 nM), respectively. *Panels E* and *F* represent the combination of ENA-78 and TVR-IL-8 and of IL-8 and TVR-IL-8, respectively. All panels are at 25× magnification.

inhibited both bFGF-induced (10 nM) maximal endothelial cell chemotaxis by 65% ($p < 0.05$) (Fig. 6*a*) and corneal neovascularization (five of six corneas; $n = 6$ corneas for each cytokine) (Fig. 6*b*). Endothelial cell viability, as determined by the exclusion of trypan blue, was unchanged in the presence or absence of the TVR-IL-8 mutant (data not shown). In addition, ELR-MIG (10 nM) induced angiogenic responses in 8 of 10 corneas, as compared with wild-type MIG, which induced an angiogenic response in only 1 of 7 corneas (Fig. 7, *A–D*). Interestingly, MIG (10 nM) inhibited the angiogenic response of ELR-MIG in five of six corneas (Fig. 7, *E* and *F*). These data further support the importance of the ELR motif as a domain for mediating angiogenic activity. Similar to the synthetic ELR-IP-10 (36), ELR-MIG in a concentration of 10 pM to 100 nM failed to induce neutrophil chemotaxis (data not shown).

DISCUSSION

The CXC chemokine family of chemotactic cytokines are polypeptide molecules that appear, in general, to have proinflammatory activities. In monomeric forms, they range from 7 to 10 kDa and are characteristically basic heparin-binding proteins. They display four highly conserved cysteine amino acid residues with the first two cysteines separated by a nonconserved amino acid residue (the CXC cysteine motif). The CXC chemokines are all clustered on human chromosome 4 (q12-q21), and exhibit between 20 and 50% homology on the amino acid level (31–34). Over the last 2 decades, several human CXC chemokines have been identified, including PF4, NH_2-terminal truncated forms of platelet basic protein (connective tissue activating protein-III, β-thromboglobulin, neutrophil-activating protein-2), IL-8, GRO-α, GRO-β, GRO-γ, ENA-78, GCP-2, IP-10, and MIG (31–34, 38). The ubiquitous nature of CXC chemokine production by a variety of cells suggest that these cytokines may play a role in mediating biological events other than leukocyte chemotaxis.

We hypothesized that members of the CXC chemokine family may exert disparate effects in mediating angiogenesis as a function of the presence or absence of the ELR motif for primarily four reasons. First, members of the CXC chemokine family that display binding and activation of neutrophils share the highly conserved ELR motif that immediately precedes the first cysteine amino acid residue, whereas, PF4, IP-10, and MIG lack this motif (35, 36). Second, IL-8 (contains ELR motif) mediates both endothelial cell chemotactic and proliferative activity *in vitro* and angiogenic activity *in vivo* (28), and, in addition, endogenous IL-8 has been found to represent a major angiogenic factor that mediates net angiogenic activity of human nonsmall cell lung cancer (42). In contrast, PF4 (lacking the ELR motif) has been shown to have angiostatic properties (27), and attenuates growth of tumors *in vivo* (45). Third, the interferons (IFN-α, IFN-β, and IFN-γ) are all known inhibitors of wound repair, especially angiogenesis (18, 46–49). These cytokines, however, up-regulate IP-10 and MIG from a number of cells, including keratinocytes, fibroblasts, endothelial cells, and mononuclear phagocytes (38, 50). Finally, we and others have found that IFN-α, IFN-β, and IFN-γ are potent inhibitors of the production of monocyte-derived IL-8, GRO-α, and ENA-78 (51, 52), supporting the notion that IFN-α, IFN-β, and IFN-γ may shift the biological balance of ELR- and non-ELR-CXC chemokines toward a preponderance of angiostatic (non-ELR) CXC chemokines.

In this study, we demonstrated that the members of the CXC chemokine family behave as either angiogenic or angiostatic

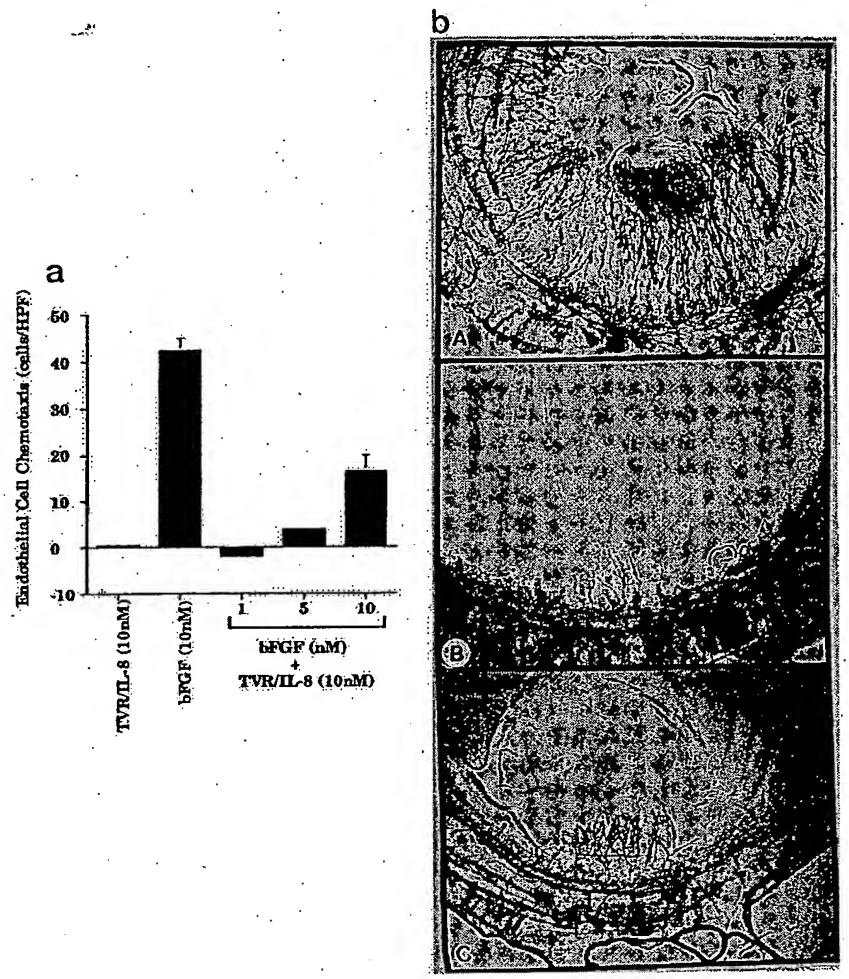

FIG. 6. **Endothelial chemotaxis (*part a*) and rat cornea neovascularization (*part b*) in response to the presence or absence of varying concentrations of bFGF and the IL-8 mutein, TVR-IL-8 (10 nM).** *Part a* is the endothelial chemotaxis in response to the presence or absence of varying concentrations of bFGF (1–10 nM), TVR-IL-8 (10 nM), or in combination of varying concentrations of IL-8 with TVR-IL-8 (10 nM). To demonstrate specific migration, background (unstimulated control) migration (cells/HPF) was subtracted. *Part b, panels A–C* is rat cornea neovascularization in response to bFGF (10 nM), TVR-IL-8 (10 nM), and the combination of bFGF and TVR-IL-8 at 25× magnification, respectively.

factors, depending upon the presence or absence of the ELR motif, respectively. This was supported using both *in vitro* (endothelial cell chemotaxis) and *in vivo* (rat cornea neovascularization) analyses. The evidence *in vitro* of directed (chemotaxis not chemokinesis by checkerboard analysis) migration in response to varying concentrations of ELR-CXC chemokines, IL-8, ENA-78, and the MIG mutein ELR-MIG, and the absence *in vivo* of leukocyte infiltration in the rat cornea during ELR-CXC chemokine-induced neovascularization, supports the direct role ELR-containing CXC chemokines play in mediating angiogenic activity. In contrast, CXC chemokines lacking the ELR motif, PF4, IP-10, MIG, and the two IL-8 muteins DLQ-IL-8 and TVR-IL-8, behave as potent angiostatic regulators of neovascularization, inhibiting not only the angiogenic activity of ELR-CXC chemokines, but also the structurally unrelated angiogenic factor, bFGF. Thus, the ELR motif appears to be essential for dictating the angiogenic activity of the CXC chemokines.

These findings are compatible with the ability of ELR-containing CXC chemokines to bind to both endothelial cells and neutrophils. However, the non-ELR muteins of wild-type IL-8, as well as IP-10 and MIG, inhibited ELR-CXC chemokine-induced angiogenesis but not neutrophil chemotaxis. The finding that IP-10 and MIG block other ELR-CXC chemokine-induced functions, *i.e.* angiogenesis, is unprecedented (53). Moreover, the muteins of wild-type IL-8, as well as IP-10 and MIG, also inhibited the angiogenic activity of the unrelated cytokine, bFGF, suggesting that a receptor system(s) other than the IL-8 receptor may be operative on endothelial cells, which allows the angiostatic CXC chemokines to regulate both ELR-CXC chemokine and bFGF-induced angiogenic activity. This contention is further supported with the evidence that equimolar concentrations of mutant and wild-type IL-8 do not result in a 50% restoration of the endothelial cell chemotactic effect. This response is most likely due to the use of another "receptor" by the angiostatic CXC chemokines. While the Duffy antigen receptor for chemokines has been identified on post-capillary venule endothelial cells (54), this receptor binds not only ELR-CXC chemokines, but also MCP-1 and RANTES (55). We have found that these latter two CC chemokines are not chemotactic for endothelial cells (data not shown).

While the NH_2-terminal ELR motif appears to be essential for angiogenic activity of CXC chemokines, it is uncertain whether the angiostatic properties of the non-ELR-CXC chemokines tested are due to the absence of the ELR motif. In particular, bFGF binds to low affinity cell surface receptors on endothelia that appear to be sulfate proteoglycans (47, 56), and IL-8 specific binding to endothelial cells can be inhibited by preincubation with either heparin or heparan sulfate (57). One can speculate that, in the absence of the ELR motif, a potential mechanism exists by which another amino acid domain, perhaps within the COOH terminus of PF4, IP-10, MIG, TVR-IL-8, and DLQ-IL-8 may compete with either ELR-CXC chemokines or bFGF for proteoglycan binding sites and thus prevent endothelial cell activation and angiogenesis. It also possible, however, that the angiostatic effects of CXC chemokines lacking

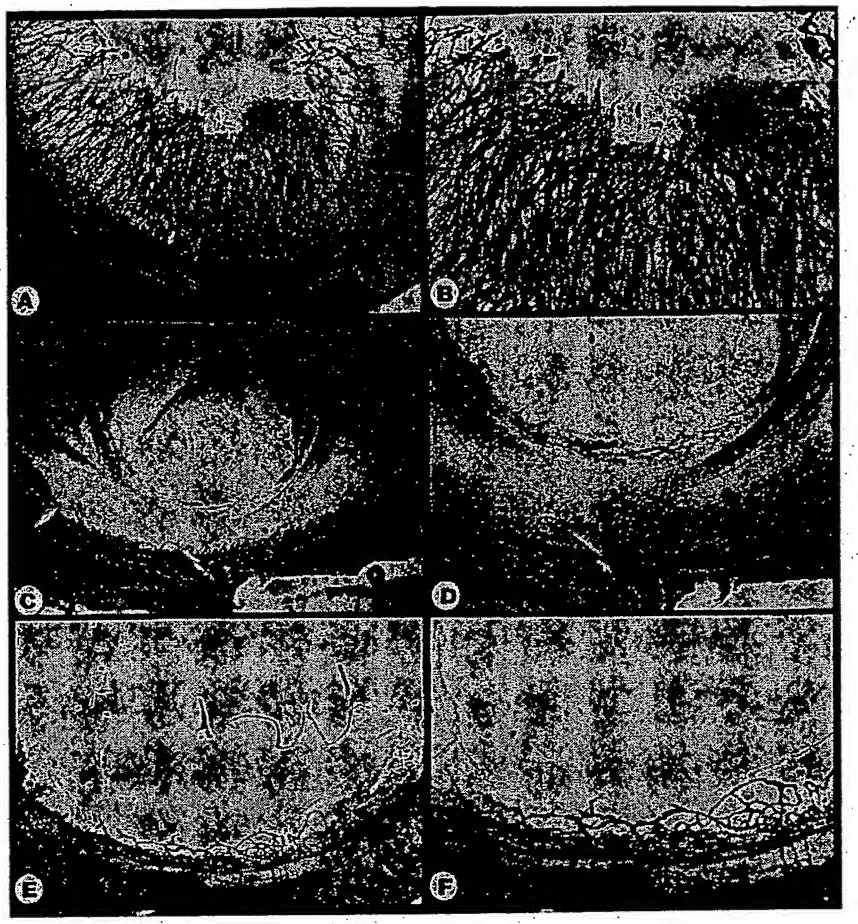

FIG. 7. **Rat cornea neovascularization in response to the MIG mutein, ELR-MIG, MIG, and the combination of ELR-MIG and MIG.** *Panels A* and *B* represents the cornea neovascular response to ELR-MIG (10 nM) at 25 and 50×, respectively. *Panels C* and *D* represent the cornea neovascular response to MIG (10 nM) at 25 and 50× magnification, respectively. *Panels E* and *F* represent the cornea neovascular response to the combination of ELR-MIG and MIG at 25 and 50× magnification, respectively.

the ELR motif are not directly competitive in nature, but are rather mediated through an independent receptor system. Studies in our laboratories are currently addressing these issues.

The interferons have been shown to inhibit wound repair and tumorigenesis through a presumed antiproliferative and angiostatic mechanism (46–49). While the expression of IL-8, GRO-α, and ENA-78 can be induced by a variety of factors, including TNF and IL-1, these chemokines are down-regulated by IFN-γ (51, 52). In contrast, IP-10 and MIG expression is up-regulated by IFN-γ (38, 50). This suggests that the disparate activity of the CXC chemokines as angiogenic or angiostatic factors may be physiologically relevant. The finding that IP-10 and MIG are potent angiostatic factors suggests that IFN-γ, in part, may mediate its angiostatic activity through the local stimulation of production of IP-10 and MIG and by down-regulation of the expression of the angiogenic CXC chemokines, such as IL-8 and ENA-78. This suggests that the magnitude of local IFN-γ expression by mononuclear cells during wound repair, chronic inflammation, or tumorigenesis may be a pivotal event in regulating both angiogenic (through negative feedback) and angiostatic (through positive feedback) CXC chemokine production.

Thus, our findings suggest that the ELR motif is the functional domain that dictates the angiogenic activity of the CXC chemokines, and supports the contention that members of the CXC chemokine family may exert disparate effects in mediating angiogenesis. The magnitude of the expression and relative concentrations of either angiogenic or angiostatic CXC chemokines during neovascularization may thus significantly contribute to the regulation of net angiogenesis during either wound repair, chronic inflammation, or tumorigenesis.

Acknowledgments—We thank Carla Forte (Bayer Corp., West Haven, CT) for technical help during the course of this work and Ghislain Opdenakker (University of Leuven, Leuven, Belgium) for critical review of this manuscript.

REFERENCES

1. Folkman, J., and Cotran, R. (1978) *Int. Rev. Exp. Pathol.* 16, 207–248
2. Auerbach, R. (1981) *Lymphokines* Vol. IV, Academic Press, New York
3. Folkman, J. (1985) *Adv. Cancer Res.* 43, 175–203
4. Folkman, J., and Klagsbrun, M. (1987) *Science* 235, 442–444
5. Leibovich, S. J., and Weisman, D. M. (1988) *Prog. Clin. Biol. Res.* 266, 131–145
6. Engerman, R. L., Pfaffenenbach, D., and Davis, M. D. (1967) *Lab Invest.* 17, 738–743
7. Tannock, I. F., and Hayashi, S. (1972) *Cancer Res.* 32, 77–82
8. Bouck, N. (1990) *Cancer Cells* 2, 179–85
9. Folkman, J., Watson, K., Ingber, D., and Hanahan, D. (1989) *Nature* 339, 58–61
10. Brem, H., and Folkman, J. (1975) *J. Exp. Med.* 141, 427–433
11. Lee, A., and Langer, R. (1983) *Science* 221, 1185–1187
12. Madri, J. A., Pratt, B. M., and Tucker, A. M. (1988) *J. Cell Biol.* 106, 1375–1384
13. Ingber, D. E., Madri, J. A., and Folkman, J. (1986) *Endocrinology* 119, 1768–1775
14. Ingber, D. E., and Folkman, J. (1988) *Lab. Invest.* 59, 44–51
15. Maragoudakis, M. E., Sarmonika, M., and Panoutscaopoulou, M. (1988) *J. Pharmacol. Exp. Ther.* 244, 729–733
16. Shapiro, R., and Vallee, B. L. (1987) *Proc. Natl. Acad. Sci. U.S.A.* 84, 2238–2241
17. Sato, N., Fukuda, K., Nariuchi, H., and Sagara, N. (1987) *J. Natl. Cancer Inst.* 79, 1383–1391
18. Sidky, Y. A., and Borden, E. C. (1987) *Cancer Res.* 47, 5155–5161
19. Peterson, H.-I. (1986) *Anticancer Res.* 6, 251–254
20. Homandberg, G. A., Kramer-Bjerke, J., Grant, D., Christianson, G., and Eisenstein, R. (1986) *Biochim. Biophys. Acta* 874, 61–71
21. Taylor, S., and Folkman, J. (1982) *Nature* 297, 307–312
22. Crum, R., Szabo, S., and Folkman, J. (1985) *Science* 230, 1375–1378
23. Lee, K., Erturk, E., Mayer, R., and Cockett, A. T. K. (1987) *Cancer Res.* 47,

5021
24. Good, D. J., Polverini, P. J., Rastinejad, F., LeBeau, M. M., Lemons, R. S., Frazier, W. A., and Bouck, N. P. (1990) *Proc. Natl. Acad. Sci. U. S. A.* **87**, 6624–6628
25. O'Reilly, M. S., Holmgren, L., Shing, Y., Chen, C., Rosenthal, R. A., Moses, M., Lane, W. S., Cao, Y., Sage, E. H., and Folkman, J. (1994) *Cell* **79**, 315–328
26. Brooks, P. C., Montgomery, A. M. P., Rosenfeld, M., Reisfeld, R. A., Hu, T., Klier, G., and Cheresh, D. A. (1994) *Cell* **79**, 1157–1164
27. Maione, T. E., Gray, G. S., Petro, J., Hunt, A. J., Donner, A. L., Bauer, S. I., Carson, H. F., and Sharpe, R. J. (1990) *Science* **247**, 77–79
28. Koch, A. E., Polverini, P. J., Kunkel, S. L., Harlow, L. A., DiPietro, L. A., Elner, V. M., Elner, S. G., and Strieter, R. M. (1992) *Science* **258**, 1798–1801
29. Strieter, R. M., Kunkel, S. L., Elner, V. M., Martonyl, C. L., Koch, A. E., Polverini, P. J., and Elner, S. G. (1992) *Am J. Pathol.* **141**, 1279–1284
30. Hu, D. E., Hori, Y., and Fan, T. P. D. (1993) *Inflammation* **17**, 135–143
31. Baggiolini, M., Walz, A., and Kunkel, S. L. (1989) *J. Clin. Invest.* **84**, 1045–1049
32. Miller, M. D., and Krangel, M. S. (1992) *Crit. Rev. Immunol.* **12**, 17–46
33. Baggiolini, M., Dewald, B., and Moser, B. (1994) *Adv. Immunol.* **55**, 97–179
34. Proost, P., De Wolf-Peeters, C., Conings, R., Opdenakker, G., Billiau, A., and Van Damme, J. (1993) *J. Immunol.* **150**, 1000–1010
35. Hebert, C. A., Vitangcol, R. V., and Baker, J. B. (1991) *J. Biol. Chem.* **266**, 18989–18994
36. Clark-Lewis, I., Dewald, B., Geiser, T., Moser, B., and Baggiolini, M. (1993) *Proc. Natl. Acad. Sci. U. S. A.* **90**, 3574–3577
37. Kunkel, T. A., Roberts, J. D., and Zakour, R. A. (1987) *Methods Enzymol.* **154**, 367–382
38. Farber, J. M. (1993) *Biochem. Biophys. Res. Comm.* **192**, 223–230
39. Sanger, F., Nicklen, S., and Coulson, A. R. (1977) *Proc. Natl. Acad. Sci. U. S. A.* **74**, 5463–5467
40. Messing, J. (1983) *Methods Enzymol.* **101**, 20–78
41. Laemmli, U. K. (1970) *Nature* **227**, 680–685
42. Smith, D. R., Polverini, P. J., Kunkel, S. L., Orringer, M. B., Whyte, R. I., Burdick, M. D., Wilke, C. A., and Strieter, R. M. (1994) *J. Exp. Med.* **179**, 1409–1415
43. Strieter, R. M., Kunkel, S. L., Showell, H., Remick, D. G., Phan, S. H., Ward, P. A., and Marks, R. M. (1989) *Science* **243**, 1467–1469
44. Strieter, R. M., Phan, S. H., Showell, H. J., Remick, D. G., Lynch, J. P., Genord, M., Raiford, C., Eskandari, M., Marks, R. M., and Kunkel, S. L. (1989) *J. Biol. Chem.* **264**, 10621–10626
45. Sharpe, R. J., Byers, H. R., Scott, C. F., Bauer, S. I., and Maione, T. E. (1990) *J. Natl. Cancer Inst.* **82**, 848–853
46. Clark, R. A. F. (1993) *J. Dermatol. Surg. Oncol.* **19**, 693–70
47. Klagsbrun, M., and D'Amore, M. (1991) *Annu. Rev. Physiol.* **53**, 217–239
48. Pober, J. S., and Cotran, R. S. (1990) *Pathol. Rev.* **70**, 427–451
49. Stout, A. J., Gresser, I., and Thompson, D. (1993) *Int. J. Exp. Path.* **74**, 79–85
50. Kaplan, G., Luster, A. D., Hancock, G., and Cohn, Z. (1987) *J. Exp. Med.* **166**, 1098–1108
51. Gusella, G. L., Musso, T., Bosco, M. C., Espinoza-Delgado, I., Matsushima, K., and Varesio, L. (1993) *J. Immunol.* **151**, 2725–2732
52. Schnyder-Candrian, S., Strieter, R. M., Kunkel, S. L., and Walz, A. (1995) *J. Leukocyte Biol.* **57**, 929–935
53. Dewald, B., Moser, B., Barella, L., Schumacher, C., Baggiolini, M., and Clark-Lewis, I. (1992) *Immunol. Lett.* **32**, 81–84
54. Hadley, T. J., Lu, Z., Wasniowska, K., Martin, A. W., Peiper, S. C., Hesselgesser, J., and Horuk, R. (1994) *J Clin. Invest.* **94**, 985–991
55. Neote, K., Darbonne, W., Ogez, J., Horuk, R., and Schall, T. (1993) *J. Biol. Chem.* **268**, 12247–12249
56. Moscatelli, D. (1987) *J. Cell. Physiol.* **131**, 123–130
57. Schonbeck, U., Brandt, E., Peterson, F., Flad, H.-D., and Loppnow, H. (1995) *J. Immunol.* **154**, 2375–2383

Simple Method for Quantitation of Enhanced Vascular Permeability[1] (34695)

KEIJI UDAKA,[2] YUKO TAKEUCHI, AND HENRY Z. MOVAT[3]

Division of Experimental Pathology, Department of Pathology, University of Toronto, Toronto, Ontario, Canada

The wall of certain vessels (venules and capillaries) of the microcirculation represent the blood–tissue barrier. This barrier is freely permeable to water, electrolytes, and small molecules, but only slightly permeable to proteins. The term "increased vascular permeability" refers to an alteration of this barrier, leading to an accelerated rate of passage of plasma proteins into the extravascular tissues: exudation. This phenomenon leads to swelling, which is one of the cardinal features of acute inflammation. Exudation is closely linked to other vascular phenomena, such as hyperemia and stasis. It has been generally accepted that some vital dyes, such as Evans blue, trypan blue or pontamine sky blue, given intravenously, become bound to plasma proteins, particularly to albumin. Therefore, the accumulation of such dyes in inflammatory lesions indicates exudation of plasma proteins. However, evaluation of experimental results in such tests often lacks precision. The present paper describes a simple physicochemical assay for the quantitative measurement of enhanced vascular permeability.

Material and Methods. Adult male albino rabbits, both male and female albino guinea pigs and female Wistar rats were used.

Dye extraction method. Evans blue was injected intravenously in concentrations of 60 mg/kg for rabbits and rats and 20 mg/kg for guinea pigs, respectively. Inflammatory skin lesions were produced by intradermal injections of various inflammatory agents. The skin lesions were punched out with a standard steel punch (1.5–2.5 cm in diameter. To each piece of skin containing the lesion, 4.0 ml of formamide (Fisher Scientific Co. Ltd.) was added and incubated at 45° for 72–96 hr or at 65° for 24–36 hr. If necessary, the incubation time was prolonged, until the blue color of the skin completely disappeared. After filtration with glass filter (Pyrex, coarse; 1.0 cm in diameter), the optical density of the filtrate was measured at 620 mμ in a Zeiss PMQ II spectrophotometer. The total amount of dye can be calculated by means of a standard calibration curve.

Simultaneous radioassay and dye extraction. Evans blue (doses as above) were injected intravenously mixed with ^{125}RISA (radioiodinated human serum albumin; Charles Frosst and Co., Montreal, Canada). The ratio of ^{125}RISA to Evans blue was 1 μCi/mg for studies in rabbits and guinea pigs and ⅓ μg/mg for experiments in rats. The punched out pieces of skin, containing the lesion, were placed in tubes containing 4 ml of formamide. First the radioactivity was measured in a γ-scaler (Model 4204 Nuclear Chicago), calibrated with cesium (44,000 counts ± 500/min) and known amounts of ^{125}RISA. Subsequently, the Evans blue was extracted and the amount of dye was determined as described above.

Experiments to test vascular permeability. As known chemical mediators, synthetic bradykinin (Sandoz, Montreal, Canada), histamine (histamine base, Fisher Scientific Co., Toronto, Canada) and serotonin (serotonin sulfate, Upjohn Co., Kalamazoo, Michi-

[1] Part of this work was presented at the 11th Canadian Federation of Biological Societies, Kingston, Ontario, 1968. This study was supported by Grants MA-1251 and MA-2660 of the Medical Research Council of Canada.

[2] MRC Research Scholar.

[3] MRC Research Associate.

gan) were selected. Each of them was suspended in buffered (pH 7.4) saline at the following concentrations: bradykinin, 10 μg/ml; histamine, 100 μg/ml; and serotonin, 1 μg/ml. They were further diluted if necessary before use. Volumes of 0.1 ml of each sample were injected intradermally with 27-gauge hypodermic needles into the abdominal skin of rabbits and the back of guinea pigs and rats which had received Evans blue with ^{125}RISA intravenously. Unless otherwise stated, 30 min later, the animals were killed with sodium Nembutal (Upjohn Co., Kalamazoo, Michigan) and the extravasated dye and the radioactivity of the punched out skin were determined.

As an experimental model of inflammation, the following two types of inflammation were used. (i) The Arthus reaction: This was elicited in the abdominal skin of BSA-immunized rabbits according to methods previously described (1). Unless otherwise stated, 0.1 ml of antigen (2.5 mg of bovine serum albumin (BSA); Mann Research Lab., New York) was injected intradermally at 48, 24, 12, 6, 4.5, 3, 2, 1 hr, 30, 10, and 5 min before injecting Evans blue and ^{125}RISA. (ii) Thermal injury was induced in the abdominal skin of rabbits at 56° ± 0.25 for 20 sec, by using the burning apparatus of Sevitt (2), slightly modified. Lesions were induced at 6, 5, 4, 2.5, 1 hr and at 20 and 5 min before injecting dye and ^{125}RISA. Thirty min later, the animals were killed and the extravasated dye and radioactivity were measured as described above.

Results. The relationship between extravasated dye and radioactivity of skin lesions. First, the radioactivity of skin lesions of varying intensities was determined. Then following formamide extraction, the total amount of extravasated dye (μg) in a particular skin lesion, was calculated by means of the standard calibration curve. As shown in Fig. 1, a linear response was obtained between about 1000 and 13,000 counts, corresponding to about 0–18 μg of Evans blue.

Recovery of Evans blue given intradermally. 0.1 ml of Evans blue was injected intradermally at various concentrations. The skin was removed 30 min after injection. The dye was extracted and measured.

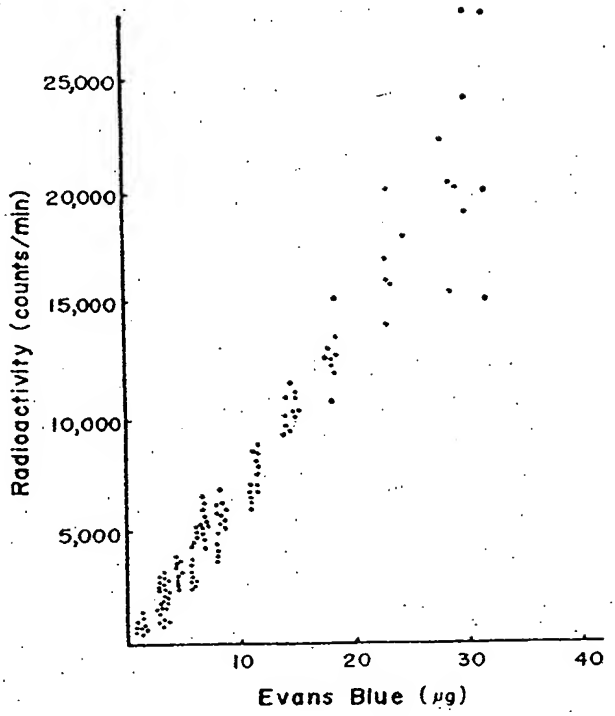

FIG. 1. The dots show radioactivity of skin lesions of varying intensity expressed as counts per minute per lesion. They also show the relationship between radioactivity of the individual skin lesions and the amount of Evans blue extracted from the same lesions.

As illustrated in Table I, the recovery of dye was over 95% in all animals tested (rabbits, guinea pigs, and rats). This shows that the dye given interdermally can be recovered from the skin almost completely.

Extraction of dye from skin sites treated with bradykinin, histamine, and serotonin.

TABLE I. Recovery of Evans Blue Given Intradermally.

Dye injected (μg)	Dye recovered (μg)[a]			Yield (av; %)
	Rabbits	Guinea pigs	Rats	
5.0	5.0	4.9	4.8	Over 96
10.0	10.1	9.8	9.8	Over 98
30.0	29.6	29.8	29.3	Over 97
50.0	48.8	49.2	48.1	Over 95
75.0	74.4	74.5	73.6	Over 98
100.0	98.2	97.6	—	Over 97

[a] Mean values of 5 experiments.

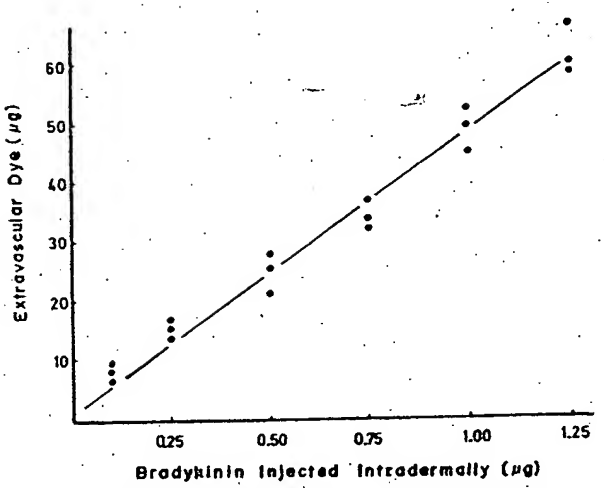

FIG. 2. Dose–response curve of bradykinin: volume injected was 0.1 ml; skin was removed 30 min after intradermal injections; Evans blue and ^{125}RISA were injected intravenously as described in the text.

0.1 ml of synthetic bradykinin was injected intradermally, in graded concentrations, into the abdominal skin of rabbits and the back of guinea pigs which had received Evans blue and ^{125}RISA intravenously. As shown in Fig. 2, the dose–response relationship shows a straight line between concentration of 0.10 and 1.25 μg/ml of bradykinin.

Similar injections, using histamine and serotonin, were given to guinea pigs and rats, respectively. The same relationship between concentrations of 0.3 and 10 μg/ml of histamine and 0.1 and 0.5 μg/ml of serotonin were obtained. These results indicate that this assay is useful for estimating increased vascular permeability in the skin induced with known chemical mediators.

Enhanced vascular permeability in experimental models. The time courses of vascular permeability in cutaneous Arthus reactions and moderate thermal injury in rabbits were tested. As shown in Fig. 3, the general pattern of vascular response appeared to be biphasic. The early response appeared in 5 min, lasted 20–30 min and decreased thereafter in both responses. The late response reached its maximum in 4–5 and 2 hr, respectively, and disappeared in 10–12 and 4–5 hr, respectively. This indicates that the assay allows accurate measurement of increased vascular permeability in cutaneous Arthus reaction and in thermal injury.

Discussion. The earliest attempts to estimate quantitatively the amounts of accumulated dye in inflamed skin sites were based on "mean lesion diameter" (3) or by comparing the color intensity with a series of color standards (4). However, evaluation of experimental results in such tests often lacks precision. Attempts to extract the dye from the skin were cumbersome in most instances. Beach and Steinetz (5) used acid digestion, Judah and Willoughby (6) pounded the skin frozen at —70°, Carr and Wilhelm (7) homo-

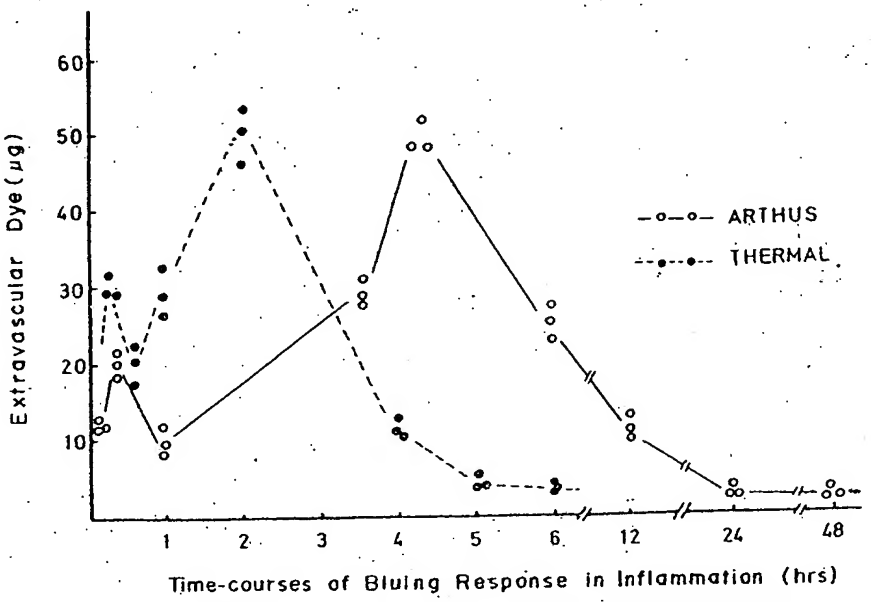

FIG. 3. Time-course of permeability changes in Arthus reaction and thermal injury.

genized the skin mechanically, whereas Nitta *et al.* (8) extracted pontamine sky blue from the skin in two steps: (a) denaturation and dehydration of tissues with dioxane, and (b) elimination of the tissue lipid with organic solvents such as methanol, ethanol, and ether.

In 1962, Frimmer and Müller (9) demonstrated that the extravasated dye could be extracted from the skin with formamide and estimated quantitatively by colorimetry. The extraction being performed at 80° for 24 hr induced a color change ranging from green to dark brown. When extracted under the conditions described in this report, no color changes were observed. Especially at 45°, the incubation time can be prolonged until the blue color of the skin completely disappears without any color changes taking place. Good results were obtained with this method in two studies in which enhanced vascular permeability has been measured (10, 11). In these studies large amounts of animals had to be used because of considerable variation in bluing from animal to animal obtained with intense bluing reactions. As shown in Fig. 1 not much scattering is obtained within a certain range. This means that the material to be tested has to be prepared in such a way as to give a bluing response not exceeding 20 μg of Evans blue or about 13,000 cpm/lesion. If a certain standard (*e.g.*, synthetic bradykinin or histamine) which falls within the linear dose–response is used in each experiment, one can compare it visually with the bluing induced by the unknown permeability factor. If the latter gives too intense a reaction it can be further diluted. The assay with the ^{125}I-labeled serum albumin is simple, sensitive and rapid. It allows quantitation within minutes after completion of the experiment.

In addition to permeability tests with known chemical mediators (Fig. 2) it was shown that this assay is applicable to the time course study of enhanced vascular permeability in cutaneous Arthus reactions and thermal injury (Fig. 3). These results show that this assay permits quantitation of enhanced vascular permeability in studies dealing with certain immune reactions and of inflammatory lesions induced with various chemical mediators and of other phlogistic agents.

Summary. A simple physicochemical assay for the quantitation of enhanced vascular permeability in inflammation was described. It was shown that the assay is applicable to the study of inflammatory lesions induced with known chemical mediators, to the study of enhanced vessel permeability associated with the Arthus reaction, and that associated with thermal injury.

1. Udaka, K., Kumamoto Med. J. 16, 55, (1963).
2. Sevitt, S., J. Pathol. Bacteriol. 61, 427 (1949).
3. Miles, A. A., and Wilhelm, D. L., Brit. J. Exp. Pathol. 36, 71 (1955).
4. Lockett, M. F., and Jarman, D. A., Brit. J. Pharmacol. Chemother. 13, 11 (1958).
5. Beach, V. L., and Steinmetz, B. G., J. Pharmacol. Exp. Ther. 131, 400 (1961).
6. Judah, J. D., and Willoughby, D. A., J. Pathol. Bacteriol. 83, 567 (1962).
7. Carr, J., and Wilhelm, D. L., Aust. J. Exp. Biol. Med. Sci. 42, 511 (1964).
8. Nitta, R., Hayashi, H., and Norimatsu, K., Proc. Soc. Exp. Biol. Med. 113, 185 (1963).
9. Frimmer, M., and Müller, F. W., Med. Exp. 6, 327 (1962).
10. Movat, H. Z., DiLorenzo, N. L., Taichman, N. S., Berger, S., and Stein, H., J. Immunol. 98, 230 (1967).
11. Movat, H. Z., and DiLorenzo, N. L., Lab. Invest. 19, 187 (1968).

Received Sept. 8, 1969. P.S.E.B.M., 1970, Vol. 133.

THROMBOSIS RESEARCH 71; 139–148, 1993
0049–3848/93 $6.00 + .00 Printed in the USA.

SUPPRESSIVE EFFECT OF HUMAN BLOOD COAGULATION FACTOR XIII ON THE VASCULAR PERMEABILITY INDUCED BY ANTI-GUINEA PIG ENDOTHELIAL CELL ANTISERUM IN GUINEA PIGS

Keizo Hirahara, Kazuhiko Shinbo, Mikiko Takahashi and Tetsuro Matsuishi
Pharma Research Laboratories, Hoechst Japan Limited, 1-3-2, Minamidai, Kawagoe-shi, Saitama, 350 Japan

(Received 12.11.1992; accepted in revised form 20.4.1993 by Editor A. Takada)

Abstract

We investigated the effect of blood coagulation factor XIII(FXIII) on enhanced permeability induced by anti-endothelial cell antiserum, that was produced by the immunization of guinea pig endothelial cells with adjuvant into rabbits repeatedly. We have found that this antiserum reacts to human and guinea pig endothelial cells but not guinea pig fibroblast cells. The permeability was enhanced by intradermal injection of 400-fold dilution of this antiserum into dorsal skin of guinea pigs. The mixture of equal volume of antiserum and FXIII was intradermally injected into dorsal skin of guinea pig after Evans blue injection, and 15 minutes later the quantity of Evans blue at the each injection site was determined. We recognized the suppressive effect of FXIII on the dye leakage. We also studied the suppressive effect on swelling induced by the antiserum. After the subcutaneous injection of the mixture of antiserum and FXIII into the back of guinea pigs, we measured the thickness of skins at the injection site after day 1, 2 and 3. As a result, FXIII significantly suppressed the swelling. We found that FXIII suppresses the acute and subacute permeability enhancement. These results suggest that FXIII plays an important role on an inflammatory site and that it may exert as an anti-inflammatory protein.

Blood coagulation factor XIII (FXIII), the last enzyme in the

Key words: Factor XIII, anti-endothelial cell antiserum, vascular permeability, anti-inflammatory protein, Schönlein Henoch purpura

blood coagulation cascade, is a transamidase that catalyzes the formation of γ - gultamyl - ε - lysyl peptide crosslinks between polypeptide chains in adjacent fibrin monomers and other plasma proteins(1,2,3). Crosslinks of each fibrin molecule caused a marked increase in the rigidity of the clot network(4). On the other hands, the crosslinks between fibrin and cellular matrix protein such as fibronectin may exert to connect fibrin molecules with the injury sites(5). It is well known that clots play an important role in the prevention of further tissue damage and in subsequent wound healing(6). Schönlein Henoch purpura (SHP) is characterized by hemorrhagic skin lesions, abdominal symptoms including gastro-intestinal bleeding, renal involvement with proteinuria and hematuria and swelling of joints(7). The symptoms are ascribed to generalized inflammation of arterioles and capillaries. That is, the local changes of the coagulation and fibrinolytic system due to immunoreaction were induced in the affected vessels. In 1977, Henriksson and colleagues described a lowering of FXIII activity during the acute phase of this disease(8). The mechanism of the decrease of FXIII activity in the acute phase of SHP has not yet been clarified. Destruction of FXIII molecules by protease derived from leukocytes which migrated into the inflammation sites has been proposed(9). In this connection, Kamitsuji and Fukui et al. reported that the administration of FXIII concentrate may contribute to the improvement of gastro-intestinal complications of SHP patients(10). Recently FXIII concentrate (Fibrogammin P) is used for the treatment of SHP patients(11). According to Matsuoka(12), Bowie et al.(13) and Ito et al.(14), this vasculitis of SHP is regarded as the immunovascular disease that antibody-antigen complexes on the vascular capillary endothelial cells enhances the vascular permeability. Consequently non-thrombocytopenic purpura caused by the injection of anti-endothelial cell antiserum(15). In the present study, we investigated whether or not human FXIII suppresses the enhancement of permeability and swelling induced by anti-endothelial cell antiserum in guinea pigs.

MATERIALS AND METHODS

Materials

Materials were purchased from the following suppliers: Dulbecco phosphate buffer, Dulbecco MEM, FCS(Gibco, USA), ECGS(Calbiochem, USA), Freund's adjuvant(Difco, USA), FITC conjugated anti-rabbit IgG(Cappel, USA), Evans blue, potassium hydroxide(KOH, Kanto Kagaku, Japan), phosphoric acid(Wako Pure Chemical, Japan), Guinea pig complement(Kyokuto, Japan), and Human FXIII(Fibrogammin P, Behringwerke, FRG).

Preparation of anti-guinea pig endothelial cell antiserum
Guinea pig endothelial cells were isolated from the main artery and vena cava(16), then cells were inoculated into tissue culture dishes and incubated for several days with Dulbecco MEM containing 15% FCS and 37.5 μg/ml ECGS till reaching confluency. Confluent monolayer was harvested by a cell scraper. The cells were rinsed twice with Dulbecco phosphate buffered saline(pH 7.2). These cells were used as an antigen for the production of anti-endothelial cell antiserum. The antiserum was obtained from rabbits immunized with emulsion of Freund's complete adjuvant with guinea pig endothelial cells, and boosted with emulsion of Freund's incomplete adjuvant. After several times of boosting, the antibody titer was measured with guinea pig endothelial cells by the methods of cytolysis and indirect immunofluorescence microscopy using FITC conjugated anti-rabbit IgG(17).

Measurement of antibody titer of anti-endothelial cell antiserum
Confluent monolayer of guinea pig endothelial cells in a 96-well plate was incubated with 50 μl of variously diluted antiserum in Dulbecco MEM-15% FCS for 30 min. The medium was then replaced to 50 μl of 5% guinea pig complement in Dulbecco MEM-15% FCS and the cells were further incubated for 30 min. After addition of 10 μl of trypan blue solution, the cell layers were photographed to evaluate the extent of cell lysis. Indirect immunofluorescence microscopy was done as follows. The antiserum was serially diluted two times. The diluted antiserum was then incubated with the main artery at room temperature for 1 hour and rinsed 3 times with Dulbecco phosphate buffer. After washing, 1000-fold dilution of FITC conjugated anti-rabbit IgG was added to the sections, incubated for 30 minutes at room temperature, and washed 3 times with Dulbecco phosphate buffer. All sections were observed by a Nikon microscope equipped with a mercury lamp. The titer was taken as a highest dilution which gave a fluorescent staining just above the background staining of normal serum controls.

Duration of activity of permeability enhancement
Measurement of permeability was studied according to Yamamoto et al.(18). A 100 μl portion of 50-fold diluted antiserum was intradermally injected into the back of a guinea pig before intravenous injection of 0.5 ml of 1 % Evans blue. After 15 minutes of the Evans blue injection, the back skins were harvested and the blue lesions were observed.

Suppressive effect of FXIII on the permeability enhancement
A 100 μl portion of either each diluted antiserum or the mixture of equal volume of FXIII and the diluted antiserum was

intradermally injected into the dorsal skin of guinea pigs after intravenous injection of Evans blue. After 15 minutes, skins were harvested and blue lesions in the skins were observed.

Extraction of Evans blue from guinea pig skins
Evans blue was extracted from skins, soaked with 1 ml of 1 M KOH solution, and incubated at 37°C overnight. After the incubation, 3 ml of 0.6 N phosphoric acid and 3 ml of FRIGEN(Behringwerke, FRG), a defatting agent, was added to each tube and mixed for 30 sec. with a Vortex mixer. Each tube was centrifuged at 3000 rpm for 15 minutes, and the absorbance of the supernatant was measured at 620 nm(19).

Suppressive effect of FXIII on the swelling
One milliliter of equal volume mixture of FXIII and the intact antiserum was subcutaneously injected into the dorsum of guinea pigs. After days 1, 2 and 3, the skins were harvested and the thickness was measured with a slide caliper at injection sites as a marker of swelling. The swelling was shown by the difference of the thicknesses between a injection and a non-injection site.

RESULTS

Characterization of polyclonal anti-guinea pig endothelial cell antiserum
The antibody titer was determined with guinea pig endothelial cells by the methods of cytolysis and indirect immunofluoresence microscopy using FITC conjugated anti-rabbit IgG. As a result, the 50% cytolysis was observed by the 60-fold dilution of antiserum, and the fluorescence was observed by 400-fold dilution. The antiserum exhibited the reactivity with not only guinea pig but also human endothelial cells. However it did not react with guinea pig fibroblasts. When the cryosection of the main artery of a guinea pig was used for the indirect immunofluorescence test, the fluorescence was observed on the inner membrane which was seemed to be endothelial cell. It was also found that the antiserum reacted with the extracellular matrix proteins produced by endothelial cells(data not shown).

Enhanced permeability
First, we studied whether this antiserum induced the permeability in guinea pigs. The variation of permeability after intradermal injection is shown in Fig. 1. The permeability reached the maximum within 5 minutes. This activity for enhancing the permeability almost disappeared within 30 minutes after the injection. This permeability enhancing phenomenon was classified as a short lasting reaction. We next investigated the dose response of this antiserum. As shown in Fig. 2, the activity of

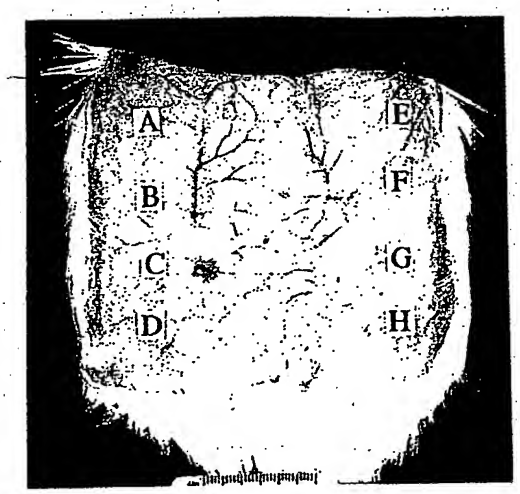

FIG. 1.

Time course of permeability enhancement induced by anti-endothelial cell antiserum. Antiserum was injected into a guinea pig at varying times before intravenous dye injection. Time 0 means an intradermal injection immediately after intravenous dye injection. (A): antiserum, 60 min, (B): antiserum, 30 min, (C): antiserum, 0 min, (D): saline, 30 min, (E): rabbit serum, 60 min, (F): rabbit serum, 30 min, (G): rabbit serum, 0 min, (H): saline, 0 min

enhancing the permeability is recognized by 400-fold dilution of antiserum. The effect of FXIII was examined on the vascular permeability induced by the antiserum. In this experiment, the mixture of antiserum was injected with various concentration of FXIII. As shown in Fig. 3, FXIII shows the suppressive effect on the dye leakage in a dose dependent fashion. We obtained a result that both 200-fold and 400-fold diluted antiserum exhibit the same tendency. Thus the effect of FXIII was examined in 10 guinea pigs and the dye leakage was measured in extravascular space. As shown in Fig. 4, FXIII exhibited the suppressive effect in a dose dependent manner.

Suppressive effect of FXIII on the swelling

When the antiserum was subcutaneously injected into a dorsal skin of guinea pig, edema, in addition to hemorrhage was observed at injection site(20). Thus we examined the suppressive effect of FXIII on the swelling. On injecting the mixture of FXIII and antiserum, the edema was significantly suppressed by FXIII on day 1 and 2(Fig. 5). This result indicates that FXIII suppresses the permeability in the acute and the subacute phase as well.

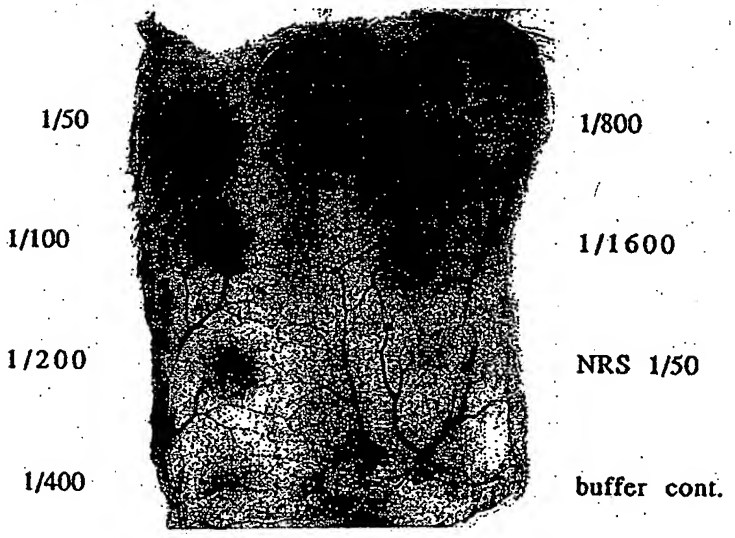

FIG. 2.

Dose response of anti-endothelial cell antiserum in a guinea pig. Each sample was injected immediately after a intravenous dye leakage. NRS: Normal rabbit serum

DISCUSSION

For more than 20 years after its detection of FXIII, many authors have reported that a clotting factor, FXIII, influenced a lot of other systems and thus it was often termed a connective tissue factors (21). The fibrin stabilizing effect is an example of general properties of this factor which crosslinks proteins with suitably configurated ε - lysyl- and γ - glutamyl - residues. Many kinds of proteins are listed as substrates for FXIII, e.g. fibrin(1), collagen(22), fibronectin(5), actin(23) and factor V(24). In this context, the binding of biogenic amines to proteins by FXIII may also participate in the elimination of toxic substances like histamine. FXIII concentrate has been recently used not only for the promotion of the wound healing but also for the treatment of Shönlein Henoch Purpura(SHP)(6,10). The clinical effects of FXIII on SHP are probably due to the stabilization of microvasculature leading to a reduction of the leakage at inflammatory sites. Pilger et al(25) has reported that FXIII shows the suppressive/sealing effect in a screlodermia patient. However none of these reports showed the sealing/suppressive effect on the permeability by FXIII in animal studies. This vasculitis of SHP is regarded as the immunovascular disease that

the vascular permeability is enhanced by the formation of the antigen-antibody complex not with standing ambiguity of trigger which may include drugs, foods, insect bites or bacterial infections(11,12,13,14). Thus we tried to demonstrate the suppressive effect of FXIII on permeability enhancement induced by anti-endothelial cell antiserum. As shown in Figs. 1 and 2, anti-endothelial cell antiserum induces the enhancement of permeability. This phenomenon can be caused by factors such as complement fragments and histamine etc. which are produced by the activation of complement system after complex formation of antiserum with endothelial cells(11,12,13,14). As this phenomenon shows the dose dependent manner by antiserum, condition of SHP patients may be influenced seriously depending on the extent of the antibody generation. SHP patients show the increase of plasma level of IgA and the imbalance of serum IgG subclass and IgM(13,14,26). As shown in Figs. 3, 4 and 5, FXIII suppresses the vascular permeability in acute phase and the edema in subacute phase. These results are supported by some clinical studies. Kamitsuji et al.(10) and Fukui et al.(11) have reported that FXIII shows the suppressive effect on the swelling of joints of SHP patients.

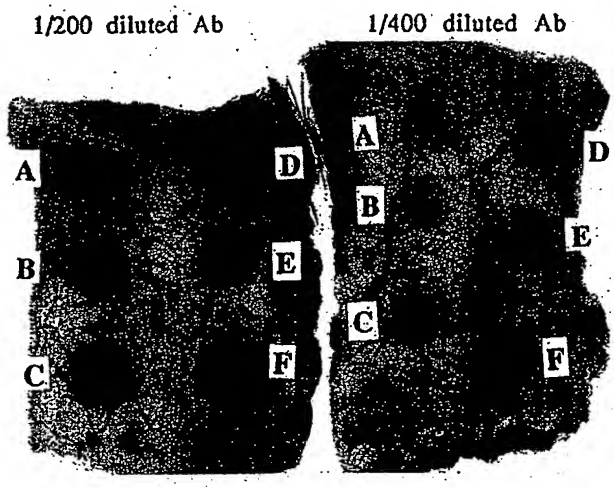

FIG. 3.

Suppressive effect of FXIII on the permeability enhancement induced by anti-endothelial cell antiserum. FXIII was used with the final concentration at a injection site of (A), 3.0 U; (B), 1.5 U; (C), 0.75 U; (D), 0.38 U; (E), medium control. The mixture of FXIII and either 200- or 400- fold diluted antiserum was injected immediately after the intravenous injection of dye.

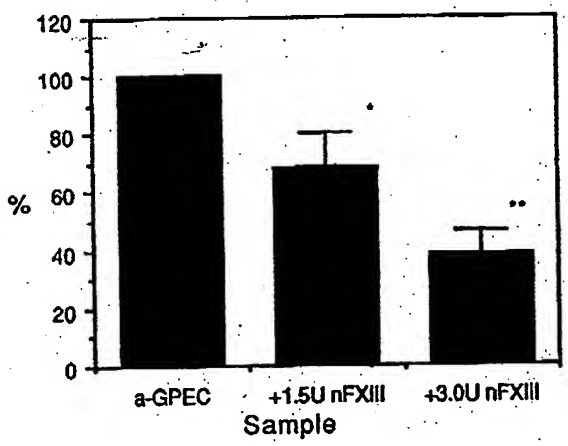

FIG. 4

Suppressive effect of FXIII on the permeability induced by anti-guinea pig endothelial cell antiserum. Extraction of Evans blue at the injection site was according to the materials and methods. n=10, *: $p<0.05$, **: $p<0.01$ In this experiment, we used the 300-fold diluted anti-endothelial cell antiserum as a permeability inducer. FXIII was mixed with antiserum, then the mixture was injected intradermally.

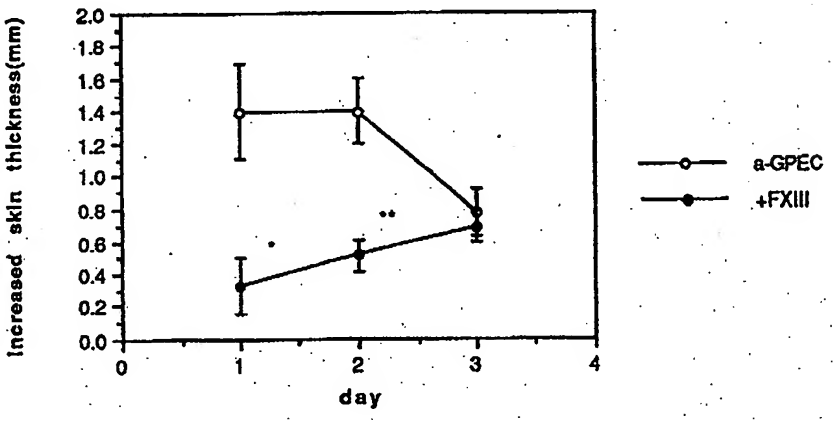

FIG. 5.

Effect of FXIII on the swelling induced by anti-guinea pig endothelial cell antiserum. Open circle (o) denotes the antiserum alone. Closed circle (●) denotes the FXIII plus antiserum. n=5, *: $p<0.05$, **: $p,0.01$

Pilger et al.(25) reported that FXIII also shows the suppressive effect on vascular permeability in sclerodermia patients. These results suggest that FXIII may crosslink cellular matrices to prevent the opening of the space between cells(27) and that it may crosslink the enhancing factors for the permeability(21). We have succeeded in demonstrating the suppressive effect of FXIII on vascular permeability in an animal study. This study indicates that FXIII may play a crucial role in an inflammatory site. Consequently it seems that FXIII therapies are necessary for the treatment of some inflammatory diseases (28,29).

REFERENCES

1. ROBBINS, K.C. A study of the comparison of fibrinogen to fibrin. AM. J. Physiol., *142*, 581-588, 1944
2. KESKI-OJA, J., MOSHER, D.F. and VAHERI, A. Crosslinking of a major surface-associated glycoprotein (fibronectin) catalyzed by blood coagulation factor XIII. Cell, *9*, 29-35, 1976
3. ICHINOSE, A., TAMAKI, T. and AOKI, N. FXIII mediated cross-linking of NH2-terminal peptide of alpha-2 plasmin inhibitor to fibrin. FEBS-letter, *153*, 369-371, 1983
4. SHEN, L. and LORAND, L. Contribution of fibrin stabilization to clot strength. J. Clin. Invest., *71*, 1336-1341,1983
5. OKADA, M., BLOMBÄCK, B., DER CHANG, M. and HOROBITZ, B. Fibronectin and fibrinogen structure. J. Biol. Chem., *260*, 1811-1820, 1985
6. MISHIMA, Y., NAGAO, F., ISHIBIKI, K., MATSUDA, M. and NAKAMURA, N. Faktor XIII in der Behandlung postoperativer therapierefraktärer Wundheilungsstorungen. Chirurg, *55*, 803-808, 1984
7. FYE, K.H. and SACK, K.E. Basic and Clinical Immunology, In: *Rheumatic disease*, STITES, D.P., STOBO, J.D., FUDENBERG, H.H. and WELLS, J.V. (eds.), p449, Lange Medical Publications, California, (1982)
8. HENRIKSSON, P., HENDERNER, U. and NILSSON, I.M. Factor XIII (fibrin stabilizing factor) in Henoch-Schönlein's purpura. Acta. Pediatr. Scand., *66*, 273-277, 1977
9. HENRIKSSON, P., NILSSON, I.M., OKLSSON, K. and STENBERG, P. Granulocyte elastase activation and degradation of factor XIII. Thromb. Res., *18*, 343-351, 1980
10. KAMITSUJI, H., TANI, K., YASUI, M., TANIGUCHI, A., TAIRA, K., TSUKADA, S., IIDA, Y., KANNKI, H. and FUKUI, H. Activity of blood coagulation Factor XIII on a prognostic indicator in patients with Henoch-Schönlein purpura. Eur. J. Pediatr., *146*, 519-523, 1987
11. FUKUI, H., KAMITSUJI, H., NAGAO, T., YAMADA, K., AKATSUKA, J., INAGAKI, M., SHIKE, S., KOBAYASHI, Y., YOSHIOKA, K., MAKI, S., SHIRAHATA, A., MIYAZAKI, S., NAKASHIMA, M. and TANAKA, S. Clinical evaluation of a pasteurized factor XIII concentrate administration in Henoch-Schönlein Purpura. Thromb. Res. *56*, 667-675, 1989
12. MATSUOKA, M., Hemorrhagic factors and Thrombosis, In: *Purpura Schönlein-Henoch*, p245-246, Kinbara Shuppan, Tokyo (1981)
13. BOWIE, W.E.J. and OWEN, C.A.Jr Hemostasis and Thrombosis, In: *Non thrombocytopenic vascular disorders*, COLMAN, R.W., HIRSH, J, MARDER, U.J. and SALZMAN, E.W. (eds.), p816-824, Lippincott, Philadelphia, 1987

14. ITO, T. and FUJIMAKI, M. Intergated handbook of internal medicine, In: *Schönlein-Henoch purpura*, IMURA, H., OGATA, E., TAKAKU, S. and TARUI, S.(eds.), p296-300, Nakayama Shupann, Tokyo
15. WILSON, C.B., COLE, E.R., ZANETTI, M. and MAMPASO, F.M. Basic and Clinical Immunology, In: *Renal disease*, STITES, D.P., STOBO, J.D., FUDENBERG, H.H. and WELLS, J.V. (eds.), p557-575, Lange Medical Publication, California (1978)
16. MITSUI, Y. and IMAMURA, J. Isolation and Culture for Functional Cells, In: *Endothelial cells.*, MITSUI, J., TAKAGI, R., ICHIHARA, A., SEKIGUTI, M. and MURAMATSU, T.(eds.) p227-229, Maruzen, Tokyo (1987)
17. WICK, G., BAUNDNER, S. and HERZOG, F. Immunofluorescence, p47-51, Die Medizinishe Verlagsgesellschaft, Marburg (1987)
18. Yamamoto, T., Chemical Mediators of Inflammation and Immunity, In; *Role of Hageman factor in enhancing vascular permeability.*, CHOEN, S., HAYASHI, H., SAITO, K. and TAKADA, A. (eds.), p129-143, Academic Press, New York (1986)
19. KATAYAMA, S., SHIONOYA, H. and OHTAKE, S. A new method for extraction of extravasated dye in the skin and influence of fasting stress on passive cutaneous anaphylaxis in guinea pigs and rats. Microbiol. Immunol. Biol., *22*, 89-101, 1987
20. SHINBO, K., HIRAHARA, K., TAKAHASHI, M. and MATSUISHI, T. Suppressive effect of factor XIII on the hemorrhage induced by anti-endothelial cell antiserum. Int. J. Hematol., *54*(suppl 1), 276, 1991
21. KARGES, H.E. and CLEMENS, R. Factor XIII: Enzymatic and clinical aspects. Behring Inst. Mitt. *82*, 43-58, 1988
22. SORIA, A., SORIA, C. and BOULARD, C. Fibrin stabilizing factor (FXIII) and collagen polymerization. Experientia, *31*, 1355-1357, 1975
23. CHOEN, J., BLANKENBERG, T.A., BORDEN, B., KAHN, D.R. and VEIS, A. Factor XIIIa-catalyzed crosslinking of platelet and muscle. Regulation by nucleotides. Biochem. Biophys. Acta., *628*, 365-375, 1980
24. FRANCIS, R.T., MACDONAGH, J. and MANN, K.G. Factor V is a substrate for the transamidase factor XIIIa. J. Biol. Chem., *261*, 9787-9797, 1986
25. PILGER, E., BERTUCH, H., ULREICH, A. and RAINER, F. Capillary permeability in connective tissue disease.: Influence of Fibrogammin P-therapy, Thromb. Haemostas. *58*, 81, 1987
26, TRYGSTAD, C.W. and STIEHM, E.R. Elevated serum IgA globulin in anaphylactoid purpura. Pediatrics, *47*, 1023-1029, 1971
27. TAKAHASHI, M., SHINBO, K., HIRAHARA, K. and MATSUISHI, T. Effect of activated factor XIII on increase in permeability of human umbilical vein endothelial cell layer. The XXIV Congress of International Society of Hematology in London (abstract), 1992
28. GALOWAY, M.J., MAKIE, M.J. and MACVERRY, B.A. Reduced levels of factor XIII in patients with chronic inflammatory bowel disease. Clin. Lab. Haemat., *5*, 427-428, 1983
29. KURATSUJI, T., OKIMA, T., FUKUMOTO, T., SHIMIZU, S., IWASAKI, Y., TOMITA, Y., MEGURO, T. and YAMADA, K. Factor XIII deficiency in antibiotic-associated pseudomembranous colitis and its treatment with Factor XIII concentrate. Haemostas., *11*, 229-234, 1982

Waterbury, *ibid.*, p. 340; H. Felback, J. Childress, G. Somero, *Nature (London)* 293, 291 (1981).
15. U. Laemmli, *Nature (London)* 227, 680 (1970).
16. G. Fairbanks, T. Steck, D. Wallach, *Biochemistry* 10, 2606 (1971).
17. S. Panyim and R. Chalkley, *Arch. Biochem. Biophys.* 130, 337 (1969); T. Poole, B. Leach, W. Fish, *Anal. Biochem.* 60, 596 (1974).
18. Funds for the vessels D.S.R.V. *Alvin*, R.V. *Lulu*, and R.V. *New Horizon* were provided by NSF. Research was supported by NSF grants OCE78-08852 and OCE78-08933 (to J. J. Childress), OCE78-10458 (to J. F. Grassle), and PCM 80-12854 and PCM 78-21784 (to R.C.T.). This work was made possible by the physical and intellectual efforts of many people, including the captains and crews of the vessels named above. We thank B. Smithie and R. Hessler for collection of the East Pacific Rise clam blood and J. J. Childress for supplying the Galápagos Rift Valley clam blood. This article is contribution No. 43 of the Galápagos Rift Biology Expedition.

10 June 1982; revised 12 November 1982

Tumor Cells Secrete a Vascular Permeability Factor That Promotes Accumulation of Ascites Fluid

Abstract. *Tumor ascites fluids from guinea pigs, hamsters, and mice contain activity that rapidly increases microvascular permeability. Similiar activity is also secreted by these tumor cells and a variety of other tumor cell lines in vitro. The permeability-increasing activity purified from either the culture medium or ascites fluid of one tumor, the guinea pig line 10 hepatocarcinoma, is a 34,000- to 42,000-dalton protein distinct from other known permeability factors.*

Abnormal accumulation of fluid commonly accompanies solid and particularly ascites tumor growth (*1*). To investigate the mechanism of tumor ascites formation, we measured the rates of influx and efflux of ^{125}I-labeled human serum albumin (HSA) at various times after the implantation of tumor cells in the peritoneal cavities of guinea pigs. We detected a markedly increased influx of HSA as early as 1 hour after intraperitoneal injection of guinea pig line 10 hepatocarcinoma cells, which provoke a substantial accumulation of ascites fluid (Table 1). In contrast, efflux of HSA from the peritoneal cavities of animals bearing line 10 tumors did not change significantly, even with progressive tumor growth (*2*).

To establish whether the increased influx of fluid induced by tumor cells reflects an alteration in vessel permeability, we injected animals intravenously with colloidal carbon. Examination of the peritoneal cavities of strain 2 guinea pigs, Syrian hamsters, and A/Jax mice bearing syngeneic ascites tumors (line 10, HSV-NIL8, and TA3-St, respectively) revealed that many venules of the peritoneal wall, diaphragm, mesentery, and gastrointestinal serosal surfaces were heavily labeled with colloidal carbon, indicating increased permeability; comparable vessels in control animals were not labeled.

These observations suggest that tumor ascites may be attributable to alterations in the permeability of vessels lining the peritoneum. To investigate the basis for this increased permeability, we used the Miles assay (*3*) to test ascites fluid for the presence of factors that increase vascular permeability (Table 2 and Fig. 1). Ascites fluid from line 10 guinea pig and TA3-St mouse carcinomas and the HSV-NIL8 hamster sarcoma all markedly increased local cutaneous vascular permeability. The increase was evident after 1 minute and maximal within 5 to 10 minutes. By contrast, platelet-poor plasma samples from the same species (Table 2 and Fig. 1) and oil-induced peritoneal exudate fluids (*4*) had little or no activity. The tumor ascites permeability-increasing activity was not inhibited by soybean trypsin inhibitor (1000 μg/ml); therefore, it is not PF/dil (*5*), a permeability factor unmasked when serum is diluted ≥ 1:100 (*6*).

We previously reported that line 10 tumor cells release a vascular permeability–increasing activity in serum-free culture (*7*). This activity is not inhibited by soybean trypsin inhibitor (200 μg/ml), and its production by cells in vitro requires protein synthesis (complete inhibition by 20 μg of cycloheximide per milliliter). Many other tumor cell lines also release permeability-increasing activity in serum-free culture, including guinea pig 104 C1 fibrosarcoma, hamster HSV-NIL8 sarcoma, rat sarcomas B77 Rat 1 and RR 1022, and mouse TA3-St carcinoma, MOPC 21 myeloma, and polyoma BALB/c 3T3 sarcoma. Line 1 guinea pig hepatocarcinoma cells release one-fourth the activity released by line 10 cells, a finding that may explain the relative ability of these cells to promote HSA influx (Table 1) and ascites fluid accumulation (the volume of line 1 ascites fluid was routinely one-fourth that of line 10). Oil-induced guinea pig peritoneal exudate cells (> 70 percent macrophages) neither increase the influx of HSA into the peritoneum (Table 1) nor secrete detectable permeability-increasing activity in vitro. Guinea pig fibroblasts and smooth muscle cells release approximately one-eighth the activity released by comparable numbers of line 10 cells (*8*).

We next purified both the ascites and tissue culture permeability factors from a single tumor, the line 10 guinea pig carcinoma. Permeability-increasing activities from both sources chromatographed identically as single peaks on columns containing Sephadex G-150, heparin-Sepharose, or hydroxylapatite (*9*) and electrophoresed as a single peak with an apparent molecular weight of 34,000 to 42,000 on sodium dodecyl sulfate–polyacrylamide gels (Fig. 2). Using the heparin-Sepharose, hydroxylapatite, and electrophoretic steps in tandem, we purified the permeability-increasing activity approximately 1200-fold from serum-free conditioned medium and approximately 10,000-fold from ascites fluid. As little as 200 ng (5×10^{-12} mole) of the purified material increased vascular permeability to a degree equivalent to that induced by 1.25 μg (4×10^{-9} mole) of histamine.

Rabbits immunized with the purified permeability factor secreted by line 10 cells in vitro produced an immunoglobulin G (IgG) that bound and neutralized virtually all the permeability-increasing activity in undiluted line 10 and line 1 tumor ascites fluids (Table 2) and in line 10 and line 1 culture media. This antibody also blocked the peritoneal influx that follows intraperitoneal injection of line 10 tumor cells (Table 1). In every

Table 1. Peritoneal vessel permeability. Guinea pigs (400 g) were injected intraperitoneally with 3×10^7 line 1 or line 10 tumor cells (*17*) or with peritoneal exudate cells in Hanks balanced salt solution (HBSS) and immediately thereafter were injected intravenously with ^{125}I-labeled HSA (5×10^6 dis/min). One hour later the animals were exsanguinated under ether anesthesia, and peritoneal fluid was collected following intraperitoneal injection of 20 ml of heparinized (10 U/ml) HBSS. For each animal total radioactivity in the ascites fluid was determined and normalized for that in the blood: influx of HSA was computed as the ratio of total disintegrations per minute in peritoneal fluid to those per milliliter of blood. Net influx was determined by subtracting influx values for control animals. Values are means ± standard errors ($N = 4$).

Type of cells injected intraperitoneally	Net peritoneal influx of HSA
Line 1	0.09 ± 0.04
Line 10	0.41 ± 0.08
Line 10 + immune IgG (2 mg)	0.11 ± 0.03
Peritoneal exudate	0

Table 2. Dermal vessel permeability, as determined by the Miles assay (7), of depilated guinea pigs were injected intravenously with ^{125}I-labeled HSA (1.3×10^7 dis/min) in 1 ml of saline containing 0.5 percent Evans Blue dye. Samples to be tested for permeability-increasing activity, in isotonic solution and at neutral *p*H, were injected intradermally in a volume of 0.1 ml. After 20 minutes the animals were exsanguinated under ether anesthesia. Test sites were excised and quantitated for ^{125}I in a gamma counter. The number of net disintegrations per minute extravasated was determined by subtracting values for control sites injected with saline. Each animal also received a series of intradermal histamine injections; these sites served as reference points for the calculation of histamine equivalents. B.L., below limit of quantitation (0.6 μg histamine).

Substance injected intradermally	Net disintegrations per minute ^{125}I-HSA extravasated (mean ± standard error) (N = 3 to 7)	Histamine equivalent* (μg)
Hamster plasma	70 ± 176	B.L.
Hamster ascites (HSV-NIL8)	15,309 ± 1,508	1.3
Guinea pig plasma	1,989 ± 1,070	B.L.
Line 1 ascites	69,609 ± 6,850	5.5
Line 1 ascites + preimmune IgG (80 μg)	70,321 ± 2,567	5.5
Line 1 ascites + immune IgG (80 μg)	3,935 ± 1,568	B.L.
Line 10 ascites	92,472 ± 4,886	10.0
Line 10 ascites + preimmune IgG (80 μg)	93,756 ± 1,171	10.0
Line 10 ascites + immune IgG (80 μg)	7,187 ± 930	B.L.
Line 10 serum-free culture supernatant†		
After 1 hour of culture	1,054 ± 60	B.L.
After 5 hours of culture	3,610 ± 295	0.7
After 24 hours of culture	21,565 ± 617	2.5

*A plot of net disintegrations per minute extravasated in response to histamine versus the logarithm of the number of micrograms of histamine injected generated a straight line (histamine range, 0.6 to 10 μg). †Derived from cultures containing 2.5×10^6 cells per milliliter.

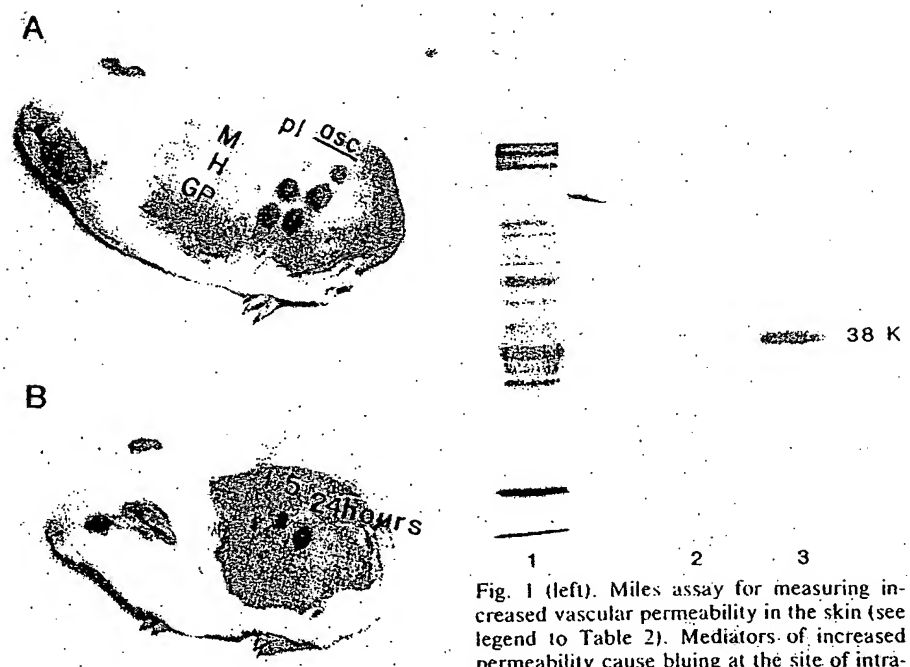

Fig. 1 (left). Miles assay for measuring increased vascular permeability in the skin (see legend to Table 2). Mediators of increased permeability cause bluing at the site of intradermal injection within 5 minutes, whereas control substances such as saline elicit no response. Abbreviations in (A): *pl*, control plasma; *asc*, ascites fluid; *M*, mouse TA3-St tumor; *H*, hamster HSV-NIL8 tumor; and *GP*, guinea pig line 10 tumor. In (B), line 10 cells were cultured (1×10^6 cell/ml) in serum-free Dulbecco's modified Eagle's medium and conditioned media was harvested at 1, 5, and 24 hours as indicated. Fig. 2 (right). Resolution of the permeability-increasing activity on sodium dodecyl sulfate–polyacrylamide slab gels (*16*). Samples were electrophoresed without reduction at 4°C in a 7.5 percent polyacrylamide gel containing 0.1 percent sodium dodecyl sulfate and washed for 1 hour at 4°C in 2.5 percent Triton X-100 and then in phosphate-buffered saline for 1 hour. The gel was sliced, individual slices were extracted, and dialyzed extracts were tested for activity by the Miles assay. Track 1 shows the stained pattern of concentrated line 10 serum-free culture medium. All the activity in track 1 (total recovery was regularly 50 percent) was confined to two adjacent slices (reelectrophoresed in tracks 2 and 3) composing the 34,000 to 42,000 molecular weight region. Line 10 ascites fluid permeability-increasing activity was found to electrophorese identically (molecular weight 34,000 to 42,000) with the activity in line 10 culture medium.

munization (preimmune IgG) was without effect. The IgG from immunized animals (immune IgG) also neutralized the permeability-increasing activity released in culture by an unrelated tumor, the 104 C1 guinea pig fibrosarcoma (*10*), but not the activity of guinea pig PF/dil or the low levels of activity released by guinea pig fibroblasts or smooth muscle cells.

As determined by light and electron microscopy, line 10 permeability factor did not cause endothelial cell damage or mast cell degranulation. Vessels responded equally well to multiple challenges with equivalent doses of line 10 permeability factor administered 30 minutes apart; the effect of a single intradermal injection was rapid (evident within 5 minutes) and transient (little residual increased permeability was detectable 20 minutes after injection), providing further evidence that line 10 permeability factor is not toxic to blood vessels. It does not resemble bradykinin (molecular weight, 1200), plasma kallikrein (108,000), or leukokinins (2500). Leukokinins (*11*) are generated in ascites fluids under nonphysiological conditions (*p*H 3.8 and 37°C for 24 hours) by a mechanism sensitive to 1 μ*M* pepstatin A. Line 10 permeability factor is present in fresh, unmanipulated ascites fluid (*p*H 6.4 to 6.9), and its action is unaffected by 20 μ*M* pepstatin A. Lymphocyte permeability factors with molecular weights of 12,000 (*12*) and 39,000 (*13*) have been reported; however, unlike line 10 permeability factor, the latter increases vascular permeability only after a latent period of 20 minutes. The effects of line 10 permeability factor are not mediated by histamine. Guinea pigs treated with the antihistamines mepyramine (5 μmole/kg, subcutaneously) plus cimetidine (500 μmole/kg) (*14*) responded normally to line 10 permeability factor, although the action of 20 μg of histamine was blocked. It is also unlikely that the effects of this factor are mediated through prostaglandin synthesis. Neither systemic (14 μmole/kg, intraperitoneally) nor local (2 nmole, intradermally) treatment with indomethacin (*15*) affected the response of vessels to the permeability factor.

In conclusion, vessels lining the peritoneal cavities of guinea pigs, hamsters, and mice bearing ascites tumors display markedly greater permeability than do the same vessels in control animals. This increased permeability is apparently due to the presence in ascites fluid of a potent permeability factor not found in normal plasma or serum. The permeability factors found in guinea pig line 10

culture medium or ascites fluids appear to be identical. In addition, they are antigenically related to permeability factors produced by guinea pig line 1 or 104 C1 tumor cells. Secretion of permeability-increasing activity appears to be a common feature of tumor cells, and may contribute to the abnormal accumulation of fluid associated with neoplastic disease.

Note added in proof: The immune IgG raised against line 10 permeability factor also neutralizes the rat dermal vessel permeability-increasing activity released by Walker rat carcinoma cells in culture. Preimmune IgG has no neutralizing effect.

DONALD R. SENGER
STEPHEN J. GALLI
ANN M. DVORAK
CAROLE A. PERRUZZI
V. SUSAN HARVEY
HAROLD F. DVORAK

Departments of Pathology, Beth Israel Hospital, and Harvard Medical School, and Charles A. Dana Research Institute, Beth Israel Hospital, Boston, Massachusetts 02215

References and Notes

1. P. M. Gullino, in *Cancer 3: A Comprehensive Treatise*, F. F. Becker, Ed. (Plenum, New York, 1975), pp. 327–354; M. Green, *Principles of Cancer Treatment* (McGraw-Hill, New York, 1982), pp. 237–243.
2. Clearance of labeled HSA from the peritoneal cavity was not impaired in tumor-bearing animals at any interval. For example, 7 days after intraperitoneal injection of 3×10^7 line 10 tumor cells, 58.4 ± 4.2 percent (mean ± standard error) of the HSA (90 to 95 percent precipitable with trichloroacetic acid) remained in the peritoneal cavities after 2 hours; 56 ± 1.15 percent remained in the controls.
3. A. A. Miles and E. M. Miles, *J. Physiol. (London)* **118**, 228 (1952).
4. M. E. Hammond and H. F. Dvorak, *J. Exp. Med.* **136**, 1518 (1972).
5. A. A. Miles and D. L. Wilhelm, *Br. J. Exp. Pathol.* **36**, 71 (1955).
6. It has been shown that PF/dil is activated Hageman factor (clotting factor XIIa or αHFa) [H. Z. Movat, in *Handbook of Experimental Pharmacology*, vol. 25, *Supplement*, E. G. Erdos, Ed. (Springer-Verlag, Berlin, 1979), p. 1], an activity totally inhibited by 5 μg of soybean trypsin inhibitor per milliliter [A. A. Miles and O. D. Ratnoff, *Br. J. Exp. Pathol.* **45**, 328 (1964)]. We confirmed this finding and therefore conclude that the activity present in undiluted ascites fluid is not PF/dil. However, a ≥ 1:50 dilution of line 10 guinea pig ascites fluid in saline with 0.38 percent sodium citrate in plastic tubes unmasked a second permeability factor activity which, like PF/dil, was inhibited completely by soybean trypsin inhibitor. Because this inhibitable activity was not expressed unless ascites fluid was diluted substantially, we concluded that it was not likely to be responsible for inducing tumor ascites in vivo. Therefore we focused our attention on the permeability-increasing activity in undiluted ascites fluid.
7. H. F. Dvorak *et al.*, *J. Immunol.* **122**, 166 (1979).
8. The cells were cultured in the presence of 10 percent guinea pig serum because protein synthesis by fibroblasts is decreased in the absence of serum.
9. Activities from both ascites fluid and serum-free culture medium bound completely to both heparin-Sepharose and hydroxylapatite. Columns were eluted with linear gradients; ascites and culture medium activities coeluted from heparin-Sepharose as a peak centered at 0.40*M* NaCl–0.01*M* PO_4 (*p*H 7.0) and from hydroxylapatite at 0.25*M* sodium phosphate (*p*H 7.0). To avoid complicating our analysis of diluted ascites fluid fractions with unmasked PF/dil (*7*), we added soybean trypsin inhibitor (20 μg/ml) to all ascites fluid column fractions before assay.
10. C. H. Evans and J. A. DiPaolo, *Cancer Res.* **35**, 1035 (1975).
11. L. M. Greenbaum, in *Handbook of Experimental Pharmacology*, vol. 25, *Supplement*, E. G. Erdos, Ed. (Springer-Verlag, Berlin, 1979), p. 91.
12. A. Sobel and G. La Grue, in *Lymphokine Reports*, E. Pick, Ed. (Academic Press, New York, 1980), vol. 1, pp. 211–230.
13. J. L. Maillard, E. Pick, J. L. Turk, *Int. Arch. Allergy Appl. Immunol.* **42**, 50 (1972).
14. D. A. A. Owen *et al.*, *Br. J. Pharmacol.* **69**, 615 (1980). Both injections were given 30 minutes before skin testing.
15. J. S. Stoff, R. M. Rosa, P. Silva, F. H. Epstein, *Am. J. Physiol.* **241**, F231 (1981). Intraperitoneal injections were given 1 and 25 hours before skin testing. For intradermal injections, indomethacin was mixed with test substances.
16. U. K. Laemmli, *Nature (London)* **227**, 680 (1970).
17. B. Zbar, H. T. Wepsic, H. J. Rapp, J. Whang-Peng, T. Borsos, *J. Natl. Cancer Inst.* **43**, 821 (1969); B. Zbar, I. Bernstein, T. Tanaka, H. J. Rapp, *Science* **170**, 1217 (1970).
18. We thank B. Wildi, J. Feder, and R. D. Rosenberg for help and advice, J. Osage for technical assistance, and B. Zbar, R. Hynes, R. Garcia, T. Isomura, and J. Codington for cells. Supported by a grant from the Monsanto Company.

12 October 1982

Yolk Pigments of the Mexican Leaf Frog

Abstract. *Eggs of the Mexican leaf frog contain blue and yellow pigments identified as biliverdin and lutein, respectively. Both pigments are bound to proteins that occur in crystalline form in the yolk platelet. The major blue pigment is biliverdin IX α. The eggs vary in color from brilliant blue to pale yellow-green depending on the amount of each pigment. These pigments may provide protective coloration to the eggs.*

While studying the lipid composition of the eggs and embryos of the Mexican leaf frog, *Agalychnis dacnicolor* (*1*), we observed that their green coloration was due to the presence of two pigments, one blue and one yellow, which together produce blue, blue-green, or yellow-green eggs. We have now identified the major blue pigment as biliverdin IX α and the major yellow pigment as lutein. The presence of the latter pigment is not surprising since lutein is widely distributed among plants and animals (*2*). Biliverdin occurs less often as a pigment, although it has been found in the dog placenta, in the shells of bird eggs, in the skin of fishes and amphibians (*2*, *3*), in the eggs and larvae of the tobacco hornworm (*4*), and in the serum and eggs of *Xenopus* (*5*). It seems likely that the utilization of these two pigments by *A. dacnicolor* evolved as a mechanism for producing green eggs. The green coloration of leaf frog eggs, which are laid on green vegetation, may afford camouflage to protect eggs and embryos from predation. However, as far as we can ascertain, there have been no definitive studies on the adaptive value of green eggs, although the ecological implications deriving from a two-pigment system for egg coloration are apparent.

Six different batches of *A. dacnicolor* eggs (100 to 250 eggs) varying in color from brilliant blue to yellow-green were extracted with a 1:1 mixture of chloroform and methanol and a mixture of acetone and hydrochloric acid to obtain the yellow and blue pigments. The pigments were separated by column chromatography on silicic acid. Chloroform eluted the yellow pigment, and acetone eluted the blue pigment. The pigments were further purified by preparative thin-layer chromatography (TLC). The yellow and blue pigments were localized in lipid-rich yolk platelets.

Yolk platelets, which were pale blue-green or pale yellow, were obtained by collagenase treatment of homogenized eggs, followed by differential centrifugation. Analysis by light microscopy of the isolated fresh yolk platelets revealed rounded rectangular platelets of different sizes, and electron microscopy showed that the platelets consisted of closely stacked crystalline arrays about 70 Å thick.

The ultraviolet to visible spectra of the silicic acid column–purified pigments from different eggs are given in Fig. 1, a and b. The blue pigment has major bands at 372 to 376 nm and 640 to 690 nm. The yellow pigments have major bands at 442 to 444 nm and 470 to 471 nm. The relative amount of the yellow and blue pigments in the various eggs was determined by the ratio of the absorbance at 442 nm to that at 650 nm. This ratio was correlated with the color of the egg. The ratio of brilliant blue eggs was 1.15, that of blue eggs was 1.7 to 2.3, that of green eggs was 3.4 to 3.6, and that of yellow-green eggs was 10.4.

The blue pigment has properties consistent with a biliverdin. Both the blue pigment and biliverdin (Sigma) were converted to methyl esters by treatment with methanolic HCl (Supelco). The dimethyl esters were purified by preparative TLC (Merck-Darmstadt silica gel 60 plates) using chloroform and methanol 9:1. Both had identical relative mobility (R_f) values of 0.62, and gave a purple

CLIN. CHEM. 38/1, 71–75 (1992)

Development of Time-Resolved Immunofluorometric Assay of Vascular Permeability Factor

Kiang-Teck Yeo, Tracy M. Sioussat, James D. Faix, Donald R. Senger, and Tet-Kin Yeo

We describe a two-site time-resolved immunofluorometric assay for guinea pig vascular permeability factor (VPF) for quantifying VPF in different biological fluids. Antibody against the carboxy terminus (C-IgG) is immobilized on microtiter wells, and antibody against the amino terminus (N-IgG) is labeled with Eu^{3+}-chelate. Line 10 tumor culture medium, known to be rich in VPF, is assayed in a two-step incubation. Bound Eu^{3+} is then quantified by dissociation into a fluorescent enhancement solution, with measurement of the time-resolved fluorescence. The analytical sensitivity is 0.35 VPF unit, and the intra-assay CV is about 20%. The assay is specific for VPF, because pre-treatment with the appropriate C- or N-peptide, or pre-extraction of VPF, greatly decreases fluorescence. The VPF immunoassay is highly correlated (r^2 = 0.94) with the Miles permeability assay, the classical bioassay of VPF. In addition, the immunofluorometric assay is about 30-fold more sensitive than the Miles assay.

Additional Keyphrases: *vascular endothelial growth factor · angiogenesis · line 10 tumor culture medium · bioassay compared*

Vascular permeability factor (VPF), which is secreted by various tumor cells, is a highly conserved protein (M_r 34 000–42 000) with potent vascular permeability-enhancing activity that causes accumulation of ascites fluid associated with tumor growth (*1, 2*).[1] In addition, recent studies have shown that VPF is similar or identical to vascular endothelial growth factor (VEGF), a mitogen specific for endothelial cells (*3–7*). Thus, tumor-secreted VPF (VEGF) may promote tumor angiogenesis directly by its mitogenic activity for endothelium. VPF (VEGF) may also elicit angiogenesis indirectly by its vascular permeability effect, which causes extravasation of plasma proteins, including fibrinogen, and deposition of an extravascular fibrin gel, which provokes ingrowth of vascular endothelial cells (*8*). Currently, the precise role of VPF (VEGF) in the pathogenesis of solid tumor growth is an area of intense investigation. Important to this investigation is the development of a simple, sensitive, and specific assay for VPF, preferably one that can be used for assaying VPF in various biological fluids and tissue homogenates.

VPF was first measured by using the Miles assay (*9*), which measures the extravasation of intravenously injected Evans Blue dye into the dermis of guinea pigs in response to intradermal injections of VPF (*1*). The amount of accumulated dye can be quantified by extraction and measuring the absorbance at 620 nm (*10*). The Miles assay has been used widely to detect VPF in cell-free culture medium of tumor cells as well as in tumor ascites fluid (*1, 2*). However, this assay is not specific because it will detect permeability changes in response to other inflammatory mediators besides VPF. Also, fluids from different animal species cannot be used because foreign proteins commonly elicit nonspecific permeability changes, leading to a false-positive Miles test.

We report here a sensitive and specific immunofluorometric assay for detecting VPF. Antibodies raised against the C-terminus of VPF (C-IgG) were immobilized on microtiter wells and served as the "capture" antibody. Antibodies raised against the amino terminus of VPF (N-IgG) were labeled with Eu^{3+}-chelate and served as the "detector" antibody. In the presence of VPF, a "sandwich" configuration is formed. After the final wash step, bound Eu^{3+} is dissociated in the presence of β-diketone, forming a highly fluorescent chelate that can be read in a time-resolved fluorometer. This approach is termed "dissociation enhanced lanthanide fluoroimmunoassay," or DELFIA (*11–14*). The reagents and equipment required are commercially available.

Materials and Methods

Reagents. DELFIA Eu^{3+}-labeling kits were purchased from Pharmacia-LKB Nuclear, Inc. (Gaithersburg, MD). Each kit contained 0.2 mg of labeling reagent [N^1-(*p*-isothiocyanatobenzyl)-diethylenetriamine-N^1,N^2,N^3,N^3-tetraacetate-Eu^{3+}], a 100 nmol/L Eu^{3+} standard, highly purified bovine serum albumin (BSA; 75 g/L in Tris · HCl, pH 7.8 plus, NaN_3, 0.5 g/L) stabilizer, enhancement solution (per liter, 15 μmol of 2-naphthoyltrifluoroacetone, 50 μmol of tri-*n*-octylphosphine oxide, 100 mmol of acetic acid, 6.8 mmol of potassium hydrogen phthalate, and 1.0 g of Triton X-100 detergent), assay buffer (Tris · HCl solution, pH 7.8, containing BSA, bovine gamma globulin, Tween 40, diethylenetriaminepentaacetic acid, and NaN_3, 0.5 g/L), and wash concentrate solution (25-fold concentration of Tris · HCl/NaCl, pH 7.8, plus Tween 20) (*11–14*). PD-10 columns, Sepharose CL-6B, and Sephadex G-50 were from Pharmacia LKB Biotechnology (Piscataway, NJ). Macrosolute concentrators were from Amicon (Danvers, MA). Maxisorp microtiter plates and strips (96-well) were obtained from Nunc

Department of Pathology, Beth Israel Hospital and Harvard Medical School, and Charles A. Dana Research Institute, 330 Brookline Ave., Boston, MA 02215.

[1] Nonstandard abbreviations: VPF, vascular permeability factor; VEGF, vascular endothelial growth factor; C-IgG, antibody against carboxy terminus of VPF; N-IgG, antibody against amino terminus of VPF; ELISA, enzyme-linked immunosorbent assay; and BSA, bovine serum albumin.

Received July 9, 1991; accepted November 14, 1991.

Inc. (Naperville, IL). Serum-free medium (HL-1) was purchased from Ventrex Labs. Inc. (Portland, ME). Hemoglobin crystals were from Sigma Chemical Co. (St. Louis, MO). The GammaGone IgG removal device was from Genex Corp. (Gaithersburg, MD).

Buffers. The labeling buffer was 50 mmol/L $NaHCO_3$, pH 8.5, containing NaCl, 9 g/L. The elution buffer was 50 mmol/L Tris · HCl, pH 7.8, containing 9 g of NaCl and 0.5 g of NaN_3 per liter. The coating buffer contained phosphate-buffered saline, pH 7.0, and the blocking reagent was 30 g/L hemoglobin solution.

Polyclonal antibodies. Polyclonal antibodies were raised against two synthetic peptides that correspond to the N- and C-termini of guinea pig VPF (designated N-IgG, C-IgG, respectively). In the single letter code, the 25-amino acid sequence of the N-terminus is APMAEGEQKPREVVKFMDVYKRSYC (*15*), and the 20-amino acid sequence of the C-terminus is YKARQLELNERTCRCDKPRR (*4*). The C-terminal peptide was synthesized by Multiple Peptide Systems (San Diego, CA), and both peptides were used for generation of antibodies in rabbits as described (*15*), except that the C-terminal peptide was coupled to keyhole limpet hemocyanin with bis-diazo benzidine. The antibodies (N-IgG and C-IgG) were affinity-purified from rabbit antisera by using the respective peptides coupled to CNBr-Sepharose (Pharmacia LKB). Bound antibodies were eluted from Sepharose–peptide columns with 0.1 mol/L glycine, pH 2.5, and the activity against each peptide was determined by an ELISA (*16*). Briefly, we used a 1 g/L solution of peptide in 10 mmol/L NaCl and 10 mmol/L Tris, pH 8.5, to coat a 96-well microtiter plate. After blocking with normal human serum (100 mL/L) in phosphate-buffered saline, we added the respective anti-peptide IgG solution (200-, 2000-, or 10 000-fold dilution). Antibody binding was detected with a peroxidase-labeled goat anti-rabbit antibody (Kirkegaard and Perry Labs. Inc., Gaithersburg, MD) with 2,2′-azino-di-[3-ethylbenzthiazoline sulfonate] as the enzyme substrate. Color development was determined with a THERMOmax microplate reader at 405 nm (Molecular Devices, Menlo Park, CA). All affinity-purified IgG preparations retained strong anti-peptide activities, even at 10 000-fold dilution. Moreover, both N-IgG and C-IgG (when bound to Protein A–Sepharose) adsorbed VPF efficiently from solution, as determined with the Miles vessel permeability assay (T. Sioussat et al., manuscript in preparation).

Eu^{3+}-labeling of N-IgG. We performed Eu^{3+}-labeling of the affinity-purified N-IgG according to the DELFIA kit protocol with some modifications and pooled and concentrated the affinity-purified antisera to ~0.5 g/L, using an Amicon Macrosolute concentrator. The PD-10 column was pre-equilibrated with 40 mL of labeling buffer, and 2 mL of the antisera (0.5 g/L) was loaded on the column. We rinsed the column with labeling buffer, collected 1.0-mL fractions, and measured the absorbance at 280 nm with a Model U-2000 spectrophotometer (Hitachi Instruments Inc., Danbury, CT 06810). Fractions corresponding to peak absorbance were pooled, and concentrated to ~1 mL, which typically contained 1.5 g/L IgG concentration (we used an absorptivity value of 1.34 for 1 g/L of IgG solution to calculate IgG concentration). We added 1.0 mL of the IgG solution to 0.2 mg of labeling reagent (containing the Eu^{3+}-chelate) and mixed it gently on a rotator for 16 h at room temperature.

Purification of Eu^{3+}-labeled IgG. Sepharose CL-6B was poured into a 1.5 × 30 cm column to a height of 18 cm. Next, we added pre-swollen Sephadex G-50 to a height of 28 cm and equilibrated the column with 180 mL of elution buffer. The Eu^{3+}-labeled IgG reaction mixture was added and fractionated on this column. We rinsed the column with elution buffer, collected 60 1-mL fractions, and measured their absorbance at 280 nm. We diluted a small aliquot of each fraction 10 000-fold with enhancement solution and determined the fluorescence with a 1232 DELFIA time-resolved fluorometer (Pharmacia Diagnostics, Fairfield, NJ), in which a pulsed xenon flash at 340 nm and electronic gating were used to detect fluorescence at 613 nm between 400 and 800 μs after the excitation flash.

Characterization of Eu^{3+}-labeled N-IgG. Fractions corresponding to peak IgG absorbance (280 nm) and fluorescence were pooled (usually, fractions 25 to 33) and the resulting absorbance (280 nm) and fluorescence (10 000-fold dilution) were determined. The yield of Eu^{3+}/IgG was calculated as described in the DELFIA kit protocol (typically, 10 Eu^{3+}/IgG). To increase the stability of the Eu^{3+}-labeled N-IgG, purified BSA was added to a final concentration of 1.0 g/L.

Coating of microtiter strips. We added 50 μL of a 50-fold dilution of C-IgG (stock concentration of 0.64 g/L in phosphate-buffered saline) to each well of the microtiter strips, and incubated the plate overnight at 4 °C on a shaker. Thereafter, we washed the wells six times with DELFIA wash buffer, and blocked by incubation with 30 g/L hemoglobin solution at 20 °C for 2 h with gentle shaking. Plates were washed six times with DELFIA wash buffer before use.

Line 10 cell cultures. Line 10 tumor cells from guinea pig were grown as suspension cultures in serum-free defined medium HL-1 as described previously (*17*). Conditioned line 10 medium, which contains large amounts of VPF, was centrifuged and frozen at −70 °C to serve as calibrators.

Immunoassay procedure. We used freshly coated microtiter strips on the same day to assay VPF. We added 50 μL of various dilutions of line 10 conditioned media (using HL-1 medium as the diluent) to each well and incubated at 20 °C for 2 h with gentle shaking. After six washes with wash buffer, we added 50 μL of Eu^{3+}-labeled N-IgG (diluted appropriately in assay buffer), incubated for another 2 h at 20 °C, and again washed six times. Finally, we dispensed 200 μL of enhancement solution into each well, and after 5 min of gentle shaking, read the absorbance of the plate in the 1232 DELFIA fluorometer.

Miles vessel permeability assay. We assayed the bio-

activity of VPF in the line 10 culture medium preparations, using the Miles assay as described previously (*1*, *17*).

Results

Preparation and purification of Eu^{3+}-labeled N-IgG. Eu^{3+} labeling of affinity-purified antibodies directed against the N-terminal region of VPF was performed as described in *Materials and Methods*. The Sepharose 6B/Sephadex G-50 chromatographic profile in Figure 1 shows two distinct peaks. The first peak (I) corresponds to Eu^{3+}-labeled N-IgG, and the second peak (II) represents unreacted Eu^{3+}-chelate. For this reason, we showed in a separate experiment that >90% of the fluorescence associated with peak I could be removed by an IgG-removing device (Gammagone), indicating that peak I comprised mainly Eu^{3+}-labeled N-IgG. We pooled fractions 25–33, corresponding to Eu^{3+}-labeled N-IgG, and determined the corrected protein concentration to be 115 mg/L (using the absorptivity value of 1.34 mentioned above, with corrections for absorbance of the thiourea bonds of ~0.008 *A* per μmol/L). We calculated the specific activity of the Eu^{3+}-labeled N-IgG to be ~10 Eu^{3+}/IgG, using a 1 nmol/L Eu^{3+} standard as described in the DELFIA kit protocol.

Optimization of VPF immunoassay. To determine the optimal dilution of Eu^{3+}-N-IgG, we studied the effect of various amounts of N-IgG on the VPF binding curve. Microtiter plate wells were immobilized with a constant amount (225 ng/well) of C-IgG. Because pure VPF is not available, we used line 10 tumor cell conditioned medium, which is rich in VPF (*17*), to standardize the assay. We used the same lot of line 10 conditioned medium in all experiments. The concentration of VPF was expressed in arbitrary units, i.e., 100 units is defined as the amount of VPF in our batch of undiluted line 10 tumor cell conditioned medium. We arbitrarily defined "signal" as the fluorescence obtained with undiluted line 10 conditioned medium, and "noise" as the nonspecific fluorescence associated with HL-1 medium (0 unit). Thus, the signal-to-noise ratio is defined as $\text{fluorescence}_{100\ \text{units}}/\text{fluorescence}_{0\ \text{unit}}$. The effect of varying the N-IgG dilution (from five- to 50-fold) is shown in Figure 2*A*. We determined that 50-fold diluted N-IgG gave a maximal signal-to-noise ratio of 83 (Figure 2*B*).

In a separate experiment, we studied the effect of varying the C-IgG dilution, keeping Eu^{3+}-N-IgG constant at 115 ng/well. As shown in Figure 3, we obtained a maximal signal-to-noise ratio of 89 with 30-fold diluted C-IgG (1000 ng/well). However, because of our limited supply of C-IgG, we decided to use a 50-fold dilution of C-IgG (640 ng/well) to coat the microtiter wells; at this concentration, the signal-to-noise ratio was close to maximal at 80. For all subsequent experiments, we coated microtiter plate wells with 50-fold dilution of C-IgG, and bound VPF was detected with 50-fold dilution of Eu^{3+}-N-IgG.

Sensitivity and intra-assay CV of VPF immunoassay. To assess the analytical sensitivity of the VPF assay, we prepared line 10 conditioned medium corresponding to 0.25 unit, 0.50 unit, and 1.00 unit by diluting with HL-1 medium, then assayed these 10 times. HL-1 medium devoid of VPF served as the zero standard. The sensitivity or minimal detectable dose (defined as +2 SD above the zero standard), determined by extrapolation from the standard curve, was ~0.35 unit (Figure 4*A*). The intra-assay CV was <20% at 0.50 unit (Figure 4*B*).

Specificity of VPF immunoassay. Because the format of this assay depended on C-IgG as the capture antibody and Eu^{3+}-N-IgG as the detector antibody, we used peptides corresponding to the N- and C-termini of VPF to demonstrate the assay specificity. As shown in Figure 5, inclusion of C-VPF, N-VPF, or both peptides in the assay inhibited the binding of VPF in line 10 medium by ~80%. In addition, when VPF was selectively removed from line 10 conditioned medium (by unlabeled N-IgG followed by incubation with Protein A–Sepharose and

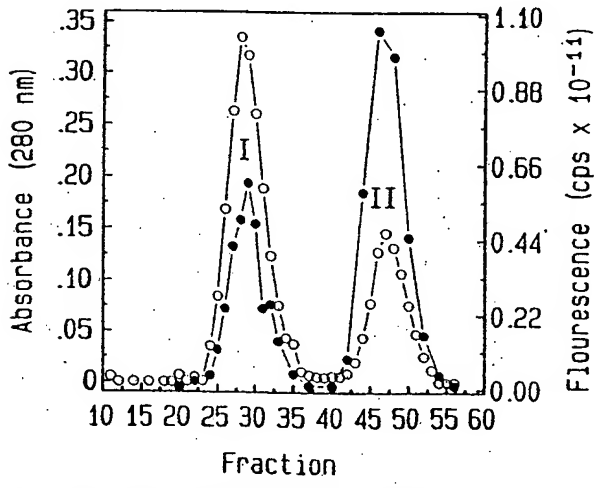

Fig. 1. Chromatographic profile of Eu^{3+}-labeled N-IgG

Absorbance at 280 nm (○) and fluorescence (●) were determined on fractions collected from a Sepharose 6B/Sephadex G-50 column. Each fraction was diluted 10 000-fold before fluorescence measurements, and results were expressed as total counts/s. Peak I denotes the Eu^{3+}-labeled N-IgG and peak II represents the free Eu^{3+}-chelate. Typical labeling yield is ~10 Eu^{3+} per IgG molecule

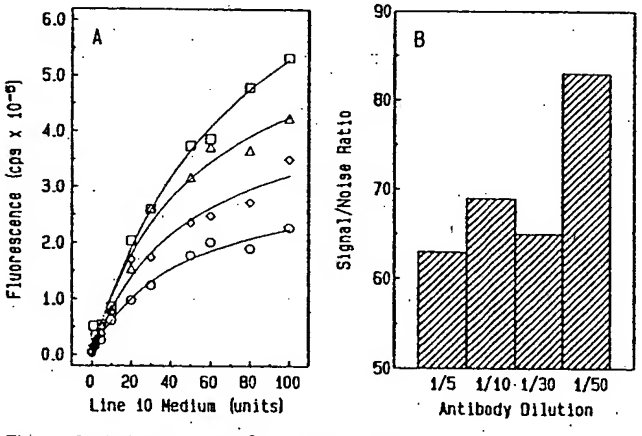

Fig. 2. Optimization of Eu^{3+}-labeled N-IgG

Eu^{3+}-labeled N-IgG was used at various titers (at constant C-IgG) to determine the optimal titer. Signal-to-noise ratio is arbitrarily defined as $\text{fluorescence}_{(100\ \text{units})}/\text{fluorescence}_{(0\ \text{unit})}$. *A:* calibration curves at 50-fold (○), 30-fold (◇), 10-fold (△), and fivefold (□) dilution of N-IgG. *B:* effect of antibody dilutions on the signal-to-noise ratio

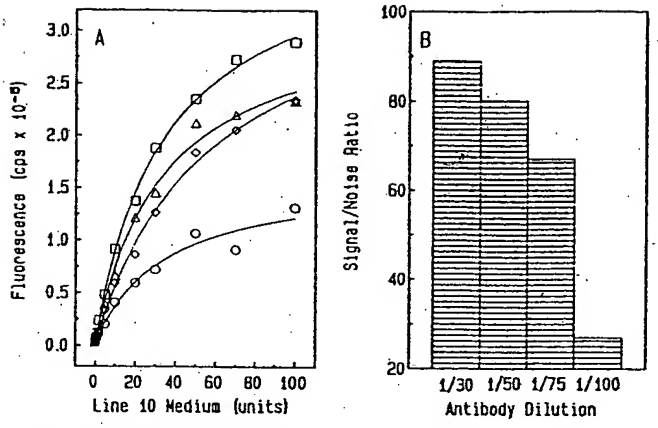

Fig. 3. Optimization of C-IgG

A: C-IgG was coated at 100-fold (○), 75-fold (◇), 50-fold (△), and 30-fold (□) dilution, at constant Eu^{3+}-labeled N-IgG concentration to determine the optimal concentration for the assay. *B*: effect of antibody dilutions on the signal-to-noise ratio

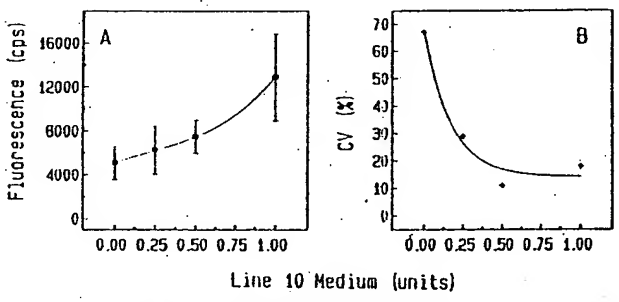

Fig. 4. Sensitivity and intra-assay CV of VPF immunofluorometric assay

Each point in *A* represents the mean of 10 determinations, and the *error bar* represents ±2 SD. *B*: intra-assay CV of VPF as a function of VPF dose

centrifugation), little fluorescent signal remained in the supernatant solution. In addition, when guinea pig serum containing platelet-derived growth factor and other growth factors was assayed, no VPF was detected (data not shown).

Correlation of VPF immunoassay with Miles permeability assay. We prepared and tested various concentrations of VPF from line 10 medium in both the Miles permeability assay and the VPF immunofluorometric assay. For the Miles assay, the amount of local dye development due to VPF permeability-enhancing activity was quantified by absorbance at 620 nm as described earlier (*17*). The VPF immunofluorometric assay was more sensitive than the Miles permeability assay; at a dose of 0.35 unit of VPF, the immunoassay gave values that were markedly different from zero (Figure 4*A*). In contrast, the sensitivity of the Miles permeability assay extended to only ~10 units (Figure 6). There was an excellent linear correlation (r^2 = 0.94) between the Miles permeability assay and the VPF immunoassay at VPF concentrations >10 units (Figure 6, inset).

Discussion

Immunofluorometric assays involving Eu^{3+}-chelate as the label are characterized by low-end sensitivity and

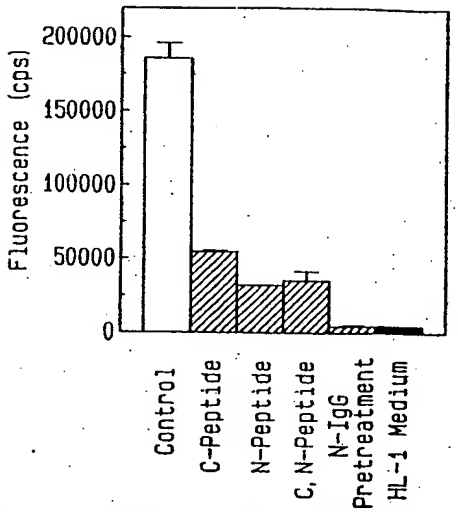

Fig. 5. Specificity of VPF immunofluorometric assay

Line 10 medium was used as the positive control and HL-1 medium was the negative control. C-peptide of VPF (final concentration 80 mg/L) was included during the first incubation with the sample. The N-peptide (final concentration 80 mg/L) was pre-incubated with the Eu^{3+}-labeled N-IgG and added during the second incubation. N-IgG pretreatment refers to line 10 medium that has been pre-extracted for VPF by using the N-IgG. *Error bars* denote ± SEM

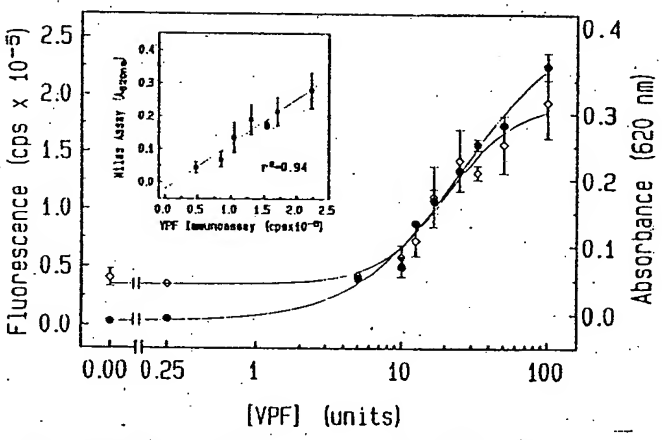

Fig. 6. Correlation of VPF immunoassay and Miles assay

Line 10 conditioned media at various concentrations were prepared for Miles assay (◇) and VPF fluoroimmunoassay (●) by diluting with HL-1 medium. Each point and its respective *error bar* represent the mean ± SEM of duplicate determinations. For the Miles assay, two animals were used to generate each point. *Inset*: correlation of the Miles and the VPF immunoassay at concentrations >10 units

wide dynamic range. The principles underlying these advantages have been reviewed recently (*18*). The large Stokes shift of Eu^{3+}-chelate and the time-resolved nature of the fluorometric measurements yield a high signal-to-noise ratio. Because of the longer decay time of the Eu^{3+}-chelate (>500 μs), readings can be determined between 400 and 800 μs to decrease nonspecific fluorescence, which typically has shorter decay times (~0.01 μs). This feature minimizes the endogenous nonspecific fluorescence of various biological specimens, making it especially attractive as a method to measure VPF in both tumor cell culture medium and in biological fluids.

We prepared affinity-purified N- and C-termini antibodies to guinea pig VPF and used the DELFIA approach

to develop a sensitive and specific immunofluorometric assay of VPF. We also demonstrated that our fluoroimmunoassay provides a quantitative measure of VPF in line 10 tumor cell culture medium. Although absolutely pure VPF is unavailable for standardization, we showed good correlation between the VPF immunoassay and the Miles bioassay with line 10 medium, thus confirming that the immunoassay is measuring bioactive VPF. We are confident that the immunoassay is measuring VPF in the physiologically relevant range because the dynamic range correlates well with the dynamic range of the Miles bioassay.

The VPF immunofluorometric assay has a minimal detection limit of 0.35 unit, and is ~30 times more sensitive than the Miles permeability assay. In addition, the immunoassay is much more precise and simpler to perform, is readily automatable, and can measure several specimens rapidly and inexpensively. In a separate study, we used the VPF immunoassay to measure VPF in ascites fluid, serum, and urine to study the potential role of VPF in tumor-elicited ascites fluid accumulation (*19*). We have also currently adapted the VPF immunofluorometric assay to measure VPF in human fluids to study its potential diagnostic utility in the pathogenesis of tumor metastases and the often accompanying fluid accumulation found in pleural and peritoneal cavities (*19*).

We thank Lisa Freter, Cheryl Hart, and the staff of the Clinical Chemistry Laboratory for their technical assistance. We also thank Dr. Harold F. Dvorak for his critical review of this work. This work was supported by USPHS NIH grant nos. CA-28471 and CA-50453 (to H.F.D.), and by grant no. CA-43967 (to D.R.S.) from the National Cancer Institute.

References

1. Senger DR, Galli SJ, Dvorak AM, Perruzzi CA, Harvey VS, Dvorak HF. Tumor cells secrete a vascular permeability factor that promotes accumulation of ascites fluid. Science 1983;219:983–5.
2. Senger DR, Perruzzi CA, Feder J, Dvorak HF. A highly conserved vascular permeability factor secreted by a variety of human and rodent tumor cell lines. Cancer Res 1986;46:5629–32.
3. Leung DW, Cachianes G, Kuang WJ, Goeddel DV, Ferrara N. Vascular endothelial growth factor is a secreted angiogenic mitogen. Science 1989;246:1306–9.
4. Keck PJ, Hauser SD, Krivi G, et al. Vascular permeability factor, an endothelial cell mitogen related to PDGF. Science 1989;246:1309–12.
5. Conn G, Bayne ML, Soderman DD, et al. Amino acid and cDNA sequences of a vascular endothelial cell mitogen that is homologous to platelet-derived growth factor. Proc Natl Acad Sci USA 1990;87:2628–32.
6. Connolly DT, Olander JV, Heuvelman D, et al. Human vascular permeability factor: isolation from U937 cell. J Biol Chem 1989;264:2017–24.
7. Connolly DT, Heuvelman DM, Nelson R, et al. Tumor vascular permeability factor stimulates endothelial growth and angiogenesis. J Clin Invest 1989;84:1470–8.
8. Dvorak HF, Harvey VS, Estrella P, et al. Fibrin containing gels induce angiogenesis. Implications for tumor stroma generation and wound healing. Lab Invest 1987;57:673–86.
9. Miles AA, Miles EM. Vascular reactions to histamine, histamine-liberator, and leukotaxine in the skin of guinea pigs. J Physiol (London) 1952;118:228–57.
10. Udaka K, Takeuchi Y, Movat HZ. Simple method for quantitation of enhanced vascular permeability. Proc Soc Exp Biol Med 1970;133:1384–7.
11. Soini E, Kojola H. Time-resolved fluorometer for lanthanide chelates—a new generation of nonisotopic immunoassays. Clin Chem 1983;29:65–8.
12. Hemmilä I, Dakubu S, Mukkala VM, Siitari H, Lövgren T. Europium as a label in time-resolved immunofluorometric assays. Anal Biochem 1984;137:335–43.
13. Hemmilä I. Fluoroimmunoassays and immunofluorometric assays [Review]. Clin Chem 1985;31:359–70.
14. Soini E, Lövgren T. Time-resolved fluorescence of lanthanide probes and applications in biotechnology. Crit Rev Anal Chem 1987;18:105–54.
15. Senger DR, Connolly DT, Van De Water L, Feder J, Dvorak HF. Purification and NH_2-terminal amino acid sequence of guinea pig tumor-secreted vascular permeability factor. Cancer Res 1990;50:1774–8.
16. Engvall E. Enzyme immunoassay ELISA and EMIT. Methods Enzymol 1980;70:419–39.
17. Yeo TK, Senger DR, Dvorak HF, Freter L, Yeo KT. Glycosylation is required for efficient transport but not for permeability-enhancing activity of vascular permeability factor (vascular endothelial growth factor). Biochem Biophys Res Commun 1991;179:1568–75.
18. Diamandis EP, Christopoulos TK. Europium chelate labels in time-resolved fluorescence immunoassays and DNA hybridization assays [Review]. Anal Chem 1990;62:1149A–57A.
19 Yeo KT, Wang H, Nagy JA, et al. Vascular permeability factor levels in line 1 and line 10 ascites tumors and human fluids [Abstract]. J Cell Biol 1991;115:421A.

EXHIBIT I

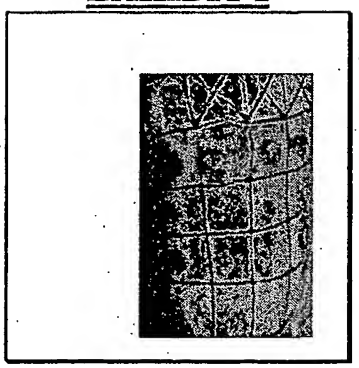

in vivo *3:* 279-284 (1989)

Immunocompetence Status as Related to Growth Progression of Mouse MOPC-315 Plasmacytoma

G. RASHID[1], R. OPHIR[1], M. PECHT[2] and S. BEN-EFRAIM[1]

[1]*Department of Human Microbiology, Sackler School of Medicine, Tel Aviv University, Tel-Aviv 69978:*
[2]*Department of Cell Biology, The Weizmann Institute of Science, Rehovot, Israel*

Abstract. *The immunocompetence status of mice bearing MOPC-315 plasmacytoma was determined at various days after tumor inoculation. Changes in T and B-cell functions appeared gradually. The allogeneic response of spleen cells from BALB/c tumor-bearing mice against C57BL spleen cells was impaired from the 4th day after the tumor inoculation (nonpalpable tumor stage). The primary antibody response in vitro against SRBC was depressed at 18 days, and the mitogenic response of splenic cells to PHA and to LPS was depressed at 25 days after the tumor inoculation. T cells taken from day 18 tumor-bearing mice partially suppressed the MLR response of normal splenocytes. Mice bearing large MOPC-315 tumors responded less to SRBC immunization than normal, noninoculated mice. The relative percentage of Lyt 1, Lyt 2 and L3T4 T-cell subsets decreased starting from the 11th day after tumor inoculation.*

Previous studies have established that murine plasmacytomas suppress B-cell responses such as decrease in antibody titers (1, 2, 3), decrease in response to B-cell mitogens (4), and impairment in generation of primary antibody response *in vivo* (2, 5, 6, 7, 8). In one report (6) it was claimed that secondary antibody response was not affected in mice bearing plasmacytomas, whereas in another work (9) suppression of secondary antibody response was also described. It has been suggested that plasmacytomas primarily affect B-cell responsiveness (8). However, in other works impairment of T-cell responses was also described such as low response to PHA stimulation (4, 10, 11) and induced decrease by tumor cells of specific antitumor cytotoxic response of T cells (12). The decrease in responsiveness to T and B-cell mitogens in plasmacytomas was attributed to the suppressive activity of macrophages in tumor-bearing animals (10). Differences were found among plasmacytomas in their ability to suppress antibody response. It is of interest in this respect that in two instances (3, 4) the primary antibody response to SRBC was found to be normal in mice bearing MOPC-315 plasmacytoma.

Most of the work reported previously was done in mice bearing large plasmacytoma tumors. In some instances in which the immunological responsiveness was examined at various stages of tumor growth, no full concomitant comparison was made between the effect of plasmacytoma presence on T and B-cell functions at various stages of tumor growth.

The aim of the present work was to determine concomitantly changes in various T and B-cell functions as related to progression of MOPC-315 tumor growth.

Correspondence to: Dr. Shlomo Ben-Efraim.

Key Words: Immunocompetence, MOPC-315 plasmacytoma, growth progression.

Materials and Methods

Mice. Male BALB/c mice, 8-12 weeks old, from the breeding colony of the Tel-Aviv University and male C57BL mice from the breeding colony of the Hebrew University, Jerusalem, Israel, were used.

Tumor. The MOPC-315 plasmacytoma was maintained by serial s.c. inoculation of 1×10^5 tumor cells or i.p. inoculation of 1×10^6 cells into syngeneic BALB/c mice. For experiments, the mice were inoculated s.c. with 1×10^5 tumor cells. This dose kills all the mice in 32 days. The tumor was excised, minced with scissors in RPMI medium (GIBCO, Grand Island, NY, USA) and single-cell suspensions were prepared by mechanical disruption of the tissue. (13). The viability, as determined by trypan blue dye (0.1%) exclusion, always exceeded 85%.

Spleen-cell preparations. Single spleen-cell suspensions were prepared by mechanical disruption and the viability as determined by trypan blue dye (0.1%) always exceeded 95%. The spleen cells were washed three times in plain RPMI medium (serum-free) before use. A splenic T-enriched fraction was obtained by passage through a nylonwool column (14). Depletion from most macrophages was achieved by passage through a glasswool column (15). The glasswool adherent fraction (mostly macrophages) was eluted from the column by washing with warm (37°C) EDTA-PBS (15). The T-cell population was removed from the intact spleen-cell population or from the T+B enriched fraction by treatment with monoclonal antiThy 1,2 antibody (F7D5, Booth, England) and fresh guinea pig serum complement (16).

Mitogenic stimulation. Assays of lymphocyte stimulation were performed

0258-851X/89 $2.00+.40

by a micromethod using an automatic harvester (17). Spleen cells were incubated for 3 days in RPMI complete medium in flat bottom Limbro plates at 37°C in a humidified atmosphere containing 5% CO_2. The complete medium consisted of plain RPMI medium supplemented with 10% fetal calf serum (FCS: Beit-Haemek, Israel), penicillin (100 u/ml) and streptomycin (100 µg/ml). Phytohemagglutinin (PHA, Wellcome, Beckenham, England, 0.1 µg/culture) or LPS (*E. coli* 0.55:B5, Difco, USA, 100 µg/culture) were added to spleen cell cultures containing 2×10^5 cells at the beginning of the incubation time. ^{3}H-thymidine (Nuclear Research Center, Negev, Israel, 1 µCi/culture) was added for the last 6 h of incubation. The quantities of mitogens used were found to be optimal in preliminary experiments. The cpm represent means ± SE of 12 parallel samples.

Mixed lymphocyte reaction (MLR). Allogeneic stimulation of BALB/c splenocytes by C57BL spleen cells was determined. C57BL spleen cells were treated with mitomycin C (MC, Sigma, St. Louis, MO, USA. 50 µg MC/1×10^7 cells) for 30 min at 37°C. Equal quantities of 4×10^5 BALB/c spleen cells and of MC-treated C57BL spleen cells were mixed and cultured in 200 ml of complete RPMI medium supplemented with 2-ME (Sigma, St. Louis, MO, USA) at a final concentration of 5×10^{-5} M. The cultures were incubated for 4 days in Falcon flat bottom plates at 37°C. ^{3}H-thymidine (1 µCi/culture) was added for the last 6 h of incubation. Each combination mixture was performed in 12 parallel samples and the results represent means of cpm+SE.

Primary antibody response in vitro. The generation of primary antibody response *in vitro* against Sheep Red Blood Cells (SRBC) antigen entity was determined by a MicroMarbrook method (18). The «in» phase contained 2×10^6 spleen cells and 2×10^6 SRBC in a total volume of 100 µl separated by a dialysis membrane from the «out» phase containing 2ml of RPMI complete medium supplemented with 2-ME. The cultures were incubated for 4 days at 37°C. The number of PFC was determined by a liquid hemolytic-plaque assay method (19). The antibody response was evaluated by counting the number of specific antibody forming cells: Plaque-forming cells (PFC) in cultures with SRBC minus No. of PFC in corresponding cultures without SRBC.

In vivo immunizations. The primary antibody response *in vivo* to SRBC was determined by enumerating specific splenic PFC at 4 days after i.p. injection of 5×10^8 SRBC in BALB/c mice. The Delayed Type Hypersensitivity (DTH) response was determined at 4 days after i.v. injection of 1×10^6 SRBC in BALB/c mice. The DTH determinations were based on evaluation of specific footpad swelling (f.p. thickness before or after injection) at 24 h after f.p. injection of 1×10^8 SRBC. The f.p. swelling in the footpad injected with SRBC was compared with that measured in the adjacent pad injected with PBS alone.

Immunofluorescence by flow cytometry. For indirect immunofluorescence, spleen cells (1×10^6 cells in 50 ml, in PBS containing 2% FCS and 0.1% sodium azide) were incubated with r at monoclonal antibodies anti Lyt 1, anti Lyt 2 and anti L3T4 (Becton-Dickinson, Mountain View, CA, USA), in a final volume of 100 µl for 30 min on ice. After three washings the cells were incubated with FITC labelled affinity purified rabbit anti-rat IgG (Bio-Makor, Israel). Controls received secondary antibody only. Stained cells were analyzed in a fluorescence activated cell sorter FACS-440 (Becton-Dickinson). Fluorescence signals were gated on the forward angle light scatter "live" cells peak. Ten thousand gated events were collected and positively stained cells calculated after subtraction of controls.

Statistical analysis. The significance of differences was determined by Student's t-test for ^{3}H-thymidine incorporation experiments and by the double-tailed Mann-Whitney *U* test for the other experiments. Differences were considered significant when $p<0.05$.

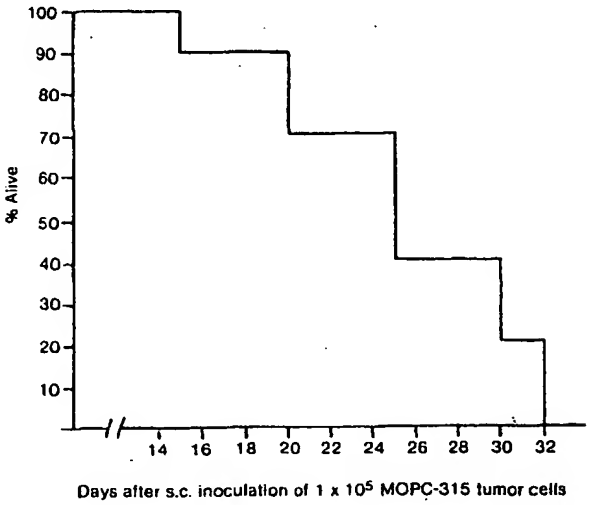

Figure 1. *Survival time of BALB/c mice following subcutaneous inoculation of 1×10^5 MOPC-315 tumor cells; 10 mice per group.*

Results

Kinetics of survival after tumor inoculation. BALB/c mice were inoculated s.c. with 1×10^5 MOPC-315 tumor cells (Figure 1). Approximately 50% of mice died within 25 days after inoculation and all mice died with tumors by the 32nd day after inoculation. Thus various tests for immunocompetence could be carried out at various times after inoculation for up to 25 days.

Immunological responsiveness in vitro

Mitogenic stimulation. The blastogenic response to PHA stimulation of T-enriched fraction of spleen cells from MOPC-315 tumor-bearing mice was determined on days 4, 11, 18 and 25 after inoculation (Table I). Significant decrease in the ability to respond to PHA stimulation was observed only at 25 days after inoculation. The response to stimulation by LPS of a T+B spleen-cell enriched fraction (glasswool nonadherent) was also depressed at 25 days after inoculation (Table I).

Antigenic stimulation. The allogeneic response of a T-enriched spleen-cell fraction from MOPC-315 tumor-bearing mice was already significantly depressed on the 4th day after inoculation, *i.e.* at a stage when palpable tumors are not yet detected. The allogeneic response remained low during all the observation period, up to 25 days after inoculation (Table II).

In another series of experiments, MC-treated splenic T cells that originate from tumor-bearing mice at different days after tumor inoculation, were added to an allogeneic mixture

Table I. *In vitro blastogenic response of spleen cells from MOPC-315 tumor-bearing mice.*

Exp. No.[a]	Spleen-cell origin[b]	Spleen-cell population[c]	Mitogen[d]	^{3}H-Thymidine incorporation[e] cpm ± SE without mitogen	with mitogen	% of control[f]	p[g]
I	N			1.822 ± 529	9.136 ± 1.546		
	TB-4	T	PHA	609 ± 70	9.023 ± 324	99	NS
II	N			1.066 ± 161	4.515 ± 811		
	TB-11	T	PHA	1.296 ± 214	4.059 ± 482	90	NS
III	N			1.302 ± 118	18.282 ± 2.074		
	TB-18	T	PHA	1.411 ± 156	16.672 ± 4.646	91	NS
IV	N			1.166 ± 140	19.351 ± 1.504		
	TB-25	T	PHA	1.461 ± 219	3.948 ± 457	20	<0.002
V	N			204 ± 30	24.240 ± 1.760		
	TB-25	T+B	LPS	309 ± 46	9.359 ± 922	39	=0.002

[a] Exps. III and V were repeated twice with similar results. Exp. IV was repeated 4 times with similar results.
[b] TB: tumor-bearing mice; spleen cells taken at various days after s.c. inoculation of 1×10^5 MOPC-315 tumor cells; N: noninoculated mice belonging to the same batch as corresponding TB mice.
[c] T: nylonwool nonadherent populations; T+B: glasswool nonadherent population.
[d] PHA: 0.1 μg/culture; LPS: 100 μg/culture.
[e] 2×10^5 cells/culture were incubated for 72 h in the absense or presence of mitogen; ^{3}H-thymidine (1 μCi/culture) was added for the last 6 h of incubation; mean cpm of 12 parallel samples.
[f] % calculated by reference to mean cpm in corresponding normal cultures incubated with the mitogen.
[g] Comparison between individual cpm in mitogen stimulated cultures from TB mice and corresponding cultures from N mice; NS: non singificant.

containing normal effector BALB/c spleen cells. As shown in Table III, T cells that originated from tumor-bearing mice partially suppressed the MLR response of a normal splenic population, at the 18th day after inoculation. A similar suppressive effect was observed when the added splenic cells were collected at days 17, 21 or 24 after tumor inoculation (results not shown).

The generation of primary antibody response to SRBC *in vitro* was significantly reduced in spleen-cell cultures taken at least 18 days after the tumor inoculation (Table IV). Experiments performed with spleen cells taken on the 25th day after inoculation showed that the deficiency in the antibody response potential resides in the T+B (glasswool nonadherent fraction) (Table V). Reconstitution experiments were carried out in order to find out whether the deficiency in antibody response potential is due to impairment of T-cell function and/or to impairment in the ability of B-cell population to generate antibodies. Table VI shows that the addition of T cells from tumor-bearing mice to a normal MΦ+B population resulted in a significant decrease in antibody response. B cells from tumor-bearing mice were also deficient in their ability to produce antibodies in cultures supplied with normal MΦ and T cells (Table VII).

Immune response in vivo *of tumor-bearing mice.* Tumor-bearing mice were immunized with SRBC on the day of tumor inoculation (day o) or on the 24th day after tumor inoculation and the number of antibody-forming cells in their spleens was determined on the 4th day after immunization. The antibody response was significantly lower in 24-Day tumor-bearing mice than in noninoculated mice or in mice immunized on the day of inoculation (Table VIII). In another series of experiments, day «o», 11-day or 24-day tumor-bearing mice were sensitized with SRBC i.v. and the delayed-type-hypersensitivity response was determined 4 days later by f.p. injection of the antigen. The DTH response was significantly lower in the groups of Day 11 and Day 24 tumor-bearing mice than in noninoculated mice or Day «0» mice (Table IX).

Table II. *Allogeneic response of splenic T cells from MOPC-315 tumor-bearing mice.*

Origin of T spleen population[a]	^{3}H-Thymidine incorporation[b] Δcpm ± SE	% of control[c]	p[d]
N	29,216 ± 2,208		
TB-2	25,357 ± 1,419	87	NS
TB-4	7,366 ± 2.015	25	<0.002
TB-11	13,532 ± 2,041	46	<0.002
TB-18	13,108 ± 1,733	45	<0.002

[a] See Table I for designations.
[b] ^{3}H-thymidine (1 μCi/culture) added for the last 6 h of incubation; mean cpm values of 12 parallel samples: mean cpm in allogeneic cultures minus mean cpm in corresponding syngeneic cultures; allogeneic mixture: BALB/c responder cells × C57BL stimulator cells; 4×10^5 responder cells × 4×10^5 mitomycin treated stimulator cells per culture; 96 h old cultures.
[c] % of Δcpm values from cultures with «N» responder cells.
[d] Comparison between individual cpm in allogeneic mixtures with responder cells from tumor-bearing mice and corresponding cultures from «N» mice; mean cpm from corresponding syngeneic mixtures was subtracted; NS: Not Significant.
The experiment was repeated 3 times with similr results.

Phenotype expression of splenic T cells of tumor-bearing mice.

Table III. *Effect of addition of splenic T cells from MOPC-315 tumor-bearing mice on allogeneic response (MLR)*[a]

Origin of added T cells[b]	^{3}H-thymidine incorporation in presence of various dilutions of added T cells[c]			
	1/2 % of control	1/4 % of control	1/8 % of control	1/16 % of control
N	–	–	–	–
TB-2	95	144	124	107
TB-4	126	142	132	118
TB-11	86	99	88	103
TB-18	39(<0.001)[d]	65(<0.01)	77(<0.02)	104

[a] 4×10^5 BALB/c spleen cells were cultured with 4×10^5 MC-treated C57BL spleen cells; cpm in allogeneic mixtures without addition of T cells was 27.677 ± 3.074 (8 parallel cultures).
[b] N: noninoculated mice; TB: tumor-bearing mice, spleen cells taken at various days (2, 4, 11, 18) after inoculation.
[c] T cells were inactivated by MC and than added to allogeneic mixtures in various dilutions: 1/2 represents 2×10^5 T cells/culture; ^{3}H-thymidine (1 μCi/culture) was added for the last 6 h of 72 h incubation period; cpm means were calculated from 8 parallel samples; % of control was calculated by reference to mean cpm in cultures supplemented with «N» T cells: 17.742 ± 1.523, 20.156 ± 731, 22.239 ± 1.587 and, 24.326 ± 1.901 in presence of 1/2, 1/4, 1/8, 1/16 «N» T cells respectively.
[d] Calculated by reference to corresponding cultures containing added «N» T cells; all the other differences were not significant.
The experiment was repeated twice with similar results.

Table IV. *Primary antibody, response in vitro to SRBC by spleen cells from MOPC-315 tumor-bearing mice.*

Origin of spleen cells[a]	Mean specific PFC/10^6 cells ± SE[b]	p[c]
N	813 ± 51	
TB-11	629 ± 96	NS
TB-18	6 ± 4	<0.001
TB-25	0	<0.001

[a] 2×10^6 cells/culture; N: normal, noninoculated mice; TB: spleen cells taken at various days (11, 18, 25) after tumor inuculation.
[b] Number of plague-forming cells in 4-day cultrues with SRBC minus the number of PFC in corresponding cultures without SRBC; means ± SE of 12 parallel samples.
[c] Comparison between individual specific PFC in cultures of «N» group and TB cultures; NS: Not Significant.
Te experiment was repeated once with TB-11 and TB-18 groups and 3 times with TB-25 group; similar results were obtained.

Table V. *Primary antibody response in vitro of splenic T+B enriched fraction from MOPC-315 tumor-bearing mice*[a].

Origin of spleen cells	Spleen-cell population[b]	Normal MØ added[c]	Specific PFC±SE 10^6/cells	p[d]
N	Intact	–	462 ± 153	
TB-25	Intact	–	7 ± 12	<0.001
N	GWNA	2×10^4	174 ± 50	
TB-25	GWNA	2×10^4	13 ± 14	<0.001
N	GWNA	4×10^4	305 ± 180	
TB-25	GWNA	4×10^4	4 ± 3	<0.001

[a] See Table IV for details.
[b] Intact: unfractionated spleen-cell population; GWNA: glasswool nonadherent (T+B enriched) fraction of spleen cells.
[c] Splenic MØ from normal, noninoculated mice added per 2×10^6 cultures.
[d] Calculated by comparison with No of specific PFC in cultures of «N» spleen cells. 12 Parallel samples for each type of culture.
Experiment repeated with similar results.

Table VI. *Effect of addition of splenic T cells from MOPC-315 tumor-bearing mice on the in vitro antibody response to SRBC in cultures of normal splenic MØ+B cells*[a].

Origin of spleen cells	Spleen-cell population[b]	T cells origin[c]	added %	Specific PFC±SE per 10^6 cells	p[d]
N	Intact	–		234 ± 28	
TB-25	Intact	–		0	=0.004
N	MØ+B	N	7.5	217 ± 55	
	MØ+B	TB-25	7.5	22 ± 8	=0.02
N	MØ+B	N	15.0	343 ± 69	
	MØ+B	TB-25	15.0	39 ± 15	=0.002
N	MØ+B	N	30.0	398 ± 62	
	MØ+B	TB-25	30.0	22 ± 9	=0.002

[a] See Table IV for details.
[b] Intact: unfractionated spleen-cell population; MØ+B: spleen-cell population depleted of T cells by treatment with anti Thy 1,2+c.
[c] Nylonwool nonadherent fraction; % added by rapport to 2×10^6 normal splenic cells/culture.
[d] Calculated by comparison with individual PFC readings in corresponding normal cultures (intact or supplied with «N» T cells): 12 parallel samples for each type of culture.
Experiment repeated with similar results.

As shown in Table X, no marked changes in Lyt 1, Lyt 2 and L3T4 subsets were observed on the 4th day after inoculation. Decreases in the relative percentage of Lyt 1, Lyt 2 and L3T4 subsets were observed in most of the experiments performed with spleen cells of Day-11 tumor-bearing mice and were especially marked on the 18th day after tumor inoculation.

Discussion

It has previously been demonstrated that plasmacytomas of various types may induce suppression of immune responses, especially as related to B-cell functions (2, 4, 5, 6, 7, 8, 10, 11). In this paper an effort was made to determine concomitantly changes in T and B-cell functions induced by MOPC-315 plasmacytoma at different times after tumor inoculation. The main finding emerging from the present work is that changes in T and B-cell functions do not all occur at the same stage of tumor growth but appear gradually during progression of the growth of the MOPC-315 tumor. Thus the allogeneic response potential is already decreased at a very early stage of tumor growth (at 4 days after tumor inoculation), *i.e.* at a stage when a palpable tumor is not yet detected. On the other hand, the ability of spleen cells from tumor-bearing mice to generate a primary antibody response

Table VII. *In vitro antibody response to SRBC of splenic B cells originated from BALB/c mice bearing large MOPC-315 tumors*[a].

Origin of spleen cells	Spleen-cell population[b]	B cells origin[c]	added %	Specific PFC±SE per 10^6 cells	p[d]
N	Intact	–		241 ± 64	
TB-25	Intact	–		0	<0.001
N	MØ+T	N	50	173 ± 50	
	MØ+T	TB-25	50	10 ± 7	=0.002
N	MØ+T	N	60	193 ± 61	
	MØ+T	TB-25	60	9 ± 3	=0.05
N	MØ+T	N	75	139 ± 83	
	MØ+T	TB-25	75	3 ± 0.3	=0.002

[a] See Table IV for details.
[b] Intact: unfractionated spleen-cell population; MØ+T: eluted glasswool adherent fraction+nylonwool nonadherent fraction.
[c] Glasswool nonadherent fraction depleted of T cells; % out of total number of 2×10^6 cells/culture.
[d] Calculated by comparison with individual PFC readings in corresponding normal cultures. 12 parallel samples for each type of culture. Experiment repeated with similar results.

Table VIII. *In vivo antibody response to SRBC of mice bearing MOPC-315 tumors*[a].

Group[b]	Specific PFC/10^6 spleen cells ± SE[c]	p[d]
N	7.992 ± 960	
TB-0	7.233 ± 1.743	NS
TB-24	1.353 ± 133	=0.002

[a] SRBC injected i.p. 5×10^8 cells/0.5 ml; spleen cells collected and pooled on the 4th day after immunization; 5 mice per group.
[b] N: Normal, noninoculated mice; TB: mice inoculated with 1×10^5 MOPC-315 tumor cells s.c.; SRBC injected either on the day of inoculation (TB-0) or 24 days after inoculation (TB-24).
[c] Means of 12 parallel samples.
[d] By comparison with individual specific PFC in «N» group. Experiment repeated with similar results.

Table IX. *Delayed Type Hypersensitivity (DTH) response of mice bearing MOPC-315 tumors*[a].

Group[b]	Footpad[c]	Footpad measurements (10^{-3}cm units±SE)[d] Before f.p. injection	24 h after f.p. injection	Specific swelling	p[e]
N	L	1.56 ± 0.01	1.68 ± 0.03		
	R	1.56 ± 0.01	2.00 ± 0.10	0.32	
TB-0	L	1.58 ± 0.01	1.63 ± 0.02		
	R	1.58 ± 0.01	2.00 ± 0.08	0.37	NS
TB-11	L	1.58 ± 0.01	1.60 ± 0.07		
	R	1.58 ± 0.01	1.75 ± 0.17	0.15	<0.05
TB-24	L	1.56 ± 0.01	1.60 ± 0.01		
	R	1.56 ± 0.01	1.55 ± 0.10	−0.015	<0.005

[a] SRBC injected i.v. 1×10^6 cells/0.2 ml; groups of 5 mice.
[b] N: normal, noninoculated mice; TB: mice inoculated with 1×10^5 MOPC-315 tumor cells i.p. and sensitized at various times after inoculation: 0, 11 or 24 days.
[c] L: Left footpad, R: right footpad.
[d] Mice injected on the 4th day after the SRBC injection with 0.05 ml control buffer (left pad) or 1×10^8 SRBC/0.05 ml (right pad); specific swelling (DTH response): difference between R f.p. thickness and L f.p. thickness at 24h after the f.p. injection. The experiment was repeated twice with similar results.
[e] By comparison with individual specific swellings in the N group.

Table X. *Phenotypic distribution of splenic T-cell population from MOPC-315 tumor-bearing mice.*

Origin of splenic T cells[a]	% positive with phenotype marker[b] Lyt-1	Lyt-2	L3T4
N	70	33	43
TB-4	62	35	40
TB-11	43	22	23
TB-18	38	20	21

[a] N: Normal, noninoculated mice; TB: tumor-bearing mice at various days after inoculation (4, 11 and 18); nylonwool nonadherent T-enriched fraction (app. 30% of the total splenic population).
[b] Pools of 6 spleen cells were used for fluorescence sorter determinations. Experiments with TB-4 and TB-11 cells were repeated 5 times and with N and TB-18 cells 8 times.

in vitro was significantly depressed only on the 25th day after inoculation and the response to LPS was found to be also depressed in Day 25 tumor-bearing mice. It seems that at least at a later stage of tumor development (Day 18 after tumor inoculation) increase in suppressor T-cell activity might be involved in the reduction of allogeneic response potential. The spleens of MOPC-315 tumor-bearing mice contain a high percentage of tumor cells at least from the 11th day after the tumor inoculation (20). These tumor cells are adherent to glasswool column (20) and to the nylonwool column (results not shown). Accordingly, the decrease in allogeneic response of a T-enriched (nylonswool nonadherent) population and of antibody response of a T+B enriched (glasswool nonadherent) population is due to an induced change in potential of spleen cells from tumor-bearing mice and not to the presence of viable tumor cells in the test cultures. The use of a microtechnique for generation of primary antibody response *in vitro* allowed us to determine whether the deficiency induced by the presence of the tumor is on the level of MΦ, T or B-cell functions. We showed that addition of splenic macrophages from noninoculated mice was not able to restore antibody response potential in a T+B enriched population of tumor-bearing mice. We also found that splenic T cells from tumor-bearing mice were deficient in their ability to promote generation of antibody response in cultures containing normal MΦ and normal B cells and that B cells from spleens of tumor-bearing mice were markedly impaired in their ability to produce antibodies in cultures reconstituted with normal MΦ and T cells. It seems, therefore, that both T and B-cell functions are impaired during progression of MOPC-315 tumor growth as expressed in antigenic stimulation and mitogenic stimulation assays. The

finding that cell-mediated antigenic stimulation (allogeneic response) is already decreased at a very early stage of tumor growth, whereas T-mitogenic stimulation is decreased only at a late stage, might be explained by the fact that antigenic stimulation involves a more restricted number of T cells than polyclonal mitogenic stimulation. The impairment in T-cell function was also expressed in the generation of antibody response *in vitro* in cultures containing T cells from tumor-bearing mice. The deficiency in T-cell function might be due to impairment of T-helper activity and/or emergence of suppressor T cells. In this respect our data indicate a decrease in the relative percentage of Lyt 1, Lyt 2 and L3T4 populations starting from day 11 after tumor inoculation.

Several assumptions have been made in order to explain the induced decrease in immunocompetence of tumor-bearing subjects including plasmacytomas. Thus it was claimed that P815 mastocytoma tumor cells secrete a factor which stimulate the appearance of suppressor T cells (21, 22). As regards MOPC-315, it was reported that tumor cells release a factor of high molecular weight which induces spleen cells to release an immunosuppressive factor (23). We also found (results not shown) that MOPC-315 tumor cells release factor(s) suppressing T and B-cell activities. Decrease in the immunocompetence of MOPC-315 tumor-bearing mice might also be due to the described shifts in the pattern of spleen-cell population caused by the tumor presence: occurrence of metastatic tumor cells (20) and increase in percentage of splenic macrophages (24, 25).

Although a complete kinetic study was not made on the immunological responsiveness *in vivo* of tumor-bearing mice, it might be of interest to mention that both antibody and DTH responses to SRBC were depressed in mice bearing large MOPC-315 tumors.

In conclusion: we showed here that mice bearing MOPC-315 tumors are immunodepressed in T and B-cell functions and that this impairment appears gradually during the progression of tumor growth.

Acknowledgements

The excellent technical assistance of Mrs. Anna Jackman is gratefully acknowledged. This work was supported by an endowment raised by Meir and Rebeca Heinik in memory of their late son Joseph Heinrichson. This paper was drafted during a sabbatical stay of one of us (S. B-E) in the Institute of Pharmacology, Faculty of Medicine, Erasmus University, Rotterdam, as a Fellow of the Integrated Cancer Center, Rotterdam.

References

1 Carlson PJ and Smith F: Effect of plasma cell tumor on antibody production by mouse spleen cells. Proc Soc Exp Biol Med *127:* 212-215, 1968.
2 Fahey JL and Humphrey JH: Effects of transplantable plasma cell tumors on antibody responses in mice. Immunology *5:* 110-115, 1962.
3 Fenton MR and Havas HF: The effects of plasmacytoma on serum immunoglobulin levels of BALB/c mice. J Immunol *114:* 793-801, 1975.
4 Brus I, Brent J and Hollander VP: Lymphocyte defect in plasmacytoma bearing mice. Br J Cancer *37:* 545-552, 1978.
5 Havas HF and Schiffman G (1978) The effect of an IgM plasmacytoma (TEPC-183) on the primary immune response of BALB/c mice. Immunology *34:* 1-8, 1978.
6 Zolla S: The effect of plasmacytoma on the immune response of mice. J Immunol *108:* 1039-1048, 1972.
7 Zolla S, Naor O and Tanapatchaiyopong P: Cellular basis of immunodepression in mice with plasmacytoma. J Immunol *112:* 2068-2076, 1978.
8 Zolla-Pazner S, Sullivan B and Richardson D: Cellular specificity of plasmacytoma-induced immunosuppression. J Immunol *117:* 563-568, 1976.
9 Havas JF, Schiffman G, Fenton MR, Goodis A and Braverman S: Immunosuppression of the primary and secondary immune response by an IgM plasmacytoma (TEPC-183). Immunology *36:* 191-197, 1979.
10 Padarathsingh ML, Dean JH, Jerrels TR, McCoy JL, Lewis DD and Northing JW: Evidence for and characterization of suppressor cells in BALB/c mice bearing ADJ-PC5 plasmacytomas. J Natl Cancer Inst *62:* 1235-1241, 1979.
11 Padarathsingh ML, McCoy JL, Dean JH, Lewis DD, Northing JW and Law LW: Examination of general and tumor-specific cell-mediated immune response in mice bearing progressively growing plasmacytoma. J Natl Cancer Inst *58:* 1701-1707, 1977.
12 Giorgi JV and Warner NL: Tumor immunity to murine plasma-cell tumors. VIII Immunosuppression of the generation of cytotoxic T cells by murine plasma tumor lines. Int J Cancer *32:* 629-635. 1983.
13 Mokyr MB, Braun DP, Usher F, Reiter H and Dray S: The development of *in vitro* and *in vivo* antitumor cytoxicity in noncytotoic MOPC-315 tumor-bearing spleen cells "educated" *in vitro* with MOPC-315 tumor cells. Cancer Immunol Immunother *4:* 143-150, 1978.
14 Julius MH, Simpson E and Herzenberg LA: A rapid method for the isolation of functional thymus derived murine lymphocytes. Eur J Immunol *3:* 645-649, 1973.
15 Lowy I and Bussard AE: A simple method for the removal of antibody forming cells from whole spleen cell population. J Immunol Methods *5:* 107-110, 1974.
16 Ben-Efraim S, Halperin D, Reuben C, Dar O and Weiss DW: Effect of methanol extraction residue (MER) tubercle bacillus fraction on the production of antibodies *in vitro*. II Effects on macrophage and lymphocyte populations. Cell Immunol *86:* 33-45, 1984.
17 Oppenheim JJ and Rosenstreich DL: Lymphocyte transformation: Utilization of automatic harvesters. *In:* Bloom BK, David JR (eds). *In: vitro* methods in cell-mediated and tumor immunity. Academic Press, New York, San Francisco, London, 1976, p. 593.
18 Eipert EF, Adorini L and Couderc J: A miniaturized *in vitro* diffusion culture system. J Immunol Methods *22:* 283-292, 1978.
19 Cunningham AJ and Szenberg A: Further improvements in the plaque technique for detecting single antibody forming cells. Immunology *14:* 599-600, 1968.
20 Mokyr MB, Hengst JCD, Przepiorka D and Dray S: Augmentation of antitumor cytotoxicity of MOPC-315 tumor bearer spleen cells by depletion of dinitrophenol adherent cells prior to *in vitro* immunization. Cancer Res *39:* 3928-3934, 1979.
21 Argyris BF: Activation of suppressor cells by syngeneic tumor transplantation in mice., Cancer Res *38:* 1269-1273, 1978.
22 Argyris BF and Delustro F: Immunologic unresponsiveness of mouse spleen sensitized to allogeneic tumors. Cell Immunol *28:* 390-403, 1977.
23 Katzman JA: Myeloma induced immunosuppression: A multistep mechanism. J Immunol *121:* 1405-1409, 1978.
24 Mokyr MB, Braun DP and Dray S: Augmentation of antitumor cytotoxicity in MOPC-315 tumor bearer spleen cells by depletion of glassadherent cells prior to *in vitro* activation. Cancer Res *39:* 785-792, 1979.
25 Ye QW, Mokyr MB, Pyle JM and Dray S: Suppression of antitumor immunity by macrophage in spleens of mice bearing a large MOPC-315 tumor. Cancer Immunol Immunother *16:* 162-169, 1984.

Received July 20, 1989
Accepted August 16, 1989

American Journal of Pathology, Vol. 156, No. 6, June 2000

In Vivo Expression of the Novel CXC Chemokine BRAK in Normal and Cancerous Human Tissue

Mitchell J. Frederick,* Ying Henderson,* Xiaochun Xu,† Michael T. Deavers,‡ Aysegul A. Sahin,‡ Hong Wu,† Dorothy E. Lewis,§ Adel K. El-Naggar,‡ and Gary L. Clayman*¶

From the Departments of Head and Neck Surgery, Clinical Cancer Prevention,† Pathology,‡ and Cancer Biology,¶ The University of Texas M. D. Anderson Cancer Center; and the Department of Immunology,§ Baylor College of Medicine, Houston, Texas*

Using differential display, we cloned a gene with reduced expression in short-term explants of head and neck squamous cell carcinoma (HNSCC) tumors compared to cultured normal oral epithelial cells. The differentially expressed gene was identical to the recently cloned CXC chemokine BRAK, which is ubiquitously expressed in normal tissue extracts but is absent from many tumor cell lines *in vitro*. To define the cell populations expressing BRAK *in vivo, in situ* mRNA hybridization was performed on normal and cancerous tissues from six different histological sites. The predominant normal cell type constitutively expressing BRAK *in vivo* was squamous epithelium. Expression in tumors was heterogeneous, with the majority of HNSCCs and some cervical squamous cell carcinomas (SCCs) showing loss of BRAK mRNA. Although absent in unstimulated peripheral blood mononuclear cells, high levels of BRAK were consistently found in infiltrating inflammatory cells (with lymphocyte morphology) in nearly all cancers examined. Furthermore, BRAK expression was demonstrated in B cells and monocytes, after stimulation of peripheral blood mononuclear cells with lipopolysaccharide. This study demonstrates for the first time up-regulation of BRAK mRNA by inflammatory cells in the tumor microenvironment and lost expression from certain cancers *in vivo*. The data suggest that BRAK may have a role in host-tumor interactions. *(Am J Pathol 2000, 156:1937–1950)*

Cancer is a multistep process involving perturbations of numerous genes. Using differential display reverse transcription-based polymerase chain reaction (DDRT-PCR) to identify differences in gene expression between short-term explants of human head and neck squamous cell carcinoma (HNSCC) cells and the normal oral epithelium from which they were derived, we isolated and sequenced a gene that was expressed at lower levels in HNSCC. Based on structural homology of the predicted protein, the gene was identified as a novel member of the human α (CXC) chemokine family. An independent group has simultaneously cloned the same gene and are calling it BRAK.[1] BRAK was identified by Hromas et al[1] by translating expressed sequence tags (ESTs) derived from breast and kidney carcinoma libraries and was found to be expressed ubiquitously in RNA from normal tissue extracts, but absent from a variety of *in vitro* established tumor cell lines. The origin of cells expressing BRAK in normal tissue has not been investigated, nor is the function of BRAK known.

Chemokines are a superfamily of small cytokines that selectively attract and activate leukocytes and a variety of other cell types.[2] Although their primary function appears to be directing leukocyte migration and endothelial transmigration, it is now clear that these small cytokines play a role in a variety of homeostatic and disease processes, including development, hematopoiesis, allergies, inflammatory syndromes, angiogenesis, and cancer.[2–5] The majority of chemokines are expressed in response to some stimuli, but several are constitutively produced.[2,4,5] In this study, we characterize the full-length cDNA encoding BRAK, examine by *in situ* hybridization the cell populations expressing this novel chemokine in normal and cancerous tissues from six different histological sites, and define populations of leukocytes capable of expressing BRAK.

Materials and Methods

Explants and Tumor Cell Lines

Explantation of human normal oral epithelial cells and HNSCC was performed using a protocol established by Dr. Peter Sacks (Memorial Sloan-Kettering Hospital, New York). Surgically removed specimens were histopatho-

Supported in part by grants from the National Institute of Dental Research 1-P50-DE11906 (93-9), a National Institute of Health First Investigator Award (R29 DE11689-01A1), a Training of the Academic Head and Neck Surgical Oncologist Core support grant (T32 CA60374-03 to G. L. C.), the Betty Berry Cancer Research Fund, the Michael A. O'Bannon Foundation Cancer Research Fund, a Cancer Center grant (NIH-NCI-CA16672), and a Physicians Referral Service grant from The University of Texas M. D. Anderson Cancer Center.

Accepted for publication February 16, 2000.

Address reprint requests to Dr. Gary L. Clayman, Department of Head and Neck Surgery, Box 69, University of Texas M.D. Anderson Cancer Center, 1515 Holcombe, Houston, TX 77030.

logically verified, minced, placed epithelial side up (for normal), and allowed to adhere and grow in AmnioMAX medium (Gibco BRL, Grand Island, NY). At first passage, contaminating fibroblasts were removed with cold trypsin, and remaining normal oral epithelial cells or HNSCC recovered by further trypsinization were seeded into 10-cm plates containing KGM growth medium (Clonetics, San Diego, CA). Tu-177, Tu-182, Tu-212, Tu-159, Tu-167, Tu-138, and MDA 1483 are established human HNSCC lines derived from larynx, tonsil, larynx, tongue, floor of the mouth, lip, and retromolar trigone, respectively, and have previously been characterized.[6;7] All tumor lines were passaged in Dulbecco's minimum essential medium containing 10% fetal bovine serum (FBS), glutamine, penicillin, and streptomycin.

DDRT-PCR

Total RNA was isolated from explants with the TRI reagent (Molecular Research, Cincinnati, OH), and contaminating DNA was removed by DNase I treatment. DDRT-PCR was performed using a kit (Display Systems, Los Angeles, CA) that employs 24 arbitrary upstream primers and nine downstream primers (dT11VN). PCR products labeled with [α-^{33}P]dATP were resolved by nondenaturing polyacrylamide gels and excised following autoradiography. Recovered fragments were reamplified, cloned into the pCR-TRAP plasmid (GeneHunter, Nashville, TN), and sequenced.

Nucleic Acid Searches and Sequence Alignments

The BLASTN and BLASTP searches were performed using the National Center for Biotechnology Information website (http://www.ncbi.nlm.nig.gov/), and open reading frames were identified using the ExPasy website translation tool software (http://expasy.hcuge.ch/www/dna.html). Multiple protein sequence alignments and subsequent phylogenetic analysis were performed using the ClustalW Multiple Sequence Alignment Program (at http://www2.ebi.ac.uk/clustalw/). Pairwise sequence alignment between BRAK cDNA and the BAC clone was accomplished with the LALIGN program at Genestream (http://vega.crbm.cnrs-mop.fr/bin/lalign-guess.cgi), and exon/intron boundaries were confirmed using the HSPL program available at the Baylor College of Medicine Search Launcher (http://kiwi.imgen.bcm.tmc.edu:8088/search-launcher/launcher.html).

Northern Blots

Total RNA (7.5 μg/sample) isolated from cell lines or biopsy specimens was fractionated by agarose-formaldehyde gel electrophoresis, transferred to a Hybond-N+ membrane (Amersham, Arlington Heights, IL), and hybridized with a α-^{32}P-labeled 213-bp probe complementary to the entire coding region of BRAK. The same BRAK probe was also hybridized to a multitissue poly A$^+$ RNA blot purchased from Clontech (Palo Alto, CA).

In Situ *mRNA Hybridization*

A total of 52 archival formalin-fixed paraffin-embedded specimens containing cancerous and/or adjacent normal tissue were obtained from 44 patients diagnosed with cancer of the head and neck, colon, kidney, cervix, breast, or ovary. In addition, one of the normal cervical samples was taken from a healthy volunteer who did not have cancer. *In situ* sense and antisense probe templates were prepared by amplifying a 367-bp fragment of BRAK cDNA (nucleotides 474–840), using sense and antisense primers modified with either T7 or SP6 sequences. The resulting templates were then transcribed with a digoxigenin RNA labeling kit (Boehringer Mannheim, Indianapolis, IN). After deparaffinization, proteinase K treatment, and hybridization, digoxigenin riboprobes were detected with the Genius 3 Nucleic acid kit (Boehringer Mannheim), which contains an anti-digoxigenin alkaline phosphatase-conjugated antibody and chromogenic substrate 5-bromo-4-chloro-3-indolyl phosphate/nitroblue tetrazolium (BCIP/NBT), which appears as a purplish-brown precipitate. All slides were evaluated by two investigators, including a clinical pathologist. Tumor or corresponding normal tissue was scored + when $\geq$10% total cells present showed staining, or cells from more than one microscopic field under a 10× objective lens contained areas with $\geq$10% cells staining positive. Tumor or normal tissue was scored $\pm$ when only a single microscopic field under a 10× objective contained $\geq$10% cells staining positive on an entire slide. Staining was qualified as weak when the intensity of positively staining cells was less than 50% of that observed with normal squamous epithelium of the tongue. Inflammatory and stromal cells were considered + when multiple fields under a 10× objective contained positively staining cells with a signal intensity similar to that of normal squamous epithelium of the tongue, and as "weak+" when multiple fields contained positively staining cells with an intensity less than 50% of that observed with normal squamous epithelium of the tongue. All tissues failing to meet at least one of the above criteria were considered negative (−).

Reverse Transcription-Based PCR

RNA was isolated from cells using TRI reagent according to suppliers' instructions, except that glycogen was added as a carrier molecule. Up to 2 μg total RNA was reverse-transcribed in a final reaction volume of 25 μl containing 200 ng random hexamers (PE Applied Biosystems, Foster City, CA), 1× first stand synthesis buffer (Gibco BRL), 0.4 mmol/L each of the deoxynucleoside triphosphates, 10 mmol/L dithiothreitol, 1 μl RNase inhibitor (Boehringer Mannheim), and 200 U SuperScript II reverse transcriptase (Gibco BRL). For sorted cells (ie, $<3 \times 10^6$ total), the entire RNA yield was reverse-transcribed in 25 μl. After cDNA synthesis, residual RNA was

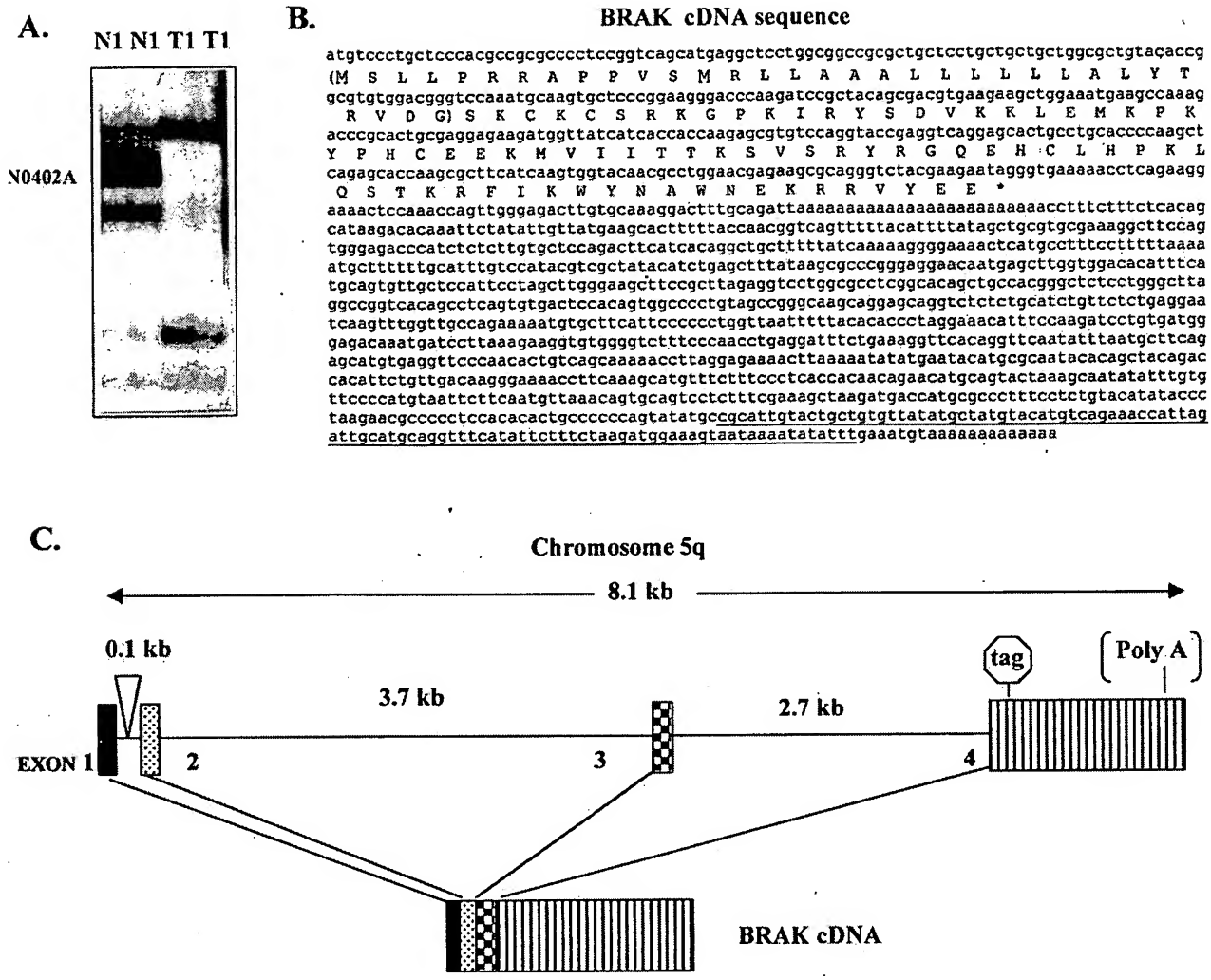

Figure 1. Molecular cloning of BRAK. **A:** Portion of a differential display gel comparing gene fragments from short-term explants of normal epithelial cells (N1) and squamous tumor cells (T1) derived from patient 1 with SCC of the tongue. **B:** Complete cDNA sequence of BRAK with predicted signal peptide (in parentheses) and amino acids of mature chain. The two potential methionine start sites appear in larger font. The asterisk indicates the stop codon, and the underlined sequence was derived from cloning and sequencing gene fragment N0402A. **C:** Schematic diagram of the genomic structure of the BRAK gene. The size interval between introns is indicated but is not to scale with the size of exons.

removed by digestion with 1 U RNase H (Boehringer Mannheim) at 37°C for 20 minutes. For PCR, 4 μl of cDNA reaction was amplified in a final volume of 30 μl containing 1× Mg^{2+}-free *Taq* buffer, 50 μmol/L each deoxynucleoside triphosphate, 1.5 mmol/L Mg^{2+}, 0.5 μmol/L gene-specific primers, and 1.5 U Promega *Taq* enzyme. PCR amplification was performed at 94°C for 30 seconds, followed by 35 cycles of 94°C for 30 seconds, 60°C for 20 seconds, 72°C for 50 seconds, and a final extension at 72°C for 7 minutes. PCR products were resolved by agarose electrophoresis and stained with ethidium bromide. BRAK-specific primers (derived from exons II and IV) amplifying a 233-bp amplicon were 5′-GTCCAAATGCAAGTGCTCCC-3′ (sense) and 5′-TTCTTCGTAGACCCTGCGCT-3′ (antisense). Primers (derived from sequences in exons II, III, and IV) specific for glyceraldehyde-3-phosphate dehydrogenase (GAPDH) amplifyinga 231-bp fragment were 5′-ACGGATTTGGTCG TATTG-3′ (sense) and 5′-TGATTTTGGAGGGATCTC-3′ (antisense).

Peripheral Blood Mononuclear Cells and Cell Sorting

Heparinized whole blood obtained from healthy volunteers by venipuncture was separated over Histopaque 1077 (Sigma, St. Louis, MO) to obtain peripheral blood mononuclear cells (PBMCs). PBMCs were cultured in RPMI containing 10% FBS, with glutamine, penicillin, and streptomycin additives before stimulations. Phorbol 12-myristate 13-acetate (PMA), calcium ionophore A23187, and lipopolysaccharide (LPS) were purchased from Sigma. Phytohemagglutinin (PHA) and pokeweed mitogen (PWM) were from GibcoBRL, and recombinant human interferon-γ (rhIFN-γ) was from R&D (Minneapolis, MN). Recombinant human tumor necrosis factor (TNF) and interleukin-2 (IL-2) were generous gifts from Dr. Elizabeth Grimm (University of Texas M. D. Anderson Cancer Center, Houston, TX). PBMCs were stimulated for 6–8 hours with PMA (10 ng/ml), calcium ionophore (0.5 μM), PHA (1.5% final concentration), PWM (1.5% final concen-

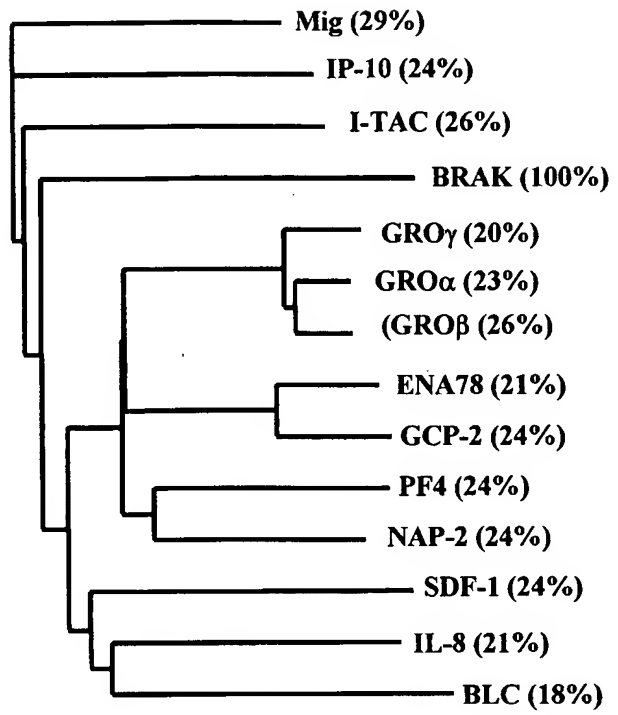

Figure 2. Phylogenetic relationship of all known human CXC chemokines. A ClustalW alignment of BRAK with known human CXC genes was used to generate the phylogenetic tree. The numbers in parentheses indicate the percentage amino acid identity with BRAK.

tration), LPS (0.5 μg/ml), TNF (500 U/ml), IFN-γ (200 U/ml), or IL-2 (500 U/ml). Subsequent to stimulation, nonadherent and adherent cells (harvested by EDTA treatment) were pooled and either used directly for RNA isolation or stained with antibodies for cell sorting. Phycoerythrin-cyanine 5-conjugated CD33, phycoerythrin-conjugated CD3, and fluorescein isothiocyanate-conjugated CD19 recognizing cell surface markers on monocytes, T cells, and B cells, respectively, were purchased from Beckman Coulter (Miami, FL). Cells were sorted, using a high-pressure Beckman Coulter ALTRA flow cytometer, into subpopulations that were >95% pure.

Results

Isolation of BRAK cDNA

Short-term primary explants were established using tumor and normal biopsies from a patient with invasive SCC of the tongue, and extracted mRNA was used for DDRT-PCR. One of the gene fragments identified, N0402A (Figure 1A), was expressed at much lower levels in the tumor explants (T1) compared to normal (noncancerous) oral epithelial explants (N1). After the 120-bp gene fragment N0402A was cloned and sequenced, a BLASTN search identified more than 95% homology with an EST (W73085), which was subsequently matched to the tentative human consensus (THC) sequence THC221548 in the TIGR Human Gene Index database. Although THC221548 contained 1105 bp of sequence, no long open reading frames (ORFs) were apparent. A series of successive BLASTN searches using end sequence information linked THC221548 to a set of homologous ESTs containing an ORF. Because the translation initiation start site was missing from the ESTs with the ORF, 5′ rapid amplification of cDNA ends (RACE) was used to define upstream nucleotides. The cDNA including the translation start site, remaining ORF, and 3′ untranslated sequence was determined to be at least 1533 bp long (Figure 1B) and was deposited in GenBank (accession number AF144103) formerly under the name NJAC. Continuity between ESTs with the ORF and the sequence of the differentially expressed gene fragment N0402A (shown as the underlined sequence in Figure 1B) was confirmed by PCR amplification and sequencing of the contiguous cDNA fragment. The ORF predicted a protein 111 amino acids long, with two potential methionine translation start sites separated from each other by just 11 amino acids. Starting from the second methionine start site, the protein is 100% identical to the recently cloned BRAK (GB AF073957) gene, which encodes a precursor protein of 99 amino acids.[1] BRAK belongs to the CXC subfamily, all members of which contain a total of four conserved cysteine resides, with the first two separated by a nonconserved amino acid. At the nucleic acid level, the differentially expressed gene and BRAK were also 100% identical over the region encoding the second methionine residue to a stretch of "A" residues following the TAG termination codon; however, our sequence contained an additional 1066 untranslated nucleotides that were not determined for BRAK. The theoretical cleavage site of the BRAK signal peptide was predicted to occur immediately before the sequence SKCK, using the SignalP V1.1 software available at http://www.cbs.dtu.dk/services/SignalP/ (regardless of which upstream methionine start site was chosen) and is thus identical to the cleavage site previously predicted.[1]

Chromosomal Localization of BRAK and Characterization of Genomic Sequence

A search of the STS database using the entire BRAK cDNA yielded a 99% match between the human STS marker TIGR-A002I14 (which maps to chromosome 5q23–5q31) and a 120-bp stretch of BRAK cDNA from bp 1255 to bp 1314, which was previously unpublished. This is the same chromosomal area that Hromas et al[1] mapped BRAK to, based on sequence homology between nucleotides in the open reading frame and a genomic BAC clone. The STS marker TIGR-A002I14 localizes to the BAC clone AC005738 that contains 134 kb of genomic sequence from human chromosome 5 and encodes the entire BRAK gene. Alignment between BRAK cDNA and the genomic sequences in the BAC clone identified four exons that span an 8.1-kb region of genomic DNA (Figure 1C). Exon and intron boundaries were confirmed using the HSPL program that predicts RNA splice sites (available on the web through the Baylor College of Medicine Search Launcher at http://kiwi.imgen.bcm.tmc.edu:8088/search-launcher/launcher.htm). Exon 1 is at least 100 bp, includes two potential "ATG" start sites,

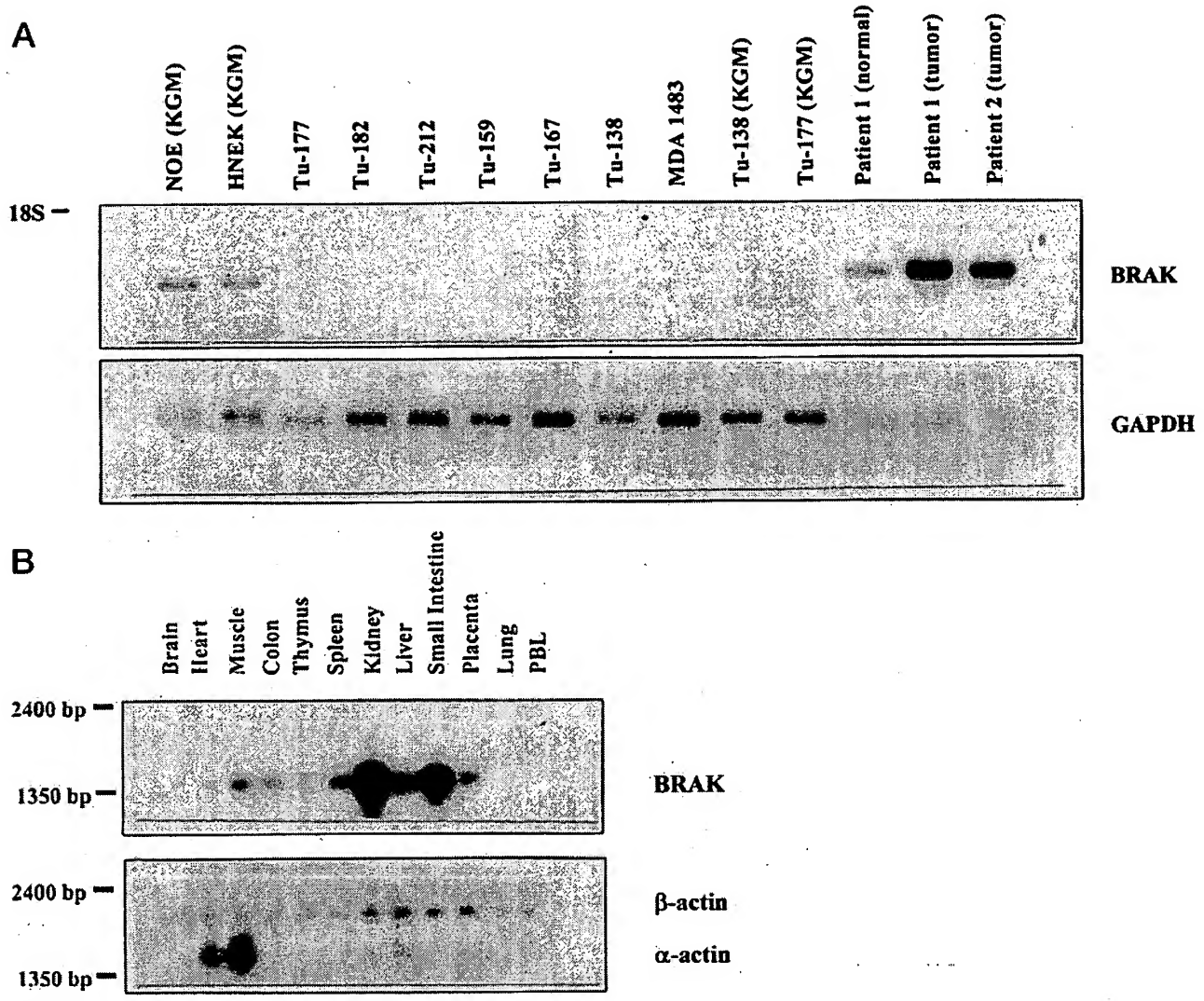

Figure 3. Detection of BRAK mRNA by Northern blotting. **A:** Northern analysis of BRAK expression in short-term explants of normal oral epithelial (NOE) cells, cultured normal epidermal keratinocytes (HNEKs), established HNSCC lines grown in regular or KGM growth medium, and biopsy specimens, including normal tongue epithelium (patient 1), invasive HNSCC of the tongue (patient 1), and invasive HNSCC of the buccal region (patient 2). **B:** Multiple tissue-Poly A mRNA Northern blot probed for BRAK (**top**) or stripped and reprobed with a sequence complementary to β-actin. In some tissues, the β-actin probe also cross-hybridizes to α-actin.

and encodes for all but one of the amino acids in the putative signal peptide. Exons 2 (106 bp) and 3 (115 bp) encode the majority of the remaining BRAK peptide, and exon 4, which is the largest (1182 bp), encodes the terminal four amino acids, stop codon, and potential polyadenylation site. A search of the genomic sequences 1650 bp upstream of the translational start site did not reveal any interferon response elements as are found in IP-10; however, several AP-2 and Sp1 binding sites were detected.

Phylogenetic Relationship of BRAK to Other CXC Chemokine Family Members

A multiple sequence alignment comparing the predicted mature BRAK peptide with the 13 other known human CXC chemokines was performed and used to generate the phylogenetic tree in Figure 2. BRAK has the greatest homology with Mig (29% amino acid identity) and appears to have diverged from most CXC chemokines very early in evolution.

Expression of BRAK mRNA by Northern Analysis

A fragment of BRAK cDNA corresponding to the entire coding region was used to probe a Northern blot containing total RNA extracted from cultured cells as well as flash-frozen biopsy specimens from HNSCC patients (Figure 3A). A single 1.5-kb band corresponding to BRAK mRNA was evident in RNA extracted from both cultured normal oral epithelial cells and cultured human normal epidermal keratinocytes (HNEKs). BRAK mRNA was completely absent from a panel of seven established

Table 1. Summary of BRAK Expression in Head and Neck Tissue*

Case	Specimen	Adjacent normal	Tumor	Inflammatory cells	Other stromal†
1	Normal tongue adjacent to buccal SCC	Squamous epithelium +	N.P.	–	–
2	Tongue SCC (moderately diff.)	Squamous epithelium + Dysplasia +.	–	Weak +	–
3	Tongue SCC (poorly diff.)	N.P.‡	–	Weak +	+
4	Metastatic tongue SCC	N.P.	–	–	–
5	Tongue SCC (moderately diff.) metastatic to lymph node	N.P.	Weak +/–	–	–
6	Tongue SCC metastatic to lymph node	N.P.	+	+	–
7	Laryngeal SCC (moderately diff.)	Squamous epithelium +	–	+	–
8	Laryngeal SCC (well diff.)	Squamous epithelial +	–	–	–
9	Laryngeal SCC	Basal layer weak +	N.P.	–	–
10	Laryngeal SCC (moderately diff.)	N.P.	–	–	–
11	Laryngeal SCC (poorly diff.) metastatic to lymph node	N.P.	–	+	–
12	Buccal SCC (moderately diff.)	Squamous epithelium + Dysplasia +	–	+	+
13	Buccal SCC	N.P.	+	–	–
14	Pharyngeal SCC (moderate to poorly diff.)	N.P.	–	–	–
15	Soft palate SCC (poorly diff.)	N.P.	+	+	–
Total		6/6 +	4/13 +	5/15 + 2/15 weak	2/15 +

*For definitions of +, +/–, weak, and –, see *Materials and Methods*.
†Predominantly fibroblasts.
‡N.P., not present in sample.

HNSCC tumor lines. To determine whether the differential expression might have been due to the different culture mediums used, two HNSCC lines (Tu-138 and Tu-177) were cultured for 30 hours with KGM medium (used for growing normal oral epithelial cells and keratinocytes). BRAK mRNA was undetectable from these tumor cell lines, regardless of their growth in KGM medium. As expected, BRAK mRNA was also detected in RNA extracted from a nonneoplastic normal tongue epithelial tissue biopsy. However, BRAK was found in specimens from two patients with SCC of the tongue (patient 1) and buccal region (patient 2). The results of the Northern blot in Figure 3A have been confirmed by relative RT-PCR in separate experiments (data not shown).

BRAK mRNA expression was also examined using a multitissue poly A^+ mRNA blot (Figure 3B). BRAK expression (after normalization to β-actin) was highest in kidney, followed by small intestine, spleen, colon, muscle, liver, brain, placenta, thymus, and heart. BRAK was not detected in lung or unstimulated peripheral blood lymphocytes. Absence of BRAK mRNA expression from fresh PBL (as well as monocytes) has also been confirmed by RT-PCR (data not shown).

Several CXC chemokine family members are up-regulated by IL-1β, TNF, or IFN-γ. Therefore, the ability of these cytokines to up-regulate BRAK expression in HNEKs was examined *in vitro*. No increased expression of BRAK mRNA was apparent after incubation with any of these cytokines, regardless of whether HNEKs were cultivated in complete KGM medium or basal medium lacking the usual growth factor additives (data not shown).

In Situ *Detection of BRAK mRNA in Head and Neck Tissue*

Because HNSCC lines were all negative for BRAK message, *in situ* mRNA hybridization studies were undertaken to identify which cell populations within tumors and adjacent nonneoplastic tissues were expressing this chemokine. A digoxigenin-labeled antisense RNA probe to BRAK was hybridized to paraffin sections containing tumor or adjacent nonneoplastic tissue from HNSCC patients; a summary of the results appears in Table 1. Strong expression of BRAK mRNA was detected in all layers of nonneoplastic squamous epithelium (basal to superficial) derived from the tongue and buccal mucosa and anatomically as far caudal as the true vocal cord of the larynx (Figure 4). Although most of the nonneoplastic tissues were adjacent to cancerous areas and theoretically could have been altered, in at least one case the normal tongue biopsy specimen expressing BRAK (Figure 4A) was derived from a patient with a contralateral buccal SCC. In addition, murine BRAK is 98% identical to the human gene at the amino acid level,[1] and we have also been able to detect its expression in normal mouse tongue from undiseased animals by Northern blotting (data not shown). BRAK mRNA was absent from nine of 13 HNSCCs (Table 1) derived from areas of the tongue (Figure 4C), buccal mucosa (Figure 4L), pharynx, and larynx (Figure 4J). Strong expression of BRAK mRNA in inflammatory cells (Figure 4D) adjacent to tumors was a

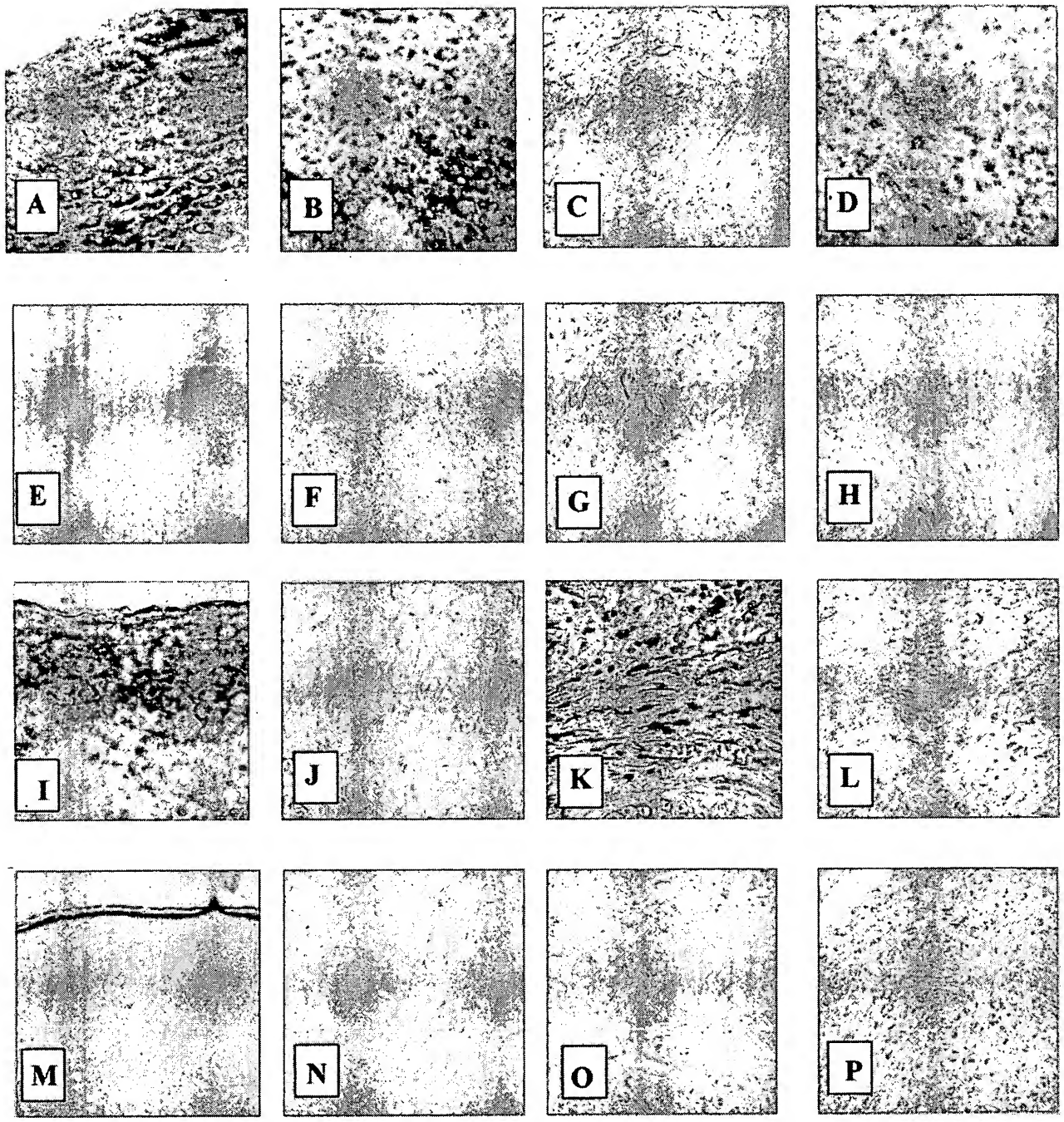

Figure 4. *In situ* hybridization analysis of BRAK mRNA expression in head and neck tissue. A digoxigenin-labeled antisense (**A–D** and **I–L**) or control sense (**E–H** and **M–P**) probe generated from the middle portion of BRAK cDNA was hybridized to paraffin sections. **A:** Detectable BRAK expression in normal tongue. **B:** BRAK expression in a dysplastic region of the tongue. **C:** Absence of BRAK from a metastatic SCC of the tongue. **D:** Numerous inflammatory cells expressing BRAK in the vicinity of a SCC of the tongue (tumor not visible). **E–H:** Sense controls of corresponding regions in consecutive sections. **I:** Detection of BRAK in normal squamous epithelium from the true vocal cord. **J:** Absence of BRAK from a laryngeal SCC. **K:** Numerous inflammatory and stromal cells, showing expression of BRAK adjacent to a buccal SCC (**bottom of picture**) that does not make the chemokine. **L:** Absence of BRAK from a buccal SCC. **M–P:** Sense controls of the corresponding regions stained on consecutive sections. Original magnifications, ×200.

frequent finding (ie, five of 15 cases) in HNSCC, and high levels of mRNA occasionally occurred in stromal fibroblasts (Figure 4K) adjacent to tumors as well. Expression was also observed in dysplastic epithelium from the tongue (Figure 4B) and occasionally in endothelial cells (data not shown). The *in situ* hybridization data were consistent with absence of expression in the panel of HNSCC cell lines and suggest that BRAK expression may be down-regulated or lost by tumor cells during development or progression of cancer *in vivo*.

Table 2. BRAK Expression in Gynecological Tissues*

Tissue	Specimen	Adjacent normal	Tumor	Inflammatory cells	Other stromal†
Breast					
1	Ductal carcinoma (high grade)	N.P.‡	–	+	+
2	Ductal carcinoma (high grade)	N.P.	–	–	–
3	Ductal carcinoma (high grade)	Lobular unit +/–	–	+	+
4	Ductal carcinoma (intermediate grade)	N.P.	–	–	–
5	Ductal carcinoma (intermediate grade)	Lobular unit –	–	–	–
Cervix					
1	Normal undiseased cervix	Squamous epithelium + Columnar epithelium –	N.P.	–	–
2	Normal cervix (adjacent to ovarian carcinoma)	Squamous epithelium + Columnar epithelium –	N.P.	Weak +	Weak +
3	Squamous carcinoma (moderately diff.)	Normal squamous epithelium +.	+	+	+
4	Squamous carcinoma (poorly diff.)	Hyperplastic epithelium +	–	–	–
5	Squamous carcinoma (poorly diff.)	N.P.	+	+	+
6	Squamous carcinoma (poorly diff.)	Squamous epithelium + Columnar epithelium –	–	Weak +	Weak +
7	Squamous carcinoma (moderately diff.)	N.P.	+	+	+
Ovarian					
1	Normal ovary	Columnar epithelium –	N.P.	N.P.	–
2	Serous carcinoma (high grade)	N.P.	–	N.P.	–
3	Serous carcinoma (high grade)	N.P.	–	–	–
4	Serous carcinoma (high grade)	N.P.	–	N.P.	–
5	Serous carcinoma (high grade)	N.P.	–	–	–

*For definitions of +, +/–, weak, and –, see *Materials and Methods*.
†Predominantly fibroblasts.
‡N.P., not present in sample.

In Situ *Detection of BRAK mRNA in Gynecological Tissues*

Although BRAK was originally identified from ESTs derived from breast and kidney cancer libraries, *in vitro* expression was absent from a panel of established breast cancer cell lines.[1] Therefore, the cell types expressing BRAK mRNA were examined in cancerous and nonneoplastic tissues derived from breast and other gynecological sites. Table 2 summarizes the results of *in situ* mRNA hybridization in these tissues. Although the vast majority of normal breast lobules were negative, weak expression of BRAK could be detected in an isolated area of normal breast lobules (Figure 5A). Within these lobules, expression was mostly confined to the inner luminal epithelium. No BRAK mRNA was detected in five of five invasive ductal carcinomas of the breast (eg, Figure 5B). However, strong expression of BRAK mRNA was detected in inflammatory and stromal cells immediately adjacent to some of the breast carcinomas (Table 2).

High levels of BRAK mRNA were detected in nonneoplastic squamous epithelium from the exocervix in four of four cases but was absent from the adjacent columnar epithelium that lined the endocervix. An example of expression in the exocervical squamous epithelium from a healthy volunteer is shown in Figure 5C. Similar to the head and neck mucosa, all layers of the exocervical squamous epithelium expressed BRAK. Expression in the cervical SCC was heterogeneous, with three of five tumors showing strong expression (eg, Figure 5D) and two of five tumors failing to express BRAK. There was also a strong propensity for expression of BRAK mRNA in inflammatory and stromal cells adjacent to the cervical SCCs (Table 2). In contrast, no BRAK mRNA was found in normal ovary tissue or in four ovarian carcinomas studied.

In Situ *Detection of BRAK mRNA in Kidney and Colorectal Tissues*

On the multitissue blot in Figure 3B, high levels of BRAK were found in the kidney and colon. It was therefore of interest to determine the cell types responsible for BRAK expression in these tissues. Although BRAK was also highly expressed in the small intestine, this region was excluded from our *in situ* analysis, as cancers from this site are uncommon. Table 3 summarizes the findings in kidney and colorectal tissue. Expression in normal proximal and distal tubules of the kidney was consistently detected but was sometimes weak. BRAK mRNA was strongly detected in nonneoplastic transitional epithelium of the renal calyx (Figure 5I) that was adjacent to a transitional cell carcinoma of the renal pelvis, which also expressed high levels of BRAK (Figure 5J). Renal cell carcinoma of the clear type is by far the most frequent kidney tumor that occurs; however, these tumors were all negative for BRAK mRNA by *in situ* hybridization (Table 3). As with the other cancers, BRAK mRNA was found in inflammatory and stromal cells adjacent to the renal carcinomas.

Normal columnar epithelium found in the colorectal region was negative for BRAK in four of four cases (eg, Figure 5K). Normal goblet cells were also negative, except for weak staining in one specimen that contained many adjacent positively staining inflammatory cells. Expression in the colon cancers was heterogeneous. Two

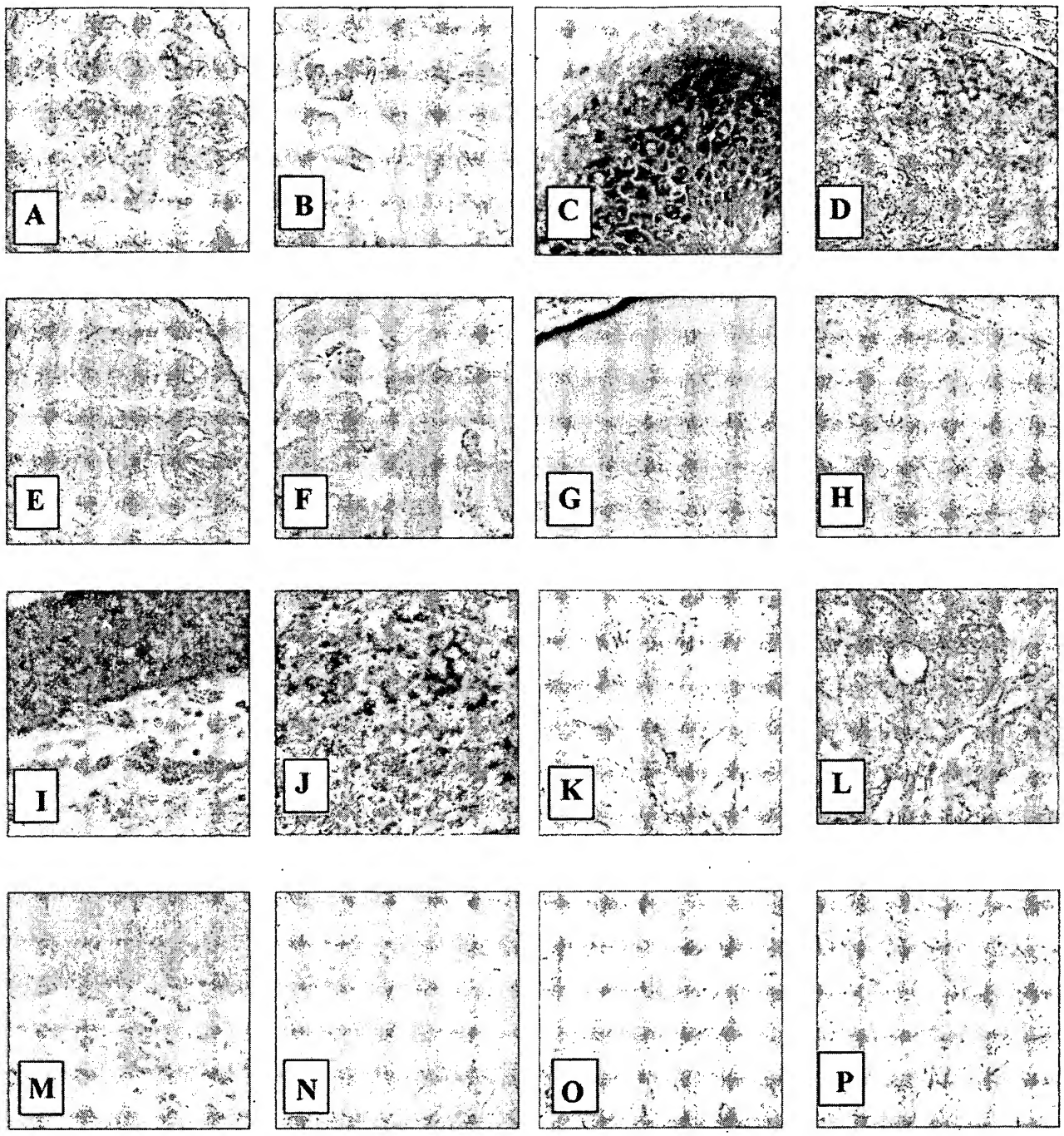

Figure 5. *In situ* hybridization analysis of BRAK mRNA expression in other tissues. A digoxigenin-labeled antisense (**A–D** and **I–L**) or control sense probe (**E–H** and **M–P**) generated from the middle portion of BRAK cDNA was hybridized to paraffin sections. **A:** Weak expression of BRAK in a cluster of normal breast lobules. **B:** Absence of BRAK in an invasive breast ductal carcinoma. **C:** Detection of BRAK in normal squamous epithelium from the exocervix of a healthy volunteer. **D:** Heterogeneous expression of BRAK in a cervical SCC. **E–H:** Sense controls of corresponding regions in consecutive sections. **I:** Detection of BRAK in normal transitional epithelium from the renal calyx. **J:** A transitional squamous carcinoma from the renal pelvis expressing BRAK. **K:** Absence of BRAK from normal columnar epithelium of the colon. **L:** Weak BRAK expression in a colon adenocarcinoma. **M–P:** Sense controls of the corresponding regions stained on consecutive sections. Original magnifications, ×200.

colorectal adenocarcinomas were completely negative, whereas one colon adenocarcinoma was strongly positive. Weak expression of BRAK was found in one colon adenocarcinoma (Figure 5L) and in a squamous carcinoma of the anorectal region. High levels of BRAK mRNA were observed in inflammatory cells in 100% of colorectal cancers (Table 3) and in one benign adenoma, which was itself negative for BRAK. Stromal fibroblasts also expressed BRAK in the majority of colorectal cancers studied.

Table 3. BRAK Expression in Colorectal and Renal Tissue*

Tissue	Specimen	Adjacent normal	Tumor	Inflammatory cells	Other stromal†
Colorectal					
1	Rectal adenocarcinoma (moderately diff.)	Columnar epithelium − Goblet cells −	−	+	+
2	Colon adenocarcinoma (moderately diff.)	N.P.‡	Weak +	+	Weak +
3	Dysplastic adenoma of colon	Columnar epithelium N.P. Goblet cells − Dysplasia −	N.P.	+	−
4	Colon adenocarcinoma (poorly diff.)	Columnar epithelium − Goblet cells −/+	+	+	+
5	Colon adenocarcinoma (moderately diff.)	Columnar epithelium − Goblet cells −	−	+	−
6	Anorectal squamous carcinoma (moderate to well diff.)	Columnar epithelium − Goblet cells −	Weak +	+	+
Renal					
1	Clear cell carcinoma	Distal tubules weak + Proximal tubules weak + Glomeruli −	−	−	+
2	Clear cell carcinoma	Distal tubules weak + Proximal tubules weak + Glomeruli −	−	−	−
3	Leiomyosarcoma of kidney	Distal tubules + Proximal tubules + Glomeruli weak +	−	Weak +	−
4	Clear cell carcinoma	Distal tubules weak + Proximal tubules weak + Glomeruli −	−	+	+
5	Transitional carcinoma of renal pelvis	Distal tubules + Proximal tubules + Glomeruli − Transitional epithelium +	+	+	−

*For definitions of +, +/−, weak, and −, see *Materials and Methods*.
†Predominantly fibroblasts.
‡N.P., not present in sample.

Morphology of Inflammatory Cell Populations Expressing BRAK

Expression of BRAK in inflammatory cells adjacent to tumors was a frequent finding. Examples of inflammatory cells expressing BRAK from cancer of the soft palate, colon, and breast are shown in Figure 6. Hematoxylin and eosin (H&E) staining of consecutive sections from these regions revealed numerous inflammatory cells with lymphoid morphology. In the soft palate specimen there were numerous plasma cells and small lymphocytes (Figure 6J). However, the majority of inflammatory cells present in the colon adenocarcinomas had a morphology consistent with small lymphocytes (eg, Figure 6K). In the breast cancers as well, there were predominantly small lymphocytes in the inflammatory areas expressing BRAK (eg, Figure 6L).

BRAK Expression in PBMC

Because *in situ* mRNA hybridization consistently demonstrated expression of BRAK in inflammatory cells with the morphology of lymphocytes, we sought further proof that this subpopulation of cells was capable of making BRAK mRNA. The riboprobe used to detect BRAK could not be used successfully in combination with immunohistochemistry techniques. Therefore, the question was addressed *in vitro*. Freshly isolated PBMCs from healthy volunteers were cultured with various stimuli, and extracted RNA was examined for the presence of BRAK mRNA by RT-PCR, using BRAK-specific primers from exons II and IV. A 236-bp BRAK-specific fragment was amplified by RT-PCR from PBMCs cultured in the presence of either PMA/calcium-ionophore or LPS, but not other stimuli (Figure 7A). No BRAK expression was detected in RNA extracted from freshly isolated PBMCs or after overnight culture in medium containing 10% FBS. The plasmid pCMV-BRAKfg, which contains the entire coding portion of cDNA from the BRAK gene, served as a gene-specific positive control. The integrity of the cDNA used in PCR reactions was confirmed by amplifying a portion of the housekeeping gene glyceraldehyde-3-phosphate dehydrogenase (GAPDH) (Figure 7A, bottom gel). As there were a number of biopsy specimens in which plasma cells (B cells) were detected by H&E staining in the vicinity of BRAK-positive inflammatory cells (eg, Figure 6J), it was possible that B cells were making BRAK mRNA after *in vitro* stimulation of PBMC with LPS. Con-

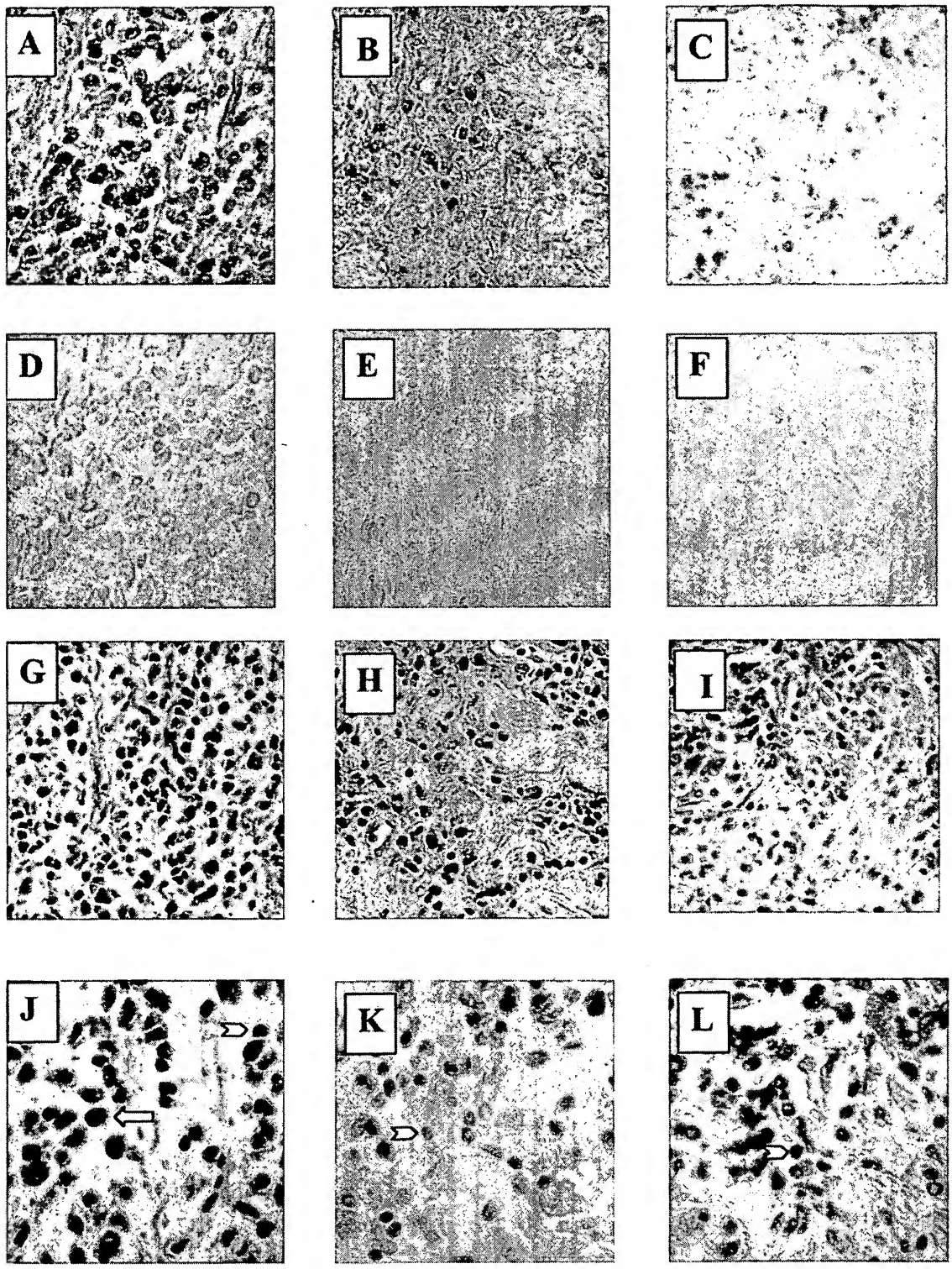

Figure 6. BRAK expression by infiltrating inflammatory cells in various tissues. A digoxigenin-labeled antisense (**A–C**) or control sense (**D–F**) probe generated from the middle portion of BRAK cDNA was hybridized to paraffin sections. The same regions were stained with hematoxylin and eosin (H&E) on consecutive sections. Original magnifications: **G–I**, ×200; **J–L**, ×400. **A:** Numerous inflammatory cells expressing BRAK adjacent to a soft palate SCC (tumor not visible). **B:** Detection of BRAK in scattered inflammatory cells adjacent to a colon adenocarcinoma (tumor not visible). **C:** Expression of BRAK by inflammatory cells that have infiltrated a breast ductal carcinoma that is itself negative for BRAK. **G–I:** H&E stains of corresponding regions. **J:** At higher magnification, many small and larger lymphocytes can be seen to be localizing to the same area where inflammatory cells positive for BRAK were evident adjacent to the soft palate SCC. An **arrowhead** indicates a small lymphocyte, and the full **arrow** points to an example of a plasma cell. **K:** Higher magnification of inflammatory cells adjacent to the colon adenocarcinoma. An example of a cell with morphology indicative of a small lymphocyte is shown by the **arrowhead**. **L:** Higher magnification of inflammatory cells infiltrating the breast ductal carcinoma. An example of a cell with morphology indicative of a small lymphocyte is shown by the **arrowhead**.

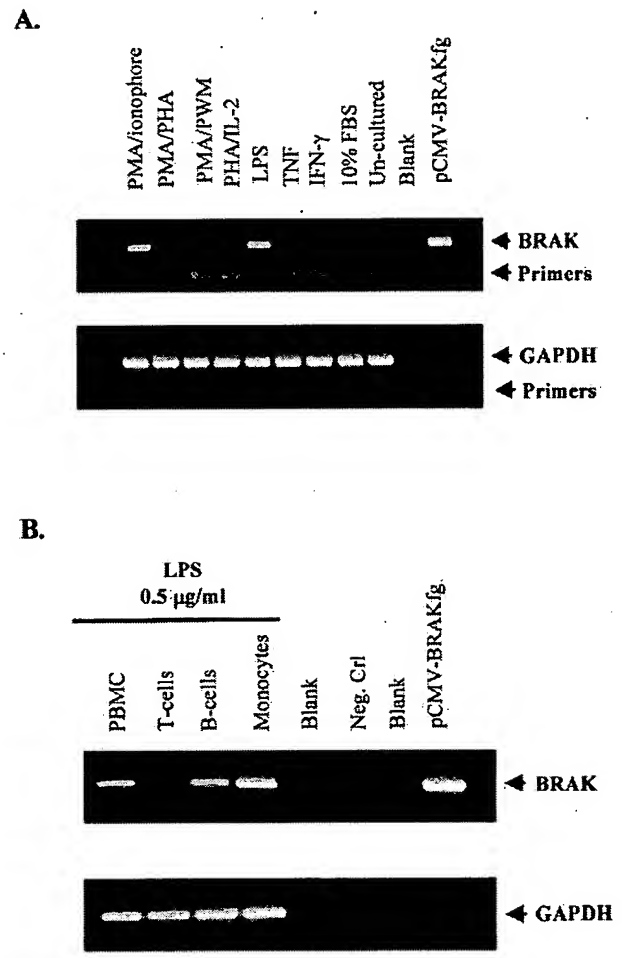

Figure 7. RT-PCR detection of BRAK in stimulated PBMCs. **A:** PBMCs (2×10^6/ml) were stimulated for 8 hours with various agents as described in Materials and Methods, and extracted RNA was analyzed by RT-PCR for the presence of a BRAK message, using gene specific primers (**top gel**). Plasmid pCMV-BRAKfg contains the entire coding region of BRAK cDNA and was used as a positive control. To control for the integrity of cDNA synthesis and PCR amplification, the same RT reaction was also subjected to PCR to amplify GAPDH (**bottom gel**). **B:** PBMCs (2×10^6/ml) were stimulated for 6 hours with 0.5 μg/ml LPS and then sorted into populations of T cells, B cells, or monocytes, based on the expression of cell surface markers. RNA was extracted from unsorted or purified populations and subjected to RT-PCR analysis as in **A**. The negative control (Neg. Crl) reaction was amplified without cDNA to rule out cross-contamination.

sequently, PBMCs were stimulated with LPS for 6 hours and then separated into T-cell, monocyte, and B-cell subpopulations, using a flow cytometer based on expression of the cell surface markers CD3 (T cells), CD33 (monocytes), and CD19 (B cells). The monocyte marker CD33 was chosen in lieu of CD14 to sort monocytes, because the latter recognizes the LPS receptor and could have confounded interpretation of the results. Preliminary analysis indicated that the CD33 marker was present on 85% of CD14+ monocytes before and after stimulation with LPS and was not expressed by T cells or B cells (data not shown). Granulocytes that can also express CD33 were removed from the starting population during purification of PBMC on Histopaque gradients, and any residual granulocytes were gated out during sorting. Because of limiting amounts of RNA, RT-PCR with BRAK-specific primers was again used to detect BRAK expression. After stimulation with LPS, BRAK RNA was detected in unsorted PBMC, B cells, and monocytes, but not in the T-cell population (Figure 7B, top gel). GAPDH, however, was detected in all populations examined (Figure 7B, bottom gel).

Discussion

BRAK is a novel member of the CXC chemokine family that was identified in our laboratory because of reduced expression in short-term primary tumor explants derived from a patient with invasive SCC of the tongue. Previously it was reported that BRAK is ubiquitously expressed in normal tissues and conspicuously absent from a variety of established *in vitro* tumor cell lines.[1] Because no information was available with regard to the actual cell populations that express BRAK *in vivo*, the primary focus of this study was to address this question by using *in situ* mRNA hybridization.

In the normal tissues examined, the predominant cell type constitutively expressing the highest levels of BRAK mRNA was squamous cell epithelium from the upper aerodigestive tract and exocervix. We have also detected high levels of BRAK mRNA in normal squamous epithelium from the skin (data not shown). Expression was found to extend from the basal to the superficial layers of squamous epithelium in both mucosal and skin tissues. In contrast, columnar epithelium from the endocervix and colon failed to express BRAK. There was weak and focal expression in normal epithelium that lines breast lobules. Distal and proximal tubules of the kidney consistently expressed BRAK, but the levels were sometimes weak. The latter results may explain the relatively strong signal for BRAK mRNA that we and Hromas et al[1] detected in kidney tissue on poly A^+ mRNA Northern blots. As tubules are a main component of the kidney, even modest amounts of BRAK mRNA at the cellular level could produce a strong signal in whole tissue homogenates. However, the ubiquitous expression of BRAK mRNA in other tissues on poly A^+ blots could be due to contaminating cell populations present in whole tissue extracts. It is clear that BRAK mRNA can be made at high levels by inflammatory and stromal cells.

Normal human lymphocytes from blood do not express BRAK mRNA by Northern analysis or even by the more sensitive technique of RT-PCR. Yet high levels of BRAK were consistently detected in infiltrating inflammatory cells with lymphocyte morphology in the vast majority of cancers we studied. This would suggest that factors in the environment of the tumor could be up-regulating BRAK expression. In freshly isolated PBMCs from healthy volunteers, BRAK expression was detectable by RT-PCR after stimulation with either LPS or PMA/calcium ionophore. When LPS-stimulated PBMCs were separated by flow cytometry, BRAK expression was found in both B-cell and monocyte populations, but not in CD3+ T cells. These *in vitro* experiments provide independent corroborative evidence that inflammatory cells are capable of BRAK expression. Furthermore, plasma cells (B cells)

were frequently found in consecutive sections in the immediate vicinity of inflammatory cells positive for BRAK by *in situ* mRNA hybridization and therefore could be one of the leukocyte subtypes expressing BRAK mRNA in cancerous tissues. Final confirmation of the inflammatory cell phenotype expressing BRAK will have to await the production of a BRAK-specific antiserum that can be used in immunohistochemistry. It is currently unknown which population of cells expresses BRAK after stimulation of PBMCs with PMA/calcium ionophore, and it cannot be ruled out that T cells or natural killer cells could express BRAK given the appropriate stimulus. The ability of local factors to up-regulate BRAK may also explain why certain colon adenocarcinomas were capable of expressing the chemokine, despite the fact that adjacent normal columnar epithelium (which presumably gives rise to these cancers) did not express BRAK.

In vivo expression of BRAK mRNA in tumors was more heterogeneous than would be predicted from our own data with established tumor cell lines and the study from Hromas et al.[1] Because squamous epithelium appears to be a predominant cell type constitutively expressing BRAK mRNA, issues regarding whether down-regulation occurs in cancer are best studied in tumors derived from these cells. Most head and neck cancers originate from squamous epithelium, and the majority of cervical cancers are SCCs that arise from the squamocolumnar junction of the exocervix. Normal squamous epithelium from both of these regions constitutively expressed BRAK. Yet the majority of HNSCCs and two of six cervical SCCs failed to express BRAK mRNA. Thus there does indeed appear to be loss of BRAK mRNA occurring in certain tumors. Most breast cancers, however, arise from the same epithelium that gives rise to normal lobular units. As the *in vivo* expression in normal lobular units was rare, it would not necessarily be expected for breast adenocarcinomas to produce BRAK mRNA. This is also true of ovarian cancer, because the normal ovary does not appear to express BRAK either. On the other hand, expression in colon cancer had an interesting pattern. The normal columnar epithelium (that gives rise to the majority of adenocarcinomas) had no BRAK expression, yet in some cases there was weak or even strong expression in the corresponding colorectal tumors. That coexpression of BRAK mRNA in subpopulations of inflammatory cells was found in 100% of the colorectal cancers studied raises the possibility that BRAK mRNA could even be up-regulated in certain tumors because of locally produced factors.

At present, the role of BRAK in the biology of tumors is unknown and there are no existing data regarding the function of an active recombinant protein. However, three lines of evidence suggest that there could be some involvement in host-tumor interactions. First, down-regulation of BRAK was observed in certain tumors. Second, up-regulation of BRAK was a ubiquitous finding in infiltrating inflammatory cells in numerous cases. Third, there is increasing evidence implicating chemokines in the regulation of tumor growth.[2;8–12 10–13] The chemokines MCP-1,[14] mTCA3,[15] RANTES,[16] IP-10,[13] and Mig[17] have all been shown to cause tumor regression or slow growth of tumors in mice when transfected into various tumor cell lines or directly administered to mice. In contrast, expression of GROα, and IL-8 leads to increased tumorigenicity.[18;19]

BRAK belongs to the CXC chemokine subfamily, certain members of which have been shown to regulate the angiogenesis needed for solid tumor growth.[2;20–22] CXC chemokines can be subdivided according to the presence or absence of the amino acid motif "glutamic acid-leucine-arginine (ELR)". Several ELR$^+$ CXC chemokines stimulate migration of endothelial cells *in vitro* and induce angiogenesis *in vivo*, whereas ELR$^-$ chemokines inhibit endothelial cell chemotaxis and block angiogenesis mediated by ELR$^+$ chemokines, basic fibroblast growth factor, and vascular endothelial growth factor.[20–22] Evidence that the ELR motif determines whether CXC chemokines inhibit or stimulate angiogenesis comes from studies employing recombinant chimeric proteins.[21] BRAK lacks the ELR motif and may therefore turn out to be an angiogenesis inhibitor.

A plethora of data exists supporting the idea that the balance of angiogenic and angiostatic chemokines can alter the *in vivo* growth of tumors.[12;18;20;22] Recently, the antitumor properties of IL-12 have been shown to be mediated by secondary induction of the angiostatic CXC chemokines IP-10 and Mig in both immunocompetent[11] and T-cell-deficient mice.[12] While the angiostatic behavior of certain CXC chemokines is a plausible explanation for their antitumor properties, there also appears to be an immunological mechanism in some cases. Murine plasmacytomas and mammary carcinomas transfected with the CXC chemokine IP-10 become infiltrated by lymphocytes and are rejected by immunocompetent mice but not by immunodeficient nude mice.[10] Further studies are needed to determine whether BRAK behaves like an angiogenesis inhibitor or simply like a chemotactic factor. The fact that many other CXC family members regulate tumor growth is intriguing, because BRAK expression is lost in certain tumors and is frequently expressed by infiltrating inflammatory cells. An understanding of the biological significance, however, must await definition of the functional properties belonging to this novel chemokine.

Note Added in Proof

While this manuscript was in press, the murine homologue of BRAK (BMAC) was described and found to stimulate chemotaxis of B cells and monocytes. Sleeman MA, Fraser JK, Murison JG, Kelly SL, Pestidge RL, Palmer DJ, Watson JD, Kumble KD: B cell- and monocyte-activating chemokine (BMAC), a novel non-ELF α-chemokine. Int Immunol 2000, 12:677–689.

Acknowledgments

We thank Drs. Michael Hudson, Michael Gilcrease, Marc Levy, and Jeffrey Scott for their competent technical assistance, and Paula Holton for organizing and coordinating the procurement of specimens.

References

1. Hromas R, Broxmeyer HE, Kim C, Nakshatri H, Christopherson K, Azam M, Hou YH: Cloning of BRAK, a novel divergent CXC chemokine preferentially expressed in normal versus malignant cells. Biochem Biophys Res Commun 1999, 255:703–706
2. Wang JM, Deng X, Gong W, Su S: Chemokines and their role in tumor growth and metastasis. J Immunol Methods 1998, 220:1–17
3. Baggiolini M: Chemokines and leukocyte traffic. Nature 1998, 392: 565–568
4. Baggiolini M, Dewald B, Moser B: Human chemokines: an update. Annu Rev Immunol 1997, 15:675–705
5. Gale LM, McColl SR: Chemokines: extracellular messengers for all occasions? Bioessays 1999, 21:17–28
6. Sacks PG: Cell, tissue and organ culture as in vitro models to study the biology of squamous cell carcinomas of the head and neck. Cancer Metastasis Rev 1996, 15:27–51
7. Carey TE, Hay RJ, Park J-G, Gazdar A: Atlas of Human Tumor Cell Lines. San Diego, Academic Press, 1994, pp 79–119
8. Luan J, Shattuck-Brandt R, Haghnegahdar H, Owen JD, Strieter R, Burdick M, Nirodi C, Beauchamp D, Johnson KN, Richmond A: Mechanism and biological significance of constitutive expression of MGSA/GRO chemokines in malignant melanoma tumor progression. J Leukoc Biol 1997, 62:588–597
9. Arenberg DA, Kunkel SL, Polverini PJ, Morris SB, Burdick MD, Glass MC, Taub DT, Iannettoni MD, Whyte RI, Strieter RM: Interferon-gamma-inducible protein 10 (IP-10) is an angiostatic factor that inhibits human non-small cell lung cancer (NSCLC) tumorigenesis and spontaneous metastases. J Exp Med 1996, 184:981–992
10. Luster AD, Leder P: IP-10, a -C-X-C- chemokine, elicits a potent thymus-dependent antitumor response in vivo. J Exp Med 1993, 178:1057–1065
11. Tannenbaum CS, Tubbs R, Armstrong D, Finke JH, Bukowski RM, Hamilton TA: The CXC chemokines IP-10 and Mig are necessary for IL-12-mediated regression of the mouse RENCA tumor. J Immunol 1998, 161:927–932
12. Kanegane C, Sgadari C, Kanegane H, Teruya-Feldstein J, Yao L, Gupta G, Farber JM, Liao F, Liu L, Tosato G: Contribution of the CXC chemokines IP-10 and Mig to the antitumor effects of IL-12. J Leukoc Biol 1998, 64:384–392
13. Sgadari C, Angiolillo AL, Cherney BW, Pike SE, Farber JM, Koniaris LG, Vanguri P, Burd PR, Sheikh N, Gupta G, Teruya-Feldstein J, Tosato G: Interferon-inducible protein-10 identified as a mediator of tumor necrosis in vivo. Proc Natl Acad Sci USA 1996, 93:13791–13796
14. Hoshino Y, Hatake K, Kasahara T, Takahashi Y, Ikeda M, Tomizuka H, Ohtsuki T, Uwai M, Mukaida N, Matsushima K: Monocyte chemoattractant protein-1 stimulates tumor necrosis and recruitment of macrophages into tumors in tumor-bearing nude mice: increased granulocyte and macrophage progenitors in murine bone marrow. Exp Hematol 1995, 23:1035–1039
15. Laning J, Kawasaki H, Tanaka E, Luo Y, Dorf ME: Inhibition of in vivo tumor growth by the beta chemokine, TCA3. J Immunol 1994, 153: 4625–4635
16. Mule JJ, Custer M, Averbook B, Yang JC, Weber JS, Goeddel DV, Rosenberg SA, Schall TJ: RANTES secretion by gene-modified tumor cells results in loss of tumorigenicity in vivo: role of immune cell subpopulations. Hum Gene Ther 1996, 7:1545–1553
17. Sgadari C, Farber JM, Angiolillo AL, Liao F, Teruya-Feldstein J, Burd PR, Yao L, Gupta G, Kanegane C, Tosato G: Mig, the monokine induced by interferon-gamma, promotes tumor necrosis in vivo. Blood 1997, 89:2635–2643
18. Luca M, Huang S, Gershenwald JE, Singh RK, Reich R, Bar-Eli M: Expression of interleukin-8 by human melanoma cells up-regulates MMP-2 activity and increases tumor growth and metastasis. Am J Pathol 1997, 151:1105–1113
19. Owen JD, Strieter R, Burdick M, Haghnegahdar H, Nanney L, Shattuck-Brandt R, Richmond A: Enhanced tumor-forming capacity for immortalized melanocytes expressing melanoma growth stimulatory activity/growth-regulated cytokine beta and gamma proteins. Int J Cancer 1997, 73:94–103
20. Moore BB, Keane MP, Addison CL, Arenberg DA, Strieter RM: CXC chemokine modulation of angiogenesis: the importance of balance between angiogenic and angiostatic members of the family. J Invest Med 1998, 46:113–120
21. Strieter RM, Polverini PJ, Kunkel SL, Arenberg DA, Burdick MD, Kasper J, Dzuiba J, Van Damme J, Walz A, Marriott D: The functional role of the ELR motif in CXC chemokine-mediated angiogenesis. J Biol Chem 1995, 270:27348–27357
22. Arenberg DA, Polverini PJ, Kunkel SL, Shanafelt A, Hesselgesser J, Horuk R, Strieter RM: The role of CXC chemokines in the regulation of angiogenesis in non-small cell lung cancer. J Leukoc Biol 1997, 62:554–562

International Immunology, Vol. 12, No. 5, pp. 677–689

B cell- and monocyte-activating chemokine (BMAC), a novel non-ELR α-chemokine

Matthew A. Sleeman, Jonathon K. Fraser, James G. Murison, Sharon L. Kelly, Ross L. Prestidge, David J. Palmer, James D. Watson and **Krishnanand D. Kumble**

Genesis Research and Development Corp. Ltd, PO Box 50, Auckland, New Zealand

Keywords: chemotaxis, inflammation, migration, nude mice, tumour

Abstract

A novel α-chemokine, designated KS1, was identified from an EST database of a murine immature keratinocyte cDNA library. The EST has 94% similarity to a recently cloned human gene, BRAK, that has no demonstrated function. Northern analysis of mouse and human genes showed detectable mRNA in brain, intestine, muscle and kidney. Tumour panel blots showed that BRAK was down-regulated in cervical adenocarcinoma and uterine leiomyoma, but was up-regulated in breast invasive ductal carcinoma. KS1 bound specifically to B cells and macrophages, as well as two B cell lines, CESS and A20, and a monocyte line, THP-1. KS1 showed no binding to naive or activated T cells. In addition, KS1 stimulated the chemotaxis of CESS and THP-1 cells but not T cells. The s.c. injection of KS1 creates a mixed inflammatory response in Nude and C3H/HeJ mice. The above data indicates that KS1 and its human homologue represents a novel non-ELR α-chemokine that may have important roles in trafficking of B cells and monocytes. We propose the name B cell- and monocyte-activating chemokine (BMAC) for this molecule to reflect the described biological functions.

Introduction

Chemokines are a large family of small peptides that are involved in the trafficking of leukocytes around the body. They consist of proteins between 8 and 12 kDa in size with a number of conserved cysteines that form two disulphide bridges (1–3). The chemokine superfamily is currently classified with respect to the number and position of the first cysteines, CC, CXC, CX_3C and C. The two main groups are (i) the CXC or α-chemokines, defined by a single amino acid separating the first two cysteines, and (ii) the CC or β-chemokines, with the first two cysteines being contiguous. The α-chemokines can be further subdivided into two groups depending on whether they contain a Glu–Leu–Arg (ELR) motif immediately prior to the first cysteine (1). Initially, these molecules were thought to only be involved in stimulating an inflammatory response by promoting chemotaxis of leukocytes from the peripheral blood to sites of inflammation. IL-8 was one of the first chemokines identified and was shown to promote neutrophil migration (4–6). Since then the chemokine family has grown to >50 members (http://cytokine.medic.kumamoto-u.ac.jp/CFC/CK/chemokine.html) with every leukocyte population having its own particular subset of chemokines and chemokine receptors. The non-ELR α-chemokines currently consist of six members whose chemotactic functions are highly diverse (7–13), in contrast to the neutrophil migration-promoting ELR chemokines, and are of great interest for their therapeutic potential in areas other than leukocyte migration. PF-4, IP-10 and Mig have all been shown to have anti-angiogenic properties in a range of tumour models (14–16). SDF-1α has been shown to competitively block viral entry in HIV strains that uniquely use CXCR4 as their co-receptor for infection (17,18). The potential of this therapeutic approach is supported by the observation that high circulating levels of β-chemokines can confer a degree of immunity on those exposed to HIV (19). Recently, a non-ELR α-chemokine, BRAK, was identified by screening human EST databases (20). Function has yet to be assigned for this molecule, although it has been postulated to have a role in oncogenesis. We have identified the murine homologue of this gene, the responding cell types for this new chemokine and propose a new name that reflects its biological activity.

Correspondence to: M. Sleeman

Transmitting editor: M. Feldmann

Received 10 September 1999, *accepted* 28 January 2000

Methods

Chemicals and reagents

Recombinant human stromal derived factor-1α and human IL-2 were purchased from PeproTech (Rocky Hill, NJ). The following primary anti-murine antibodies were obtained from PharMingen (San Diego, CA), I-A^k (A_α^k) biotin (clone 11-5.2), CD19–FITC (Clone 1D3), CD4–FITC (clone RM4-5), CD8a–FITC (clone 53-6.7), rat IgG2a–FITC (R35-95) and mouse IgG2b–biotin (clone 49.2). The secondary antibody goat anti-human IgG–phycoerythrin (PE) and streptavidin–PE were purchased from Southern Biotechnology Associates (Birmingham, AL), and the streptavidin–alexa 488 from Molecular Probes (Eugene, OR).

Bioinformatic analysis

An oligo-d(T)-primed directionally cloned murine immature keratinocyte cDNA library was constructed from poly(A)$^+$ RNA using a ZAP express cDNA kit (Stratagene, La Jolla, CA) following the manufacturer's protocol. The library was mass excised and colonies randomly selected for sequencing. High-throughput single-pass sequence from the 5′ end of the clones was obtained on ABI377 sequencers (Perkin Elmer, Foster City, CA). Novel sequences were analysed using BLAST (21), Prosite (Swiss Institute of Bioinformatics, University of Geneva) and SignalP V1.1 (Center for Biological Sequence Analysis, Technical University of Denmark), and the Phylip package (University of Washington) to define similarities to known gene families or motifs.

Sequence and cloning of KS1

The full-length sequence of KS1 was obtained by subcloning and sequence primer walking. The coding region, without the predicted signal sequence, was PCR amplified using Klentaq polymerase (Clontech, Paolo Alto, CA) and KS1 as template, using the following sequences 5′-CATGCCATGGCGTCCAAGTGTAAGTGTTCCCGGAAGGGG-3′ and 5′-CATGCCATGGCTAATGGTGGTGATGGTGATGTTCTTCGTAGACCCTGCGCTTCTC-3′ as forward and reverse oligonucleotides respectively. The product was purified using a PCR purification kit (Qiagen, Valencia, CA), digested with NcoI and ligated into pET16B (Novagen, Madison, WI) to obtain the sequence in frame with the C-terminal $(His)_6$ tag. In addition to this we cloned the full-length coding region into a eukaryotic expression vector, pIGFc, using 5′-GGAATTCCATGAGGCTCCTGGCGGCCGCGCTGCTC-3′ and 5′-ACGGATCCACTTACCTGTTTCTTCGTAGACCCTGCGCTTCTCGTT-3′ as forward and reverse primers respectively. PCR products were prepared as above and ligated into pIGFc to obtain the sequence in-frame with human IgG1 Fc present in the vector. All constructs were confirmed by automated sequencing.

Northern analysis

KS1 probe was PCR amplified using Taq polymerase (Qiagen) with 5′-ACGCGTCGACATGAGGCTCCTGGCGGC-3′ and 5′-TCGTCCAGATCTTTCTTCGTAGACCCTGCGCTT-3′ as forward and reverse oligonucleotides respectively. BRAK probe was PCR amplified from human keratinocyte cDNA using Taq polymerase (Qiagen) with 5′-ACGCGTCGACATGAGGCTCCTGGCGGCCGCGCTGCTC-3′ and 5′-ATAAGATCTTTCTTCGTAGACCCTGCGCTTC-3′ as forward and reverse oligonucleotides respectively. Probe identity was confirmed by sequencing. PCR products were labelled with [α-^{32}P]dCTP (3000 Ci/mmol, NEN/Life Science products, Boston, MA) using 25 ng of DNA in a Rediprime II random-primed labelling system (Amersham Pharmacia, Piscataway, NJ). Human multiple tissue northern blots (Clontech) were hybridized with a 300 bp PCR product (nucleotides 1–300 bp of the BRAK coding sequence) following the manufacturer's protocol (Clontech). A human tumour panel blot (Invitrogen, Calsbad, CA) was hybridized with the probe prepared as described above, in 6×SSC buffer, 2×Denhardt reagent, 2% SDS, 120 μg heparin and 100 μg yeast tRNA (Boehringer Mannheim, Mannheim, Germany) at 65°C for 18 h. RNA for mouse tissue blots was isolated using Trizol reagent (Life Technologies, Grand Island, NY) and 20 μg total RNA loaded per lane in a 1% formaldehyde agarose gel, transferred to Hybond N+ membrane (Amersham) and hybridized with the radiolabelled PCR product (nucleotides 1–300 bp of the KS1 coding sequence). Mouse tissue blots were hybridized as described for the tumour panel blots. All blots were washed under stringent conditions as specified by the manufacturers or by standard protocols (22). Northern blots were exposed to X-ray film at –80°C and developed at various times up to 7 days. Both the tumour panel blot and human tissue blots were re-probed, as described previously, with a 500 bp β-actin probe as a loading control.

Expression and purification of recombinant KS1

A C-terminal $(His)_6$ tag fusion protein of KS1 was expressed in BL21(DE3) *Escherichia coli* cells (Novagen). One litre cultures were induced at an OD_{600} of 0.5 with 1 mM IPTG and harvested after 3 h. All subsequent procedures were performed on ice. The pellet was re-suspended in lysis buffer (20 mM Tris–HCl, pH 8.0, 1 mM PMSF, 10 mM β-mercaptoethanol, 1% NP-40) and sonicated using a Virsonic ultrasonicator (Virtis, Gardiner, NY) fitted with the miniprobe at 20% output for 4×15 s bursts with 15 s intervals. The sonicate was centrifuged in a JA20 rotor at 18,000 r.p.m. for 10 min at 4°C. The resultant pellet was washed twice for 1 h each in lysis buffer containing 0.5% CHAPS and solubilized in 20 mM Tris–HCl, pH 8.0, containing 6 M guanidine–HCl and 0.5 M NaCl. The $(His)_6$ fusion protein was isolated by chromatography using nickel chelating Sepharose FF resin (0.5 ml column; Pharmacia). After loading, the column was washed sequentially with 20 volumes of binding buffer (6 M urea, 0.5 M NaCl and 20 mM Tris–HCl, pH 8.0), 20 volumes of 0.5% sodium deoxycholate in binding buffer and 20 volumes of binding buffer containing 20 mM imidazole. The protein was eluted with 10 volumes 300 mM imidazole in binding buffer. The eluate was dialysed against binding buffer and re-chromatographed as above. Fusion protein in the eluate was then refolded by dialysis against 1 l of 4 M urea, 20 mM Tris–HCl, pH 7.5, overnight while 1 l of 20 mM Tris–HCl, pH 7.5, was pumped into the dialysis beaker at a rate of 1 ml/min. The refolded protein was finally dialysed against 20 mM Tris–HCl, pH 7.5, containing 10% (w/v) glycerol. Preparations obtained were >95% pure as determined by SDS–PAGE using FragmeNT Analysis

A

```
-202                                                          GC
-200  AGCACCCAGC GCCAAGCGCA CCAGGCACCG CGACAGACGG CAGGAGCACC
-150  CATCGACGGG CGTACTGGAG CGAGCCGAGC AGAGCAGAGA GAGGCGTGCT
-100  TGAAACCGAG AACCAAGCCG GGCGGCATCC CCCGGCCGCC GCACGCACAG
-50   GCCGGCGCCC TCCTTGCCTC CCTGCTCCCC ACCGCGCCCC TCCGGCCAGC

1    ATG AGG CTC CTG GCG GCC GCG CTG CTC CTG CTG CTC CTG GCG
1     M   R   L   L   A   A   A   L   L   L   L   L   A

43   CTG TGC GCC TCG CGC GTG GAC GGG TCC AAG TGT AAG TGT TCC
15    L   C   A   S   R   V   D   G   S   K   C   K   C   S

85   CGG AAG GGG CCC AAG ATC CGC TAC AGC GAC GTG AAG AAG CTG
29    R   K   G   P   K   I   R   Y   S   D   V   K   K   L

127  GAA ATG AAG CCA AAG TAC CCA CAC TGC GAG GAG AAG ATG GTT
43    E   M   K   P   K   Y   P   H   C   E   E   K   M   V

167  ATC GTC ACC ACC AAG AGC ATG TCC AGG TAC CGG GGC CAG GAG
57    I   V   T   T   K   S   M   S   R   Y   R   G   Q   E

211  CAC TGC CTG CAC CCT AAG CTG CAG AGC ACC AAA CGC TTC ATC
71    H   C   L   H   P   K   L   Q   S   T   K   R   F   I

253  AAG TGG TAC AAT GCC TGG AAC GAG AAG CGC AGG GTC TAC GAA
85    K   W   Y   N   A   W   N   E   K   R   R   V   Y   E

295  GAA TAG GGTGGACGAT CATGGAAAGA AAAACTCCAG GCCAGTTGAG AGA
295   E  ***

344  CTTCAGC AGAGGACTTT GCAGATTAAA ATAAAAGCCC TTTCTTTCTC ACA
394  AGCATAA GACAAATTAT ATATTGCTAT GAAGCTCTTC TTACCAGGGT CAG
444  TTTTTAC ATTTTATAGC TGTGTGTGAA AGGCTTCCAG ATGTGAGATC CAG
494  CTCGCCT GCGCACCAGA CTTCATTACA AGTGGCTTTT TGCTGGGCGG TTG
544  GCGGGGG GCGGGGGGAC CTCAAGCCTT TCCTTTTTAA AATAAGGGGT TTT
594  GTATTTG TCCATATGTC ACCACACATC TGAGCTTTAT AAGCGCCTGG GAG
644  GAACAGT GAGCATGGTT GAGACCGTTC ACAGCACTAC TGCTCCGCTC CAG
694  GCTTACA AAGCTTCCGC TCAGAGAGCC TGGCGGCTCT GTGCAGCTGC CAC
744  AGGCTCT CCTGGGCTTA TGACTGGTCA GAGTTTCAGT GTGACTCCAC TGT
794  GGCCCCT GTTGCAGGGC AATTGGGAGC AGGTCCTTCT ACATCTGTGC CTA
844  GAGGAAC TCAGTCTACT TACCAGAAGG AGCTTCATCC CCACCCCACC CCC
894  ACCCGCA CCCCAGCTCA TTCCCCTGTC ACGACCAGGC AAGTGATCCT TAA
944  AGGAGCT GGGTCTTTTT CTTGCAAACT GAGGGTTTCT GAAAGGTCGG CTG
994  CTTTGGT AGAAGATGCT TCTGAGGCAT CCAAAGTCCC CAGCAGTGTG AGA
1044 AAATGAT TCTCGATGTT CGGGAGGACA AGGGAAGATG CAGGATTAGA TGC
1094 AGGACAC ACAGCCAGAG CTACACATCC TCTTGGCAAT GGGAGCTCCC CCC
1144 CCCCAAA GCTTTGTTTC TTTCCCTCAC CCCAACAGAA AGTGCACTCC CCC
1194 TCAGTGA ATACGCAAAC AGCACTGTTC TCTGAGTTAG GATGTTAGGA CGA
1244 TCCTGCG CCCTGCCCTC TCCTGTGTAC ATATTGCCTT CAGTACCCCT CCC
1294 CCACCCC ATGCCACACA CTGCCCCTCA TTAGAGGCCG CACTGTATGG CTG
1344 TGTATCT GCTATGTAAA TGCTGAGACC CCTGAGTGCT GCATGCAGGT TTC
1394 ATGTTCT TTCTAAGATG AAAAGAGAAA GTAATAAAAT ATATTTGAAG TTC
1444 CCCAAAA AAAAAAAAAA A
```

B

```
KS1        .......... .........M RLLAAA...L LLLLLALCAS RVDGS..... ..KCKCSRKG
BRAK       .......... .........M RLPAAA...L LLLLLALYTA RVDGS..... ..KCKCSRKG
mCrg-2     .......... .......... MNPSAAVIFC LILLGLSGTQ GIPLAR.... TVRCNCIHID
mMig       .......... .......... MKSAVLFLLG IIFLEQCGVR GTLVIR.... NARCSCISTS
mSDF-1     .......... .......... MDAKVVAVLA LVLAALCISD GKPVSLS... .YRCPCRFFE
mBLC       .......... .........M RLSTAT...L LLLLASCLSP GHGILEAHYT NLKCRCSGVI
mMIP-2     .........M AP.....PTC RLLSAALVLL LLLATNHQAT GAVVAS.... ELRCQCLKTL
mKC        .........M IP.....ATR SLLCAA...L LLLATSRLAT GAPIAN.... ELRCQCLQTM
mLix       MSLQLRSSAH IPSGSSSPFM RMAPLA.FLL LFTLPQHLAE AAPSSVIAAT ELRCVCLTVT

Consensus                                                          c c

KS1        PK.IRYSDVK KLEMKPKYPH CSEKMVIVTT KSMSRYRGQE HCLHPKLQST KRFI....KW
BRAK       PK.IRYSDVK KLEMKPKYPH CSEKMVIITT KSVSRYRGQE HCLHPKLQST KRFI....KW
mCrg-2     DGPVRMRAIG KLEIIPASLS CPRVEIIATM KK....NDEQ RCLNPESKTI KNLM....KA
mMig       RGTIHYKSLK DLKQFAPSPN CNKTEIIATL K.....NGDQ TCLDPDSANV KKLMKEWEKK
mSDF-1     SH.IARANVK HLKILN.TPN CALQIVARLK N.....NNRQ VCIDPKLKWI QEYL...EKA
mBLC       STVVGLN1ID RIQVTPPGNG CPKTEVVIWT K.....MKKV ICVNPRAKWL QRLLRHVQSK
mMIP-2     PR.VDFKNIQ SLSVTPPGPH CAQTEVIATL K.....GGQK VCLDPEAPLV QKII....QK
mKC        AG.IHLKNIQ SLKVLPSGPH CTQTEVIATL K.....NGRE ACLDPEAPLV QKIV....QK
mLix       PK.INPKLIA NLEVIPAGPQ CPTVEVIAKL K.....NQKE VCLDPEAPVI KKII....QK

Consensus                          C                  C

KS1        YNAWNE.KRR VYEE..... ..........
BRAK       YNAWNE.KRR VYEE..... ..........
mCrg-2     FSQKRS.KRA P........ ..........
mMig       INQKKKQKRG KKHQKNMKNR KPKTPQSRRR SRKTT
mSDF-1     LNKRLKM... .......... ..........
mBLC       SLSSTPQAPV SKRRAA.... ..........
mMIP-2     ILNKGK.AN. .......... ..........
mKC        MLKGVP.K.. .......... ..........
mLix       ILGSDK.KKA KRNALAVERT ASVQ......

Consensus
```

C

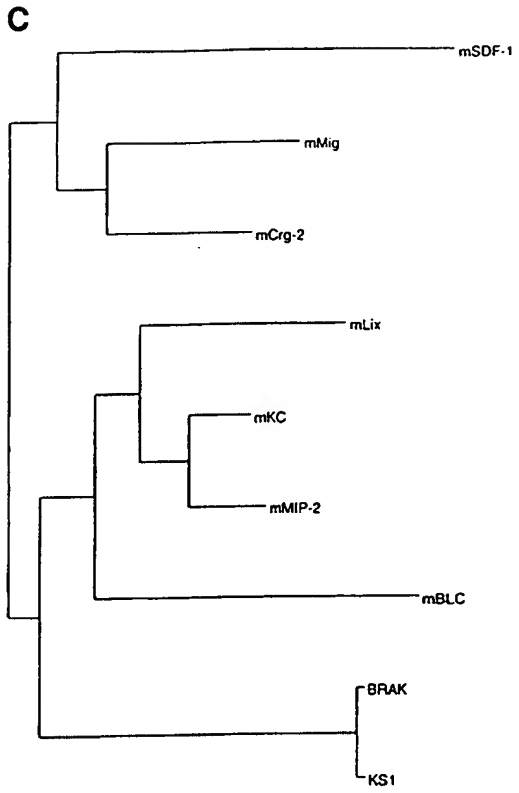

Fig. 1. (A) The nucleotide sequence of KS1 cDNA is shown along with the deduced amino acid sequence using the single letter code. The 5′ untranslated region is indicated by negative numbers. The underlined N-terminal amino acids represent the predicted leader sequence and the stop codon is denoted by '***'. The poly-adenylation signal is marked by a double underline. The sequence data is available from GenBank under accession no. AF144754. (B) Comparison of the complete open reading frame of KS1 with its human homologue BRAK and with the mouse α-chemokines mCrg-2, mMig, mSDF-1, mBLC, mMIP-2, mKC and mLIX. An additional five residues are present in KS1 and BRAK between cysteine 3 and cysteine 4 that have not previously been described for chemokines. (C) A phylogenetic tree of KS1 was constructed against current murine α-chemokines using Phylip software version 3.57c, and programs protdist and neighbour joining. The figure represents the degree of divergence between each of the family members. The branch lengths are proportional to the numbers of substitutions, based on the amino acid homology, the level of conservation between the different amino acid residues and the rate of evolution. GenBank accession nos for the sequences are (from top to bottom): L12030, M34815, M86829, U27267, J04596, X53798, AF044196, AF073957 and AF144754.

Package (Molecular Dynamics, Sunnyvale, CA). Endotoxin contamination of purified KS1 was determined using a limulus amebocyte lysate assay kit (Biowhittaker, Walkersville, MD). Endotoxin levels were <0.1 ng/μg of protein. Internal amino acid sequencing was performed on tryptic peptides of KS1 by the Protein Sequencing Unit at the University of Auckland, New Zealand.

An Fc fusion protein was produced by expression in HEK 293 T cells. Using 35 μg of KS1pIGFc DNA to transfect 6×10^6 cells/flask, 200 ml of KS1 Fc-containing supernatant was produced. The Fc fusion protein was isolated by chromatography using an Affiprep Protein A resin (0.3 ml column; BioRad, Hercules, CA). After loading, the column was washed with 15 ml of PBS, followed by a 5 ml wash of 50 mM Na citrate, pH 5.0. The protein was then eluted with 6 column volumes of 50 mM Na citrate, pH 2.5, collecting 0.3 ml fractions in tubes containing 60 μl of 20 mM Tris–HCl, pH 7.5. Fractions were analyzed by SDS–PAGE and pooled.

Cell isolation and culture

Murine spleens, thymus, peripheral lymph node and bone marrow cells for flow cytometric analysis were obtained from C3H/

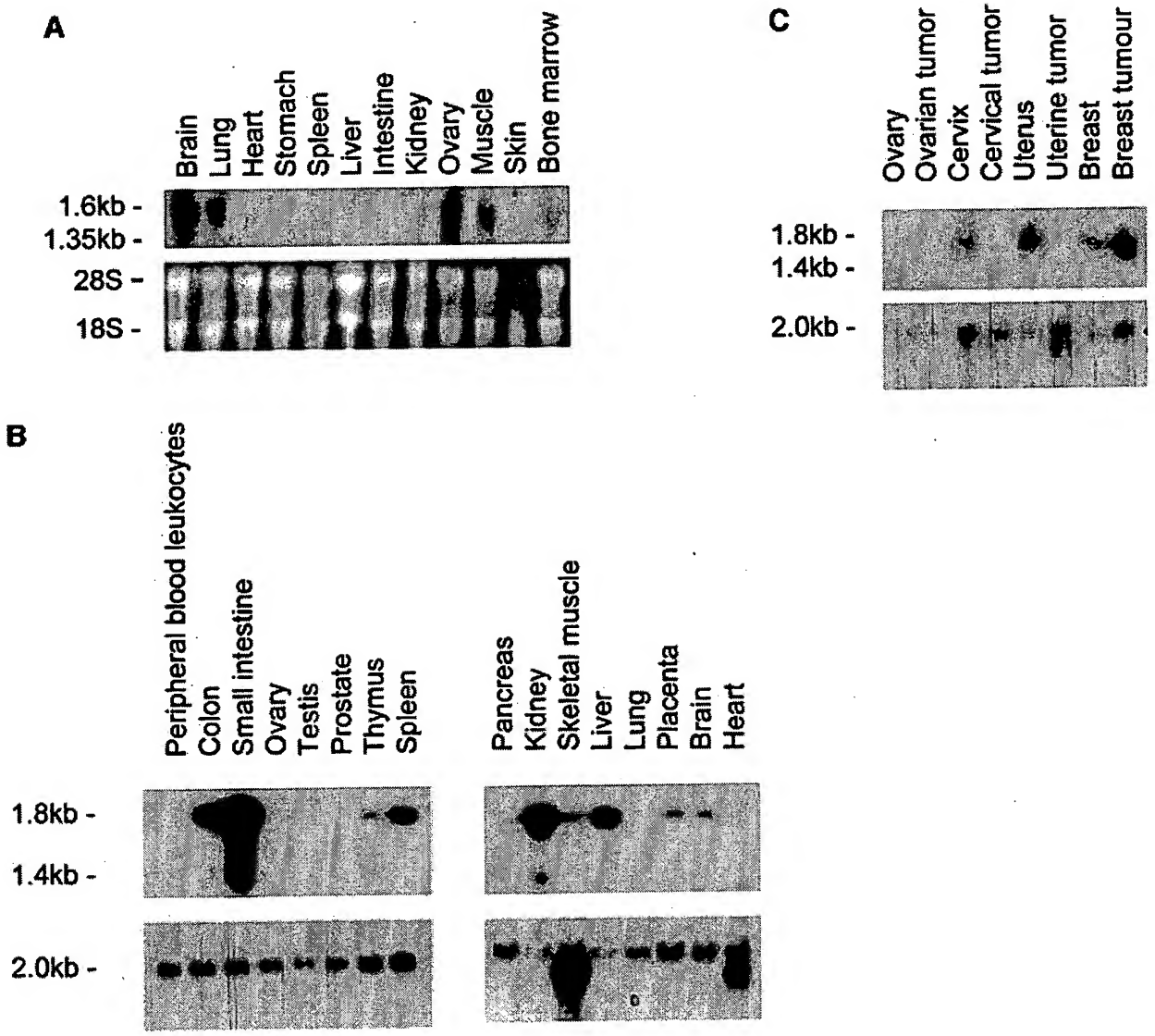

Fig. 2. (A). Northern blot analysis of KS1 mRNA in various murine tissues. The upper panel shows the level of expression in these tissues, whereas the lower panel illustrates equal loading of total RNA from these tissues. The position of the 1.35 kb RNA marker is indicated as is the position of 1.6 kb KS1; 28S and 18S ribosomal bands are also indicated. (B) Northern blot of BRAK mRNA in various human tissues as a comparison with murine expression. Human multiple tissue blots were purchased from Clontech. (C) Northern blot analysis of BRAK mRNA in tumor versus normal tissue. Tumor panel blots were purchased from Invitrogen. The northern blot directly compares four different tumors with their respective normal tissue. The upper panels of the human blots shows the level of expression of BRAK, whereas the lower panel demonstrates the level of β-actin expression. The position of the 1.4 kb RNA marker and 1.8 kb BRAK message is indicated

HeJ mice, erythrocytes were lysed using ACK lysis buffer (0.15 M NH_4Cl, 1 mM $KHCO_3$ and 0.1 mM Na_2EDTA). Peritoneal exudate cells (PEC) were obtained by i.p. lavage from C3H/HeJ mice. In brief, euthanized mice were injected with 2×4 ml volumes of 0.02% EDTA/PBS into the peritoneal cavity using an 18 gauge needle. Cells were then drawn out from the peritoneal cavity, pelleted and washed in PBS prior to further analysis. Murine IL-2-activated T cells were cultured as described below. Briefly, splenocytes were activated with 2 μg/ml concanavalin A (Con A) (Sigma, St Louis, MO) in the presence of 5% FBS in DMEM supplemented with 2 mM L-glutamine (Sigma), 1 mM sodium pyruvate (Life Technologies), 0.77 mM L-asparagine (Sigma), 0.2 mM arginine (Sigma), 160 mM penicillin G (Sigma), 70 mM dihydrostreptomycin sulfate (Boehringer Mannheim) and 50 μM 2-mercaptoethanol, for 3 days followed by addition of recombinant human IL-2 (PeproTech) at 10 ng/ml. Cytokine was added at 3 day intervals for 9–21 days. Peripheral blood mononuclear cells (PBMC) were isolated in heparin (10U/ml) containing tubes from human donors and purified on a Ficoll-Hypaque (Pharmacia) gradient by centrifugation at 900 *g* for 20 min with no brake. PBMC were aspirated from the interface, washed and re-suspended in HBSS, 20 mM HEPES, 0.5% BSA and used directly for assays. Human IL-2-activated T cells were cultured as described below. Briefly, PBMC were activated with 0.1% phytohemagglutinin (PHA) (Gibco/BRL) in the presence of 5% FBS in RPMI supplemented with 2 mM L-glutamine (Sigma), 160 mM penicillin G (Sigma), 70 mM dihydrostreptomycin sulphate (Boehringer Mannheim) and 50 μM 2-mercaptoethanol, for 3 days followed by addition of recombinant human IL-2 (PeproTech) at 10 ng/ml. CESS, THP-1 and Jurkat

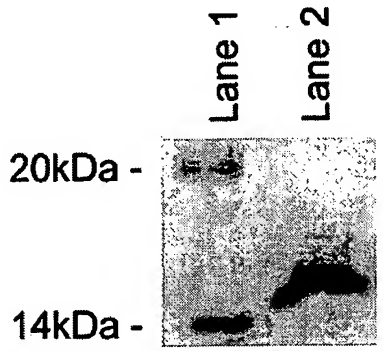

Fig. 3. Analysis of purified $(His)_6$KS1 fusion protein by SDS–PAGE. Protein was resolved on a 12% acrylamide denaturing gel and stained with Coomassie blue. Lane 1, mol. wt standards; lane 2, 5 μg of purified $(His)_6$KS1 protein.

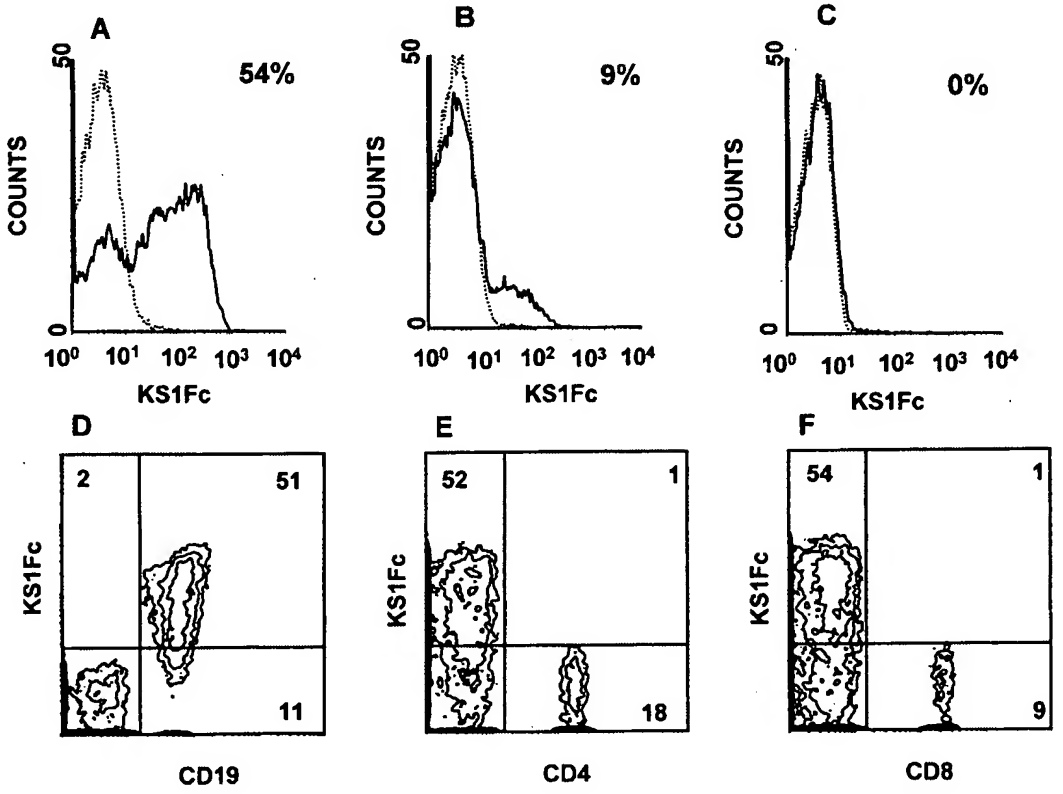

Fig. 4. Flow cytometric analysis of KS1Fc binding to murine splenocytes, peripheral lymph node cells and thymocytes. Cells were labelled with KS1Fc or negative control protein EGBFc and visualized with a two-step staining procedure using goat anti-human–PE. Ten thousand gated events were analysed for each of the experiments. (A) Binding of KS1Fc was detected on murine splenocytes and (B) peripheral lymph node cells as compared with the negative control, EGBFc. (C) Alternatively, KS1Fc showed no binding to thymocytes when compared to negative control. The phenotype of the $KS1Fc^+$ splenocytes was determined using two-color analysis with the following antibody markers. (D) Murine splenocytes were double positive for KS1Fc and CD19 (D) but not for CD4 (E) or CD8a (F) cells. KS1Fc (solid line), EGBFc (dotted line).

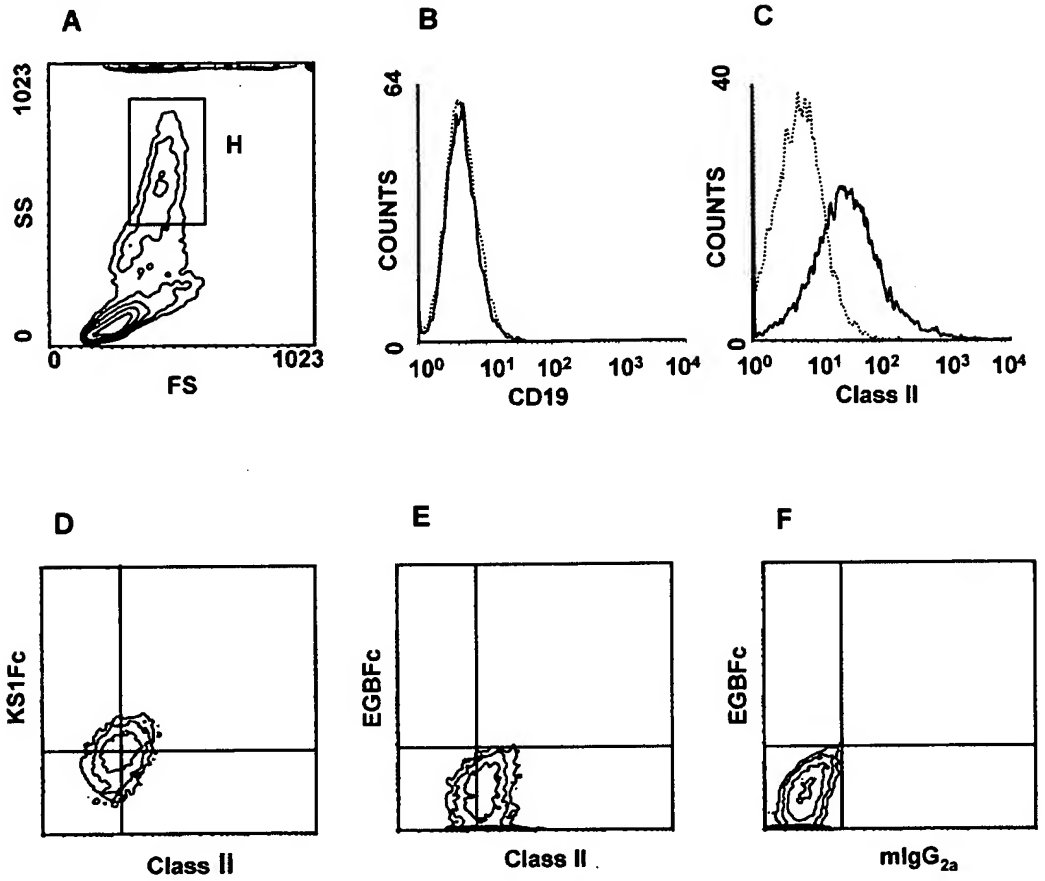

Fig. 5. Flow cytometric analysis of KS1Fc binding to monocytes from PEC. Ten thousand gated events were analysed for each of the experiments. Forward (FS) versus side scatter (SS) histogram of PEC (A). All subsequent histograms were gated on region H. Cells from this region were $CD19^-$ (B) [CD19 (solid line), rIgG2a (dotted line)] and MHC class II^+ (C) [MHC class II (solid line), mIgG2a (dotted line)]. Two-colour analysis shows that MHC class II^+ cells are positive for KS1Fc (D) and not the control protein, EGBFc (E). The matching isotype for MHC class II, mIgG2a, showed no non-specific binding (F).

cells were maintained in complete RPMI as described previously, whereas A20 cells were grown in 5% FBS in DMEM supplemented with 2 mM L-glutamine (Sigma), 1 mM sodium pyruvate (Life Technologies), 0.77 mM L-asparagine (Sigma), 0.2 mM arginine (Sigma), 160 mM penicillin G (Sigma) and 70 mM dihydrostreptomycin sulphate (Boehringer Mannheim).

Flow cytometric binding studies

Binding of KS1 to cells was tested in the following manner. Cells (5×10^5) were resuspended in 3 ml of wash buffer (2% FBS and 0.2% sodium azide in PBS) and pelleted at 4°C, 200 *g* for 5 min. Ig Fc receptors were blocked with 1% goat serum in wash buffer for 30 min on ice. Cells were washed, pelleted, resuspended in 50 µl of KS1Fc at 10 µg/ml and incubated for 30 min on ice. After incubation the cells were prepared as before and resuspended in 50 µl of goat anti-human IgG–PE at 1 µg/ml and incubated for 30 min on ice. Cells were washed and resuspended in 250 µl of wash buffer containing 40 ng/ml propidium iodide (Sigma) to exclude any dead cells. A purified Fc tagged plant protein (EGBFc) was used, at 10 µg/ml, as a negative control in place of KS1Fc to determine non-specific binding. For two-colour staining, cells were incubated with one of the following antibodies prior to staining with KS1Fc or EGBFc, anti-CD4–FITC, anti-CD8a–FITC, anti-CD19–FITC and rat IgG2a–FITC at 10 µg/ml. Biotinylated Ia^k and its isotype control, mouse IgG2b–biotin, were used to identify MHC class II^+ cells and detected using streptavidin–alexa 488. Ten thousand gated events were analysed on a log scale using a FITC, PE and propidium iodide filter arrangement with peak transmittance at 525, 575 and 675 nm respectively with a bandwidth of 10 nm on an Elite cell sorter (Coulter, Hileah, FL). To determine KS1Fc binding to human cell lines CESS, THP-1 and Jurkat, and to reduce level of non-specific binding, both KS1Fc and control protein EGBFc were biotinylated using the Sigma biotinylation kit (Sigma BK-101) as described in the manufacturer's protocols. Human cells were labelled with KS1Fc–biotin or EGBFc–biotin as described previously and then detected with streptavidin–PE. Cold competition was performed by adding various concentrations of $(His)_6$KS1 at 4°C as a competitor prior to labelling with KS1Fc. An equivalent concentration of $(His)_6$GV14B, an identically expressed unrelated bacterial protein, was used as control in competition experiments.

Chemotaxis assays

Cell migration in response to KS1 was tested using a 48-well Boyden chamber (Neuro Probe, Cabin John, MD) as described

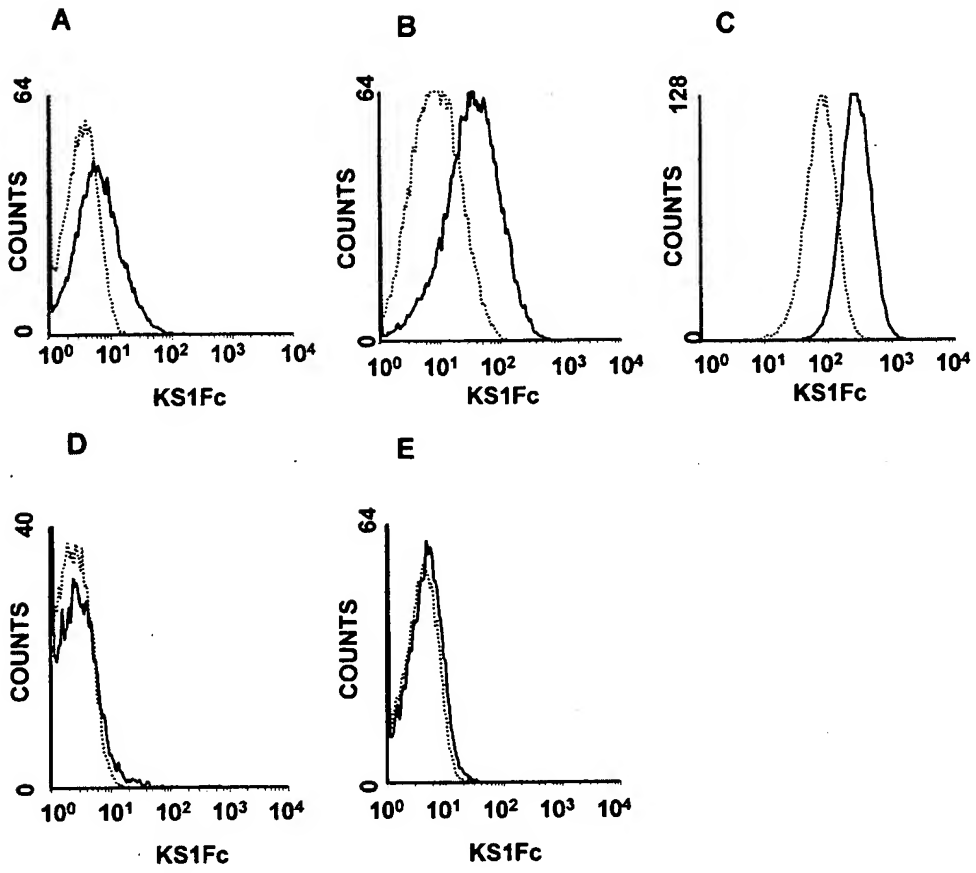

Fig. 6. Flow cytometric analysis of KS1Fc binding to murine and human cell lines. Murine cells were labelled with KS1Fc or negative control protein EGBFc and visualized with a two-step staining procedure using goat anti-human IgG–PE. Human cell lines were labelled with KS1Fc–biotin or negative control EGBFc–biotin and visualized with a two-step staining procedure using streptavidin–PE. Ten thousand gated events were analysed for each of the experiments. Enhanced KS1Fc binding was detected on A20 (A), CESS (B) and THP-1 (C) cells but not on Con A IL-2-activated T cells (D) or Jurkat T cells (E). KS1Fc (solid line), EGBFc (dotted line).

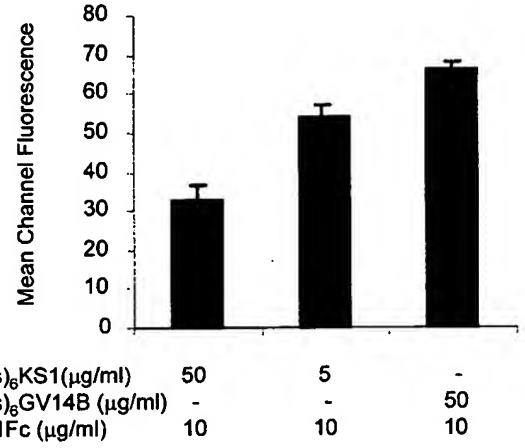

Fig. 7. Cold competition of KS1Fc binding with increasing concentrations of $(His)_6$KS1. KS1Fc binding on murine splenocytes was inhibited by increasing concentrations of $(His)_6$KS1 protein, whereas it was not influenced by the negative control protein, $(His)_6$GV14B. Ten thousand gated events were analysed for each experiment. Values are the geometric mean channel fluorescence ± SD obtained for duplicate samples and are representative of two individual experiments.

in the manufacturer's protocol. In brief, agonists were diluted in HBSS, 20 mM HEPES, 0.5% BSA and added to the bottom wells of the chemotactic chamber. Cells were re-suspended in the same buffer at 3×10^5 cells/50 μl. Top and bottom wells were separated by a PVP-free polycarbonate filter with a 5 μm pore size for CESS and THP-1 cells or 3 μm pore size for splenocytes and lymphocytes. Cells were added to the top well and the chamber incubated for 2 h for THP-1 and 4 h for CESS cells, splenocytes and lymphocytes in a 5% CO_2 humidified incubator at 37°C. After incubation the filter was fixed and cells scraped from the upper surface. The filter was then stained with Diff-Quik (Dade Behring Diagnostics, Deerfield, IL) and the number of migrating cells counted in five randomly selected high-power fields. The results are expressed as a migration index defined as: migration index = no. of test migrated cells/no. of control migrated cells. Assays were repeated in triplicate.

In vivo experiments

BalbcByJ Hfh11 *nu/nu* (Nude) and C3H/HeJ inbred mice strains used for all experiments were maintained in house. C-terminal $(His)_6$KS1 (20 μg) was injected into the left footpads of either Nude or C3H/HeJ mice in triplicate. The right foot of each animal was injected with an equal volume of 20 mM Tris–HCl, pH 7.5.

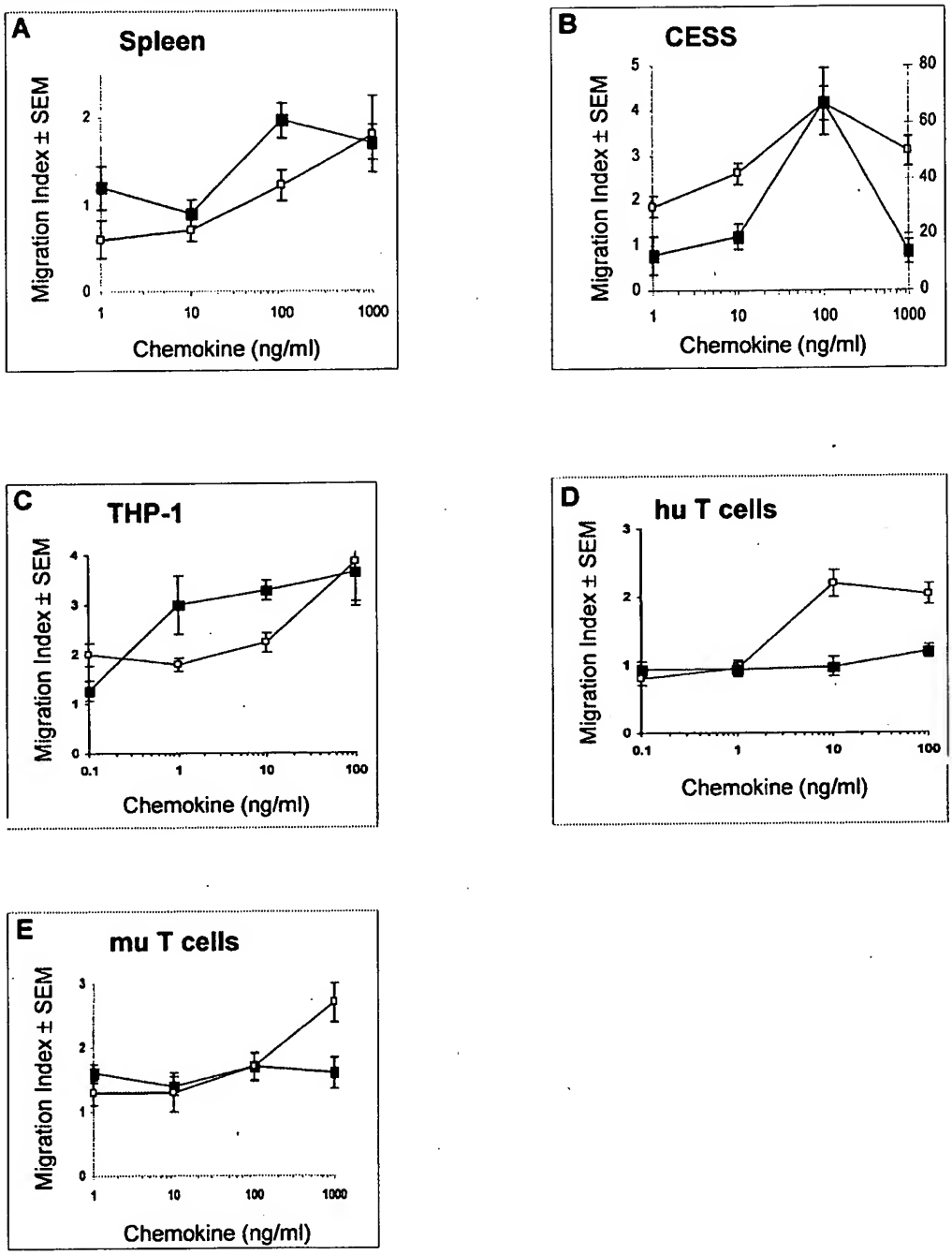

Fig. 8. Chemotactic activities of recombinant KS1. Chemotaxis assays were performed using a 48-well modified Boyden chamber with varying concentrations of KS1 (■) or SDF1α (□). Five randomly selected regions per well were chosen and the number of cells counted under high-power field microscopy. The migration index was calculated by the following formula: migration index = no. of test migrated cells/no. of control migrated cells. (A) Chemotactic activity of murine spleen cells. (B) Chemotactic activity of the B cell line CESS, left *y*-axis is migration to KS1 whereas right *y*-axis is migration to SDF1α. (C) Chemotactic activity of the monocyte leukemia cell line THP-1. (D) Chemotactic activity of PHA IL-2-activated T cells and (E) chemotactic activity of Con A IL-2-activated murine T cells. Values are the mean migration index ± SEM obtained for triplicate wells and are representative of two individual experiments.

Mice were sacrificed after 18 h, and feet dissected and fixed in 3.7% formol saline. All tissues were sectioned and stained with haemotoxylin & eosin. Histology was performed at Agro-Quality (Auckland, NZ). Photomicrography was performed on a Leica compound microscope and images prepared using Adobe Photoshop.

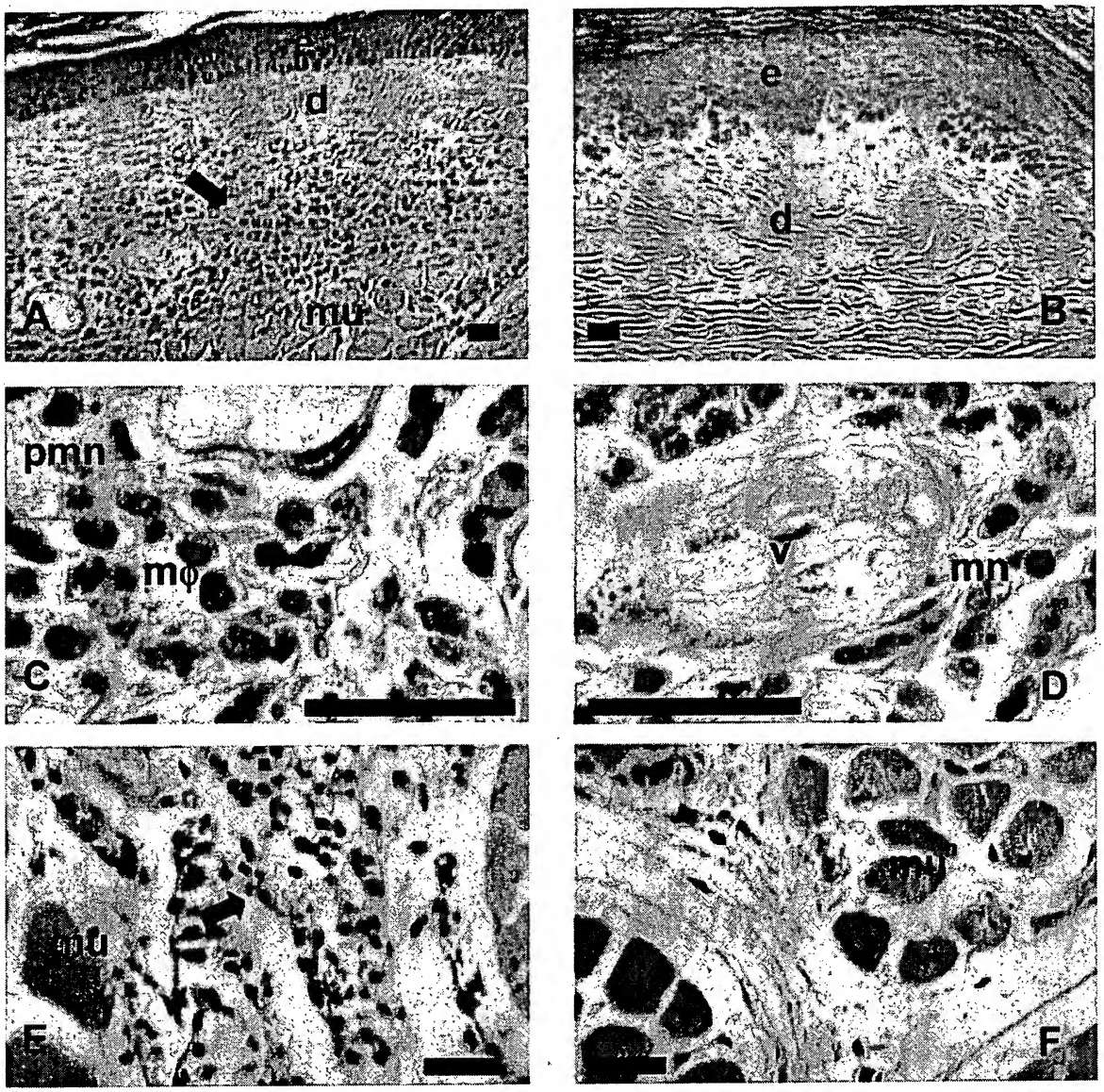

Fig. 9. Inflammatory response of Nude and C3H/HeJ mice upon s.c. injection of KS1. Each group of three mice was injected with $(His)_6$KS1 per group. Mice were injected in the left footpad with $(His)_6$KS1. Equal volumes of Tris buffer were injected into the right footpads as controls. Feet were biopsied after 18 h and haemotoxylin & eosin sections prepared. (A) Nude mice demonstrate a mixed inflammatory response upon injection with KS1, as indicated by an arrow. (B) No inflammation is apparent in the footpad injected with Tris buffer control. (C and D) High-power magnification (×100 objective) of cells in Nude mouse inflammation indicates the presence of monocytes, mononuclear cells and polymorphonuclear cells. (E) A mixed inflammatory response was also present in C3H/Hej mice as denoted by an arrow. (F) No inflammation was detectable in footpads injected with the negative control. Abbreviations: mu, muscle; v, vein; e, epidermis; d, dermis; mϕ, monocyte; mn, mononuclear; and pmn, polymorphonuclear cells. Scale bar = 50 μm.

Results

Identification of KS1 cDNA sequence

A directionally cloned cDNA library was constructed from immature murine keratinocytes and submitted for high-throughput sequencing. Sequence data from a clone designated KS1 showed 35% identity over 74 amino acids with rat macrophage inflammatory protein (MIP)-2B and 32% identity over 72 amino acids with its murine homologue. The insert of 1633 bp (Fig. 1A) contained an open reading frame of 300 bp with a 5′ untranslated region of 202 bp and a 3′ untranslated region of 1161 bp (this sequence is available from GenBank under accession no. AF144754). A poly-adenylation signal of AATAAA is present 19 bp upstream of the poly(A) tail. The predicted mature polypeptide is 77 amino acids in length containing four conserved cysteines with no ELR motif.

The putative signal peptide cleavage site between Gly22 and Ser23 was predicted by the hydrophobicity profile. The full-length sequence was then screened against the EMBL database using the BLAST program, and showed 92.6, 94 and 93.6% identity at the nucleotide level with human EST clones AA643952, AA865643 and HS1301003 respectively. A recently described human α-chemokine, BRAK, has 94% identity with KS1 at the protein level (20). The alignment of KS1, BRAK and other murine α-chemokines is shown in Fig. 1B. The phylogenetic relationship between KS1 and other α-chemokine family members was determined using the Phylip package (Fig. 1C). KS1 and BRAK demonstrate a high degree of divergence from the other α-chemokines supporting the relatively low homology shown in the multiple alignment.

Tissue expression of KS1 and BRAK

Tissue distribution of KS1 by Northern hybridization showed high expression in brain, ovary, lung and muscle, with low levels of expression in bone marrow. The transcript size on the Northern blot of 1.6 kb was the same size as the full-length cDNA sequence. BRAK was highly expressed in small intestine, colon and kidney, with moderate to low levels in liver, spleen, thymus, placenta, brain and pancreas. BRAK mRNA could also be detected in skeletal muscle and heart. Expression could not be detected in ovary, testis or prostate. The transcript size of BRAK was ~1.8 kb, which is similar to KS1 (Fig. 2B). As non-ELR α-chemokines have been implicated as having angiostatic properties, BRAK expression levels were tested in a variety of tumours and compared to normal tissue. BRAK was expressed in normal uterine and cervical tissue, whereas it was completely down-regulated in their respective tumours, uterine leiomyoma and cervical adenocarcinoma (Fig. 2C). Conversely, BRAK was expressed in breast tissue but was up-regulated in breast invasive ductal carcinoma (Fig. 2C).

Recombinant expression of KS1

Recombinant C-terminal $(His)_6$KS1 was a homogenous protein with an apparent molecular mass of 15 kDa (Fig. 3). Internal sequencing of the 15 kDa protein gave the peptide sequence WYNAWNEK, confirming that the observed sequence is identical to that predicted from the cDNA sequence. The isoelectric point was predicted to be 10.26 using DNASIS (Hitachi Software Engineering, Yokohama, Japan). Recombinant KS1Fc, expressed and purified using Protein A-affinity column chromatography, revealed a protein with a molecular mass of 43 kDa corresponding to the predicted size plus the Fc fusion tag (data not shown).

Flow cytometric analysis of KS1 binding

Fc tagged KS1 (KS1Fc) was used to determine the cell types which express the receptor for this chemokine. KS1Fc bound to 54% of splenocytes and 9% peripheral lymph node cells (Fig. 4A and B). No positive binding was identified in thymocytes (Fig. 4C). Dual labelling experiments with antibodies to cell surface antigens showed that KS1Fc bound B cells in spleen (Fig. 4D) but not CD4 or CD8 T cells (Fig. 4E and F). KS1Fc also bound to the B cells in peripheral lymph node cells but not the T cells (data not shown). The matched isotype control for CD19, CD8 and CD4, rIgG2a–FITC, showed no positive labelling (data not shown).

Additionally, we screened peritoneal exudate cells (PEC) to determine whether KS1Fc bound monocytes. Forward and side scatter histograms from PEC were used to identify the monocyte population in region H (Fig. 5A). Cells in region H were $CD19^-$ (Fig. 5B), but were MHC class II^+ (Fig. 5C) indicating that they were monocytes and not B cells. Dual labelling experiments showed that all the cells in region H were double positive for MHC class II and KS1Fc (Fig. 5D). The control protein, EGBFc, showed no binding to the MHC class II^+ cells from region H (Fig. 5E). The matched isotype control for MHC class II, mIgG2a–biotin, showed no positive labelling (Fig. 5F).

As many non-ELR chemokines stimulate activated T cells we analysed KS1Fc binding to Con A-activated splenocytes grown in the presence of 10 ng/ml IL-2 for 9 days. All cells were positive for the activation marker CD69, and consisted of 63% CD4 cells and 37% CD8 cells (data not shown). KS1Fc showed no positive binding to these cells (Fig. 6D). KS1Fc also bound to the murine B cell line, A20 (Fig. 6A), and the human B lymphoblastoid cell line, CESS (Fig. 6B). Additionally, KS1Fc bound to the monocyte leukemia cell line THP-1 (Fig. 6C) but not Jurkat T cells (Fig. 6E). Preliminary analysis identifies B cells and monocytes as responsive cells for KS1. To demonstrate specificity $(His)_6$KS1 was used in cold competition with KS1Fc against murine splenocytes. Increasing concentrations of $(His)_6$KS1 reduced the level of binding of KS1Fc (Fig. 7), as demonstrated by a decrease in the mean channel fluorescence, to murine splenocytes. An equivalent concentration of a non-specific $(His)_6$-tagged protein, GV14B, showed no decrease in mean channel fluorescence when co-incubated with KS1Fc (Fig. 7). The ability of $(His)_6$KS1 to competitively inhibit the binding of KS1Fc validates the hypothesis that this reagent bound via the KS1 receptor.

$(His)_6$KS1 induces chemotaxis in B cells and monocytes

Flow cytometric analysis revealed that KS1 specifically bound to B cells and monocytes. We determined whether KS1 could stimulate the chemotaxis of these cells using a modified Boyden chamber. $(His)_6$KS1 induced a concentration-dependant migration in murine splenocytes, with optimal activity at 100 ng/ml (Fig. 8A). In addition, $(His)_6$KS1 stimulated the migration of the B lymphoblastoid cell line, CESS, and the monocyte line, THP-1 (Fig. 8B and C). However, unlike SDF-1α, KS1 did not stimulate the migration of either human or murine activated T cells (Fig. 8D and E).

$(His)_6$KS1 induces inflammation in vivo

To determine whether KS1 was active *in vivo* and whether T cells are required for an inflammatory response we injected Nude mice s.c. with $(His)_6$KS1. Histological examination of mouse footpads injected s.c. with $(His)_6$KS1 showed a leukocyte infiltrate (Fig. 9A). The inflammation was of a mixed phenotype with evidence of mononuclear cells and polymorphonuclear cells (Fig. 9C and D). No obvious inflammation was apparent in the feet of mice injected with Tris, the buffer excipient (Fig. 9B). To confirm that this inflammation was due to $(His)_6$KS1 and not endotoxin we repeated the experiment

in LPS-insensitive C3H/HeJ mice. $(His)_6$KS1-injected footpads from these mice showed a similar inflammatory response to the Nude mice (Fig. 9E) with the buffer excipient-injected footpads having no marked inflammation (Fig. 9F).

Discussion

We have identified some of the biological activities of a novel non-ELR α-chemokine, KS1, and described its tissue distribution. The cDNA was similar to a recently cloned human gene called BRAK (20). Homology of KS1 to BRAK was 94% at the protein level, indicating it as the murine homologue of this gene. To date no known function has been described for BRAK. KS1 and BRAK appear to be distant relatives of the non-ELR α-chemokines as was shown by their phylogenetic relationship. There are five additional residues (KS1, SMSRY and BRAK, SVSRY), between cysteines 3 and 4 of the conserved cysteines, which is not consistent with the predicted Prosite motif for α-chemokines. The predicted N-terminus of the mature protein upstream of the first cysteine has only two residues in contrast to other non-ELR α-chemokines. Furthermore, KS1 has a lysine in place of an arginine immediately prior to the first cysteine. The conservation of a highly basic residue, typically arginine, prior to the first conserved cysteine has been postulated as a requirement for binding to the receptor (1). The amino acid substitutions between KS1 and BRAK in the mature peptide are conservative, indicating that these differences are likely to be insignificant.

KS1 tissue distribution in mouse and BRAK in human is unusual for α-chemokines in that it is highly expressed in normal non-lymphoid tissues. Although expression levels are different between mouse and human, KS1 and BRAK are expressed in brain and muscle. Differences between mouse and human expression profiles have been described for other chemokines (23–25), and are thought to reflect pathological changes of the particular donor. In contrast to the reported expression profile for BRAK (20), we found BRAK was expressed at higher levels in small intestine, colon and kidney. Additionally, the predominant band ran at 1.8 kb rather than 2.5 kb as reported earlier (20), raising the possibility of splice variance. Alternative splicing has previously been described as a property of some chemokines, for example LARC/MIP3α (23).

As non-ELR α-chemokines have been shown to have angiostatic function (15,16,26,27), we investigated BRAK expression in normal versus tumour tissue. The blot revealed that BRAK is expressed in non-malignant breast, uterine and cervical tissues. With good expression in human breast and kidney it is not surprising that BRAK was identified from breast and kidney EST. From the tumour expression data we saw two patterns emerge, either BRAK was up-regulated in breast invasive ductal carcinoma or, in the case of uterine leiomyoma and cervical adenocarcinoma, BRAK mRNA was undetectable. The reason for the disparate trends in expression levels from the different tumours is unclear at this stage and may be related to differences in cancer pathology. Furthermore, these biopsies were likely derived from a single patient and may not reflect the majority of cases. Nevertheless, it would be of interest to determine whether BRAK added directly to tumour models of these cancers could alter malignancy.

KS1 had a predicted size of 9.4 kDa; however, the purified $(His)_6$KS1 protein had an apparent size of 15 kDa which could not be accounted for by the additional histidine residues. This discrepancy between the predicted and apparent size has previously been reported for a number of chemokines (28,29), and is thought to be due to the highly basic nature of these proteins.

The high degree of homology between KS1 and BRAK suggested that they would be active on both mouse and human cell types. This was demonstrated by flow cytometric analysis which showed that KS1 binds directly to mouse and human B cells and monocytes. Furthermore, KS1 induced chemotaxis on both mouse and human cells. This phenomenon of rodent chemokines stimulating human cells has been previously described for a number of different chemokines (30–32). We clearly defined B cells and monocytes, and not T cells, as target cells for KS1 by binding studies. The only other non-ELR α-chemokine to bind to these cells is SDF-1α; however, SDF-1α also binds to T cells (17,18,33). We were able to confirm that KS1 stimulates B cells and monocytes but not T cells in migration assays using a range of different cell types. In the case of splenocytes and THP-1 cells, SDF-1α and KS1 stimulated equivalent levels of migration; however, CESS cells were 15-fold more responsive to SDF1α than KS1.

As the *in vitro* data indicated that B cells and monocytes respond to KS1, we tested its inflammatory properties by injecting Nude mice with the protein. Mice injected s.c. with $(His)_6$KS1 showed a mixed inflammatory response. As Nude mice have no T cells this supported the *in vitro* data that $(His)_6$KS1 promotes extravasation of cells other than T cells. As seen with the Nude mice, C3H/HeJ also had an inflammatory response to $(His)_6$KS1, demonstrating that the response in the Nude mice was $(His)_6$KS1 specific and not due to endotoxin. Although we have demonstrated the ability of KS1 to stimulate chemotaxis of B cells and monocytes, we do not rule out the possibility that other haemopoetic or non-haemopoetic cells might respond to KS1.

The majority of non-ELR α-chemokines have been shown to be chemotactic for activated T cells; however, KS1 did not cause the migration of these cells. Therefore, this raises the question of which receptor does KS1 utilize? There are currently only three known chemokine receptors that bind non-ELR α-chemokines: CXCR3, the receptor for I-TAC (12), Mig and IP-10 (34); CXCR4, the receptor for SDF-1α (17,18); and CXCR5, the receptor for BCA-1 (13). As we have shown that KS1 does not stimulate T cells it is unlikely that it is binding via CXCR4. Furthermore, it is unlikely to bind via CXCR3, a receptor on activated T cells, as we can demonstrate no activity on Con A IL-2-activated T cells. This then leaves CXCR5; however, this receptor has only been demonstrated on B cells and not monocytes. Therefore, the likelihood of KS1 acting via a novel receptor merits further investigation.

The biological function of a novel chemokine, initially identified as KS1, is described. KS1 has a broad expression in non-lymphoid tissue, altered expression levels in tumours and a role in trafficking of B cells and monocytes. Therefore, we propose the name B cell- and monocyte-activating chemokine

(BMAC) for this molecule to reflect its described biological functions

Acknowledgements

We are grateful to Dr Paul Tan for his helpful comments with the manuscript, Dr Matthew Glenn and Dr Ilkka Havukkala for maintenance of the EST database, and Stewart Whiting for managing the animal facility. We are also grateful to Dr Annette McGrath for assistance with the bioinformatic analysis. We also appreciate the support of the Functional Genomics group at Genesis Research and Development Corp. Ltd, Auckland, NZ and Immunex Corp., Seattle, WA.

Abbreviations

BMAC	B cell- and monocyte-activating chemokine
Con A	concanavalin A
ELR	Glu–Leu–Arg
MIP	macrophage inflammatory protein
PBMC	peripheral blood mononuclear cells
PE	phycoerythrin
PEC	peritoneal exudate cells
PHA	phytohaemagglutinin

References

1 Baggiolini, M., Dewald, B. and Moser, B. 1997. Human chemokines: an update. *Annu. Rev. Immunol.* 15:675.
2 Rollins, B. J. 1997. Chemokines. *Blood* 90:909.
3 Gale, L. M. and McColl, S. 1999. Chemokines: extracellular messengers for all occasions? *BioEssays* 21:17.
4 Walz, A., Peveri, P., Aschauer, H. and Baggiolini, M. 1987. Purification and amino acid sequencing of NAF, a novel neutrophil activating factor produced by monocytes. *Biochem. Biophys. Res. Commun.* 149:755.
5 Yoshimura, T., Matsushima, K., Tanaka, S., Robinson, E. A., Appella, E., Oppenheim, J. J. and Leonard, E. J. 1987. Purification of a human monocyte derived neutrophil chemotactic factor that has peptide sequence similarity to other host defense cytokines. *Proc. Natl Acad. Sci. USA* 84:9233.
6 Schroder, J.-M., Mrowietz, U., Morita, E. and Christophers, E. 1987. Purification and partial biochemical characterization of a human monocyte derived, neutrophil-activating peptide that lacks interleukin 1 activity. *J. Immunol.* 139:3474.
7 Deuel, T. F., Senior, R. M., Chang, D., Griffin, G. L., Henrikson, R. L. and Kaiser, E. T. 1981. Platelet factor 4 is chemotactic for neutrophils and monocytes. *Proc. Natl Acad. Sci. USA* 78:4584.
8 Luster, A. D., Unkeless, J. C. and Ravetch, J. V. 1985. Gamma-interferon transcriptionally regulates an early-response gene containing homology to platelet proteins *Nature* 315:672.
9 Luster, A. D. and Ravetch, J. V. 1987. Biochemical characterization of a γ-interferon inducible cytokine (IP-10). *J. Exp. Med.* 166:1098.
10 Farber, J. M. 1993. HuMIG: a new human member of the chemokine family of cytokines. *Biochem. Biophys. Res. Commun.* 192:223.
11 Nagasawa, T., Kikutani, H. and Kishimoto, T. 1994. Molecular cloning and structure of a pre-B-cell growth-stimulating factor. *Proc. Natl Acad. Sci. USA* 91:2305.
12 Cole, K. E., Strick, C. A., Paradis, T. J., Ogborne, K. T., Loetscher, M., Gladue, R. P., Lin, W., Boyd, J. G., Moser, B., Wood, D. E., Sahagan, B. G. and Neote, K. S. 1998 Interferon-inducible T cell alpha chemoattractant (I-TAC): a novel non-ELR CXC chemokine with potent activity on activated T cell through selective high affinity binding to CXCR3. *J. Exp. Med.* 187:2009.
13 Legler, D. F., Loestcher, M., Roos, R. S., Clark-Lewis, I., Baggiolini, M. and Moser, B. 1998. B cell-attracting chemokine 1, a human CXC chemokine expressed in lymphoid tissues, selectively attracts B lymphocytes via BLR1/CXCR5. *J. Exp. Med.* 187:655.
14 Maione, T. E., Gray, G. S., Petro, J., Hunt, A. J., Donner, A. L., Bauer, S. I., Carson, H. F. and Sharpe, R. J. 1990. Inhibition of angiogenesis by recombinant human platelet factor-4 and related peptides. *Science* 247:77.
15 Angiolillo, A. L., Sgadari, C., Taub, D. D., Liao, F., Farber, J. M., Maheshwari, S., Kleinman, H. K., Reaman, G. H. and Tosato, G. 1995. Human interferon-inducible protein 10 is a potent inhibitor of angiogenesis *in vivo*. *J. Exp. Med.* 182:155.
16 Sgadari, C., Farber, J. M., Angiolillo, A. L., Liao, F., Teruya-Feldstein, J., Burd, P. R., Yao, L., Gupta, G., Kanegane, C. and Tosato, G. 1997. Mig, the monokine induced by interferon γ, promotes tumour necrosis *in vivo*. *Blood* 89:2635.
17 Bleul, C. C., Farzan, M., Choe, H., Parolin, C., Clark-Lewis, I., Sodroski, J. and Springer, T. A. 1996. The lymphocyte chemoattractant SDF-1 is a ligand for LESTR/fusin and blocks HIV-1 entry. *Nature* 382:829.
18 Oberlin, E., Amara, A., Bachelerie, F., Bessia, C., Virelizier, J. L., Arenzana-Seisdedos, F., Schwartz, O., Heard, J. M., Clark-Lewis, I., Legler, D. F., Loetscher, M., Baggiolini, M. and Moser, B. 1996. The CXC chemokine SDF-1 is the ligand for LESTR/fusin and prevents infection by T-cell-line-adapted HIV-1. *Nature* 382:833.
19 Zagury, D., Lachgar, A., Chams, V., Fall, L. S., Bernard, J., Zagury, J. F., Bizzini, B., Gringeri, A., Santagostino, E., Rappaport, J., Feldman, M., O'Brien, S. J., Burny, A. and Gallo, R. C. 1998. C–C chemokines, pivotal in protection against HIV type 1 infection. *Proc. Natl Acad. Sci. USA* 95:3857.
20 Hromas, R., Broxmeyer, H. E., Kim, C., Nakshtri, H., Christopherson, K., II, Azam, M. and Hou, Y.-H. 1999. Cloning of BRAK, a novel divergent CXC chemokine preferentially expressed in normal versus malignant cells. *Biochem. Biophys. Res. Commun.* 255:703.
21 Altschul, S. F., Gish, W., Miller, W., Myers, E. W. and Lipman, D. J. 1990. Basic local alignment search tool. *J. Mol. Biol.* 215:403.
22 Sambrook, J., Fritsch, E. F. and Maniatis, T. 1989. *Molecular Cloning: A Laboratory Manual*, 2nd edn, p. 7.39. Cold Spring Harbor Laboratory Press, Cold Spring Harbor, NY.
23 Tanaka, Y., Imai, T., Baba, M., Ishikawa, I., Uehira, M., Nomiyama, H. and Yoshie, O. 1999. Selective expression of liver and activation-regulated chemokine (LARC) in intestinal epithelium in mice and humans. *Eur. J. Immunol.* 29:633
24 Hromas, R., Gray, P. W., chantry, D., godiska, R., Krathwohl, M., Fife, K., Bell, G. I., takeda, J., Aronica, S., Gordon, M., Cooper, S., Broxmeyer, H. E. and Klemsz, M. J. 1997. Cloning and characterization of exodus, a novel beta-chemokine. *Blood* 89:3315.
25 Hieshima, K., Imai, T., Opdenakker, G., van Damme, J., Kusuda, J., tei, H., Sakaki, Y., Takatsuki, K., Miura, R., Yoshie, O. and Nomiyama, H. 1997. Molecular cloning of a novel CC chemokine liver and activation-regulated chemokine (LARC) expressed in liver. Chemotactic activity for lymphocytes and gene localization on chromosome 2. *J. Biol. Chem.* 272:5846.
26 Tannenbaum, C. S., Tubbs, R., Armstrong, D., Finke, J. H., Bokowski, R. M. and Hamilton, T. A. 1998. The CXC chemokine IP-10 and Mig are necessary for IL-12 mediated regression of the mouse RENCA tumour. *J. Immunol.* 161:927.
27 Kanegane, C., Sgadari, C., Kanegane, H., Teruya-Feldstein, J., Yao, L., Gupta, G., Farber, J. M., Liao, F., Liu, L. and Tosato, G. 1998. Contribution of the CXC chemokines IP-10 and Mig to the antitumor effects of IL-12. *J. Leuk. Biol.* 64:384.
28 Richmond, A., Balentien, E., Thomas, H. G., Flaggs, G., Barton, D. E., Spiess, J., Bordoni, R., Francke, U. and Derynck, R. 1988. Molecular characterization and chromosomal mapping of melanoma growth stimulatory activity, a growth factor structurally related to β-thromboglobulin. *EMBO J.* 7:2025.
29 Liao, F., Rabin, R. L., Yannelli, J. R., Koniaris, L. G., Vanguri, P. and Farber, J. M. 1995 Human Mig: biochemical and functional characterization. *J. Exp. Med.* 182:1301.
30 Wuyt, A., Haelens, A., Proost, P., Lenaerts, J. P., Conings, R., Opdenakker, G. and van Damme, J. 1996. Identification of mouse granulocyte chemotactic protein-2 from fibroblasts and epithelial cells. Functional comparison with natural KC and macrophage inflammatory protein-2. *J. Immunol.* 157:1736.
31 Abdullah, F., Ovadia, P., Feuerstein, G., Neville, L. F., Morrison,

R., Mathiak, G., Whiteford, M. and Rabinovici, R. 1997. The novel chemokine mob-1: involvement in adult respiratory distress syndrome. *Surgery* 122:303.

32 Patel, V. P., Kreider, B. L., Li, Y., Li, H., Leung, K., Salcedo, T., Nardelli, B., Pippalla, V., Gentz, S., Thotakura, R., Parmelee, D., Gentz, R. and Garotta, G. 1997. Molecular and functional characterization of two novel human C–C chemokines as inhibitors of two distinct classes of myeloid progenitors. *J. Exp. Med.* 185:1163.

33 Bleul, C. C., Fuhlbrigge, R. C., Casasnovas, J. M., Aiuti, A. and Springer, T. A. 1996. A highly efficacious lymphocyte chemoattractant, stromal cell-derived factor 1 (SDF-1). *J. Exp. Med.* 184:1101.

34 Weng, Y., Siciliano, S. J., Waldburger, K. E., Sirotina-Meisher, A., Staruch, M. J., Daugherty, B. L., Gould, S. L., Springer, M. S. and DeMartino, J. A. 1998. Binding and functional properties of recombinant and endogenous CXCR3 chemokine receptors. *J. Biol. Chem.* 273:18288.

[CANCER RESEARCH 64, 8262–8270, November 15, 2004]

BRAK/CXCL14 Is a Potent Inhibitor of Angiogenesis and a Chemotactic Factor for Immature Dendritic Cells

Thomas D. Shellenberger,[1] Mary Wang,[1] Manu Gujrati,[4] Arumugam Jayakumar,[1] Robert M. Strieter,[5] Marie D. Burdick,[5] Constantin G. Ioannides,[2] Clayton L. Efferson,[2] Adel K. El-Naggar,[3] Dianna Roberts,[1] Gary L. Clayman,[1] and Mitchell J. Frederick[1]

Departments of [1]Head and Neck Surgery, [2]Gynecologic Oncology, and [3]Molecular Pathology, University of Texas M.D. Anderson Cancer Center, Houston, Texas; [4]Department of Otorhinolaryngology, University of Kentucky, Lexington, Kentucky; and [5]Department of Medicine, Division of Pulmonary and Critical Care Medicine, University of California, Los Angeles, California

ABSTRACT

BRAK/CXCL14 is a CXC chemokine constitutively expressed at the mRNA level in certain normal tissues but absent from many established tumor cell lines and human cancers. Although multiple investigators cloned BRAK, little is known regarding the physiologic function of BRAK or the reason for decreased expression in cancer. To understand the possible significance associated with loss of BRAK mRNA in tumors, we examined the pattern of BRAK protein expression in normal and tumor specimens from patients with squamous cell carcinoma (SCC) of the tongue and used recombinant BRAK (rBRAK) to investigate potential biological functions. Using a peptide-specific antiserum, abundant expression of BRAK protein was found in suprabasal layers of normal tongue mucosa but consistently was absent in tongue SCC. Consistent with previous *in situ* mRNA studies, BRAK protein also was expressed strongly by stromal cells adjacent to tumors. In the rat corneal micropocket assay, BRAK was a potent inhibitor of *in vivo* angiogenesis stimulated by multiple angiogenic factors, including interleukin 8, basic fibroblast growth factor, and vascular endothelial growth factor. *In vitro*, rBRAK blocked endothelial cell chemotaxis at concentrations as low as 1 nmol/L, suggesting this was a major mechanism for angiogenesis inhibition. Although only low affinity receptors for BRAK could be found on endothelial cells, human immature monocyte-derived dendritic cells (iDCs) bound rBRAK with high affinity (*i.e.*, K_d, ~2 nmol/L). Furthermore, rBRAK was chemotactic for iDCs at concentrations ranging from 1 to 10 nmol/L. Our findings support a hypothesis that loss of BRAK expression from tumors may facilitate neovascularization and possibly contributes to immunologic escape.

INTRODUCTION

To identify genes associated with the malignant phenotype of head and neck squamous cell carcinoma (SCC), we previously used differential display of matched tumor explants and normal oral squamous epithelial cells. One of the genes down-regulated in tumor specimens was BRAK/CXCL14, which encodes a novel chemokine (1). BRAK was independently cloned by Hromas *et al.* (2) and was found in normal kidney and breast tissues but was absent in the majority of established tumor cell lines. The work of multiple investigators (1–4) formed an early consensus that BRAK mRNA was constitutively expressed in normal tissues but was absent in a variety of transformed cells. The absence of BRAK from many tumor cell lines (1, 2) and head and neck SCC tumor specimens (1) is of currently unknown biological significance. Moreover, little is known regarding the physiologic functions of this gene.

To date, three groups of investigators have examined the chemotactic properties of BRAK for leukocytes and reported disparate results. Among cells proposed to respond to BRAK by various investigators are prostaglandin E_2–treated monocytes (5), cell lines from B-cell and monocytic cell lineages (3), neutrophils, and dendritic cells (4). A plausible explanation for the lack of agreement could be the different sources of BRAK used by investigators, which included a synthetic polypeptide, a murine homologue, and unpurified conditioned supernatants from transfected mammalian cells. The recent availability of commercially purified recombinant human BRAK (rBRAK) should allow for better study of the physiologic targets and functions of the *BRAK* gene.

Although there are few published articles focusing on BRAK, one common finding appears to be the persistent absence of BRAK mRNA from established tumor cell lines despite constitutive expression in normal tissues. Consistent with these findings, we previously showed by *in situ* hybridization that BRAK mRNA is abundantly expressed in normal squamous mucosa but absent from a majority of head and neck SCC tumors (1). A role for chemokines in cancer is supported by evidence that these molecules can regulate fundamental biological processes, including tumor-associated angiogenesis, activation of host tumor-specific immunity, and autocrine stimulation of tumor growth (6–12).

Chemokines are classified into subfamilies based on variations in a structural motif of conserved aminoproximal cysteine residues and include the CXC, CC, CX_3C, and the C families. BRAK belongs to the CXC family, which can be further subdivided by the presence or absence of a conserved "Glu-Leu-Arg" (ELR) motif at the NH_2 terminus. ELR(+) CXC chemokines, such as GRO-α/CXCL1, IL-8/CXCL8, and ENA-78/CXCL5, are angiogenic, whereas ELR(−) CXC chemokines induced by interferon, such as PF-4/CXCL4, IP-10/CXCL10, and MIG/CXCL9, are angiostatic (10, 13–16). Although not induced by interferon (1), BRAK does lack an ELR motif similar to the angiostatic CXC chemokines. However, the role of BRAK in the regulation of angiogenesis remains to be established.

Chemokine action is mediated via members of the seven-transmembrane domain G protein–coupled receptors, which bind multiple ligands within chemokine subfamilies (17, 18). However, the receptors and mechanisms by which chemokines inhibit chemotaxis of endothelial cells currently are unknown. Although the angiostatic chemokines γ-interferon–inducible protein (IP-10), MIG, and I-TAC mediate chemotaxis of activated T cells through binding the high affinity chemokine receptor CXCR3 (19), there is little evidence that CXCR3 is involved in inhibition of endothelial cell chemotaxis. Although endothelial cells reportedly express low levels of CXCR3 (20, 21), a recent publication suggests that only the mRNA splice variant termed CXCR3B is present in these cells (22). This putative receptor was reported to mediate growth arrest of endothelial cells in response to PF-4 and IP-10. However, a role

Received 6/10/04; revised 8/9/04; accepted 9/8/04.

Grant support: The University of Texas M.D. Anderson Cancer Center SPORE in Head and Neck Cancer Development Award, P50 CA97007.

The costs of publication of this article were defrayed in part by the payment of page charges. This article must therefore be hereby marked *advertisement* in accordance with 18 U.S.C. Section 1734 solely to indicate this fact.

Note: Supplementary data for this article can be found at Cancer Research Online (http://cancerres.aacrjournals.org).

Requests for reprints: Mitchell J. Frederick, Department of Head and Neck Surgery, University of Texas M.D. Anderson Cancer Center, 1515 Holcombe Boulevard, Houston, TX 77030. E-mail: mfrederi@mdanderson.org.

for CXCR3B in inhibition of endothelial chemotaxis has not been investigated. The chemokine receptor that binds BRAK currently has not been identified.

On the basis of the loss of BRAK mRNA in head and neck SCC, as well as a structural relationship to other angiostatic CXC chemokines, we hypothesized that BRAK might inhibit angiogenesis. In this report, we examine the expression of BRAK protein in SCC of the tongue and confirm the antiangiogenic effect of this chemokine. We also show that rBRAK is a potent chemoattractant for human immature monocytic-derived dendritic cells (iDCs) through a specific high affinity receptor for BRAK.

MATERIALS AND METHODS

Reagents. Recombinant human cytokines including rBRAK, interleukin 8 (IL-8), vascular endothelial growth factor (VEGF), basic fibroblast growth factor (bFGF), IP-10, stromal cell–derived factor 1 (SDF-1), BLC/BCA, macrophage inflammatory protein 1α (MIP-1α), monocyte chemoattractant protein 1 (MCP-1), RANTES, TARC, MIP-3α, and MIP-3β were obtained from Peprotech (Rocky Hill, NJ). Human BRAK was iodinated by Amersham Biosciences (Piscataway, NJ) to a specific activity of 1250 Ci/mmol using the lactoperoxidase method. The [^{125}I]–IL-8 (2200 Ci/mmol) and [^{125}I]-Bolton Hunter–labeled IP-10 (2200 Ci/mmol) were purchased from Perkin-Elmer Life Sciences (Boston, MA), and [^{125}I]-bFGF (1000 Ci/mmol) was from Amersham Biosciences.

Immunohistochemistry. Rabbit antiserum to BRAK was raised against two synthetic peptides derived from the amino and COOH-terminal sequence of BRAK, which contained minimal homology to other chemokines. Whole antiserum was affinity purified using the synthetic peptides and confirmed to specifically react with BRAK and not other chemokines by Western blot analysis (data not shown). Immunohistochemistry was performed using reagents supplied in an alkaline phosphatase rabbit Vectastain ABC kit (Vector Labs, Burlingame, CA). Cryostat sections were fixed in cold acetone, washed, incubated in PBS containing 0.05% Triton X-100, and blocked overnight at 4°C with normal goat serum blocking solution. After a PBS/Triton wash, sections were incubated in avidin blocking solution (Vector Labs), washed again in PBS/Triton, and further incubated in biotin blocking solution (Vector Labs). Following additional washes, sections were incubated with rabbit anti-BRAK or normal rabbit IgG at a final concentration of 3 μg/mL in PBS/Triton at 4°C overnight. Sections then were rinsed in PBS/Triton, incubated with biotinylated goat antirabbit serum for 30 minutes, washed in PBS, and incubated with Avidin:Biotinylated enzyme complex reagent. After rinsing with water, sections were incubated with 5-bromo-4-chloro-3-indolyl phosphate/nitroblue tetrazolium substrate, counterstained with nuclear fast red, dehydrated, and mounted under coverslips. The specificity of the antibody in immunohistochemistry was validated by preincubating anti-BRAK antiserum with a 500-fold molar excess of immunizing BRAK peptides.

Cell Lines and Cell Cultures. Primary cultures of human umbilical vein endothelial cells (HUVECs) and human dermal microvascular endothelial cells (HMECs) were purchased from Cambrex Biosciences (Walkersville, MD), maintained in medium 131 plus microvascular growth supplement (Cascade Biologicals, Portland, OR), and cultured on gelatin-coated flasks. Murine lung microvascular endothelial cells (LEII), provided by Dr. Kari Alitalo (Helsinki, Finland), were grown in Dulbeco's modified Eagle's medium (DMEM) supplemented with 10% fetal bovine serum (FBS). The iDCs were derived from peripheral blood monocytes as described previously (23). In brief, mononuclear cells from healthy volunteers were isolated over Histopaque, labeled with CD14 microbeads (Miltenyi Biotec, Auburn, CA), the CD14-positive population isolated with an MACS LS separation column (Miltenyi Biotec), and placed in a magnetic field. Purified CD14-positive cells (1×10^6/mL) were cultured in RPMI containing 10% FBS, 1000 units/mL IL-4 (R&D Systems, Minneapolis, MN), and 1050 units/mL granulocyte macrophage colony-stimulating factor (R&D Systems) for 6 to 7 days. By adding lipopolysaccharide (1 μg/mL) on day 4 of culture, mature dendritic cells were generated. Dendritic cells were phenotyped by staining with phycoerythrin-conjugated anti-CD83, allophycocyanin–conjugated anti-CD14, and FITC-conjugated anti-CD1a (all obtained from PharMingen, San Diego, CA). The iDCs were typically CD14 negative, CD83 negative, and 95% CD1a positive by flow cytometry, whereas mature dendritic cells were >80% CD83/CD1a positive and CD14 negative.

Chemotactic Assays. *In vitro* endothelial chemotaxis assays were performed in a 48-well chemotaxis chamber (Neuro Probe, Gaithersburg, MD) using an 8-μm pore-sized filter precoated with type IV collagen. Cytokines known to stimulate migration of endothelial cells (IL-8, bFGF, or VEGF) were added at 10 ng/mL to the bottom wells of chemotaxis chambers containing assay medium, rBRAK, or IP-10. Following starvation in DMEM containing 0.1% FBS for 2 hours, HUVECs or HMECs were trypsinized, seeded at 12,500 cells per well in the upper chamber, and allowed to migrate for 4 hours at 37°C. Unmigrated cells were scraped from the tops of filters, which were fixed, stained with Dif Quik (Baxter Scientific, Deerfield, IL), and mounted under oil immersion. Migratory cells were counted from nine random high-power fields from each well. The mean counts of cells from multiple wells were averaged and plotted graphically along with the SE of the means. Chemotaxis assays were repeated at least three times. Results were analyzed for significance using the honest statistical difference test of unequal Ns.

Chemotaxis of dendritic cells also was measured in a microchemotaxis chamber using an 8-μm pore-sized polyvinyl pyrrolidone-free filter (uncoated). Assay media alone or in combination with rBRAK or MIP-1α were placed in the bottom wells. Dendritic cells were seeded at 50,000 cells per well in the upper chambers and allowed to migrate for 90 minutes at 37°C. To determine the effects of abolishing the chemotactic gradient, rBRAK was added to the upper and lower wells of the chemotactic chamber. In other experiments, dendritic cells were pretreated overnight with 100 ng/mL pertussis toxin. Fixation, mounting, cell counting, and statistical analysis were performed as described for endothelial cells.

Rat Corneal Micropocket Assay. *In vivo* angiogenesis was examined using a modification of the rat corneal micropocket assay as described previously (24). Essentially, 5 μL hydron pellets were prepared with cytokines (maintaining a polymer to cytokine ratio of 4:1) and polymerized overnight in the presence of UV light. Male Long Evans rats (2 months old) were anesthetized via intraperitoneal injection of mixture containing ketamine (63 mg/mL), atropine (0.7 mg/mL), and xylazine (3.6 mg/mL) in a volume to deliver a ketamine dose of 150 mg/kg body weight. An ophthalmic solution of 0.5% proparacaine hydrochloride was applied to corneas for local anesthesia, and corneal micropockets were created using microsurgical technique. Six days following implantation of rehydrated pellets, rats were reanesthetized with ketamine/atropine/xylazine mixture, given 0.2 mL of heparin (5000 units/mL) intraperitoneally, perfused with 10 mL of a 1:1 solution of colloidal carbon (Sanford Design Higgins Waterproof Drawing Ink, black India 4415; Sanford, Bellwood, IL) and normal saline via direct intracardiac injection, and sacrificed. Globes were harvested and fixed in 4% paraformaldehyde overnight. Dissected corneas were mounted and imaged with a microscope equipped with a digital camera.

Image analysis was carried out using Image Pro Plus software (Media Cybernetics, Silver Spring, MD) to measure the area of neovascularization and calculate the total vascularity by summing the pixel intensities over the area of neovascularization. Data were analyzed using a one-way ANOVA test. All of the animals were handled in accordance with the University of Texas/M.D. Anderson Department of Veterinary Medicine, and an Institutional Animal Care Use Committee approved the procedures.

The optimal dose of angiogenic cytokine per pellet was determined to be 100 ng for IL-8, 50 ng for bFGF, and 200 ng for VEGF. Pellets containing angiogenic cytokines alone were implanted into the right eyes of rats, whereas pellets containing the combination of angiogenic cytokines plus rBRAK were placed into the opposite eye (*i.e.*, left eye) of the same animals.

Competitive Binding Assays. HUVECs and HMECs were plated at 75,000 cells per well in 24-well plates and left in growth medium overnight at 37°C. Before experiments, cells were washed twice with PBS and once with wash buffer containing 50 mmol/L HEPES, 1 mmol/L calcium chloride, 5 mmol/L magnesium chloride, 500 mmol/L sodium chloride, and 1% bovine serum albumin (BSA) adjusted to pH 7.4. Cells then were incubated with 0.1 nmol/L [^{125}I]-BRAK, [^{125}I]–IP-10, or [^{125}I]-FGF and increasing concentrations of unlabeled rBRAK, IP-10, bFGF, or heparin sodium in binding buffer (wash buffer containing no sodium chloride) for 2 hours at 4°C. Cells then were washed three times, and bound radioactivity extracted with 1 N sodium hydroxide was measured in a gamma counter. In some experiments, the concentration of NaCl in washes was changed to either 0.15 mol/L (to detect

low affinity receptors) or 2 mol/L NaCl (to detect high affinity receptors). Total binding was determined in the absence of unlabeled ligand. Nonspecific binding was determined in an excess (*i.e.*, 1 μmol/L) of unlabeled ligand and was usually <20% total binding. Percent specific binding then was calculated using the formula:

$$\%\text{Specific binding} = \frac{\text{Sample counts} - \text{NSB}}{\text{Total binding} - \text{NSB}} \times 100\%$$

Values for the K_d and maximum number of receptors per cell (β_{max}) were calculated using GraphPad Prism V4.0 software (GraphPad Software, Inc., San Diego, CA). Binding of [^{125}I]-FGF to LEII cells was essentially as described for HUVECs, except assays were performed in six-well plates containing 500,000 cells/plate, and wash buffer routinely contained 2 mol/L NaCl to remove ligand from low affinity sites.

Binding assays for dendritic cells were performed as described previously for nonadherent cells (25). In brief, cells were washed in PBS and resuspended to obtain 750,000 cells/100 μL of binding buffer containing 75 mmol/L HEPES, 1 mmol/L calcium chloride, 5 mmol/L magnesium chloride, 150 mmol/L sodium chloride, and 1% BSA at a pH of 7.4. The cell suspension was incubated with 0.5 nmol/L [^{125}I]-BRAK and either increasing concentrations of unlabeled BRAK or 25 nmol/L unlabeled chemokines for 90 minutes at 4°C. Following incubation, the binding reaction was centrifuged through a binding column containing a 300 μL mixture of pthalate and bispthalate oil (4:1) to separate cells from unbound radiolabeled ligand. Binding columns were snap frozen in a dry ice/EtOH bath, and the bottoms containing the cell pellet were cut off for counting in a gamma counter.

Binding to Immobilized IL-8 and bFGF. Binding assays were performed on immobilized cytokines as described previously (26). Ninety-six–well HB isoplates (Perkin-Elmer) were coated with 15 ng of IL-8 or bFGF in 100 μL of 0.1 mol/L carbonate buffer (pH 8.5) overnight at 4°C. Plates then were washed three times with PBS containing 0.05% Tween-20 and once with PBS alone. Blocking was performed with 1% BSA in PBS for 2 hours at room temperature, followed by three washes with PBS/Tween-20 and an additional PBS wash. Fifty microliters of a 0.1% BSA solution in PBS with or without unlabeled competitor ligands at various concentrations then were added to the plate. Subsequently, 50 μL of PBS/0.1% BSA containing 4 nmol/L [^{125}I]-BRAK was added to each well. After 1 hour at 37°C, the plate was washed four times with 0.05% Tween-20 in PBS; scintillation fluid was added to the wells; and the radioactivity was counted in a MicroBeta TriLux scintillation counter (Perkin-Elmer).

RESULTS

BRAK Protein Is Abundantly Expressed in Normal Mucosa and Absent from SCC Tumors of the Tongue. Our previous demonstration that BRAK mRNA is abundant in normal squamous mucosa but absent from many head and neck SCC tumors (1) led to our analysis of BRAK protein expression in tumor specimens. Immunohistochemistry with antiserum raised against BRAK peptides was performed on frozen section specimens of tumor and adjacent normal tissue derived from patients with SCC of the tongue. Intense staining for BRAK protein was observed in the suprabasal layers of histologically normal squamous epithelium of tongue (Fig. 1*A*) but found to be virtually absent in an adjacent SCC of the tongue from the same patient (Fig. 1*C*). Control normal rabbit immunoglobulin in the absence of BRAK antiserum showed negative staining (Fig. 1*B* and *D*). Similar results showing intense suprabasal expression of BRAK in normal squamous epithelium of tongue were observed in an additional three patients, whereas BRAK staining was weak or absent in six of eight tongue SCC samples examined (data not shown). The specificity of the BRAK antiserum was confirmed by preincubating specimens of normal mucosa with antiserum in the presence of a 500-fold molar excess of immunizing peptides, which led to a substantial reduction in staining intensity (See Supplementary Fig. 1). Strong expression of BRAK protein also was observed in stromal fibroblasts adjacent to nests of tongue SCC that were clearly negative for BRAK (See Supplementary Fig. 2).

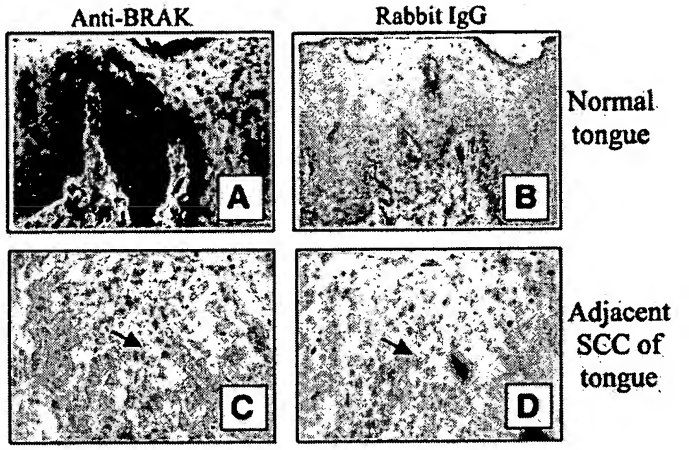

Fig. 1. BRAK protein expression is abundant in normal tongue but absent from SCC of the tongue. Cryostat sections containing normal tongue (*A, B*) or adjacent SCC of the tongue (*C, D*) from the same patient were incubated with rabbit anti-BRAK serum (*A, C*) or control normal rabbit IgG (*B, D*). The center of a tumor nest is indicated by an arrow.

rBRAK Protein Inhibits Chemotaxis of Human Endothelial Cells Stimulated by IL-8, bFGF, and VEGF. We investigated the effects or rBRAK on migration of HUVECs and HMECs *in vitro*. Initial findings indicated that rBRAK did not stimulate the chemotaxis of either of these human endothelial cells. Therefore, we examined whether rBRAK would block chemotaxis of endothelial cells stimulated by IL-8, bFGF, and VEGF. In HUVECs, profound inhibition of the chemotactic response stimulated by IL-8 (Fig. 2*A*) or bFGF (Fig. 2*B*) occurred at rBRAK concentrations of 10 ng/mL ($P < 0.008$), 50 ng/mL ($P < 0.0002$), or 100 ng/mL ($P < 0.0002$). In HMECs, a similar profound inhibition of the chemotactic response stimulated by either cytokine (Fig. 2*C* and *D*) occurred at all three concentrations of rBRAK ($P < 0.0002$). The potency of rBRAK inhibition is shown alongside that of IP-10, a member of the CXC subfamily that is known to block endothelial cell migration (ref. 27; Fig. 2). Complete inhibition of chemotaxis was shown at 100 ng/mL rBRAK by the reduction of migrating cells to the level of control conditions without cytokine. The inhibitory response in HUVECs was concentration dependent and reached maximal inhibition at 100 ng/mL. However, in HMECs a nearly complete inhibitory response was reached at the lowest concentration of 10 ng/mL (*i.e.*, 1 nmol/L), and inhibition persisted at higher concentrations. Nearly identical results were found for the inhibition of chemotaxis stimulated by VEGF at the same rBRAK concentrations (data not shown). Chemotactic assays were repeated a minimum of three times, with similar results obtained.

rBRAK Protein Inhibits Angiogenesis in the Rat Corneal Micropocket Assay. Our findings in endothelial cell migration led us to investigate the effects of rBRAK on angiogenesis *in vivo* using a rat corneal micropocket assay. Because rBRAK did not stimulate angiogenesis in the rat cornea, we studied the effects of rBRAK in the presence of cytokines known to stimulate angiogenesis, including IL-8 (27), bFGF (28), and VEGF (29). In the corneal micropocket assay, rBRAK profoundly inhibited the angiogenic response stimulated by IL-8, bFGF, or VEGF.

The typical dense angiogenic response to 100 ng IL-8 alone is shown in Fig. 3 (*top*), in which IL-8 alone was implanted in the right eye of the animal, whereas inhibition of the response is shown in the animal's left eye, in which 100 ng of rBRAK was combined with IL-8. Similar results were found with inhibition of angiogenesis

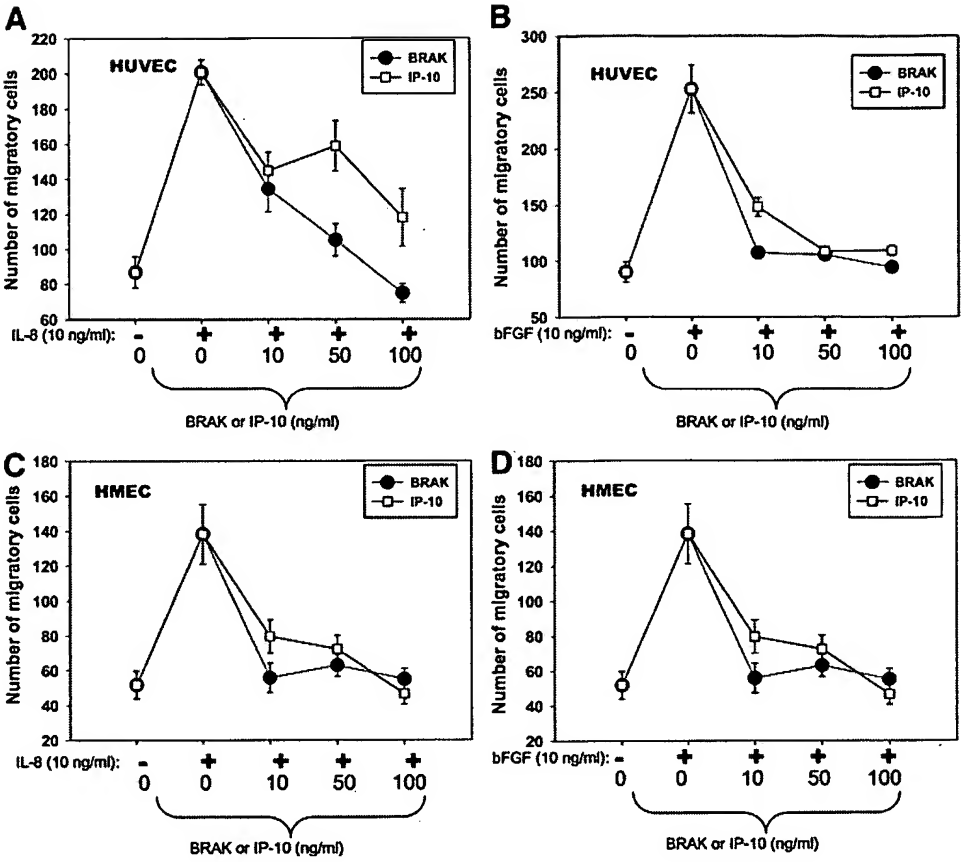

Fig. 2. BRAK inhibits the chemotaxis of endothelial cells. Cytokines were added at the specified concentrations to the bottoms of a 48-well microchemotaxis chamber that was sealed with an 8-μm pore-sized filter and upper gasket. HUVECs (*A, B*) or HMECs (*C, D*) were seeded at 12,500 cells per well in the upper chamber and allowed to migrate for 4 hours at 37°C. Filters then were scraped to remove top cells, fixed, and stained with Dif Quik before mounting under immersion oil. Using a microscope (×200), migratory cells were counted from nine random fields from each well. The mean count of cells from multiple wells (four to six wells) then was averaged and plotted graphically along with the SE of the means (*error bars*). Significance values are reported in the text.

stimulated by 50 ng of bFGF (Fig. 3, *middle*) and 200 ng of VEGF (Fig. 3, *bottom*) by the introduction of 100 ng of rBRAK.

Computer-assisted image analysis was used to objectively quantitate the area of neovascularization and total vascularity, thus allowing comparisons to be made between the right eye (angiogenic substance alone) and the left eye (angiogenic substance plus 100 ng rBRAK) for each group of 12 animals. For corneas implanted with IL-8 plus rBRAK, the reduction in area of neovascularization ranged from 34.9% to 88.1% with a mean reduction of 68.7% ($P < 0.001$). The reduction in total vascularity ranged from 44.0% to 91.6% with a mean reduction of 67.6% ($P < 0.001$). For assays in which bFGF was introduced as the angiogenic cytokine, rBRAK caused a 58.4 ± 14.0% mean reduction in area of neovascularization ($P < 0.01$) and a 58.9 ± 16.1% mean reduction in total vascularity ($P < 0.05$). For assays in which VEGF was introduced as the angiogenic cytokine, rBRAK caused a similar reduction in both parameters ($P < 0.03$). The ability of rBRAK to inhibit corneal neovascularization induced by IL-8, bFGF, and VEGF has been confirmed in two independent experiments. Neutralizing BRAK antibody was found to attenuate the inhibition of angiogenesis when added to the combination of IL-8 and rBRAK in pellets, indicating that the angiostatic properties were attributable to rBRAK itself and not a contaminant of the commercial chemokine (See Supplementary Fig. 3).

rBRAK Ligand Binds Low Affinity Sites that Are Competed by Heparin Sodium. The time-dependent binding of [^{125}I]-rBRAK to HUVECs was examined by incubating cells with 0.1 nmol/L labeled rBRAK for increasing time points at 4°C. Binding required 2 hours to reach equilibrium (Fig. 4*A*). To characterize the receptor for rBRAK on HUVECs, a homologous competitive binding assay was performed by incubating cells with 0.1 nmol/L of [^{125}I]-BRAK in the presence of increasing concentrations of competing, unlabeled rBRAK. An IC_{50} of 300 nmol/L was measured for unlabeled BRAK (Fig. 4*B*), which amounts to a K_d of ~300 nmol/L when the Cheng and Prusoff equation is applied. The number of receptors per cell or B_{max} calculated was on the order of several million, consistent with low affinity binding sites on HUVECs. High affinity receptors were undetectable even by pretreatment with acid wash or by varying the salt concentrations of the binding and wash conditions. Similar results were found with HMECs (data not shown). Thus, only low affinity binding sites for rBRAK could be shown on either HUVECs or HMECs.

The binding of chemokine and growth factor ligands to endothelial cells has been shown through low affinity binding sites on cell surface glycosaminoglycans, such as heparin moieties (30–33), and can be overcome in the presence of excess, free glycosaminoglycan. To determine the presence of such interaction between rBRAK and glycosaminoglycans, a competitive binding assay was performed in HUVECs or HMECs by incubating cells with 0.1 nmol/L [^{125}I]-rBRAK in the presence of increasing concentrations of heparin sodium. Heparin sodium effectively blocked [^{125}I]-rBRAK binding to both types of endothelial cells (Fig. 4*C*).

The CXC chemokine IP-10, which like rBRAK inhibits endothelial cell chemotaxis and angiogenesis, has been reported to bind high affinity receptors on endothelial cells (34). The inability to detect such high affinity receptors for BRAK on endothelial cells led us to investigate HUVECs for the binding of IP-10. A competitive binding assay was performed by incubating HUVECs with 0.1 nmol/L [^{125}I]-IP-10 in the presence of increasing concentrations of unlabeled IP-10 or rBRAK. An IC_{50} and K_d for unlabeled IP-10 at ~2 nmol/L was found (Fig. 4*D*). Unlabeled rBRAK did not compete for the binding of [^{125}I]-IP-10 in HUVECs, suggesting that rBRAK and IP-10 act via disparate receptors.

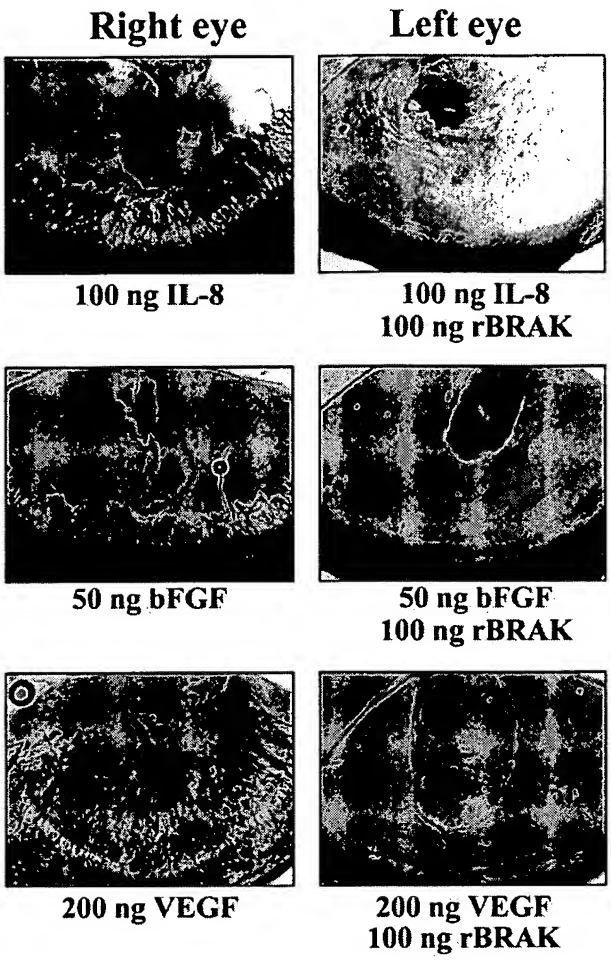

Fig. 3. BRAK inhibits *in vivo* angiogenesis mediated by multiple angiogenic factors. The angiogenic cytokines IL-8 (*top*), bFGF (*middle*), or VEGF (*bottom*) were added alone to pellets (right eye) or in combination with rBRAK (left eye) and implanted in rat corneas for 6 days. Animals were perfused with India ink to visualize blood vessels, and corneas were fixed and mounted for analysis.

Recombinant BRAK Protein Binds Immobilized IL-8 and bFGF and Inhibits Binding of bFGF to High Affinity Receptors. Several groups have hypothesized that chemokines inhibit angiogenesis through direct interaction with angiogenic ligands (26, 35, 36). To determine the presence of such interactions between BRAK and angiogenic ligands, we performed binding assays using IL-8 or bFGF immobilized on 96-well plates. Preliminary results showed that [^{125}I]-rBRAK bound to immobilized IL-8 or bFGF with high affinity as compared with binding of control wells coated with immobilized BSA alone. A competitive binding assay was performed by incubating immobilized IL-8 with 0.2 nmol/L [^{125}I]-rBRAK in the presence of increasing concentrations of unlabeled BRAK or IL-8. As shown in Fig. 5*A*, [^{125}I]-rBRAK binds immobilized IL-8 with high affinity and an IC_{50} of 2 nmol/L, whereas unlabeled, soluble IL-8 did not block [^{125}I]-rBRAK binding even at high concentration. Similar results are shown in Fig. 5*B* for the binding [^{125}I]-rBRAK to immobilized bFGF, in which labeled rBRAK also binds bFGF with high affinity and an IC_{50} of 2 nmol/L. In contrast to IL-8, unlabeled soluble bFGF did inhibit [^{125}I]-rBRAK binding to immobilized bFGF.

Considering that the interaction of ligands with low affinity binding sites on cell surface glycosaminoglycans may facilitate the action of chemokines and growth factors on endothelial cells, we investigated the effects of rBRAK and heparin sodium on the binding of bFGF to low affinity receptors on HUVECs. A competitive binding assay was performed by incubating cells with 0.1 nmol/L [^{125}I]-bFGF in the presence of increasing concentration of unlabeled rBRAK or heparin sodium under low salt wash conditions. Unlabeled rBRAK did not block binding of [^{125}I]-bFGF to HUVECs (Fig. 5*C*) even at 1 μmol/L. This concentration is 100 times higher than that required for inhibition in the chemotactic assays. Conversely, incubation with heparin sodium at 10 μg/mL resulted in near complete competition of binding by [^{125}I]-bFGF (Fig. 5*C*).

We next examined whether BRAK could interfere with binding of bFGF to high affinity receptors on endothelial cells by increasing the salt concentration in washes (*i.e.*, 2 mol/L NaCl). In preliminary experiments, binding of [^{125}I]-bFGF to HUVECs and HMECs was barely measurable following high salt washes, suggesting that receptor numbers were low. Therefore, the murine microvascular endothe-

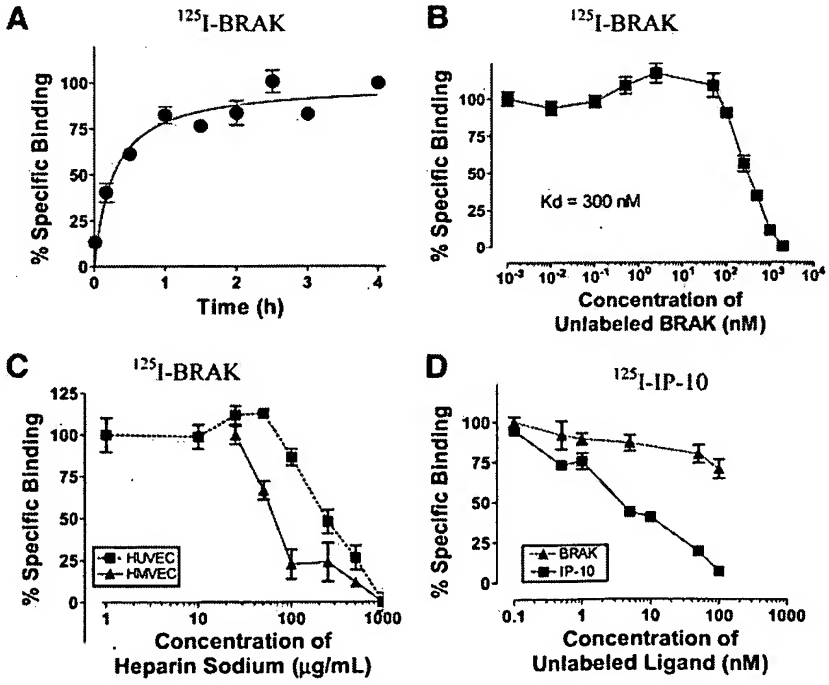

Fig. 4. Binding of BRAK and IP-10 to endothelial cells. *A*. Kinetics of binding saturation were examined by incubating 75,000 cells per well with 0.1 nmol/L [^{125}I]-BRAK for increasing amounts of time at 4°C. Saturation by labeled ligand occurred at 2 hours. *B*. A homologous competitive binding assay was performed using 75,000 HUVECs per well incubated with 0.1 nmol/L [^{125}I]-BRAK and increasing concentrations of unlabeled rBRAK for 2 hours at 4°C. A K_d of 300 nmol/L for BRAK indicated only low affinity receptors. *C*. HUVECs or HMECs (75,000 cells per well) were incubated with 0.1 nmol/L [^{125}I]-BRAK and increasing concentrations of heparin sodium for 2 hours at 4°C. *D*, HUVECs incubated with 0.1 nmol/L [^{125}I]–IP-10 for 2 hours at 4°C in the presence of increasing concentrations of either unlabeled IP-10 or rBRAK. A high affinity receptor was found for IP-10, for which BRAK did not compete. Nonspecific binding was determined in the presence of excess unlabeled ligand and was usually <20% total binding.

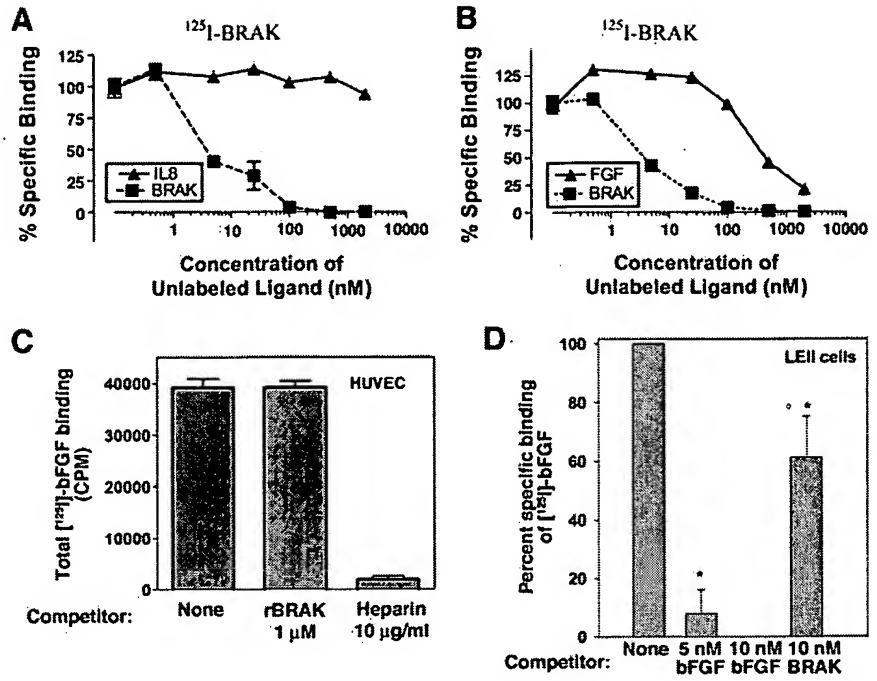

Fig. 5. Interaction between BRAK and angiogenic factors. Fifteen nanograms of IL-8 (*A*) or bFGF (*B*) were preabsorbed onto the surface of a 96-well ELISA plate and subsequently incubated with 2 nmol/L [^{125}I]-BRAK and increasing concentrations of the indicated unlabeled cytokine for 1 hour at 37°C. Nonspecific binding was determined in parallel wells precoated with BSA and was <20% of what bound to either immobilized IL-8 or bFGF. The ability of excess BRAK (1 μmol/L) to block binding of [^{125}I]-bFGF to low affinity receptors on HUVECs was examined in *C*. The percent specific binding of [^{125}I]-bFGF to high affinity receptors on murine LEII cells was examined in the presence of either unlabeled bFGF or rBRAK (*D*). *Binding was significantly different in the presence of unlabeled bFGF ($P < 0.001$) or rBRAK ($P < 0.05$) compared with no competitor (none).

lial cell line LEII was chosen to study the binding of bFGF to high affinity receptors. In the absence of unlabeled competitor, [^{125}I]-bFGF specific binding to LEII cells was clearly detectable following high salt washes. In the presence of 5 nmol/L unlabeled bFGF, specific binding of [^{125}I]-bFGF to LEII cells was reduced to 8% of the levels detected in the absence of competitor (Fig. 5*D*). At 10 nmol/L unlabeled bFGF, binding was completely blocked (Fig. 5*D*). When unlabeled rBRAK was used at 10 nmol/L (*i.e.*, 100 ng/mL), which was the optimal concentration for inhibiting endothelial cell chemotaxis, there was a 40% reduction ($P < 0.05$) in the amount of [^{125}I]-bFGF that bound to high affinity receptors on LEII cells.

rBRAK Protein Stimulates Chemotaxis of iDCs. The absence of detectable high affinity receptors on human endothelial cells prompted us to investigate the existence of potential BRAK receptors on other cell types. Such receptors would likely exist on cells that exhibited a positive chemotactic response to rBRAK. The findings of Kurth *et al.* (5) that rBRAK attracts monocytes pretreated with prostaglandin E_2 led us to examine the effects of rBRAK on the chemotaxis of other monocyte-derived cells under similar prostaglandin pretreatment conditions. Because the chemotactic response of mature dendritic cells to CCL19 and CCL21 also is up-regulated following prostaglandin E_2 treatment (37, 38), we also studied the effects of rBRAK on the migration of these cells. The maturation of dendritic cells was achieved by cultivation with lipopolysaccharide and confirmed by flow cytometry, which showed >80% of cells with a CD83/CD1a-positive phenotype (data not shown). Although mature dendritic cells pretreated with prostaglandin E_2 were not induced to migrate, we unexpectedly discovered that iDCs manifested a chemotactic response to rBRAK, even in the absence of prostaglandin pretreatment.

Thus, we further studied chemotaxis of iDCs derived from CD14-positive monocytes. Phenotypically, iDC cells were CD14/CD83 negative but 95% CD1a positive by flow cytometry (data not shown). Stimulation of iDC chemotaxis occurred at 10, 50, and 100 ng/mL of rBRAK and reached maximal response at 50 ng/mL (Fig. 6*A*). The potency of rBRAK is similar to that of MIP-1α (Fig. 6*A*), another chemokine known to stimulate chemotaxis of iDCs (39). Similar results were found in three independent experiments using iDCs derived from unrelated donors.

To determine whether abolishing the chemotactic gradient of rBRAK effects the migration of iDCs, experiments were performed by adding various concentrations of rBRAK to the upper and lower wells of the microchemotaxis chamber. The experiment depicted in Fig. 6*B* shows that chemotaxis of iDCs in response to rBRAK is abrogated by adding rBRAK to upper and lower wells. Abolishing the gradient of rBRAK resulted in only random migration of cells similar to the conditions of media alone. Consistent with what has been described for many other chemokines, supraoptimal concentrations of BRAK (*i.e.*, >1.0 μg/mL) were inhibitory for chemotaxis, and pretreatment of iDCs with pertussis toxin completely blocked chemotaxis (data not shown).

rBRAK Ligand Binds a High Affinity Receptor on iDCs. Our finding that rBRAK stimulates chemotaxis of iDCs led us to investigate these cells for the presence of a high affinity chemokine receptor capable of binding rBRAK. Homologous competitive binding assays were performed by incubating iDCs with 0.5 nmol/L [^{125}I]-BRAK in the presence of increasing concentrations of unlabeled rBRAK or 25 nmol/L unlabeled CXC chemokine. Fig. 6*C* shows the high affinity binding of rBRAK to iDCs with an IC_{50} of 2 nmol/L. Calculations revealed a K_d of 2.2 nmol/L and an estimated 20,000 receptors sites per cell, consistent with high affinity binding. IL-8, IP-10, SDF-1, and BCA did not compete with rBRAK for this high affinity receptor (Fig. 6*D*). Binding experiments were repeated twice using iDCs from two unrelated donors. The CC chemokines MIP-1α, MCP-1, RANTES, TARC, MIP-3α, and MIP-3β also failed to compete with [^{125}I]-BRAK binding to high affinity receptors on iDCs (data not shown).

DISCUSSION

In this study, we validated our previous findings for BRAK mRNA by confirming the abundant expression of BRAK protein in normal squamous mucosa and the absence of protein in tumors derived from the same tissue of origin. These findings give rise to the hypothesis that loss of BRAK may allow tumor cells to gain a selective advantage

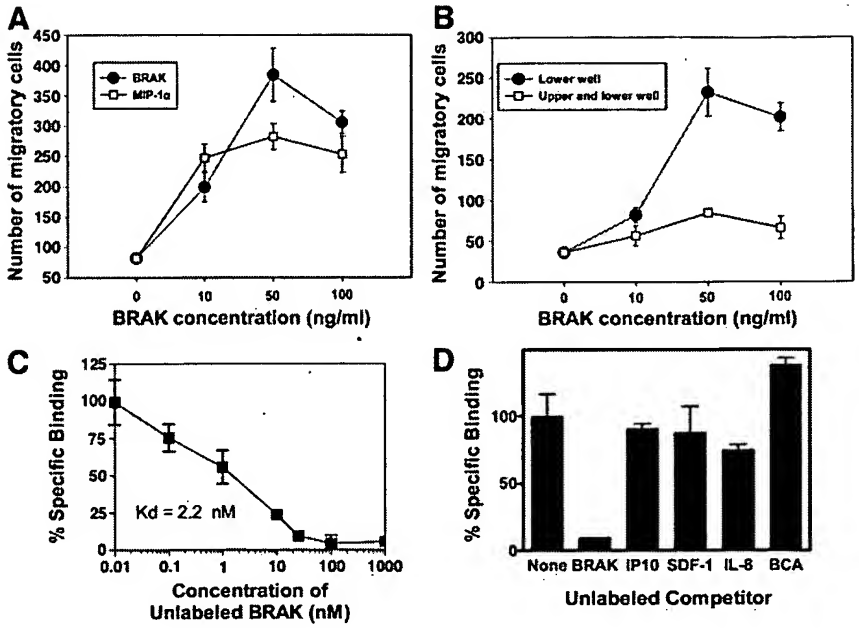

Fig. 6. BRAK is chemotactic for iDCs and binds to high affinity receptors. *A*. Six-day-old cultures of iDCs were seeded in upper wells of a 48-well chemotaxis chamber containing various concentrations of either rBRAK or MIP-1a in the lower chambers. *B*, checkerboard analysis in which increasing concentrations of rBRAK were added to the lower wells of the chemotaxis chamber and resulted in cell migration (●). Adding increasing, equivalent concentrations of rBRAK to upper and lower wells abolished the chemotactic gradient and abrogated the migration of iDCs (□). Chemotaxis assays were performed for 90 minutes at 37°C, and migratory cells were counted. The mean of the averages from replicate wells is depicted along with error bars corresponding to the SE. *C*, homologous competitive binding assay in which 75,000 iDCs were incubated with 0.2 nmol/L [^{125}I]-BRAK and increasing concentrations of unlabeled rBRAK for 1.5 hours at 4°C. A K_d of 2.2 nmol/L was calculated in the experiment shown. *D*, heterologous competitive binding assay in which 750,000 iDCs per tube were incubated with 0.5 nmol/L [^{125}I]-BRAK and no competitor or unlabeled competitor at 25 nmol/L for 1.5 hours at 4°C. Nonspecific binding was determined in the presence of excess (1 μmol/L) unlabeled rBRAK. All of the reactions were performed in triplicate, and error bars represent the SD of triplicate measurements.

in vivo. Central to explaining the implications for the loss of BRAK in tumors is an understanding of the normal biological function of BRAK. However, little progress has been made in understanding BRAK function since the gene was cloned >5 years ago (2).

Our data establish BRAK as a potent inhibitor of *in vivo* angiogenesis in the rat corneal micropocket assay. Neovascularization induced by multiple angiogenic factors was inhibited to a high degree at a biologically relevant dose of rBRAK. Although qualitative assessment of corneal images was sufficient to show a profound inhibition of neovascularization, we also developed a quantification method that provided objective evidence. Concurrence between separately defined parameters for the area of neovascularization and the total vascularity was found in each experimental group of 12 animals for angiogenesis in response to IL-8, bFGF, or VEGF. Finally, the specificity of inhibition was shown with a neutralizing antibody to BRAK.

Our findings of nearly complete inhibition of human endothelial cell migration in response to multiple chemotactic stimuli with 10 ng/mL rBRAK place BRAK alongside IP-10 and MIG (27) as ELR(−) CXC chemokines that are potent inhibitors of endothelial cell chemotaxis. Because angiogenesis occurs by a stepwise process of events that includes the migration and proliferation of endothelial cells accompanied by the formation of three-dimensional tubelike structures, inhibition of any one of these events is sufficient to interrupt *in vivo* angiogenesis. We found only a slight effect of BRAK on proliferation of endothelial cells (data not shown). Similar to the reported effects of IP-10 and PF-4 on proliferation (16, 26, 40), inhibition of proliferation required BRAK concentrations >1 μmol/L. Concentrations of chemokine up to 1000-fold greater than those required to inhibit chemotaxis suggest a limited role for BRAK in regulating endothelial cell proliferation. Thus, inhibition of endothelial migration appears to be a major mechanism by which BRAK interrupts *in vivo* angiogenesis.

A high affinity binding receptor for BRAK could not be shown on either HUVEC or HMEC lines. Several mechanisms can interfere with the detection of a high affinity binding site for ligands and may be overcome by varying conditions in receptor binding assays. Labeled ligand can bind to an abundance of low affinity cell surface receptors (*e.g.*, surface glycosaminoglycans), which can obscure high affinity receptors and can be overcome by increasing the salt concentration in washes. We found that a 2 mol/L NaCl wash solution sufficient to disrupt the binding of [^{125}I]-BRAK to immobilized heparin agarose beads (data not shown) did not reveal the presence of a high affinity receptor on HUVECs. Second, occupation of receptors by endogenous ligand before incubation can block binding of labeled ligand and can be overcome by acid stripping the cells to remove endogenous ligand. Pretreatment of HUVECs with an acid wash did not unmask a high affinity receptor. However, we cannot exclude the possibility that such receptors exist at levels beneath the capability of detection in binding assays.

A high affinity receptor for IP-10 is present on HUVECs as shown previously by Soejima *et al.* (34), and BRAK does not compete with IP-10 for this receptor. It currently is unknown whether this high affinity IP-10 receptor is the CXCR3B variant reported by Lasagni *et al.* (22). Nevertheless, our evidence suggests that BRAK does not bind CXCR3B because [^{125}I]-BRAK failed to bind with high affinity to ACHN cells (data not shown), a human kidney adenocarcinoma line reported to express abundant levels of this receptor (22). Rather, our findings of low affinity receptor sites for BRAK with K_d of ~300 nmol/L are consistent with cell surface glycosaminoglycan heparin moieties and are supported by the demonstration of competition of [^{125}I]-BRAK binding by soluble heparin in HUVECs and HMECs.

Interaction of ligands with cell surface glycosaminoglycans facilitates the specific receptor binding and signal transduction of angiogenic cytokines, such as IL-8, $VEGF_{165}$, and bFGF (30–33). The demonstration that PF-4 inhibits the binding of bFGF and $VEGF_{165}$ to endothelial cells mediated through glycosaminoglycans (26, 35) supports a proposed mechanism that chemokines may inhibit angiogenesis by competing for cell surface glycosaminoglycan binding sites (40). Our observation that BRAK binds immobilized heparin and the finding of low affinity receptor sites on endothelial cells support such a mechanism. However, we found that unlabeled BRAK at concentrations up to 1 μmol/L could not block the binding of [^{125}I]-FGF to low affinity receptors on HUVECs. Therefore, competition with angiogenic cytokines for glycosaminoglycan binding sites does not appear responsible for the inhibition of endothelial cell chemotaxis mediated by BRAK.

Several published reports (26, 35, 36) support the hypothesis that angiostatic chemokines can inhibit angiogenic ligands by direct interaction. PF-4 has been shown to bind immobilized bFGF or $VEGF_{165}$ *in vitro* and to interfere with bFGF dimerization. Our data suggest that

BRAK may act through a similar mechanism because rBRAK bound with high affinity to immobilized bFGF (*i.e.*, $IC_{50} < 10$ nmol/L). The concentration of soluble bFGF required to block [^{125}I]-BRAK binding to immobilized bFGF also was consistent with concentrations found by Perollet *et al.* (26) required to block PF-4 binding to immobilized bFGF. Our findings that unlabeled rBRAK could inhibit binding of bFGF to high affinity receptors further support a mechanism of direct interaction between BRAK and bFGF. Although [^{125}I]-BRAK bound to immobilized IL-8 with a similar affinity, competition for [^{125}I]-BRAK binding by excess soluble IL-8 did not occur at concentrations up to 2 μmol/L, suggesting that oligomerization of IL-8 may be necessary for interaction with BRAK.

A clear consensus is lacking regarding the cellular target spectrum of chemotaxis in response to BRAK. An explanation could be the disparity in sources of BRAK protein used by various investigators before the recent commercial availability of rBRAK. One study used a COOH-terminal histidine-tagged protein corresponding to the murine homologue BMAC (97% identical to human) and found chemotaxis of human B-cell and monocytic cell lines but not resting or activated T cells (3). Another reported that micromolar concentrations of chemically synthesized BRAK peptide were chemotactic for prostaglandin E_2–stimulated human monocytes but not for dendritic cells or other leukocyte subsets (5). A third group used unpurified BRAK (*e.g.*, MIP-2γ) from supernatants of transfected mammalian cells to show chemotaxis for human neutrophils and dendritic cells but not other leukocyte subsets (4). Consistent in these reports is the finding that BRAK does not appear chemotactic for resting or activated T cells. Although each group reported chemotactic activity for a monocyte-derived cell type, the activation or differentiation requirements varied among reports.

Our data unequivocally show that human BRAK is chemotactic for iDCs at 10 ng/mL of purified rBRAK. These findings were validated with the abrogation of a chemotactic response by abolishing the concentration gradient. Consistent with the action of chemokines through G protein–coupled receptors, BRAK-mediated chemotaxis of iDCs was sensitive for pertussis toxin. Moreover, BRAK bound to high affinity receptors on iDCs with a K_d of 2.2 nmol/L. The binding of [^{125}I]-BRAK to dendritic cells in our assays occurred at concentrations comparable with those of the chemotaxis assay and consistent with those of other chemokines. Although the identity is presently unknown, the demonstration of a receptor for BRAK on dendritic cells opens new opportunities for its characterization. Competitive binding assays using a panel of chemokine ligands with known receptors indicate that BRAK does not bind any of the currently known CXC receptors nor does BRAK bind any of the known CC receptors found on dendritic cells.

In summary, we found that BRAK protein is constitutively expressed in normal squamous mucosa of the tongue but absent in SCC tumors arising from this site. We showed that BRAK is a potent inhibitor of endothelial cell chemotaxis and angiogenesis in response to multiple angiogenic factors. Supporting that the loss of BRAK expression might dysregulate host immune mechanisms, we found that BRAK is chemotactic for iDCs. Therefore, the potential biological implications of rBRAK in SCC of the head and neck, either systemically introduced or pharmacologically induced, require further investigation.

Note Added in Proof

During preparation of this manuscript, Allinen *et al.* (Cancer Cell 2004;6:17–32) reported that CXCL14 (BRAK) is up-regulated in the myoepithelial stromal cells adjacent to invasive breast carcinomas and that breast carcinoma tumor lines bind BRAK and respond with chemotaxis and increased invasion. These observations are in agreement with our current findings that BRAK/CXCL14 protein is highly expressed in stromal fibroblasts immediately adjacent to nests of tongue SCC and suggest that breast carcinomas may express the same high affinity receptor for BRAK as iDCs.

REFERENCES

1. Frederick MJ, Henderson Y, Xu X, et al. In vivo expression of the novel CXC chemokine BRAK in normal and cancerous human tissue. Am J Pathol 2000;156: 1937–50.
2. Hromas R. Broxmeyer HE, Kim C, et al. Cloning of BRAK, a novel divergent CXC chemokine preferentially expressed in normal versus malignant cells. Biochem Biophys Res Commun 1999;255:703–6.
3. Sleeman MA, Fraser JK, Murison JG, et al. B cell- and monocyte-activating chemokine (BMAC), a novel non-ELR α-chemokine. Int Immunol 2000;12:677–89.
4. Cao X, Zhang W, Wan T, et al. Molecular cloning and characterization of a novel CXC chemokine macrophage inflammatory protein-2 γ chemoattractant for human neutrophils and dendritic cells. J Immunol 2000;165:2588–95.
5. Kurth I, Willimann K, Schaerli P, et al. Monocyte selectivity and tissue localization suggests a role for breast and kidney-expressed chemokine (BRAK) in macrophage development. J Exp Med 2001;194:855–61.
6. Homey B, Muller A, Zlotnik A. Chemokines: agents for the immunotherapy of cancer? Nat Rev Immunol 2002;2:175–84.
7. Frederick MJ, Clayman GL. Chemokines in cancer. Expert Rev Mol Med 2001;1–18.
8. Moore BB, Keane MP, Addison CL, Arenberg DA, Strieter RM. CXC chemokine modulation of angiogenesis: the importance of balance between angiogenic and angiostatic members of the family. J Investig Med 1998;46:113–20.
9. Wang JM, Deng X, Gong W, Su S. Chemokines and their role in tumor growth and metastasis. J Immunol Methods 1998;220:1–17.
10. Belperio JA, Keane MP, Arenberg DA, et al. CXC chemokines in angiogenesis. J Leukoc Biol 2000;68:1–8.
11. Haghnegahdar H, Du J, Wang D, et al. The tumorigenic and angiogenic effects of MGSA/GRO proteins in melanoma. J Leukoc Biol 2000;67:53–62.
12. Arya M, Patel HR, Williamson M. Chemokines: key players in cancer. Curr Med Res Opin 2003;19:557–64.
13. Arenberg DA, Polverini PJ, Kunkel SL, et al. The role of CXC chemokines in the regulation of angiogenesis in non-small cell lung cancer. J Leukoc Biol 1997;62: 554–62.
14. Maione TE, Gray GS, Petro J, et al. Inhibition of angiogenesis by recombinant human platelet factor-4 and related peptides. Science 1990:247:77–9.
15. Arenberg DA, Keane MP, DiGiovine B, et al. Epithelial-neutrophil activating peptide (ENA-78) is an important angiogenic factor in non-small cell lung cancer. J Clin Investig 1998;102:465–72.
16. Angiolillo AL, Sgadari C, Taub DD, et al. Human interferon-inducible protein 10 is a potent inhibitor of angiogenesis in vivo. J Exp Med 1995;182:155–62.
17. Zlotnik A, Morales J, Hedrick JA. Recent advances in chemokines and chemokine receptors. Crit Rev Immunol 1999;19:1–47.
18. Baggiolini M, Dewald B, Moser B. Human chemokines: an update. Annu Rev Immunol 1997;15:675–705.
19. Rossi D, Zlotnik A. The biology of chemokines and their receptors. Annu Rev Immunol 2000;18:217–42.
20. Salcedo R, Resau JH, Halverson D, et al. Differential expression and responsiveness of chemokine receptors (CXCR1–3) by human microvascular endothelial cells and umbilical vein endothelial cells. FASEB J 2000;14:2055–64.
21. Romagnani P, Annunziato F, Lasagni L, et al. Cell cycle-dependent expression of CXC chemokine receptor 3 by endothelial cells mediates angiostatic activity. J Clin Investig 2001;107:53–63.
22. Lasagni L, Francalanci M, Annunziato F, et al. An alternatively spliced variant of CXCR3 mediates the inhibition of endothelial cell growth induced by IP-10, Mig, and I-TAC, and acts as functional receptor for platelet factor 4. J Exp Med 2003;197: 1537–49.
23. Skelton L, Cooper M, Murphy M, Platt A. Human immature monocyte-derived dendritic cells express the G protein-coupled receptor GPR105 (KIAA0001, P2Y14) and increase intracellular calcium in response to its agonist, uridine diphosphoglucose. J Immunol 2003;171:1941–9.
24. Fournier GA, Lutty GA, Watt S, Fenselau A, Patz A. A corneal micropocket assay for angiogenesis in the rat eye. Investig Ophthalmol Vis Sci 1981;21:351–4.
25. Lowenthal JW MTSH. Measurement of lymphokine receptors. Curr Protocol Immunol Suppl 1997;6.1.1–6.1.15.
26. Perollet C, Han ZC, Savona C, Caen JP, Bikfalvi A. Platelet factor 4 modulates fibroblast growth factor 2 (FGF-2) activity and inhibits FGF-2 dimerization. Blood 1998;91:3289–99.
27. Strieter RM, Polverini PJ, Kunkel SL, et al. The functional role of the ELR motif in CXC chemokine-mediated angiogenesis. J Biol Chem 1995;270:27348–57.
28. Loughman MS, Chatzistefanou K, Gonzalez EM, et al. Experimental corneal neovascularisation using sucralfate and basic fibroblast growth factor. Aust NZ J Ophthalmol 1996;24:289–95.
29. Nissen NN, Polverini PJ, Koch AE, et al. Vascular endothelial growth factor mediates angiogenic activity during the proliferative phase of wound healing. Am J Pathol 1998;152:1445–52.
30. Hoogewerf AJ, Kuschert GS, Proudfoot AE, et al. Glycosaminoglycans mediate cell surface oligomerization of chemokines. Biochemistry 1997;36:13570–8.

31. Kuschert GS, Coulin F, Power CA, et al. Glycosaminoglycans interact selectively with chemokines and modulate receptor binding and cellular responses. Biochemistry 1999;38:12959–68.
32. Aviezer D, Levy E, Safran M, et al. Differential structural requirements of heparin and heparan sulfate proteoglycans that promote binding of basic fibroblast growth factor to its receptor. J Biol Chem 1994;269:114–21.
33. Wang D, Sai J, Richmond A. Cell surface heparan sulfate participates in CXCL1-induced signaling. Biochemistry 2003;42:1071–7.
34. Soejima K, Rollins BJ. A functional IFN-γ-inducible protein-10/CXCL10-specific receptor expressed by epithelial and endothelial cells that is neither CXCR3 nor glycosaminoglycan. J Immunol 2001;167:6576–82.
35. Gengrinovitch S, Greenberg SM, Cohen T, et al. Platelet factor-4 inhibits the mitogenic activity of VEGF121 and VEGF165 using several concurrent mechanisms. J Biol Chem 1995;270:15059–65.
36. Chadderton NS, Stringer SE. Interaction of platelet factor 4 with fibroblast growth factor 2 is stabilised by heparan sulphate. Int J Biochem Cell Biol 2003;35:1052–5.
37. Luft T, Jefford M, Luetjens P, et al. Functionally distinct dendritic cell (DC) populations induced by physiologic stimuli: prostaglandin E(2) regulates the migratory capacity of specific DC subsets. Blood 2002;100:1362–72.
38. Scandella E, Men Y, Gillessen S, Forster R, Groettrup M. Prostaglandin E2 is a key factor for CCR7 surface expression and migration of monocyte-derived dendritic cells. Blood 2002;100:1354–61.
39. Rubbert A, Combadiere C, Ostrowski M, et al. Dendritic cells express multiple chemokine receptors used as coreceptors for HIV entry. J Immunol 1998;160:3933–41.
40. Luster AD, Greenberg SM, Leder P. The IP-10 chemokine binds to a specific cell surface heparan sulfate site shared with platelet factor 4 and inhibits endothelial cell proliferation. J Exp Med 1995;182:219–31.

Modulation of CXCL14 (BRAK) Expression in Prostate Cancer

Steven R. Schwarze,[1] Jun Luo,[2] William B. Isaacs,[2] and David F. Jarrard[1]*

[1]Department of Surgery, Division of Urology, University of Wisconsin Medical School, Molecular and Environmental Toxicology and the University of Wisconsin Comprehensive Cancer Center, Madison, Wisconsin
[2]Department of Oncology and Urology, Johns Hopkins University School of Medicine, Baltimore, Maryland

BACKGROUND. Recent studies suggest inflammatory processes may be involved in the development or progression of prostate cancer. Chemokines are a family of cytokines that can play several roles in cancer progression including angiogenesis, inflammation, cell recruitment, and migration.
METHODS. Real-time quantitative RT-PCR, in situ RNA hybridization, laser capture microscopy, immunohistochemistry, and cDNA array based technologies were used to examine CXCL14 (BRAK) expression in paired normal and tumor prostate. To determine the role CXCL14 expression has on cancer progression, LAPC4 cells were engineered to overexpress mouse or human CXCL14, and xenograft studies were performed.
RESULTS. CXCL14 RNA expression was observed in normal and tumor prostate epithelium and focally in stromal cells adjacent to cancer. CXCL14 mRNA was significantly upregulated in localized prostate cancer and positively correlated with Gleason score. CXCL14 levels were unchanged in BPH specimens. LAPC4 cells expressing CXCL14 resulted in a 43% tumor growth inhibition ($P = 0.019$) in vivo compared to vector only xenografts.
CONCLUSIONS. CXCL14 mRNA upregulation is a common feature in prostate cancer. The finding that CXCL14 expression inhibits tumor growth suggests this gene has tumor suppressive functions. *Prostate 64: 67–74, 2005.* © 2005 Wiley-Liss, Inc.

KEY WORDS: **chemokine; cancer; inflammation; xenograft**

INTRODUCTION

Several recent findings suggest that inflammation is present in the prostate and may play a central role in the development of prostate cancer. Chronic inflammation commonly occurs in the prostate and is closely associated with a histological phenotype termed focal prostatic glandular atrophy [1,13]. Histochemical staining with Ki-67 shows that focal atrophic lesions contain actively dividing cells and, therefore, they have been appropriately termed proliferative inflammatory atrophy (PIA). The strongest case for the hypothesis that inflammation plays a central role in prostate cancer comes from recent studies of hereditary prostate cancer. To date, only two genes, *Ribonuclease L (RNaseL)* and *macrophage scavenging receptor 1* (MSR1), have been associated with familial prostate cancer and both function in host immune responses [3–5,9]. The identification of two independent susceptibility genes integral to this process is strong evidence implicating inflammatory, possibly macrophage-mediated, events in prostate carcinogenesis.

Chemokines are a family of small, secreted chemotactic cytokines. Most chemokines have four cysteine residues and, depending on the motif displayed by the first two cysteine residues, they have been classified into CXC, CC, C, and CXC3 classes (reviewed in [6]). In addition to their role in the migration of hematopoetic

Grant sponsor: National Institutes of Health; Grant number: R01CA97131; Grant sponsor: University of Wisconsin George M. O'Brien Urology Research Center; Grant number: 1P50DK065303; Grant sponsor: Department of Defense Prostate Cancer Research Program; Grant number: DAMD17-02-1-0163.

*Correspondence to: David F. Jarrard, MD, Department of Surgery, University of Wisconsin, 600 Highland Avenue, K6/530, Madison, WI 53792. E-mail: jarrard@surgery.wisc.edu

Received 7 August 2004; Accepted 21 September 2004
DOI 10.1002/pros.20215
Published online 13 January 2005 in Wiley InterScience (www.interscience.wiley.com).

cells and inflammation, members of the CXC chemokine class are also involved in regulating angiogenesis and proliferation. To date, several CXC chemokines (CXCL1, CXCL6, CXCL8, and CXCL12) are known angiogenic factors capable of stimulating endothelial cell migration that results in increased blood supply to the tumor. In contrast, other CXC chemokines (CXCL9, CXCL10, CXCL11) are angiostatic factors that can inhibit endothelial cell chemotaxis [19,23]. The proliferative effects of two CXC chemokines, CXCL1 and CXCL8, are well characterized. CXCL1 (GROα) was initially identified and characterized as an autocrine growth factor for melanoma cells [18]. This gene also acts as a growth factor for some human adenocarcinoma cell lines derived from the lung and stomach and in human malignant pancreatic cells [8,24]. Similarly, CXCL8 enables autocrine growth regulation in melanoma cells and numerous epithelial cell lines [2,8,17]. Therefore, in addition to chemotactic activities, altering the expression of many CXC chemokines also modulates tumor progression.

CXCL14 is a novel CXC chemokine of 77 amino acids. CXCL14 mRNA expression is constitutive in normal tissues with the highest expression in epithelial cell types [10]. Consistent with chemokine attraction of hematopoetic cells, CXCL14 induces migration in the activated macrophage THP-1 cell line and other cells of macrophage lineages including monocytes and dendritic cells [7,10,22]. From these studies, it is hypothesized that CXCL14 may play a role in the maturation of monocytes to macrophages and dendritic cells. Currently, the CXCL14 receptor is unknown.

Although RNaseL and MSR1 are likely involved in mediating a small number of hereditary prostate cancers, a dysregulated immune regulatory gene has not been identified in a large fraction of prostate cancer specimens. Through a screen to identify genes induced in a model of aging prostate epithelial cells (cellular senescence), we identified CXCL14 expression to be consistently upregulated [20]. Here we demonstrate that CXCL14 is reproducibly elevated at the mRNA level in localized prostate cancers and this alteration is positively associated with cancer progression. The inhibition of LAPC4 xenograft growth and the previous demonstration that cancer cell lines and solid tumors infrequently express this gene [7], suggests CXCL14 protein expression may be selected against during tumor development.

MATERIALS AND METHODS

Procurement of Human Prostate Tissues

Fresh frozen prostate tissue samples (36) used for cDNA microarray analysis were collected from 1993 to 2000 and were analyzed at Johns Hopkins under a protocol exemption for this tissue bank approved by The Johns Hopkins Medicine Institutional Review Board. Prostate tissue samples used for quantitative RT-PCR analysis, in situ RNA hybridization, and laser capture microscopy were obtained from the University of Wisconsin Hospital and Clinics under a University of Wisconsin Institution Review Board protocol (45 CFR 46.101(b)). Normal tumor pairs were selected based on the availability of paired sections containing predominantly adenocarcinoma cells (in the case of the cancer samples) or normal epithelial cells (in the case for paired normal samples) from the same patient. Trimmed prostate blocks were cut into 10-micron sections in a cryostat followed by RNA extraction using previously described procedure [11]. The first and last section from each sample was H&E stained for pathological confirmation and calculation of the percentage of glandular cells by a pathologist. The average percentage of epithelial content in the BPH samples is 51% (SD = 9.9), while the normal prostate samples contains epithelial cells averaged at 68% (SD = 16.1), and the prostate tumor samples at 69% (SD = 16.3). Normal prostate tissue for laser capture microscopy studies was obtained from the prostates of patients undergoing cystoprostatectomy for bladder cancer treatment. Linear regression analysis was carried out with Mstat 4.01 software.

Quantitative RT-PCR Analysis

Total RNA was isolated using the RNeasy RNA isolation kit (Qiagen, Valencia, CA), DNase treated, and 1 μg was used to prepare cDNA. Quantitative RT-PCR was performed by monitoring in real time the increase in fluorescence of the SYBR Green dye as described using a iCycler detection system (Bio-Rad, Hurcules, CA) [15,26]. For comparison of transcript levels between samples, a standard curve of cycle thresholds for several serial dilutions of a cDNA sample was established. This value was used to calculate the relative abundance of each gene. These values were then normalized to the relative amounts of 18S cDNA. All PCR reactions were performed in duplicate. Sequences of primers used for PCR analysis are available upon request.

cDNA Microarray Expression Analysis

Microarrays used in this study were fabricated in the Johns Hopkins Oncology Microarray Core and contained 11904 human IMAGE clones (http://image.llnl.gov/). The experimental design, total RNA extraction, labeling, hybridization, image analysis, and data analysis were modified based on the protocols described previously [12]. Total RNA was extracted from each of the samples as described, amplified once using

the MessageAmp aRNA kit (Ambion, Austin, TX) using an input of 500 ng of total RNA, labeled by direct incorporation Cy3-dUTP (Amersham Biosciences, Piscataway, NJ) in a reverse transcription reaction using random primers and Superscript II reverse transcriptase (Invitrogen, Carlsbad, CA). Expression profiles were generated by co-hybridization of each of 59 Cy3-labeled probes with a Cy5-labeled common reference sample, prepared from a pool of two BPH specimens as described [11] and its RNA similarly amplified. The expression profile for each sample was represented as intensity ratios of sample/reference for each of the 11904 ESTs. Expression ratios for CXCL14 were extracted from the corresponding EST clone represented by IMAGE clone ID 345034 on the array.

In Situ RNA Hybridization

Human CXCL14 cDNA corresponding to the entire open reading frame was cloned into pGEM3Z (Promega, Madison, WI). Digoxigenin labeled sense and anti-sense RNA was transcribed in vitro using SP6 and T7 polymerases, respectively, according to the manufacturer's directions (Roche Applied Science, Indianapolis, IN). Ten-micron cryostat sections were cut, fixed in 4% paraformaldehyde for 5 min and washed in PBS. Slides were incubated for 30 min at 37°C in 1 μg/ml of proteinase K. Slides were rinsed in DEPC-treated water and incubated in 0.25% acetic anyhydride in 0.1 M triethanolamine for 10 min. Next, the samples were dehydrated in increasing (70%, 95%, and 100%) ethanol concentrations for 3 min each and allowed to dry. Tissue sections were blocked in 0.1 mg/ml yeast tRNA in hybridization buffer [4×SSC; 10% dextran sulfate; 1× Denhardt's solution (0.02% Ficoll® 400, 0.02% polyvinyl pyrolidone, 0.02% bovine serum albumin); 1 mg/ml salmon sperm DNA] at 60°C for 2 hr. To hybridize, 10 ng/ml of anti-sense or sense (negative control) probe was added to hybridization buffer, plastic coverslipped, sealed with rubber cement, and incubated in a humidified chamber overnight. The following day the slides were washed twice in 4× SSC/0.2% DTT for 15 min at room temperature followed by a 30-min incubation at 37°C with 0.03 mg/ml RNase A in Tris buffered Saline (TBS; 10 mM Tris pH 7.4, 100 mM NaCl). Slides were then washed in 2× SSC/0.1% DTT at room temperature for 30 min, followed by a 0.1× SSC/0.1% DTT wash at 60°C for 30 min. The tissue was blocked in PBS containing 0.1% Triton X-100 and 2% normal sheep serum (NSS; Sigma). An anti-digoxigenin alkaline phosphatase antibody (Roche Applied Science) was added 1:1,000 in TBS containing 1% NSS and 0.1% Triton X-100 and incubated for 2 hr at room temperature. The antibody was washed twice for 10 min in TBS and once in AP detection buffer [10 mM Tris (pH 9.5), 100 mM NaCl, 50 mM $MgCl_2$]. Alkaline phosphatase activity was detected by incubating in the detection buffer 0.18 mg/ml BCIP, 0.34 mg/ml NBT, and 240 μg/ml levamisole.

Laser Capture Microscopy

Ten-micron frozen sections were cut, mounted on Superfrost Plus slides (Fisher Scientific, Pittsburg, PA), and immediately placed on dry ice. Tissue was dehydrated in the following ethanol series for 1 min each: 50%, 60%, 70%, and 80%. Samples were then placed in 100% ethanol for 20 min and followed by three washes for 1 min each. Slides were air dried 1 hr. Capturing of epithelial and stromal tissue was performed on the Acturus PixCell II (Acturus, Mountain View, CA) laser capture system.

Stable Cell Line Generation

The human and mouse CXCL14 open reading frame was cloned into the pBABE puro retroviral expression vector and verified by sequence analysis (GenBank accession BC003513 and AF144754, respectively). Replication-defective retrovirus was generated as described [21] and added to proliferating LAPC4 cells. After 24 hr, complete media (DMEM + 5% FBS) was added. LAPC4 cells were treated with 2 μg/ml of puromycin (EMD Biosciences, San Diego, CA) at 48-hr post-transduction. The selection was carried out for 1 week at which point all non-transduced cells were not viable. CXCL14 expression was determined by RT-PCR.

LAPC4 Xenograft Propagation

LAPC4 cells containing the pBABE puro vector or the pBABE puro stably expressing human or mouse CXCL14 were trypsinized, washed, and resuspended in DMEM at 1×10^7 cells/ml. An equal volume of Matrigel (Becton Dickinson) was added on ice, and 0.2 ml of the mixture subcutaneously injected into the ventral inguinal region of 10 athymic nude mice per group (Harlan, Indianopolis, IN). Tumor size was monitored bi-weekly. Tumor volume was calculated by $(L \times W^2)/2$. Tumor volume measurements began on day 7 post-injection and were terminated when the average tumor volume reached 500 mm^3. Following euthanasia, tumors were excised and weighed. Statistical determinations were carried out with the Mstat 4.01 software using the Wilcoxon's rank sum test.

BrdU Incorporation

Cells were fed with fresh media 24 hr prior to 5-bromo-2′-deoxy-uridine (BrdU) labeling. LAPC4 cells were BrdU labeled (Sigma, St. Louis, MO) for 30 min,

harvested, and processed using an anti-BrdU monoclonal primary antibody followed by a goat anti-mouse FITC conjugated secondary according to the manufacturer's directions (Becton-Dickinson Immunocytometry Systems (B-D), San Jose, CA). Cells were analyzed with a FACScan (B-D) and the percentage of BrdU positive cells (10,000-gated events) determined using CellQuest software (B-D). Statistical determinations were carried out with the Mstat 4.01 software using the Wilcoxon's rank sum test.

CD31 Immunostaining

Cryostat sections (10 μM) were mounted on Superfrost Plus slides and fixed for 1 min in 10% neutral buffered formalin. The slides were rinsed in 1× PBS and blocked for endogenous peroxidase for 5 min in 3% H_2O_2. DAKO Protein Block (DAKO Corporation, Carpinteria, CA) was added for 10 min. A 1:50 dilution of the MEC13.3 rat anti-CD31 monoclonal antibody (BD Pharmingen) was made in DAKO antibody diluent (DAKO Corporation) and added to the tissue section for 1 hr at room temperature. Slides were rinsed in three changes of 1×TBS (DAKO Corporation) and 5 μg/ml of biotinylated rabbit anti-rat IgG (Vector Laboratories, Burlingame, CA) was added for 15 min at room temperature. Slides were rinsed in three changes of TBS and incubated for 15 min in Streptavidin-HRP (DAKO Corporation). Slides were rinsed three times in TBS and developed with DAB (Pierce Biotechnology, Rockford, IL). Slides were counterstained with 1:10 hematoxylin, blued in 37 mM ammonia, dehydrated, and mounted in permount.

Three representative areas on each immunostained slide were digitally imaged. Vessels were counted and averaged for each animal. Statistical determinations were carried out with the Mstat 4.01 software using the Wilcoxon's rank sum test.

RESULTS

Paired specimens consisting of normal and tumor prostate tissue were analyzed for CXCL14 mRNA expression levels. Prior to homogenization, all specimens were examined histologically and only those containing greater than 90% pure tumor or pure normal prostate tissue were used for subsequent analysis. CXCL14 mRNA levels were determined by two independent methodologies. First, 25 localized normal-tumor prostate tissue pairs were analyzed by cDNA microarray analysis. These studies showed that CXCL14 mRNA was induced in 22/25 of the tumor samples compared to their paired normal tissue with an average fold increase of 6.7 ($P < 0.001$) (Fig. 1A). Nine unpaired benign prostatic hyperplasia (BPH) samples demonstrated no significant change in

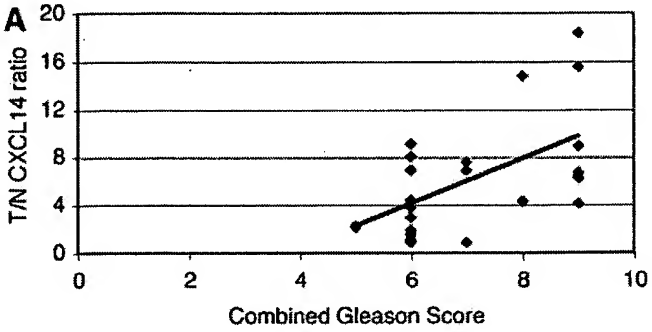

B

Sample	T:N CXCL14 ratio
NP/TP26	15
NP/TP27	14
NP/TP28	9
NP/TP29	15
NP/TP30	146
NP/TP31	49
NP/TP32	3.4
NP/TP33	1.1

Fig. 1. CXCL14 levels are induced in localized prostate cancer and correlate with cancer grade. **A**: Paired normal and tumor prostate specimens were analyzed with cDNA microarrays for CXCL14 expression. The ratio of tumor to normal expression was calculated and plotted with the Gleason's score of each tumor specimen. Linear regression analysis was performed on the scatter plot and the CXCL14 expression was found to increase with increasing grade of cancer ($r = 0.57$, $P = 0.009$). **B**: Paired normal and tumor prostate specimens were analyzed for CXCL14 expression using real-time quantitative RT-PCR. Total RNA was isolated and cDNA prepared. Quantitative RT-PCR (QPCR) was performed by monitoring SYBR green fluorescence from reactions containing CXCL14 or 18S rRNA specific primers. Following standardization with the 18S rRNA expression, the ratio of the tumor to normal expression was determined.

CXCL14 expression (data not shown). The fold CXCL14 expression change was plotted against the Gleason's score for each specimen, and linear regression analysis was performed to determine if gene expression and prostate cancer grade were associated. CXCL14 expression was found to positively correlate with prostate cancer aggressiveness ($P = 0.009$) (Fig. 1A).

Real-time quantitative PCR (QPCR) was used to confirm the CXCL14 mRNA induction observed with cDNA arrays. Seven of eight intermediate grade prostate tumors (Gleason score 5–7) exhibited increased CXCL14 mRNA levels compared to their normal pair (Fig. 1B). Thus, CXCL14 mRNA induction appears to be a common feature of most localized prostate tumors.

Next, we wished to examine the cell types responsible for CXCL14 expression in the normal and cancerous prostate. Laser capture microscopy was used to separate epithelial or stromal components. First, four normal prostate samples were obtained from cystoprostatectomy specimens not containing cancer to

avoid potential global CXCL14 expression changes in normal tissues adjacent to prostate tumor. RNA was isolated from laser capture dissected tissue, converted to cDNA, and analyzed by QPCR. Epithelial tissue contained 17 ± 2.3-fold higher CXCL14 mRNA levels than stromal tissue in normal prostate tissue (data not shown). In microdissected prostate cancer tissues, CXCL14 expression was consistently greater in tumor epithelium than in paired normal epithelium (Fig. 2A). Tumor stroma demonstrated increased CXCL14 mRNA in two of four samples.

A

Specimen	Tissue	T:N CXCL14 ratio
NP/TP34	Epithelium	3.5
	Stroma	35
NP/TP35	Epithelium	16
	Stroma	1.0
NP/TP36	Epithelium	71
	Stroma	1.0
NP/TP37	Epithelium	2.8
	Stroma	18

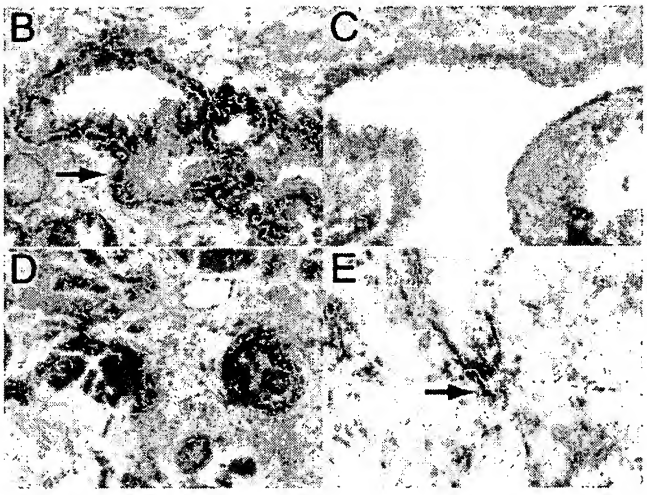

Fig. 2. CXCLI4 mRNA localization in normal and tumor prostate tissue. **A**: Laser capture microscopy was used to separate epithelium and stroma from paired localized prostate tumor specimens and adjacent normal tissue. CXCLI4 expression was determined by QPCR as described in Figure I. The values represent the ratio of the tumor to normal expression in both the epithelium and stroma. **B–E**: A complementary (anti-sense) or sense (negative control) mRNA probe corresponding to the entire secreted CXCLI4 reading frame was in vitro transcribed in the presence of digoxigenin-labeled UTP. The probe was then hybridized overnight, RNase treated, and washed under stringent conditions. An alkaline phosphatase anti-digoxigenin antibody was applied to detect the probe and developed with NBT/BCIP overnight. Intense CXCLI4 mRNA staining was detected in basal epithelium (arrow) from normal prostate tissue treated with the anti-sense probe (B). No staining was observed in the same specimen stained with the sense probe (C). In prostate tumor samples, CXCLI4 expression was present in tumor epithelium (D) and intensely stained sporadic stromal regions (arrow) (E).

In situ RNA hybridization techniques were also employed to verify and further define CXCL14 expression. Digoxigenin labeled probes corresponding to the entire CXCL14 open reading frame were hybridized to normal and tumor paired prostate cryosections. This methodology revealed that CXCL14 mRNA expression occurred predominantly from the basal epithelial cell type in normal prostate tissue (Fig. 2B). CXCL14 was highly expressed in the tumor epithelium (Fig. 2C). However, stromal staining was intermittent with occasional regions exhibiting high levels of expression in fibroblast-like cells (Fig. 2D). These localization experiments demonstrate in normal tissue that CXCL14 expression occurs predominantly in the basal epithelium. In prostate cancer, CXCL14 expression is consistently upregulated in tumor epithelium with focal regions of intense stromal expression.

To address the effect of increased CXCL14 expression on prostate tumor progression, xenograft studies were carried out in nude mice utilizing the LAPC4 prostate cancer cell line. LAPC4 cells do not express detectable amounts of CXCL14 [20]. LAPC4 cells were transduced with retrovirus containing either human or mouse CXCL14 or vector alone. A polyclonal cell population was selected with puromycin and CXCL14 expression verified by reverse transcriptase PCR. One million LAPC4 cells were injected with Matrigel into the inguinal fat pad of 30 nude mice. Tumor volume increased similarly in each group for 2 weeks (Fig. 3A). Beginning at day 23 post-injection, both the mouse and human CXCL14 expressing LAPC4 xenograft tumors exhibited a reduced tumor volume compared to the vector only LAPC4 xenografts. At termination (day 37), tumors were excised and weighed to accurately determine volume (Fig. 3B). Human CXCL14 expressing LAPC4 xenografts were significantly smaller ($P = 0.023$) than the vector only controls. Mouse CXCL14 expressing LAPC4 xenografts exhibited the same trend, however the size reduction did not reach significance ($P = 0.082$). When combining both hCXCL14 and mCXCL14, tumor volumes were 43% smaller ($P = 0.019$).

To examine how CXCL14 may be altering tumor growth, histology was examined by H&E staining paraffin embedded sections. Infiltration by neutrophils or monocytes was not apparent (data not shown). To ensure CXCL14 had no effect on proliferation in vitro, LAPC4 cells were BrdU labeled to determine rates of DNA synthesis. The percentage of cells actively undergoing DNA synthesis was not different in those cells expressing CXCL14 compared to the vector only control (Fig. 4A). To determine the effect of CXCL14 expression on endothelial cell recruitment, we stained the xenograft tissue for CD31, an endothelial cell marker. The microvessel density in multiple tumors

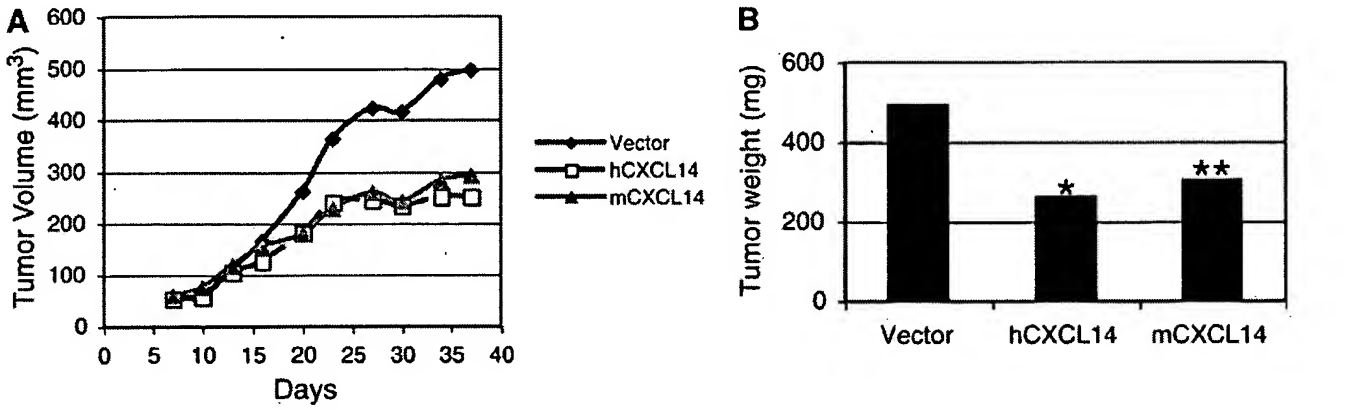

Fig. 3. Effect of CXCLI4 expression on LAPC4 xenograft tumor growth in nude mice. LAPC4 prostate cancer cells were transduced with retrovirus containing vector only (pBABE) or human or mouse CXCLI4 (hCXCLI4 and mCXCLI4, respectively). Transduced cells were selected with puromycin, and a polyclonal population was used for tumor formation studies. LAPC4 cells were co-injected with Matrigel into the inguinal fat pad of nude mice. **A**: Tumor volume was measured bi-weekly and the average tumor volume for each group plotted. **B**: Tumors were excised and tumor mass averaged and plotted. Tumors expressing hCXCLI4 were 47% smaller than vector only LAPC4 tumors (** indicates $P = 0.023$). Likewise, mCXCLI4 expression reduced tumor volume by 38% (* indicates $P = 0.082$). When combining the hCXCLI4 and mCXCLI4 groups, CXCLI4 expression resulted in tumors 43% smaller than the vector transduced tumors ($P = 0.019$).

from each group was determined. No significant difference in CD31 positive vessel density was noted (Fig. 4B).

DISCUSSION

We report for the first time that CXCL14 mRNA induction is consistently found in localized prostate cancers. In total, we analyzed 36 paired normal and tumor prostate tissue specimens and 33 (92%) exhibited elevated CXCL14 mRNA expression. Furthermore, expression increased with increasing cancer grade. These studies are in contrast to head and neck cancers in which CXCL14 mRNA is conspicuously absent [7]. Using microdissection and in situ RNA hybridization techniques, we found the constitutive expression in normal tissue to be derived predominantly from epithelial cells. In prostate cancer, CXCL14 mRNA induction was also consistently observed in tumor epithelium. In addition, focal areas of increased fibroblast expression were found in the stromal compartment of tumors. These regions of stromal expression have also been demonstrated in fibroblasts adjacent to squamous cell carcinomas [7]. Although chemokines are commonly expressed from white blood cell types, CXCL14 expression was not observed in any inflammatory cell type in prostate cancer. Thus, increased CXCL14 RNA expression is a specific and common finding in prostate cancers.

Steady-state CXCL14 mRNA upregulation is a common feature in localized prostate cancer and it will

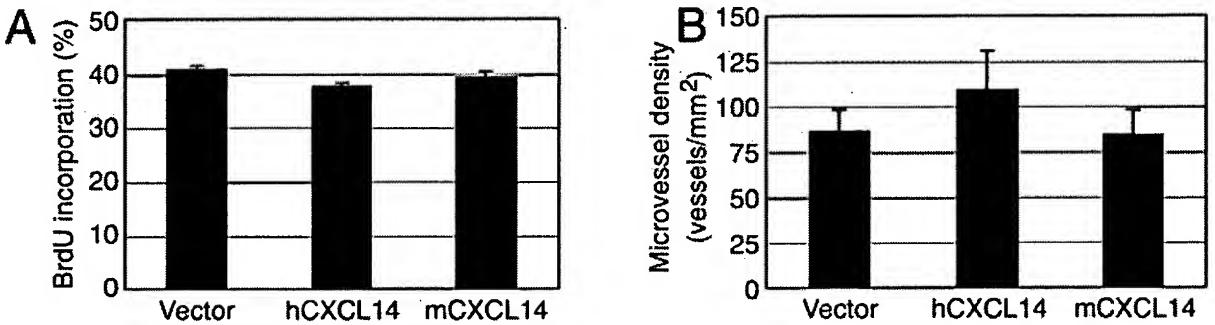

Fig. 4. Effect of CXCLI4 expression on proliferation and endothelial cell recruitment. **A**: Proliferation of LAPC4 cells expressing either human or mouse CXCLI4 or vector only transduced control cells was determined in vitro. Cells were pulsed with BrdU and detected by immunofluorescence and flow cytometry. The average of three experiments ± the standard deviation is shown. CXCLI4 had no significant effect on proliferation rates. **B**: Xenografts (above) were cryosectioned and probed with an anti-CD3l antibody to detect endothelial cells. Vessels were imaged, counted, and the average of multiple images from three xenografts in each group quantitated ± the standard deviation. No significant difference was found between the groups.

be extremely important to verify this finding on the protein level. To this end, we generated a polyclonal anti-CXCL14 antibody and performed immunohistochemistry and Western analysis on prostate specimens. However, our efforts to detect CXCL14 in vivo have been largely unsuccessful (1 ng sensitivity by Western analysis). The development of ELISA reagents, as for the majority of other chemokines and cytokines, will allow for much more sensitive (picogram level) and accurate protein quantitation. CXCL14 protein expression may not only be a good biomarker of prostate cancer, but also may play a fundamental role in cancer progression.

We generated data supporting a tumor suppressive role for CXCL14 in prostate cancer. Both human and mouse CXCL14 repressed the growth of LAPC4 xenografts. LAPC4 cells were utilized, as this is the only prostate cancer cell line that permits high levels of CXCL14 protein expression (unpublished observations). Both human and mouse CXCL14 were tested in this experiment to guarantee interaction with the, as of yet unidentified, CXCL14 receptor. If acting in an autocrine fashion, human CXCL14 should interact with the LAPC4 cells. If acting in a paracrine manner the mouse host cells should interact with the murine CXCL14. However, human and mouse CXCL14 vary by only two conserved amino acids (I36 to V36; V40 to M40) and it is likely that the human ligand can interact with the mouse receptor and vice versa. The latter scenerio is likely as both chemokines were able to slow tumor growth in vivo.

Several analyses were performed to address the mechanism of CXCL14 induced growth repression, however in vitro cellular proliferation was unaltered and microvessel density was unchanged in vivo. In addition, inflammation was not observed in the xenografts. CXCL14 has been shown to attract monocytes in vitro [10], which are present in the athymic nude mice we utilized. It is unclear if CXCL14 is unable to recruit monocytes in vivo, or if the athymic condition renders monocytes unable to be recruited. Similar studies have been reported on the involvement of the chemokine CXCL8 (IL-8) and its receptor, CXCR2, in prostate cancer progression. Through blocking CXCL8, a chemokine induced in the serum of patients with localized and metastatic prostate cancer [25], xenograft tumor growth could be inhibited in the immune compromised *scid* mouse [14]. Together these studies indicate that modulating chemokine expression can have an effect on tumor growth in prostate xenograft models in the absence of modulating inflammatory processes. Obviously, caveats exist with the use of xenografts to study tumor progression, especially when examining chemokines in immune deficient mice.

In addition to inflammatory cell recruitment, chemokines have numerous effects in cancer including the modulation of angiogenesis, tumor cell migration and cellular proliferation [16,23,24]. Our data presented here in LAPC4 xenografts suggest CXCL14 has tumor suppressive properties. Furthermore, CXCL14 is down-regulated and not expressed in the majority of cancer cell lines and head and neck cancers [7,20]. Further studies will need to be performed examining CXCL14 regulation, principally its protein translation and degradation, as well as identifying its receptor before its role in prostate cancer progression are clearly understood.

REFERENCES

1. Bennett BD, Richardson PH, Gardner WA. 1993. Histopathology and cytology of the prostatitis. Philadelphia: Saunders W.B. Company.
2. Brew R, Erikson JS, West DC, Kinsella AR, Slavin J, Christmas SE. 2000. Interleukin-8 as an autocrine growth factor for human colon carcinoma cells in vitro. Cytokine 12:78–85.
3. Carpten J, Nupponen N, Isaacs S, Sood R, Robbins C, Xu J, Faruque M, Moses T, Ewing C, Gillanders E, Hu P, Bujnovszky P, Makalowska I, Baffoe-Bonnie A, Faith D, Smith J, Stephan D, Wiley K, Brownstein M, Gildea D, Kelly B, Jenkins R, Hostetter G, Matikainen M, Schleutker J, Klinger K, Connors T, Xiang Y, Wang Z, De Marzo A, Papadopoulos N, Kallioniemi OP, Burk R, Meyers D, Gronberg H, Meltzer P, Silverman R, Bailey-Wilson J, Walsh P, Isaacs W, Trent J. 2002. Germline mutations in the ribonuclease L gene in families showing linkage with HPC1. Nat Genet 30:181–184.
4. Casey G, Neville PJ, Plummer SJ, Xiang Y, Krumroy LM, Klein EA, Catalona WJ, Nupponen N, Carpten JD, Trent JM, Silverman RH, Witte JS. 2002. RNASEL Arg462Gln variant is implicated in up to 13% of prostate cancer cases. Nat Genet 32:581–583.
5. Diaz-Guerra M, Rivas C, Esteban M. 1997. Activation of the IFN-inducible enzyme RNase L causes apoptosis of animal cells. Virology 236:354–363.
6. Fernandez EJ, Lolis E. 2002. Structure, function, and inhibition of chemokines. Annu Rev Pharmacol Toxicol 42:469–499.
7. Frederick MJ, Henderson Y, Xu X, Deavers MT, Sahin AA, Wu H, Lewis DE, El-Naggar AK, Clayman GL. 2000. In vivo expression of the novel CXC chemokine BRAK in normal and cancerous human tissue. Am J Pathol 156:1937–1950.
8. Fujisawa N, Sakao Y, Hayashi S, Hadden WA 3rd, Harmon CL, Miller EJ. 2000. Alpha-chemokine growth factors for adenocarcinomas; a synthetic peptide inhibitor for alpha-chemokines inhibits the growth of adenocarcinoma cell lines. J Cancer Res Clin Oncol 126:19–26.
9. Hassel BA, Zhou A, Sotomayor C, Maran A, Silverman RH. 1993. A dominant negative mutant of 2-5A-dependent RNase suppresses antiproliferative and antiviral effects of interferon. Embo J 12:3297–3304.
10. Kurth I, Willimann K, Schaerli P, Hunziker T, Clark-Lewis I, Moser B. 2001. Monocyte selectivity and tissue localization suggests a role for breast and kidney-expressed chemokine (BRAK) in macrophage development. J Exp Med 194:855–861.
11. Luo J, Duggan DJ, Chen Y, Sauvageot J, Ewing CM, Bittner ML, Trent JM, Isaacs WB. 2001. Human prostate cancer and benign

prostatic hyperplasia: Molecular dissection by gene expression profiling. Cancer Res 61:4683–4688.

12. Luo J, Dunn TA, Ewing CM, Walsh PC, Isaacs WB. 2003. Decreased gene expression of steroid 5 alpha-reductase 2 in human prostate cancer: Implications for finasteride therapy of prostate carcinoma. Prostate 57:134–139.
13. McNeal JE, 1988. Normal histology of the prostate. Am J Surg Pathol 12:619–633.
14. Moore BB, Arenberg DA, Stoy K, Morgan T, Addison CL, Morris SB, Glass M, Wilke C, Xue YY, Sitterding S, Kunkel SL, Burdick MD, Strieter RM. 1999. Distinct CXC chemokines mediate tumorigenicity of prostate cancer cells. Am J Pathol 154:1503–1512.
15. Morrison TB, Weis JJ, Wittwer CT. 1998. Quantification of low-copy transcripts by continuous SYBR Green I monitoring during amplification. Biotechniques 24:954–958, 960, 962.
16. Muller A, Homey B, Soto H, Ge N, Catron D, Buchanan ME, McClanahan T, Murphy E, Yuan W, Wagner SN, Barrera JL, Mohar A, Verastegui E, Zlotnik A. 2001. Involvement of chemokine receptors in breast cancer metastasis. Nature 410: 50–56.
17. Norgauer J, Metzner B, Schraufstatter I. 1996. Expression and growth-promoting function of the IL-8 receptor beta in human melanoma cells. J Immunol 156:1132–1137.
18. Richmond A, Thomas HG. 1986. Purification of melanoma growth stimulatory activity. J Cell Physiol 129:375–384.
19. Rossi D, Zlotnik A. 2000. The biology of chemokines and their receptors. Annu Rev Immunol 18:217–242.
20. Schwarze SR, DePrimo SE, Grabert LM, Fu VX, Brooks JD, Jarrard DF. 2002. Novel pathways associated with bypassing cellular senescence in human prostate epithelial cells. J Biol Chem 277:14877–14883.
21. Schwarze SR, Fu VX, Jarrard DF. 2003. Cdc37 enhances proliferation and is necessary for normal human prostate epithelial cell survival. Cancer Res 63:4614–4619.
22. Sleeman MA, Fraser JK, Murison JG, Kelly SL, Prestidge RL, Palmer DJ, Watson JD, Kumble KD. 2000. B cell- and monocyte-activating chemokine (BMAC), a novel non-ELR alpha- chemokine. Int Immunol 12:677–689.
23. Strieter RM, Polverini PJ, Kunkel SL, Arenberg DA, Burdick MD, Kasper J, Dzuiba J, Van Damme J, Walz A, Marriott D, Chan SY, Roczniak S, Shanafelt AB. 1995. The functional role of the ELR motif in CXC chemokine-mediated angiogenesis. J Biol Chem 270:27348–27357.
24. Takamori H, Oades ZG, Hoch OC, Burger M, Schraufstatter IU. 2000. Autocrine growth effect of IL-8 and GROalpha on a human pancreatic cancer cell line, Capan-1. Pancreas 21: 52–56.
25. Veltri RW, Miller MC, Zhao G, Ng A, Marley GM, Wright GL Jr, Vessella RL, Ralph D. 1999. Interleukin-8 serum levels in patients with benign prostatic hyperplasia and prostate cancer. Urology 53:139–147.
26. Wittwer CT, Herrmann MG, Moss AA, Rasmussen RP. 1997. Continuous fluorescence monitoring of rapid cycle DNA amplification. Biotechniques 22:130–131, 134–138.

Loss of New Chemokine CXCL14 in Tumor Tissue Is Associated with Low Infiltration by Dendritic Cells (DC), while Restoration of Human CXCL14 Expression in Tumor Cells Causes Attraction of DC Both In Vitro and In Vivo[1]

Galina V. Shurin,* Robert Ferris,[†§] Irina L. Tourkova,* Lori Perez,* Anna Lokshin,* Levent Balkir,* Bobby Collins,[¶] Gurkamal S. Chatta,[‡] and Michael R. Shurin[2*†]

Breast and kidney-expressed chemokine (BRAK) CXCL14 is a new CXC chemokine with unknown function and receptor selectivity. The majority of head and neck squamous cell carcinoma (HNSCC) and some cervical squamous cell carcinoma do not express CXCL14 mRNA, as opposed to constitutive expression by normal oral squamous epithelium. In this study, we demonstrate that the loss of CXCL14 in HNSCC cells and at HNSCC primary tumor sites was correlated with low or no attraction of dendritic cell (DC) in vitro, and decreased infiltration of HNSCC mass by DC at the tumor site in vivo. Next, we found that recombinant human CXCL14 and CXCL14-positive HNSCC cell lines induced DC attraction in vitro, whereas CXCL14-negative HNSCC cells did not chemoattract DC. Transduction of CXCL14-negative HNSCC cell lines with the human CXCL14 gene resulted in stimulation of DC attraction in vitro and increased tumor infiltration by DC in vivo in chimeric animal models. Furthermore, evaluating the biologic effect of CXCL14 on DC, we demonstrated that the addition of recombinant human CXCL14 to DC cultures resulted in up-regulation of the expression of DC maturation markers, as well as enhanced proliferation of allogeneic T cells in MLR. Activation of DC with recombinant human CXCL14 was accompanied by up-regulation of NF-κB activity. These data suggest that CXCL14 is a potent chemoattractant and activator of DC and might be involved in DC homing in vivo. ***The Journal of Immunology,*** **2005, 174: 5490–5498.**

The destructive disease head and neck squamous cell carcinoma (HNSCC)[3] annually afflicts 40,000 new persons in the United States (1), and 3,000,000 new cases develop worldwide annually (2, 3). Despite improvements in therapy and diagnosis, the overall survival rate of generally 50% for persons diagnosed with HNSCC has remained practically unchanged over the last two decades (1). For this reason, new therapeutic strategies need to be developed to treat HNSCC and the evaluation of alternative treatment strategies for patients with this malignancy is highly justified. Immunotherapy has a long history, but is only rarely considered as the treatment of choice. However, it seems that increasing efficacy of immunotherapy will make it one of the possible therapeutic options.

Specific active immunotherapy is based on the principle that malignant cells contain immunogenic determinants against which an antitumor immune response can be induced. Dendritic cells (DC) that acquire Ags from tumor cells are able to induce and regulate specific antitumor immunity. Several clinical trials have been initiated to evaluate the efficacy of DC-based immunotherapies in cancer, including stimulation of endogenous DC (4–6). However, it is still unclear why endogenous DC do not mediate efficient antitumor immunity in cancer patients. Whereas successful immunotherapy requires a functional immune system, a defect in the immune response may contribute to tumor growth. Such defects include active suppression of immune cells including DC by the tumor causing disturbed longevity and cell dysfunction (7, 8). For instance, it has been shown that many tumor cell lines, including melanoma and colon adenocarcinoma can effectively chemoattract DC in vitro, modulate their phenotype, and eventually, severely damage DC mobility (9). From this point of view, recent reports about loss of certain chemokines in several tumors, including HNSCC, initially sound surprising (10–12). However, it is conceivable to hypothesize a new mechanism of tumor escape: loss of certain chemokines by tumor cells results in a low attraction of DC, decreased number of tumor-infiltrating DC and thus inhibited ability of the immune cells to recognize tumor and initiate specific antitumor immune responses. In fact, analysis of phenotype and distribution of immunocompetent cells in oral leukoplakia with different levels of dysplasia revealed that the levels of immune effector cells varied according to the degree of dysplasia (13). Examining distribution of $S100^+$ DC in the tumor tissues and regional lymph nodes of 60 patients with HNSCC, Deng et al. (14) reported that the $S100^+$ DC density in tumor tissues was correlated with the tumor histologic grade, and the density of $S100^+$ DC was significantly higher in regional lymph nodes without tumor than in those with metastases. A similar conclusion was reported after

Departments of *Pathology, [†]Immunology, [‡]Medicine, and [§]Otolaryngology, University of Pittsburgh Medical Center, Pittsburgh, PA 15213; and [¶]Department of Oral Medicine and Pathology, University of Pittsburgh School of Dental Medicine, Pittsburgh, PA 15261

Received for publication December 3, 2004. Accepted for publication February 8, 2005.

The costs of publication of this article were defrayed in part by the payment of page charges. This article must therefore be hereby marked *advertisement* in accordance with 18 U.S.C. Section 1734 solely to indicate this fact.

[1] This work was supported in part by National Institutes of Health Grant 2RO1 CA084270 (to M.R.S.) and University of Pittsburgh Cancer Institute Pilot Research grant (to G.V.S.).

[2] Address correspondence and reprint requests to Dr. Michael R. Shurin, Clinical Immunopathology, Room 5725 Children's Hospital of Pittsburgh-Medical Towers, University of Pittsburgh Medical Center, 200 Lothrop Street, Pittsburgh, PA 15213. E-mail address: shurinmr@upmc.edu

[3] Abbreviations used in this paper: HNSCC, head and neck squamous cell carcinoma; SCC, squamous cell carcinoma; DC, dendritic cell.

0022-1767/05/$02.00

evaluation of 36 cases of primary HNSCC of the lip mucosa or vermillion border for the correlation between tumor-associated DC density and tumor grade, mitotic rate, diameter, ulceration, depth of invasion, muscle invasion, and metastasis (15). Goldman et al. (16) have determined that survival and recurrence rates for patients with squamous cell carcinoma (SCC) of the tongue correlate with the degree of DC infiltration of the primary tumor or adjacent tongue tissue. Patients who had greater numbers of $CD1a^+$ DC adjacent to tumor had better survival and decreased recurrence rates. These suggest that the distribution of DC subsets in HNSCC may reflect the degree of tumor immunity induced in the host-bearing HNSCC. Altogether, these suggest a functional role of DC in the immune response to HNSCC. Localized absence of DC might impair mucosal immunologic protection, allow microbial colonization, and enhance carcinogenesis. However, the mechanisms and chemokines responsible for DC homing and accumulation in HNSCC are unknown.

The various members of chemokine are subdivided into four families known as either the CXC, C-C, C, and CX3C, or the α, β, γ, and δ subfamilies, respectively (17). Approximately 50 human chemokines and 20 receptors are currently known. This large number reflects the highly complex traffic pattern of blood leukocytes, including granulocytes, monocytes, lymphocytes, and DC. Accumulating evidence indicates critical regulatory roles for chemokines during the development of metastatic tumors by stimulating angiogenesis and tumor growth. In addition, by regulating immunity, chemokines critically regulate antitumor immune responses and chronic inflammation such as that associated with various neoplasias (18–20).

Breast and kidney-expressed chemokine (BRAK) CXCL14 is a new CXC chemokine with unknown function and receptor selectivity (11, 12, 21). CXCL14 transcripts are highest in human kidney, small intestine, and liver tissues and expressed constitutively by a variety of epithelia including the basal keratinocytes and dermal fibroblasts of skin (21). Importantly, Hromas et al. (12) reported that CXCL14 mRNA was expressed ubiquitously in normal tissues, but absent in a variety of in vitro established tumor cell lines. Moreover, using differential display and in situ mRNA hybridization, Frederick et al. (11) have recently reported that squamous epithelium constitutively express CXCL14, whereas expression in tumors was heterogeneous, with the majority of HNSCC and some cervical SCC showing loss of CXCL14 mRNA. This study demonstrates for the first time up-regulation of CXCL14 mRNA in the inflammatory sites in the tumor microenvironment and lost expression from certain cancers in vivo. The loss of expression in tumors and the presence of CXCL14 in nonmalignant tissues suggest that this chemokine may play a role in host-tumor interactions. It is also possible that down-regulation of the CXCL14 gene expression in tumor cells might be beneficial for tumor growth. However, the role of CXCL14 in the regulation of migration of DC in cancer and their biologic significance has not yet been investigated.

In the present work, we have established new in vitro and in vivo models to address the chemotactic interaction among human DC, CXCL14, and HNSCC tumor cells. We have demonstrated that HNSCC tissues are low in tumor infiltrating DC although DC are present in oral dysplasia lesions. Decreased infiltration of HNSCC by DC was correlated with no or low expression of CXCL14 protein at the tumor site. However, intense CXCL14 staining was observed in oral dysplasia (premalignant) lesions. Furthermore, we showed that CXCL14 is a potent DC chemoattractant in vitro and in vivo and DC are recruited to genetically modified CXCL14-expressing HNSCC cells. In addition to being potent DC chemoattractant, CXCL14 also increased functional activity of DC, which was associated with increased activity of NF-κB.

Materials and Methods

Tumor cell lines and tissues

Human SCC-15, prostate adenocarcinoma LNCaP, and melanoma FemX cell lines were obtained from American Type Culture Collection. The HNSCC PCI-13, PCI-16, and PCI-4B cell lines were prepared from HNSCC tumors (22). Conditioned medium from normal human lymph node cell suspensions served as a positive control. Tumor cells were maintained in RPMI 1640 medium supplemented with 10% heat-inactivated FCS, 100 U/ml penicillin, 100 μg/ml streptomycin, 0.2 mM L-glutamine, 1 mM sodium pyruvate, and 0.1 mM HEPES (Invitrogen Life Technologies).

The immunohistochemical studies were performed on a variety of formalin-fixed and paraffin-embedded tissue sections, including normal oral tissue (7 blocks), oral epithelial hyperplasia (8 blocks), and oral SCC (8 blocks).

Mice

Male C.B-17 SCID ($T^{-/-}$, $B^{-/-}$) mice, 6- to 8-wk-old were obtained from Taconic Farms. Animals were maintained in pathogen-free facility under the controlled temperature, humidity, and a 12-h light to dark cycle.

Immunohistochemistry

Monoclonal Abs recognizing CD83, CD1a (Immunotech), CD11c (DAKO), and S-100 (Sigma-Aldrich) were used for the detection of DC infiltration in formalin-fixed and paraffin-embedded tumor tissue sections. Five-micrometer sections were cut, mounted on positively precharged slides (Superfrost Plus; Fisher Scientific), and allowed to dry overnight at 56°C to ensure optimal adhesion. The sections were deparaffinized and rehydrated. After endogenous peroxidase quenching (0.3% H_2O_2 in PBS for 30 min), Ags were retrieved by boiling the sections in 1 mM EDTA/NaOH solution, pH 8.0, in a microwave oven for three cycles (5 min each). Appropriately diluted mouse anti-human Abs against CD83 (1/50), CD1a (nondiluted), CD11c (1/100), and S-100 protein (1/1000) were applied to each section. Immunohistochemistry was performed using an avidin-biotin peroxidase technique. Staining was developed with peroxidase and amino-9-ethylcarbazole or diaminobenzidine (Vector Laboratories).

Expression CXCL14 protein in tissue sections and tumor cell lines was determined with anti-CXCL14 mAbs (1/100, overnight incubation; R&D Systems). Staining with normal murine IgG2a was performed as a negative control for CXCL14 stain. Immunohistochemical and immunocytochemical staining was performed using avidin-biotin peroxidase technique described.

Transduction of HNSCC cell lines with the CXCL14 encoding vector

Frederick et al. (11) have demonstrated expression of CXCL14 in PBMC stimulated with LPS. We isolated total RNA from human PBMC activated with *Escherichia coli* LPS (0.5 μg/ml; Sigma-Aldrich) for 6 h using the TriReagent (Molecular Research Center) and according to the supplier's instructions. Up to 2 μg of total RNA was reverse-transcribed in a final reaction volume of 25 μl containing 2.5 μM oligonucleotides, 1× reaction buffer (Invitrogen Life Technologies), 0.5 mM each of dNTP (Invitrogen Life Technologies), 10 mM DTT, 1 μl of RNase inhibitor (Boehringer Mannheim), and 200 U of Superscript II reverse transcriptase (Invitrogen Life Technologies). For PCR, 4 μl of cDNA was amplified in a final volume of 30 μl containing 1× *Taq* buffer, 50 μM each dNTP, and 2.5 U of *Taq* polymerase enzyme (Invitrogen Life Technologies). Primers for human CXCL14 were: 5′-CAG GTC GAC ATG AGG CTC CTG GCG GCC GCG and 3′-CGG GGA TCC CTA TTC TTC GTA GAC CCT GCG. PCR amplification was performed at 94°C for 10 min, followed by 35 cycles at 94°C for 1 min, 64°C for 1 min, 72°C for 1 min, and a final extension at 72°C for 10 min. PCR products were resolved by agarose electrophoresis and stained with ethidium bromide. To construct a eukaryotic expression vector, the CXCL14 gene was cloned into pCR3.1 plasmid. The PCR products were purified using QIAEX II gel extraction kit (Qiagen) and cloned into pCR3.1 mammalian expression vector using the Eukaryotic TA Expression kit (Invitrogen Life Technologies) according to the manufacturer's instructions.

Human HNSCC primary cell line PCI-16 was transfected with the human CXCL14 gene using Effectene Transfection Reagent (Qiagen) according to the supplier's instructions. Briefly, tumor cells were counted and plated at 70% density in 10-cm petri dish 1 day before the transfection. On the next day, the

medium was removed, the cells were washed in HBSS (Invitrogen Life Technologies), and transfection mixture containing 2 μg of DNA was added to the tumor cells. The cells were incubated with a transfection mixture at 37°C for 6 h. After incubation, fresh medium (RPMI 1640, 10% FCS) was added and tumor cells were incubated at 37°C for additional 48 h. Next, transfected tumor cells were split and fresh medium containing 1 mg/ml geneticin (Invitrogen Life Technologies) was added for selection of transfected cells. Culture medium with geneticin was changed twice a week for 2–3 mo. Expression of CXCL14 protein was confirmed by Western blot (recombinant human CXCL14 served as a positive control; RDI) and immunocytochemistry.

RT-PCR

Analysis of mRNA expression of human chemokines in normal oral mucosa and HNSCC tissues was performed using RT-PCR technique. RNA was extracted from five normal mucosae and five oral SCC specimens, transcribed into cDNA using 200 U of superscript reverse transcriptase, and cDNA was amplified with 2.5 U of *Taq* polymerase using 1.5 pM of the primers specific for MIP-3α, MIP-3β, CXCL8, and GAPDH. RT-PCR was conducted as described earlier (23).

Generation of human monocyte-derived DC

CD14-derived DC were generated as described earlier (24). Briefly, PBMC were isolated from buffy coats by Ficoll gradient centrifugation. The PBMC were further plated at 10^7 cells/well in 2 ml of AIM-V medium (Invitrogen Life Technologies) in six-well plates. After 1-h incubation at 37°C in a humidified 5% CO_2 atmosphere, nonadherent cells were removed and adherent monocytes were gently washed with warm AIM-V medium. Adherent monocytes were cultured with recombinant human GM-CSF (1000 U/ml; PeproTech) and IL-4 (1000 U/ml; PeproTech) in complete RPMI 1640 medium for 7 days. Maturation of DC was stimulated by additional supplementation with 20 ng/ml TNF-α (PeproTech) on day 6.

Analysis of DC migration and chemotaxis in vitro and in vivo

Spontaneous and chemokine-induced migration of DC in vitro was assessed in the Transwell system with DC placed in the upper chamber (10^6 cells/ml, 100 μl) and chemokines added to the bottom chamber (600 μl) in a 4-h migration assay. Cell migration was measured in 48-well Transwell plates (5-μm pores; Corning Costar). Recombinant human MIP-1α (10–20 ng/ml; PeproTech), synthetic chemotactic peptide *N*-fMLP (0.5–5 μg/ml; Sigma-Aldrich) and recombinant human CXCL14 (5–200 ng/ml; RDI) were diluted in RPMI 1640 medium contained 1% FBS (assay medium), and 600-μl aliquots were placed in the lower chamber of Transwell plates. Assay medium was used to measure a spontaneous migration of DC. After 4-h incubation at 37°C, the Transwell inserts were removed and cells from the lower chamber were collected. Cells transmigrated through the 5-μm pore size membrane were acquired on FACScan (BD Biosciences) for 60 s. Data are reported as mean number of transmigrated cells from triplicate wells.

To test whether human tumor cell lines produce chemokines that attract DC, cell-free conditioned media were collected from FemX, LNCaP, and different HNSCC cell lines. Tumor cells were seeded at 1×10^6 in 4 ml of assay medium. Twenty-four hours later, cell-free supernatant was collected and centrifuged. Conditioned medium from normal human lymph node cell suspensions served as a positive control. Tumor-conditioned or control media were placed in the lower chamber of the Transwell plate and migration of DC was assessed as previously described.

Trafficking of DC in vivo was assessed in immunodeficient SCID mice (Taconic Farms) bearing human CXCL14-positive or CXCL14-negative PCI-16 HNSCC. Mice were injected s.c. with 10^7 CXCL14-positive or CXCL14-negative HNSCC cells and 2×10^6 human DC labeled with fluorescent dye 5-sulfofluorescein diacetate/succinimidyl ester (SFDA/SE, 2.5 μM; Molecular Probes) were injected i.v. 1 wk after tumor cells administration. Tumors were harvested 48 h later and tissue sections were analyzed by confocal microscopy and immunohistochemistry with anti-CD1a Abs.

Flow cytometry

Expression of DC specific markers was determined as described earlier (25) by flow cytometry on a FACSCalibur (BD Biosciences) using the following Abs: CD14-FITC, HLA-DR-PE (BD Biosciences), CD1a-PE, CD40-PE, CD80-PE, CD83-PE, (Immunotech/Coulter), and CD86-FITC (BD Pharmingen). The analyses were done using the CellQuest software (BD Biosciences).

MLR assay

MLR assays were performed to evaluate the effect of CXCL14 on the ability of human DC to stimulate proliferation of allogeneic T cells. Control and CXCL14-treated (200 ng/ml) DC were added in triplicates in graded doses (10^2–10^6 cells per well) to T cells (1×10^5 per well) in round-bottom 96-well plates. Proliferation of T cells was measured 72 h later by incorporation of [^{3}H]thymidine (1 μCi/well; DuPont-NEN) added for the last 16 h. Cells were harvested onto GF/C glass fiber filter paper (Whatman) and isotope incorporation was assessed by 1450 MicroBeta TRILUX liquid scintillation counter (Wallac). The counts were expressed as cpm ± SEM.

NF-κB activity assay

Monocyte-derived DC were treated with CXCL14 200 ng/ml for 0–30 min. TNF-α (50 ng/ml, 15 min) served as a well-known activator of NF-κB in DC. Nuclear extract from Jurkat cells was used as an internal control. The effect of CXCL14 on NF-κB activation in DC was determined using a method developed by Active Motif. This method was developed in an ELISA format and uses binding of the active form of NF-κB to immobilized oligonucleotides corresponding to NF-κB nuclear consensus site 5′-GGGACTTTCC-3′. The assay was performed according to the manufacturer's specifications.

We additionally quantitated NF-κB in DC by an activity assay recently developed by Marligen Biosciences using a Luminex technology. The assay is based on a specific binding of transcription factors to cognate sequences on labeled probes. Nuclear extracts were incubated with a mixture of PE-conjugate oligonucleotides containing appropriate cognate DNA binding sequences. This mixture was then incubated with a digestion reagent. In the presence of active transcription factors, label remains associated with the probes, whereas it is removed in the absence of transcription factor binding. Finally, the oligonucleotides were captured onto distinctly colored agarose microspheres that allow each of the reactions to be individually scored, and the quantitative signal generated by the label was detected with a Bio-Plex (Bio-Rad) reader. The amount of label remaining correlates with the amount of active transcription factor derived from the nuclear extract. This format allows better sensitivity and dynamic range than does EMSA. Furthermore, quantitative results allow comparisons among treatments. The assays were performed according to manufacturer's protocol.

Statistical analysis

For a single comparison of two groups, the Student *t* test was used after evaluation for normality. If data distribution was not normal, a Mann-Whitney rank sum test was performed. For the comparison of multiple groups, one- or two-way ANOVA was applied. For all statistical analysis, the level of significance was set at a probability of 0.05 to be considered significant. All experiments were repeated at least two or three times. Data are represented as the mean ± SEM.

Results

Immunohistochemical analysis of human HNSCC tissues for infiltration by DC and expression of CXCL14

First, we confirmed and expanded the published data concerning the reduction of DC numbers in the tumor mass when compared with nonmalignant tissues (14, 15). We analyzed a variety of paraffin specimens of HNSCC and oral dysplastic lesions for the presence of CD1a, S-100, CD83, and CD11c DC by immunohistochemistry. The biopsy specimens were from different patients diagnosed with mild to moderate dysplasia from oral mucosal sites, including buccal mucosa, lateral tongue, and floor of the mouth. For comparison, specimens were also obtained from patients diagnosed with invasive HNSCC from similar oral mucosal sites. The results of the analysis of multiple oral epithelial hyperplasia, and oral SCC specimens suggest that CD83- and CD11c-positive DC were essentially absent in HNSCC tissues, and the numbers of CD1a- and S-100-positive DC were markedly lower in the tumor tissues than in oral dysplasia lesions (Fig. 1*A*). These data allowed us to hypothesize that DC migration into the HNSCC tissues might be inhibited compared with their migration to the hyperplastic or premalignant lesions. It is likely that chemokines

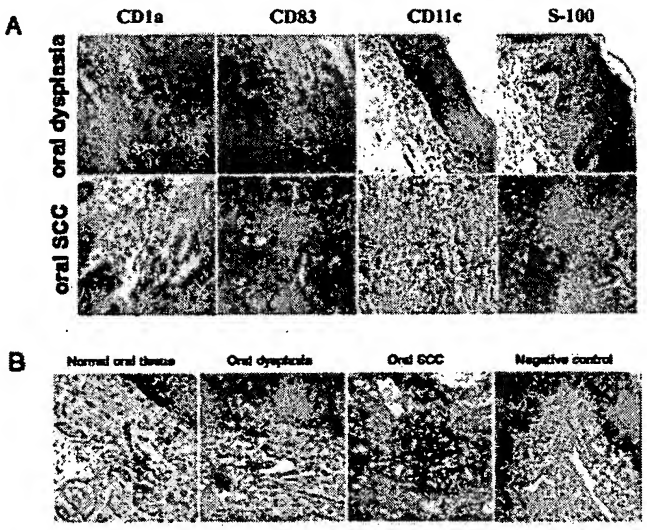

FIGURE 1. Immunohistochemical evaluation of tumor-infiltrating DC (*A*) and CXCL14 expression (*B*) in HNSCC, oral dysplasia, and normal oral tissue specimens. Five-micrometer sections were dried overnight, dewaxed, rehydrated, followed by Ag retrieval with 1 mM EDTA/NAOH solution (see *Materials and Methods*). *A*, For evaluating tumor-infiltrating DC, the following DC-specific Abs were used: CD83, CD1a, CD11c, and S-100. Secondary Abs were biotinylated with goat anti-mouse. *B*, For detection of CXCL14 expression in HNSCC tissues anti-CXCL14 Abs or control murine IgG2a were applied to the tissues overnight. Biotinylated horse anti-mouse secondary Abs were added for 30 min. Staining was developed with amino-9-ethylcarbazole and counterstained with hematoxylin. Positive staining is red-brown. The representative immunohistochemical data from the analysis of 10–12 specimens are shown.

are, at least in part, responsible for differential homing of DC in normal and malignant tissues.

To test whether decreased infiltration of HNSCC by DC might be associated with a low expression of chemokines, we have measured expression of DC attracting chemokines in HNSCC and normal mucosa tissues by RT-PCR. Our data revealed similar mRNA expression of MIP-3α (CCL20) and MIP-3β (CCL19) in HNSCC and normal mucosa (Fig. 2). These chemokines interact with CCR6 and CCR7, expressed on immature and mature DC, respectively. Given that expression of new chemokine CXCL14 mRNA was reported to be lost in different tumors (11, 12), we also examined CXCL14 protein in different human tissues by immunohistochemistry. Because expression of CXCL14 in tissues has been previously determined only by in situ hybridization (11, 12), we

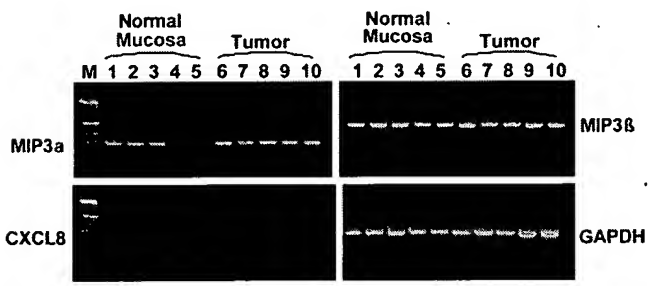

FIGURE 2. Analysis of chemokine mRNA expression in normal oral mucosa and HNSCC tissues by RT-PCR. mRNA was extracted from normal mucosa and HNSCC specimens, transcribed into cDNA using 200 U of superscript reverse transcriptase, and cDNA was amplified with 2.5 U *Taq* polymerase using 1.5 pM of the primers specific for MIP-3α, MIP-3β, CXCL8, and GAPDH, as described in *Materials and Methods*. The results of a representative experiment are shown (n = 3).

have developed a new immunohistochemical procedure to analyze CXCL14 protein in paraffin-embedded tissues. Fig. 1*B* demonstrates that both normal oral mucosa tissues (n = 7) and oral dysplasia specimens (n = 8) were strongly positive for CXCL14, whereas HNSCC tissues (n = 8) were low or negative for CXCL14 staining. Thus, these data suggest that CXCL14 protein is lost in human HNSCC, which led us to the hypotheses that low infiltration of HNSCC by DC might be associated with the lost expression of certain chemokines (i.e., CXCL14) and whether CXCL14 is chemoattractive for DC.

Chemoattractive properties of CXCL14 and tumor cell lines toward DC

To determine whether DC could be attracted by a CXCL14, we compared its chemotactic activity toward DC with the known DC chemokines. Analysis of DC migration revealed that CXCL14 and two control DC chemokines fMLP, a prototypic bacterial chemotactic stimulus (26) and MIP-1α (27), all dose-dependently chemoattracted human DC (Fig. 3*A*). For example, in the presence of 20 ng/ml MIP-1α migration of immature DC reached 6360 $\pm$ 650 cells/min vs 3620 $\pm$ 380 cells/min spontaneously transmigrated in control wells ($p < 0.05$). A comparable chemoattraction of DC (5960 $\pm$ 568 cells/min, $p < 0.05$) was also detected in the presence of 200 ng/ml (20 nM) CXCL14 (Fig. 3*A*). Thus, CXCL14 is a potent DC chemokine with a chemoattractive activity in the nanograms per milliliter range.

Next question was whether CXCL14 chemoattracts both immature and mature DC. Fig. 3*B* demonstrates that only immature, but not mature DC, are chemoattracted by CXCL14. These data are in agreement with Shellenberger et al. (28) and the general concept that immature DC are attracted to nonlymphoid tissues where a number of potent DC chemokines, including CXCL14, may be ubiquitously expressed.

In the next set of experiments, we tested whether human tumor cell lines, including different HNSCC, prostate adenocarcinoma, and melanoma, might produce chemokines that could attract human DC in vitro. Cell-free conditioned media were collected from FemX melanoma, LNCaP prostate adenocarcinoma, and HNSCC cell lines SCC-15, PCI-13, PCI-16, PCI-38, and PCI-4B as described in *Materials and Methods*. Conditioned medium from normal human lymph node cell suspensions served as a positive control. Fig. 3*C* demonstrates that conditioned media from FemX melanoma cells (5620 $\pm$ 483 vs 3630 $\pm$ 250 cells in control, $p < 0.005$), normal lymph node cells (5880 $\pm$ 602 cells, $p < 0.005$), and PCI-4B (6340 $\pm$ 436 cells, $p < 0.005$), but not from LNCaP (3920 $\pm$ 286 cells) and HNSCC lines PCI-13 (3720 $\pm$ 405), PCI16 (3320 $\pm$ 241), and SCC-15 (3390 $\pm$ 301) ($p > 0.1$), displayed chemoattractive activity toward human DC. Selective attraction of DC by several tumor cell lines raises the question whether it might correlate with the expression of CXCL14.

The next series of experiments focused on evaluating the expression of CXCL14 protein in different human tumor cell lines. Tumor cells were cultured on microscopic slides for 48–72 h, and CXCL14 protein was detected by the immunocytochemical procedure. Human PBMC-derived monocytes stimulated with 0.5 μg/ml LPS for 6 h served as a positive control for the expression of CXCL14. Nonstimulated PBMC were used as a negative control. We found that all tested tumor cells, with the exception of PCI4B and FemX, were CXCL14-negative (Fig. 3*D*). Thus, HNSCC cell line SCC-15 and primary HNSCC cell lines PCI-13, PCI-16, and PCI-38 as well as prostate adenocarcinoma cell line LNCaP express no CXCL14 protein. Interestingly, CXCL14-negative HNSCC cell lines did not attract DC in a chemotaxis assay,

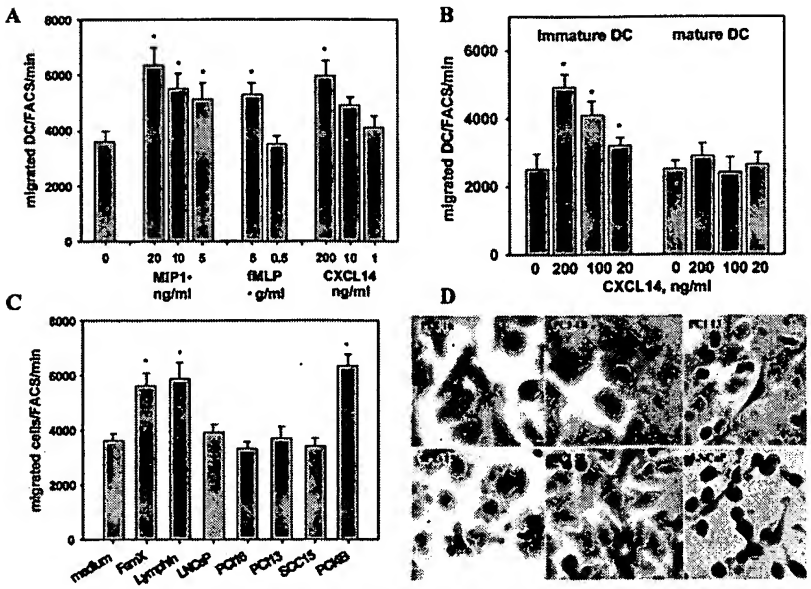

FIGURE 3. Analysis of migration of human DC toward different chemokines and tumor cell lines in vitro. DC were generated from $CD14^+$ monocytes, and DC chemotaxis was assessed in the 5-μm pore size Transwell system in 4-h migration assay. The numbers of transmigrated DC were determined by a 60 s FACScan analysis of triplicate samples. *A*, Comparative analysis of DC migration toward three chemokines revealed a chemoattractive potential of CXCL14. The results of a representative experiment are shown as mean ± SEM. Three independent experiments have shown similar results. *B*, Immature (GM-CSF + IL-4, Day 6), but not mature (GM-CSF + IL-4 + TNF-α, Day 8) DC migrate toward CXCL14. The representative results are shown as mean ± SEM ($n = 4$). *, $p < 0.05$, one-way ANOVA and *t* test. *C*, Differential chemoattraction of human DC to different human tumor cell lines. The results from three independent experiments are shown and presented as the mean ± SEM. *, $p < 0.05$, Student *t* test. *D*, Immunohistochemical evaluation of CXCL14 expression in tumor cell lines was done as described in *Materials and Methods*. Note the correlation between CXCL14 expression in tumor cell lines (*D*) and their chemoattractive potential toward DC in a migration assay (*C*).

whereas CXCL14-expressing cell lines PCI-4B and FemX demonstrated significant chemoattractive potential for DC in the same assay (Fig. 3*D*).

Migration of DC toward CXCL14-transduced tumors in vitro and in vivo

Our results indirectly support the hypothesis that DC are chemoattracted toward CXCL14-producing cells and do not migrate toward at least certain types of tumors that have lost expression of this chemokine. To test this possibility in direct in vitro and in vivo experiments, we have generated a vector encoding human CXCL14, which was used for a stable transduction of human CXCL14-negative HNSCC cell lines. The HNSCC cell line PCI-16 was transfected with the human CXCL14 gene and, after selection, expression of CXCL14 protein was confirmed by Western blot (Fig. 4*A*). These data suggest that CXCL14-negative tumor cells could be efficiently engineered to produce high levels of CXCL14 protein. Functional activity of synthesized CXCL14 protein in tumor cells was next tested in in vitro and in vivo experiments.

Next we demonstrated that human HNSCC tumor cells transduced with the CXCL14 gene attract significantly higher levels of human DC both in vitro and in vivo. First, cell-free supernatants from CXCL14-negative wild type PCI-16 cultures and PCI-16 cells transduced with CXCL14 were collected and tested for the attraction of human monocyte-derived DC in the chemotaxis assay. Fig. 4*B* shows that wild type PCI-16 cells did not attract DC (2100 ± 77 vs 2500 ± 105 cells transmigrated in control wells), whereas CXCL14-expressing PCI-16 cells were chemoattractive for DC (6400 ± 135 transmigrated cells, $p < 0.05$). Together with the results demonstrating no attraction of DC toward control neo-transduced tumor cells, this suggests that CXCL14-transduced tumor cells release biologically active CXCL14 protein. Second, we evaluated trafficking of human DC labeled with a fluorescent dye in SCID mice in vivo. Fluorescent-labeled human DC were i.v. injected in immunodeficient SCID mice ($n = 5$) bearing both wild type (or control neo-transduced) and CXCL14-transduced PCI-16 cells for 7 days. Two days later, tumors were harvested and fluorescent cells were examined on 6-μm sections immediately by confocal microscopy. The results revealed that infiltration of CXCL14-expressing tumors by labeled DC was significantly higher than in wild type or neo-transduced tumors in all tested mice (Fig. 4*C*). Similar data were obtained when nonlabeled human DC were i.v. transferred in SCID mice ($n = 5$) bearing PCI-16/wild type (or neo-transduced) and PCI-16/CXCL14 and infiltration of tumors by injected DC was assessed 48 h later by immunohistochemistry. Fig. 4*D* demonstrates that the levels of accumulation of $CD1a^+$ human DC in CXCL14-expressing tumors were markedly higher than the number of DC in control tumors. Thus, these results suggest that the recovery of CXCL14 expression in HNSCC cells is associated with increased attraction of DC both in vitro and in vivo.

Regulation of DC function by CXCL14

We next tested whether CXCL14, in addition to being a DC chemoattractant, may also increase functional activity of DC. We first examined whether CXCL14 alters phenotype characteristics of DC. Fig. 5 shows that the addition of 200 ng/ml CXCL14 to DC markedly up-regulated expression of CD83, HLA-DR, CD86, and CD80 molecules when compare with CXCL14-untreated DC. For example, the percentage of $CD83^+$ cells increased from 8.4 ± 0.9% in control DC cultures to 38.0 ± 2.3% in DC cultures treated with CXCL14 ($p < 0.01$). The same pattern was observed for the expression of CD86 and CD80 molecules on DC (Fig. 5). Interestingly, not only the percentage of DC expressing the specific markers was up-regulated after addition of CXCL14, but also the

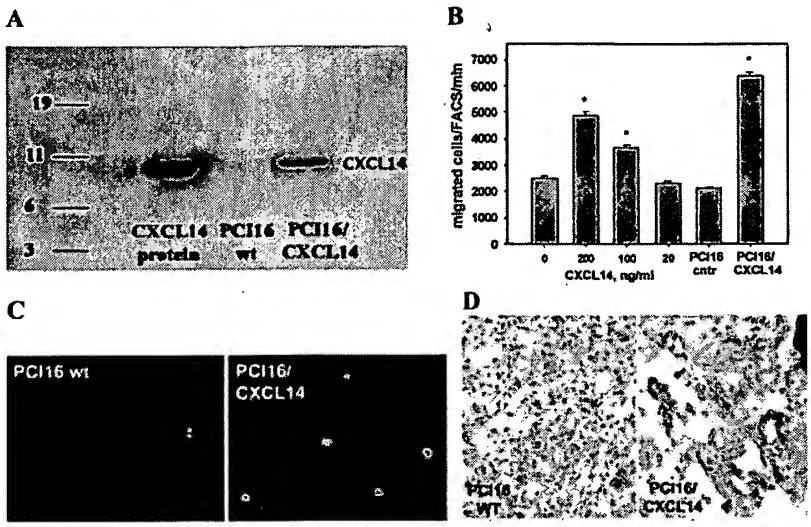

FIGURE 4. Transduction of CXCL14-negative human HNSCC cell line PCI-16 with the CXCL14 gene resulted in expression of high levels of CXCL14 protein. Primary HNSCC cells PCI-16 were transduced with the human CXCL14 gene as described in *Materials and Methods*. Immunocytochemical analysis of CXCL14-positive cells was assessed by Western Blot (*A*) as described in *Materials and Methods*. Recombinant human CXCL14 protein served as a positive control. *B*, CXCL14-transduced HNSCC cells secrete functionally active protein, which exhibits significant chemoattractive potential toward human DC in vitro (*B*) and in vivo (*C* and *D*). PCI-16 cells were transduced with the human CXCL14 gene and after selection with G148 supernatants obtained from wild type (wt) and CXCL14-transduced PCI-16 tumor cells were tested for their ability to attract DC in Transwell-based cell migration assay (*B*). Medium and CXCL14 served as negative and positive controls, respectively. *, $p < 0.05$ vs medium (one-way ANOVA, $n = 5$). *C* and *D*, PCI-16 wild type or PCI-16/CXCL14 tumor cells (10^7 cells per mouse) were injected s.c. in SCID mice on day 1. Sulfofluorescein diacetate/succinimidyl ester (SFDA/SE)-labeled or nonlabeled human DC (2×10^6 cells) were injected i.v. on day 7 and all tumors were harvested 48 h later. Tissue sections were analyzed by confocal microscopy (*C*) or immunohistochemistry with anti-CD1a Abs (red staining) (*D*) as described in *Materials and Methods*. The results from a representative experiment ($n = 3$) are shown.

levels of CD83, CD86, CD80, and HLA-DR expression on DC were significantly up-regulated (Fig. 5). For instance, the mean fluorescence intensity values for CD83 and HLA-DR markers were increased from 4.4 ± 0.5 in control DC to 15.9 ± 1.4 ($p < 0.01$) on DC treated with CXCL14 and from 123.6 ± 5.8 to 287.7 ± 9.9 ($p < 0.01$), respectively (Fig. 5). Thus, it is conceivable that CXCL14 stimulates maturation of DC.

Further confirmation of the biologic activity of CXCL14 was obtained in the MLR assay using DC generated from different donors with or without the addition of 200 ng/ml CXCL14 (Fig. 6*A*). Significantly higher induction of allogeneic T cell proliferation by CXCL14-treated DC ($p < 0.01$), as compared with untreated DC, was observed. For instance, at DC to T cell ratio 1:30, uptake of [^{3}H]thymidine increased from 17252 ± 897 cpm in control to 30385 ± 689 cpm ($p < 0.01$) in group treated with CXCL14.

To explore the molecular mechanisms of CXCL14-mediated activation of DC, monocyte-derived DC were treated with CXCL14 (200 ng/ml) and TNF-α (50 ng/ml). The levels of p65 in nuclear extracts were determined using NF-κB Transcription Factor Assay kit. TNF-α served as a well-known activator of NF-κB in DC. Nuclear extract from Jurkat cells was used as internal control. We demonstrated that activation of DC with CXCL14 was accompanied by a significant up-regulation of NF-κB activity in DC up to 200% ($p < 0.01$) (Fig. 6*B*). Next, these data were confirmed and further explored by using Luminex-based technique for analyzing NF-κB activation (Fig. 6*C*). The results also demonstrated that CXCL14 is a strong inducer of NF-κB activation in human DC. Interestingly, the kinetic analysis of transcription factor activity revealed that NF-κB activation induced in DC by CXCL14 was delayed compared with TNF-α-induced activation reaching the maximum at 30 min (Fig. 6*C*).

In summary, these data suggest that CXCL14, in addition to being DC attractant, also increases functional activity of DC.

Discussion

We have demonstrated that expression of a new DC chemokine, CXCL14, is frequently lost in HNSCC tissues, which was accompanied by a low infiltration of the tumor by DC. We speculate that low levels of HNSCC infiltration by DC may be due to a low or absent expression of CXCL14 in tumor cells. It is well known that homing of leukocytes to the sites of hemopoiesis, Ag priming, immune surveillance, and inflammation largely depends on the presence of chemokines (29). The presence of DC, macrophages, and lymphocytes in solid tumors is regulated by local production of chemokines by tumor and stromal cells. In particular, CC chemokines are the major determinants of macrophage and lymphocyte infiltration in carcinomas of the breast and cervix, sarcomas, and gliomas (30). CCL2 (MCP-1) has been implicated in mediating macrophage infiltration into breast (19) and ovarian cancers (31), whereas CCL5 levels correlate with the extent of CD8 T cell infiltrate in ovarian tumors (20). It is conceivable to speculate that immature DC might be constitutively recruited to CXCL14-expressing tissues. This would allow DC and monocytes to leave the circulation and enter these tissues in the absence of inflammation. On the contrary, the loss of CXCL14 expression in malignant tissues may explain a decreased rate of DC attraction and thus augments efficacy of tumor escape mechanisms.

CXCL14 was initially named BRAK because it was identified in human breast and kidney derived cells (12). CXCL14 (KS1, Kec, BMAC, NJAC, MIP-2γ) is a chemokine with an as yet unknown function and receptor selectivity (11, 12, 21). The mature sequences of CXCL14 and its murine analog SK1 contain 77 amino acids and are unique with regard to the short N-terminal end of only two amino acids (Ser-Lys), preceding the first of four chemokine-typical Cys residues. The most closely related chemokines, MIP-2α and MIP-2β, share ~30% amino acid identity with CXCL14. Kurth et al. (32) have recently provided evidence that

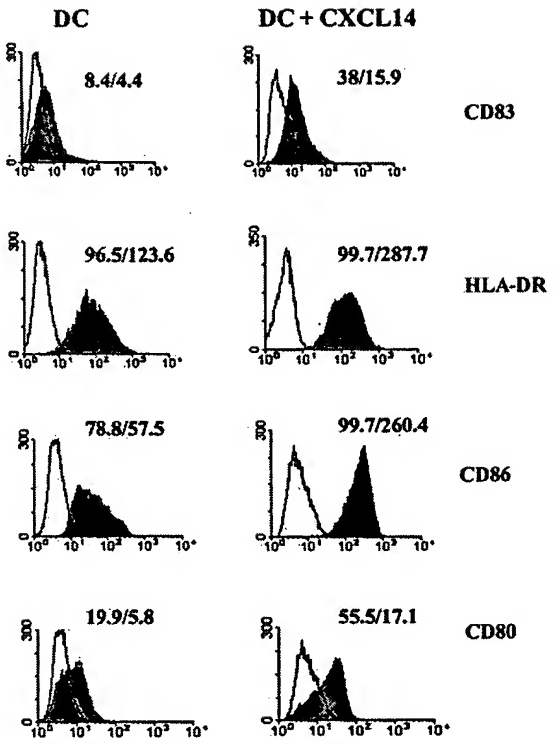

FIGURE 5. CXCL14 up-regulated DC maturation. Monocyte-derived DC were coincubated with CXCL14 (200 ng/ml, 72 h) and surface expression of CD83, CD80, CD86, and HLA-DR was assessed by FACScan. Both the percentage and the mean fluorescent intensity (%/MFI) are demonstrated. The results of a representative experiment are shown (n = 3).

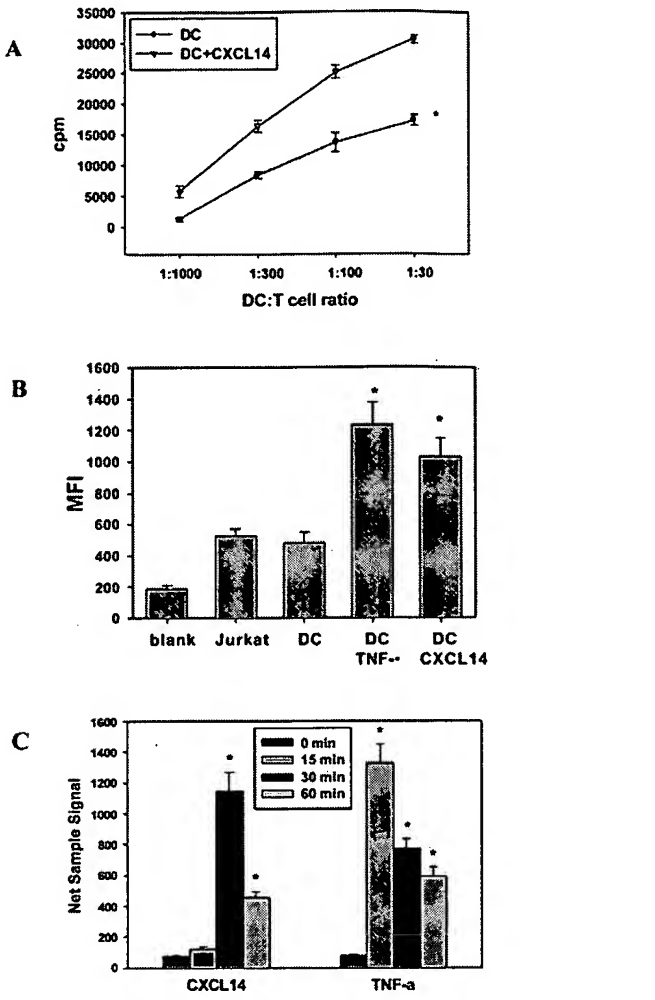

FIGURE 6. CXCL14 stimulated APC function of human DC and up-regulates activation of NF-κB. *A*, CXCL14 (200 ng/ml, daily day 3–6) significantly up-regulates Ag-presenting activity of human DC in vitro, as was determined in an allogeneic MLR assay. Data are shown as mean ± SEM. *, $p < 0.01$, two-way ANOVA (n = 3). *B*, Monocyte-derived DC were treated with CXCL14 (200 ng/ml, 30 min) and p65 was assessed in nuclear extracts as described in *Material and Methods*. TNF-α (50 ng/ml, 15 min) served as well-known activator of NF-κB in DC. Nuclear extract from Jurkat cells was used as an internal control. The levels of p65 in nuclear extracts were determined using NF-κB Transcription Factor Assay kit (Active Motif). Data are expressed as mean ± SEM from two independent experiments. *, $p < 0.05$ (ANOVA). *C*, NF-κB activity in human DC was determined 0, 15, 30, and 60 min after stimulation with CXCL14 (200 ng/ml) or TNF-α (50 ng/ml) using Luminex-based technique as described in *Materials and Methods*. The results are shown as mean ± SEM from two independent experiments. *, $p < 0.01$ (ANOVA).

CXCL14 is not a chemoattractant for peripheral blood T cells, B cells, and NK cells or neutrophils and is selectively chemotactic for monocytes activated by the cyclic AMP-elevating agents PGE_2 and forskolin. The authors proposed that once monocytes enter tissues in response to local inflammation, PGE_2 at the site renders them responsive to the high levels of CXCL14 in these tissues, attracting them to the subepithelial locations where they mature into macrophages. In contrast, others have reported that CXCL14 regulates trafficking of B cells (21), is a potent chemoattractant for neutrophils, and weak or inactive for DC, monocytes, NK cells, and T and B lymphocytes (33). Thus, the data on the biologic role of CXCL14 for chemoattraction of immune cells are controversial.

Our results demonstrate that human recombinant CXCL14 and CXCL14-transduced HNSCC cell line PCI-4B are potent inducers of DC migration in vitro and in vivo, whereas CXCL14-negative HNSCC cell lines and prostate adenocarcinoma cell line LNCaP do not attract DC in a chemotaxis assay. Several laboratories demonstrated that CXCL14 mRNA is constitutively expressed in normal tissues, but absent in a number of tumors (11, 12, 34). The majority of HNSCC and some cervical SCC show loss of CXCL14 mRNA. Analysis of the expression of 20,000 genes in human prostate epithelial cells passaged to senescence revealed the CXCL14 gene among three genes whose expression was uniformly lost in human prostate cancer cell lines and xenografts (34). The loss of expression in tumors and the presence of CXCL14 in nonmalignant tissues suggest that this chemokine may play a role in host-tumor interactions. It is also possible that down-regulation of the CXCL14 gene expression in tumor cells might be beneficial for tumor growth. In agreement, our new data revealed that the growth of CXCL14-transduced murine HNSCC cell line B7E3/6 in syngeneic BALB/c mice was significantly inhibited in comparison with wild type tumors, which was associated with high infiltration by DC and $CD8^+$ T cells (G. V. Shurin, R. Ferris, I. L. Tourkova, L. Perez, G. S. Chatta, and M. R. Shurin, manuscript in preparation).

Importantly, a leukocyte and chemokine balance in tumors can be manipulated. When murine tumors are engineered to overexpress certain chemokines, the increased intratumoral infiltrate stimulates antitumor responses. For instance, overexpression of CCL19 (MIP-3β) mediated rejection of murine breast tumors in an NK cell and CD4 T cell-dependent mechanism (35). CCL21 (6Ckine) reduced growth of colon adenocarcinoma in mice using a similar pathway (36). Overproduction of CCL20 (MIP-3α) might activate tumor-specific CTLs by attracting DC (37), whereas overproduction of secondary lymphoid tissue chemokine by DC may

enhance T cell recruitment and immune priming to tumor-associated Ags (38). In fact, injection of recombinant secondary lymphoid tissue chemokine in the axillary lymph node region in mice with bilateral multifocal pulmonary adenocarcinomas led to a marked reduction in tumor burden with extensive lymphocytic and DC infiltration of the tumors and enhanced survival (39). Together with clinical evidence demonstrating that infiltration of tumor mass by DC is associated with a better patient survival, these results suggest that regulated induction of DC migration into the tumor site might induce efficient antitumor immune responses. However, there are no data on whether CXC cytokines play a role in attraction of immune cells to the tumor site and inducing antitumor immunity. We have shown, that genetic modification of CXCL14-negative PCI-16 HNSCC cell line with the CXCL14 gene results in stimulation of DC attraction in vitro and increased infiltration of the tumor by DC in vivo. In fact, we have shown on a murine HNSCC model that CXCL14-expressing tumors were highly infiltrated by $CD11c^+$ DC suggesting their potential role in developing antitumor immune response at the tumor site (G. V. Shurin, R. Ferris, I. L. Tourkova, L. Perez, A. Lokshin, L. Balkir, B. Collins, G. S. Chatta, and M. R. Shurin, manuscript in preparation).

Next, we evaluated the effect of CXCL14 on DC function. It is known that chemokines may regulate cellular adhesion, proliferation, and cell survival (10, 18, 40). Based on the current knowledge of the life cycle of DC, it has been postulated that chemokines can play an important role at several stages of DC development (18). Basal chemokine production and expression at the surface of endothelial cells can mediate DC precursor recruitment into peripheral tissues, which is important for the maintaining DC levels within tissues. Once in the tissue, chemokines, such as MIP-1α, MIP-1β, MIP-3α, MIP-5, MCP-3, MCP-4, RANTES, TECK, and SDF-1 (41), may participate in differentiation of DC precursors into immature DC that are programmed to pick up and process Ag(s). Upon initiation of an inflammatory response, chemokines that recruit immature DC may be up-regulated, resulting in DC accumulation within the tissue. When DC have matured, they enter tissue-draining lymphatic vessels and migrate to the T cell zones in secondary lymphoid organs under the influence of chemokines produced there, such as MIP-3β and 6Ckine. In the T cell zones, DC can produce chemokines that stimulate DC-T cell interaction, thereby enhancing the likelihood of clonal selection (18, 41). Our data show that CXCL14 chemoattracts only immature, but not mature DC, which is in agreement with the concept that nonlymphoid tissue chemokines should attract immature DC. Importantly, we demonstrated that CXCL14 also activated DC through NF-κB-mediated pathways and up-regulated expression of costimulatory molecules on DC as well as enhanced the proliferation of allogeneic T cells in MLR. Thus our results support the hypothesis that CXCL14 might be a novel DC chemokine regulating their homing and activation in nonlymphoid tissues.

Disclosures

The authors have no financial conflict of interest.

References

1. Greenlee, R. T., M. B. Hill-Harmon, T. Murray, and M. Thun. 2001. Cancer statistics. *CA Cancer J. Clin. 51:15.*
2. Wong, D. T., R. Todd, T. Tsuji, and R. B. Donoff. 1996. Molecular biology of human oral cancer. *Crit. Rev. Oral Biol. Med. 7:319.*
3. Neville, B. W., and T. A. Day. 2002. Oral cancer and precancerous lesions. *CA Cancer J. Clin. 52:195.*
4. Becker, Y. 1992. Anticancer role of dendritic cells (DC) in human and experimental cancers: a review. *Anticancer Res. 12:511.*
5. Janjic, B. M., G. Lu, A. Pimenov, T. L. Whiteside, W. J. Storkus, and N. L. Vujanovic. 2002. Innate direct anticancer effector function of human immature dendritic cells. I. Involvement of an apoptosis-inducing pathway. *J. Immunol. 168:1823.*
6. Triozzi, P. L., R. Khurram, W. A. Aldrich, M. J. Walker, J. A. Kim, and S. Jaynes. 2000. Intratumoral injection of dendritic cells derived in vitro in patients with metastatic cancer. *Cancer 89:2646.*
7. Shurin, M. R., and D. I. Gabrilovich. 2001. Regulation of dendritic cell system by tumor. *Cancer Res. Ther. Control 11:65.*
8. Shurin, G. V., Z. R. Yurkovetsky, and M. R. Shurin. 2003. Tumor-induced dendritic cell dysfunction. In *Mechanisms of Tumor Escape.* A. Ochoa, ed. Harwood Academic Publishers, p. 115.
9. Remmel, E., L. Terracciano, C. Noppen, P. Zajac, M. Heberer, G. C. Spagnoli, and E. Padovan. 2001. Modulation of dendritic cell phenotype and mobility by tumor cells in vitro. *Hum. Immunol. 62:39.*
10. Brault, M. S., and R. A. Kurt. 2003. Chemokines and antitumor immunity: walking the tightrope. *Int. Rev. Immunol. 22:199.*
11. Frederick, M. J., Y. Henderson, X. Xu, M. T. Deavers, A. A. Sahin, H. Wu, D. E. Lewis, A. K. El-Naggar, and G. L. Clayman. 2000. In vivo expression of the novel CXC chemokine BRAK in normal and cancerous human tissue. *Am. J. Pathol. 156:1937.*
12. Hromas, R., H. E. Broxmeyer, C. Kim, H. Nakshatri, K. Christopherson, II, M. Azam, and Y. H. Hou. 1999. Cloning of BRAK, a novel divergent CXC chemokine preferentially expressed in normal versus malignant cells. *Biochem. Biophys. Res. Commun. 255:703.*
13. Bondad-Palmario, G. G. 1995. Histological and immunochemical studies of oral leukoplakia: phenotype and distribution of immunocompetent cells. *J. Philippines Dental Assoc. 47:3.*
14. Deng, Y., X. Yuan, and Z. Chen. 1997. Immunobiological significance of S-100 protein positive dendritic cells ($S\text{-}100^+$DC) in patients with oral squamous cell carcinoma. *Zhonghua Kou Qiang Yi Xue Za Zhi. 32:174.*
15. Wei, N., and S. R. Tahan. 1998. $S100^+$ cell response to squamous cell carcinoma of the lip: inverse correlation with metastasis. *J. Cutaneous Pathol. 25:463.*
16. Goldman, S. A., E. Baker, R. J. Weyant, M. R. Clarke, J. N. Myers, and M. T. Lotze. 1998. Peritumoral CD1a-positive dendritic cells are associated with improved survival in patients with tongue carcinoma. *Arch. Otolaryngol. Head Neck Surg. 124:641.*
17. Rollins, B. J. 1997. Chemokines. *Blood 90:909.*
18. McColl, S. R. 2002. Chemokines and dendritic cells: a crucial alliance. *Immunol. Cell Biol. 80:489.*
19. Ueno, T., M. Toi, H. Saji, M. Muta, H. Bando, K. Kuroi, M. Koike, H. Inadera, and K. Matsushima. 2000. Significance of macrophage chemoattractant protein-1 in macrophage recruitment, angiogenesis, and survival in human breast cancer. *Clin. Cancer Res. 6:3282.*
20. Negus, R. P., G. W. Stamp, J. Hadley, and F. R. Balkwill. 1997. Quantitative assessment of the leukocyte infiltrate in ovarian cancer and its relationship to the expression of C-C chemokines. *Am. J. Pathol. 150:1723.*
21. Sleeman, M. A., J. K. Fraser, J. G. Murison, S. L. Kelly, R. L. Prestidge, D. J. Palmer, J. D. Watson, and K. D. Kumble. 2000. B cell- and monocyte-activating chemokine (BMAC), a novel non-ELR α-chemokine. *Int. Immunol. 12:677.*
22. Heo, D. S., C. Snyderman, S. M. Gollin, S. Pan, E. Walker, R. Deka, E. L. Barnes, J. T. Johnson, R. B. Herberman, and T. L. Whiteside. 1989. Biology, cytogenetics, and sensitivity to immunological effector cells of new head and neck squamous cell carcinoma lines. *Cancer Res. 49:5167.*
23. Wang, J., L. Xi, J. L. Hunt, W. Gooding, T. L. Whiteside, Z. Chen, T. E. Godfrey, and R. L. Ferris. 2004. Expression pattern of chemokine receptor 6 (CCR6) and CCR7 in squamous cell carcinoma of the head and neck identifies a novel metastatic phenotype. *Cancer Res. 64:1861.*
24. Shurin, M. R. 2003. Preparation of human dendritic cells for tumor vaccination. In *Methods in Molecular Biology. Cytokines and Colony Stimulating Factors: Methods and Protocols.* vol. 215. D. K. a. W. Kiess, ed. Humana Press, Totowa, NJ, p. 437.
25. Shurin, G. V., M. R. Shurin, S. Bykovskaia, J. Shogan, M. T. Lotze, and E. M. Barksdale, Jr. 2001. Neuroblastoma-derived gangliosides inhibit dendritic cell generation and function. *Cancer Res. 61:363.*
26. Sozzani, S., F. Sallusto, W. Luini, D. Zhou, L. Piemonti, P. Allavena, J. Van Damme, S. Valitutti, A. Lanzavecchia, and A. Mantovani. 1995. Migration of dendritic cells in response to formyl peptides, C5a, and a distinct set of chemokines. *J. Immunol. 155:3292.*
27. Sozzani, S., P. Allavena, A. Vecchi, and A. Mantovani. 2000. Chemokines and dendritic cell traffic. *J. Clin. Immunol. 20:151.*
28. Shellenberger, T. D., M. Wang, M. Gujrati, A. Jayakumar, R. M. Strieter, M. D. Burdick, C. G. Ioannides, C. L. Efferson, A. K. El-Naggar, D. Roberts, et al. 2004. BRAK/CXCL14 is a potent inhibitor of angiogenesis and a chemotactic factor for immature dendritic cells. *Cancer Res. 64:8262.*
29. Moser, B., and P. Loetscher. 2001. Lymphocyte traffic control by chemokines. *Nat. Immunol. 2:123.*
30. Bottazzi, B., N. Polentarutti, R. Acero, A. Balsari, D. Boraschi, P. Ghezzi, M. Salmona, and A. Mantovani. 1983. Regulation of the macrophage content of neoplasms by chemoattractants. *Science 220:210.*
31. Bottazzi, B., P. Ghezzi, G. Taraboletti, M. Salmona, N. Colombo, C. Bonazzi, C. Mangioni, and A. Mantovani. 1985. Tumor-derived chemotactic factor(s) from human ovarian carcinoma: evidence for a role in the regulation of macrophage content of neoplastic tissues. *Int. J. Cancer 36:167.*
32. Kurth, I., K. Willimann, P. Schaerli, T. Hunziker, I. Clark-Lewis, and B. Moser. 2001. Monocyte selectivity and tissue localization suggests a role for breast and kidney-expressed chemokine (BRAK) in macrophage development. *J. Exp. Med. 194:855.*

33. Cao, X., W. Zhang, T. Wan, L. He, T. Chen, Z. Yuan, S. Ma, Y. Yu, and G. Chen. 2000. Molecular cloning and characterization of a novel CXC chemokine macrophage inflammatory protein-2γ chemoattractant for human neutrophils and dendritic cells. *J. Immunol. 165:2588.*
34. Schwarze, S. R., S. E. DePrimo, L. M. Grabert, V. X. Fu, J. D. Brooks, and D. F. Jarrard. 2002. Novel pathways associated with bypassing cellular senescence in human prostate epithelial cells. *J. Biol. Chem. 277:14877.*
35. Braun, S. E., K. Chen, R. G. Foster, C. H. Kim, R. Hromas, M. H. Kaplan, H. E. Broxmeyer, and K. Cornetta. 2000. The CC chemokine CKβ-11/MIP-3β/ELC/Exodus 3 mediates tumor rejection of murine breast cancer cells through NK cells. *J. Immunol. 164:4025.*
36. Vicari, A. P., S. Ait-Yahia, K. Chemin, A. Mueller, A. Zlotnik, and C. Caux. 2000. Antitumor effects of the mouse chemokine 6Ckine/SLC through angiostatic and immunological mechanisms. *J. Immunol. 165:1992.*
37. Fushimi, T., A. Kojima, M. A. Moore, and R. G. Crystal. 2000. Macrophage inflammatory protein 3α transgene attracts dendritic cells to established murine tumors and suppresses tumor growth. *J. Clin. Invest. 105:1383.*
38. Terando, A., B. Roessler, and J. J. Mule. 2004. Chemokine gene modification of human dendritic cell-based tumor vaccines using a recombinant adenoviral vector. *Cancer Gene Ther. 11:165.*
39. Sharma, S., M. Stolina, L. Zhu, Y. Lin, R. Batra, M. Huang, R. Strieter, and S. M. Dubinett. 2001. Secondary lymphoid organ chemokine reduces pulmonary tumor burden in spontaneous murine bronchoalveolar cell carcinoma. *Cancer Res. 61:6406.*
40. Nakashima, E., A. Oya, Y. Kubota, N. Kanada, R. Matsushita, K. Takeda, F. Ichimura, K. Kuno, N. Mukaida, K. Hirose, et al. 1996. A candidate for cancer gene therapy: MIP-1α gene transfer to an adenocarcinoma cell line reduced tumorigenicity and induced protective immunity in immunocompetent mice. *Pharm. Res. 13:1896.*
41. Caux, C., S. Ait-Yahia, K. Chemin, O. de Bouteiller, M. C. Dieu-Nosjean, B. Homey, C. Massacrier, B. Vanbervliet, A. Zlotnik, and A. Vicari. 2000. Dendritic cell biology and regulation of dendritic cell trafficking by chemokines. *Springer Semin. Immunopathol. 22:345.*